FEBRUARY 2025
VOLUME 84
ISSUE
2

ANNALS OF THE RHEUMATIC DISEASES

THE EULAR JOURNAL

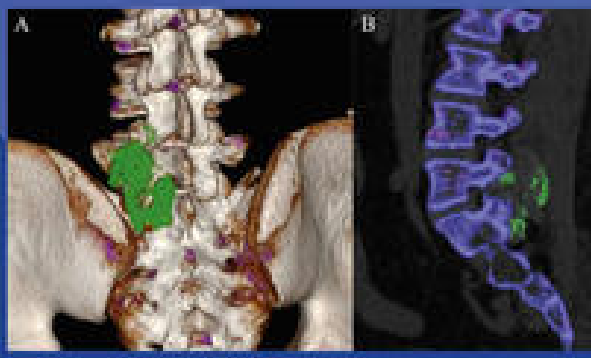

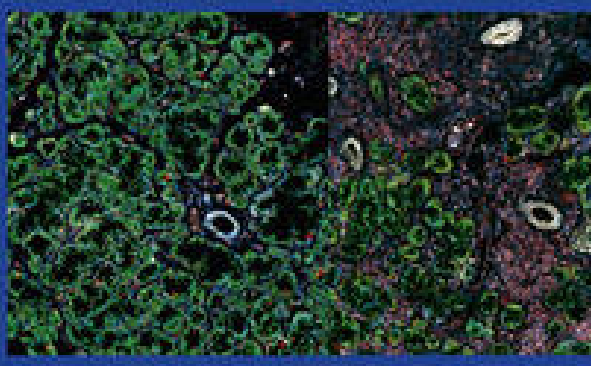

ELSEVIER

eular
EUROPEAN ALLIANCE OF ASSOCIATIONS FOR RHEUMATOLOGY

The home of innovative rheumatology research

Ann Rheum Dis 84 (2025) 153–157

Contents lists available at ScienceDirect

Annals of the Rheumatic Diseases

journal homepage: https://www.sciencedirect.com/journal/annals-of-the-rheumatic-diseases

Viewpoint

Cure as a treatment target in rheumatoid arthritis and systemic sclerosis—achievable aim or mission impossible? FOREUM stimulates new industry-academia collaboration

Kenneth Frank Baker[1,2], Julia Spierings[3], Martin Brom[4], Timothy Radstake[5], Emma Smith[6], Roberta Weiss[7], Gerd R. Burmester[8,*], FOREUM Boot Camp Working Group member

[1] *Translational and Clinical Research Institute, Newcastle University, Newcastle upon Tyne, UK*
[2] *Rheumatology Department, Newcastle upon Tyne Hospitals NHS Foundation Trust, Newcastle upon Tyne, UK*
[3] *Rheumatology and Clinical Immunology, Universitair Medisch Centrum Utrecht, Utrecht, The Netherlands*
[4] *Novartis, Basel, Switzerland*
[5] *AbbVie Inc, Cambridge, Massachusetts, USA*
[6] *UCB, Slough, UK*
[7] *Pfizer, Collegeville, Pennsylvania, USA*
[8] *Department of Rheumatology and Clinical Immunology, Charité - Universitätsmedizin Berlin, Berlin, Germany*

Keywords:
treatment
rheumatoid arthritis
scleroderma
systemic

The past 25 years have witnessed a remarkable revolution in outcomes for patients living with rheumatoid arthritis (RA). Historically, uncontrolled joint inflammation was commonplace leading to inexorable joint destruction, disability and mortality. In contrast, well over half of patients diagnosed with RA in the modern era can now achieve disease remission through a combination of early diagnosis, treat-to-target drug escalation and a pathogenesis-driven introduction of novel therapeutics [1]. With disease remission now an achievable treatment target in RA, can—and should—we aim higher to achieve disease cure?

Management of systemic sclerosis (SSc) is different from RA because of the multiorgan character and complex pathophysiology. Organ complications can be life-threatening and in many patients SSc severely reduces quality of life and limits daily functioning. Although progress in disease management still lags behind that of RA, SSc mortality has steadily decreased over the past two decades [2] due to improved disease monitoring and new treatment strategies targeting autoimmunity, fibrosis and vasculopathy [3]. Furthermore, there is an ongoing shift towards early treatment and defining very early stages of SSc to create a window for intervention and prevention of progression towards SSc, analogous to the developments in RA [4].

In this white paper, we summarise discussions and key learning points from the first FOREUM Boot Camp—an ambitious and innovative initiative to foster collaboration and sharing of ideas and experience between world-leading European rheumatology academics and major pharmaceutical companies. The focus of this boot camp, held over 3 days in March 2024, was remission and cure in RA and SSc. FOREUM Foundation for Research is promoting health in individuals with rheumatic and musculoskeletal diseases (RMDs) through excellent effective research (https://www.foreum.org/). A full collection of summaries of the contribution made at the boot camp can be obtained via the following link: (https://www.foreum.org/foreum_academy.cfm).

*Correspondence to Dr. Gerd R. Burmester.
E-mail address: gerd.burmester@charite.de (G.R. Burmester).
Handling editor Josef S. Smolen

https://doi.org/10.1136/ard-2024-226772
Received 13 September 2024; Accepted 15 October 2024

REMISSION VERSUS CURE: WHAT IS THE DIFFERENCE?

The concept of disease cure has been established for centuries, even featuring in the Latin lexicon as *restitutio ad integrum*, meaning 'restoration to original condition'. In contrast, remission as a medical term is a relatively modern concept with origins in the field of oncology. Following eradication of detectable malignancy through surgery, radiotherapy and/or chemotherapy/immunotherapy, a patient is said to be 'in remission'. Following a period in remission without relapse of malignancy, a patient is then said to be 'cured'—the time period differs for different malignancies, but many studies focus on 5-year survival rates as analogous to cure. These concepts are relatively straightforward to formulate for conditions caused by clearly defined 'foreign' agent, such as a malignancy composed of transformed cancer cells, or an infection driven by an exogenous pathogen. However, despite being frequently discussed in the context of RMDs, the concepts of remission and cure are more difficult to define in the dynamic dysregulation of endogenous immunity that underpins RMD pathogenesis.

In the context of RMDs, remission refers to the absence (or near-absence) of symptoms and signs of the disease. Thus, a patient in remission still has disease, but the symptoms have been controlled or eliminated for a period of time. Remission is usually achieved through the use of immunomodulatory drugs, and usually most patients require ongoing treatment to keep the disease under control (ie, on-drug remission). After a prolonged period of remission, some patients may choose to taper and potentially stop treatment, achieving drug-free remission. Transition between these states is dynamic, such that an individual patient may move bidirectionally between active disease, on-drug remission and drug-free remission throughout their disease course (figure 1). In contrast, cure refers to a specific subset of patients in drug-free remission who have regained a state of enduring immune tolerance, such that they are no longer at increased risk of disease relapse compared with the healthy population. In essence, transition to cure is thus unidirectional, that is, once cure is achieved, there is no (or at least negligible) risk of transition back to a disease state.

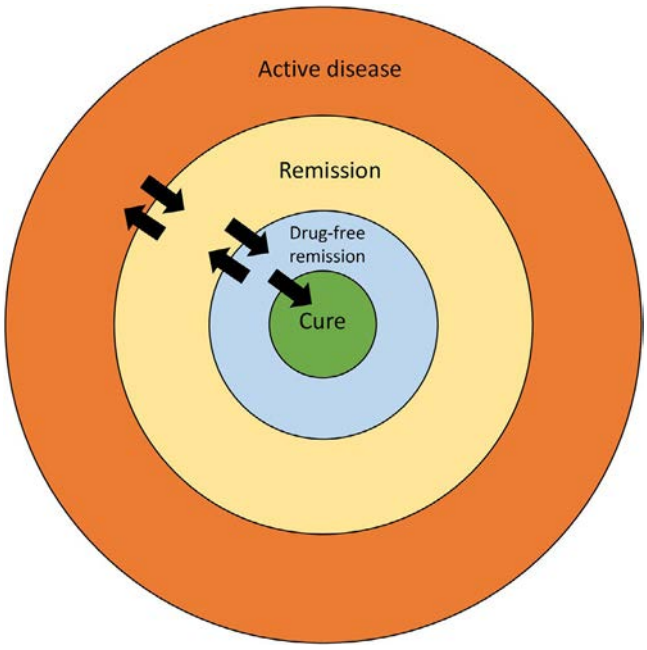

Figure 1. Aiming for cure in immune-mediated autoinflammatory diseases. Patients with active disease can achieve remission with drug treatment, of whom some can later stop therapy to achieve drug-free remission. Cure represents a subset of drug-free remission, in which patients are free of disease with no (or neglible) risk of disease recurrence. Developed from concepts discussed by Schett *et al* [16].

STRATEGIES TO ACHIEVE CURE AND DRUG-FREE REMISSION: IMMUNE RESET AND IMMUNE NUDGE

Two related but distinct strategies have been identified to achieve cure in future clinical practice: 'immune reset' and 'immune nudge' (John Isaacs, personal communication). In the immune reset approach, a single or short period of treatment is administered to restore immune homeostasis and regain long-lasting immune tolerance without further drug treatment. Autologous haematopoetic stem cell transplantation (AHSCT) is believed to reset the immune system but has been variably successful in autoimmune disease in terms of longstanding drug-free remission and toxicity. Before the biological disease-modifying antirheumatic drug era, AHSCT has been used in RA but most patients required post-transplant immunosuppressive drugs to maintain remission [5]. In SSc, specifically in early diffuse cutaneous SSc (dsSSc), AHSCT stops disease progression and reverses skin thickening, achieving long-term drug-free remission in around 80% of patients [6–8]. AHSCT is therefore included in the treatment armamentarium for dcSSc and used in routine clinical practice in experienced centres. However, because of higher risk of severe complications, AHSCT is only used in patients with high risk of severe organ damage and therefore not a treatment for all patients. Given these limitations, other approaches to reset the immune system are needed. Indeed, recent observations from the use of anti-CD19 chimeric antigen receptor T cell (CAR-T) therapy in a research setting for the treatment of systemic lupus erythematosus [9] open a new way to explore this.

In contrast, the immune nudge approach proposes application of a short period of treatment to push the immune system back towards homeostasis, but which would require repeated application at infrequent intervals to maintain this. Between treatments, the patient would be in drug-free remission with an underlying immune system indistinguishable from that of a healthy individual; however, without repeated treatment the disease would eventually relapse. In some respects, this approach mirrors the current use of rituximab in the treatment of RA and other RMDs, although with the additional resolution of underlying immunopathology.

BARRIERS TO ACHIEVING CURE IN CLINICAL PRACTICE

Despite widespread interest from academia, industry and patients in the concept of cure, we are still far from achieving this in routine clinical practice. A crucial barrier to the development of curative therapies is our current inability to define drug-free remission and cure at a molecular and/or cellular level. This makes it impossible to define when these states are achieved, and prevents a quantitative measure of the effectiveness of therapeutic approaches towards them.

Second, there are numerous potential therapeutic targets continually expanding the possibilities for achieving a cure; however, there is a limited number of patients available for recruitment to clinical trials. This is especially true for rarer

diseases such as SSc or hard-to-recruit phases of disease, such as asymptomatic individuals at risk of developing RA.

Third, our current definitions of disease are primarily based on clinical symptoms and signs, which can mask extensive heterogeneity in immunopathology and consequently lead to a wide range of responses to targeted immunotherapies. The resulting variability in treatment response poses a significant confounding factor in the evaluation of clinical trials.

Fourth, cure may be difficult, if not impossible, to achieve in patients with end-organ damage where ongoing symptomatology may persist despite absence of active inflammation. Furthermore, extended delay of treatment initiation may result in distinct or recalcitrant immune dysregulation (eg, through epigenetic and metabolic modification), [10] making cure harder to achieve in this patient population.

Finally, despite widespread enthusiasm for the concept of cure, there remains several regulatory hurdles to overcome in the approval and licencing of novel curative therapeutics. Recent years have witnessed a clear shift in acceptable phase III clinical trial outcome measures, with regulators moving away from numerical improvement of disease activity scores (eg, American College of Rheumatology and EULAR response measures) towards the attainment of well-defined clinical states (eg, Disease Activity Score in 28 joints (DAS28)-defined disease states) that are known to have tangible and meaningful long-term benefits for patients [11,12]. Therefore, our current lack of biomarkers to define drug-free remission and cure, and the current lack of long-term outcome data for patients achieving these states, poses challenges for clinical trial design and regulatory approval of this novel class of therapeutics [13].

HOW CAN THESE BARRIERS BE OVERCOME?

Despite the formidable barriers to the development and eventual deployment of curative therapies in clinical practice, there are several strategies and tools by which these can be overcome. First, the identification and validation of biomarkers of immune tolerance would provide a precise immunological roadmap towards cure, and the means to measure progress towards cure at an individual patient level [14]. Such biomarkers will likely be related to underlying disease immunopathology, and thus will be different between different molecular subtypes of disease both between and within individual RMDs. In addition, in systemic autoimmune diseases biomarkers could also be organ-specific, as observations from studies confirm distinct processes in different tissues (eg, skin and lung in SSc). Beyond identification and validation of these biomarkers, robust assays will need to be developed which conform to regulatory standards and are both acceptable to patients and cost-effective for healthcare providers.

Second, to study the effectiveness of targeted immunological therapies for disease cure, there is a pressing need to enrich patient cohorts based on underlying immunopathology [15]. By moving away from clinical classification criteria towards mechanistic definitions of disease at a molecular and cellular level, we should be able to maximise therapeutic effect size in clinical trials, enabling a more accurate assessment of the effectiveness of tolerising therapies.

Third, by coupling these immunological definitions of disease with innovative trial designs (eg, umbrella and basket platform trials), it should be possible to maximise clinical trial impact through harmonisation of protocols and clinical end points, while simultaneously avoiding counterproductive competition for recruitment between individual studies.

Fourth, strategies to achieve disease cure may be enhanced by novel treatment approaches at earlier stages of disease, including those at risk of developing disease. Earlier treatment to rapidly suppress inflammation, or prevent development of deleterious immune dysregulation in at-risk individuals, has the potential to make cure easier to achieve in a broader group of patients.

Finally, there is a need to better understand and quantify the benefits of achieving cure in terms of tangible clinical benefit to patients, as well as health economic impact for healthcare providers and wider society. This requires long-term follow-up of patients in drug-free remission and cure, combined with longitudinal biological sampling and clinical data annotation.

CONCLUSION

All of the above challenges are considerable, but not insurmountable. The enthusiasm to achieve cure is shared among academia, industry and patients alike, and greater collaboration between all of these stakeholders can help to make cure a future clinical reality. The EULAR Network of Trial centres, a new initiative by the EULAR Research Centre, is an example of how this could be achieved at scale by bringing together a network of clinical trial centres, patient partner involvement, clinical trial toolkits and trial capacity and training to better interface with industry partners to accelerate translational RMD research. Through close collaboration and shared purpose, we can have the ambition and means to move beyond remission in RMDs, to achieve a future where disease cure and even *restitutio ad integrum* are attainable targets for the majority of our patients.

Contributors

KFB and JS wrote the first draft of the manuscript based on discussions and summaries provided by the Working Group. MB, TR, ES, RW and GRB reviewed the manuscript and approved the final version. KFB is the guarantor of this work.

Funding

The Boot Camp was funded by the Foundation for Research in Rheumatology (FOREUM). KFB is funded by a National Institute for Health and Care Research (NIHR) Advanced Fellowship (NIHR303620), and is supported by the NIHR Newcastle Biomedical Research Centre.

Disclaimer

The views expressed in this publication are those of the authors and not necessarily those of the NIHR, NHS or the UK Department of Health and Social Care.

Competing interests

KFB: grant support from Pfizer; consultancy fees from Modern Biosciences, Versus Arthritis; Chair of Versus Arthritis Research Advisory Group. MB: employee of Novartis; stockholder of Novartis, Sandoz. TR: employee and stockholder of AbbVie. ES: employee of UCB. RW: employee of Pfizer; stockholder of Bristol Myers Squibb, Johnson and Johnson, Tevva, AstraZeneca, Pfizer. GRB: consultancy fees from AbbVie, BMS, Alphasigma, Lilly, Pfizer, UCB, Janssen, Novartis; honoraria from AbbVie, BMS, Alphasigma, Lilly, Pfizer, UCB, Janssen, Novartis. JS has no conflicts of interest to declare. FOREUM Boot Camp Working Group—JWJB: participation on data safety

monitoring board/advisory board related to gout; President of the FOREUM Board of Trustees. APC: consulting fees from BMS, AbbVie, GlaxoSmithKline (GSK), Janssen, Galapagos; honoraria from BMS, AbbVie, Galapagos, Janssen; advisory board participation for GSK, Galvani; Chair of EULAR Research Sub-Committee. JHWD: consultant relationships with and participation on the speaker or advisory boards of AbbVie, Active Biotech, Anamar, ARXX, AstraZeneca, Bayer Pharma, Boehringer Ingelheim, Calliditas Therapeutics, Celgene, Galapagos, Genentech, GSK, Inventiva, Janssen, Novartis, Pfizer, Roche, UCB; research funding from Anamar, Argenx, ARXX, BMS, Bayer Pharma, Boehringer Ingelheim, Cantargia, Celgene, CSL Behring, Galapagos, GSK, Inventiva, Kiniksa, Lassen, Sanofi-Aventis, RedX, UCB; travel support from AstraZeneca, Boehringer Ingelheim, AbbVie, SOBI; stockholder in 4D Science, FibroCure; receipt of equipment, materials, drugs, medical writing, gifts or other services from Boehringer Ingelheim; CEO of 4D Science and Scientific Lead of FibroCure. OD: research grants from Kymera, Mitsubishi Tanabe, Boehringer Ingelheim; consultancy fees from 4P-Pharma, AbbVie, Acceleron, Alcimed, Altavant Sciences, Amgen, AnaMar, ARXX, AstraZeneca, Blade Therapeutics, Bayer, Boehringer Ingelheim, Catalyze Capital, Corbus Pharmaceuticals, CSL Behring, EMD Serono, Galapagos, Glenmark, Gossamer, Horizon, Janssen, Kymera, Lupin, Medescape, Merck, Miltenyi Biotec, Mitsubishi Tanabe, Nkarta, Novartis, Orion, Prometheus Biosciences, Redxpharma, Roivant, Topadur, UCB; honoraria from Bayer, Boehringer Ingelheim, Janssen, Medscape; patent issued 'mir-29 for the treatment of systemic sclerosis' (US8247389, EP2331143); board/leadership positions for FOREUM Foundation, ERS/EULAR guidelines, EUSTAR, SCQM (Swiss Clinical Quality Management in Rheumatic Diseases), Swiss Academy of Medical Sciences, Hartmann Müller Foundation; co-founder of Citus AG. CAG: employee of AbbVie; stockholder in AbbVie. DMG: employee of UCB Pharma; scientific advisory board member for SynOA Therapeutics; stockholder in GSK, UCB Pharma. MH: employee of Pfizer; stockholder of Pfizer. BL: employee of UCB. RL: consultancy fees from AbbVie, UCB, Novartis, Eili-Lilly; honoraria from UCB, Eli Lilly, Novartis, Viatris, Galapagos; support for attending meetings and/or travel from Novartis; FOREUM Scientific Chair, OARSI Board member, Royal Belgian Society Board member. RS: employee of Pfizer. AMH-V: research grants from Boehringer Ingelheim, Janssen; consultancy fees from AbbVie, ARXX Therapeutics, BMS, Boeringer Ingelheim, Genentech, Janssen, Merck Sharp & Dohme, Pliant Therapeutics, Roche, Werfen; honoraria from Boehringer Ingelheim, Janssen, Medscape, Merck Sharp & Dohme, Novartis, Roche; travel support from Boehringer Ingelheim; CTD-ILD ERS/EULAR convenor and EULAR study group leader on the lung in rheumatic and musculoskeletal diseases. IMcI: research grants from AbbVie, Amgen, BMS, Causeway Therapeutics, Cabaletta, Dextera, Eli Lilly, Gilead, Janssen, Monatai, Novartis, Pfizer, Sanofi, UCB, Compugen, AstraZeneca, Moonlake; consultancy fees from AbbVie, Amgen, BMD, Causeway Therapeutics, Cabaletta, Dextera, Eli Lilly, Gilead, Janssen, Montai, Novartis, Pfizer, Sanofi, UCB, Compugen, AstraZeneca, Moonlake; board/leadership positions with NHS Greater Glasgow & Clyde Health Board, Versus Arthritis and University of Glasgow; stockholder for Causeway Therapeutics, Compugen, Cabaletta, Dextera. SO: employee of Novartis; stockholder of Novartis; travel support from Novartis; patents with Novartis; receipt of equipment, materials, drugs, medical writing, gifts or other services from Novartis. CP: consultancy fees for AbbVie, Sanofi, Janssen, Exagen, AnaptysBio, Novartis, Kinikska; contract research for AbbVie, Sanofi, Janssen and Novartis; honoraria from AbbVie, Sanofi, Janssen. LR-B: employee of AbbVie; stockholder in AbbVie; support for attending meetings and/or travel from AbbVie. RV: consultancy fees from Allucent, Anada; honoraria from IOIBD; travel support from IOIBD.

Patient and public involvement

Patients and/or the public were not involved in the design, or conduct, or reporting, or dissemination plans of this research.

Patient consent for publication

Not applicable.

Ethics approval

Not applicable.

Orcid

Kenneth Frank Baker: http://orcid.org/0000-0002-6735-2911
Julia Spierings: http://orcid.org/0000-0002-2546-312X
Gerd R. Burmester: http://orcid.org/0000-0001-7518-1131

REFERENCES

[1] Brown P, Pratt AG, Hyrich KL. Therapeutic advances in rheumatoid arthritis. BMJ 2024;384:e070856. doi: 10.1136/bmj-2022-070856.
[2] Yen EY, Singh DR, Singh RR. Trends in Systemic Sclerosis Mortality Over Forty-Eight Years, 1968-2015: A US Population-Based Study. Arthritis Care Res (Hoboken) 2021;73:1502–10. doi: 10.1002/acr.24411.
[3] Volkmann ER, Andréasson K, Smith V. Systemic sclerosis. Lancet 2023;401:304–18. doi: 10.1016/S0140-6736(22)01692-0.
[4] Lescoat A, Bellando-Randone S, Campochiaro C, et al. Beyond very early systemic sclerosis: deciphering pre-scleroderma and its trajectories to open new avenues for preventive medicine. Lancet Rheumatol 2023;5:e683–94. doi: 10.1016/S2665-9913(23)00212-6.
[5] Snowden JA, Kapoor S, Wilson AG. Stem cell transplantation in rheumatoid arthritis. Autoimmunity 2008;41:625–31. doi: 10.1080/08916930802198550.
[6] Burt RK, Shah SJ, Dill K, et al. Autologous non-myeloablative haemopoietic stem-cell transplantation compared with pulse cyclophosphamide once per month for systemic sclerosis (ASSIST): an open-label, randomised phase 2 trial. Lancet 2011;378:498–506. doi: 10.1016/S0140-6736(11)60982-3.
[7] van Laar JM, Farge D, Sont JK, et al. Autologous hematopoietic stem cell transplantation vs intravenous pulse cyclophosphamide in diffuse cutaneous systemic sclerosis: a randomized clinical trial. JAMA 2014;311:2490–8. doi: 10.1001/jama.2014.6368.
[8] Sullivan KM, Goldmuntz EA, Keyes-Elstein L, et al. Myeloablative Autologous Stem-Cell Transplantation for Severe Scleroderma. N Engl J Med 2018;378:35–47. doi: 10.1056/nejmoa1703327.
[9] Müller F, Taubmann J, Bucci L, et al. CD19 CAR T-Cell Therapy in Autoimmune Disease - A Case Series with Follow-up. N Engl J Med 2024;390:687–700. doi: 10.1056/NEJMoa2308917.
[10] Vuscan P, Kischkel B, Joosten LAB, et al. Trained immunity: General and emerging concepts. Immunol Rev 2024;323:164–85. doi: 10.1111/imr.13326.
[11] EMA. Guideline on clinical investigation of medicinal products for the treatment of rheumatoid arthritis. 2017. Available: https://www.ema.europa.eu/en/documents/scientific-guideline/guideline-clinical-investigation-medicinal-products-treatment-rheumatoid-arthritis_en.pdf.
[12] FDA. Guidance for industry rheumatoid arthritis: developing drug products for treatment - draft guidance. US Food and Drugs Admin; 2013. Available: https://www.fda.gov/media/86066/download.
[13] Aiyegbusi OL, di Ruffano LF, Retzer A, et al. Outcome selection for tissue-agnostic drug trials for immune-mediated inflammatory diseases: a systematic review of core outcome sets and regulatory guidance. Trials 2022;23:42. doi: 10.1186/s13063-022-06000-w.
[14] Baker KF, Sim JPX, Isaacs JD. Biomarkers of tolerance in immune-mediated inflammatory diseases: a new era in clinical management? Lancet Rheumatol 2021;3:e371–82. doi: 10.1016/S2665-9913(21)00069-2.

[15] Tanaka H, Okada Y, Nakayamada S, et al. Extracting immunological and clinical heterogeneity across autoimmune rheumatic diseases by cohort-wide immunophenotyping. Ann Rheum Dis 2024;83:242–52. doi: 10.1136/ard-2023-224537.

[16] Schett G, Emery P, Tanaka Y, et al. Tapering biologic and conventional DMARD therapy in rheumatoid arthritis: current evidence and future directions. Ann Rheum Dis 2016;75:1428–37. doi: 10.1136/annrheumdis-2016-209201.

Ann Rheum Dis 84 (2025) 158–168

Contents lists available at ScienceDirect

Annals of the Rheumatic Diseases

journal homepage: https://www.sciencedirect.com/journal/annals-of-the-rheumatic-diseases

Recommendation

Development of CARRA/PReS-endorsed consensus Core and Expanded Datasets in childhood-onset systemic lupus erythematosus for international registry-based research

Rebecca E. Sadun[1], Jennifer C. Cooper[2], Alexandre Belot[3], Tadej Avcin[4], Amita Aggarwal[5], Jenny Ainsworth[6,7], Alisha Akinsete[8], Stacy P. Ardoin[9], Michael W. Beresford[6,7], Lynette Bortey[10], Hermine I. Brunner[11], Joyce C. Chang[12], Coziana Ciurtin[13], Ashley Daftary[14], Barbara Eberhard[15], Candace H. Feldman[16], Christian M. Hedrich[6,7], Aimee O. Hersh[17], Linda T. Hiraki[18,19], David A. Isenberg[13], Sylvia Kamphuis[20], Andrea M. Knight[18,19], Lou Lambert[10], Deborah M. Levy[18,19], Stephen D. Marks[21,22], Naomi Maxwell[10], Angela Migowa[23], Katharine Moore[2], Seza Ozen[24], Rosalind Ramsey-Goldman[25], Angelo Ravelli[26], Bryce B. Reeve[27], Tamar B. Rubinstein[28], Claudia Saad-Magalhaes[29], Sujata Sawhney[30], Laura E. Schanberg[31], Emily von Scheven[32], Christiaan Scott[33,34], Mary Beth Son[12], Gladys Tony[35], Elissa R. Weitzman[12], Scott E. Wenderfer[36,37], Alisha Woodside[35], Laura B. Lewandowski[38], Eve MD Smith[6,7,*], the CARRA SLE Committee and PReS Lupus Working Party

[1] *Departments of Medicine and Pediatrics, Duke University School of Medicine, Durham, North Carolina, USA*
[2] *Department of Pediatrics, University of Colorado Anschutz Medical Campus, Aurora, Colorado, USA*
[3] *Service de Pediatrie, Centre Hospitalier Universitaire de Lyon, Lyon, France*
[4] *Department of Allergology, Rheumatology and Clinical Immunology, University Medical Centre, Ljubljana, Slovenia*
[5] *Department of Clinical Immunology and Rheumatology, Sanjay Gandhi Post Graduate Institute of Medical Sciences, Lucknow, Uttar Pradesh, India*
[6] *Department of Women's & Children's Health, University of Liverpool, Liverpool, UK*
[7] *Department of Paediatric Rheumatology, Alder Hey Children's NHS Foundation Trust, Liverpool, UK*
[8] *Department of Pediatrics, Hospital for Special Surgery, New York, New York, USA*
[9] *Departments of Medicine and Pediatrics, The Ohio State University College of Medicine, Columbus, Ohio, USA*
[10] *TARGET LUPUS PPIE Group, University of Liverpool, Liverpool, UK*
[11] *Department of Pediatrics, University of Cincinnati, Cincinnati, Ohio, USA*

*Correspondence to Dr. Eve MD Smith.
E-mail address: esmith8@liverpool.ac.uk (E.M. Smith).
Social media: @AlexandreBelot (A. Belot), @Elissa_Weitzman (E. R. Weitzman), @PedsLupusRenal (S. E. Wenderfer), @evemdsmith_eve (E. M. Smith)
Handling editor Josef S. Smolen
RES, JCC and AB are joint first authors.
LBL and EMS are joint senior authors.

https://doi.org/10.1136/ard-2024-226528

[12] Department of Pediatrics, Harvard Medical School, Boston, Massachusetts, USA
[13] Centre for Rheumatology, University College London, London, UK
[14] University of Nevada Reno School of Social Work, Reno, Nevada, USA
[15] Department of Pediatrics, Hofstra Northwell School of Medicine at Hofstra University, Hempstead, New York, USA
[16] Division of Rheumatology, Inflammation and Immunity, Brigham and Women's Hospital, Boston, Massachusetts, USA
[17] The University of Utah School of Medicine, Salt Lake City, Utah, USA
[18] Division of Rheumatology and Department of Pediatrics, The Hospital for Sick Children, Toronto, Ontario, Canada
[19] Division of Rheumatology, University of Toronto Temerty Faculty of Medicine, Toronto, Ontario, Canada
[20] Erasmus MC University Medical Center, Rotterdam, The Netherlands
[21] NIHR Great Ormond Street Hospital Biomedical Research Centre, University College London, London, UK
[22] Institute of Child Health and Department of Paediatric Nephrology, Great Ormond Street Hospital for Children NHS Foundation Trust, London, UK
[23] Department of Pediatrics, The Aga Khan University Medical College East Africa, Nairobi, Kenya
[24] Department of Pediatrics, Hacettepe University, Ankara, Turkey
[25] Department of Medicine, Northwestern University Feinberg School of Medicine, Chicago, Illinois, USA
[26] Direzione Scientifica, IRCCS Istituto Giannina Gaslini and Dipartimento di Neuroscienze, Riabilitazione, Oftalmologia, Genetica e Scienze Materno-Infantili, Università degli Studi di Genova, Genova, Italy
[27] Departments of Population Health Sciences and Pediatrics, Duke University School of Medicine, Durham, North Carolina, USA
[28] Children's Hospital at Montefiore, New York, New York, USA
[29] Pediatric Rheumatology Division, Faculdade de Medicina de Botucatu, Universidade Estadual Paulista (UNESP), Botucatu, Brazil
[30] Institute of Child Health, Paediatric Rheumatology Division, Sir Ganga Ram Hospital, New Delhi, India
[31] Department of Pediatrics, Duke University School of Medicine, Durham, North Carolina, USA
[32] Department of Pediatrics, University of California San Francisco, San Francisco, California, USA
[33] Department of Child and Adolescent Health, University of Cape Town, Rondebosch, South Africa
[34] Division of Pediatric Rheumatology, University of Ottawa, Ottawa, Ontario, Canada
[35] Patient/Caregiver Representative, Childhood Arthritis and Rheumatology Research Alliance, Milwaukee, Wisconsin, USA
[36] Department of Pediatrics, The University of British Columbia, Vancouver, Columbia, Canada
[37] BC Children's Hospital, Vancouver, Columbia, Canada
[38] National Institutes of Health, National Institute of Arthritis and Musculoskeletal and Skin Diseases, Bethesda, Maryland, USA

ARTICLE INFO

Article history:
Received 6 August 2024
Accepted 25 September 2024

Keywords:
Child
Lupus Erythematosus
Systemic
Lupus Nephritis
Outcome Assessment
Health Care
Patient Reported Outcome Measures

ABSTRACT

Objectives: Childhood-onset systemic lupus erythematosus (cSLE), representing 15%–20% of individuals with SLE, has been difficult to study globally due to differences between registries. This initiative, supported by Childhood Arthritis Rheumatology Research Alliance (CARRA) and Paediatric Rheumatology European Society (PReS), aims to create Core and Expanded cSLE Datasets to standardise and enhance research worldwide.

Methods: 21 international cSLE experts and 4 patients participated in a Delphi process (questionnaires, 2 topic-specific focus groups and 3 virtual consensus meetings) to create 2 standardised cSLE datasets. The Core cSLE Dataset was designed to include data essential to meaningful clinical research across many settings. The Expanded cSLE Dataset was designed for centres able to consistently collect data to address broader research questions. Final data items for the Core and Expanded datasets were determined by consensus defined as >80% agreement) using an adapted nominal group technique and voting.

Results: The resulting Core cSLE Dataset contains 46 items, including demographics, clinical features, laboratory results, medications and significant adverse events. The Expanded cSLE Dataset adds 26 additional items and includes patient-reported outcomes. Consensus was also achieved regarding the frequency and time points for data collection: baseline, quarterly follow-up visits, annually and flare visits.

Conclusion: Standardised Core and Expanded cSLE Datasets for registry-based international cSLE research were defined through the consensus of global experts and patient/caregiver representatives, endorsed by CARRA and PReS. These datasets incorporate disease-specific and patient-specific features, optimised for diverse settings to facilitate international collaborative research for children and adolescents with SLE worldwide.

INTRODUCTION

Children and adolescents with childhood-onset systemic lupus erythematosus (cSLE) generally experience more severe disease manifestations when compared with people with adult-onset SLE (aSLE) [1–3]. Patients with cSLE experience more active and aggressive disease, greater medication burden and more frequent involvement of internal organs, such as renal, haematological and neuropsychiatric manifestations [4–7]. Children with cSLE have a higher standardised mortality rate when compared with people who develop lupus in adulthood (aSLE) [8,9].

Several cSLE registries exist worldwide, each intended to enhance our understanding of the epidemiology, phenotypes and prognosis of cSLE while also providing the opportunity to capture real-world data on medication response rates and toxicities [2,10,11]. Due to the rarity of cSLE, however, the study of specific disease manifestations remains underpowered using existing individual registries. Treatment paradigms for cSLE are currently based predominantly on adult lupus trial data, supplemented with data from relatively small paediatric clinical trials and observational studies [11,12]. It remains unclear in which instances children with cSLE have similar treatment responses to individuals with aSLE, and many cSLE manifestations, such as neuropsychiatric disease, are still understudied. Furthermore, there is regional variability in the manifestations of cSLE that likely influences diagnosis, surveillance, treatment response and prognosis of the disease [13]. These challenges highlight the need for international clinical research that focuses specifically on cSLE [2,14,15]. Importantly, registry data from large cohorts serve as a powerful tool for unifying data collection for this rare and clinically heterogeneous disease to establish prognosis and determine optimal treatment and long-term safety.

The three largest existing cSLE registries are (1) the Childhood Arthritis and Rheumatology Research Alliance (CARRA) Registry, which has enrolled approximately 1500 cSLE patients from the USA and Canada, (2) the UK JSLE Cohort Study and Repository, which has enrolled over 850 patients from across the United Kingdom [2,11,14] and (3) the Juvenile Inflammatory Rheumatism (JIR) Lupus Cohort (Pedialup), which includes more than 600 cSLE patients from 96 centres across 11 countries in and around Europe [10]. These three registries are independent inception cohorts, and while they share similar goals, they differ in several aspects, including inclusion and exclusion criteria, data items, and data collection time points. Although data from each registry have been useful in characterising the regional cohorts, data collection differences between the registries have hindered the combination of data for inter-registry analyses.

For this study, we assembled an international group of clinicians and researchers with extensive expertise in cSLE research, alongside patient and caregiver representatives, to reach consensus on common data items for cSLE.

METHODS

Background and development

cSLE Expert Committee: A committee of international cSLE experts from CARRA, the Paediatric Rheumatology European Society (PReS), the UK JSLE Cohort Study, the JIR Cohort, the Paediatric Society of the African League Against Rheumatism, the Asia-Pacific League Against Rheumatism and the Pan American League Against Rheumatism along with patient/caregiver partners, developed a prototype Core and Expanded cSLE dataset. This cSLE Expert Committee was composed of 21 practising clinicians with extensive clinical and/or research experience of cSLE (15 paediatric rheumatologists, 4 combined adult medicine/paediatric trained or adult-trained rheumatologists, and 2 paediatric nephrologists who specialise in lupus nephritis, representing 10 countries across 5 continents). Although SLE is a systemic autoimmune disease that can affect any organ system, treatment is often determined by severe lupus nephritis, which led to the selection of rheumatologists and nephrologists in the consensus expert panel. The cSLE Patient/Caregiver members of the committee included two parents of patients with cSLE and three young adults with cSLE, now over 18 years old, who provided valuable patient-centred perspectives.

The cSLE Expert Committee was tasked with reaching consensus on the data items to include in a Core cSLE Dataset that would have sufficient detail to support meaningful clinical research across a broad array of research aims but also be streamlined enough to remain feasible for use at centres with limited research infrastructure. Experts were asked to reach consensus on additional data items to include in an Expanded cSLE dataset that would allow centres with sufficient research infrastructure to collect data needed to answer more expansive research questions. In both the Core and the Expanded datasets, emphasis was placed on defining each data item for a broad array of participating centres, considering countries beyond those currently participating in cSLE registry work to include regions of the world not yet represented.

To identify potential data items for inclusion, the CARRA/PReS Co-PI Committee (RS, JCC, EMDS, AB and LBL) compiled all data items used by current registries in North America and Europe, namely CARRA, the UK JSLE Cohort Study and the JIR Cohort; these data items were then supplemented by a literature review. From these items, the CARRA/PReS Co-PI Committee curated a list of potential data items as a starting point for the Delphi process. The cSLE Expert Committee was tasked with considering which items should be included in either ‘Core’ or ‘Expanded’ datasets. We defined ‘Core’ data items as the essential components for registry-based research on cSLE, aiming to streamline data entry to a maximum of approximately 15 min per patient visit. ‘Expanded’ dataset items refer to those that could significantly enhance the understanding of cSLE but are not essential for effectiveness research—and due to the additional time and effort required for their entry, the inclusion of these data would likely be feasible primarily at centres with a more robust research infrastructure.

cSLE expert Delphi process

Premeeting Delphi surveys: The cSLE Expert Committee participated in two initial rounds of Delphi surveys to identify areas of agreement and disagreement ahead of the first virtual consensus meeting. The first Delphi survey was completed by 20 out of 21 experts and was administered through a piloted, custom-made, online Qualtrics questionnaire. Participants reviewed all variables currently collected in the existing CARRA, UK JSLE Cohort Study and JIR registries. For each data item, participants were asked whether to include the item in the Core or Expanded datasets, or in neither; they were also asked to determine the appropriate frequency for collecting each data item. Experts were encouraged to provide free text comments explaining their reasoning. Experts were also given the opportunity to suggest additional data items for consideration. The results of the first Delphi survey informed a second Delphi survey, which was also administered through Qualtrics and was completed by all 21 experts. This survey presented the summary scores from the first survey, along with key free-text comments (anonymised). In the second Delphi survey, experts were asked to reflect on the results from the first Delphi survey for each item and indicate whether they could agree with the majority response for that item.

Consensus meeting 1

The first virtual consensus meeting was conducted over 8 hours on two consecutive days. An adapted nominal group

technique (NGT) methodology was used, led by a non-voting facilitator, to discuss and vote on data items to be included in the Core cSLE Dataset. Consensus was defined prior to the start of the meeting as >80% agreement. All 21 experts who participated in the Delphi survey were invited, and 20 were able to attend. In addition, four patients/caregivers attended the virtual consensus meeting and had full, equal voting rights. cSLE Expert Committee members were sent premeeting materials to review, including a summary of the Delphi results, a summary of relevant literature and a voting guide that summarised the results of the second Delphi survey. All items were reviewed during the meeting using NGT. For items that did not reach consensus for inclusion or exclusion after the first vote, we proceeded with discussion, statement refinement, and ultimately a re-vote until consensus was attained or it was clear that consensus would not be achieved.

The group voted to create focus groups to consider two especially complex topics: (1) how to best capture discrimination experienced by patients with cSLE and (2) what patient-reported outcomes (PROs) to include in the Expanded cSLE Dataset. The focus groups provided an opportunity to discuss existing literature in depth and get input from specialists in the relevant fields. These two topics, alongside items that did not reach a consensus at meeting 1 (including which laboratory values should be captured in a continuous fashion vs as categorical data), we sought additional input from specialists before reconvening for another consensus meeting. A third round of Delphi surveys was subsequently carried out to gauge opinions on these topics. Specialists' insights and recommendations, along with the results of third-round voting, were presented to the cSLE Expert Committee members at consensus meeting 2.

Focus groups

PROs: Two separate focus groups were convened to examine the optimal utilisation of PROs in cSLE. The first group included five individuals diagnosed with cSLE and only four members of the CARRA-PReS Co-PI committee members; this smaller group of physicians aimed to help patients feel comfortable speaking freely and sharing their experiences without intimidation from a large group of cSLE experts. A summary of the discussion from this focus group was presented at a subsequent larger focus group, which included CARRA-PReS Co-PI committee members, one adult and eight paediatric rheumatologists with expertise in using PROs in SLE, two PRO methodology experts and two patients. At the conclusion of this 2-hour session, a consensus recommendation statement on PROs was drafted to be reported to the full cSLE Expert Committee at the second consensus meeting.

Capturing perceived discrimination: The initial consensus group identified racism and discrimination as important influences on health outcomes in cSLE. Racism can happen on many levels: systemic, institutional and individual [16]. While racism has a vast impact on health, it can be difficult to measure at the individual level. Minoritised individuals can experience discrimination based on many factors, such as race, gender identity or age [17]. Discrimination describes individual mistreatment and the perception of unjust treatment without specific cause. A focus group consisting of nine individuals with expertise in understanding the health effects of racism and other forms of discrimination, including one adult rheumatologist, eight paediatric rheumatologists, a social work professor and one patient was convened to discuss ways to efficiently capture the experiences of patients with cSLE regarding discrimination. The nine voting focus group members, along with CARRA-PReS Co-PI committee members, patients and caregivers, met to review existing tools for assessing patient experiences with racism and discrimination, ultimately developing a consensus recommendation statement that was reported to the full cSLE Expert Committee at the consensus meeting 2.

Consensus meeting 2

A second consensus meeting was held virtually over 1 day to finalise laboratory data collection units and to review the results of the aforementioned focus groups in order to select PRO measures for inclusion in the Expanded dataset. All cSLE experts, patients and caregivers who participated in the first meeting were invited, with 20 out of 21 experts and all 4 patients/caregivers participating in the second meeting. In addition, a non-voting PRO expert (BBR), not present during the first consensus meeting, joined the second meeting to offer technical input on PRO measures. Consensus was achieved on all remaining items during consensus meeting 2 (figure 1).

Patient and public involvement

Patients and parents from the USA and Europe actively participated in the design, conduct and dissemination of this research. The cSLE Patient/Caregiver committee included two parents and three young adults with cSLE, each now older than 18 years old, providing patient-centred perspectives. They attended all virtual consensus meetings with full, equal voting rights. They also joined a focus group to identify key domains for capturing the patient experience using PRO measures, and participated as voting members in a PRO expert focus group. Additionally, they joined a focus group to discuss PROs for efficiently capturing cSLE patients' experiences with discrimination. Finally, patients and parents reviewed this manuscript. For all of these important efforts and contributions, they are included in this paper as named authors.

RESULTS

Core cSLE Dataset

Voting members of the consensus meetings achieved >80% agreement on the minimal core data items that were deemed crucial for collection in all international cSLE registries. Tables 1 and 2 summarise the data items voted into the Core cSLE Dataset and the recommended frequency for data collection.

Demographics: Demographic data items that can be consistently collected between international cohorts are shown in table 1. Following extensive discussion relating to whether race, ethnicity or ancestry should be collected, self-reported ancestry was deemed to be most appropriate for inter-registry research, using the specific question, ‘What region(s) of the world do your ancestors come from?‘ and respondents can select all that apply. However, individual cohorts may choose to collect these data in an additional way, as appropriate for their country or region.

Initial presentation, classification criteria and family history: The SLICC 2012 [18] and EULAR/American College of Rheumatology (EULAR/ACR) 2019 classification criteria [19] were both voted into for collection at the initial visit and annual update, to capture cSLE features experienced over time. Data on the patient's initial presentation and family history of SLE in a first-degree relative should also be collected at baseline and annually, to capture the evolution of the disease and new family history (see table 1).

Baseline, routine follow-up visits (every 3 months) and unscheduled/emergency disease flare visits: There was

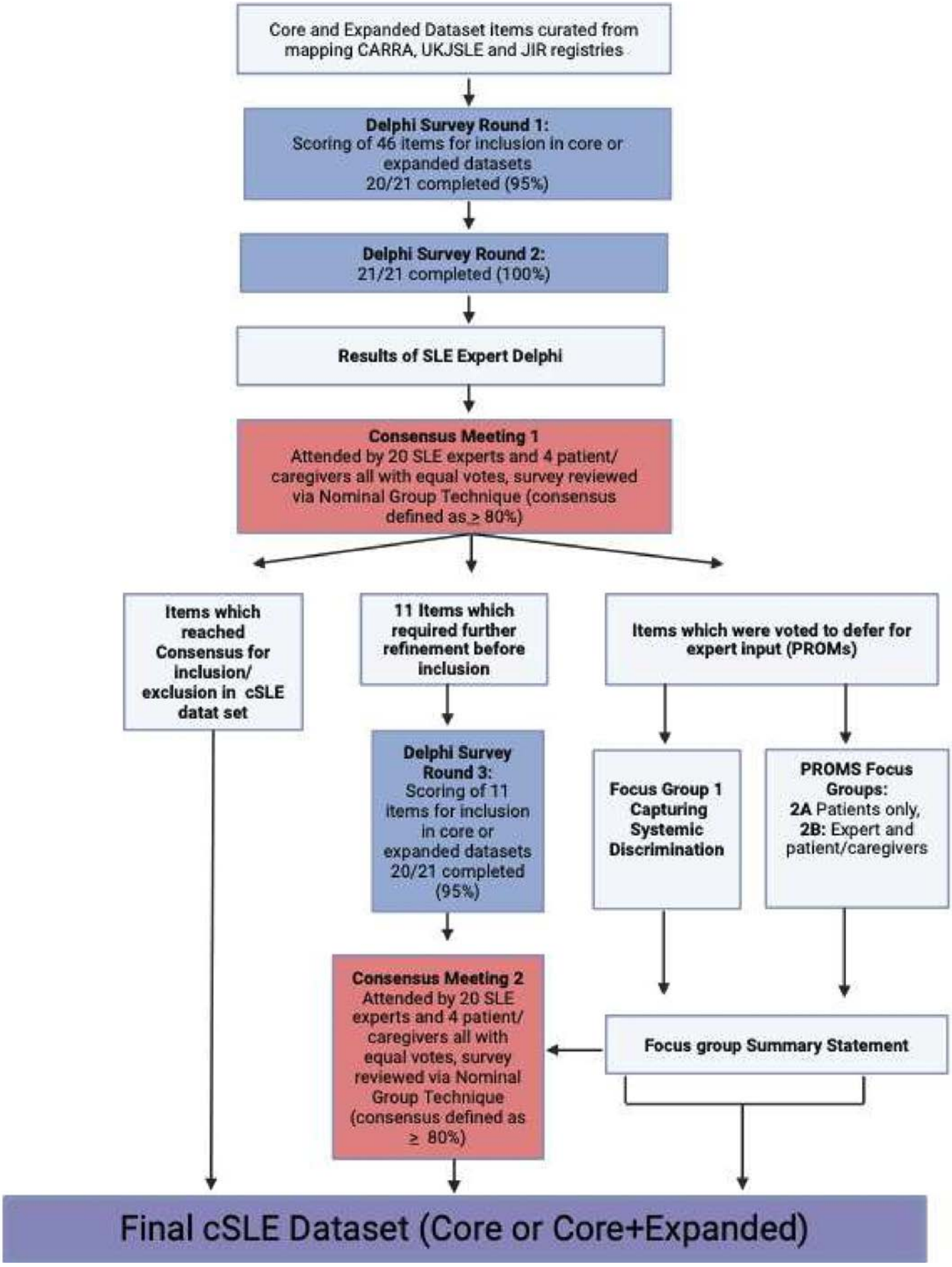

Figure 1. Methods used to create Core and expanded cSLE datasets. CARRA, Childhood Arthritis Rheumatology Research Alliance; cSLE, childhood-onset systemic lupus erythematosus; JIR, Juvenile Inflammatory Rheumatism; PROMS, Patient-Reported Outcomes Measurement System.

Table 1
Core cSLE dataset: data items

Section	Frequency of data collection			
	Baseline	Follow-up	Annually	Flare/AE
Demographics: DOB, country of residence, sex assigned at birth, gender identity, ancestry*	*			
Family history: SLE in a first-degree relative	*		*	
SLE onset: Date of SLE symptoms and date of SLE diagnosis	*		*	
SLE vs evolving/incomplete SLE vs other rheumatic or CTD	*		*	
SLE classification criteria: SLICC 2012 + EULAR/ACR 2019	*		*	
Basic observations: blood pressure, height, weight	*	*	*	*
Menarche status (age of menarche) and menstrual cycle status (currently menstruating, yes/no)	*	*	*	*
Disease activity: SLEDAI-2K, PGA, patient/parent global assessment of disease activity	*	*	*	*
SLICC Damage Index			*	
Investigations: CBC, CRP, ESR, Cr, Alb, IgG, ANA, ENA, dsDNA, APLs, C3/C4, UPC, urine dip/microscopy, kidney biopsy (ISN/RPS class, biopsy date)	*	(frequency and format of data shown in table 2)		
Medications	*	*	*	*
Corticosteroids				
Total daily dose of oral prednisolone (or equivalent)				
Number or intravenous corticosteroid pulses since last visit				
Immunomodulators/biologics (detailed data collection)				
Mycophenolate mofetil (dose, frequency, stop/start dates)				
Cyclophosphamide (dose of each infusion, route, infusion dates, stop/start dates)				
Rituximab (dose (mg) of each infusion, date of each infusion, stop/start dates)				
Belimumab (dose, route, frequency, stop/start dates)				
Other immunosuppressants/biologics (used Y/N, stop/start dates)				
Chloroquine, hydroxychloroquine, azathioprine, ciclosporin A, methotrexate, tacrolimus, voclosporin, anifrolumab, ofatumumab, ocrelizumab, obinutuzumab, JAKi, IVIG, other immunosuppressant (free text)				
Other medications				
Antihypertensives (ACEi, AT2 RB, Ca2 + channel blocker, blocker, diuretic), lipid-lowering agents, aspirin, anticoagulants (warfarin, other oral anticoagulant, subcutaneous LMWH), contraceptives (oestrogen containing, progesterone only, implantable/intrauterine), antidepressants, antiepileptics, bisphosphonates				
Significant adverse events	*	*	*	*
Hospitalisation (reason, level of care), ESRD, dialysis (start/stop date, indication: acute kidney injury or chronic dialysis >3 months), kidney transplant, death (cause), pregnancy (date, outcome), malignancy (type)				

Minimum of 80% consensus for inclusion of each data item.
ACEI, ACE inhibitors; ACR, American College of Rheumatology; Alb, serum albumin; ANA, antinuclear antibody; APLs, antiphospholipid antibodies; AT2 RB, angiotensin 2 receptor blocker; Ca^{2+}, calcium; CBC, complete blood count; C3/C4, complement factor 3 or 4; Cr, serum creatinine; CRP, C reactive protein; cSLE, childhood-onset SLE; CTD, connective tissue disease; DOB, date of birth; DsDNA, anti-double stranded DNA; ENA, extractable nuclear antigens; ESR, erythrocyte sedimentation rate; ESRD, end stage renal disease; ISN/RPS, International Society of Nephrology/Renal Pathology Society; IV, intravenous; JAKi, Janus Kinase inhibitor; LMWH, low-molecular-weight heparin; PGA, Physicians Global Activity; SLE, systemic lupus erythematosus; SLEDAI-2K, Systemic Lupus Erythematosus Disease Activity Index 2000; SLICC 2012, Systemic Lupus International Collaborating Clinics SLE Classification Criteria; SLICC, Systemic Lupus International Collaborating Clinics; UPC, urine protein creatinine ratio; Urine dip, urine dipstick; Y/N, yes/no.
* Self-identified ancestry, including a multiple-choice question with responses including Africa, East Asia, South Asia, Southeast Asia, Caribbean, Europe, Middle East/North Africa, South America, Indigenous/Native Population.

consensus to collect blood pressure, height, weight, menarche and menstrual cycle status, disease activity (Systemic Lupus Erythematosus Disease Activity Index 2000, SLEDAI-2K) [20], medication information and significant adverse events at each visit. The experts agreed that the SLICC Standardised Damage Index (SDI) [21] should be collected annually (see table 1).

Laboratory tests: Haematology, biochemistry, immunology and pathology laboratory investigations that reached consensus for inclusion in the Core cSLE Dataset are listed in table 1, with the frequency and format of data varying according to the specific test, as summarised in table 2.

Data collection time points: There was a 100% consensus that registry data collection time points should include the time of diagnosis, follow-up visits at least every 3 months and urgent visits due to a flare or significant adverse event.

Expanded cSLE Dataset

Additional data items that reached consensus for inclusion in the Expanded cSLE Dataset are shown in table 3, and notable additions are discussed below.

Disease activity and damage: Disease activity assessment for the Expanded dataset should include a BILAG-2004, to enable a more detailed and comprehensive assessment of disease activity than the SLEDAI-2K [22]. UK-based experts shared their experience using the BILAG-2004 in clinical practice, and ease of use and the now available 'Easy BILAG' tool, which includes a colour-coded scoring system [23]. As in the Core cSLE Dataset, annual reporting of the SLICC-SDI was supported, including parental height to allow for the assessment of growth failure as a potential damage item.

Kidney biopsy data: In addition to ISN-RPS classification [24], the Expanded dataset should collect key histopathological features associated with renal outcomes, including the presence of thrombotic microangiopathy, percent cellular crescents, percent glomerulosclerosis, presence of interstitial fibrosis and/or tubular atrophy, and the modified NIH disease activity and chronicity indices [25], when available.

Genetic testing results: With increasing recognition of lupus caused by single gene mutations or a combination of two (or more) high-impact alleles [26–28] underlying primary immune dysregulation in cSLE, and given wider availability of genetic

Table 2
Core cSLE dataset investigations—data format and frequency of collection

Investigations	Data format	Frequency of data collection			
		Baseline	Follow-up	Annually	Flare/AE
Laboratory tests					
Complete blood cell counts WCC, Hgb, Plts, ANC, ALC	Continuous value + low vs normal vs elevated	*	*	*	*
C reactive protein	Continuous value + normal/low versus elevated	*	*	*	*
Erythrocyte sedimentation rate	Continuous value + normal/low vs elevated	*	*	*	*
Serum creatinine	Continuous value + normal/low vs elevated	*	*	*	*
Serum albumin	Continuous value + low vs normal/elevated	*	*	*	*
Total IgG	Continuous value + low vs normal/elevated				*
Complements C3 and C4	Continuous value + low vs normal/elevated	*	*	*	*
Serologies					
ANA ≥1:80	Positive vs negative	*			
ENA (anti-Smith, anti-SSA, anti-SSB, anti-RNP)	Positive vs negative	*			
Anti-dsDNA titre	Continuous value + normal/low vs elevated	*	*	*	*
Lupus anticoagulant	Positive vs negative	*		*	
Anti-cardiolipin IgG, IgM	Continuous value + elevated vs negative/normal	*		*	
Anti-Beta-2-glycoprotein IgG, IgM	Continuous value + elevated vs negative/normal	*		*	
Urine studies					
Urine dipstick protein	Categorical (6 categories)	*	*	*	*
Urine dipstick specific gravity	Categorical (7 categories)	*	*	*	*
Urine dipstick leucocytes and blood	Categorical (5 categories each)	*	*	*	*
Urine microscopy red blood cells	Categorical (0–5 or >5 cells per hpf)	*	*	*	*
Urine microscopy white blood cells	Categorical (0–5 or >5 cells per hpf)	*	*	*	*
Urine microscopy red blood cell casts	Present vs absent	*	*	*	*
Urine protein to creatinine ratio	Continuous value for each + continuous for ratio w/ ratio reporting of normal/low vs elevated	*	*	*	*
Kidney biopsy data					
ISN/RPS Classification	ISN/RPS class (1–6), date(s) of biopsy(ies)	*	*	*	*

*denotes the frequncy of data collection for each investigation.
ALC, absolute lymphocyte count; ANA, antinuclear antibody; ANC, absolute neutrophil count; CBC, complete blood count; C3/C4, complement factor three or 4; cSLE, childhood-onset systemic lupus erythematosus; ENAs, extractable nuclear antigens; ESR, erythrocyte sedimentation rate; Hgb, haemoglobin; Hpf, high powered field; ISN/RPS, International Society of Nephrology/Renal Pathological Society; SSB, Sjögren Syndrome B.

testing, the expert panel voted to include whether or not a patient had genetic testing relevant to SLE, and if they had a known or suspected pathologic variant.

Laboratory tests: Laboratory tests for the Expanded dataset include additional investigations for haemolytic anaemia, CH50, anti-C1q antibodies, and yearly assessment of routine screening investigations for thyroid disease, diabetes, cholesterol and vitamin D.

Comorbidities: The experts reached a consensus on the collection of data on additional autoimmune conditions and primary immunodeficiency. Both tuberculosis and HIV status were deemed important, due to significant implications for patient care and outcomes worldwide. Additionally, a diagnosis of depression was highlighted as an important comorbidity to incorporate into the Expanded cSLE Dataset.

PRO measures: During the first PRO focus group, which consisted entirely of patients, patients prioritised the collection of patient-reported symptoms of fatigue, depression and anxiety. Regarding PRO administration, patient-participants recommended that PRO assessments performed within routine clinical visits should take no more than 5–10 min to complete. During the second PRO focus group, in which patient perspectives were presented to a group of clinician cSLE experts, recommendations were developed, as described in online supplemental file 1. In brief, the PRO expert group and patient representatives agreed that fatigue (100%), depression (92%), anxiety (82%) and a global health (82%) measures should all be collected. To achieve this, they recommended the use of the corresponding Patient-Reported Outcomes Measurement Information System (PROMIS) Paediatric short-forms, which exist in multiple languages and have been validated extensively, including in cSLE, with the existence of normative data and the ability to link scores from paediatric to adult-versions of PROMIS [29–31]. Patients raised some concerns about the ability of the PROMIS fatigue short-form to fully capture the mental and cognitive fatigue described by SLE patients. Despite this, they voiced that it was the best available instrument, preferring its brief recall period (past 7 days), question clarity, brevity, evidence for its validity and ability to link scores to those from adult versions of PROMIS fatigue measures, as compared with other fatigue PRO measures. During the second consensus meeting, the experts agreed with the recommendations from the PRO focus groups that PROMIS Paediatric short-forms for fatigue, depression, anxiety and global health should be collected within the Expanded dataset (all ≥80% consensus), with the expectations that these would take no more than 10 min to complete. Children aged >8 years are expected to be able to complete PROMIS paediatric measures, with parent proxy measures available for younger patients.

Importantly, all cSLE experts agreed that the depression and anxiety PRO measures should only be implemented at sites that already have mental health screening and support as part of their clinical protocol, or sites where the PROMIS depression and anxiety scores could be reviewed in real time, during the clinical visit, by members of the clinical team. It was recommended that future work should focus on enhancing registry workflows to enable all PRO results to be available to clinicians during patient encounters, enabling conversations about information disclosed about patients' symptoms.

Discrimination: Following extensive discussion and review of existing tools, the expert panel voted to use the Everyday Discrimination Scale short-form [32,33] (online supplemental file

Table 3
Expanded cSLE dataset—data items, format and frequency of collection

Data item	Data format	Frequency of data collection			
		Baseline	Follow-up	Annually	Flare/AE
Family history (first-degree relatives)					
Primary Sjögren syndrome	Yes or no	*		*	
Rheumatoid arthritis	Yes or no	*		*	
Antiphospholipid syndrome	Yes or no	*		*	
Other autoimmune disease	Yes or no, options + free text if yes	*		*	
Disease activity					
BILAG-2004 Index	Domain and total scores	*	*	*	*
SLE-related damage					
Parental height (for final adult height estimate)	Continuous value	*			
Significant adverse events					
Hydroxychloroquine maculopathy	Yes or no, date if yes	*	*	*	*
Laboratory investigations					
Anti-C1q antibody	Positive or negative	*	*	*	*
Ferritin	Continuous value	*	*	*	*
Direct coombs	Positive or negative	*	*	*	*
Lactate dehydrogenase	Low/normal versus elevated	*	*	*	*
Haptoglobin	Low versus normal/elevated	*	*	*	*
Total complement activity (CH50)	Continuous value	*	*	*	*
Thyroid stimulating hormone	Continuous value			*	
Haemoglobin A1c	Continuous value			*	
Cholesterol panel (TC, TG, LDL, HDL)	Continuous values			*	
25-hydroxy vitamin D	Low versus normal/elevated			*	
Genetic testing					
Confirmed or suspected monogenic lupus	Yes or no	*		*	
DNA collected/sequenced	Yes or no	*		*	
Known or suspected mutation/variant	Yes or no, free text if yes	*		*	
Kidney biopsy data (initial/subsequent biopsies)					
Modified NIH disease activity index	0–24 scale	*	*	*	*
Modified NIH disease chronicity index	0–12 scale	*	*	*	*
Cellular crescents	Percentage of glomeruli	*	*	*	*
Sclerosis	Percentage of glomeruli	*	*	*	*
Thrombotic microangiopathy present	Yes or no	*	*	*	*
Interstitial fibrosis present	Yes or no	*	*	*	*
Tubular atrophy present	Yes or no	*	*	*	*
Comorbidities					
Sjögren syndrome	Yes or no	*		*	
Autoimmune thyroid disease	Yes or no	*		*	
Other autoimmune disease	Yes or no, options + free text if yes	*		*	
Primary immunodeficiency	Yes or no	*		*	
Tuberculosis	Yes (latent/active) or no	*		*	
HIV	Yes or no	*		*	
Depression	Yes or no	*		*	
Patient-reported outcome measures					
Recommended to be available in real time to treating clinician					
Everyday Discrimination Scale Short-Form Ages 14+ years	5 questions	*		*	
PROMIS Paediatric Fatigue Short-Form Ages 8–17 years	10 questions	*	*	*	*
PROMIS Paediatric Global Health Ages 8–17 years	7 questions	*	*	*	*
PROMIS Paediatric Anxiety Short-Form* Ages 8–17 years	8 questions	*	*	*	*
PROMIS Paediatric Depressive Symptoms Short-Form* Ages 8–17 years	8 questions	*	*	*	*

Minimum of ≥80% consensus is required for inclusion of each data item.
*PROMIS Pediatric measures should not replace standard mental health screening.
BILAG, British Isles Lupus Assessment Group; cSLE, childhood-onset systemic lupus erythematosus; HDL, high-density lipoprotein; LDL, low-density lipoprotein; NIH, National Institutes of Health; PROMIS, Patient-Reported Outcomes Measurement Information Systems; TC, total cholesterol; TG, triglycerides.

2), which is validated for individuals ages 14 years and older in multiple languages and cultural settings [34]. The Everyday Discrimination Scale short-form consists of five questions assessing day-to-day discrimination experiences. Affirmative responses lead to inquiries about frequency and perceived discrimination reasons (eg, ancestry or national origin, gender, race, age, religion, sexual orientation, height, weight, other aspects of physical appearance, education or income level), which may vary by geography (eg, in some locations, tribe, shade of skin colour or refugee status may be relevant).

Consensus was achieved to include the Everyday Discrimination Scale short-form within the Expanded dataset for patients aged ≥14 years (88% agreement). It was recommended that in the future, an additional question about healthcare

discrimination should be considered. Of note, socioeconomic status indicators, such as household income, postal code and parent/caregiver occupation, were considered for inclusion in the Expanded dataset but did not reach consensus due to concerns about intrusiveness and potential discomfort for families.

Items not reaching consensus: Multiple items did not reach consensus for inclusion in the consensus datasets, and therefore, were not recommended for inclusion (online supplemental file 3).

DISCUSSION

cSLE represents one of the most challenging paediatric rheumatic diseases globally [3,9,35]. In this international initiative, recognised experts in cSLE achieved consensus on data items essential for cSLE registries. This achievement is a significant advancement in the standardisation of cSLE data collection and will enhance our ability to perform cross-registry research. Funded by a collaborative grant from PReS and CARRA, there is a strong commitment to this initiative among the international paediatric rheumatology community. The standardised datasets are designed to facilitate future collaborative international cSLE research that is patient-centred, reflecting the diverse experiences and needs of children with SLE across the globe. It is crucial to emphasise that while the development of a similar dataset for aSLE is underway, the cSLE work provides valuable insights and will serve as a foundation to inform ongoing efforts.

The development a Core cSLE Dataset, which can be completed in 15 min in all settings, as well as a more comprehensive Expanded cSLE Dataset for centres able to collect additional data, allows for research that is both wide-ranging and inclusive of diverse settings. The broader scope of the Expanded cSLE Dataset incorporates more detailed family history, comorbidities, in-depth kidney biopsy and laboratory data, and genetic findings; it adds depth to the data, through the inclusion of the BILAG-2004 [22], alongside SLEDAI-2K [36] for disease activity, and it includes the 2019 EULAR/ACR classification criteria [19], to enable broad validation of these criteria in cSLE. These enhancements are expected to deepen our understanding of the impact of cSLE while creating avenues for addressing more complex research questions.

The involvement of patient and caregiver advocates had a substantial impact at every phase of this initiative, significantly influencing the composition of the final datasets. Patients and family members are the experts in the lived experience of cSLE, and they provided invaluable input to this effort [37]. Patient insights led to the adaptation of content, shaped the data administration methods and led the group to set a goal for a maximum amount of time (10 min) that is acceptable for patients to complete all PROs, given that patients recounted negative, even distressing experiences while completing PROs. In addition, direct patient input resulted in the omission of certain data items that patient representatives felt to be intrusive and upsetting.

Expert consensus among researchers, clinicians, patients and caregivers underscored the importance of PROs in understanding the full impact of cSLE on individuals. While PROMIS measures are publicly available for noncommercial use by researchers without charge in paper format, there is a fee for electronic integration into data collection. Fatigue was prioritised as a critical area for assessment within the Expanded cSLE Dataset, in recognition of its profound influence on quality of life and the limited scope with which it is currently evaluated. Patients and caregivers suggested that a future goal should be the development of a cSLE-specific PROMIS Fatigue short-form, drawing from the PROMIS Pediatric Fatigue item bank but tailored to fully capture the physical as well as the cognitive fatigue experience by cSLE patients.

The quality of life domains of depression and anxiety were prioritised by all, reflecting their prevalence in cSLE, as well as their impact on SLE outcomes. Of note, there was unanimous agreement on the need for immediate communication of severe depressive symptoms reported in PRO measures to the clinical team, thereby ensuring urgent clinical intervention alongside registry data collection. Importantly, all patients who participated in the PRO focus group believed their PRO measure responses were being used for clinical purposes in addition to research, and the patients believed their healthcare providers were actively monitoring PRO responses in real time. This feedback emphasised the need for brief, clear and repeated explanations of the use of PROs, alongside a robust plan for a timely response to psychological distress.

Patients, caregivers and clinician cSLE experts from across the world agreed that racism and discrimination significantly affect health outcomes [38,39], emphasising the need for the expanded dataset to incorporate a measure of perceived discrimination. Informed by a systemic racism and discrimination focus group, the consensus voting panel agreed that the five-item Everyday Discrimination Scale [34] short-form for adolescents 14 years or older was the most time-efficient way to capture experiences of discrimination. Broad utilisation of the Everyday Discrimination Scale would allow for multinational validation in cSLE.

We acknowledge several study limitations. First, all meetings and focus groups were conducted exclusively in English, necessitating English language proficiency for participation. The dataset was constructed based on three current cSLE registries, which have all been developed in high-resource nations. In addition, it is important to note that while multiple subspecialties and five continents were represented among the experts, patients and caregivers, the majority of contributors were paediatric and adult rheumatologists and nephrologists from Europe and North America. Some of the rheumatologists in the consensus groups have expertise in neuropsychiatric SLE or cardiovascular disease in SLE. Future consensus groups to oversee revisions of this dataset could include other specialties involved in caring for cSLE, such as dermatology or neurology. Furthermore, while the Core cSLE Dataset was crafted to be practical for all clinicians or researchers, clinical environments lacking research support may find even the 15 min time frame burdensome. Currently, existing registries capture most of the Core cSLE Dataset and a significant proportion of the Expanded cSLE Dataset. Existing registries will need to develop a plan to implement the collection of the Core and Extended cSLE Dataset Items, which will require funding and alterations to existing registry infrastructure, including a plan for electronic integration of PROMIS measures, which are only available without a fee when used in paper format, which may be suboptimal in some settings. It is important to note that the Core and Expanded cSLE Datasets are intended to be iteratively refined to remain contemporary as they are integrated into established registries and implemented within new registries across diverse settings. Researchers will need to develop methods to compare historic data to the updated unified methods.

CONCLUSION

We present the first standardised Core and Expanded datasets for cSLE research, established by an international consensus process that included cSLE researchers, clinicians, patients and caregivers and was endorsed by CARRA and PReS. The integration of standardised cSLE datasets will mark a significant

advancement in enabling the expansion of research to achieve robust global collaborations. The relatively low prevalence and high phenotypic heterogeneity of cSLE have thus far been an obstacle to clinical research. Now, through unified data collection efforts, we can collaboratively pursue a broad range of clinical research questions with greater statistical power to advance cSLE care. Although defining guidance for standardising translational biosample collection is beyond the scope of this project, the proposed datasets will also facilitate contemporary lines of cSLE research, including the investigation of the underlying mechanisms of cSLE, the genetic basis of disease susceptibility, long-term patient outcomes, prognostic factors, cSLE treat-to-target initiatives [40], real-world comparative effectiveness and long-term safety, and a fuller understanding of the impact on health-related quality of life in affected children and adolescents. The development of these consensus-derived datasets represents a major strategic step towards the advancement of cSLE research, facilitating international collaboration and patient-centred studies designed to improve outcomes for children worldwide. Through consensus and standardisation of data collection globally, this initiative sets a new standard for cSLE registries in the field of paediatric rheumatology.

Acknowledgments

This project was funded by the CARRA/PReS Collaborative Award, and the authors wish to acknowledge the ongoing Arthritis Foundation financial support of CARRA. The authors would like to thank Katherine Cowan, Anne Dennos, François Hofer, Carla Roberts and Laura Whitty for their invaluable contributions. In addition, we are grateful to CARRA leadership and the CARRA SLE Committee, PReS leadership and SLE working party for their support of this project. We would like to thank the CARRA Registry, the JIR Lupus Cohort (Pedialup) study, and the UK JSLE Cohort Study and Repository, led by and the UK's Experimental Arthritis Treatment Centre for Children, for providing access to their data dictionaries and experience in developing and collecting real-world data in cSLE. Furthermore, we are grateful to all those individuals and centres who support these studies, and to all the patients and families who have helped inform and contribute data by participating in them.

Contributors

AB, EMDS, JCC, LBL and RS developed the Delphi surveys, organised and facilitated the consensus meeting and wrote the first version of the manuscript. AAggarwal, AH, AMK, AM, AR, CC, CMH, CS, CS-M, DL, DAI, EvS, GT, HIB, KM, LB, LTH, LL, LES, MWB, MBS, NM, SA, SK, SM, SO, SA, SW and TA participated as voting members of the consensus meetings, contributing to decisions regarding items to be included in the Core and Expanded datasets. AD, AAkinsete, AW, BE, BBR, CF, ERW, JC, RR-G and TBR participated in a task force meeting, making intellectual contributions to the decisions regarding which PROs to incorporate. All authors reviewed and approved the final draft of the manuscript. EMDS is the guarantor. RS, JCC, AB, are Co-first authors. EMDS and LBL are Co-last authors.

Funding

This research was funded by the inaugural CARRA/PReS Collaborative Research Award (JXR30630). LBL was funded by the NIAMS Intramural Program.

Competing interests

None declared.

Patient and public involvement statement

Patients and parents from the USA and Europe actively participated in the design and conduct of this research. The cSLE Patient/Caregiver committee included two parents and three young adults with childhood-onset SLE, now over 18 years old, providing patient-centred perspectives. They attended all virtual consensus meetings with full, equal voting rights. They joined a focus group to identify key domains and assess the patient experience using PRO measures, voting on the most important domains to be captured and participated in a PRO expert focus group with cSLE consensus group experts and additional PRO researchers. Additionally, they were involved in discussions on efficiently capturing cSLE patients' experiences with discrimination. Patients and parents reviewed the manuscript reporting the Core and Expanded cSLE datasets and are appropriately included as named authors.

Patient consent for publication

Not applicable.

Ethics approval

This study was reviewed and declared exempt from IRB review by the Duke Universtiy IRB (Pro #00110693).

Supplementary materials

Supplementary material associated with this article can be found in the online version at doi:10.1136/ard-2024-226528.

Orcid

Rebecca E. Sadun: http://orcid.org/0000-0001-7768-3565
Alexandre Belot: http://orcid.org/0000-0003-4902-5332
Amita Aggarwal: http://orcid.org/0000-0002-2187-5186
Michael W. Beresford: http://orcid.org/0000-0002-5400-9911
Hermine I. Brunner: http://orcid.org/0000-0001-9478-2987
Coziana Ciurtin: http://orcid.org/0000-0002-8911-4113
Christian M. Hedrich: http://orcid.org/0000-0002-1295-6179
Linda T. Hiraki: http://orcid.org/0000-0002-6690-8148
David A. Isenberg: http://orcid.org/0000-0001-9514-2455
Angelo Ravelli: http://orcid.org/0000-0001-9658-0385
Laura E. Schanberg: http://orcid.org/0000-0002-1913-6472
Mary Beth Son: http://orcid.org/0000-0002-7394-2862
Elissa R. Weitzman: http://orcid.org/0000-0003-1299-0008
Eve MD Smith: http://orcid.org/0000-0002-8371-7597

REFERENCES

[1] Bader-Meunier B, Armengaud JB, Haddad E, et al. Initial presentation of childhood-onset systemic lupus erythematosus: a French multicenter study. J Pediatr 2005;146:648–53. doi: 10.1016/j.jpeds.2004.12.045.
[2] Smitherman EA, Chahine RA, Beukelman T, et al. Childhood-Onset Lupus Nephritis in the Childhood Arthritis and Rheumatology Research Alliance Registry: Short-Term Kidney Status and Variation in Care. Arthritis Care Res (Hoboken) 2023;75:1553–62. doi: 10.1002/acr.25002.

[3] Watson L, Leone V, Pilkington C, et al. Disease activity, severity, and damage in the UK juvenile–onset systemic lupus erythematosus cohort. Arthritis & Rheumatism 2012;64:2356–65. doi: 10.1002/art.34410.
[4] Brunner HI, Gladman DD, Ibañez D, et al. Difference in disease features between childhood-onset and adult-onset systemic lupus erythematosus. Arthritis Rheum 2008;58:556–62. doi: 10.1002/art.23204.
[5] Hersh AO, von Scheven E, Yazdany J, et al. Differences in long-term disease activity and treatment of adult patients with childhood- and adult-onset systemic lupus erythematosus. Arthritis Rheum 2009;61:13–20. doi: 10.1002/art.24091.
[6] Mina R, Brunner HI. Pediatric lupus—are there differences in presentation, genetics, response to therapy, and damage accrual compared with adult lupus? Rheum Dis Clin North Am 2010;36:53–80. doi: 10.1016/j.rdc.2009.12.012.
[7] Massias JS, Smith EMD, Al-Abadi E, et al. Clinical and laboratory characteristics in juvenile-onset systemic lupus erythematosus across age groups. Lupus (Los Angel) 2020;29:474–81. doi: 10.1177/0961203320909156.
[8] Chiche L, Jourde-Chiche N, Bader-Meunier B, et al. Acute pancreatitis as a cause of mortality in pediatric systemic lupus erythematosus: Results of a multiple cause-of-death analysis in France. Semin Arthritis Rheum 2016;46:e6–7. doi: 10.1016/j.semarthrit.2016.03.009.
[9] Ambrose N, Morgan TA, Galloway J, et al. Differences in disease phenotype and severity in SLE across age groups. Lupus (Los Angel) 2016;25:1542–50. doi: 10.1177/0961203316644333.
[10] Cabrera N, Lega J-C, Kassai B, et al. Safety of biological agents in paediatric rheumatic diseases: A real-life multicenter retrospective study using the JIR-cohorte database. Joint Bone Spine 2019;86:343–50. doi: 10.1016/j.jbspin.2018.08.003.
[11] Smith EMD, Egbivwie N, Jorgensen AL, et al. Real world treatment of juvenile-onset systemic lupus erythematosus: Data from the UK JSLE cohort study. Clin Immunol 2022;239:109028. doi: 10.1016/j.clim.2022.109028.
[12] Smith E, Al-Abadi E, Armon K, et al. Outcomes following mycophenolate mofetil versus cyclophosphamide induction treatment for proliferative juvenile-onset lupus nephritis. Lupus (Los Angel) 2019;28:613–20. doi: 10.1177/0961203319836712.
[13] Massias JS, Smith EM, Al-Abadi E, et al. Clinical and laboratory phenotypes in juvenile-onset Systemic Lupus Erythematosus across ethnicities in the UK. Lupus (Los Angel) 2021;30:597–607. doi: 10.1177/0961203320984251.
[14] Vazzana KM, Daga A, Goilav B, et al. Principles of pediatric lupus nephritis in a prospective contemporary multi-center cohort. Lupus (Los Angel) 2021;30:1660–70. doi: 10.1177/09612033211028658.
[15] Weill O, Decramer S, Malcus C, et al. Familial and syndromic lupus share the same phenotype as other early-onset forms of lupus. Joint Bone Spine 2017;84:589–93. doi: 10.1016/j.jbspin.2016.12.008.
[16] Abubakar I, Gram L, Lasoye S, et al. Confronting the consequences of racism, xenophobia, and discrimination on health and health-care systems. Lancet 2022;400:2137–46. doi: 10.1016/S0140-6736(22)01989-4.
[17] Potter L, Zawadzki MJ, Eccleston CP, et al. The Intersections of Race, Gender, Age, and Socioeconomic Status: Implications for Reporting Discrimination and Attributions to Discrimination. Stigma Health 2019;4:264–81. doi: 10.1037/sah0000099.
[18] Petri M, Orbai A, Alarcón GS, et al. Derivation and validation of the Systemic Lupus International Collaborating Clinics classification criteria for systemic lupus erythematosus. Arthritis & Rheumatism 2012;64:2677–86. doi: 10.1002/art.34473.
[19] Aringer M, Costenbader K, Daikh D, et al. 2019 European League Against Rheumatism/American College of Rheumatology classification criteria for systemic lupus erythematosus. Ann Rheum Dis 2019;78:1151–9. doi: 10.1136/annrheumdis-2018-214819.
[20] Bombardier C, Gladman DD, Urowitz MB, et al. Derivation of the SLEDAI. A disease activity index for lupus patients. The Committee on Prognosis Studies in SLE. Arthritis Rheum 1992;35:630–40. doi: 10.1002/art.1780350606.
[21] Gladman D, Ginzler E, Goldsmith C, et al. The development and initial validation of the Systemic Lupus International Collaborating Clinics/American College of Rheumatology damage index for systemic lupus erythematosus. Arthritis Rheum 1996;39:363–9. doi: 10.1002/art.1780390303.
[22] Isenberg DA, Rahman A, Allen E, et al. BILAG 2004. Development and initial validation of an updated version of the British Isles Lupus Assessment Group's disease activity index for patients with systemic lupus erythematosus. Rheumatology (Oxford) 2005;44:902–6. doi: 10.1093/rheumatology/keh624.
[23] Carter LM, Gordon C, Yee C-S, et al. Easy-BILAG: a new tool for simplified recording of SLE disease activity using BILAG-2004 index. Rheumatology (Oxford) 2022;61:4006–15. doi: 10.1093/rheumatology/keab883.
[24] Weening JJ, D'Agati VD, Schwartz MM, et al. The classification of glomerulonephritis in systemic lupus erythematosus revisited. Kidney Int 2004;65:521–30. doi: 10.1111/j.1523-1755.2004.00443.x.
[25] Bajema IM, Wilhelmus S, Alpers CE, et al. Revision of the International Society of Nephrology/Renal Pathology Society classification for lupus nephritis: clarification of definitions, and modified National Institutes of Health activity and chronicity indices. Kidney Int 2018;93:789–96. doi: 10.1016/j.kint.2017.11.023.
[26] Belot A, Rice GI, Omarjee SO, et al. Contribution of rare and predicted pathogenic gene variants to childhood-onset lupus: a large, genetic panel analysis of British and French cohorts. Lancet Rheumatol 2020;2:e99–109. doi: 10.1016/S2665-9913(19)30142-0.
[27] Almlöf JC, Nystedt S, Leonard D, et al. Whole-genome sequencing identifies complex contributions to genetic risk by variants in genes causing monogenic systemic lupus erythematosus. Hum Genet 2019;138:141–50. doi: 10.1007/s00439-018-01966-7.
[28] Charras A, Haldenby S, Smith EMD, et al. Panel sequencing links rare, likely damaging gene variants with distinct clinical phenotypes and outcomes in juvenile-onset SLE. Rheumatology (Oxford) 2023;62:SI210–25. doi: 10.1093/rheumatology/keac275.
[29] Jones JT, Carle AC, Wootton J, et al. Validation of Patient-Reported Outcomes Measurement Information System Short Forms for Use in Childhood-Onset Systemic Lupus Erythematosus. Arthritis Care Res (Hoboken) 2017;69:133–42. doi: 10.1002/acr.22927.
[30] Weitzman ER, Gaultney A, von Scheven E, et al. Construct validity of Patient-Reported Outcomes Measurement Information System Paediatric measures in juvenile idiopathic arthritis and systemic lupus erythematosus: cross-sectional evaluation. BMJ Open 2023;13:e063675. doi: 10.1136/bmjopen-2022-063675.
[31] Translations promis. Available: https://www.healthmeasures.net/explore-measurement-systems/promis/intro-to-promis/available-translations/117-available-translations; 2023.
[32] Williams DR, Yan Y, Jackson JS, et al. Racial Differences in Physical and Mental Health: Socio-economic Status, Stress and Discrimination. J Health Psychol 1997;2:335–51. doi: 10.1177/135910539700200305.
[33] Sternthal MJ, Slopen N, Williams DR. RACIAL DISPARITIES IN HEALTH: How Much Does Stress Really Matter? Du Bois Rev 2011;8:95–113. doi: 10.1017/S1742058X11000087.
[34] Kim G, Sellbom M, Ford K-L. Race/ethnicity and measurement equivalence of the Everyday Discrimination Scale. Psychol Assess 2014;26:892–900. doi: 10.1037/a0036431.
[35] Tamirou F, Costedoat-Chalumeau N, Medkouri G, et al. Disease severity of proliferative lupus nephritis in Maghrebians. Lupus (Los Angel) 2018;27:1387–92. doi: 10.1177/0961203318772016.
[36] Gladman DD, Ibañez D, Urowitz MB. Systemic lupus erythematosus disease activity index 2000. J Rheumatol 2002;29:288–91.
[37] Kennedy I. Patients are experts in their own field. BMJ 2003;326:1276–7. doi: 10.1136/bmj.326.7402.1276.
[38] Kolasinski SL, Neogi T, Hochberg MC, et al. 2019 American College of Rheumatology/Arthritis Foundation Guideline for the Management of Osteoarthritis of the Hand, Hip, and Knee. Arthritis Care & Research 2020;72:149–62. doi: 10.1002/acr.24131.
[39] Drenkard C, Bao G, Dennis G, et al. Burden of Systemic Lupus Erythematosus on Employment and Work Productivity: Data From a Large Cohort in the Southeastern United States. Arthritis Care & Research 2014;66:878–87. doi: 10.1002/acr.22245.
[40] Smith EMD, Aggarwal A, Ainsworth J, et al. Towards development of treat to target (T2T) in childhood-onset systemic lupus erythematosus: PReS-endorsed overarching principles and points-to-consider from an international task force. Ann Rheum Dis 2023;82:788–98. doi: 10.1136/ard-2022-223328.

Ann Rheum Dis 84 (2025) 169–187

Contents lists available at ScienceDirect

Annals of the Rheumatic Diseases

journal homepage: https://www.sciencedirect.com/journal/annals-of-the-rheumatic-diseases

Recommendation

Expert consensus recommendations for the diagnosis and treatment of chronic non-bacterial osteitis (CNO) in adults

Elizabeth Winter[1,2,*], Olaf Dekkers[2,3], Caroline Andreasen[4], Salvatore D'Angelo[5], Natasha Appelman-Dijkstra[1,2], Simone Appenzeller[6], Gunter Assmann[7], Judith Bubbear[8], Oana Bulaicon[1,2], Roland Chapurlat[9], Varvara Choida[10,11], Gavin P.R. Clunie[12], Dimitrios Daoussis[13], Torsten Diekhoff[14], Marcel Flendrie[15], Olivier Fogel[16,17], Roba Ghossan[18], Hermann Girschick[19], Femke van Haalen[1], Neveen Hamdy[1,2], Barbara Hauser[20,21], Christian Hedrich[22], Philip Helliwell[23], Kay Geert Hermann[24], Antonella Insalaco[25], Anne Grethe Jurik[26], Mitsumasa Kishimoto[27], Willem Lems[28], Paivi Miettunen[29], Burkhard Muche[30], Ana Navas Cañete[1,31], Natalia Palmou-Fontana[32], Frits Smit[1,33,34], James Teh[35], Charlotte Verroken[36], Kurt de Vlam[37], Daniel Wendling[38], Wei Zhou[39], Hans-Georg Zmierczak[36], Anne Leerling[1,2,3]

[1] *Center for Bone Quality, Leiden University Medical Center, Leiden, The Netherlands*
[2] *Department of Internal Medicine, Division of Endocrinology, Leiden University Medical Center, Leiden, The Netherlands*
[3] *Department of Clinical Epidemiology, Leiden University Medical Center, Leiden, The Netherlands*
[4] *Department of Rheumatology and Internal Medicine, Gødstrup Hospital, Herning, Denmark*
[5] *Department of Health Science, University of Basilicata, Potenza, Italy*
[6] *Departamento de Clínica Médica. Facultade de Ciências Medicas da UNICAMP, Universidade Estadual de Campinas, Campinas, Brazil*
[7] *Department of Rheumatology, Ruhr-Universitat Bochum, Bochum, Germany*
[8] *Department of Rheumatology, Royal National Orthopaedic Hospital, London, UK*
[9] *Service de Rheumatologie et Pathologie osseuse, Hopital Edouard Herriot, INSERM UMR 1033 and University of Lyon, Lyon, France*
[10] *Department of Rheumatology, Homerton Healthcare NHS Foundation Trust, London, UK*
[11] *University College London, London, UK*
[12] *Department of Rheumatology, Cambridge University Hospital NHS Foundation Trust, Cambridge, UK*
[13] *Department of Rheumatology, University of Patras Medical School, Patras, Greece*
[14] *Department of Radiology, Charité Universitätsmedizin Berlin, Berlin, Germany*
[15] *Department of Rheumatology, Sint Maartenskliniek, Nijmegen, The Netherlands*
[16] *Department of Rheumatology, Paris Saint Joseph Hospital, Paris, France*
[17] *Department of Rheumatology, Cochin Hospital, Paris, France*
[18] *Department of Rheumatology, Hospital Cochin, Paris, France*

*Correspondence to Dr. Elizabeth M. Winter.
E-mail address: e.m.winter@lumc.nl (E. Winter).
Social media: @FogelOlivier (O. Fogel)
Handling editor Josef S. Smolen.

https://doi.org/10.1136/ard-2024-226446

[19] Department of Pediatrics, Vivantes Klinikum im Friedrichshain, Berlin, Germany
[20] Rheumatic Diseases Unit, Western General Hospital, Edinburgh, UK
[21] Centre for Genomic and Experimental Medicine, MRC Institute of Genetics and Cancer, Western General Hospital, Edinburgh, UK
[22] Department of Women's and Children's Health, University of Liverpool, Liverpool, UK
[23] Academic Unit of Musculoskeletal Medicine, University of Leeds, Leeds, UK
[24] Department of Radiology, Charite Universitatsmedizin Berlin, Berlin, Germany
[25] Department of Paediatric Rheumatology, Ospedale Pediatrico Bambino Gesu, Roma, Italy
[26] Department of Radiology, Aarhus University Hospital, Aarhus, Denmark
[27] Department of Nephrology and Rheumatology, Kyorin University, Mitaka, Tokyo, Japan
[28] Department of Rheumatology, Amsterdam University Medical Centres, Amsterdam, The Netherlands
[29] Department of Paediatrics, University of Calgary McCaig Institute for Bone and Joint Health, Calgary, Alberta, Canada
[30] Department of Rheumatology, Charite Universitatsmedizin Berlin, Berlin, Germany
[31] Department of Radiology, Leiden University Medical Center, Leiden, The Netherlands
[32] Department of Rheumatology and Pediatric Rheumatology, Immunology Group, Hospital Universitario Marques de Valdecilla, Santander, Cantabria, Spain
[33] Department of Radiology, Division of Nuclear Medicine, Leiden University Medical Center, Leiden, The Netherlands
[34] Department of Nuclear Medicine, Alrijne Hospital Location Leiderdorp, Leiderdorp, The Netherlands
[35] Department of Radiology, Nuffield Orthopaedic Centre Girdlestone Memorial Library, Oxford, UK
[36] Department of Endocrinology, Unit for Osteoporosis and Metabolic Bone Diseases, Ghent University, Gent, Belgium
[37] Department of Rheumatology, Universitaire Ziekenhuizen Leuven, Leuven, Belgium
[38] Department of Rheumatology, Universite de Franche-Comte, Besancon, France
[39] Department of Rheumatology, Beijing Tiantan Hospital, Beijing, China

ARTICLE INFO

Article history:
Received 19 July 2024
Accepted 1 November 2024

Keywords:
epidemiology
outcome and process assessment
health care
tumor necrosis factors
magnetic resonance imaging

ABSTRACT

Background: There is considerable practice variation in labelling, diagnosis and treatment of adults with sterile bone inflammation. We developed a expert consensus recommendations on the disease definition, diagnosis and treatment of this rare condition.
Methods: Systematic literature review and Grading of Recommendations, Assessment, Development and Evaluations-based appraisal of evidence, two Delphi surveys and three digital and in-person consensus meetings with a multidisciplinary expert panel and patient representatives.
Results: A consensus disease definition was developed and the term 'chronic non-bacterial osteitis' (CNO) is proposed to describe adults with sterile bone inflammation. For initial imaging evaluation of adults with suspected CNO, the panel recommends MRI or otherwise CT combined with nuclear imaging. Whole-body imaging at initial evaluation can be considered for diagnostic and prognostic purposes. Suggested first-line treatment in adults with active CNO includes non-steroidal anti-inflammatory drugs/cyclooxygenase 2-inhibitors. Second-line treatment preferably consists of intravenous bisphosphonates, and otherwise tumour necrosis factor-α inhibitors. Choice between them should be individualised, considering the presence of additional inflammatory features. The panel further discusses outcome measures, follow-up and management of adverse events and complications.
Conclusions and future perspectives: These expert consensus recommendations are intended to support healthcare professionals worldwide in their care for adults with CNO. They also lay the groundwork for establishing international patient registries, translational research lines and multicentre trials, all of which are urgently required.

INTRODUCTION

Sterile bone inflammation (SBI) represents a rare and heterogeneous disease spectrum that affects children and adults [1]. Various terms are currently in use to describe patients with SBI, including chronic nonbacterial osteomyelitis, chronic recurrent multifocal osteomyelitis (CRMO), synovitis, acne, pustulosis, hyperostosis, osteitis (SAPHO) syndrome, diffuse sclerosing osteomyelitis (DSO), pustulotic arthro- osteitis (PAO), sternocostoclavicular hyperostosis (SCCH) and more [2]. The disease definition of SBI is complex, owing to its broad clinical presentation and overlap with other autoinflammatory musculoskeletal and non-musculoskeletal disorders [3–5]. In adults, SBI mostly manifests as osteitis of the anterior chest wall, but the vertebrae, mandible and pelvis may also be involved [6]. Initial radiological signs comprise bone marrow oedema and osteolysis, while progressive structural alterations secondary to inflammation include sclerosis, hyperostosis, erosion, soft tissue ossification and joint ankylosis [7]. Apart from bone inflammation, patients may present with a range of other autoinflammatory features, including musculoskeletal features (inflammatory arthritis, sacroiliitis, dactylitis, enthesitis), dermatological features (palmoplantar pustulosis (PPP), psoriasis, hidradenitis suppurativa, severe acne), uveitis and inflammatory bowel disease [2,8]. The clinical management of SBI presents major challenges. Unifying diagnostic criteria are lacking, pathophysiology is largely unknown and there are no standard outcome measures or evidence-based treatment modalities [9,10]. Individuals with SBI

endure high disease burden due to bone pain impacting daily functioning, and, especially without timely treatment, are at risk for complications such as skeletal deformities, compromised joint functionality, neurovascular entrapment or vertebral fractures [7,11–15]. The provision of care for patients with SBI is fragmented, spread across diverse medical disciplines such as rheumatology, orthopaedic surgery and endocrinology, with wide variety in (off-label) treatment strategies [2]. Clearly, consensus recommendations and a research agenda are necessary steps towards clinical advancement for SBI. Recognising this imperative, we convened a consensus group to formulate a disease definition, to choose an overarching name for the SBI spectrum, systematically develop recommendations for the diagnosis and treatment and develop a research agenda.

We concentrate on chronic non-bacterial osteitis (CNO) that occurs in adulthood, acknowledging the distinct clinical differences between adult-onset and paediatric-onset forms of the disease. Patients with adult-onset CNO typically present with lesions confined to one or two areas in the axial skeleton. In contrast, childhood-onset CNO often follows a recurrent multifocal pattern, also involving appendicular bones, and is more clearly associated with systemic inflammation [1,16]. While the recommendations focus on adult (-onset) CNO, we recognise that paediatric patients wth CNO may transition into adulthood with ongoing disease activity. The applicability of these recommendations to such individuals will depend on the extent to which their disease resembles the adult phenotype, thereby ensuring that management strategies are appropriately tailored to their specific clinical characteristics. The consensus recommendations are intended to support healthcare professionals worldwide, especially those who are not situated at expert centres and encounter very limited numbers of adults with SBI. These generally include secondary care specialists working in rheumatology, endocrinology, clinical osteology, orthopaedics, radiology and nuclear medicine. Although we recognise the limited evidence supporting diagnostic and therapeutic recommendations for adults with SBI, we are confident that they represent a valuable synthesis of the best-available literature and clinical expertise. As such, it has the potential to enhance care for adults with SBI while future studies are awaited. The initial stage in developing recommendations for diagnosis and treatment involved choosing a unified name for the spectrum of SBI. After thoughtful discussion, the expert panel and patient representatives chose the term ‘CNO’ for this spectrum, with distinctions made based on age—adult CNO or paediatric CNO. The reasoning behind this is detailed later in this document, but from this point, for clarity, we will refer to the patient population of interest as ‘*adult CNO*’.

METHODS

This consensus project was initiated by ATL and EMW from the Center for Bone Quality of the Leiden University Medical Center. The project’s scope was adults with SBI (previously labelled as chronic non-bacterial osteomyelitis, CRMO, SAPHO, PAO, SCCH, DSO and henceforth designated as adult CNO). The bone marrow oedema syndrome, traumatic causes of bone marrow oedema, spontaneous osteonecrosis and genetic syndromes like Majeed or deficiency of the interleukin (IL)-1 receptor antagonist were considered beyond the scope. The expert consensus recommendations were developed and reported according to the Appraisal of Guidelines Research and Evaluation-Recommendations Excellence (see online supplemental file S1 for reporting checklist) [17] and endorsed by The European Calcified Tissue Society, The European Reference Network of Rare Bone Diseases (formally) and European Society of Endocrinology (pending final publication). An overview of the project’s steps is outlined in figure 1. As a first step, we conducted a physician survey study mapping current clinical practices for adults with CNO, which is published elsewhere [18]. Based on this, the domains of interest for the consensus recommendations were

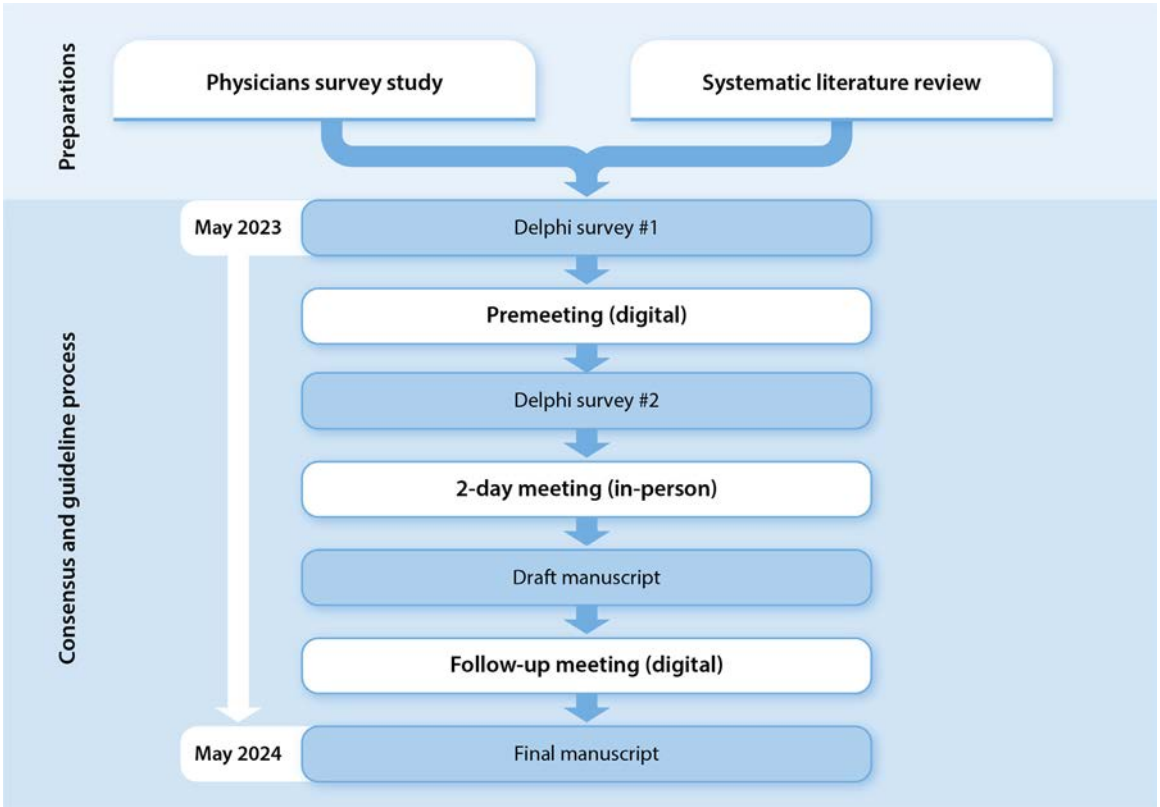

Figure 1. Schematic overview of consensus process.

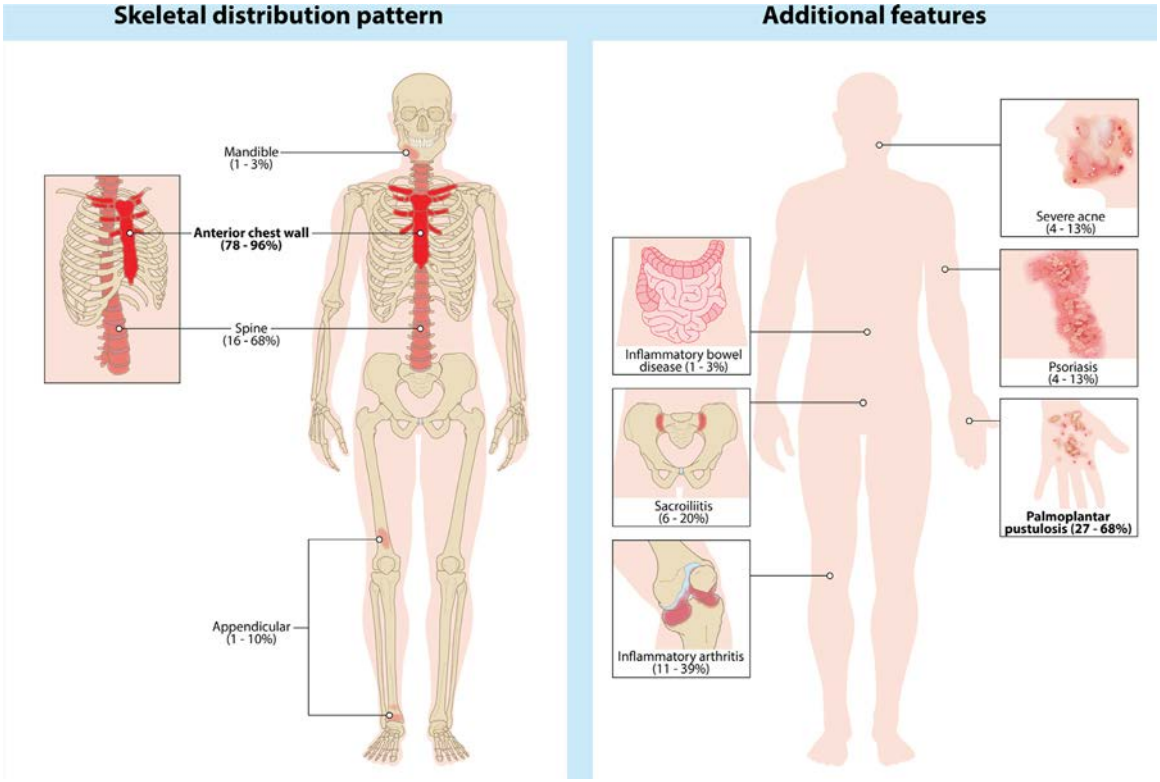

Figure 2. Visual representation of disease definition of adult CNO; skeletal distribution pattern of osteitis (left) and additional (extra)-skeletal features (right). Reported as 95% CI.

chosen (see online supplemental file S2 for complete list). For all domains, a systematic literature review was performed and results were synthesised into summary of evidence tables, also including the survey study results (online supplemental file S3). Methods used for the systematic literature review with appraisal of evidence, including the Grading of Recommendations, Assessment, Development and Evaluations approach as outlined in the Cochrane Handbook for Systematic Reviews of Interventions [19] are detailed in online supplemental file S4. In-detail descriptions of the expert panel constitution and the decision-making process are presented in online supplemental file S4 as well. Briefly, we assembled a diverse and inclusive expert panel via inviting (a) all participants of the aforementioned physician survey study, (b) experts via relevant international networks and societies and (c) authors of scientific studies on CNO. Input from patient representatives was arranged with the Dutch CNO patient association. With the summary of evidence as resource for expert panel members, the consensus recommendations were subsequently developed over the course of two Delphi survey rounds (results outlined in online supplemental files S5 and S6) and three meetings (two digital and a 2-day in-person). All domains of interest were reviewed in the in-person meeting, as well as a research agenda. Ultimately, the complete panel assessed the final recommendations using a 0–10 Likert scale, where 0 represented no agreement and 10 signified full agreement. The metrics of agreement are presented in the recommendation tables, which include the mean score, SD and the percentage of panel members who rated the recommendation 8/10 or higher.

CONSENSUS STATEMENT: DISEASE DEFINITION

Based on the systematic literature review, Delphi results and panel discussions, it became evident that CNO represents a rare and clinically heterogeneous disease spectrum (see also online supplemental file S3, Q1A and Q1B for supportive evidence). It is not known whether the full spectrum shares the same autoinflammatory mechanisms, or whether it entails multiple (partially) distinct conditions. The connection between adult CNO and musculoskeletal rheumatic diseases such as axial spondyloarthritis (axSpA) and psoriatic arthritis (PsA), which share similar features, remains similarly ambiguous, as does the link between adult and paediatric disease. Despite these uncertainties, the panel proposes the following disease definition to capture the concept of adult CNO (figure 2).

CNO in adults is a condition characterised by SBI, which affects one or multiple bones, and primarily manifests in the anterior chest wall. Adult CNO may exhibit different temporal patterns, including monophasic, chronic or relapsing-remitting. Typical imaging characteristics of bone inflammation include bone marrow oedema, osteolysis, increased tracer uptake on nuclear imaging and in later stages, sclerosis, erosions, hyperostosis (seen as endosteal and periosteal thickening), soft tissue ossification and ankylosis [7,11,20–26] (see online supplemental file S2, Q2A and Q2B for supportive evidence). While isolated bone inflammation is the most common presentation, additional features that may be seen are:

- Musculoskeletal: inflammatory arthritis, sacroiliitis and possibly enthesitis and dactylitis.
- Non-musculoskeletal: PPP, psoriasis, hidradenitis suppurativa, severe acne and rarely uveitis and inflammatory bowel disease.

Regarding the skeletal distribution, the panel recognises that the frequency of involvement sites is difficult to accurately estimate, due to three factors. First, estimates from published cohorts may be subject to referral bias, as certain distribution patterns prompt referral to specific specialists (eg,

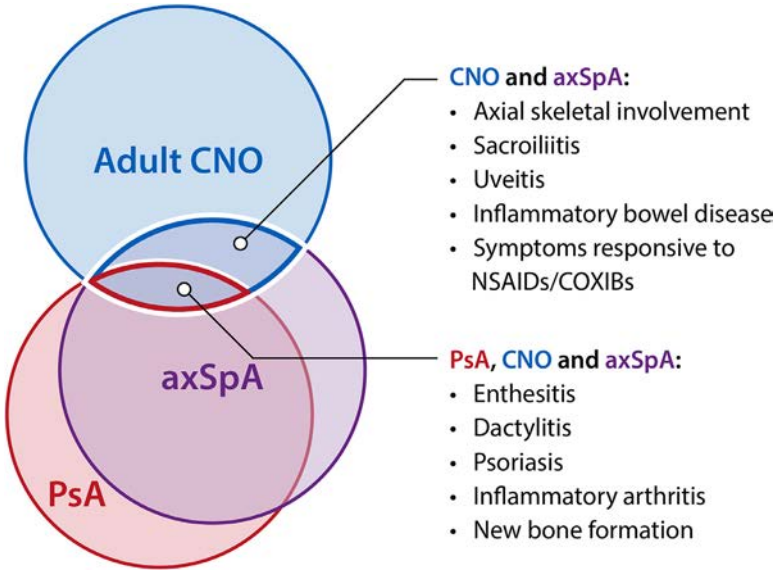

Figure 3. Venn diagram displaying conceptual overlap between adult chronic non-bacterial osteitis (CNO) and axial spondyloarthritis (axSpA) and psoriatic arthritis (PsA) based on features seen in the multiple conditions. COXIB, cyclooxygenase-2 inhibitor; NSAID, non-steroidal anti-inflammatory drug.

rheumatologists for multifocal appendicular involvement, orthopaedic evaluation for a unifocal lesion, anterior chest wall involvement and associated shoulder dysfunction). Second, the involvement of certain sites may be easier and faster to diagnose over others, which may distort estimates. Third, the presence of silent lesions in up to 67% of patients and the lack of routine whole-body imaging contribute to the potential underestimation of specific skeletal involvement sites [20]. Notwithstanding, the panel identifies the anterior chest wall, including the clavicles, upper ribs and sternum, as the most frequently involved sites, which is supported by recent meta-analyses reporting involvement rates between 78% and 96% [2]. Following this, the spine, appendicular skeleton, jaw and pelvis may be involved [2,6,24,28]. Based on clinical experience (without available supporting literature), the panel reports that most patients exhibit multifocal involvement, although cases affecting a single bone are also recognised.

Adult CNO may exhibit various additional features, some of which lead a clinical overlap with axSpA and PsA (figure 3). Although all features are susceptible to potential over-reporting or under-reporting, the most prominent among these is the presence, or history of PPP, reported in 37%–68% of patients. Additionally, non-erosive peripheral arthritis is observed in 11%–39% of cases, followed by psoriasis (4%–14%) and severe acne (4%–13%) [2,29–32]. Uveitis, dactylitis, enthesitis, erosive arthritis, hidradenitis suppurativa, tonsillitis, periodontitis and inflammatory bowel disease have been documented in a few CNO cases, although prevalence estimates are highly uncertain [33–35]. Despite this variety of features, the panel's experience is that the vast majority of adult patients with CNO present with isolated osseous disease.

The panel recognises that adult patients with CNO present mainly with bone pain, but symptomatology may vary significantly depending on the sites and the presence of additional features. According to recent literature, the typical age of presentation falls within the range of 29–46 years, and 60%–73% of the patients are female [2] (see online supplemental file S3, Q1C for supportive evidence). In early CNO, physical examination findings may reveal local soft-tissue swelling, erythema, tenderness and impairment of function. CNO may progress over time to the point where bony swelling becomes apparent, but due to the frequent diagnostic delay, patients often present with a bony swelling already at first consultation. According to the panel's clinical experience, systemic symptoms such as fever or unexplained weight loss are rare (fever noted in up to 14%, as reported in literature) and warrant further investigation to exclude other causes than CNO [2].

CONSENSUS STATEMENT: NOMENCLATURE

The panel unanimously recognises that the multitude of names for 'adults with SBI' is confusing, inconvenient and burdensome for patients (see online supplemental file S3, Q3 for overview). From various names currently in use, several are deemed unsuitable by the panel, such as SCCH (too descriptive and narrow), PAO (excluding patients without PPP) and CRMO (a recurrent multifocal pattern is rare in adults). Although SAPHO is a widely recognised term, its broad scope makes it poorly applicable to the majority of patients who never develop additional features, leaving the S, A and P of the acronym largely unfulfilled. This idea is echoed by patient representatives, who prefer a concise name, not laden with features that often do not occur. Alternatively, 'chronic non-bacterial osteomyelitis' effectively captures the core disease feature, is short and inclusive and has recently been adopted in the paediatric community. However, the panel perceives that the term 'osteitis' better suits the pathology than 'osteomyelitis'. Therefore, CNO has been proposed to represent 'adults with SBI' in clinical and research practice. For paediatric CNO, a transition from 'osteomyelitis' to 'osteitis' is also anticipated. The panel recommends discontinuing the use of other historical names, both in adults and children.

GENERAL RECOMMENDATIONS

R1: Consider referral to an expert centre for all adult patients with CNO, and refer difficult-to-treat patients if not done initially

Rationale

Due to the rarity of the condition and the limited evidence on diagnostics and treatment, the panel suggests considering referral to an expert centre for all patients, and specifically recommends referral of all difficult-to-treat patients if not done already (see 'Treatment recommendations' section). Depending on healthcare system, expert centres may include tertiary referral centres, specific government-appointed facilities and centres that are part of reference networks for rare diseases (table 1). The panel and patient representatives further recognise that a hub-and-spoke care model, involving periodic assessments at an

Table 1
General recommendations

General recommendations	Level of evidence for clinical utility (see online supplemental file S3)	LoA, mean±SD	LoA, % ≥8
R1: consider referral to an expert centre for all adult patients with CNO, and refer difficult-to-treat patients if not done initially.	°°°	9.51±0.77	97.30%
R2: adults with CNO should be diagnosed and treated by a multidisciplinary team, led by an expert in this disease, preferably a rheumatologist. In the absence of a rheumatologist, a specialist with expertise in autoinflammatory and bone-related disorders should assume this role. The team should involve musculoskeletal imaging experts and other medical specialists according to the presence of additional features.	°°°	9.51±0.80	97.30%
R3: aim for long-term follow-up in all patients. When follow-up is discontinued, inform patients that their condition may return with similar but different features and involvement sites in the future.	°°°	9.54±0.73	97.30%

° indicates 4-point scale ranging from very low to low to moderate to high according to the Grading of Recommendations, Assessment, Development and Evaluations approach.
CNO, chronic non-bacterial osteitis; LoA, level of agreement.

expert centre with follow-up and treatment administered at nearby clinics, would be a patient-friendly approach, minimising travel while ensuring expertise with larger patient numbers.

R2: Adults with CNO should be diagnosed and treated by a multidisciplinary team, led by an expert in this disease, preferably a rheumatologist. In the absence of a rheumatologist, a specialist with expertise in autoinflammatory and bone-related disorders should assume this role. The team should involve musculoskeletal imaging experts and other medical specialists according to the presence of additional features

Rationale

Adults with CNO should ideally be diagnosed and managed by a multidisciplinary team, preferably led by a rheumatologist. In the absence of a rheumatologist, another specialist with expertise in autoinflammatory and bone-related disorders, such as an endocrinologist or a clinician-osteologist, may take on this role, depending on the healthcare system (see online supplemental file S3, Q4 for current overview and quality appraisal). Close collaboration with musculoskeletal imaging experts is necessary in all patients, and other disciplines should be involved as necessary if additional features are present.

R3: Aim for long-term follow-up in all patients. When follow- up is discontinued, inform patients that their condition may return with similar but different features and involvement sites in the future

Rationale

The panel agreed that development of new (rather than evolving existing) bone lesions is very rare in adults. Only in the anterior chest wall it is observed that more bones become involved in the inflammatory process, for example, progressing from one clavicle into rib and manubrial lesions. In other body parts, like the spine, the involvement of bones is usually already 'complete' at presentation. However, there are no known predictors to identify patients at risk for new lesions [36–38], the disease may follow a relapsing-remitting course, and additional features like skin manifestations may occur long before or after the presentation of osteitis. Therefore, long-term follow-up in all patients is recommended. The frequency of follow-up visits varies according to local protocols, healthcare organisation policies, patient-specific factors and importantly, treatment type. Generally, the panel considers it advisable to schedule follow-up visits 3–6 months after the initial diagnosis, and with larger intervals (eg, every 12–24 months) after clinical stabilisation.

DIAGNOSTIC RECOMMENDATIONS

Across the different stages of diagnostic evaluation, differential diagnoses to consider in adults with suspected CNO include infectious osteomyelitis, malignant bone tumours, other rheumatic musculoskeletal diseases, Tietze's syndrome, metabolic bone diseases and sternoclavicular subluxation (table 2, figure 4). Clinical findings suggestive of these diagnoses are listed in table 3.

R4: Perform clinical evaluation with specific attention for additional features and fulfilment of axSpA and PsA classification criteria. Consider diagnostic involvement of relevant medical disciplines

Rationale

In adults with suspected CNO, the panel recommends performing a thorough clinical evaluation including history of initial and presenting complaints, full medical history and family history of autoinflammatory or autoimmune diseases in first-degree relatives [39]. Atraumatic bone pain persisting for over 6 weeks, with inflammatory properties such as pain irrespective of motion, or during the night, is suggestive of CNO [1,8,40–42]. The patient should be assessed for other inflammatory features (figure 2). Involvement from a dermatologist, ophthalmologist and gastroenterologist can be considered depending on suspected features. It also is recommended to review whether there is fulfilment of classification criteria for axSpA or PsA, as this may have implications for clinical management.

R5: Conduct routine laboratory investigation with full blood and differential count, inflammatory markers, renal function, alkaline phosphatase, calcium, 25-hydroxy-vitamin D, parathyroid hormone levels and phosphate. Consider on case- by-case basis (eg, for differential diagnosis or pretreatment evaluation): bone turnover makers, anti-CCP, RF, HLA-B27

Rationale

The panel acknowledges that most laboratory markers of inflammation lack specificity for adult CNO, but may be used to investigate differential diagnoses [2] (see online supplemental

Table 2
Diagnostic recommendations

Diagnostic recommendations	Level of evidence for clinical utility (see online supplemental file S3)	LoA, mean±SD	LoA, % ≥8
R4: perform clinical evaluation with specific attention for additional features (figure 2) and fulfilment of axSpA and PsA classification criteria. Consider diagnostic involvement of relevant medical disciplines.	°°°	9.51±0.65	100.00%
R5: conduct routine laboratory investigation with full blood and differential count, inflammatory markers, renal function, alkaline phosphatase, calcium, 25-hydroxy-vitamin D, parathyroid hormone levels and phosphate. Consider on case-by-case basis (eg, for differential diagnosis or pretreatment evaluation): bone turnover makers, anti-CCP, RF, HLA-B27.	°°°	9.27±0.87	97.30%
R6: perform imaging of the suspected region, giving priority to a modality suitable for assessing both activity and structural changes. MRI should be preferred but combined [^{99}mTc]Tc-HDP SPECT/CT or PET/CT with a bone-seeking radiotracer are reasonable alternatives.	°°°	9.32±1.53	94.59%
R7: consider performing whole-body imaging in all patients at initial evaluation to map clinically silent, but radiologically active lesions. Whole-body MRI (with sagittal spinal images) should be preferred, but [^{99}mTc]Tc-HDP SPECT/CT, PET/CT with a bone-seeking radiotracer or bone scintigraphy alone are reasonable alternatives.	°°°	8.92±1.79	86.49%
R8: do not perform routine bone biopsies. Reserve bone biopsies for cases with inconclusive imaging and/or suspicion of malignancy or infectious osteomyelitis.	°°°	9.51±0.73	100.00%

° indicates 4-point scale ranging from very low to low to moderate to high according to the Grading of Recommendations, Assessment, Development and Evaluations approach. See table 3 for differential diagnoses. See table 4 for advantages and disadvantages of MRI versus CT + nuclear imaging.
Anti-CCP, anticitrullinated protein antibodies; axSpA, axial spondyloarthritis; CNO, chronic non-bacterial osteitis; HLA-B27, human leucocyte antigen B27 typing; LoA, level of agreement; [^{99}mTc]Tc-HDP SPECT/CT, technetium-labelled hydroxymethylene diphosphonate single positron emission CT; PET, positron emission tomography; PsA, psoriatic arthritis; RF, rheumatoid factor.

file S3, Q5 for supportive evidence). As part of the initial evaluation, the panel recommends routinely measuring complete blood count with white blood cell differential, and inflammation markers to assess the degree of systemic inflammation. Renal function should be included to assess the safety of medications. Alkaline phosphatase, calcium, 25-hydroxy-vitamin D, phosphate and parathyroid hormone levels should routinely be measured to exclude other metabolic bone diseases, such as osteomalacia, Paget's disease or hypophosphatasia. The following tests can be considered on a case-by-case basis:

- Bone turnover markers such as serum procollagen type I N propeptide (P1NP) and C-terminal telopeptide (CTx); these can be determined, preferably in fasting blood samples, to aid the evaluation of other metabolic bone diseases [43–45].
- Anticitrullinated protein antibodies (anti-CCP) and rheumatoid factor (RF); in patients presenting with inflammatory (erosive) polyarthritis, elevated levels may support a diagnosis of rheumatoid arthritis.
- Human leucocyte antigen B27 (HLA-B27) typing; in cases with axial involvement or inflammatory back pain, these may support the diagnosis of axSpA. HLA-B27 positivity has so far not been shown to be associated with adult CNO.

R6: Perform imaging of the suspected region, giving priority to a modality suitable for assessing both activity and structural changes. MRI should be preferred but combined [^{99}mTc]Tc-HDP SPECT/CT or PET/CT with a bone-seeking radiotracer are reasonable alternatives

Rationale

Imaging of the clinically suspected region plays a pivotal role in the diagnosis of adult CNO. The panel agrees that the goals of imaging at initial evaluation are to (1) visualise characteristic features associated with the condition, thereby aiding the diagnostic process and informing on prognosis and (2) assess inflammatory disease activity, should a diagnosis of CNO be confirmed. Achieving both goals using a single scan is feasible with either MRI or CT combined with a bone scintigraphy technique. Examples of the latter are technetium-labelled hydroxymethylene diphosphonate single positron emission CT ([^{99}mTc]Tc-HDP SPECT/CT) and positron emission tomography (PET)/CT with a boneseeking radiotracer such as sodium fluoride [7,23,46–48] (see online supplemental file S3, Q6A and Q6B for supportive evidence). The specific scan properties of MRI and [^{99}mTc] Tc-HDP SPECT/CT or PET/CT are listed in table 4. The panel recommends MRI for the initial evaluation of adult CNO, but considers [^{99}mTc]Tc-HDP SPECT/CT or PET/CT a reasonable alternative, for the following reasons.

CT provides excellent visualisation of structural changes secondary to inflammation, which are often already seen at initial evaluation owing to diagnostic delays [7]. These include sclerosis, erosions, hyperostosis (seen as endosteal and periosteal thickening), soft tissue ossification and ankylosis [7,20–25] (see online supplemental file S3, Q2A and Q2B for supportive evidence). Structural changes are useful for the diagnosis of CNO due to their specificity, and are valuable for prognosis since they reflect the degree of accumulated skeletal damage. Structural changes are well visualised with CT, which can conveniently be combined with bone scintigraphy techniques ([^{99}mTc]Tc-HDP SPECT/CT or PET/CT) to evaluate disease activity, with increased radiotracer uptake representing heightened osteoblastic activity. Of note, bone scintigraphy *without* CT is inadequate for diagnosis of CNO, as radiotracer uptake is highly non-specific and correlation with structural features is thus crucial. A disadvantages of [^{99}mTc]Tc-HDP SPECT/CT and PET/CT is that it only detects patients with CNO with structural changes that have accumulated over time. As awareness for

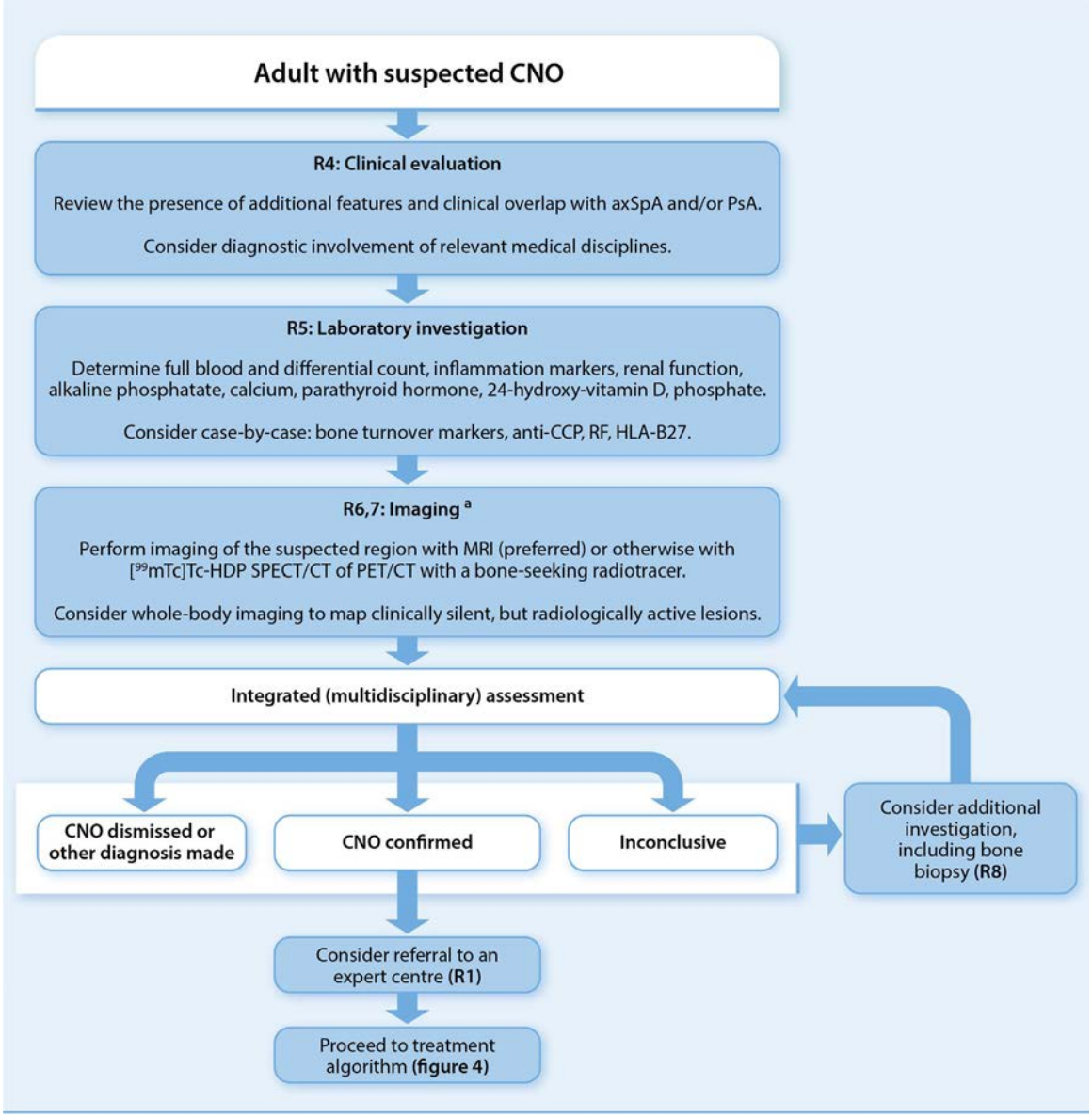

Figure 4. Diagnostic algorithm for adult CNO. ANA, antinuclear antibody and immunofluorescence pattern; anti-CCP, anticitrullinated protein antibodies; CNO, chronic non-bacterial osteitis; HLA-B27, human leucocyte antigen B27 typing; PET, positron emission tomography; RF, rheumatoid factor; [^{99}mTc]Tc-HDP SPECT/CT, technetium-labelled hydroxymethylene diphosphonate single positron emission CT. [a]See table 4 for advantages and disadvantages of MRI and CT + nuclear imaging.

CNO is rising, the panel anticipates physicians encountering patients earlier in their disease course, in which other features like bone marrow oedema and osteolysis are more prominent (see online supplemental file S3, Q2A and Q2B for supportive evidence). Although bone marrow oedema lacks specificity due to its occurrence in other conditions and also healthy individuals [21,25,46,49,50], the panel concurs that this feature is generally helpful in the diagnostic process, particularly if it is seen in typical skeletal sites for CNO (eg, anterior chest wall, spine and mandible). The key relevance of bone marrow oedema as an early and activity-related disease feature requires a preference for the use of MRI. Other advantages of MRI include the detection of soft tissue involvement and neurovascular structures, and the lack of ionising radiation. Although somewhat less optimal than CT, MRI also provides fair visualisation of structural changes (see online supplemental file S3, Q2C for supportive evidence). Based on their properties, the panel recommends MRI for the initial evaluation of adult CNO, but agrees that CT with nuclear imaging ([^{99}mTc]Tc-HDP SPECT/CT or PET/CT with bone-seeking radiotracer) are other reasonable options. A combination of MRI and CT may be used in certain circumstances. The panel also acknowledges that CT provides better visualisation of the anterior chest wall, as CT can detect subtle structural changes and is less affected by breathing artefacts [7,51]. The panel agrees that plain radiographs are of limited use for adult CNO, as they have low sensitivity, do not provide information about disease activity and are less suitable to assess the anterior chest wall, spine and mandible [7,52]. Furthermore, the progression of these lesions over time can provide critical information, aiding in the exclusion of differential diagnoses. Hence, previous imaging should be given considerable attention in the diagnostic process. This approach may render repeated examinations unnecessary or assist in selecting a complementary imaging technique in complex cases.

Table 3
Differential diagnostic considerations in suspected adult CNO

Differential diagnosis	Specifically consider when presentation includes:
Infectious osteomyelitis	Systemic symptoms such as fever and chills, presumable port of entry, solitary bone lesion, significantly elevated CRP or ESR, bactaeremia
Malignant bone tumour	Unexplained weight loss, solitary bone lesion with quick growth, cortical destruction or perpendicular periosteal new bone formation on imaging
Psoriatic arthritis	Psoriasis (current, history or family history in first-degree relatives), inflammatory articular disease (joint, spine, entheseal), nail dystrophy, dactylitis, juxta-articular new bone formation on hand or foot radiography
Axial spondyloarthritis	Inflammatory back pain, sacroiliitis, asymmetrical inflammatory arthritis, enthesitis, dactylitis, uveitis, psoriasis, inflammatory bowel disease, pain responsive to NSAIDs, family history, HLA-B27 positivity, elevated CRP
Rheumatoid arthritis	Symmetrical polyarthritis, specifically of small joints, characteristic erosions, anti-CCP or RF positivity, elevated CRP or ESR
Osteoarthritis	Older age at onset, history of strain or occurrence at dominant side, osteoarthritis in other locations, bony swelling (depending on site; may be seen with sternoclavicular involvement), subchondral sclerosis or cysts, characteristic osteophytes and joint space narrowing on imaging
Tietze's syndrome	Pain in costosternal transitions, unilateral, self-limiting symptoms after weeks-months and not due to intercostal enthesitis in psoriatic arthritis
Paget's disease	Family history, pelvic or skull localisation, raised alkaline phosphatase, deformities, characteristically mixed osteolytic and osteosclerotic aspect on imaging, age of onset usually >50 years
Osteomalacia	Generalised bone pain and muscle weakness, low serum phosphate, elevated alkaline phosphatase, low 25-hydroxy-vitamin D, increased parathyroid hormone, bone demineralisation on imaging
Hypophosphatasia	Generalised bone pain and muscle weakness, dental abnormalities, low alkaline phosphatase levels, bone demineralisation on imaging, mixed lytic and sclerotic lesions
Fibrous dysplasia	Bone deformities, neurological symptoms in case of skull involvement, other endocrinopathies in case of McCune-Albright syndrome, expansive, lytic, ground-glass lesions on imaging
Anterior sternoclavicular subluxation	Recent trauma, unilateral swelling of sternoclavicular joint, history of connective tissue disorder like Ehlers-Danlos syndrome
Bone bruise	Recent trauma, adjacent trauma-related lesions, self-limiting symptoms after 1–2 months

Other rare differential diagnoses for CNO in adults: (osseous manifestations of) sarcoidosis, gout, Langerhans cell histiocytosis, osteonecrosis with certain involvement sites (eg, avascular osteonecrosis), ascorbic acid deficiency, Erdheim-Chester disease.
Anti-CCP, anticitrullinated protein antibodies; CNO, chronic non-bacterial osteitis; CRP, C reactive protein; ESR, erythrocyte sedimentation rate; HLA, human leucocyte antigen; NSAIDs, non-steroidal anti-inflammatory drugs; RF, rheumatoid factor.

R7: Consider performing whole-body imaging in all patients at initial evaluation to map clinically silent, but radiologically active lesions. Whole-body MRI (with sagittal spinal images) should be preferred, but [^{99}mTc]Tc-HDP SPECT/CT, PET/CT with a bone-seeking radiotracer or bone scintigraphy alone are reasonable alternatives

Rationale

The panel extensively deliberated whether routine whole-body imaging is advisable for the diagnosis and initial evaluation of adult CNO. It is known that up to 67% of patients may have clinically silent, but radiologically active lesions, which remain undetected if imaging is only conducted in clinically suspect areas [11,20,23,27] (see online supplemental file S3, Q6C for supportive evidence). According to the panel, performing routine whole- body imaging at initial evaluation offers two key advantages. First, it allows for accurate mapping of the disease, potentially supporting the CNO diagnosis when lesions follow a specific distribution. Second, whole-body imaging may affect clinical management when numerous silent lesions may be interpreted as more severe or aggressive disease, or when silent lesions carry a complication risk (eg, vertebral collapse with highly active spinal lesion). However, it should be stressed that it is unclear whether identifying these silent lesions will lead to better patient outcomes (see online supplemental file S3, Q6C for appraisal of evidence). The panel, therefore, *suggests* considering routine whole-body imaging at the initial evaluation of adult CNO. The panel emphasises that whole-body imaging is not a strict prerequisite for diagnosis, and should not come at the expense of good- quality regional imaging. Techniques to be considered include whole-body MRI (with sagittal images of the spine), [^{99}mTc] Tc-HDP SPECT/CT, PET/CT or plain bone scintigraphy.

Table 4
Relevant scan properties of [^{99}mTc] Tc-HDP SPECT/CT or PET/CT versus MRI for initial evaluation of adult CNO

Feature	[^{99}mTc]Tc-HDP SPECT/CT or PET/CT	MRI
Detection of new bone formation	Very good	Fair
Detection of bone inflammation	Fair (visualised through bone turnover)	Good
Detection of soft tissue inflammation	Poor	Good
Ease of performance	Good	Fair
Ease of interpretation	Fair	Poor
Ionising radiation	Considerable	None
Contraindications	Few	Metal, claustrophobia

CNO, chronic non-bacterial osteitis; [^{99}mTc]Tc-HDP SPECT/CT, technetium-labelled hydroxymethylene diphosphonate single positron emission CT; PET, positron emission tomography.

R8: Do not perform routine bone biopsies. Reserve bone biopsies for cases with inconclusive imaging and/or suspicion of malignancy or infectious osteomyelitis

Rationale

The panel recommends against routinely perform bone biopsies in adults with suspected CNO and considering these only in cases where the recommended imaging is inconclusive, and/or

suspicion of malignancy or infectious osteitis is high. Suspicion of malignancy is raised in scenarios characterised by involvement of a single bone, atypical locations for CNO, rapid lesion growth, evidence of cortical destruction on imaging, the presence of overt and/or severe systemic symptoms such as unexplained weight loss. Infection may be more likely in patients with fever, significantly raised inflammation parameters, a suspected infection source or confirmed bacteraemia.

TREATMENT RECOMMENDATIONS

The diverse clinical presentation of adult CNO renders formulating uniform treatment recommendations challenging. These recommendations thus centre on *osteitis* and its associated morbidity, the core feature of the disease. In patients with additional features and/or fulfilment of criteria for axSpA and PsA, established treatment protocols should be followed, with treatment preferably targeting both osteitis and the additional feature(s). Furthermore, it should be stressed that the treatment recommendations for adult CNO are largely based on low-level evidence and expert opinion. Currently, all drugs listed are used off-label based mainly on evidence from observational studies and case reports (table 5, figure 5).

R9: Use the following treatment goals and outcome measures in CNO management

- **Relieving symptoms, as evaluated by bone pain likely caused by osteitis.**
- **Maintaining/Regaining functional capacity, as evaluated by range of motion, fatigue, patient-reported functional capacity and quality of life.**
- **Reducing inflammation, as evaluated by focal inflammatory signs on physical examination (if present), inflammation markers (if previously raised) and radiological signs of inflammation such as bone marrow oedema or increased tracer uptake in the clinically and/or radiologically suspect lesions.**
- **Preventing (the progression of) structural musculoskeletal damage.**

Rationale

Clinicians and patient representatives identified four treatment goals and associated outcome measures in adult CNO. Recognising that validated sets of outcome measures are yet to be developed, the following is meant as a practical tool to support clinical management. The panel unanimously agrees that the patient's well-being should be the primary consideration across all goals. However, laboratory test results and imaging findings may help to assess if symptoms can be attributed to active disease, since pain may also derive from neuropathic or nociplastic mechanisms and structural changes in the skeleton [53].

1. *Relieve symptoms*: the panel recommends pain as the main outcome measure, preferably measuring its severity on a visual analogue scale or numerical rating scale. While acknowledging the relevance of other types of pain to the patient, the focus should be on pain that can reasonably be attributed to osteitis.
2. *Regain and maintain functional capacity*: the panel recommends that this goal is evaluated by assessing the active and passive range of motion in the affected part of the skeleton and patient-reported outcomes such as fatigue and quality of life, which can be measured with standardised questionnaires such as Brief Pain Inventory and Health Assessment Questionnaire Disability Index [54,55].
3. *Reduce inflammation*: the panel emphasises that this is an important treatment goal, as inflammation contributes to symptoms in the acute phase, and likely to risk of skeletal damage over time. Outcome measures include bone pain that is likely caused by osteitis (just as in goal 1), focal inflammatory signs on physical examination (if present at initial evaluation), inflammation markers (if elevated at initial evaluation) and radiological signs of inflammation such as bone marrow oedema and increased tracer uptake in the clinically and/or radiologically suspect lesions. For the latter, the panel emphasises that longitudinal studies are needed to elucidate the validity, utility and clinical relevance of bone marrow oedema or tracer uptake as an outcome measure, as it is known that both may persist despite resolution of symptoms (see online supplemental file S3, Q2C for summary of evidence) [56,57]. The relevance of asymptomatic bone marrow oedema or tracer uptake may depend on the location(s) and extent of disease, and may influence treatment decisions in some cases to protect the structural integrity of functionally important joints and bones and reduce the risk of complications.
4. *Prevent (the progression of) structural musculoskeletal damage*: this is monitored by imaging studies that depict secondary structural changes, as well as indirectly by the clinical assessment.

The panel recommends that the caring team should discuss and agree on treatment goals with patients before the start of treatment, as goals may vary among individuals and across different stages of the disease and influence treatment response evaluation (see R11).

R10: Assess disease activity based on clinical symptoms (bone pain likely caused by osteitis) and radiological measures (bone marrow oedema or increased tracer uptake in the clinically and/or radiologically suspect lesions). Include the presence of focal inflammatory signs and elevation of inflammation markers if applicable

The following categories can be used as guidance:

1. **Corresponding clinical symptoms and radiological disease activity: consider these patients as active CNO and initiate treatment.**
2. **Neither clinical symptoms nor radiological disease activity: consider these patients as inactive CNO and do not start treatment.**
3. **Clinical symptoms without radiological disease activity: consider these patients as probably inactive CNO, and first investigate other causes of pain.**
4. **Radiological disease activity without clinical symptoms: consider these patients as having no clinically relevant CNO activity, and decide on treatment in shared decision.**

Rationale

Defining disease activity in adult CNO is challenging due to the lack of evidence supporting existing definitions and measures. According to the panel, disease activity assessment should primarily be based on clinical symptoms of bone pain likely caused by osteitis, and radiological measures of bone marrow

Table 5
Treatment recommendations

Treatment recommendations	Level of evidence (see online supplemental file S3)	LoA, mean±SD	LoA, % ≥8
R9: use the following treatment goals and outcome measures in CNO management: • Relieving symptoms, as evaluated by bone pain likely caused by osteitis. • Maintaining/Regaining functional capacity, as evaluated by range of motion, fatigue, patient-reported functional capacity and quality of life. • Reducing inflammation, as evaluated by focal inflammatory signs on physical examination (if present), inflammation markers (if previously raised) and radiological signs of inflammation such as bone marrow oedema or increased tracer uptake in the clinically and/or radiologically suspect lesions. • Preventing (the progression of) structural musculoskeletal damage.	°°°	9.24±1.01	97.30%
R10: disease activity assessment at initial evaluation (see text for further details) • Assess disease activity based on clinical symptoms (bone pain likely caused by osteitis) and radiological measures (bone marrow oedema or increased tracer uptake in the clinically and/or radiologically suspect lesions). Include the presence of focal inflammatory signs and elevation of inflammation markers if applicable. The following categories can be used as guidance: 1. Corresponding clinical symptoms and radiological disease activity: consider these patients as *active CNO* and initiate treatment. 2. Neither clinical symptoms nor radiological disease activity: consider these patients as *inactive CNO* and do not start treatment. 3. Clinical symptoms without radiological disease activity: consider these patients as *probably inactive CNO*, and first investigate other causes of pain. 4. Radiological disease activity without clinical symptoms: consider these patients as *likely not having clinically relevant CNO activity*, and decide on treatment in shared decision.	°°°	9.16±0.76	100.00%
R11: treatment response evaluation during follow-up (see text for further details) • Conduct a treatment response evaluation between treatment steps, primarily based on clinical measures, but integrate radiological and biochemical measures as appropriate. • Declare sufficient/insufficient response based on improvement, no change or worsening on relevant measures, with the individual patient context and predetermined treatment goals as reference.	°°°	9.27±0.69	100.00%
R12: general treatment recommendations • Provide patient education and lifestyle recommendations. • Consider physiotherapy and dental examination. • Short courses of oral prednisolone or intra-articular glucocorticoid injections may be considered as bridging options, awaiting the effect of other agents, throughout the treatment steps. Avoid the long-term use of glucocorticoids.	°°°	9.05±1.37	91.89%
R13: first-line treatment • Start NSAIDs/COXIBs in maximum tolerated and approved dosage in adults with active CNO. – Consider directly adding/advancing to second-line treatment in patients with spinal bone lesions with risk of vertebral collapse and in patients presenting with significant accumulated skeletal damage. • Evaluate treatment response at 2–4 weeks: – In case of sufficient response, continue and re-evaluate response at 12 weeks. Consider tapering or ondemand treatment in case of sustained sufficient response. – In case of insufficient response at 2–4 weeks or later, consider an NSAID/COXIB rotation or add/advance to second-line treatment.	°°°	9.30±0.81	100.00%
R14: second-line treatment • Start IVBP (generally preferred) or TNFi, depending on patient characteristics. • csDMARDs can be considered, especially in patients with inflammatory polyarthritis, but it is not necessary to trial these before considering TNFi. • Evaluate treatment response at 3–6 months: – In case of sufficient response, continue and re-evaluate response at 6–12 months. Consider tapering in case of sustained sufficient response. – In case of insufficient response, exchange for TNFi or IVBP or consider combination therapy. Similarly, reevaluate response at 6–12 months. Consider tapering (one-by-one) in case of sustained sufficient response.	°°°	9.05±0.81	97.30%
R15: third-line treatment • Refer patients with insufficient response to IVBP and TNFi (or combined) to an expert centre, where a range of other third-line treatment options may be considered (see text for details).		9.54±0.65	100.00%
R16: complications and adverse effects of treatment • Be aware of the neurovascular complications in patients with anterior chest wall involvement and of the risk of vertebral fractures in patients with spinal involvement. • Monitor adverse treatment effects according to established guidelines.		9.46±0.77	100.00%

° indicates 4-point scale ranging from very low to low to moderate to high according to the Grading of Recommendations, Assessment, Development and Evaluations approach. See table 6 for agents and dosages to consider.
axSpA, axial spondyloarthritis; CNO, chronic non-bacterial osteitis; COXIB, cyclooxygenase-2 inhibitor; csDMARD, conventional synthetic disease-modifying antirheumatic drug; IVBP, intravenous bisphosphonates; LoA, level of agreement; NRS, numerical rating scale; NSAID, non-steroidal anti-inflammatory drug; PsA, psoriatic arthritis; TNFi, tumour necrosis factor-α inhibitors.

oedema/increased tracer uptake in the clinically and/or radiologically suspect lesions. Clinical signs of focal inflammation and elevated inflammatory markers may contribute to the overall assessment, but they are observed in only a small number of patients, making them limitedly informative for the majority. Using clinical symptoms and radiological parameters as leading reflectors of disease activity, the panel identified four main categories of patients as guidance.

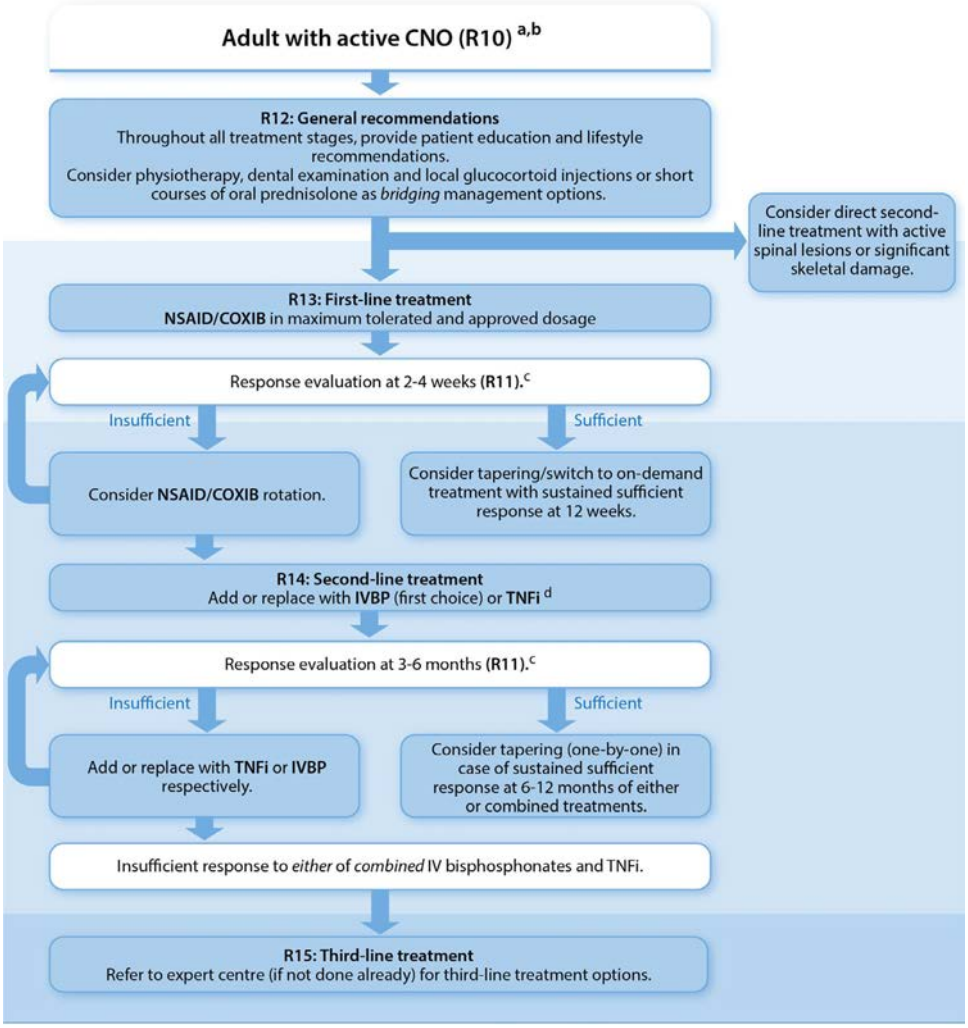

Figure 5. Treatment algorithm for adult CNO. axSpA, axial spondyloarthritis; CNO, chronic non-bacterial osteitis; COXIB, cyclooxygenase-2 inhibitor; csDMARD, conventional synthetic disease-modifying antirheumatic drug; IVBP, intravenous bisphosphonates; NSAID, non-steroidal anti-inflammatory drug; PsA, psoriatic arthritis; TNFi, tumour necrosis factor-α inhibitors. [a]Active CNO defined as corresponding clincal and radiological disease activity, optionally with focal inflammatory signs and/or elevated inflammation parameters. See **R10** for details. [b]In case of additional features or clinical overlap with axSpA and/or PsA, follow established treatment protocols and align with treatment for osteitis where possible. [c]Declare sufficient/ insufficient response based on clinical measures mainly, but integrate radiologic and biochemical measures as appropriate, with the individual patient context and predetermined treatment goals as reference. See **R11** for details. [d]csDMARDs may be consided as step 2 treatments too, especially in cases with concomitant polyarthritis.

1. *Corresponding clinical symptomsand radiological disease activity*: this category of patients should be regarded as having *active CNO*. These patients may exhibit focal inflammatory signs and elevated inflammation markers as well, but these are not required to speak of active CNO. The panel recommends that treatment is initiated in patients with active CNO.
2. *Neither clinical symptoms nor radiological disease activity*: this category of patients should be regarded as *inactive CNO*. Should elevated inflammation markers be seen, alternative causes should be investigated as the relation to CNO is less likely. The panel recommends that these patients do not require treatment.
3. *Clinical symptoms without radiological disease activity*: the panel would consider these patients as probably *inactive CNO*, and recommends evaluating other causes of pain before treating osteitis. Myalgia, central sensitisation, neuropathic pain and pain originating from structural changes, such as mechanical issues related to ankylosis, are potential alternative causes [53].
4. *Radiological disease activity without clinical symptoms*: the panel leans towards classifying this group as having no clinically relevant CNO activity, particularly if there are no focal inflammatory signs or elevated inflammation markers. This classification is based on the lack of evidence that treating patients with asymptomatic radiological activity improves outcomes. Similarly, there is no evidence that withholding treatment in such cases results in worse outcomes. In addition, common imaging methods, such as [^{99}mTc]Tc-HDP SPECT/CT, can reveal imprinted tracer uptake patterns regardless of symptoms [58]. Since the panel recommends prioritising patient symptoms in clinical management, this typically means refraining from treatment in cases of asymptomatic radiological activity. It is important to recognise that, although this is a patient-centred approach, it disregards subclinical osteitis, which could, in theory, cause long-term skeletal damage. Therefore, the decision to start treatment should be made through careful shared decision-making. Particular cases in which treatment may be justified despite the absence of pain are those in which radiological activity poses a direct risk of complications, such as highly active spinal lesions or imminent vertebral collapse. In such cases, patients should be counselled on the potential burdens and benefits of treatment as part of the shared decision-making process (see also R14).

R11: Conduct a treatment response evaluation between treatment steps, primarily based on clinical measures, but integrate radiological and biochemical measures as appropriate. Declare sufficient/insufficient response based on improvement, no change or worsening on relevant measures, with the individual patient context and predetermined treatment goals as reference

Rationale

Defining treatment response criteria for adult CNO presents several challenges. First, the prognostic value of various outcome measures is unknown. Additionally, response may manifest in one domain (eg, reduced bone pain caused by osteitis) but not in others (eg, persistent bone marrow oedema or increased tracer uptake in the clinically and/or radiologically suspect region). Lastly, determining response adequacy is always partly subjective, contingent on baseline conditions and individual patient context. Hence, the assessment of treatment response should be made by the treating physician, integrating clinical, biochemical (if applicable) and radiological measures within the patient's context and predetermined treatment goals. As guidance, the panel outlines three common scenarios:

1. *Improvement in all disease activity domains*: an improvement in clinical and radiological activity, along with biochemical measures (if applicable) is an all-round effect and thus can be considered as *sufficient response*.
2. *No change or worsening in all disease activity domains*: unchanged or worsened clinical and radiological activity along with biochemical measures (if applicable) can be considered as *insufficient response*.
3. *Improvement in some, but not all disease activity domains*: inconsistent effect on clinical and radiological measures, along with biochemical measures (if applicable) may be considered as *sufficient or insufficient*, depending on patient context and treatment goals.

The panel wishes to stress that, despite the importance of radiological measures in declaring treatment response, routine follow-up imaging is not required in all patients. In patients with evident clinical (and optionally biochemical) improvement, follow-up imaging is not essentially required to confirm sufficient response. Naturally, in patients with lack of or differential clinical or biochemical improvement, *local* follow-up imaging is helpful to incorporate radiological response in the final assessment and to facilitate shared decision-making. Apart from treatment response evaluations, local follow-up imaging may also be considered if the differential diagnosis needs to be explored further, or when new symptoms arise or complications such as vascular occlusion, nerve compression or fractures are suspected. Routine follow-up whole-body scans are not typically recommended after the initial evaluation but may be a valid option in specific cases, such as for patients with extensive disease which is difficult to assess with local imaging.

R12: Use the following as general treatment recommendations:

- **Provide patient education and lifestyle recommendations**
- **Consider physiotherapy and dental examination**
- **Consider short courses of oral prednisolone or intraarticular glucocorticoid injections as bridging options, awaiting the effect of other agents. Avoid the long-term use of glucocorticoids.**

R12: As general treatment recommendations: provide patient education and lifestyle recommendations, consider physiotherapy and dental examination, and consider short courses of oral prednisolone or intra-articular glucocorticoid injections as bridging options, awaiting the effect of other agents. Avoid the long-term use of glucocorticoids

Rationale

The panel recommends that patient education should be given (specifically because CNO is a rare disorder and often diagnosed after significant delay). Lifestyle recommendations are to be given to all patients as well, including smoking cessation, weight control and regular physical activity, thereby contributing to general health. The panel recommends considering physiotherapy in adult patients with CNO to optimise physical functioning. Dental examination may further be considered, to evaluate the presence of concomitant infections which have been suggested to be associated with CNO [35,59–64], as well as to ensure adequate dental hygiene before the start bisphosphonate therapy to mitigate the small risk of osteonecrosis of the jaw. Regarding the use of glucocorticoids, the panel agreed that intra-articular glucocorticoid injections may provide short-term relief in patients with joint involvement and can be considered when awaiting the effect of other treatments (see online supplemental file S3, Q13 for summary of evidence). The same also holds for oral glucocorticoids, which may be helpful as bridging option in short courses with fast tapering. As the evidence supporting glucocorticoids in CNO is scarce, management should in no way rely on these agents, also given their adverse effect profile [37,65,66]. Glucocorticoids may even pose controversial effects, as they promote bone resorption, possibly worsening the accelerated bone turnover that is seen in CNO lesions. However, exact impact of glucocorticoids on CNO lesions, and its relevance in clinical practice, is unknown.

R13: As first-line treatment, start non-steroidal antiinflammatory drugs/cyclooxygenase-2 inhibitors in maximum tolerated and approved dosage in adults with active CNO. Consider directly adding/advancing to second-line treatment in patients with spinal bone lesions with risk of vertebral collapse and in patients presenting with significant accumulated skeletal damage

- **Evaluate treatment response at 2–4 weeks after initiation**
- **In case of sufficient response, continue and re-evaluate response at 12 weeks. Consider tapering or on-demand treatment in case of sustained sufficient response.**
- **In case of insufficient response at 2–4 weeks or later, consider a non-steroidal anti-inflammatory drug (NSAID)/cyclooxygenase-2 inhibitor (COXIB) rotation or add/advance to second-line treatment.**

Rationale

It should be emphasised that no randomised controlled trials (RCTs) exist to inform the optimal treatment choice and duration in adult CNO. As first-line treatment in adults with active CNO, panel recommends starting NSAIDs/COXIBs in maximum tolerated and approved dosage for 2–4 weeks. This may be followed by a trial of another NSAID/COXIB if the first did not provide benefit or was not tolerated [67,68] (see online supplemental file S3, Q10 for summary of evidence). For patients with prior NSAIDs/COXIBs usage, it is advisable to confirm adherence to the most optimal regimens. The panel

recommends treatment response evaluation at 2–4 weeks after initiation. In patients with sufficient response, treatment can be continued; switching to on-demand treatment or dose tapering can be considered with sustained sufficient response at 12 weeks. For patients with insufficient response at 2–4 weeks (or later if response was initially sufficient), the panel suggests adding/advancing to second-line treatments. Direct progression, without NSAID/ COXIB trial, to second-line treatments is suggested for:

- Patients with spinal bone lesions with risk of vertebral collapse, for example, due to extensive bone marrow oedema in a full vertebral body [69,70]. The panel specifically suggests starting intravenous bisphosphonates (IVBP) in these patients directly (with the addition of tumour necrosis factor-α inhibitors (TNFi) if indicated based on additional features).
- Patients with significant accumulated skeletal damage, for example, existing vertebral collapse or severe joint or vertebral ankylosis and erosions.

For both groups, it should be noted that evidence on better clinical outcomes with earlier and more aggressive treatment is lacking, making this a fully eminence-based suggestion.

R14: As second-line treatment, start IVBP (generally preferred) or TNFi, depending on patient characteristics. Conventional synthetic disease-modifying antirheumatic drugs can be considered, especially in patients with inflammatory polyarthritis, but it is not necessary to trial these before considering TNFi

- **Evaluate treatment response at 3–6 months**
- **In case of sufficient response, continue and re-evaluate response at 6–12 months. Consider tapering in case of sustained sufficient response.**
- **In case of insufficient response, exchange for TNFi or IVBP or consider combination therapy. Similarly, re-evaluate response at 6–12 months. Consider tapering (one-by-one) in case of sustained sufficient response.**

Rationale

As second-line treatment, the panel recommends IVBP and TNFi as reasonable treatment options (see table 6 for specific agents and dosages to consider, see online supplemental file S3, Q11 for summary of evidence) [2,32,38,43,44,71–103]. Conventional synthetic disease-modifying antirheumatic drugs (csDMARDs) may be considered in this treatment line as well, especially in cases with inflammatory polyarthritis, but the majority of the panel recognises that there is more supportive observational evidence for IVBP and TNFi in the treatment of osteitis [2,32,37,71,89,91,104–107]. In any case, the panel considers it unnecessary to trial csDMARDs before considering TNFi, like it is required in, for example, rheumatoid arthritis. Regarding IVBP and TNFi, the panel recommends IVBP as the first preferred option, due to the more favourable adverse effects profile (see also R16), lower costs, the fact that IVBP allow for on-demand treatment courses and the relative ease of discontinuing treatment. IVBP are specifically recommended in patients with active spinal lesions, although it should be noted there are no data on whether IVBP can prevent complications in these patients. TNFi may be preferred over IVBP in patients with primarily axial involvement, sacroiliitis or additional features like inflammatory arthritis uveitis or inflammatory bowel disease (resembling an axSpA phenotype). Ultimately, the choice should be based on patient profile, contraindications to particular treatments, cost considerations, logistics and patient factors and preferences, including pregnancy considerations in females. During second-line treatment, NSAIDs/ COXIBs can be maintained when having been partially effective. Response evaluation to IVBP and TNFi is recommended at 3–6 months after initiation. In patients with sufficient response, the panel suggests continuing treatment and re-evaluate at 6–12 months (from baseline). While there is no evidence on the preferred treatment duration in adult CNO, the panel majority suggests that after 6–12 months of sustained sufficient response, dose or interval tapering can be considered. In this decision, the risk of flare after treatment discontinuation should be weighed against the negative consequences of long-term treatment, including complications (see also *R16*) and patient burden. In patients with an insufficient response at 3–6 months, switching to TNFi or IVBP, or considering combination therapy, may be appropriate, with a similar re-evaluation at 6–12 months. In case of combination therapy and sustained sufficient response at 6–12 months, taper the first-started drug first, and consider tapering the second-started drug after another 6–12 months of sustained sufficient response.

If disease reactivation occurs during tapering, treatment may be resumed. However, if disease remains inactive during tapering, the panel suggests it may be appropriate to discontinue treatment at a certain point, depending on patient-specific

Table 6
Agents and dosages to consider for main treatment classes

Class	Agents and dosages to consider in active treatment phase (non-tapering dosages) ***Of note: these depend on local regulations and guidelines***
NSAIDs/COXIBs	Naproxen 375–1100 mg/day in two doses Diclofenac starting at 150 mg/day in divided doses, maintenance 75–100 mg/day in divided doses Indomethacin 150 mg/day in divided doses Ibuprofen 1800 mg/day in divided doses Celecoxib 200–400 mg/day in divided doses Etoricoxib 90 mg/day (or temporarily 120 mg/day) Piroxicam 20 mg/day in one dose Meloxicam 15 mg/day in one dose
IVBP	Pamidronate intravenously 3 × 30 mg on 3 consecutive days, every 3 months* Pamidronate intravenously 45–90 mg (or 1 mg/ kg), every month or every 3 months* Zoledronate intravenously 5 mg, according to symptoms†
TNFi	Infliximab 3–5 mg/kg intravenously at 0, 2 and 6 weeks, and henceforth 3–5 mg/kg every 6–8 weeks or subcutaneously 120 mg/2 weeks Etanercept 50 mg/week, subcutaneously Adalimumab 40 mg/2 weeks, subcutaneously Golimumab 50 mg/4 weeks, subcutaneously (may be increased to 100 mg depending on weight) Certolizumab 400 mg/4 weeks or 200 mg/2 weeks, subcutaneously (compatible with all trimesters of pregnancy [118])

* According to clinical experience of the panel, pamidronate seems to be more effective for pain reduction than zoledronate.
† Zoledronate carries logistical advantages, with—generally—fewer infusions and associated admissions, thereby decreasing treatment burden and costs.
CNO, chronic nonbacterial osteitis; COXIB, cyclooxygenase-2 inhibitor; IVBP, intravenous bisphosphonates; NSAID, non-steroidal anti-inflammatory drugs; TNFi, tumour necrosis factor-α inhibitors.

factors and at the discretion of the physician. On disease reactivation after a drug-free period, previously effective treatment regimens may be restarted.

R15: Refer patients with insufficient response to IVBP and TNFi (or combined) to an expert centre, where a range of other third-line treatment options may be considered

Rationale

Difficult-to-treat patients with insufficient response to first-line and second-line treatments need to be referred to an expert centre if not already done, to optimise management. Strategies may include the re-evaluation of diagnosis (possibly by bone biopsy, if not performed initially), re-evaluation of disease activity (addressing the question of whether persistent pain likely derives from ongoing inflammation, or may have alternative sources as outlined before), referral to a pain specialist in case of suspected neuropathic or nociplastic pain, optimisation of comorbidity management and psychosocial support. In cases of a confirmed active disease, IL-17 inhibitors (IL-17i), Janus kinase inhibitors (JAKi) or IL-12/23i, and IL-23i are third-line pharmacological treatment options, but it should be noted that evidence on these treatment options is even more limited (see online supplemental file S3, Q12 for summary of evidence). IL-17i may be specifically considered in patients with overlapping features of axSpA or PsA, such as sacroiliitis, dactylitis, enthesitis, psoriasis, although paradoxical psoriatic skin lesions have been reported in patients with CNO with PPP. JAKi has been reported to improve both osteitis and skin manifestations of the CNO spectrum, and may be administered if not contra-indicated based on cardiovascular risk profile and cancer risk. IL-23i has mostly been evaluated in CNO patients with PPP, with joined efficacy for skin and osteitis symptoms. For IL-12/23i, reported effects on osteitis are yet highly inconsistent. Concerning surgical intervention, the panel underscores the scarcity and variability of data in adult CNO (see online supplemental file S3, Q12 for summary of evidence). Due to the invasive nature of surgical procedures, and challenging anatomical regions such as the anterior chest wall and spine, the panel suggests that consideration for surgery should be reserved for cases with evident hyperostotic complications and localised disease. Any decision for surgery should involve a multidisciplinary team comprising internal and surgical background physicians situated at an expert centre.

R16: Be aware of the neurovascular complications in patients with anterior chest wall involvement and of the risk of vertebral fractures in patients with spinal involvement. Monitor adverse treatment effects according to established guidelines

Rationale

During follow-up, clinicians should be aware of the neurovascular complications in patients with anterior chest wall involvement, such as subclavian vein obstruction and thoracic outlet syndrome, and of the small risk of vertebral or clavicular fractures should these bones be involved [25,108–111] (see online supplemental file S3, Q15 for summary of evidence). Regarding adverse treatment effects, the panel recommends following established guidelines. Briefly, physicians should be aware of gastrointestinal and cardiovascular side effects of NSAIDs/COX-IBs. For patients receiving IVBP, common side effects include acute phase reactions, which may be reduced with dose spread, longer infusion times or additional anti-inflammatory medication in severe cases (table 6) [112]. Rare but serious complications include atypical femoral fractures and osteonecrosis of the jaw [113]. These complications have mainly been seen in oncological patients; the absolute risk for patients with CNO appears very low. This may be due to the relatively low cumulative dosage received as compared with those needed to treat tumour-induced hypercalcaemia. Risk may be further reduced by ensuring good dental hygiene before treatment and seeking surgical advice in case of dental procedures under bisphosphonate treatment. Patients receiving TNFi predominately face a higher infection risk and should be monitored accordingly. It is conventional practice that these patients are screened for latent infection and vaccinated for relevant pathogens before start of treatment [114]. Also, there is some evidence suggesting that anti-TNF-α can trigger psoriasis ('paradoxical psoriasis') and this has been reported in several CNO cases [80,82,115] (see online supplemental file S3, Q11 for summary of evidence). Since adult CNO has a clear female predisposition and frequently occurs at childbearing age, it is imperative to provide explicit guidance on the safety of various medications before, during and after pregnancy and nursing [2].

CONCLUSIONS AND FUTURE PERSPECTIVES

This international initiative developed a first consensus statement regarding the disease definition of adults with SBI. It was agreed by the panel collectively to label this disease spectrum as CNO in adults (adult CNO), and no longer use terms like SAPHO syndrome, SCCH, PAO and CRMO. Building on this shared definition and name, the panel developed a first set of multidisciplinary consensus recommendations for diagnosis and treatment of adult CNO. The main goal of this document is to assist clinicians in providing optimal care for their patients, as well as to limit practice variation and standardise care pathways over disciplines and countries.

A major challenge encountered during the development of recommendations was the scarcity of high-quality evidence, as large-scale epidemiological studies and RCTs specific to CNO are lacking. Consequently, the recommendations largely rely on expert opinion, small cohort studies and case reports. Recognising the importance of ongoing research into CNO, the consensus recommendations serve as a foundation for future collaborative studies. As part of the in-person meeting of this initiative, future research priorities were defined by the panel and patients representatives (box 1).

Of priority, the establishment of an international registry for adult patients with CNO is necessary to close the gaps in current knowledge on the clinical, laboratory and radiological course of the disease. A minimal dataset for a CNO registry as proposed by the panel is provided in online supplemental file S7. As direct spin-off of this initiative, possibilities are explored to build an international registry. Requirements for such a registry include formal governance structures that safeguard data access and management, as well as the infrastructure for patients to enter patient-reported outcome measures through digital questionnaires [116]. Candidate research questions to be addressed by the registry include regional comparison of clinical phenotype, incidence of new bone lesions and structural skeletal damage during follow-up and the prognostic relevance of asymptomatic radiological inflammation.

As for pathophysiology, an understanding of CNO's underlying mechanisms is currently limited. It is crucial to obtain both systemic and local signatures of inflammatory activity in CNO, as identification of these drivers is crucial to guide the development or repurposing of treatments. To achieve this, the

Box 1 Future research priorities as identified by consensus panel and patient representatives

Future research priorities as identified by consensus panel

Fundamentals

⇒ Development and validation of classification criteria for adult CNO.

⇒ International registry and biobank for adult patients with CNO including clinical, laboratory, radiological, treatment data, patient-reported outcomes and storage of specimens.

Pathophysiology and biomarkers

⇒ Environmental and/or genetic risk factors that trigger CNO (*specifically emphasised by patient representatives*).

⇒ Underlying mechanisms for and characteristics of pathophysiological cascade, including systemic and local inflammation, increased bone turnover and structural tissue changes; identification of therapeutic targets.

⇒ Primary drivers of site-specific nature of the disease.

⇒ Predictors/Biomarkers of disease progression or the development of new involvement sites.

⇒ Predictors/Biomarkers of response to specific treatments.

Clinical trials and drug approval

⇒ Development and validation of a (stratified) CNO disease activity score in adults to use as study end point in clinical trials, including patient-reported measures, imaging and relevant biomarkers.

⇒ Randomised clinical trials, specifically those comparing IVBP against placebo (running; EUDRACT 2020-001068-27), TNFi against placebo, IVBP against TNFi, pamidronate against zoledronate and other biologics as relevant based on translational study results. Double-blind, placebo-controlled design (allowing NSAIDs/COXIBs in both groups), followed by open-label extension.

Imaging

⇒ Prognostic relevance of radiological inflammation in patients with clinical remission, and utility of follow-up imaging in patients with clinical remission.

⇒ Diagnostic accuracy of CT (+nuclear imaging) and MRI (±nuclear imaging) in diagnosis of adult CNO, including comparative analysis.

⇒ Radiological evolution of adult CNO in larger patient numbers: frequency of progressive structural change, frequency of new lesion sites and utility of whole-body imaging at diagnosis and during follow-up.

Specifically emphasised by patient representatives

Research priorities additionally identified by patient representatives:

⇒ Strategies to reduce diagnostic delay.

⇒ Factors associated with relapse and remission.

⇒ Role of physical therapy, diet and other lifestyle factors on disease outcomes.

CNO: chronic non-bacterial osteitis, COXIB: cyclooxygenase-2 inhibitor, IVBP: intravenous bisphosphonates, NSAID: non- steroidal anti-inflammatory drugs, TNFi: tumour necrosis factor-α inhibitors.

establishment of an international biobank with systemic (peripheral blood) and local (bone or joint specimens) biomaterials is needed. Subsequently, collaboration between centres to exchange biomaterials and relevant techniques is needed (eg, immunophenotyping, gene expression profiling, spatial transcriptomics). A direct next step involves crafting a grant proposal with collaborators experienced in translational research, with the aim of launching such a project in the near future.

In the domain of treatment, there is clear need to conduct RCTs to validly assess efficacy of different treatments. An RCT comparing intravenous pamidronate against placebo is currently running, and subsequent trials should preferably compare efficacy between IVBP agents (eg, pamidronate against zoledronate), TNFi against placebo, TNFi against IVBP or other biologics based on immunological signatures as discovered in translational studies [10]. The panel deliberated that randomising patients with CNO to a placebo group is ethically acceptable, provided they have the option to receive NSAIDs/COXIBs and the placebo phase is short and succeeded by an open-label intervention phase. To conduct these trials, there is need for a set of validated classification criteria and outcome measures for adult CNO, the latter being currently underway [117].

This consensus initiative has strengths and limitations. Regarding strengths, this is the first attempt to develop recommendations for the management of adults with CNO, based on the best available evidence, international expertise and in collaboration with patient representatives. The initiative was inclusive by involving numerous disciplines from a wider range of countries, recognising the widespread experience with CNO. The involvement of the Dutch CNO patient association ensured patient representation in identifying treatment goals, outcome measures and research priorities. In addition, the inclusion of different syndromes causing SBI under a single entity, named CNO, will facilitate the conduction of larger research studies to address the unmet needs in the care of patients with CNO. Limitations of this initiative mainly pertain to the limited evidence supporting the recommendations, potentially compromising the validity of the recommendations. Nevertheless, the text consistently highlights the absence of evidence, and significant emphasis is placed on weighing the risks and benefits of specific clinical approaches. As such, the panel believes the recommendations are of value, especially given the lack of alternative resources. A second limitation is the comparatively low representation of American and Asian experts relative to those from Europe, despite considerable efforts made to include voices from all continents in the process. Recognising this gap, we designed the recommendations to be flexible, allowing it to be adapted to various healthcare systems in different countries, and aim at addressing this issue by further actively enhancing geographical diversity in future updates.

Moving forward, the next steps for this project involve the dissemination and implementation of the consensus recommendations, which requires extensive communication through relevant networks in rheumatology, endocrinology, orthopaedics, radiology and paediatric rheumatology. The panel perceives they are relatively easy to implement, as the recommendations pertain to relatively low patient numbers and were developed considering differences in the availability of diagnostic tests and treatment between healthcare systems. Despite being flexible, the recommendations offer a structured overview of diagnostic and management considerations for clinicians and helps patients understand what to expect. A potential challenge may arise from the limited reimbursement and accessibility of TNFi in certain regions. However, alternatives to TNFi are proposed. Anticipating future revisions of the recommendations, the panel hopes for further advancements in research to provide a more robust scientific foundation for updates.

Acknowledgements

The authors would like to thank Anda Kars and Evianne Smit, board members of the Dutch CNO patient association and patient representatives, for their contribution to the consensus recommendations. The authors would like to thank Timothy Bray, Martine Cohen-Solal, Matteo Colina, Davide Firinu, Victoria Furer, Nuria Guañabens, Gilles Hayem, Kassim Javaid, Aurni Jayatilleke, Karen Lindsay, Aleksander Lenert, Ron Laxer, Yasmine Makhlouf, Karen Partington, Marion Roderick, Athimalaipet Ramanan, Bing Thio, Alexander van Tongel, Marleen van de Sande, Yongdong Zhao, Marco Matucci-Cerinic and Mikhail Kostik for their contributions to the initiative, including completion

of the Delphi surveys. The authors further thank Annelies Smit for supporting the round-table session during the in-person meeting, and Zoe Konsta for her contribution to the systematic literature review. Credits for the figure graphics are extended to Manon Zuurmond, medial illustrator. The authors thank the European Calcified Tissue Society, European Reference Network of Rare Bone Diseases and European Society of Endocrinology for endorsing this initiative. During the preparation of this work, the authors used ChatGPT, solely to improve language and readability. The authors reviewed all suggested improvements and take full responsibility for the content of the publication.

Contributors

Conceptualisation: ATL and EMW. Data curation: ATL. Formal analysis: ATL. Funding acquisition: EMW. Investigation: ATL. Methodology: ATL, EMW, OMD. Supervision: ATL, EMW, OMD. Visualisation: ATL. Validation: ATL. Writing— original draft: ATL, EMW, OMD. Writing—review and editing: all authors.

Funding

This consensus initiative received financial support from Leiden University Fund (LUF) and the Dutch Research Council (NWO).

Competing interests

SD'A: consulting and speaking fees from AbbVie, Amgen, Bristol-Myers Squibb, Janssen, Lilly, MSD Italy, Novartis, Pfizer and UCB. GA: speaking fees and advisory boards of UCB, Novartis, AbbVie. DD: speaking fees and honoraria for participation in advisory boards from UCB, Pfizer, Novartis, BMS, MSD, Janssen, AbbVie, Lilly and Aenorasis. TD: speaker for Canon MS, Novartis, MSD, UCB and Roche. Advisory board: Lilly; Grant/Support: Canon MS, ASASDW: speaking fees and member of advisory board of AbbVie, BMS, MSD, Pfizer, Nordic Pharma, UCB, Novartis, Lilly, Janssen, Galapagos, Celltrion. BH: grants, personal fees and other from UCB, Kyowa Kirin, Eli Lilly, Amgen, Thornton & Ross and Gedeon-Richter and Fresenius Kabi outside the submitted work. KGH: consulting fees from AbbVie, lecture fees from MSD, Novartis, Pfizer. Co-founder of BerlinFlame. MK: received consulting fees and/or honoraria from AbbVie, Amgen, Asahi-Kasei Pharma, Ayumi Pharma, BMS, Chugai, Daiichi Sankyo, Eisai, Gilead, Janssen, Lilly, Novartis, Pfizer, Tanabe-Mitsubishi and UCB. WL: speaking fees and member of advisory boards of Amgen, UCB, Pfizer, Galapagos. EMW: speaking fees and member of advisory boards of Amgen and UCB.

Patient consent for publication

Not applicable.

Ethics approval

Not applicable.

Supplementary materials

Supplementary material associated with this article can be found in the online version at doi:10.1136/ard-2024-226446.

Orcid

Elizabeth Winter: http://orcid.org/0000-0002-0119-1588

REFERENCES

[1] Buch K, Thuesen ACB, Brøns C, et al. Chronic Non-bacterial Osteomyelitis: A Review. Calcif Tissue Int 2019;104:544–53.
[2] Leerling AT, Dekkers OM, Appelman-Dijkstra NM, et al. Clinical and therapeutic diversity in adult chronic nonbacterial osteomyelitis (CNO) of the sternocostoclavicular region: a meta-analysis. Rheumatol (Oxford) 2023;62:512–22.
[3] Koné-Paut I, Mannes I, Dusser P. Chronic Recurrent Multifocal Osteomyelitis (CRMO) and Juvenile Spondyloarthritis (JSpA): To What Extent Are They Related? J Clin Med 2023;12:453.
[4] Singhal S, Landes C, Shukla R, et al. Classification and management strategies for paediatric chronic nonbacterial osteomyelitis and chronic recurrent multifocal osteomyelitis. Expert Rev Clin Immunol 2023;19:1101–16.
[5] Kishimoto M, Taniguchi Y, Tsuji S, et al. SAPHO syndrome and pustulotic arthroosteitis. Mod Rheumatol 2022;32:665–74.
[6] Ramautar AI, Appelman-Dijkstra NM, Lakerveld S, et al. Chronic Nonbacterial Osteomyelitis of the Sternocostoclavicular Region in Adults: A Single-Center Dutch Cohort Study. JBMR Plus 2021;5:e10490.
[7] Jurik AG, Klicman RF, Simoni P, et al. SAPHO and CRMO: The Value of Imaging. Semin Musculoskelet Radiol 2018;22:207–24.
[8] Rukavina I. SAPHO syndrome: a review. J Child Orthop 2015;9:19–27.
[9] Sinnappurajar P, Roderick M, Ramanan AV. The neglected and untreated pains of CRMO and SAPHO syndrome. Rheumatol Sunnyvale 2022;61:3509–10.
[10] Leerling AT, Winter EM. Comment on: The neglected and untreated pains of CRMO and SAPHO syndrome. *Rheumatology (Oxford)* 2022;62:e12–3.
[11] Depasquale R, Kumar N, Lalam RK, et al. SAPHO: What radiologists should know. Clin Radiol 2012;67:195–206.
[12] Sonozaki H, Azuma A, Okai K, et al. Clinical features of 22 cases with ?Inter-Sterno- Costo-Clavicular Ossification? Arch Orthop Traumat Surg 1979;95:13–22.
[13] Leerling AT, Navas Cañete A, Winter EM. Chronic non-bacterial osteomyelitis in SAPHO syndrome complicated by subclavian vein obstruction. Rheumatol (Oxford) 2023;62:e355–6.
[14] Ohida H, Curuk C, Prescher H, et al. Thoracic outlet syndrome in a patient with SAPHO syndrome - A case report. Int J Surg Case Rep 2021;80:105710.
[15] Godot A, Fakih O, Prati C, et al. SAPHO syndrome and subclavian thrombosis: Simple fortuitous association? Eur J Intern Med 2020;72:103–5.
[16] Ramautar A, Appelman-Dijkstra N, Lakerveld S, et al. Clinical features of sternocostoclavicular hyperostosis: A large single Center Dutch cohort. J Bone Miner Res 2018;33.
[17] Brouwers MC, Spithoff K, Kerkvliet K, et al. Development and Validation of a Tool to Assess the Quality of Clinical Practice Guideline Recommendations. JAMA Netw Open 2020;3:e205535.
[18] Leerling AT, Clunie G, Koutrouba E, et al. Diagnostic and therapeutic practices in adult chronic nonbacterial osteomyelitis (CNO). Orphanet J Rare Dis 2023;18:206.
[19] Schünemann HJ, Vist GE, Glasziou P, et al. *Cochrane handbook for systematic reviews of interventions version 6.4*. Higgins JPT TJ, Chandler J, Cumpston M, et al, eds. Cochrane, 2023.
[20] Colina M, Trotta F. Clinical and radiological characteristics of SAPHO syndrome. Curr Rheumatol Rev 2013;9:22–7.
[21] Gao S, Deng X, Zhang L, et al. The comparison analysis of clinical and radiological features in SAPHO syndrome. Clin Rheumatol 2021;40:349–57.
[22] Sallés M, Olivé A, Perez-Andres R, et al. The SAPHO syndrome: a clinical and imaging study. Clin Rheumatol 2011;30:245–9.
[23] Himuro H, Kurata S, Nagata S, et al. Imaging features in patients with SAPHO/CRMO: a pictorial review. Jpn J Radiol 2020;38:622–9.
[24] Xu W, Li C, Zhao X, et al. Whole-spine Computed Tomography Findings in SAPHO Syndrome. J Rheumatol 2017;44:648–54.
[25] Yu M, Cao Y, Li J, et al. Anterior chest wall in SAPHO syndrome: magnetic resonance imaging findings. Arthritis Res Ther 2020;22:216.
[26] Ramautar AIE, Navas A, Winter EM, et al. Defining the imaging diagnostic criteria for adult chronic non-bacterial osteitis. JBMR Plus 2024;8:ziae024.
[27] Freyschmidt J, Sternberg A. The bullhead sign: scintigraphic pattern of sternocostoclavicular hyperostosis and pustulotic arthroosteitis. Eur Radiol 1998;8:807–12.
[28] Cao Y, Li C, Yang Q, et al. Three patterns of osteoarticular involvement in SAPHO syndrome: a cluster analysis based on whole body bone scintigraphy of 157 patients. *Rheumatology (Oxford)* 2019;58:1047–55.

[29] Okuno H, Watanuki M, Kuwahara Y, et al. Clinical features and radiological findings of 67 patients with SAPHO syndrome. Mod Rheumatol 2018;28:703–8.
[30] Akiyama Y, Sato T, Hanai S, et al. SAT0269 The Clinical Features of Sapho Syndrome in Japanese Patients: A Single Center Cohort Study. Ann Rheum Dis 2015;74:756.
[31] Asano T, Furuya MY, Fujita Y, et al. Diagnostic value of ultrasonography in synovitis- acne-pustulosis-hyperostosis-osteitis (SAPHO) syndrome: A case report. *Medicine (Baltimore)* 2018;97:e12725.
[32] Aljuhani F, Tournadre A, Tatar Z, et al. The SAPHO syndrome: a single-center study of 41 adult patients. J Rheumatol 2015;42:329–34.
[33] Ralston SH, Scott PD, Sturrock RD. An unusual case of pustulotic arthro-osteitis affecting the leg, and erosive polyarthritis. Ann Rheum Dis 1990;49:643–5.
[34] Aparicio Rovira M, Aparicio Espinar M, Gifre L, et al. AB0738 SAPHO OR PSORIATIC ARTHRITIS?: EVALUATION OF CASPAR CRITERIA IN A COHORT WITH SAPHO. Ann Rheum Dis 2020;79:1664–5.
[35] Yamamoto T, Hiraiwa T, Tobita R, et al. Characteristics of Japanese patients with pustulotic arthro-osteitis associated with palmoplantar pustulosis: a multicenter study. Int J Dermatology 2020;59:441–4.
[36] Maugars Y, Berthelot JM, Ducloux JM, et al. SAPHO syndrome: a followup study of 19 cases with special emphasis on enthesis involvement. J Rheumatol 1995;22:2135–41.
[37] Hayem G, Bouchaud-Chabot A, Benali K, et al. SAPHO syndrome: A long-term follow-up study of 120 cases. Semin Arthritis Rheum 1999;29:159–71.
[38] Colina M, La Corte R, Trotta F. Sustained remission of SAPHO syndrome with pamidronate: a follow-up of fourteen cases and a review of the literature. Clin Exp Rheumatol 2009;27:112–5.
[39] Valkema PA, Luymes CH, Witteveen JE, et al. High prevalence of autoimmune disease in the rare inflammatory bone disorder sternocostoclavicular hyperostosis: survey of a Dutch cohort. Orphanet J Rare Dis 2017;12:20.
[40] Carroll MB. Sternocostoclavicular hyperostosis: a review. Ther Adv Musculoskelet Dis 2011;3:101–10.
[41] Taylor W, Gladman D, Helliwell P, et al. Classification criteria for psoriatic arthritis: development of new criteria from a large international study. Arthritis Rheum 2006;54:2665–73.
[42] Zeidler H, Amor B. The Assessment in Spondyloarthritis International Society (ASAS) classification criteria for peripheral spondyloarthritis and for spondyloarthritis in general: the spondyloarthritis concept in progress. Ann Rheum Dis 2011;70:1–3.
[43] Solau-Gervais E, Soubrier M, Gerot I, et al. The usefulness of bone remodelling markers in predicting the efficacy of pamidronate treatment in SAPHO syndrome. *Rheumatology (Sunnyvale)* 2006;45:339–42.
[44] Andreasen CM, Jurik AG, Deleuran BW, et al. Pamidronate in chronic non-bacterial osteomyelitis: a randomized, double-blinded, placebo-controlled pilot trial. Scand J Rheumatol 2020;49:312–22.
[45] Armstrong DJ, Wright SA, Coward SM, et al. Bone marker response in chronic diffuse sclerosing osteomyelitis treated with intravenous ibandronate [8]. Ann Rheum Dis 2006;65:976–7.
[46] Cao Y, Li C, Xu W, et al. Spinal and sacroiliac involvement in SAPHO syndrome: A single center study of a cohort of 354 patients. Semin Arthritis Rheum 2019;48:990–6.
[47] Xu T, Ding H, Fan D, et al. Prospective Comparison of the Imaging Value of 99mTc-MDP Bone Scan and 68Ga-FAPI-04 PET/CT in Synovitis, Acne, Pustulosis, Hyperostosis, and Osteitis Syndrome. Clin Nucl Med 2023;48:768–74.
[48] Leerling AT, Smit F, Späth Z, et al. 18F-Sodium fluoride PET-CT visualizes disease activity in chronic nonbacterial osteitis in adults. JBMR Plus 2024;8:ziad007.
[49] Przepiera-Będzak H, Brzosko M. SAPHO syndrome: pathogenesis, clinical presentation, imaging, comorbidities and treatment: a review. Postepy Dermatol Alergol 2021;38:937–42.
[50] Weber U, Lambert RG, Rufibach K, et al. Anterior chest wall inflammation by whole-body magnetic resonance imaging in patients with spondyloarthritis: lack of association between clinical and imaging findings in a cross-sectional study. Arthritis Res Ther 2012;14:R3.
[51] Raptis CA, Ludwig DR, Hammer MM, et al. Building blocks for thoracic MRI: Challenges, sequences, and protocol design. J Magn Reson Imaging 2019;50:682–701.
[52] Khanna L, El-Khoury GY. SAPHO syndrome—a pictorial assay. Iowa Orthop J 2012;32:189–95.
[53] Leerling AT, Niesters M, Flendrie M, et al. Neuropathic and Nociplastic Pain Profiles are Common in Adult Chronic Nonbacterial Osteitis (CNO). Calcif Tissue Int 2024;114:603–13.
[54] Mendoza T, Mayne T, Rublee D, et al. Reliability and validity of a modified Brief Pain Inventory short form in patients with osteoarthritis. Eur J Pain 2006;10:353–61.
[55] Bruce B, Fries JF. The Stanford Health Assessment Questionnaire: a review of its history, issues, progress, and documentation. J Rheumatol 2003;30:167–78.
[56] Sun X, Li C, Cao Y, et al. F-18 FDG PET/CT in 26 patients with SAPHO syndrome: a new vision of clinical and bone scintigraphy correlation. J Orthop Surg Res 2018;13:120.
[57] Capponi M, Marafon DP, Rivosecchi F, et al. Chronic non-bacterial osteomyelitis (CNO): Correlation between clinical and radiological findings. Arthritis Rheumatol 2020;72:17–9.
[58] Li C, Wang L, Wu N, et al. A retrospective study of bone scintigraphy in the follow-up of patients with synovitis, acne, pustulosis, hyperostosis, and osteitis syndrome: is it useful to repeat bone scintigraphy for disease assessment? Clin Rheumatol 2020;39:1305–14.
[59] Takahara M, Hirata Y, Nagato T, et al. Treatment outcome and prognostic factors of tonsillectomy for palmoplantar pustulosis and pustulotic arthro-osteitis: A retrospective subjective and objective quantitative analysis of 138 patients. J Dermatol 2018;45:812–23.
[60] Wang Y, Xiang Y, Cao Y, et al. Tonsillectomy Leads to Remission of Bone Marrow Edema and Palmoplantar Pustulosis in Synovitis, Acne, Pustulosis, Hyperostosis, and Osteitis Syndrome. J Clin Rheumatol 2021;27:S719–20.
[61] Xiang Y, Wang Y, Cao Y, et al. Tonsillitis as a possible predisposition to synovitis, acne, pustulosis, hyperostosis and osteitis (SAPHO) syndrome. Int J of Rheum Dis 2021;24:519–25.
[62] Yamashita A, Sano T, Iwashita M, et al. A Case Report of Improved Palmoplantar Pustulosis following Periodontal Treatment and Possible Association with Diminished Systemic Subclinical Inflammation. Case Rep Dermatol Med 2021;2021:5548760.
[63] Akazawa H, Nishimura F, Maeda H, et al. Regression of pustulosis palmaris et plantaris by periodontal treatment in a subject with severe periodontitis. Int J Dermatol 2006;45:1420–2.
[64] Kouno M, Nishiyama A, Minabe M, et al. Retrospective analysis of the clinical response of palmoplantar pustulosis after dental infection control and dental metal removal. J Dermatol 2017;44:695–8.
[65] Jung J, Molinger M, Kohn D, et al. Intra-Articular Glucocorticosteroid Injection into Sternocostoclavicular Joints in Patients with SAPHO Syndrome. Semin Arthritis Rheum 2012;42:266–70.
[66] Oray M, Abu Samra K, Ebrahimiadib N, et al. Long-term side effects of glucocorticoids. Expert Opin Drug Saf 2016;15:457–65.
[67] Ramiro S, Nikiphorou E, Sepriano A, et al. ASAS-EULAR recommendations for the management of axial spondyloarthritis: 2022 update. Ann Rheum Dis 2023;82:19–34.
[68] Gossec L, Baraliakos X, Kerschbaumer A, et al. EULAR recommendations for the management of psoriatic arthritis with pharmacological therapies: 2019 update. Ann Rheum Dis 2020;79:700–12.
[69] Borzutzky A, Stern S, Reiff A, et al. Pediatric chronic nonbacterial osteomyelitis. Pediatrics 2012;130:e1190–7.
[70] Zhao Y, Wu EY, Oliver MS, et al. Consensus Treatment Plans for Chronic Nonbacterial Osteomyelitis Refractory to Nonsteroidal Antiinflammatory Drugs and/or With Active Spinal Lesions. Arthritis Care Res (Hoboken) 2018;70:1228–37.
[71] Monet M, Prati C, Guillot X, et al. Disease modifying anti rheumatic drugs in the treatment of sapho syndrome: systematic literature analysis. Ann Rheum Dis 2018:1155–6.
[72] Amital H, Applbaum YH, Aamar S, et al. SAPHO syndrome treated with pamidronate: an open-label study of 10 patients. *Rheumatology (Oxford)* 2004;43:658–61.
[73] Li C, Zhao Y, Zuo Y, et al. Efficacy of bisphosphonates in patients with synovitis, acne, pustulosis, hyperostosis, and osteitis syndrome: a prospective open study. Clin Exp Rheumatol 2019;37:663–9.
[74] Delattre E, Guillot X, Godfrin-Valnet M, et al. SAPHO syndrome treatment with intravenous pamidronate. Retrospective study of 22 patients. Joint Bone Spine 2014;81:456–8.
[75] Leerling AT, Cañete AN, Ramautar AIE, et al. Sternocostoclavicular Hyperostosis: Positive Clinical and Radiological Response on Pamidronate. Front Endocrinol (Lausanne) 2021;12:621604.
[76] Galadari H, Bishop AG, Venna SS, et al. Synovitis, acne, pustulosis, hyperostosis, and osteitis syndrome treated with a combination of isotretinoin and pamidronate. J Am Acad Dermatol 2009;61:123–5.
[77] Courtney PA, Hosking DJ, Fairbairn KJ, et al. Treatment of SAPHO with pamidronate. *Rheumatology (Oxford)* 2002;41:1196–8.
[78] Siau K, Laversuch CJ. SAPHO syndrome in an adult with ulcerative colitis responsive to intravenous pamidronate: a case report and review of the literature. Rheumatol Int 2010;30:1085–8.
[79] Wu N, Zhao Y, Tao W, et al. A single cohort, open-label study of the efficacy of pamidronate for palmoplantar pustulosis in synovitis, acne, pustulosis,

hyperostosis and osteitis (SAPHO) syndrome. Clin Exp Rheumatol 2020;38:1263–4.
[80] Hayem G, Ben M'Barek R, Toussirot E, et al. SAPHO syndrome treated by TNF alpha- blocking agents Report of 45 cases Arthritis Rheum 2010:2269.
[81] Ueno M, Miyagawa I, Miyazaki Y, et al. Efficacy and safety of guselkumab and adalimumab for pustulotic arthro-osteitis and their impact on peripheral blood immunophenotypes. Arthritis Res Ther 2022;24:240.
[82] Ben Abdelghani K, Dran DG, Gottenberg JE, et al. Tumor Necrosis Factor-α Blockers in SAPHO Syndrome: Table 1. J Rheumatol 2010;37:1699–704.
[83] Murgia G, Firinu D, Barca MP, et al. Biologics for SAPHO syndrome: A single centre experience. Allergy Eur J Allergy Clin Immunol 2015;70:418–9.
[84] Abourazzak FE, Hachimi H, Kadi N, et al. Etanercept in the treatment of SAPHO syndrome: Which place? Eur J Rheumatol 2014;1:125–8.
[85] Antoniou C, Nicolaidou E, Moustou AE, et al. Palmoplantar pustulosis with arthro- osteitis: successful treatment with etanercept and acitretin. Acad Dermatol Venereol 2009;23:854–5.
[86] Arias-Santiago S, Sanchez-Cano D, Callejas-Rubio J, et al. Adalimumab Treatment for SAPHO Syndrome. Acta Derm Venerol 2010;90:301–2.
[87] Baisya R, Gavali M, Tyagi M, et al. A Case of SAPHO Syndrome Complicated by Uveitis with Good Response to Both TNF Inhibitor and JAKinib. Case Rep Rheumatol 2023;2023:6201887.
[88] Burgemeister LT, Baeten DLP, Tas SW. Biologics for rare inflammatory diseases: TNF blockade in the SA PHO syndrome. Neth J Med 2012;70:444–9.
[89] Castellví I, Bonet M, Narváez JA, et al. Successful treatment of SAPHO syndrome with adalimumab: a case report. Clin Rheumatol 2010;29:1205–7.
[90] Crowley EL, O'Toole A, Gooderham MJ. Hidradenitis suppurativa with SAPHO syndrome maintained effectively with adalimumab, methotrexate, and intralesional corticosteroid injections. SAGE Open Med Case Rep 2018;6.
[91] De Souza A, Solomon GE, Strober BE. SAPHO syndrome associated with hidradenitis suppurativa successfully treated with infliximab and methotrexate. Bull NYU Hosp Jt Dis 2011;69:185–7.
[92] Hirohata A, Hanafusa T, Kawamoto T, et al. Infliximab for Treatment of Synovitis, Acne, Pustulosis, Hyperostosis, and Osteitis Syndrome: A Case Report. Ann Dermatol 2017;29:131.
[93] Iqbal M, Kolodney MS. Acne fulminans with synovitis-acne-pustulosis-hyperostosis- osteitis (SAPHO) syndrome treated with infliximab. J Am Acad Dermatol 2005;52:S118–20.
[94] Marí A, Morla A, Melero M, et al. Diffuse sclerosing osteomyelitis (DSO) of the mandible in SAPHO syndrome: A novel approach with anti-TNF therapy. Systematic review. J Cranio-Maxillofac Surg 2014;42:1990–6.
[95] Olivieri I, Padula A, Ciancio G, et al. Successful treatment of SAPHO syndrome with infliximab: report of two cases. Ann Rheum Dis 2002;61:375–6.
[96] Sabugo F, Liberman C, Niedmann JP, et al. Infliximab can induce a prolonged clinical remission and a decrease in thyroid hormonal requirements in a patient with SAPHO syndrome and hypothyroidism. Clin Rheumatol 2008;27:533–5.
[97] Saez-Martin LC, Gomez-Castro S, Roman-Curto C, et al. Etanercept in the treatment of SAPHO syndrome. Int J Dermatol 2015;54:e206–8.
[98] Su YS, Chang CH. SAPHO syndrome associated with acne conglobata successfully treated with etanercept. J Formos Med Assoc 2015;114:562–4.
[99] Vilar-Alejo J, Dehesa L, de la Rosa-del Rey P, et al. SAPHO Syndrome with Unusual Cutaneous Manifestations Treated Successfully with Etanercept. Acta Derm Venerol 2010;90:531–2.
[100] Wagner AD, Andresen J, Jendro MC, et al. Sustained response to tumor necrosis factor α–blocking agents in two patients with SAPHO syndrome. Arthritis & Rheumatism 2002;46:1965–8.
[101] Zhang L, Gao Z. Etanercept in the treatment of refractory SAPHO syndrome. Am J Clin Exp Immunol 2016;5:62–6.
[102] Hampton SL, Youssef H. Successful treatment of resistant SAPHO syndrome with anti-TNF therapy. BMJ Case Rep 2013;2013.
[103] Kanda R, Nakano K, Miyagawa I, et al. A case of bone destruction caused by chronic non-bacterial osteomyelitis (CNO) successfully repaired with a tumour necrosis factor-α (TNF-α) inhibitor, adalimumab. Mod Rheumatol Case Rep 2020;4:196–201.
[104] Huber CE, Judex AG, Freyschmidt J, et al. Sequential Combination Therapy Leading to Sustained Remission in a Patient with SAPHO Syndrome. Open Rheumatol J 2009;3:18–21.
[105] Misiak-Galazka M, Jeziorkowska R, Sikorska-Siudek K, et al. SAPHO syndrome: Case report. Postepy Dermatol Alergol 2012;29:136–8.
[106] Jinag C, Zhao Y, Li X, et al. Whole-body Bone Scan in the Diagnosis and Treatment of SAPHO Syndrome. J Coll Physicians Surg Pak 2022;32:S64–6.
[107] Yabe H, Kuroiwa T, Nonaka A, et al. Clinical features and treatment results of Japanese patients with sapho (synovitis-acne-pustulosis-hyperostosis-osteitis) syndrome. Arthritis Rheum 2012;64:S589–90.
[108] Li B, Li GW, Xue L, et al. Rapid remission of refractory synovitis, acne, pustulosis, hyperostosis, and osteitis syndrome in response to the Janus kinase inhibitor tofacitinib: A case report. World J Clin Cases 2020;8:4527–34.
[109] Li Y, Liu G, Zhao Y, et al. SAPHO syndrome with pathological fractures of vertebral bodies: a case report. BMC Musculoskelet Disord 2019;20:27.
[110] Xi Y, Lin Z, Chen N, et al. Clavicle fracture in SAPHO syndrome. Rheumatol (Oxford) 2024;63:e154–5.
[111] Yamamoto H, Taniguchi Y. Pustulotic Arthro-Osteitis–Related Pathological Clavicle Fracture. J Clin Rheumatol 2024;30:e123.
[112] Murdoch R, Mellar A, Horne AM, et al. Effect of a Three-Day Course of Dexamethasone on Acute Phase Response Following Treatment With Zoledronate: A Randomized Controlled Trial. J Bone Miner Res 2020;38:631–8.
[113] Kennel KA, Drake MT. Adverse effects of bisphosphonates: implications for osteoporosis management. Mayo Clin Proc 2009;84:632–7.
[114] Fragoulis GE, Nikiphorou E, Dey M, et al. 2022 EULAR recommendations for screening and prophylaxis of chronic and opportunistic infections in adults with autoimmune inflammatory rheumatic diseases. Ann Rheum Dis 2023;82:742–53.
[115] Brown G, Wang E, Leon A, et al. Tumor necrosis factor-α inhibitor-induced psoriasis: Systematic review of clinical features, histopathological findings, and management experience. J Am Acad Dermatol 2017;76:334–41.
[116] Kodra Y, Weinbach J, Posada-de-la-Paz M, et al. Recommendations for Improving the Quality of Rare Disease Registries. Int J Environ Res Public Health 2018;15:1644.
[117] Ramachandran S, Zhao Y, Ferguson PJ. Update on treatment responses and outcome measure development in chronic nonbacterial osteomyelitis. Curr Opin Rheumatol 2023;35:255–64.
[118] Russell MD, Dey M, Flint J, et al. British Society for Rheumatology guideline on prescribing drugs in pregnancy and breastfeeding: immunomodulatory anti- rheumatic drugs and corticosteroids. *Rheumatology (Oxford)* 2023;62:e48–88.

Ann Rheum Dis 84 (2025) 188–200

Contents lists available at ScienceDirect

Annals of the Rheumatic Diseases

journal homepage: https://www.sciencedirect.com/journal/annals-of-the-rheumatic-diseases

Rheumatoid arthritis

Ivarmacitinib, a selective Janus kinase 1 inhibitor, in patients with moderate-to-severe active rheumatoid arthritis and inadequate response to conventional synthetic DMARDs: results from a phase III randomised clinical trial

Jinjing Liu[1], Ying Jiang[1], Shangzhu Zhang[1], Shengyun Liu[2], Jingbo Su[2], Changsong Lin[3], Xiaohong He[4], Rui Wu[5], Lei Yang[6], Huaxiang Liu[7], Xinwang Duan[8], Shengqian Xu[9], Hui Luo[10], Jing Liu[11], Qibing Xie[12], Cundong Mi[13], Lin Chen[14], Ning Zhang[15], Huiping Gong[16], Jing Zhu[17], Yasong Li[18], Hua Wei[19], Long Qian[20], Jian Wang[21], Xiaofei Shi[22], Hongtao Jin[23], Zhenyu Jiang[24], Xi Xie[25], Feng Zhan[26], Xiuqin Geng[27], Zhaohui Zheng[28], Zhengfu Du[29], Guangchao Dong[30], Yuqi Sun[31], Xiaofeng Zeng[1,*]

[1] *Department of Rheumatology and Clinical Immunology, Peking Union Medical College Hospital, Beijing, China*
[2] *Department of Rheumatology & Immunology, The First Affiliated Hospital of Zhengzhou University, Zhengzhou, China*
[3] *Department of Rheumatology, The First Affiliated Hospital of Guangzhou University of Chinese Medicine, Guangzhou, China*
[4] *Department of Rheumatology, The Second Affiliated Hospital of Guangzhou University of Chinese Medicine (Guangdong Provincial Hospital of Chinese Medicine), Guangzhou, China*
[5] *Department of Rheumatology and Immunology, The First Affiliated Hospital, Jiangxi Medical College, Nanchang University, Nanchang, China*
[6] *Department of Rheumatology and Immunology, Zhengzhou Central Hospital, Zhengzhou, China*
[7] *Rheumatology Department, Qilu Hospital of Shandong University, Jinan, China*
[8] *Rheumatology and Immunology, The Second Affiliated Hospital of Nanchang University, Nanchang, China*
[9] *Rheumatology and Immunology Department, The First Affiliated Hospital of Anhui Medical University, Hefei, China*
[10] *Department of Rheumatology and Immunology, Xiangya Hospital, Central South University, Changsha, China*
[11] *Department of Rheumatology and Immunology Research Institute, Affiliated Hospital of North Sichuan Medical College, Nanchong, China*
[12] *Department of Rheumatology and Immunology, West China Hospital of Sichuan University, Chengdu, China*
[13] *Department of Rheumatology and Clinical Immunology, The Second Affiliated Hospital of Guangxi Medical University, Nanning, China*
[14] *Department of Rheumatic Immunity, Jilin Province People's Hospital, Changchun, China*
[15] *Rheumatology, Shengjing Hospital Affiliated to China Medical University, Shenyang, China*
[16] *Department of Rheumatology and Clinical Immunology, Peace Hospital Affiliated to Changzhi Medical College, Changzhi, China*
[17] *Department of Rheumatology and Immunology, Sichuan Provincial People's Hospital, Chengdu, China*
[18] *Department of Rheumatology and Clinical Immunology, Zhejiang Provincial People's Hospital, Hangzhou, China*
[19] *Rheumatology and Immunology Department, Northern Jiangsu People's Hospital, Yangzhou, China*

*Correspondence to Dr. Xiaofeng Zeng
E-mail addresses: zengxfpumc@163.com, xiaofeng.zeng@cstar.org.cn (X. Zeng).
Handling editor Josef S. Smolen

https://doi.org/10.1136/ard-2024-226385

[20] Department of Rheumatology and Clinical Immunology, The Second Hospital of Anhui Medical University, Anhui, China
[21] Department of Rheumatology and Clinical Immunology, The First Affiliated Hospital of Bengbu Medical College, Anhui, China
[22] Department of Rheumatology and Clinical Immunology, The First Affiliated Hospital of Henan University of Science & Technology, Luoyang, China
[23] Department of Rheumatology and Immunology, The Second Hospital of Hebei Medical University, Shijiazhuang, China
[24] Department of Rheumatic Immunity, The First Hospital of Jilin University, Changchun, China
[25] Department of Clinical Immunology, The Second Xiangya Hospital of Central South University, Changsha, China
[26] Department of Rheumatology and Immunology, Hainan General Hospital, Haikou, China
[27] Department of Rheumatology and Immunology, Xinxiang Central Hospital, Xinxiang, China
[28] Department of Clinical Immunology, Xijing Hospital, the Fourth Military Medical University, Xi'an, China
[29] Department of Rheumatology and Immunology, Yuncheng Central Hospital, Yuncheng, China
[30] Clinical Research & Development, Jiangsu Hengrui Pharmaceuticals, Shanghai, China
[31] Biometric Department, Jiangsu Hengrui Pharmaceuticals, Shanghai, China

ARTICLE INFO

Article history:
Received 8 July 2024
Accepted 4 November 2024

Keywords:
Arthritis
Rheumatoid
Antirheumatic Agents
Health-Related Quality Of Life
Autoimmune Diseases

ABSTRACT

Objective: To assess the efficacy/safety of ivarmacitinib, a selective Janus kinase (JAK) 1 inhibitor, in patients with moderate-to-severe active rheumatoid arthritis (RA) who had an inadequate response to conventional synthetic disease-modifying antirheumatic drugs (csDMARDs).

Methods: Patients were randomised (1:1:1) to receive either placebo (n = 188), ivarmacitinib 4 mg (n = 189) or ivarmacitinib 8 mg (n = 189) once daily, with background csDMARDs allowed. After 24 weeks, patients on placebo switched to ivarmacitinib 4 mg for an additional 28 weeks, while those on ivarmacitinib continued their initial dosage. The primary endpoint was the proportion of patients achieving a 20% improvement in the American College of Rheumatology response criteria (ACR20) at week 24.

Results: At week 24, ACR20 response rates were significantly higher in the ivarmacitinib 4 mg (70.4%) and 8 mg (75.1%) groups compared with the placebo group (40.4%; both $p<0.0001$). Both ivarmacitinib doses achieved numerically higher Disease Activity Score 28-joint count C reactive protein of $<2.6/\leq3.2$ response rates compared with placebo. Improvements in efficacy and patient-reported outcomes were sustained through 52 weeks and were noted in patients who switched from placebo after week 24. During the placebo-controlled period, treatment-emergent adverse events (TEAEs) occurred in 81.5% and 90.5% of patients in the ivarmacitinib 4 mg and 8 mg groups, versus 79.3% in the placebo group. Infection-related TEAEs were slightly higher in the ivarmacitinib groups.

Conclusions: Ivarmacitinib may offer a potential therapeutic option for patients with RA who have an inadequate response to csDMARDs, with a safety profile that was generally manageable over 1 year of treatment and similar to other JAK inhibitors.

Trial registration number: NCT04333771.

INTRODUCTION

Rheumatoid arthritis (RA) is a systemic autoimmune disease characterised by chronic inflammatory arthritis and, in some cases, involvement of extra-articular tissues [1]. The primary goals of RA treatment are to eliminate systemic inflammation, relieve pain, prevent joint damage and optimise quality of life and functional ability [2]. Prompt and effective treatment is crucial to preventing irreversible joint damage and long-term disability [3].

RA treatment is tailored based on disease severity, patient comorbidities and treatment response. Initial therapy typically involves a conventional synthetic disease-modifying antirheumatic drug (csDMARD), such as methotrexate, often supplemented by glucocorticoids. If the initial therapy proves inadequate, the addition of a targeted therapy, such as a biologic DMARD or a targeted synthetic DMARD like Janus kinase (JAK) inhibitors, is recommended [4,5].

Several JAK inhibitors have been approved for the treatment of RA by the US Food and Drug Administration (tofacitinib,[6] baricitinib [7], upadacitinib[8]), the European Medicines Agency (tofacitinib [6], baricitinib [7], upadacitinib [8], filgotinib [9]) and regulatory authorities in Japan (filgotinib [9], peficitinib [10]). Tofacitinib is a pan-JAK inhibitor with greater selectivity for JAK1/JAK3 and minor activity on JAK2 and tyrosine kinase 2 (TYK2) [11]. Peficitinib, another pan-JAK inhibitor, inhibits all JAK family members with similar potency [10]. Baricitinib primarily targets JAK1 and JAK2, with moderate activity against TYK2 and minimal activity against JAK3 [12]. Upadacitinib (an oral, reversible JAK inhibitor with selectivity for JAK1 over JAK2, JAK3 and TYK2) and filgotinib (a preferential JAK1 inhibitor) are noted for their greater affinity for JAK1 over other JAK isoforms [9,13].

Ivarmacitinib (formerly SHR0302), an orally administered, highly selective JAK1 inhibitor, exhibits potency and selectivity for JAK1 that is over 10-fold for JAK2, 77-fold for JAK3 and 420-fold for TYK2 (with IC50 values of 0.1, 0.9, 7.7 and 42 nM, respectively) [14,15]. A phase II clinical trial (NCT03254966) in Chinese patients with moderate-to-severe active RA, either treatment-naive or with an inadequate response to csDMARDs, demonstrated that ivarmacitinib had a rapid onset of action, leading to statistically significant improvements in American College of Rheumatology (ACR)20 response rates at 12 weeks (67.5% for 4 mg and 77.8% for 8 mg), with a safety profile similar to other JAK inhibitors [16]. This phase III study aimed to further evaluate the efficacy and safety of ivarmacitinib in

WHAT IS ALREADY KNOWN ON THIS TOPIC

- Pivotal phase III studies and long-term followup of Janus kinase (JAK) inhibitors (baricitinib, tofacitinib, upadacitinib and filgotinib) have demonstrated clinically meaningful benefits in reducing rheumatoid arthritis (RA) symptoms, with background conventional synthetic disease-modifying antirheumatic drugs (csDMARDs) allowed.
- Upadacitinib and filgotinib are noted for their greater affinity for JAK1 over other JAK isoform.
- A phase II clinical trial (NCT03254966) indicated that ivarmacitinib, a novel oral selective JAK1 inhibitor, demonstrated superiority over placebo in patients with active RA, whether treatment-naive or with an inadequate response to csDMARDs.

WHAT THIS STUDY ADDS

- This was the first phase III study to evaluate ivarmacitinib compared with placebo in patients with moderate-to-severe active RA and inadequate response to one or more csDMARDs.
- Ivarmacitinib treatment reduced RA signs and symptoms, decreased disease activity and improved physical function and quality of life; these benefits were sustained up to 52 weeks, with a safety profile similar to other JAK inhibitors.

HOW THIS STUDY MIGHT AFFECT RESEARCH, PRACTICE OR POLICY

- Based on these findings, ivarmacitinib with background csDMARDs allowed, could be considered a treatment option in patients with moderate-to-severe active RA who have an inadequate response to csDMARDs.

patients with active moderate-to-severe RA who had an inadequate response to one or more csDMARDs.

METHODS

Study design

This multicentre phase III study of ivarmacitinib, conducted at 59 sites in China, included a 24-week randomised, double-blind, placebo-controlled treatment period, followed by a 28-week blinded extension and a 4-week safety follow-up period (online supplemental figure S1). All patients provided written informed consent.

Patient inclusion and exclusion criteria

Eligible patients were aged 18–75 years and met the 2010 ACR/ European League Against Rheumatism (EULAR) classification criteria for RA diagnosis [17]. Patients had active moderate-to-severe RA, defined as ≥6 swollen and ≥6 tender joints at both screening and baseline, despite prior treatment with ≥1 csDMARD (methotrexate, leflunomide or sulfasalazine) for ≥3 months, accompanied by an erythrocyte sedimentation rate (ESR) >28 mm/hour or C reactive protein (CRP)/high-sensitivity CRP (hsCRP) >5 mg/L at screening. Patients on stable csDMARD therapy (eg, methotrexate 7.5–25.0 mg per week, sulfasalazine, leflunomide, hydroxychloroquine, penicillamine and iguratimod, either alone or in combination, except methotrexate and leflunomide) for ≥3 months and stable doses for ≥4 weeks, as well as stable doses of non-steroidal antiinflammatory drugs (NSAIDs), paracetamol or oral steroids (up to 10 mg/day prednisone equivalent), were permitted prior to randomisation. The use of up to two concomitant csDMARDs was allowed but not required. Patients not receiving csDMARDs at the time of entry were required to have a history of failure with, or inability to tolerate, at least one csDMARD. However, oral steroids exceeding 10 mg/day and strong cytochrome P450 3A inhibitors or inducers were not permitted. Key exclusion criteria included prior exposure to a JAK inhibitor, a history of inflammatory joint diseases other than RA, use of biologic DMARDs within 6 months prior to randomisation, key laboratory abnormalities (eg, white cell count $<3.0 \times 10^9$/L; absolute neutrophil count $<1.5 \times 10^9$/L; haemoglobin <90.0 g/L; platelet count $<100 \times 10^9$/L; levels of alanine aminotransferase (ALT), aspartate aminotransferase (AST) or total bilirubin above the upper limit of normal; and an estimated glomerular filtration rate <60 mL/min/1.73 m^2, calculated using the Modification of Diet in Renal Disease equation). The full eligibility criteria are listed in the online supplemental protocol.

Randomisation and blinding

Patients were randomised 1:1:1 to receive oral ivarmacitinib 4 mg or 8 mg once daily, or placebo, using a centralised interactive web response system. Randomisation was stratified by baseline csDMARD use (either methotrexate at ≥15 mg/week or leflunomide at 20 mg/day, methotrexate at <15 mg/week or leflunomide at <20 mg/day or no usage of either). After completing the initial 24-week treatment, patients in the placebo group switched to ivarmacitinib 4 mg for the additional 28-week extension period, while those who received ivarmacitinib during the 24-week period continued the same dose in a blinded extension up to week 52. All investigators, patients and the funder of the study were masked to group allocation. The active drug or matching placebo was identical in packaging.

Rescue medicine

If a patient's RA symptoms showed less than 20% improvement in both tender and swollen joint counts from baseline after 12 weeks, the investigator could adjust the patient's concomitant RA treatments. The initial rescue interventions included adjustments to NSAIDs, acetaminophen or weak opioids. If the response remained inadequate, further modifications, such as the addition or adjustment of oral glucocorticoids and/or csDMARDs, were permitted. These treatment adjustments were only allowed after the initial 12-week study period, following an efficacy assessment at that time point. Details on the principles governing the management of inadequate disease improvement are provided in online supplemental table S1. Additionally, patients were allowed to withdraw from the study at any point if they experienced poor disease control or deemed the treatment ineffective.

Treatment failure was defined as meeting any of the following criteria: (1) initiation or dose increase of csDMARDs for RA; (2) initiation of systemic immunosuppressants or biologic DMARDs for RA or (3) initiation or dose increase of oral glucocorticoids for RA, or the use of intravenous or intramuscular glucocorticoids.

Endpoints

The primary endpoint was the proportion of patients achieving the ACR20 response at week 24. Secondary endpoints included the proportion of patients achieving ACR20 at week 52; proportions of patients achieving ACR50/70, Disease Activity Score 28-joint count C reactive protein (DAS28(CRP)) of

<2.6 or ≤3.2, and changes from baseline in the Health Assessment Questionnaire-Disability Index (HAQ-DI) and Short Form 36 Physical and Mental Component Summaries (SF-36 PCS and MCS), all measured at weeks 24 and 52.

Additional efficacy endpoints included the proportions of patients achieving HAQ-DI improvement ≥0.22 [18], changes from baseline in DAS28(CRP), DAS28(ESR), Clinical Disease Activity Index (CDAI), Simplified Disease Activity Index (SDAI), and morning stiffness duration and severity at weeks 24 and 52. Post hoc analyses were conducted to assess the proportions of patients achieving low disease activity (CDAI≤10 or SDAI≤11) [19], remission (CDAI≤2.8 or SDAI≤3.3) [20], >50% or 70% improvement in CDAI or SDAI [21], HAQ-DI improvement ≥0.3 and normal function (HAQ-DI <0.5) [18] by visits.

Safety monitoring included assessments of treatment-emergent adverse events (TEAEs), treatment-emergent serious adverse events (TESAEs), laboratory tests, vital signs and 12-lead electrocardiograms, beginning at the time of informed consent and continuing until 28 days after the last administration of the study treatment. Prespecified TEAEs of special interest included serious infection, any systemic opportunistic infection, newly diagnosed malignancy, thromboembolic event, major adverse cardiac events (MACE) and liver function abnormality (the criteria are detailed in online supplemental table S2).

Statistical analyses

The sample size was calculated based on the assumption that 62% of patients would achieve an ACR20 response with ivarmacitinib compared with 40% with placebo after 24 weeks. To ensure a 98% power at a 5% significance level (two-sided) for detecting a difference between any ivarmacitinib dose and placebo, 168 patients per group were needed, based on normal approximation. Accounting for an 8% dropout rate, 550 patients were randomised, with 183 in each treatment arm.

For the primary endpoint, a hierarchical testing procedure was used to control the two-sided type I error at 0.05. The superiority of ivarmacitinib over placebo was assessed using a fixed-sequence testing method, starting with the higher dose. If the superiority of ivarmacitinib 8 mg was established, testing would proceed to assess the superiority of the 4 mg dose over placebo. Secondary and additional endpoints were not controlled for multiplicity.

The primary endpoint, along with secondary and other binary efficacy endpoints at week 24, was analysed using CochranMantel-Haenszel tests, stratified by baseline csDMARD use. Patients who discontinued or failed treatment before the efficacy assessment at week 24, or had missing values at week 24, were classified as non-responders, with non-responder imputation (NRI) applied in the analysis of these binary endpoints at week 24.

Changes from baseline in DAS28(CRP), DAS28(ESR), CDAI, SDAI, HAQ-DI and morning stiffness duration and severity at week 24 were assessed using a mixed-effects model for repeated measures based on the restricted maximum likelihood method. Baseline values served as covariates, while treatment group, visit, randomisation strata and the interaction between treatment and visit were treated as fixed effects. Patients were considered random effects, and an unstructured covariance matrix was employed.

Change from baselines in SF-36 PCS and MCS scores was analysed using analysis of covariance models, with the change from baseline value as the dependent variable, treatment group and randomisation strata as independent variables, baseline value as a covariate, and missing data imputed via the last observation carried forward method. The least squares (LS) mean changes from baseline were calculated for each group, and the LS mean difference between the treatment and placebo groups were provided, including corresponding 95% CIs and p values for pairwise comparisons.

Results for prespecified binary efficacy endpoints at scheduled visits (except week 24) were presented as the number of analysed patients divided by the number of patients who received ≥1 dose of study treatment during, using the NRI method for patients with missing data or who experienced treatment failure. For continuous endpoints at week 52, results were presented based on observed cases. In post hoc analyses, patients with missing values or who experienced treatment failure were identified as non-responders, and NRI was applied for binary efficacy endpoints.

All randomised patients who received at least one dose of the assigned study treatment were included in the full analysis set. Patients who received at least one dose of the study treatment were included in the safety analysis set. Statistical analyses were performed using SAS V.9.4 software.

RESULTS

Patient disposition and baseline characteristics

Between 14 July 2020 and 11 August 2022, 1085 patients were screened, 566 were eligible and randomised into ivarmacitinib 4 mg (n=189), 8 mg (n=189) and placebo groups (n=188). All 566 randomised patients received at least one dose of the assigned treatment. At baseline, demographic and disease characteristics were balanced across the three treatment groups (table 1).

A total of 524 (92.6%) patients completed the initial 24-week treatment period, and 496 (87.6%) completed the 52-week treatment period (figure 1). During the initial 24 weeks, more patients discontinued the study treatment due to TEAEs in the ivarmacitinib 8 mg group (3.2%) compared with the ivarmacitinib 4 mg and placebo groups (1.6% each). Discontinuation due to lack of efficacy, as determined by the patient's own perspective (with <20% improvement in both tender and swollen joint counts from baseline at their final efficacy assessment), was higher in the placebo group (3.7%) than in the ivarmacitinib 4 mg or 8 mg groups (0.5% each). Furthermore, 14 (7.4%) patients in the ivarmacitinib 4 mg group, 10 (5.3%) in the ivarmacitinib 8 mg group and 42 (22.3%) in the placebo group adjusted their concomitant medications between weeks 12 and 24 (online supplemental table S3).

Efficacy

The primary endpoint, ACR20 responses at week 24, was 70.4% in the ivarmacitinib 4 mg group and 75.1% in the ivarmacitinib 8 mg group compared with 40.4% in the placebo group (p<0.0001 for both comparisons). ACR50/70 responses at week 24 were higher following ivarmacitinib 4 mg (46.0%/22.2%), ivarmacitinib 8 mg (57.1%/31.7%) compared with placebo (15.4%/6.9%) (table 2 and figure 2). The ACR20/50/70 responses in the ivarmacitinib treatment groups diverged from those in the placebo group as early as week 2/4/8 and persisted throughout the 24-week treatment period (figure 2 and online supplemental table S4).

At week 24, the proportions of patients achieving DAS28 (CRP) ≤3.2 and DAS28(CRP) <2.6 were higher in both the

Table 1
Demographics and baseline disease characteristics

Characteristics	Placebo (n = 188)	Ivarmacitinib 4 mg (n = 189)	Ivarmacitinib 8 mg (n = 189)
Age, years	50.9±9.9	49.7±10.4	49.8±11.0
Female	161 (85.6)	172 (91.0)	158 (83.6)
Time since RA diagnosis, years	9.9±7.3	10.1±8.0	9.2±7.4
≥3 years	154 (81.9)	153 (81.0)	149 (78.8)
<3 years	34 (18.1)	35 (18.5)	40 (21.2)
ACR functional class			
I	21 (11.2)	27 (14.3)	23 (12.2)
II	118 (62.8)	105 (55.6)	116 (61.4)
III	49 (26.1)	57 (30.2)	50 (26.5)
csDMARDs use at baseline	184 (97.9)	180 (95.2)	184 (97.4)
Methotrexate	107 (56.9)	104 (55.0)	100 (52.9)
Leflunomide	72 (38.3)	74 (39.2)	79 (41.8)
Hydroxychloroquine	39 (20.7)	24 (12.7)	25 (13.2)
Iguratimod	14 (7.4)	16 (8.5)	16 (8.5)
Sulfasalazine	6 (3.2)	7 (3.7)	5 (2.6)
Chloroquine	0	1 (0.5)	0
NSAIDs	84 (44.7)	70 (37.0)	86 (45.5)
Oral glucocorticoid use	69 (36.7)	76 (40.2)	58 (30.7)
Dose, mg (prednisone equivalent)	5.9±2.6	6.1±2.7	6.2±2.7
Previous biologic DMARDs received*	50 (26.6)	52 (27.5)	43 (22.8)
TNF-α inhibitor	37 (19.7)	35 (18.5)	33 (17.5)
IL-6 inhibitor	17 (9.0)	21 (11.1)	7 (3.7)
CRP, mg/L†	15.5±17.7	18.7±20.0	19.4±18.9
ESR, mm/hour	44.5±24.1	48.2±27.7	47.5±23.6
RF-positive	158 (84.0)	155 (82.0)	155 (82.0)
Anti-CCP-positive	169 (89.9)	166 (87.8)	170 (89.9)
SJC‡	12.1±6.4	12.9±7.8	11.9±6.0
TJC‡	20.9±11.6	21.1±14.1	20.7±13.1
PtGA, 0–100 mm VAS	61.3±19.0	60.3±21.0	61.3±18.9
PGA, 0–100 mm VAS	61.6±14.3	60.9±15.7	61.6±15.3
Pain, 0–100 mm VAS	59.6±18.7	57.5±21.0	58.1±19.5
DAS28(CRP)	5.2±0.8	5.2±0.9	5.3±0.9
DAS28(ESR)	6.3±0.9	6.2±1.0	6.3±0.9
CDAI	35.4±10.5	35.0±12.2	35.1±11.7
SDAI score	37.0±10.8	36.8±12.8	37.1±12.4
HAQ-DI	1.2±0.7	1.2±0.6	1.1±0.6
SF-36 PCS	35.5±6.7	35.8±7.4	35.6±7.0
SF-36 MCS	42.1±10.8	40.8±10.8	41.8±10.9
Morning stiffness duration, min	52.7±63.7	64.1±81.9	61.6±82.2
Morning stiffness severity, 0–100 mm VAS	45.7±24.1	45.4±25.7	46.5±25.5

Data are n (%) or mean (SD) unless noted otherwise.
* Majority of these patients were treated with either a TNF-α inhibitor or an IL-6 inhibitor.
† The upper limit of normal, as detected by the central laboratory at baseline and during subsequent efficacy assessments, was 5 mg/L.
‡ Joints were assessed based on a 66–68 joint count examination.ACR, American College of Rheumatology; anti-CCP, anticyclic citrullinated protein antibody; CDAI, Clinical Disease Activity Index; CRP, C reactive protein; csDMARD, conventional synthetic DMARD; DAS28(CRP), Disease Activity Score 28 based on C reactive protein; DAS28(ESR), Disease Activity Score 28 based on erythrocyte sedimentation rate; DMARD, disease-modifying antirheumatic drug; ESR, erythrocyte sedimentation rate; HAQ-DI, Health Assessment Questionnaire Disability Index; IL-6, interleukin-6; SF-36 MCS, Short Form-36 mental component summary; NSAID, non-steroidal anti-inflammatory drug; SF-36 PCS, Short Form-36 physical component summary; PGA, Physician Global Assessment of Disease Activity; PtGA, Patient Global Assessment of Disease Activity; RA, rheumatoid arthritis; RF, rheumatoid factor; SDAI, Simplified Disease Activity Index; SJC, swollen joint count; TJS, tender joint count; TNF-α, tumour necrosis factor alpha; VAS, visual analogue scale.

ivarmacitinib 4 mg (46.0% and 29.6%) and 8 mg groups (57.1% and 39.2%) compared with placebo (15.4% and 4.8%) (table 2 and figure 3). Changes from baseline in DAS28(CRP) and DAS28(ESR) were presented in table 2, figure 3 and online supplemental figure S2.

At week 24, the proportions of patients achieving low disease activity (CDAI ≤10 or SDAI ≤11) and remission (CDAI ≤2.8 or SDAI ≤3.3), as well as those achieving >50% or 70% improvement in CDAI or SDAI, were higher with ivarmacitinib 4 mg and 8 mg compared with placebo. Additionally, the changes from baseline in CDAI and SDAI scores were numerically greater with both ivarmacitinib doses than with placebo (table 2, figure 3, online supplemental figures S3, S4).

At week 24, numerically greater improvements from baseline in HAQ-DI were observed in both ivarmacitinib groups compared with the placebo group, with a higher proportion of patients achieving HAQ-DI minimal clinically important difference (MCID; improvement ≥0.22 or ≥0.3) and normal function (HAQ-DI <0.5) (table 2, figure 3, online supplemental figure S5).

In parallel with the main efficacy endpoints, there were marked improvements in each other ACR and DAS28(CRP) core component, as well as in several patient-reported outcomes such as SF-36 PCS and MCS, and the duration and severity of morning stiffness (table 2, online supplemental table S5 and online supplemental figures S7–S10).

The efficacy of ivarmacitinib was sustained or further increased through week 52, and patients on placebo who switched to ivarmacitinib 4 mg after week 24 also demonstrated numerical improvements at week 52 compared with their

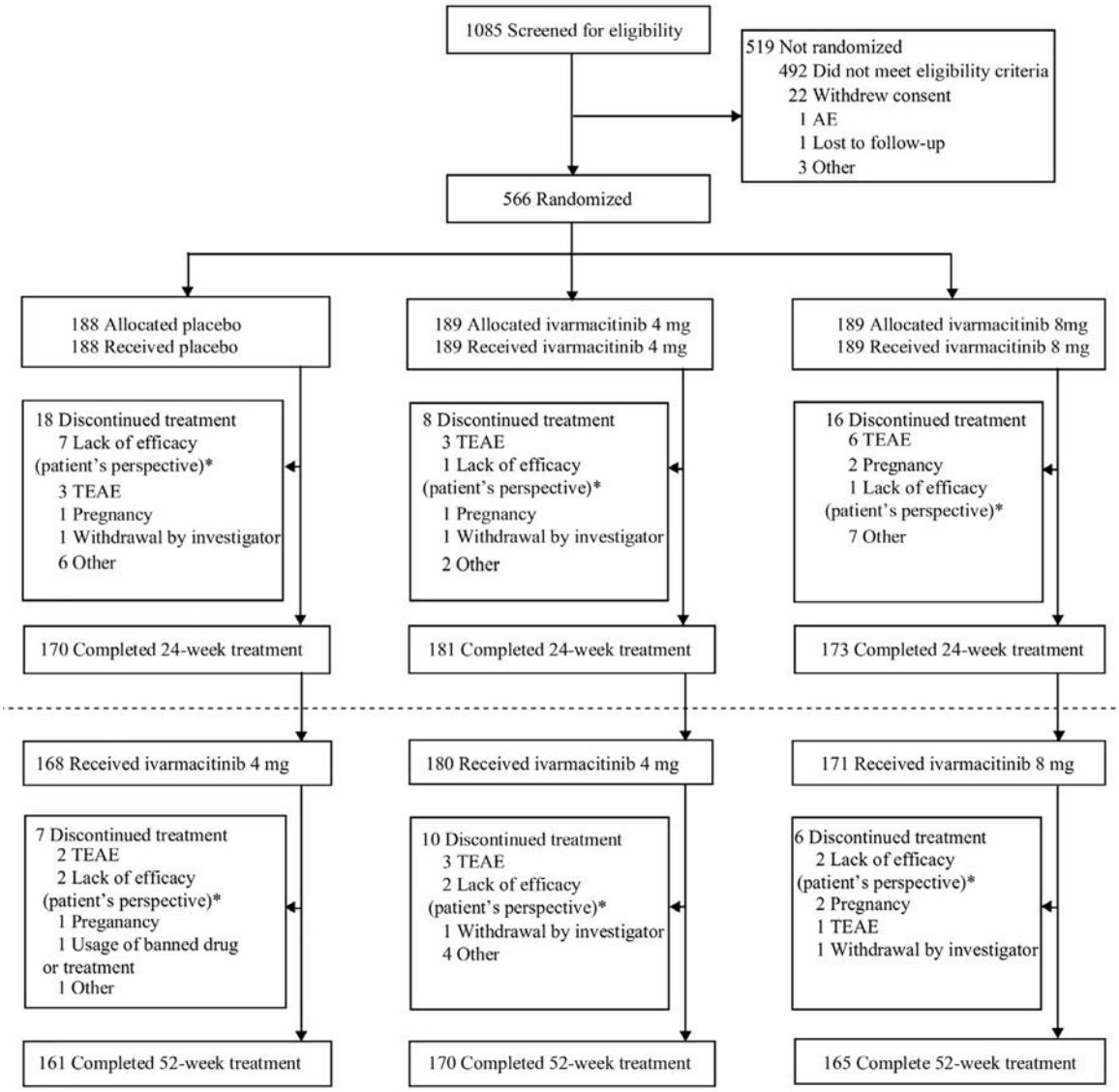

Figure 1. Patient disposition. Patients discontinued study treatment due to lack of efficacy based on their own perspective, with <20% improvement in both tender and swollen joint counts from baseline at their final efficacy assessment. AE, adverse event; TEAE, treatment-emergent adverse event.

baseline (figures 2–3, online supplemental tables S6, S7 and online supplemental figures S2–S9).

Safety

During the placebo-controlled period, a total of 474 patients (83.7%) reported TEAEs: 154 (81.5%) in the ivarmacitinib 4 mg group, 171 (90.5%) in the ivarmacitinib 8 mg group and 149 (79.3%) in the placebo group (table 3). The incidence of TEAEs appeared to be higher in the ivarmacitinib 8 mg group compared with the ivarmacitinib 4 mg group, suggesting a possible dose-response relationship. The most common TEAEs in the ivarmacitinib groups were upper respiratory tract infection (21.7% for 4 mg and 22.8% for 8 mg) and hyperlipidemia (15.3% for 4 mg and 12.2% for 8 mg). In the placebo group, the most reported TEAEs were upper respiratory tract infection (13.8%) and anaemia (11.7%). Eight patients (4.2%) in the ivarmacitinib 4 mg group, 12 (6.3%) in the ivarmacitinib 8 mg group, and 5 (2.7%) in the placebo group had ≥1 TESAE; of these, two patients in the ivarmacitinib 4 mg group (one with pneumonia and one with kidney infection), four in the ivarmacitinib 8 mg group (two with pneumonia, one with urinary tract infection, one with herpes zoster, and one with liver abscess) and one in the placebo group (urinary tract infection) had infection-related events (table 3 and online supplemental table S8).

During the extension period, TEAEs and TESAEs occurred at similar frequencies in both ivarmacitinib groups. Patients who switched from placebo to ivarmacitinib 4 mg reported more TESAEs more than those on ivarmacitinib from the baseline (table 3, online supplemental table S9). The type, frequency and severity of TEAEs in patients on ivarmacitinib, whether continued or switched during the extension, remained consistent with those observed in the placebo-controlled period.

During the placebo-controlled period, 2 patients (1.1%) in the ivarmacitinib 4 mg group (one with elevated liver enzymes and another with cervical squamous cell carcinoma), 3 (1.6%) in the ivarmacitinib 8 mg group (one with abnormal liver function and liver abscess, one with coronary arteriosclerosis and another with deep vein thrombosis), and none in the placebo group reported the prespecified TEAEs of special interest. Additionally, 12 patients reported herpes zoster: 3 (1.6%) in the ivarmacitinib 4 mg group, 5 (2.6%) in the ivarmacitinib 8 mg group and 4 (2.1%) in the placebo group. During the extension period, 4 patients (2.2%) in the ivarmacitinib 4 mg group (two with

Table 2
Efficacy endpoints at week 24 in the full analysis set

Endpoints	Placebo (n = 188)	Ivarmacitinib 4 mg (n = 189)	Ivarmacitinib 8 mg (n = 189)
Primary endpoint			
ACR20 response	76 (40.4)	133 (70.4)	142 (75.1)
Difference vs placebo, % (95% CI)	–	30.1 (20.6 to 39.7)*	34.8 (25.4 to 44.1)*
Secondary efficacy endpoints			
ACR50 response	29 (15.4)	87 (46.0)	108 (57.1)
Difference vs placebo, % (95% CI)	–	30.8 (22.0 to 39.5)†	41.7 (33.0 to 50.5)†
ACR70 response	13 (6.9)	42 (22.2)	60 (31.7)
Difference vs placebo, % (95% CI)	–	15.5 (8.5 to 22.4)†	24.9 (17.3 to 32.4)†
DAS28(CRP) <2.6	9 (4.8)	56 (29.6)	74 (39.2)
Difference vs placebo, % (95% CI)	–	24.9 (17.7 to 32.1)†	34.3 (26.7 to 41.9)†
DAS28(CRP) ≤3.2	29 (15.4)	87 (46.0)	108 (57.1)
Difference vs placebo, % (95% CI)	–	30.8 (22.0 to 39.5)†	41.7 (33.0 to 50.4)†
HAQ-DI LS mean (95% CI), mean difference from baseline	−0.21 (−0.29 to −0.13)	−0.45 (−0.53 to −0.37)	−0.51 (−0.58 to −0.43)
Change vs placebo, LS mean (95% CI), mean difference from baseline	–	−0.24 (−0.34 to −0.14)†	−0.30 (−0.40 to −0.20)†
SF-36 PCS LS mean (95% CI), mean difference from baseline	1.78 (0.67 to 2.89)	5.62 (4.52 to 6.71)	6.43 (5.33 to 7.53)
Change vs placebo, LS mean (95% CI), mean difference from baseline	–	3.84 (2.57 to 5.10)†	4.65 (3.39 to 5.91)†
SF-36 MCS LS mean (95% CI), mean difference from baseline	−0.22 (−1.68 to 1.25)	2.85 (1.40 to 4.29)	4.04 (2.58 to 5.50)
Change vs placebo, LS mean (95% CI), mean difference from baseline	–	3.06 (1.39 to 4.73)‡	4.26 (2.58 to 5.93)†
Other efficacy endpoints			
DAS28(CRP) LS mean (95% CI), mean difference from baseline	−0.84 (−1.00 to −0.67)	−1.93 (−2.09 to −1.76)	−2.36 (−2.52 to −2.19)
Change vs placebo, LS mean (95% CI), mean difference from baseline	–	−1.09 (−1.31 to −0.88)†	−1.52 (−1.74 to −1.31)†
DAS28(ESR) LS mean (95% CI), mean difference from baseline	−1.03 (−1.22 to −0.83)	−2.22 (−2.41 to −2.03)	−2.76 (−2.95 to −2.57)
Change vs placebo, LS mean (95% CI), mean difference from baseline	–	−1.19 (−1.44 to −0.94)†	−1.73 (−1.98 to −1.48)†
CDAI LS mean (95% CI), mean difference from baseline	−12.01 (−13.78 to −10.24)	−19.31 (−21.04 to −17.57)	−22.27 (−24.01 to −20.53)
Change vs placebo, LS mean (95% CI), mean difference from baseline	–	−7.30 (−9.50 to −5.09)†	−10.26 (−12.47 to −8.05)†
CDAI ≤2.8§	2 (1.1)	22 (11.6)	30 (15.9)
Difference vs placebo, % (95% CI)	–	10.7 (5.8 to 15.5)†	14.8 (9.4 to 20.2)†
CDAI ≤10§	28 (14.9)	73 (38.6)	92 (48.7)
Difference vs placebo, % (95% CI)	–	23.8 (15.2 to 32.4)†	33.8 (25.0 to 42.5)†
>50% improvement in CDAI §	59 (31.4)	111 (58.7)	124 (65.6)
Difference vs placebo, % (95% CI)	–	27.5 (17.8 to 37.1)†	34.2 (24.7 to 43.7)†
>70% improvement in CDAI §	22 (11.7)	69 (36.5)	91 (48.1)
Difference vs placebo, % (95% CI)	–	24.9 (16.6 to 33.2)†	36.4 (27.9 to 44.9)†
SDAI LS mean (95% CI), mean difference from baseline	−12.09 (−13.90 to −10.29)	−20.76 (−22.53 to −19.00)	−24.08 (−25.85 to −22.31)
Change vs placebo, LS mean (95% CI), mean difference from baseline	–	−8.67 (−10.90 to −6.44)†	−11.98 (−14.22 to −9.75)†
SDAI ≤3.3§	2 (1.1)	25 (13.2)	32 (16.9)
Difference vs placebo, % (95% CI)	–	12.2 (7.2 to 17.3) †	15.9 (10.3 to 21.4)†
SDAI ≤11§	27 (14.4)	74 (39.2)	94 (49.7)
Difference vs placebo, % (95% CI)	–	24.9 (16.4 to 33.5)†	35.4 (26.7 to 44.1)†
>50% improvement in SDAI§	53 (28.2)	112 (59.3)	126 (66.7)
Difference vs placebo, % (95% CI)	–	31.2 (21.7 to 40.7)†	38.5 (29.1 to 47.8)†
>70% improvement in SDAI§	17 (9.0)	70 (37.0)	92 (48.7)
Difference vs placebo, % (95% CI)	–	28.2 (20.2 to 36.1)†	39.6 (31.4 to 47.9) †
Morning stiffness duration LS mean (95% CI), mean difference from baseline	−25.0 (−31.2 to −18.7)	−41.4 (−47.4 to −35.4)	−40.8 (−46.8 to −34.7)
Change vs placebo, LS mean (95% CI), mean difference from baseline	–	−16.4 (−23.7 to −9.1)†	−15.8 (−23.1 to −8.5)†
Morning stiffness severity LS mean (95% CI), mean difference from baseline	−11.5 (−14.8 to −8.1)	−23.3 (−26.6 to −20.0)	−26.6 (−29.9 to −23.3)
Change vs placebo, LS mean (95% CI), mean difference from baseline¶	–	−11.8 (−15.9 to −7.7)†	−15.2 (−19.3 to −11.0)†
HAQ-DI improvement of ≥0.22**	83/172 (48.3)	121/176 (68.8)	125/172 (72.7)
Difference vs placebo, % (95% CI)	–	20.7 (10.5 to 30.8)†	24.5 (14.5 to 34.5)†
HAQ-DI improvement of ≥0.3 §,††	66/166 (39.8)	110/173 (63.6)	112/164 (68.3)
Difference vs placebo, % (95% CI)	–	24.1 (13.8 to 34.3)†	28.6 (18.4 to 38.9)†
HAQ-DI <0.5§	45 (23.9)	80 (42.3)	88 (46.6)
Difference vs placebo, % (95% CI)	–	18.7 (9.5 to 27.9)†	22.7 (13.4 to 32.0)†

Data are n (%) unless noted otherwise.
* p<0.0001 vs placebo.
† Nominal p<0.0001 vs placebo, not adjusted for multiplicity.
‡ Nominal p<0.001 vs placebo, not adjusted for multiplicity.
§ Not predefined by protocol (post hoc analyses).
¶ Detected by 0–100 mm VAS.
** Number of patients achieving a HAQ-DI improvement ≥0.22 at week 24/number of patients with a baseline HAQ-DI of ≥0.22.
†† Number of patients achieving a HAQ-DI improvement ≥0.3 at week 24/number of patients with a baseline HAQ-DI of ≥0.3.ACR, American College of Rheumatology; CDAI, Clinical Disease Activity Index; DAS28(CRP), Disease Activity Score 28 based on C reactive protein; DAS28(ESR), Disease Activity Score 28 based on erythrocyte sedimentation rate; HAQ-DI, Health Assessment Questionnaire Disability Index; LS, least squares; SDAI, Simplified Disease Activity Index; SF-36 MCS, Short Form-36 mental component summary; SF-36 PCS, Short Form-36 physical component summary; VAS, visual analogue scale.

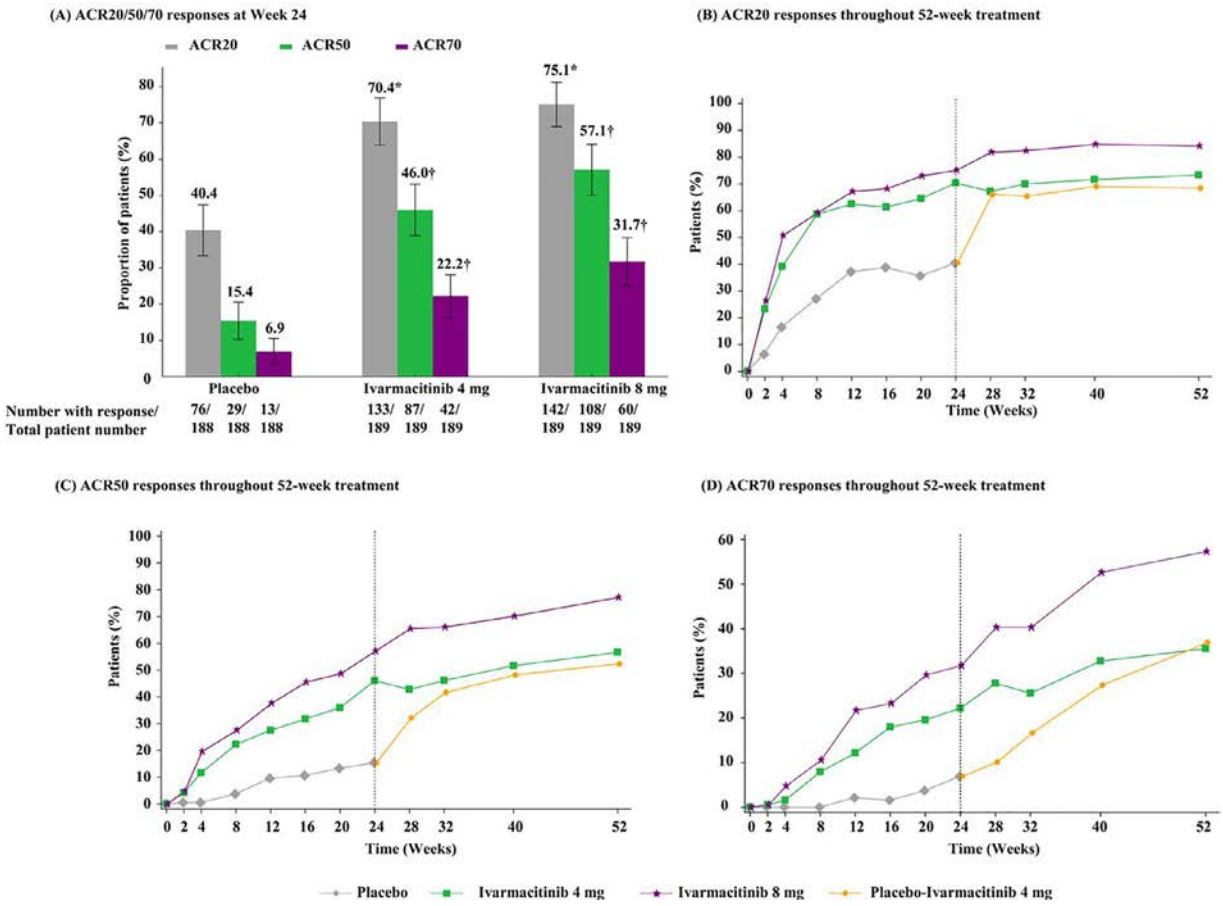

Figure 2. ACR20/50/70 responses. (A) Proportions of patients achieving ACR20/50/70 responses at week 24. (B) ACR20 responses through 52 weeks. (C) ACR50 responses through 52 weeks. (D) ACR70 responses through 52 weeks. Data are presented as % (95% CI) (A) or %(B–D). *p<0.0001 vs placebo †nominal p<0.0001 vs placebo, not adjusted for multiplicity. ACR, American College of Rheumatology response.

abnormal liver function, one with papillary thyroid cancer and another with anaplastic oligodendroglioma), 1 (0.6%) in the ivarmacitinib 8 mg group (cryptococcal pneumonia) and 2 (1.2%) in the placebo-ivarmacitinib 4 mg group (one with thalamus haemorrhage and another with deep vein thrombosis) reported prespecified TEAEs of special interest. Eight patients experienced herpes zoster: 3 (1.8%) in the placebo-ivarmacitinib 4 mg group, 1 (0.6%) in the ivarmacitinib 4 mg group and 4 (2.3%) in the ivarmacitinib 8 mg group during this period (table 3).

Up to week 24, treatment discontinuations due to TEAEs were low, with occurrences of 3 (1.6%), 7 (3.7%) and 5 (2.7%) patients for the ivarmacitinib 4 mg, ivarmacitinib 8 mg and placebo groups. During the extension period, the proportions of patients who discontinued treatment due to TEAEs remained similar across treatment groups (table 3, online supplemental tables S10, S11). No TEAEs leading to death, tuberculosis or gastrointestinal perforations were reported throughout the 52-week treatment period.

Changes from baseline in laboratory values and grade ≥3 abnormalities from weeks 0–24 and weeks 24–52 are presented in table 4. During the placebo-controlled treatment period, common hematologic abnormalities in patients treated with ivarmacitinib included increased haemoglobin levels and decreased white blood cell and neutrophil counts, most of which were grade 1/2 and not clinically relevant. However, grade 3 decreased neutrophil count and lymphopenia were more frequent in the ivarmacitinib groups compared with placebo. The mean levels of creatine kinase (CK) and liver enzymes (ALT and AST) were higher in the ivarmacitinib 4 mg and 8 mg groups than in the placebo group, but remained within the normal range. Mean changes from baseline in blood lipid levels (total cholesterol, triglycerides, LDL-C, HDL-C) increased with ivarmacitinib treatment compared with placebo, without any meaningful change in the LDL to HDL cholesterol ratio. During the extension period, these laboratory trends remained stable, with no further increases, consistent with the observations from the placebo-controlled period.

DISCUSSION

This phase III study assessed ivarmacitinib, a novel oral selective JAK1 inhibitor, to address the unmet needs for RA treatment for patients with an inadequate response to csDMARDs. The results showed statistically significant increases in ACR20 response rates by week 24 for ivarmacitinib doses of 4 mg and 8 mg once daily (70.4% and 75.1%, respectively) compared with placebo (40.4%), with background csDMARDs allowed.

Notably, the ACR20 response rates observed with ivarmacitinib (4 mg and 8 mg) were consistent with those reported in previous phase III studies of other JAK inhibitors in similar disease settings, where ACR20 response rates at week 12 or 24 served as the primary endpoint [22–25]. For instance, the ORAL SYNC phase III trial reported ACR20 response rates of 52.1% for tofacitinib 5 mg and 56.6% for 10 mg at week 24, compared with 30.8% in the placebo group [22]. In the present study, ACR20 response rates at week 12 were 62.4% with ivarmacitinib 4 mg and 67.2% with ivarmacitinib 8 mg, compared with 37.2% for

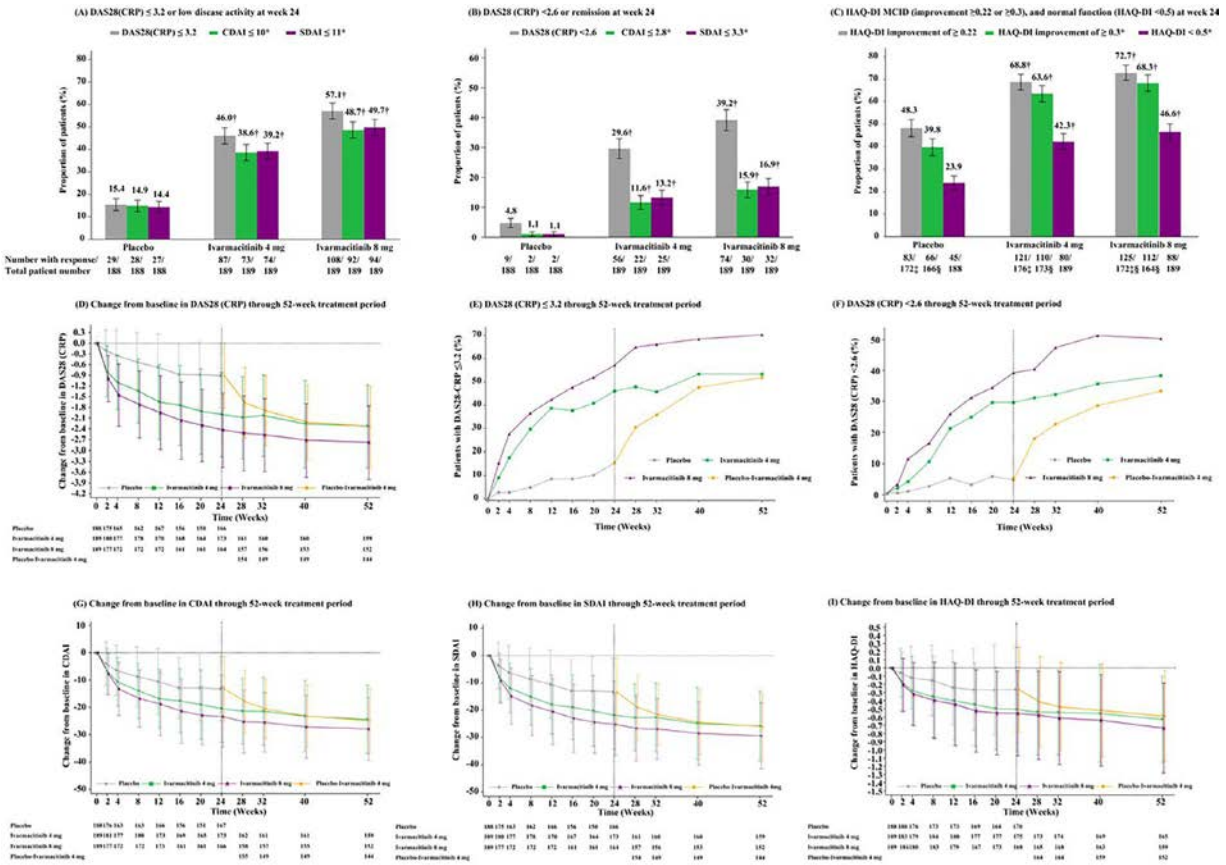

Figure 3. Disease activity and physical function. (A) Proportions of patients achieving DAS28(CRP) ≤3.2 or low disease activity (CDAI ≤10 or SDAI ≤11) at week 24. (B) Proportions of patients achieving DAS28(CRP) <2.6 or remission (CDAI ≤2.8 or SDAI ≤3.3) at week 24. (C) Proportion of patients achieving HAQ-DI MCID (improvement ≥0.22 or ≥0.3) or normal function (HAQ-DI <0.5). (D) Observed change from baseline in DAS28 (CRP) throughout 52 weeks. (E) Proportion of patients achieving DAS28(CRP) ≤3.2 through 52 weeks. (F) Proportion of patients achieving DAS28 (CRP) <2.6 through 52 weeks. (G) Observed change from baseline in CDAI throughout 52 weeks. (H) Observed change from baseline in SDAI throughout 52 weeks. (I) Observed change from baseline in HAQ-DI throughout 52 weeks. *Not predefined by protocol (post hoc analyses). †Nominal p<0.0001 vs placebo, not adjusted for multiplicity. ‡Number of patients achieving a HAQ-DI improvement ≥0.22 at week 24/number of patients with a baseline HAQ-DI of ≥0.22. §Number of patients achieving a HAQ-DI improvement ≥0.3 at week 24/number of patients with a baseline HAQ-DI of ≥0.3. Data are presented as % (95% CI) (A–C), % (E–F) and or observed mean±SD (D, G–I). DAS28(CRP), Disease Activity Score 28 based on C reactive protein; CDAI, Clinical Disease Activity Index; SDAI, Simplified Disease Activity Index; HAQ-DI, Health Assessment Questionnaire Disability Index; MCID, minimal clinically important difference.

placebo. Similarly, ACR20 responses at week 12 were 62% with baricitinib 4 mg in the RA-BUILD phase III trial [23], 64% and 66% with upadacitinib 15 mg and 30 mg in the SELECT-NEXT phase III trials [24], 57.7% and 74.5% with peficitinib 100 mg and 150 mg in the RAJ3 phase II trial [25], and 69.8% and 76.6% with filgotinib 100 mg and 200 mg in the FINCH1 phase III trial [9], compared with 30.7%–49.9% in the placebo groups of these trials. However, differences in inclusion criteria for inadequate response to csDMARDs, baseline concomitant csDMARD use, treatment duration, study regions and placebo group ACR20 response rates (influenced by geographical and temporal factors) across these studies present challenges for direct comparisons with the outcomes of the current study.

Both doses of ivarmacitinib exhibited a rapid onset of action, achieving higher ACR20/50/70 responses than placebo as early as week 2/4/8, which were either maintained or improved during long-term treatment up to week 52. Additionally, patients who switched from placebo to ivarmacitinib 4 mg after week 24 showed improvements that were sustained throughout the study. Moreover, both doses of ivarmacitinib demonstrated favourable outcomes compared with placebo when evaluated using more stringent efficacy measures that align with the EULAR recommendations and the treat-to-target strategy [5]. After 24 weeks of treatment, ivarmacitinib led to notable changes from baseline in DAS28(CRP), with 29.6%–39.2% of patients achieving DAS28(CRP) <2.6 and 46.0%–57.1% reaching DAS28(CRP) ≤3.2. In a post hoc exploratory analysis, 38.6% – 49.7% of patients receiving ivarmacitinib achieved low disease activity based on composite measures, including CDAI and SDAI, and 11.6%–16.9% met stringent criteria for clinical remission at week 24 [19,20].

Patient-reported outcomes, including pain, physical function (HAQ-DI), quality of life (SF-36 physical and mental components) and the duration and severity of morning stiffness, improved in patients treated with both doses of ivarmacitinib compared with placebo, indicating a positive impact on overall quality of life, well-being and work capability [26,27].

Numerically higher clinical responses were observed in most clinical and some patient-reported outcome domains with ivarmacitinib 8 mg compared with ivarmacitinib 4 mg; however, the study was neither designed nor powered to detect differences between these doses. This observation aligns with findings from a short-term (12 week) phase II trial involving ivarmacitinib doses ranging from 0.5 to 8 mg once daily in RA patients who were either treatment-naive or had an inadequate response to csDMARDs [16].

Table 3
Treatment-emergent adverse events through weeks 0–24 and weeks 24–52 (safety population)

	Placebo-controlled period (weeks 0–24)			Extension period (weeks 24–52)		
TEAEs, n (%)	**Placebo (n = 188)**	**Ivarmacitinib 4 mg (n = 189)**	**Ivarmacitinib 8 mg (n = 189)**	**Placebo-Ivarmacitinib 4 mg (n = 168)**	**Ivarmacitinib 4 mg (n = 180)**	**Ivarmacitinib 8 mg (n = 171)**
TEAEs	149 (79.3)	154 (81.5)	171 (90.5)	137 (81.5)	143 (79.4)	145 (84.8)
Mild	103 (54.8)	99 (52.4)	112 (59.3)	84 (50.0)	102 (56.7)	95 (55.6)
Moderate	43 (22.9)	53 (28.0)	53 (28.0)	45 (26.8)	34 (18.9)	47 (27.5)
Severe	3 (1.6)	2 (1.1)	6 (3.2)	8 (4.8)	7 (3.9)	3 (1.8)
Treatment-related TEAEs	92 (48.9)	107 (56.6)	121 (64.0)	99 (58.9)	86 (47.8)	109 (63.7)
TEAEs leading to dose discontinuation	5 (2.7)	3 (1.6)	7 (3.7)	2 (1.2)	3 (1.7)	1 (0.6)
TEAEs leading to dose interruption	9 (4.8)	15 (7.9)	20 (10.6)	9 (5.4)	18 (10.0)	12 (7.0)
Infection-related TEAEs	64 (34.0)	76 (40.2)	77 (40.7)	49 (29.2)	59 (32.8)	58 (33.9)
TESAEs*	5 (2.7)	8 (4.2)	12 (6.3)	13 (7.7)	8 (4.4)	9 (5.3)
Prespecified TEAEs of special interest	0	2 (1.1)	3 (1.6)	2 (1.2)	4 (2.2)	1 (0.6)
Serious infection†	0	0	1 (0.5)	0	0	0
Any systemic opportunistic infection‡	0	0	0	0	0	1 (0.6)
Newly diagnosed malignancy	0	1 (0.5)	0	0	2 (1.1)	0
Thromboembolic event§	0	0	1 (0.5)	1 (0.6)	0	0
MACE¶	0	0	1 (0.5)	1 (0.6)	0	0
Liver function abnormality**	0	1 (0.5)	1 (0.5)	0	2 (1.1)	0
Other TEAEs of special interest						
Herpes zoster	4 (2.1)	3 (1.6)	5 (2.6)	3 (1.8)	1 (0.6)	4 (2.3)
TEAEs occurring in ≥5% of patients in any treatment group						
Upper respiratory tract infection	26 (13.8)	41 (21.7)	43 (22.8)	26 (15.5)	25 (13.9)	29 (17.0)
Hyperlipidaemia	10 (5.3)	29 (15.3)	23 (12.2)	17 (10.1)	17 (9.4)	14 (8.2)
Hypercholesterolaemia	5 (2.7)	9 (4.8)	19 (10.1)	7 (4.2)	5 (2.8)	13 (7.6)
White cell count decreased	5 (2.7)	8 (4.2)	18 (9.5)	17 (10.1)	11 (6.1)	21 (12.3)
AST increased	6 (3.2)	6 (3.2)	17 (9.0)	9 (5.4)	10 (5.6)	23 (13.5)
Blood creatine phosphokinase increased	4 (2.1)	10 (5.3)	15 (7.9)	8 (4.8)	10 (5.6)	20 (11.7)
ALT increased	6 (3.2)	4 (2.1)	15 (7.9)	11 (6.5)	8 (4.4)	14 (8.2)
Anaemia	22 (11.7)	12 (6.3)	14 (7.4)	15 (8.9)	8 (4.4)	7 (4.1)
Urinary tract infection	9 (4.8)	8 (4.2)	12 (6.3)	7 (4.2)	12 (6.7)	9 (5.3)
Weight increased	4 (2.1)	6 (3.2)	12 (6.3)	7 (4.2)	3 (1.7)	8 (4.7)
Abdominal pain upper	5 (2.7)	4 (2.1)	11 (5.8)	2 (1.2)	1 (0.6)	1 (0.6)
Lymphocyte count decreased	5 (2.7)	9 (4.8)	9 (4.8)	6 (3.6)	14 (7.8)	15 (8.8)
Neutrophil count decreased	4 (2.1)	9 (4.8)	9 (4.8)	9 (5.4)	10 (5.6)	11 (6.4)
Platelet count decreased	2 (1.1)	4 (2.1)	9 (4.8)	5 (3.0)	3 (1.7)	9 (5.3)
Dizziness	7 (3.7)	11 (5.8)	5 (2.6)	3 (1.8)	3 (1.7)	2 (1.2)
Hepatic function abnormal	3 (1.6)	9 (4.8)	5 (2.6)	11 (6.5)	11 (6.1)	7 (4.1)
COVID-19	3 (1.6)	1 (0.5)	3 (1.6)	2 (1.2)	9 (5.0)	5 (2.9)

%, the percentage of patients relative to the total number of patients in the treatment arm. AEs were coded using MedDRA (Medical Dictionary for Regulatory Activities) Version 26.0. A TEAE is defined as an AE that either first occurred or worsened in severity after the initial dose of the study treatment.

* During the placebo-controlled period, the TESAEs by preferred term included pneumonia (3 pts), urinary tract infections (2 pts), abnormal uterine bleeding (2 pts) and one patient each for herpes zoster, liver abscess, femoral neck fracture, compression fracture, post herpetic neuralgia, hydrocephalus, myelodysplastic syndrome, uterine leiomyoma, arteriosclerosis coronary artery, arrhythmia, renal hydrocele, renal calculi, abdominal pain, kidney infection, contusion, spinal cord injury, neck injury, cervical vertebral fracture, concussion, limb injury, cervical radiculopathy, dizziness, squamous cell carcinoma of the cervix, back pain, synovial cyst, cholelithiasis, acute cholecystitis, drug eruption and spontaneous abortion (detailed in online supplemental table S8).

† Severe infection is defined as any infection that necessitates systemic antimicrobial therapy for more than two weeks, including severe systemic infections such as sepsis, pyemia and septic shock.

‡ This category includes any systemic opportunistic infection, such as active tuberculosis, disseminated herpes zoster, etc.

§ This category includes venous thrombosis (including but not limited to deep vein thrombosis), pulmonary thromboembolism, arterial thrombosis and cerebrovascular events (eg, thromboembolic stroke, transient ischaemic attack).

¶ MACE events include cardiovascular death, non-fatal myocardial infarction, non-fatal stroke, unstable angina requiring hospitalisation and heart failure necessitating hospital admission.

** Liver function abnormality is identified when one of the following criteria is met, with no other causes for the abnormality: (1) ALT or AST levels exceeding five times the ULN; (2) ALT or AST levels more than three times ULN, along with total bilirubin over two times ULN; (3) ALT or AST levels more than three times ULN, accompanied by clinical symptoms and signs indicative of hepatitis (eg, onset or aggravation of fatigue, nausea, vomiting, pain or tenderness in the right upper quadrant, fever) or an eosinophil count greater than 5%.n, number of patients; TEAE, treatment-emergent adverse event; TESAEs, treatment-emergent serious adverse events; MACE, major adverse cardiac events; AST, aspartate aminotransferase; ALT, alanine aminotransferase; ULN, upper limit of normal; pt, patient.

During the placebo-controlled period, there appeared to be a higher incidence of TEAEs in the ivarmacitinib 8 mg group compared with both the ivarmacitinib 4 mg group and the placebo group, suggesting a possible dose-response relationship with respect to overall TEAEs. However, regarding TEAEs of special interests (including serious infections, systemic opportunistic infections, newly diagnosed malignancies, thromboembolic events, MACE, liver function abnormality and herpes zoster), as well as TESAEs and TEAEs leading to treatment discontinuation, no apparent dose-dependent pattern was observed. This dose-response trend was observed only during the placebo-controlled period and was not evident for TEAEs of special interest. Furthermore, and no new safety risks commonly noted with JAK inhibitors were identified [9,23–25,28,29]. JAK inhibitors may increase infection risk in a dose-dependent manner [30]. In this phase III study, infection-related TEAEs were more frequent in patients treated with ivarmacitinib compared with placebo, with similar rates observed between the ivarmacitinib 4 mg and 8 mg groups. During the placebo-controlled period, two patients in the ivarmacitinib 4 mg group (one with pneumonia and one

Table 4
Change from baseline in laboratory values and grade ≥3 abnormalities through weeks 0–24 and weeks 24–52

	Placebo-controlled period (weeks 0–24)			Extension period (weeks 24–52)		
	Placebo (n = 188)	Ivarmacitinib 4 mg (n = 189)	Ivarmacitinib 8 mg (n = 189)	Placebo-Ivarmacitinib 4 mg (n = 168)	Ivarmacitinib 4 mg (n = 180)	Ivarmacitinib 8 mg (n = 171)
Haemoglobin, g/L	−1.7±12.1	5.4±10.2	7.4±11.0	7.5±12.1	6.8±11.2	7.4±11.5
Grade 3 anaemia, n (%)*	3 (1.6)	0	1 (0.5)	0	2 (1.1)	1 (0.6)
Neutrophils, 10^9/L	−0.3±1.6	−0.9±1.6	−1.1±1.6	−0.6±1.6	−0.9±1.7	−1.0±1.9
Grade 3 neutrophil count decreased, n (%)*	0	0	3 (1.6)	1 (0.6)	1 (0.6)	3 (1.8)
Grade 4 neutrophil count decreased, n (%)*	0	0	0	0	1 (0.6)	1 (0.6)
Lymphocytes, 10^9/L	0.0±0.5	0.1±0.5	0.2±0.4	0.0±0.5	0.0±0.5	0.0±0.4
Grade 3 lymphopenia, n (%)*	1 (0.5)	1 (0.5)	5 (2.6)	1 (0.6)	4 (2.2)	7 (4.1)
Platelets, 10^9/L	−5.2±51.1	−54.9±63.5	−68.8±61.3	−46.7±51.9	−57.2±65.4	−65.8±60.8
Grade 3 platelet count decreased, n (%)*	0	1 (0.5)	0	0	1 (0.6)	0
Grade 4 platelet count decreased, n (%)*	0	0	1 (0.5)	0	0	0
White cell count, 10^9/L	−0.3±1.7	−0.9±1.7	−1.0±1.7	−0.6±1.6	−1.1±1.9	−1.1±2.0
Grade 3 white cell count decreased, n (%)*	0	0	1 (0.5)	1 (0.6)	1 (0.6)	2 (1.2)
ALT, IU/L	1.6±12.1	5.1±17.5	5.7±16.3	4.0±18.8	3.0±11.8	5.0±15.6
Grade 3 ALT increased, n (%)*	0	1 (0.5)	1 (0.5)	0	1 (0.6)	0
AST, IU/L	0.7±8.8	4.9±11.7	6.8±12.3	3.4±10.5	3.6±7.4	5.3±9.0
Grade 3 AST increased, n (%)*	0	1 (0.5)	0	0	1 (0.6)	0
Creatinine, μmol/L	0.4±6.9	3.6±7.1	6.3±8.5	4.0±6.9	3.5±8.0	7.7±8.3
Grade 3/4 blood creatinine increased, n (%) *	0	0	0	0	0	0
CK, IU/L	2.2±41.9	41.0±40.8	75.2±136.2	47.8±62.8	45.7±51.6	65.1±64.2
Grade 3 blood CK increased, n (%)*	0	1 (0.5)	0	0	0	0
Grade 4 blood CK increased, n (%)*	0	0	1 (0.5)	0	0	0
Total cholesterol, mmol/L	0.1±0.6	0.6±0.8	0.8±0.9	0.6±0.7	0.6±0.8	0.8±0.9
Grade 3 hypercholesterolemia, n (%) *	0	2 (1.1)	1 (0.5)	0	0	0
LDL cholesterol, mmol/L	0.0±0.5	0.3±0.5	0.3±0.7	0.3±0.6	0.3±0.6	0.4±0.7
HDL cholesterol, mmol/L	0.0±0.2	0.3±0.4	0.3±0.4	0.2±0.3	0.2±0.3	0.3±0.3
LDL:HDL ratio	0.0±0.4	−0.1±0.4	−0.1±0.5	0.0±0.4	−0.1±0.5	−0.1±0.5
Triglyceride, mmol/L	0.0±0.4	0.1±0.7	0.2±0.7	0.2±0.5	0.1±0.9	0.1±0.7
Grade 3 hypertriglyceridemia, n (%) *	0	2 (1.1)	2 (1.1)	0	2 (1.1)	1 (0.6)

Absolute values are presented as mean±SD deviation change from baseline at weeks 24 and 52 unless otherwise specified. Severity was graded using Common Terminology Criteria for Adverse Events Version 4.03.

* The baseline CTCAE grades were ≤grade 2.ALT, alanine aminotransferase; AST, aspartate aminotransferase; HDL, high-density lipoprotein; LDL, low-density lipoprotein; CK, creatine kinase.

with a kidney infection) and four patients in the ivarmacitinib 8 mg group (two with pneumonia, one with a urinary tract infection, one with herpes zoster and one with a liver abscess) experienced infection-related TESAE. Among these, only the liver abscess was classified as a serious infectious event, occurring in a patient who had been hospitalised for a severe pulmonary infection 4 months earlier. The frequency of herpes zoster was low and similar across all treatment arms through week 24. Safety data remained consistent throughout the entire 52-week study. Malignancy remains a considerable concern with JAK inhibitors [31]. In the ORAL Surveillance trial, among patients with active RA despite methotrexate treatment, the incidences of malignancy were higher with tofacitinib compared with a TNF inhibitor [32]. In our study, we observed three cases of cancer: one patient with a history of leflunomide and celecoxib use, who was HPV16 positive, was diagnosed with cervical squamous cell carcinoma after taking ivarmacitinib 4 mg for over 3 months. Another patient developed papillary thyroid cancer after being on ivarmacitinib 4 mg for over 7 months. The third patient, also in the ivarmacitinib 4 mg group, involved anaplastic oligoden-droglioma in a patient with a 5-year history of methotrexate use and no baseline head CT/MRI imaging. These sporadic solid tumours did not reflect the common tumour types observed in JAK inhibitor trials nor suggest an increased incidence rate compared with other JAK inhibitors [22].

Ivarmacitinib was associated with increased haemoglobin levels, decreased white cell counts, neutrophil levels and platelet counts, as well as elevations in lipid levels, CK, creatinine, and liver enzymes (ALT and AST), consistent with findings for other JAK inhibitors [9,23–25,28,29]. A slightly higher frequency of grade 3 neutropenia and lymphopenia was observed in patients treated with ivarmacitinib compared with placebo. Treatment with ivarmacitinib slightly increased total cholesterol, LDL, HDL and triglycerides during the placebo-controlled period, without affecting the LDL-to-HDL ratio, consistent with the hypothesis that JAK inhibitor treatment may suppress elevated cholesterol ester catabolism in patients with active RA, normalising their cholesterol levels toward the range observed in healthy individuals [33]. A meta-analysis of upadacitinib trials revealed increases in LDL-C and HDL-C levels, yet no significant impact on cardiovascular disease risk during a follow-up period of up to 52 weeks [34]. Similarly, in our study, despite increases in lipid levels, the incidence of MACE among ivarmacitinib-treated patients over 52 weeks remained low. However, conclusions from a single phase 3 trial are insufficient to definitively determine whether ivarmacitinib carries a MACE risk.

The present study has several limitations. First, our findings are based on a Chinese population, which limits the generalisability to other populations, thereby lacking global diversity. Expanding future registries to include more diverse populations will be essential for broader applicability. Second, due to ethical concerns, placebo treatment was limited to 24 weeks, which restricts comparisons between placebo and ivarmacitinib beyond that period. Third, the study was not powered to compare efficacy and safety between the two active dose regimens, preventing definitive conclusions in this regard. Lastly, future studies should compare the efficacy and safety of ivarmacitinib with other JAK inhibitors in active-controlled trials.

In conclusion, ivarmacitinib at doses of 4 or 8 mg once daily was superior to placebo in reducing RA signs and symptoms, decreasing disease activity, and improving physical function over a 24-week treatment period in patients with active RA who had an inadequate response to csDMARDs. These improvements were sustained throughout the study period. Overall, both doses of ivarmacitinib demonstrated a favourable benefit-to-risk profile similar to other approved JAK inhibitors.

Contributors

XZ is the guarantor, responsible for the overall content and accepts full responsibility for the work and/or conduct of the study, with access to the data and control over the decision to publish. XZ and GD contributed to design. JinjL (Peking Union Medical College Hospital), YJ, SZ, SL, JS, CL, XH, RW, LY, HLi, XD, SX, HLu, JingL, QX, CM, LC, NZ, HG, JZ, YL, HW, LQ, JW, XS, HJ, ZJ, XX, FZ, XG, ZZ, ZD and XZ contributed to conduct/data collection. YS contributed to statistical analysis. All authorscontributed to interpretation of data. JinjL and XZ contributed to drafting of the manuscript. All authors were responsible for all content and editorial decisions. Medical writing assistance, under the direction of the authors, and editorial support was provided by Lin Dong, PhD (Jiangsu Hengrui Pharmaceuticals Co, Ltd) according to CONSORT 2010 statement: updated guidelines for reporting parallel group randomised trials (https://www.bmj.com/content/340/bmj.c332) and Good Publication Practice guidelines (http://annals.org/aim/article/2424869).

Funding

NCT04333771 RCT was funded by Jiangsu Hengrui Pharmaceuticals Co, Ltd.

Competing interests

YS and GD are employees of Jiangsu Hengrui Pharmaceuticals Co, Ltd. All other co-authors declare no competing interest.

Patient and public involvement

Patients and/or the public were not involved in the design, or conduct, or reporting, or dissemination plans of this research.

Patient consent for publication

Not applicable.

Ethics approval

This study involves human participants and was approved by This study was done in accordance with the International Council for Harmonisation Good Clinical Practice guidelines, local regulatory requirements and the ethical principles of the Declaration of Helsinki. All patients provided written, informed consent before enrolment. The study protocol was approved by an institutional review board or independent ethics committee at each study site. Participants gave informed consent to participate in the study before taking part.

Data availability statement

Data are available upon reasonable request. Data are available upon reasonable request. The data sets used and/or analyzed during the current study are available from the corresponding author on reasonable request after the product and indication has been approved by major health authorities. Data may be requested 24 months after study completion. Qualified researchers should submit a proposal to the corresponding author outlining the reasons for requiring the data. The leading clinical site and sponsor will check whether the request is subject to any intellectual property restriction. Use of data must also comply with the requirements of Human Genetics Resources Administration of China and other country or region-specific regulations. A signed data access agreement with the sponsor is required before accessing shared data.

Supplementary materials

Supplementary material associated with this article can be found in the online version at doi:10.1136/ard-2024-226385.

Orcid

Jinjing Liu: http://orcid.org/0000-0003-2150-7540
Changsong Lin: http://orcid.org/0009-0001-8049-819X
Qibing Xie: http://orcid.org/0000-0002-6727-1839
Xiaofeng Zeng: http://orcid.org/0000-0002-3883-2318

REFERENCES

[1] Di Matteo A, Bathon JM, Emery P. Rheumatoid arthritis. Lancet 2023;402:2019–33.
[2] Bullock J, Rizvi SAA, Saleh AM, et al. Rheumatoid Arthritis: A Brief Overview of the Treatment. Med Princ Pract 2018;27:501–7.
[3] Cush JJ. Rheumatoid Arthritis: Early Diagnosis and Treatment. Med Clin North Am 2021;105:355–65.
[4] Fraenkel L, Bathon JM, England BR, et al. 2021 American College of Rheumatology Guideline for the Treatment of Rheumatoid Arthritis. Arthritis Rheumatol 2021;73:1108–23.
[5] Smolen JS, Landewé RBM, Bergstra SA, et al. EULAR recommendations for the management of rheumatoid arthritis with synthetic and biological disease-modifying antirheumatic drugs: 2022 update. Ann Rheum Dis 2023;82:3–18.
[6] Traynor K. FDA approves tofacitinib for rheumatoid arthritis. Am J Health Syst Pharm 2012;69:2120.
[7] Mogul A, Corsi K, McAuliffe L. Baricitinib: The Second FDA-Approved JAK Inhibitor for the Treatment of Rheumatoid Arthritis. Ann Pharmacother 2019;53:947–53.
[8] Duggan S, Keam SJ. Upadacitinib: First Approval. *Drugs (Abingdon Engl)* 2019;79:1819–28.
[9] Combe B, Kivitz A, Tanaka Y, et al. Filgotinib versus placebo or adalimumab in patients with rheumatoid arthritis and inadequate response to methotrexate: a phase III randomised clinical trial. Ann Rheum Dis 2021;80:848–58.
[10] Markham A, Keam SJ. Peficitinib: First Global Approval. *Drugs (Abingdon Engl)* 2019;79:887–91.
[11] Harrington R, Al Nokhatha SA, Conway R. JAK Inhibitors in Rheumatoid Arthritis: An Evidence-Based Review on the Emerging Clinical Data. J Inflamm Res 2020;13:519–31.
[12] Traves PG, Murray B, Campigotto F, et al. JAK selectivity and the implications for clinical inhibition of pharmacodynamic cytokine signalling by filgotinib, upadacitinib, tofacitinib and baricitinib. Ann Rheum Dis 2021;80:865–75.
[13] Smolen JS, Pangan AL, Emery P, et al. Upadacitinib as monotherapy in patients with active rheumatoid arthritis and inadequate response to methotrexate (SELECTMONOTHERAPY): a randomised, placebo-controlled, double-blind phase 3 study. Lancet 2019;393:2303–11.
[14] Gu Y-J, Sun W-Y, Zhang S, et al. Targeted blockade of JAK/STAT3 signaling inhibits proliferation, migration and collagen production as well as inducing the apoptosis of hepatic stellate cells. Int J Mol Med 2016;38:903–11.
[15] Nielsen OH, Boye TL, Gubatan J, et al. Selective JAK1 inhibitors for the treatment of inflammatory bowel disease. Pharmacol Ther 2023;245:108402.
[16] Zeng X, Jiang Y, Yang Y, et al. A multicenter, randomized, placebo-controlled, double-blind phase 2 study of SHR0302 versus placebo in Chinese

subjects with moderate to severe active rheumatoid arthritis (RA). Arthritis Rheumatol 2020;72.
[17] Aletaha D, Neogi T, Silman AJ, et al. 2010 rheumatoid arthritis classification criteria: an American College of Rheumatology/European League Against Rheumatism collaborative initiative. Ann Rheum Dis 2010;69:1580–8.
[18] Keystone EC, van der Heijde D, Kavanaugh A, et al. Clinical, Functional, and Radiographic Benefits of Longterm Adalimumab Plus Methotrexate: Final 10-year Data in Longstanding Rheumatoid Arthritis. J Rheumatol 2013;40:1487–97.
[19] Aletaha D, Smolen J. The Simplified Disease Activity Index (SDAI) and the Clinical Disease Activity Index (CDAI): a review of their usefulness and validity in rheumatoid arthritis. Clin Exp Rheumatol 2005;23:S100–8.
[20] Felson DT, Smolen JS, Wells G, et al. American College of Rheumatology/European League Against Rheumatism provisional definition of remission in rheumatoid arthritis for clinical trials. Arthritis Rheum 2011;63:573–86.
[21] Aletaha D, Martinez-Avila J, Kvien TK, et al. Definition of treatment response in rheumatoid arthritis based on the simplified and the clinical disease activity index. Ann Rheum Dis 2012;71:1190–6.
[22] McLornan DP, Pope JE, Gotlib J, et al. Current and future status of JAK inhibitors. Lancet 2021;398:803–16.
[23] Dougados M, van der Heijde D, Chen Y-C, et al. Baricitinib in patients with inadequate response or intolerance to conventional synthetic DMARDs: results from the RA-BUILD study. Ann Rheum Dis 2017;76:88–95.
[24] Burmester GR, Kremer JM, Van den Bosch F, et al. Safety and efficacy of upadacitinib in patients with rheumatoid arthritis and inadequate response to conventional synthetic disease-modifying anti-rheumatic drugs (SELECT-NEXT): a randomised, double-blind, placebo-controlled phase 3 trial. Lancet 2018;391:2503–12.
[25] Tanaka Y, Takeuchi T, Tanaka S, et al. Efficacy and safety of peficitinib (ASP015K) in patients with rheumatoid arthritis and an inadequate response to conventional DMARDs: a randomised, double-blind, placebo-controlled phase III trial (RAJ3). Ann Rheum Dis 2019;78:1320–32.
[26] Strand V, Schiff M, Tundia N, et al. Effects of upadacitinib on patient-reported outcomes: results from SELECT-BEYOND, a phase 3 randomized trial in patients with rheumatoid arthritis and inadequate responses to biologic disease-modifying antirheumatic drugs. Arthritis Res Ther 2019;21:263.
[27] Tóth L, Juhász MF, Szabó L, et al. Janus Kinase Inhibitors Improve Disease Activity and Patient-Reported Outcomes in Rheumatoid Arthritis: A Systematic Review and Meta-Analysis of 24,135 Patients. Int J Mol Sci 2022;23:1246.
[28] Burmester GR, Cohen SB, Winthrop KL, et al. Safety profile of upadacitinib over 15 000 patient-years across rheumatoid arthritis, psoriatic arthritis, ankylosing spondylitis and atopic dermatitis. RMD Open 2023;9:e002735.
[29] Kremer J, Li Z-G, Hall S, et al. Tofacitinib in combination with nonbiologic disease-modifying antirheumatic drugs in patients with active rheumatoid arthritis: a randomized trial. Ann Intern Med 2013;159:253–61.
[30] Adas MA, Alveyn E, Cook E, et al. The infection risks of JAK inhibition. Expert Rev Clin Immunol 2022;18:253–61.
[31] Russell MD, Stovin C, Alveyn E, et al. JAK inhibitors and the risk of malignancy: a meta-analysis across disease indications. Ann Rheum Dis 2023;82:1059–67.
[32] Ozdede A, Yazıcı H. Cardiovascular and Cancer Risk with Tofacitinib in Rheumatoid Arthritis. N Engl J Med 2022;386:1766.
[33] Charles-Schoeman C, Fleischmann R, Davignon J, et al. Potential mechanisms leading to the abnormal lipid profile in patients with rheumatoid arthritis versus healthy volunteers and reversal by tofacitinib. Arthritis Rheumatol 2015;67:616–25.
[34] Makris A, Barkas F, Sfikakis PP, et al. The Effect of Upadacitinib on Lipid Profile and Cardiovascular Events: A Meta-Analysis of Randomized Controlled Trials. J Clin Med 2022;11:6894.

Ann Rheum Dis 84 (2025) 201–209

Contents lists available at ScienceDirect

Annals of the Rheumatic Diseases

journal homepage: https://www.sciencedirect.com/journal/annals-of-the-rheumatic-diseases

Rheumatoid arthritis

Disease activity of rheumatoid arthritis and kidney function decline: a large prospective registry study

Sho Fukui[1,2,3,*], Wolfgang C. Winkelmayer[4], Sara K. Tedeschi[1], Javier Marrugo[1], Hongshu Guan[1], Leslie Harrold[5,6], Heather J. Litman[6], Tomohiro Shinozaki[7], Daniel H. Solomon[1,*]

[1] *Division of Rheumatology, Inflammation, and Immunity, Brigham and Women's Hospital and Harvard Medical School, Boston, Massachusetts, USA*

[2] *Department of Emergency and General Medicine, Kyorin University, Tokyo, Japan*

[3] *Immuno-Rheumatology Center, St. Luke's International Hospital, Tokyo, Japan*

[4] *Selzman Institute for Kidney Health, Section of Nephrology, Baylor College of Medicine, Houston, Texas, USA*

[5] *Medicine, University of Massachusetts Medical School, Worcester, Massachusetts, USA*

[6] *CorEvitas LLC, Waltham, Massachusetts, USA*

[7] *Department of Information and Computer Technology, Faculty of Engineering, Tokyo University of Science, Katsushika-ku, Tokyo, Japan*

ARTICLE INFO

Article history:
Received 23 May 2024
Accepted 10 August 2024

Keywords:
Rheumatoid Arthritis
Epidemiology
Arthritis
Rheumatoid
Atherosclerosis

ABSTRACT

Introduction: Chronic kidney disease (CKD) is a common comorbidity of rheumatoid arthritis (RA). The association of longitudinal RA disease activity with long-term kidney function has remained uncertain.

Method: We analysed a multicentre prospective RA registry in the USA from 2001 to 2022. The exposure was updated time-averaged Clinical Disease Activity Index (TA-CDAI) categories from study enrolment. The primary outcome was a longitudinal estimated glomerular filtration rate (eGFR) change. Secondary outcomes included developments of CKD stage G3a (eGFR<60 mL/min/1.73 m^2) and stage G3b (eGFR<45 mL/min/1.73 m^2). Results were adjusted for relevant time-fixed and time-varying covariates.

Results: 31 129 patients (median age: 58.0 years, female: 76.3%, median eGFR: 90.7 mL/min/1.73 m^2) contributed 234 973 visits and 146 778 person-years of follow-up. Multivariable mixed-effect linear model showed an average annual eGFR decline during follow-up in the TA-CDAI-remission group of −0.83 mL/min/1.73 m^2 and estimated additional annual declines (95% CI) of −0.09 (−0.15 to −0.03) in low, −0.17 (−0.23 to −0.10) in moderate and −0.18 (−0.27 to −0.08) mL/min/1.73 m^2 in high disease activity patients. Compared with TA-CDAI remission, adjusted HRs (95% CI) for CKD stage G3a during follow-up were 1.15 (1.01 to 1.30) in low, 1.22 (1.06 to 1.40) in moderate and 1.27 (1.05 to 1.52) in high disease activity; for CKD stage G3b, 1.22 (0.84 to 1.76) in low, 1.66 (1.12 to 2.45) in moderate and 1.93 (1.16 to 3.20) in high disease activity.

Conclusions: Higher RA disease activity was associated with accelerated eGFR decline and increased risk of clinically relevant kidney dysfunction. Future intervention studies should attempt to replicate the association between RA disease activity and eGFR.

*Correspondence to Dr. Sho Fukui; Professor Daniel H. Solomon.

E-mail addresses: sfukui@bwh.harvard.edu (S. Fukui), dsolomon@bwh.harvard.edu (D.H. Solomon).

Handling editor Josef S. Smolen.

https://doi.org/10.1136/ard-2024-226156

WHAT IS ALREADY KNOWN ON THIS TOPIC

- Chronic kidney disease (CKD) is a common but underappreciated complication in patients with rheumatoid arthritis (RA).

WHAT THIS STUDY ADDS

- In this large prospective RA registry, higher RA disease activity was associated with accelerated estimated glomerular filtration rate decline over time.
- Higher RA disease activity was associated with new developments of CKD G3a and G3b in a dose-dependent manner.

HOW THIS STUDY MIGHT AFFECT RESEARCH, PRACTICE OR POLICY

- Higher RA disease activity should be recognised as a factor associated with kidney dysfunction in patients with RA.
- Future intervention studies should attempt to replicate the observed association between the disease activity of RA and kidney function.

INTRODUCTION

Systemic inflammation is closely associated with the development and progression of kidney dysfunction [1–3]. Rheumatoid arthritis (RA) is one of the most common systemic inflammatory diseases, affecting 0.6%–1.0% of the general population [4–6]. Patients with RA, particularly with higher disease activity, have well-recognised extra-articular complications such as osteoporosis [7], interstitial lung disease [8] and cardiovascular diseases (CVD) [9,10]. These complications contribute to shortened lifespans in patients with RA [11,12].

Chronic kidney disease (CKD) is a common but underappreciated comorbidity in patients with RA, affecting up to 30% of patients [13–16]. Multiple studies have identified RA as a risk factor for decreased estimated glomerular filtration rate (eGFR) [15,17], which is one domain by which CKD is defined and staged [18,19]. Reduced kidney function in patients with RA limits treatment options, such as methotrexate (MTX) and non-steroidal anti-inflammatory drugs (NSAIDs). Furthermore, patients with RA and CKD have an increased risk of morbidity and mortality by CVD regardless of other classical CVD risk factors [17,20].

Higher RA disease activity may influence kidney function. Underlying mechanisms include more nephrotoxic medication use, particularly NSAIDs, secondary amyloidosis, atherosclerotic renal disease and direct nephrotoxic effects of chronic inflammation [21,22]. Systemic inflammation in RA itself may contribute to the development and progression of multiple forms of CKD [1–3]. Higher RA disease activity is associated with systemic vascular inflammation that may play a role in atherosclerosis [23]. In addition to the increased vascular risk factors and hypertension in RA, this vascular inflammation may cause more nephrosclerosis, which is reported as a common finding of kidney biopsies in patients with RA with kidney impairment [24].

However, the direct association between longitudinal RA disease activity and the long-term trajectory of kidney function has not been thoroughly evaluated. Here, we used a large, prospective RA registry to evaluate the relationship between longitudinal RA disease activity and kidney function decline after adjusting for relevant confounders, including NSAIDs use and comorbidities over time.

METHODS

Study design and population

The CorEvitas (previously The Consortium of Rheumatology Researchers of North America) RA registry served as the database for the analyses. Details of this registry have been previously described [9,10]. In short, the CorEvitas RA registry is a prospective observational cohort of patients with RA. Data on RA including disease characteristics, disease activity, treatments and adverse events, as well as patient demographics and comorbidities, were recorded at enrolment and follow-up study visits with a typical interval of 6 months. The patients in the registry were followed from enrolment through their last study visit or until September 2022 in this study.

We included patients who were diagnosed as RA with two or more study visits in the CorEvitas RA registry from October 2001 to September 2022. Patients with less than two measurements of serum creatinine and those with missing Clinical Disease Activity Index (CDAI) or serum creatinine at enrolment were excluded. Following previous research [9], we excluded patients who received no disease-modifying antirheumatic drugs (DMARDs) treatments to improve the specificity of RA diagnosis. Patients whose eGFR at enrolment was 60 mL/min/1.73 m^2 or higher were studied in the main analysis, and those with baseline eGFR<60 mL/min/1.73 m^2 were examined in online supplemental analysis. In the main analysis, the primary population included all eligible participants without respect to disease activity. The secondary population used data from study visits where the time-averaged CDAI was stable and remained within a single category from the enrolment. In analyses involving the secondary population, if a patient's time-averaged CDAI category changed, data from that visit and all subsequent visits for that patient were excluded from the analyses.

Study outcome

The primary outcome was a longitudinal change in the eGFR from enrolment. We calculated eGFR using the race-free CKD-EPI equation [25,26]. Secondary outcomes included development (first event in time) of Kidney Disease Improving Global Outcomes CKD stage 3a or worse (ie, eGFR<60 mL/min/1.73 m^2 for more than 3 months) and stage 3b or worse (ie, eGFR<45 mL/min/1.73 m^2 for more than 3 months) [18,19].

Exposures of interest

The exposure of interest was time-averaged RA disease activity from the registry enrolment, described as the category of time-averaged CDAI, updated at each visit. Time-averaged CDAI was used for evaluating cumulative longer-term RA disease activity. Time-averaged CDAI was based on the area under the curve for longitudinal CDAI. To calculate the area under the curve at a study visit, we used all data on CDAI and visit intervals until the study visit. Time-averaged CDAI was categorised using standard thresholds [27]: remission ≤2.8, low disease activity >2.8 to 10.0, moderate disease activity >10.0 to 22.0 and high disease activity >22.0. In addition, an alternative disease activity measure, Disease-Activity Score C reactive protein (DAS-CRP), was calculated and time-averaged. This measure was also categorised using the standard thresholds [28]: remission ≤2.6, low >2.6 to 3.2, moderate >3.2 to 5.1 and high disease activity >5.1. DAS-CRP categories with modified cut-offs [29] were also used for analyses.

Table 1
Patient characteristics at study enrolment by disease activity category

	No (%) or median (IQR)				
	Total N = 31 129	Remission (CDAI≤2.8) N = 6647	Low disease activity (CDAI 2.8–10.0) N = 10 028	Moderate disease activity (CDAI 10.0–22.0) N = 8548	High disease activity (CDAI>22) N = 5906
Age, years	58 (49, 66)	58 (48, 67)	59 (50, 67)	58 (49, 66)	57 (49, 65)
Female	23 758 (76.3)	4828 (72.6)	7584 (75.6)	6688 (78.2)	4658 (78.9)
Race white	25 610 (82.3)	5548 (83.5)	8369 (83.5)	7053 (82.5)	4640 (78.6)
Hispanic	2276 (7.3)	429 (6.5)	659 (6.6)	604 (7.1)	584 (9.9)
Black	1889 (6.1)	366 (5.5)	573 (5.7)	558 (6.5)	392 (6.6)
Asian	559 (1.8)	146 (2.2)	186 (1.9)	121 (1.4)	106 (1.8)
Others	795 (2.6)	158 (2.4)	241 (2.4)	212 (2.5)	184 (3.1)
Body mass index, kg/m^2	28.4 (24.5, 33.4)	27.3 (23.9, 31.7)	28.2 (24.4, 33.0)	29.0 (24.9, 34.4)	29.2 (25.0, 34.6)
Current smoker	3847 (12.4)	598 (9.0)	1181 (11.8)	1167 (13.7)	901 (15.3)
Previous smoker	8292 (26.6)	1754 (26.4)	2681 (26.7)	2302 (26.9)	1555 (26.3)
Calendar year	2012 (2008, 2016)	2012 (2008, 2016)	2011 (2008, 2016)	2012 (2008, 2017)	2012 (2008, 2016)
eGFR, mL/min/1.73 m^2	90.7 (77.9, 101.8)	88.9 (77.2, 100.3)	89.5 (77.2, 100.8)	91.4 (78.2, 102.5)	93.6 (80.2, 103.9)
Duration of rheumatoid arthritis, years	5.00 (1, 13)	6 (2, 12)	6 (2, 13)	5 (1, 13)	5 (1, 12)
Seropositive (positive RF or ACPA)	14 926/18 390 (81.2)	3125/3775 (82.8)	4703/5746 (81.8)	4142/5156 (80.3)	2956/3713 (79.6)
CDAI	9.1 (3.5, 18.5)	1.1 (0.5, 2.0)	6.0 (4.5, 8.0)	15.0 (12.4, 18.0)	31.0 (26.0, 39.2)
CRP, mg/L	4.30 (1.6, 10.0)	3.0 (1.0, 6.0)	4.0 (1.4, 8.2)	5.0 (2.0, 11.0)	6.3 (2.2, 16.6)
Secondary Sjogren's syndrome	8495 (27.3)	1142 (17.2)	2642 (26.3)	2650 (31.0)	2061 (34.9)
Treatment					
NSAIDs	13 465/28 652 (47.0)	2527/6119 (41.3)	4364/9238 (47.2)	3903/7856 (49.7)	2671/5439 (49.1)
GC use	9779 (31.4)	1246 (18.7)	2852 (28.4)	3157 (36.9)	2524 (42.7)
GC dose in users, mg/day (prednisolone equivalent)	4.0 (3.0, 5.0)	4.0 (2.0, 4.0)	4.0 (2.0, 4.0)	4.0 (3.0, 5.0)	4.0 (4.0, 6.0)
csDMARDs					
MTX	21 311 (68.5)	4515 (67.9)	6858 (68.4)	5863 (68.6)	4075 (69.0)
Other csDMARDs	10 542 (33.9)	2031 (30.6)	3406 (34.0)	3069 (35.9)	2036 (34.5)
Biological DMARDs	14 922 (47.9)	3126 (47.0)	4659 (46.5)	4120 (48.2)	3017 (51.1)
TNF inhibitors	11 931 (38.3)	2691 (40.5)	3859 (38.5)	3184 (37.2)	2197 (37.2)
Abatacept	1531 (4.9)	226 (3.4)	428 (4.3)	483 (5.7)	394 (6.7)
IL-6 receptor inhibitors	789 (2.5)	118 (1.8)	189 (1.9)	243 (2.8)	239 (4.0)
Rituximab	685 (2.2)	91 (1.4)	183 (1.8)	216 (2.5)	195 (3.3)
JAK inhibitors	741 (2.4)	107 (1.6)	219 (2.2)	244 (2.9)	171 (2.9)
Comorbidities					
Hypertension	8244 (26.5)	1414 (21.3)	2688 (26.8)	2378 (27.8)	1764 (29.9)
Diabetes	2216 (7.1)	345 (5.2)	647 (6.5)	696 (8.1)	528 (8.9)
Dyslipidaemia	5020 (16.1)	1012 (15.2)	1659 (16.5)	1400 (16.4)	949 (16.1)

ACPA, anticitrullinated protein antibodies; CDAI, Clinical Disease Activity Index; CRP, C reactive protein; csDMARDs, conventional synthetic disease-modifying antirheumatic drugs; eGFR, estimated glomerular filtration rate; GC, glucocorticoid; NSAIDs, non-steroidal anti-inflammatory drugs; RF, rheumatoid factor.

Covariates

Time-fixed covariates were assessed at enrolment and included age, sex, race (white, Hispanic, black, Asian and others), RA duration (years) and eGFR. Seropositivity was defined as positive rheumatoid factor (RF) and/or anticyclic citrullinated peptide antibody (ACPA) at any time during the study. Secondary Sjogren's syndrome was also defined based on having both dry eyes and dry mouth at any visits during the study period. Time-varying covariates were body mass index (BMI), smoking status (current smoker or not), comorbidities (diabetes, hypertension and dyslipidaemia), both prescribed and over-the-counter NSAIDs use, daily glucocorticoid dose (mg/day, prednisolone equivalent), MTX use, non-MTX conventional synthesised DMARDs use, each of biological DMARDs use (TNF inhibitors, IL-6 inhibitors, rituximab and abatacept) and target-synthesised DMARDs (JAK inhibitors) use. Time-varying covariates were updated at each study visit in both directions (ie, from absent to present and vice versa).

Statistical analyses

We described patient characteristics at registry enrolment by CDAI category. Multiple imputations with chained equations made 20 datasets to impute missing data [30]. While CRP and seropositive status had missing values of less than 40%, the proportion of missing data in other variables was 10% or less (online supplemental table 1).

For the primary outcome of eGFR change, we applied multivariable mixed-effect linear regression with random slope and random intercept to estimate the longitudinal eGFR change from enrolment. We set time as years from study enrolment, and we included a product term for time and time-averaged CDAI categories in the models; the coefficient of the product term identified the additive difference in annual eGFR change for low, moderate and high disease activity patients compared with patients in remission. This analysis was performed both in the primary population (all patient visits) and the secondary populations (used data from visits where the time-averaged CDAI remained in one category since enrolment).

Then, we performed stratified subgroup analyses according to the following variables at enrolment: median age (≥58 or <58 years), sex (male or female), BMI (overweight or obese: ≥25.0 or non-overweight: <25.0 kg/m^2), eGFR (≥90 or <90 mL/min/1.73 m^2), RA duration (early: ≤2 years or established: >2 years), NSAIDs use (yes or no), MTX use (yes or no) and bDMARDs use (yes or no). In addition, stratified analyses by CVD factors at enrolment, including current smoking (yes or

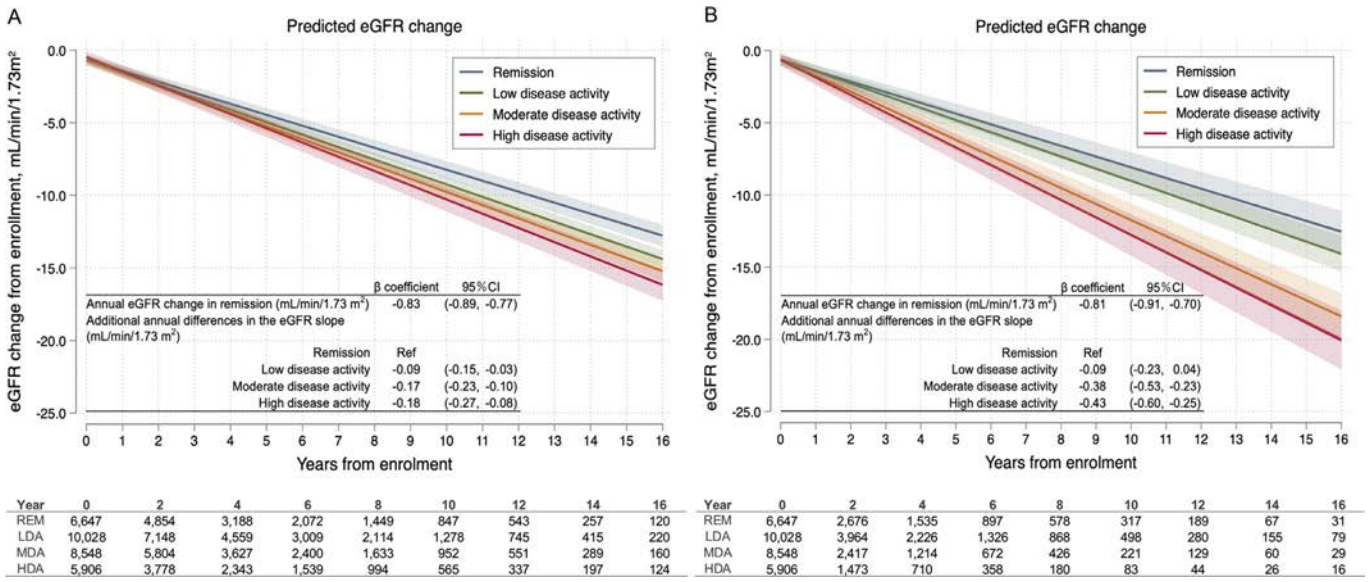

Year	0	2	4	6	8	10	12	14	16
REM	6,647	4,854	3,188	2,072	1,449	847	543	257	120
LDA	10,028	7,148	4,559	3,009	2,114	1,278	745	415	220
MDA	8,548	5,804	3,627	2,400	1,633	952	551	289	160
HDA	5,906	3,778	2,343	1,539	994	565	337	197	124

Year	0	2	4	6	8	10	12	14	16
REM	6,647	2,676	1,535	897	578	317	189	67	31
LDA	10,028	3,964	2,226	1,326	868	498	280	155	79
MDA	8,548	2,417	1,214	672	426	221	129	60	29
HDA	5,906	1,473	710	358	180	83	44	26	16

Figure 1. Estimated eGFR change by time-averaged CDAI category in the primary (A) and secondary population. (B) We calculated the predicted eGFR change for each visit of patients based on the results of multivariable mixed-effect linear regression adjusting for relevant covariates. We drew linear fitted lines with 95% CI areas by updated in time-averaged CDAI categories. Patient-specific covariates were used to estimate eGFR change in each patient. We used all visit data in this primary population analysis (A). In this secondary population analysis (B), we used data only from patient visits where the time-averaged CDAI was stable in one category from enrolment. CDAI, Clinical Disease Activity Index; DMARDs, disease-modifying antirheumatic drugs; eGFR, estimated glomerular filtration rate; HAD, high disease activity; LDA, low disease activity; MDA, moderate disease activity; REM, remission.

no), hypertension (yes or no), diabetes (yes or no), hyperlipidaemia (yes or no) and any of these CVD factors (yes or no), were also executed. Then, supplemental analyses in patients whose eGFR<60 mL/min/1.73 m^2 at enrolment were conducted. Finally, to evaluate non-linear association, we used a cubic polynomial model including quadric and cubic time from enrolment and their interaction with time-averaged CDAI categories.

For secondary outcomes (CKD stage G3a and CKD stage G3b), we performed the Kaplan-Meier survival analyses and Cox-proportional hazard regressions. The Cox proportional hazard model estimated the adjusted cause-specific HR for each time-averaged CDAI category, after controlling for both time-fixed and time-varying covariates.

Several sensitivity analyses were performed on the primary and secondary outcomes. Because of the complex relationships between RA disease activity and time-varying covariates, first, we changed time-varying covariates to time-fixed covariates at enrolment in the model. Then, we used time-averaged updated covariates instead of time-varying covariates. After that, we switched the exposure from time-averaged CDAI to DAS-CRP. Finally, we used a time-lag model where the association between outcomes at visit k and exposures at visit k−1 (k≥1; k−1 = 0 indicates enrolment) was examined to reduce the possible reverse causality. For all analyses, point estimates and 95% CIs were reported. All analyses were performed using STATA software (V.17.0, StataCorp).

Role of the funding source

The funders had no role in designing this study, data collection, statistical analysis, interpretation or the decision to approve the submission of the final manuscript.

RESULTS

Characteristics of study patients

47 547 patients had two or more study visits in the CorEvitas RA registry from October 2001 to September 2022. Patients were excluded from the study cohort for the following reasons: <2 measurements of creatinine (n = 7131 patients), baseline CDAI or serum creatinine was missing (n = 4642 patients), received no DMARDs treatment at baseline or during follow-up (n = 698 patients) and eGFR at baseline <60 mL/min/1.73 m^2 (n = 3947 patients). The final study population for the main analyses included 31 129 patients who contributed 234 973 visits and 146 778 person-years of follow-up (online supplemental figure 1).

At enrolment, the median (IQR) age was 58 (49–66) years, 76.3% of patients were female, 82.3% were white and 81.2% were seropositive (positive RF or ACPA) (table 1). Patients with higher disease activity tended to have more comorbidities and use more NSAIDs, glucocorticoids, biological DMARDs and JAK inhibitors. The median baseline eGFR was 90.7 (IQR 77.9 −101.8) mL/min/1.73 m^2. The median number of eGFR measurements during the study period was 5 (IQR 3–10) times (online supplemental figure 2). The median total follow-up was 3.5 (IQR 1.6–6.8) years. The median intervals between two consecutive visits were 0.52 (IQR 0.41–0.77) years (online supplemental figure 3). Longitudinal changes in the number of patients in each time-averaged CDAI category are visualised in online supplemental figure 2.

Disease activity of RA and eGFR slope

Patients with higher RA activity tended to have a larger absolute decline in eGFR compared with remission (online

supplemental table 2). In mixed-effect multivariable linear regression, the annualised eGFR decline in the RA remission group was −0.83 mL/min/1.73 m^2. Compared with patients in remission, the incremental additive annual mean rates of decline in eGFR (mL/min/1.73 m2) were −0.09 (95% CI −0.15 to −0.03) in low, −0.17 (95% CI −0.23 to −0.10) in moderate and −0.18 (95% CI −0.27 to −0.08) in high disease activity patients (figure 1). In the secondary population (used data from visits where time-averaged CDAI remained in one category from the enrolment), these additional changes tended to be larger with a mean annual eGFR change of −0.09 (95% CI −0.23 to 0.04) in low, −0.38 (95% CI −0.53 to −0.23) in moderate and −0.43 (95% CI −0.60 to −0.25) in high disease activity patients (figure 1).

Sensitivity analyses (using time-fixed or updated time-averaged covariates instead of time-varying covariates, alternative exposure of DAS-CRP and time-lag model) showed similar results (online supplemental table 2). The results did not change when we used modified cut-offs for DAS-CRP categories [29]. Stratified subgroup analyses showed these additional eGFR declines in higher disease activity patients were larger in early patients with RA, those with preserved renal function (eGFR≥90 mL/min/1.73 m^2) and patients who used no bDMARDs at enrolment (figure 2). The results in the subgroup analyses by CVD factors were similar to the main analysis results. The difference in annual eGFR declines tended to be slightly larger in those with any CVD factors (online supplemental figure 5). There was no clear trend between disease activity and eGFR decline in the supplementary analyses of patients with eGFR<60 mL/min/1.73 m^2 at enrolment (online supplemental table 3). Cubic polynomial models for time from enrolment showed that the differences in the eGFR decline between the groups became larger and more pronounced at later stages (online supplemental figure 3).

Disease activity of RA and development of CKD stage G3a and stage G3b

During a median follow-up of 3.5 years, 2118 patients developed CKD stage G3a (or worse) and 297 patients developed CKD stage G3b (or worse). Kaplan-Meier survival analyses demonstrated that patients with RA with higher disease activity more frequently developed CKD stage G3a and/or G3b (figure 3). The estimated adjusted HRs for new CKD G3a were 1.15 (95% CI 1.01 to 1.30) in low, 1.22 (95% CI 1.06 to 1.40) in moderate and 1.27 (95% CI 1.05 to 1.52) in high disease activity. For CKD stage G3b or worse, adjusted HRs were 1.22 (95% CI 0.84 to 1.76) in low, 1.66 (95% CI 1.12 to 2.45) in moderate and 1.93 (95% CI 1.16 to 3.20) in high disease activity when compared with remission (table 2). Larger differences were detected in the secondary population (online supplemental table 3 and figure 2). Sensitivity analyses (using time-fixed or updated time-averaged covariates instead of time-varying covariates, using DAS-CRP as an exposure and time-lag model) also showed similar dose–response associations (online supplemental table 4). Results were similar when modified cut-offs for DAS-CRP categories [29] were used.

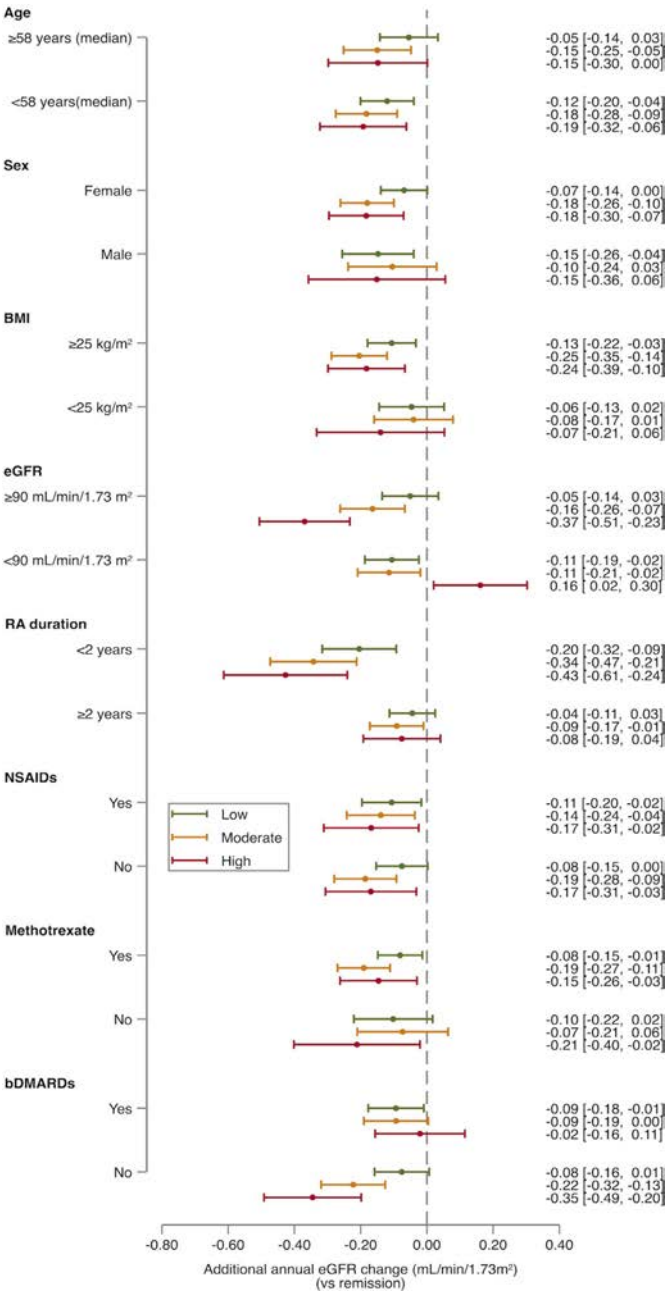

Figure 2. Subgroup analyses for associations between CDAI and annual eGFR decline. We adjusted for age, eGFR, duration of rheumatoid arthritis (RA) at enrolment, sex, race, seropositivity (rheumatoid factor or anticyclic citrullinated peptide antibody) and secondary Sjogren's syndrome as fixed covariates. Body mass index (BMI), smoking status, nonsteroidal anti-inflammatory drugs (NSAIDs) use, glucocorticoid dose, methotrexate use, non-methotrexate conventional synthesised DMARDs use, each of biological DMARDs (bDMARDs) use (TNF inhibitors, IL-6 inhibitors, rituximab and abatacept), target-synthesised DMARDs (JAK inhibitors) use and comorbidities (hypertension, diabetes and dyslipidaemia) were included as time-varying covariates. Reference was a remission group. CDAI, Clinical Disease Activity Index; DMARDs, disease-modifying antirheumatic drugs; eGFR, estimated glomerular filtration rate.

DISCUSSION

This current study evaluated the underappreciated longitudinal association between RA disease activity and changes in kidney function. After adjusting for potential confounders, we found that higher disease activity was associated with a larger annual decline in eGFR and increased rates of developing clinically relevant kidney function thresholds such as those defining CKD stage G3a and stage G3b.

Only a few studies have been published on RA disease activity and kidney outcomes. Two studies showed no association of disease activity with decreased kidney function, but these

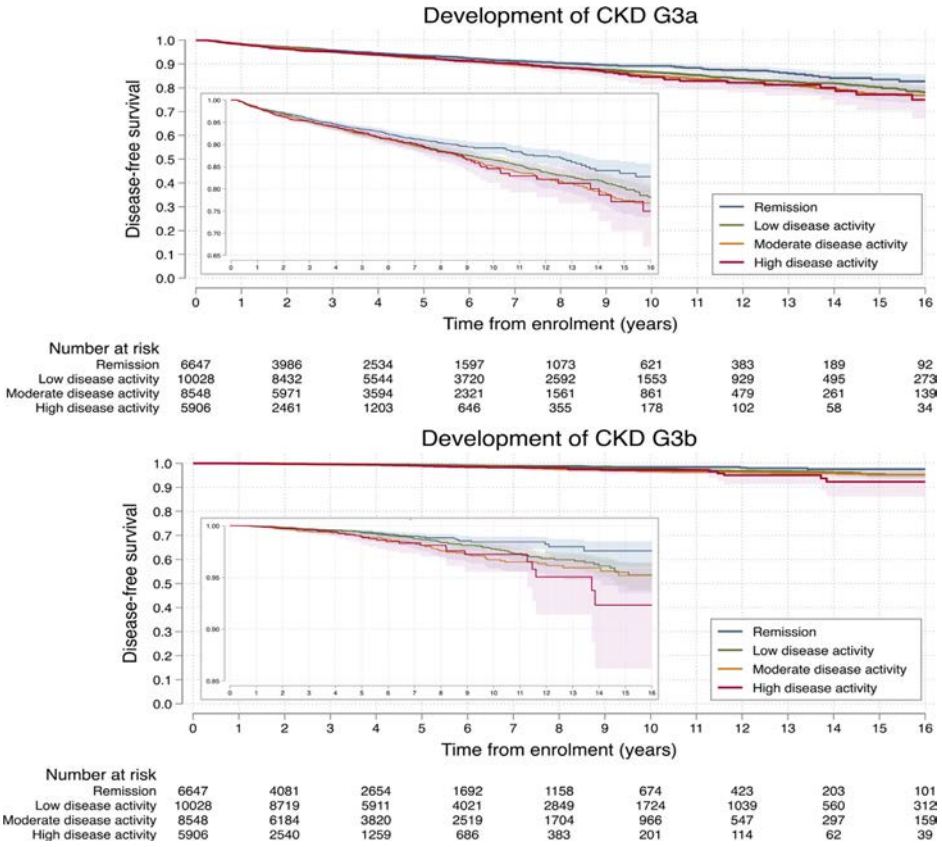

Figure 3. Disease-free survival curve for developing CKD stages G3a and G3b updated by time-averaged Clinical Disease Activity Index categories of rheumatoid arthritis. We defined CKD stage G3a as eGFR<60 mL/min/1.73 m^2 for more than 3 months and CKD stage G3b as eGFR<45 mL/min/1.73 m^2 for more than 3 months. Patients were allowed to move to other groups during the follow-up as the exposure was updated at each study visit. CKD, chronic kidney disease; eGFR, estimated glomerular filtration rate.

Table 2
Disease activity of rheumatoid arthritis and development of CKD≥G3a and ≥G3b

	CKD stage G3a or worse Adjusted HR (95%CI)	CKD stage G3b or worse Adjusted HR (95%CI)
Remission	Ref	Ref
Low disease activity	1.15 (1.01 to 1.30)	1.22 (0.84 to 1.76)
Moderate disease activity	1.22 (1.06 to 1.40)	1.66 (1.12 to 2.45)
High disease activity	1.27 (1.05 to 1.52)	1.93 (1.16 to 3.20)

We used all visit data in this primary population analysis. We used the Cox-proportional hazard model and adjusted for age, eGFR, duration of rheumatoid arthritis at enrolment, sex, race, seropositivity (rheumatoid factor or anti-cyclic citrullinated peptide antibody) and secondary Sjogren's syndrome as fixed covariates. Body mass index, smoking status, non-steroidal anti-inflammatory drugs use, glucocorticoid dose, methotrexate use, non-methotrexate conventional synthesised DMARDs use, each of biological DMARDs use (TNF tumour necrosis factor inhibitors, IL-6 inhibitors, rituximab and abatacept), target-synthesised DMARDs (JAK inhibitors) use and comorbidities (hypertension, diabetes and dyslipidaemia) were included as time-varying covariates.
CKD, chronic kidney disease; DMARDs, disease-modifying antirheumatic drugs; eGFR, estimated glomerular filtration rate; IL, interleukin; TNF, tumour necrosis factor.

studies investigated only cross-sectional associations [14,31]. One longitudinal study showed higher RA disease activity associated with a greater decrease in eGFR during a median follow-up of 1.3 years; the study did not evaluate the development of clinically relevant kidney dysfunction, such as incident CKD [32]. In another study of patients with RA using bDMARDs, 5-year averaged CDAI was higher in patients whose kidney function progressed to CKD than those without CKD progression [33]. One study found that higher baseline CRP levels over a 6-month period were associated with the onset of CKD in patients with RA [22]. This current study found a dose-dependent longitudinal association of higher RA disease activity with a larger decline in eGFR and the development of clinically relevant kidney function reductions in a large RA cohort with a relatively longer follow-up. HR can be considered similar to relative risk when the event is infrequent [34]. Based on the Kaplan-Meier estimates of CKD G3a in the remission group and adjusted HR of high RA disease activity, the estimated numbers needed to treat patients with high RA disease activity to achieve remission for preventing one CKD G3a would be 56.2 at year 5, 34.3 at year 10 and 22.4 at 15 years, if the association was causal. While the absolute differences in annual eGFR decline between disease activity categories were relatively small, we probably underestimated the difference due to the possible sarcopenia and overestimated eGFR in patients with higher RA disease activity. Based on the results from the secondary population, the eGFR would differ by 8.6 mL/min/1.73 m² after a 20-year follow-up between a patient who had consistently high disease activity and a patient who had been in remission throughout this period. This corresponds to approximately 10 years of accelerated kidney ageing.

The current study suggests that RA disease activity itself may be associated with accelerated kidney function decline. NSAID use, glucocorticoid use, diabetes and hypertension may relate to high disease activity, but these potential confounders were all included as time-varying covariates in multivariable regression models. Elevated inflammatory markers are associated with kidney dysfunction in patients with RA [22] and community-based

elderly cohort [35]. Potential aetiologies of kidney function impairment that may relate to RA disease activity and high inflammation include nephrosclerosis, amyloidosis and glomerulonephritis [21]. Based on a previous kidney biopsy study, with advancements in the treatment for RA, amyloidosis decreased over decades, and nephrosclerosis is becoming more common in patients with RA [24]. Several articles suggest mesangial-proliferative glomerulonephritis may occur in RA [36,37], and haematuria appears related to RA disease activity [38].

The results of the current study potentially suggest controlling the disease activity of RA may improve kidney outcomes. DMARD treatment improves systemic vascular inflammation in patients with RA [23] and potentially has a protective effect on nephrosclerosis. In fact, a secondary analysis of randomised controlled trials found that low-dose MTX has kidney protective effects in atherosclerotic patients [39]. Another previous study showed bDMARDs were associated with less CKD development [40]. Furthermore, chronic inflammation is an important process for the development and progression of kidney diseases, particularly diabetic kidney disease, and anti-inflammatory therapy is a potential treatment strategy for CKD [1,41].

In the current study, subgroup analyses found differences in the impact of higher disease activity on kidney function, as shown in figure 2. The influence was less pronounced in established patients with RA and high disease activity patients with mildly or moderately impaired kidney function at enrolment. As we estimated eGFR using serum creatinine in this study, long-standing RA with higher disease activity may be associated with less reliable eGFR; long-standing and active RA causes sarcopenia [42] and may result in overestimating kidney function [43]. Alternative methods, such as eGFR equations that use cystatin C, or those using timed urine collections or inulin clearance, are required to estimate kidney functions more precisely in those patients.

Strengths and limitations

This study had several strengths and limitations. Our prospective registry included a large number of patients from institutions all over the USA. Multiple study visits and longer follow-up enabled us to evaluate the longitudinal association between disease activity and kidney function outcomes over several years. Furthermore, this study used time-varying exposure and covariates, in contrast to most previous studies. We did not use principled causal analysis methods such as a marginal structural model to address possible exposure-outcome or exposure-confounder feedback. However, the results were consistent in multiple sensitivity analyses that treated confounders in different manners. We adjusted for over-the-counter NSAIDs use based on the questionnaire results, but our database did not collect details of NSAIDs. The lack of information on the types, doses and frequency of NSAIDs can be residual confounding. We acknowledge the limitation in estimating kidney function using serum creatinine and not cystatin C, but this likely biases the findings towards the null given that high disease activity leads to sarcopenia [42] and overestimating renal function [43]. We did not collect the severity of comorbidities, which may introduce residual confounding. Due to missing data at enrolment, we used information obtained after baseline to assess seropositivity. While this practice can lead to misclassification, RF and/or ACPA typically become positive years before an RA diagnosis and remain positive thereafter [44]. However, using future information may introduce potential immortal time bias. Finally, since our registry does not collect data on urinalyses and kidney biopsies, the cause and structural correlates of the decline in eGFR as well as the longitudinal association of RA activity with albuminuria cannot be determined.

CONCLUSIONS

In conclusion, we found higher RA disease activity was associated with larger declines in eGFR and the development of clinically relevant stages of CKD. This study suggests that controlling disease activity may potentially contribute to preserving kidney function in patients with RA. Further studies regarding the effect of different DMARDs on kidney function should be conducted to evaluate the potential of treatment strategies for kidney function preservation in patients with RA.

Acknowledgments

The authors would like to thank all the investigators, their clinical staff, and the patients who participate in the CorEvitas RA Registry.

Contributors

SF and DHS contributed to the original conception and design of this study, which WCW, SKT, JM, LH, HJL and TS reviewed and corrected. SF and HG collected data. SF performed data analysis with supervision from LH, HJL, TS and DHS. SF, WCW, SKT, JM and DHS initially interpreted the data, and other authors advised on the interpretation. SF drafted the original manuscript, which was critically reviewed and revised by all other authors. All authors have read and approved the final version of the manuscript. The corresponding author attests that all listed authors meet authorship criteria and that no others meeting the criteria have been omitted. SF is the guarantor.

Funding

This study was supported by funding from National Institute of Arthritis and Musculoskeletal and Skin Diseases P30 AR072577 (PI: DHS).

Competing interests

WCW reports having served as a scientific advisor or consultant to Actos, Akebia, Ardelyx, AstraZeneca, Bayer, Cadrenal, GlaxoSmithKline, Lilly, Merck, Natera, Pharmacosmos, Unicycive, Vera and Zydus. SKT reports consulting fees from Novartis. LH reports employment of CorEvitas, consultant to AbbVie, Bristol Myers Squibb, Pfizer, Roche and speakers bureau for Bristol Myers Squibb. DHS reports salary support through research contracts to his institution from CorEvitas, Janssen and Novartis.

Patient and public involvement

Patients and/or the public were not involved in the design, or conduct, or reporting, or dissemination plans of this research.

Patient consent for publication

Not applicable.

Ethics approval

This study involves human participants and all participants in the registry provided written informed consent prior to enrolment to the registry. Each participating institution obtained the appropriate institutional review board (IRB) approvals. The current study was approved by a Mass General Brigham IRB (2007P002533). Participants gave informed consent to participate in the study before taking part.

Data availability statement

No data are available. Data are not available publicly.

Supplementary materials

Supplementary material associated with this article can be found in the online version at doi:10.1136/ard-2024-226156.

REFERENCES

[1] Alicic RZ, Johnson EJ, Tuttle KR. Inflammatory Mechanisms as New Biomarkers and Therapeutic Targets for Diabetic Kidney Disease. Adv Chronic Kidney Dis 2018;25:181–91. doi: 10.1053/j.ackd.2017.12.002.

[2] Pichler R, Afkarian M, Dieter BP, et al. Immunity and inflammation in diabetic kidney disease: translating mechanisms to biomarkers and treatment targets. Am J Physiol Renal Physiol 2017;312:F716–31. doi: 10.1152/ajprenal.00314.2016.

[3] Tuttle KR. Linking metabolism and immunology: diabetic nephropathy is an inflammatory disease. J Am Soc Nephrol 2005;16:1537–8. doi: 10.1681/ASN.2005040393.

[4] Cross M, Smith E, Hoy D, et al. The global burden of rheumatoid arthritis: estimates from the global burden of disease 2010 study. Ann Rheum Dis 2014;73:1316–22. doi: 10.1136/annrheumdis-2013-204627.

[5] Helmick CG, Felson DT, Lawrence RC, et al. Estimates of the prevalence of arthritis and other rheumatic conditions in the United States. Part I. Arthritis Rheum 2008;58:15–25. doi: 10.1002/art.23177.

[6] Yamanaka H, Sugiyama N, Inoue E, et al. Estimates of the prevalence of and current treatment practices for rheumatoid arthritis in Japan using reimbursement data from health insurance societies and the IORRA cohort (I). Mod Rheumatol 2014;24:33–40. doi: 10.3109/14397595.2013.854059.

[7] Wiebe E, Huscher D, Schaumburg D, et al. Optimising both disease control and glucocorticoid dosing is essential for bone protection in patients with rheumatic disease. Ann Rheum Dis 2022;81:1313–22. doi: 10.1136/annrheumdis-2022-222339.

[8] Sparks JA, He X, Huang J, et al. Rheumatoid Arthritis Disease Activity Predicting Incident Clinically Apparent Rheumatoid Arthritis-Associated Interstitial Lung Disease: A Prospective Cohort Study. Arthritis Rheumatol 2019;71:1472–82. doi: 10.1002/art.40904.

[9] Solomon DH, Reed GW, Kremer JM, et al. Disease activity in rheumatoid arthritis and the risk of cardiovascular events. Arthritis Rheumatol 2015;67:1449–55. doi: 10.1002/art.39098.

[10] Yoshida K, Harrold LR, Middaugh N, et al. Time-Varying Association of Rheumatoid Arthritis Disease Activity to Subsequent Cardiovascular Risk. ACR Open Rheumatol 2022;4:587–95. doi: 10.1002/acr2.11432.

[11] Crowson CS, Liang KP, Therneau TM, et al. Could accelerated aging explain the excess mortality in patients with seropositive rheumatoid arthritis? Arthritis Rheum 2010;62:378–82. doi: 10.1002/art.27194.

[12] Chiu Y-M, Lu Y-P, Lan J-L, et al. Lifetime Risks, Life Expectancy, and Health Care Expenditures for Rheumatoid Arthritis: A Nationwide Cohort Followed Up From 2003 to 2016. Arthritis Rheumatol 2021;73:750–8. doi: 10.1002/art.41597.

[13] Mori S, Yoshitama T, Hirakata N, et al. Prevalence of and factors associated with renal dysfunction in rheumatoid arthritis patients: a cross-sectional study in community hospitals. Clin Rheumatol 2017;36:2673–82. doi: 10.1007/s10067-017-3804-5.

[14] Couderc M, Tatar Z, Pereira B, et al. Prevalence of Renal Impairment in Patients With Rheumatoid Arthritis: Results From a Cross-Sectional Multicenter Study. Arthritis Care Res (Hoboken) 2016;68:638–44. doi: 10.1002/acr.22713.

[15] Hickson LJ, Crowson CS, Gabriel SE, et al. Development of reduced kidney function in rheumatoid arthritis. Am J Kidney Dis 2014;63:206–13. doi: 10.1053/j.ajkd.2013.08.010.

[16] Tokoroyama T, Ando M, Setoguchi K, et al. Prevalence, incidence and prognosis of chronic kidney disease classified according to current guidelines: a large retrospective cohort study of rheumatoid arthritis patients. Nephrol Dial Transplant 2017;32:2035–42. doi: 10.1093/ndt/gfw315.

[17] Chiu H-Y, Huang H-L, Li C-H, et al. Increased Risk of Chronic Kidney Disease in Rheumatoid Arthritis Associated with Cardiovascular Complications - A National Population-Based Cohort Study. PLoS One 2015;10:e0136508. doi: 10.1371/journal.pone.0136508.

[18] Stevens PE, Levin A, Kidney Disease: Improving Global Outcomes Chronic Kidney Disease Guideline Development Work Group Members. Evaluation and management of chronic kidney disease: synopsis of the kidney disease: improving global outcomes 2012 clinical practice guideline. Ann Intern Med 2013;158:825–30. doi: 10.7326/0003-4819-158-11-201306040-00007.

[19] Kidney Disease: Improving Global Outcomes (KDIGO) CKD Work Group. KDIGO 2024 Clinical Practice Guideline for the Evaluation and Management of Chronic Kidney Disease. Kidney Int 2024;105:S117–314. doi: 10.1016/j.kint.2023.10.018.

[20] Sihvonen S, Korpela M, Mustonen J, et al. Renal disease as a predictor of increased mortality among patients with rheumatoid arthritis. Nephron Clin Pract 2004;96:c107–14. doi: 10.1159/000077372.

[21] Kapoor T, Bathon J. Renal Manifestations of Rheumatoid Arthritis. Rheum Dis Clin North Am 2018;44:571–84. doi: 10.1016/j.rdc.2018.06.008.

[22] Kochi M, Kohagura K, Shiohira Y, et al. Inflammation as a Risk of Developing Chronic Kidney Disease in Rheumatoid Arthritis. PLoS One 2016;11:e0160225. doi: 10.1371/journal.pone.0160225.

[23] Solomon DH, Giles JT, Liao KP, et al. Reducing cardiovascular risk with immunomodulators: a randomised active comparator trial among patients with rheumatoid arthritis. Ann Rheum Dis 2023;82:324–30. doi: 10.1136/ard-2022-223302.

[24] Sawamura M, Sawa N, Yamanouchi M, et al. Use of biologic agents and methotrexate improves renal manifestation and outcome in patients with rheumatoid arthritis: a retrospective analysis. Clin Exp Nephrol 2022;26:341–9. doi: 10.1007/s10157-021-02160-2.

[25] Delgado C, Baweja M, Crews DC, et al. A Unifying Approach for GFR Estimation: Recommendations of the NKF-ASN Task Force on Reassessing the Inclusion of Race in Diagnosing Kidney Disease. Am J Kidney Dis 2022;79:268–88. doi: 10.1053/j.ajkd.2021.08.003.

[26] Inker LA, Eneanya ND, Coresh J, et al. New Creatinine- and Cystatin C-Based Equations to Estimate GFR without Race. N Engl J Med 2021;385:1737–49. doi: 10.1056/NEJMoa2102953.

[27] Aletaha D, Smolen J. The Simplified Disease Activity Index (SDAI) and the Clinical Disease Activity Index (CDAI): a review of their usefulness and validity in rheumatoid arthritis. Clin Exp Rheumatol 2005;23:S100–8.

[28] Wells G, Becker J-C, Teng J, et al. Validation of the 28-joint Disease Activity Score (DAS28) and European League Against Rheumatism response criteria based on C-reactive protein against disease progression in patients with rheumatoid arthritis, and comparison with the DAS28 based on erythrocyte sedimentation rate. Ann Rheum Dis 2009;68:954–60. doi: 10.1136/ard.2007.084459.

[29] Inoue E, Yamanaka H, Hara M, et al. Comparison of Disease Activity Score (DAS)28- erythrocyte sedimentation rate and DAS28- C-reactive protein threshold values. Ann Rheum Dis 2007;66:407–9. doi: 10.1136/ard.2006.054205.

[30] White IR, Royston P, Wood AM. Multiple imputation using chained equations: Issues and guidance for practice. Stat Med 2011;30:377–99. doi: 10.1002/sim.4067.

[31] Daoussis D, Panoulas VF, Antonopoulos I, et al. Cardiovascular risk factors and not disease activity, severity or therapy associate with renal dysfunction in patients with rheumatoid arthritis. Ann Rheum Dis 2010;69:517–21. doi: 10.1136/ard.2008.105049.

[32] Onishi A, Akashi K, Yamamoto W, et al. The Association of Disease Activity and Estimated GFR in Patients With Rheumatoid Arthritis: Findings From the ANSWER Study. Am J Kidney Dis 2021;78:761–4. doi: 10.1053/j.ajkd.2021.02.338.

[33] Hanaoka H, Kikuchi J, Hiramoto K, et al. Decreased chronic kidney disease in rheumatoid arthritis in the era of biologic disease-modifying anti-rheumatic drugs. Clin Kidney J 2022;15:1373–8. doi: 10.1093/ckj/sfac036.

[34] VanderWeele TJ. Optimal approximate conversions of odds ratios and hazard ratios to risk ratios. Biometrics 2020;76:746–52. doi: 10.1111/biom.13197.

[35] Fried L, Solomon C, Shlipak M, et al. Inflammatory and prothrombotic markers and the progression of renal disease in elderly individuals. J Am Soc Nephrol 2004;15:3184–91. doi: 10.1097/01.ASN.0000146422.45434.35.

[36] Helin H, Korpela M, Mustonen J, et al. Mild mesangial glomerulopathy—a frequent finding in rheumatoid arthritis patients with hematuria or proteinuria. Nephron 1986;42:224–30. doi: 10.1159/000183671.

[37] Makino H, Yoshinaga Y, Yamasaki Y, et al. Renal involvement in rheumatoid arthritis: analysis of renal biopsy specimens from 100 patients. Mod Rheumatol 2002;12:148–54. doi: 10.3109/s101650200025.
[38] Koseki Y, Terai C, Moriguchi M, et al. A prospective study of renal disease in patients with early rheumatoid arthritis. Ann Rheum Dis 2001;60:327–31. doi: 10.1136/ard.60.4.327.
[39] Sparks JA, Vanni KMM, Sparks MA, et al. Effect of Low-Dose Methotrexate on eGFR and Kidney Adverse Events: A Randomized Clinical Trial. J Am Soc Nephrol 2021;32:3197–207. doi: 10.1681/ASN.2021050598.
[40] Sumida K, Molnar MZ, Potukuchi PK, et al. Treatment of rheumatoid arthritis with biologic agents lowers the risk of incident chronic kidney disease. Kidney Int 2018;93:1207–16. doi: 10.1016/j.kint.2017.11.025.
[41] Koshino A, Schechter M, Sen T, et al. Interleukin-6 and Cardiovascular and Kidney Outcomes in Patients With Type 2 Diabetes: New Insights From CANVAS. Diabetes Care 2022;45:2644–52. doi: 10.2337/dc22-0866.
[42] Bennett JL, Pratt AG, Dodds R, et al. Rheumatoid sarcopenia: loss of skeletal muscle strength and mass in rheumatoid arthritis. Nat Rev Rheumatol 2023;19:239–51. doi: 10.1038/s41584-023-00921-9.
[43] Okamura M, Konishi M, Butler J, et al. Kidney function in cachexia and sarcopenia: Facts and numbers. J Cachexia Sarcopenia Muscle 2023;14:1589–95. doi: 10.1002/jcsm.13260.
[44] Kelmenson LB, Wagner BD, McNair BK, et al. Timing of Elevations of Autoantibody Isotypes Prior to Diagnosis of Rheumatoid Arthritis. Arthritis Rheumatol 2020;72:251–61. doi: 10.1002/art.41091.

Ann Rheum Dis 84 (2025) 210–220

Contents lists available at ScienceDirect

Annals of the Rheumatic Diseases

journal homepage: https://www.sciencedirect.com/journal/annals-of-the-rheumatic-diseases

Rheumatoid arthritis

Peripheral blood immunophenotypic diversity in patients with rheumatoid arthritis and its impact on therapeutic responsiveness

Satoshi Kubo[1,2], Yusuke Miyazaki[2], Takahiro Nishino[3,4], Yuya Fujita[2], Michihiro Kono[3], Tsugumi Kawashima[3], Kazuyoshi Ishigaki[3,4], Katsuhide Kusaka[2], Hiroaki Tanaka[2], Masanobu Ueno[2], Yurie Satoh-Kanda[2], Yoshino Inoue[2], Yasuyuki Todoroki[1,2], Ippei Miyagawa[2], Kentaro Hanami[2], Shingo Nakayamada[2], Yoshiya Tanaka[2,*]

[1] *Department of Molecular Targeted Therapies, University of Occupational and Environmental Health, Japan, Kitakyushu, Japan*
[2] *The First Department of Internal Medicine, University of Occupational and Environmental Health, Japan, Kitakyushu, Japan*
[3] *Laboratory for Human Immunogenetics, RIKEN Center for Integrative Medical Sciences, Yokohama, Japan*
[4] *Department of Microbiology and Immunology, Keio University, Tokyo, Japan*

ARTICLE INFO

Article history:
Received 6 June 2024
Accepted 20 September 2024

Keywords:
rheumatoid arthritis
autoimmunity
T-lymphocytes

ABSTRACT

Objective: Considering the diverse aetiologies and immunodysregulatory statuses observed in each patient with rheumatoid arthritis (RA), stratification based on peripheral blood immunophenotyping holds the potential to enhance therapeutic responses to molecular targeted therapies, biological/targeted synthetic disease-modifying antirheumatic drugs (b/tsDMARDs).
Methods: Immunophenotype analysis was conducted on a cohort of over 500 b/tsDMARDs-naïve patients using flow cytometry. Patients with RA were stratified based on their immunophenotypes, and the treatment response to each targeted therapy was evaluated. Validation was performed using an additional cohort of 183 b/tsDMARDs-naïve patients with RA.
Results: Patients with RA were stratified into five clusters, two of which exhibited distinct RA phenotypes compared with controls, characterised by significant increases in $CD4^+$ effector memory T cells re-expressing CD45RA. Notably, the effectiveness of different b/tsDMARDs varied across clusters. The group using promising b/tsDMARDs was labelled as 'expected' whereas the 'non-expected' group comprised those using others. The expected group outperformed the non-expected group with higher 26-week remission rates (39.9% vs 24.6%, $p = 0.0004$) and low disease activity achievement (80.8% vs 60.2%, $p<0.0001$). Trajectory analysis showed the non-expected group's 26-week disease activity was influenced by Clinical Disease Activity Index at baseline unlike the expected group. Additionally, different molecular targeted therapies influenced the proportions of each immune cell subset variably. To validate, immunophenotyping was performed on a validation cohort. When 183 cases were grouped based on their b/tsDMARDs usage into expected/non-expected groups, the expected group had a higher remission rate ($p = 0.0021$), further confirming the observed trend.
Conclusion: Our findings offer valuable insights into the diversity of RA and potential therapeutic strategies grounded in the molecular underpinnings.

*Correspondence to Professor Yoshiya Tanaka.
E-mail address: tanaka@med.uoeh-u.ac.jp (Y. Tanaka).
Handling editor Josef S. Smolen

https://doi.org/10.1136/ard-2024-226228

WHAT IS ALREADY KNOWN ON THIS TOPIC

- Studies involving synovial membranes from patients with rheumatoid arthritis (RA) have revealed immunological diversity.
- Currently, there are no suitable biomarkers available for guiding treatment selection in phase II of the EULAR treatment recommendations.

WHAT THIS STUDY ADDS

- Immunophenotypes among patients with RA are not uniform; rather, they can be categorised into five major groups.
- Each cluster exhibited different responsiveness to various molecular targeted therapies including Janus kinase inhibitors, tumour necrosis factor inhibitors, interleukin-6 blockers and cytotoxic T lymphocyte-associated antigen 4-Ig.
- A subset identified as $CD4^+$ effector memory T cells re-expressing CD45RA exhibited an increase in several clusters, which could potentially contribute to the pathogenesis in patients with RA.

HOW THIS STUDY MIGHT AFFECT RESEARCH, PRACTICE OR POLICY

- Our study could mark a significant milestone in the pursuit of precision medicine for treating RA.

INTRODUCTION

Achieving precision medicine stands as a paramount objective across numerous diseases [1,2]. Precision medicine entails the stratification of patients to optimise therapeutic efficacy [3–5]. In the field of oncology, the identification of oncogenic mutations, coupled with the application of molecular targeted therapies tailored to these mutations, has demonstrated notable response rates [6,7]. Nevertheless, a precision medicine approach has yet to be established in any autoimmune rheumatic diseases [8–10]. Advancements in immunology, buttressed by insights gleaned from murine models, have played a pivotal role in the enhancement of rheumatoid arthritis (RA) treatment, while the heterogeneity among patients with RA has been consistently underestimated [8]. The strategy for managing RA has been delineated in the EULAR treatment recommendations, with the overarching objective of mitigating disease activity and thwarting joint destruction as the primary treatment goal [11,12]. The strategy comprises several phases, commencing treatment with methotrexate (MTX) at the onset of RA diagnosis (phase I), succeeded by combination with molecular targeted therapy in cases where MTX proves ineffective (phase II). In this treatment algorithm, an appropriate biomarker for the selection of molecular targeted therapies in phase II is still lacking. Identifying methods to select highly effective drugs from the beginning has been identified as an important clinical research agenda [11,13].

Presently, single-cell RNA sequencing affords high-resolution insights, enabling the ex vivo evaluation of patient specimens [14,15]. These analyses have unveiled the involvement of a novel cell type in the pathogenesis of RA [16,17]. In contrast to this approach, flow cytometry is acknowledged as a more conventional ex vivo methodology [18]. However, flow cytometry, despite being a more cost-effective method compared with single-cell analysis, offers valuable insights into protein expression levels.

In order to comprehend the diversity among patients with RA, we conducted an analysis of immunophenotypes in a cohort exceeding 700 biological/targeted synthetic disease-modifying antirheumatic drugs (b/tsDMARDs)-naïve patients via flow cytometry. The objective of this study was to stratify patients with RA based on immunophenotypes, laying the groundwork for the implementation of precision medicine.

METHODS

Human subjects and study design

The details of the study design are available in online supplemental methods. The overall design including patients' disposition is illustrated in online supplemental figure S1. Patients with RA who met the American College of Rheumatology/EULAR classification criteria and healthy subjects without autoimmune rheumatic diseases as controls participated in this study [19,20]. Cases from 2013 to 2021 underwent immunophenotyping for cluster classification as discovery cohort. The primary outcomes were the remission rate and the rate of achieving low disease activity at 26 weeks. Subsequently, cases from 2021 to 2023 were immunophenotyped in the same manner as the validation cohort. The primary statistical methods and power calculations were established at the beginning of the study. It was determined that 500 cases were necessary for the discovery cohort and 180 cases for the validation cohort to achieve sufficient statistical power. Further details on the power calculations can be found in the online supplemental methods.

Immune phenotyping via flow cytometry analysis

Immunophenotyping was conducted as previously described, and details can be found in online supplemental methods [21–23]. In brief, peripheral blood mononuclear cells (PBMCs) were isolated and phenotyping of immune cell subsets was conducted according to the Human Immunophenotyping Consortium protocol for comprehensive 8-colour flow cytometry analysis proposed by the National Institutes of Health/Federation of Clinical Immunology Societies, with some modifications specifically aimed at detecting T follicular helper (Tfh) cells [18]. The percentages of immunocompetent cells in immunophenotyping are presented as proportions within PBMCs.

Identification of peripheral blood cell abundance phenotypes based on immune cell type abundance

Immunophenotyping was conducted on all patients as described above, using cluster analysis to subdivide patients with RA. This subdivision was based on the percentage presence of each of the 34 immune cell subsets within the patient's PBMCs. Cluster analysis was conducted using the Ward method with Euclidean distance. Visualisation of the clusters by Uniform Manifold Approximation and Projection (UMAP) was performed using the R package umap V.0.2.9.0. The subdivisions of the clusters in the validation cohort were reclassified using the k-nearest neighbour (knn) function. More details of cluster analysis are available in online supplemental methods.

Cytoscape

Immunophenotypic figures were generated using Cytoscape, as previously described, and details can be found in online supplemental methods [23,24]. For each immune subset, the circle size was enlarged and coloured red when it was significantly elevated compared with 96 healthy controls, and reduced in size and coloured blue when it was significantly decreased.

Statistical analysis

Details have been described in online supplemental methods. A t-test was employed to detect differences in the proportion of immune cell subsets between healthy subjects and patients with RA in each cluster, with a significance level of $p<0.001$. The significance level for immunophenotypic differences between healthy subjects and patients with RA in each cluster after treatment was set at $p<0.002$. A paired t-test was used to compare the percentage of immune cell subsets before and after treatment. Differences in treatment effectiveness were evaluated using the χ^2 test after adjusting for inverse probability of treatment weighting based on propensity score (PS-IPTW), with a significance level of $p<0.05$ and the false discovery rate was calculated. To adjust for patient background bias, IPTW was used, employing propensity score matching.

RESULTS

Clinical characteristics

As the discovery cohort, 533 patients with RA who had not been treated with molecular targeted therapies were enrolled, along with 96 healthy controls without autoimmune rheumatic diseases. The patients had a mean age of 63.5 years, with 70.7% testing positive for anti-CCP antibodies (ACPA). MTX was administered in 71.1% of cases, and the mean Clinical Disease Activity Index (CDAI) was recorded at 27.1 (online supplemental table S1). Peripheral blood immunophenotyping via flow cytometry was conducted preceding the initiation of molecular targeted therapies. The immunophenotypes of the entire RA patient cohort are depicted in figure 1. In comparison with the healthy control, patients with RA exhibited pronounced aberrations in T-cell differentiation, notably marked by a substantial increase in the proportion of $CD4^+$ effector memory T cells re-expressing CD45RA (TEMRA), amounting to 6.9% as opposed to 3.7% in healthy control (figure 1). Additional observations included a reduction in $CD4^+$ central memory T cells (8.6% vs 10.8%), $CD8^+$-naïve T cells (4.4% vs 8.3%) and $CD8^+$ effector memory T cells (3.4% vs 4.8%). Within B cells, patients with RA manifested diminished frequencies of IgM memory B cells and class-switched B cells (figure 1).

On investigating these phenotypes in relation to disease activity, correlations were found between the CDAI and T helper 1 cell (Th1) and activated regulatory T cells (Treg) in the multivariate analysis (online supplemental table S2). Similarly, univariate analysis disclosed connections between ACPA titre and Tfh cells, plasmablasts and activated CD8 T cells. Nonetheless, in the multivariate analysis, ACPA values exhibited a correlation exclusively with activated CD8 T cells (online supplemental table S3).

Subgroups based on patients' background and peripheral immune phenotype

Precision medicine involves stratifying patients appropriately to achieve optimal therapeutic effects [3–5]. Therefore, before subdividing patients with RA through immunophenotyping, we assessed whether differences in treatment response could be discerned by segmenting patients based solely on their clinical backgrounds. Cluster analysis based on patient backgrounds revealed that patients with RA could be divided into five distinct clusters (figure 2A). The patient backgrounds for each cluster varied; for instance, cluster 2c predominantly consisted of younger patients with poor inflammatory responses, while cluster 5c comprised patients with very high disease activity, as detailed in online supplemental table S4. On analysing the clinical responses to molecular targeted therapies within these clusters, we observed no significant differences in response rates. Notably, all clusters demonstrated a tendency for enhanced effectiveness with Janus kinase (JAK) inhibitors, as depicted in figure 2B and detailed in online supplemental table S5. This trend may reflect the superior effectiveness of JAK inhibitors compared with other biologics in real-world clinical settings, a finding supported by several clinical trials [25–27]. These findings suggest that subclassifying patients based on existing clinical syndromes or serum markers may not effectively facilitate the development of precision medicine strategies.

Subsequently, to assess the diversity of peripheral blood immunophenotypes in patients with RA, we employed hierarchical clustering to subgroup the patients. Several statistical validations assessing the appropriateness of the number of clusters consistently indicated that five clusters were the most suitable (online supplemental figure S2A and B). As depicted in figure 2C, patients with RA were categorised into five distinct clusters, suggesting immunological heterogeneity among them. Furthermore, patients with RA were nearly evenly distributed across these clusters, as illustrated in figure 2D. To assess the similarity between stratification by immunophenotype and stratification by clinical background alone, we calculated the Adjusted Rand Index (ARI) and Normalised Mutual Information (NMI). The results, with an ARI of 0.004122 and an NMI of 0.01002, indicate that the two clustering methods produce distinct stratifications.

Next, the immunophenotypes of these clusters are illustrated in figure 2E. The figure depicts the proportions of each cell subset increased or decreased relative to 96 healthy controls in each cluster, represented by the size of the circle, with connecting lines denoting correlated cell population proportions. The clusters have been designated as peripheral blood cell abundance phenotypes (PCAPs), a naming convention inspired by the terminology used for clustering in the synovium of patients with RA [28]. In the PCAP-SD (slightly difference) cluster, there was a reduction in activated Tc1 cells and other cell types compared with healthy controls. In line with the percentage of healthy controls in the clusters (figure 2D), PCAP-LD (little difference) exhibited an immunophenotype nearly identical to that of healthy controls. PCAP-TB (T-cell and B-cell activation) manifested a simultaneous increase in activated $CD4^+$ T cells, $CD8^+$ T cells and plasmablasts, indicative of concurrent abnormalities in T-cell and B-cell differentiation. In contrast, both PCAP-T4 (TEMRA CD4) and PCAP-T4T1 (TEMRA CD4 and Th1) exhibited a pronounced augmentation in $CD4^+$ TEMRA. PCAP-T4 displayed an increase in effector memory T cells alongside $CD4^+$ TEMRA, while in PCAP-T4T1, there was an increase in Th1 cells in addition to $CD4^+$ TEMRA.

The clinical findings for these clusters are detailed in table 1. The disease activity measured by CDAI was higher in PCAP-TB. Similarly, Health Assessment Questionnaire, C reactive protein (CRP) and erythrocyte sedimentation rate (ESR) exhibited the highest values in PCAP-TB, although no discernible differences were observed among the remaining clusters. PCAP-LD exhibited the lowest mean age. These results indicated that the positivity rates of CRP and rheumatoid factor/ACPA fail to fully capture the extent of immunological dysregulation, suggesting the existence of clusters

		HC (n=96)	RA (n=533)	p value
CD4 T cells	Naive	19.7 ± 8.4	22.4 ± 12.3	0.039
	Central memory	10.8 ± 5.8	8.6 ± 5.1	<0.001
	Effector memory	11.5 ± 4.7	13.3 ± 6.8	0.016
	Terminal Effector RA	3.7 ± 4.1	6.9 ± 7.1	<0.001
	Activated	0.7 ± 0.4	0.7 ± 0.9	0.428
CD8 T cells	Naïve	8.3 ± 6.4	4.4 ± 4.1	<0.001
	Central memory	1.3 ± 1.2	1.0 ± 1.2	0.011
	Effector memory	4.8 ± 2.9	3.4 ± 3.0	<0.001
	Terminal Effector RA	6.2 ± 5.0	6.4 ± 5.2	0.687
	Activated	0.7 ± 0.7	0.9 ± 1.4	0.294
CD4 T cell subsets	Th1	8.9 ± 3.5	10.0 ± 4.1	0.018
	Activated Th1	0.3 ± 0.3	0.3 ± 0.3	0.173
	Th17	4.8 ± 2.2	4.7 ± 2.6	0.584
	Activated Th17	0.09 ± 0.06	0.07 ± 0.06	0.002
	Tfh	0.4 ± 0.2	0.4 ± 0.5	0.456
	Activated Tfh	0.05 ± 0.04	0.06 ± 0.13	0.139
	Naive Treg	0.03 ± 0.04	0.04 ± 0.12	0.468
	Memory Treg	0.6 ± 0.4	0.5 ± 0.4	0.022
	Activated Treg	0.3 ± 0.2	0.2 ± 0.2	0.003
CD8 T cell subsets	Tc1	10.3 ± 5.5	7.2 ± 4.5	<0.001
	Activated Tc1	0.4 ± 0.5	0.3 ± 0.5	0.776
	Tc17	1.3 ± 1.4	0.5 ± 0.8	<0.001
	Activated Tc17	0.02 ± 0.01	0.02 ± 0.05	0.042
B cells	Naive	3.0 ± 2.2	3.2 ± 2.3	0.512
	IgM memory	0.2 ± 0.2	0.1 ± 0.1	<0.001
	Class switched memory	0.9 ± 0.7	0.6 ± 0.6	<0.001
	Double negative	0.6 ± 0.5	0.6 ± 0.7	0.888
	Plasmablasts	0.2 ± 0.2	0.3 ± 0.4	0.234
NK cells	$CD16^+$ NK cell	11.6 ± 7.4	10.8 ± 7.7	0.851
	$CD16^-$ NK cell	0.8 ± 0.5	0.8 ± 1.0	0.365
Monocytes	Classical	13.3 ± 6.5	13.5 ± 8.4	0.766
	Non classical	1.5 ± 1.2	1.7 ± 1.5	0.299
Dendritic cells	Myeloid	1.9 ± 0.9	2.2 ± 1.5	0.128
	Plasmacytoid	0.2 ± 0.1	0.3 ± 0.2	0.037

Figure 1. Differences in the phenotype of lymphocytes, monocytes and dendritic cells and NK cells between patients with RA and healthy control subjects. The p values were calculated using Student's t-test with a significance level of p<0.001. The degrees of the change were indicated by colour compared with healthy controls (blue for decrease and red for increase). HC, healthy control; NK, natural killer; RA, rheumatoid arthritis; Tc1, cytotoxic T lymphocyte 1; Tc17, cytotoxic T lymphocyte 17; Tfh, T follicular helper cell; Th1, T helper 1 cell; Th17, T helper 17 cell; Treg, regulatory T cell.

that are indiscernible using conventional clinical symptoms and serum biomarkers.

Immunophenotypic subgroups exhibit differential responses to molecular targeted therapies

We next investigated whether these clusters could predict treatment response when using molecular targeted therapies, including tumour necrosis factor (TNF) inhibitors, interleukin (IL)-6 inhibitors, cytotoxic T lymphocyte-associated antigen 4-Ig (CTLA4-Ig) and JAK inhibitors. Online supplemental table S6 provides a detailed breakdown of the molecular targeted drugs used in each cluster, illustrating variations in the proportions of b/tsDMARDs employed across the clusters (p = 0.0401). To evaluate the effectiveness of molecular targeted therapies within the clusters, we used PS-IPTW. This approach enables adjustment for potential biases in patient backgrounds associated with each drug. Detailed patient backgrounds are presented in online supplemental tables S7–11. The analysis revealed that the drugs most likely to achieve clinical remission or low disease activity varied among the clusters (online supplemental table S12). In PCAP-SD, JAK inhibitors exhibited notable efficacy, despite their relatively low usage rate, resulting in an 86.8% rate of patients achieving clinical remission and 100% achieving low disease activity at 6 months. In PCAP-LD, alongside JAK inhibitors, IL-6 inhibitors demonstrated considerable effectiveness, with 86.4% of patients achieving low disease activity within 6 months. Within PCAP-T4, TNF inhibitors and JAK inhibitors proved highly effective, with 84.2% and 78.3% of patients achieving low disease activity after 6 months, respectively. In PCAP-T4T1, CTLA4-Ig and JAK inhibitors demonstrated noteworthy efficacy, resulting in 39.8% and 44.4% of patients

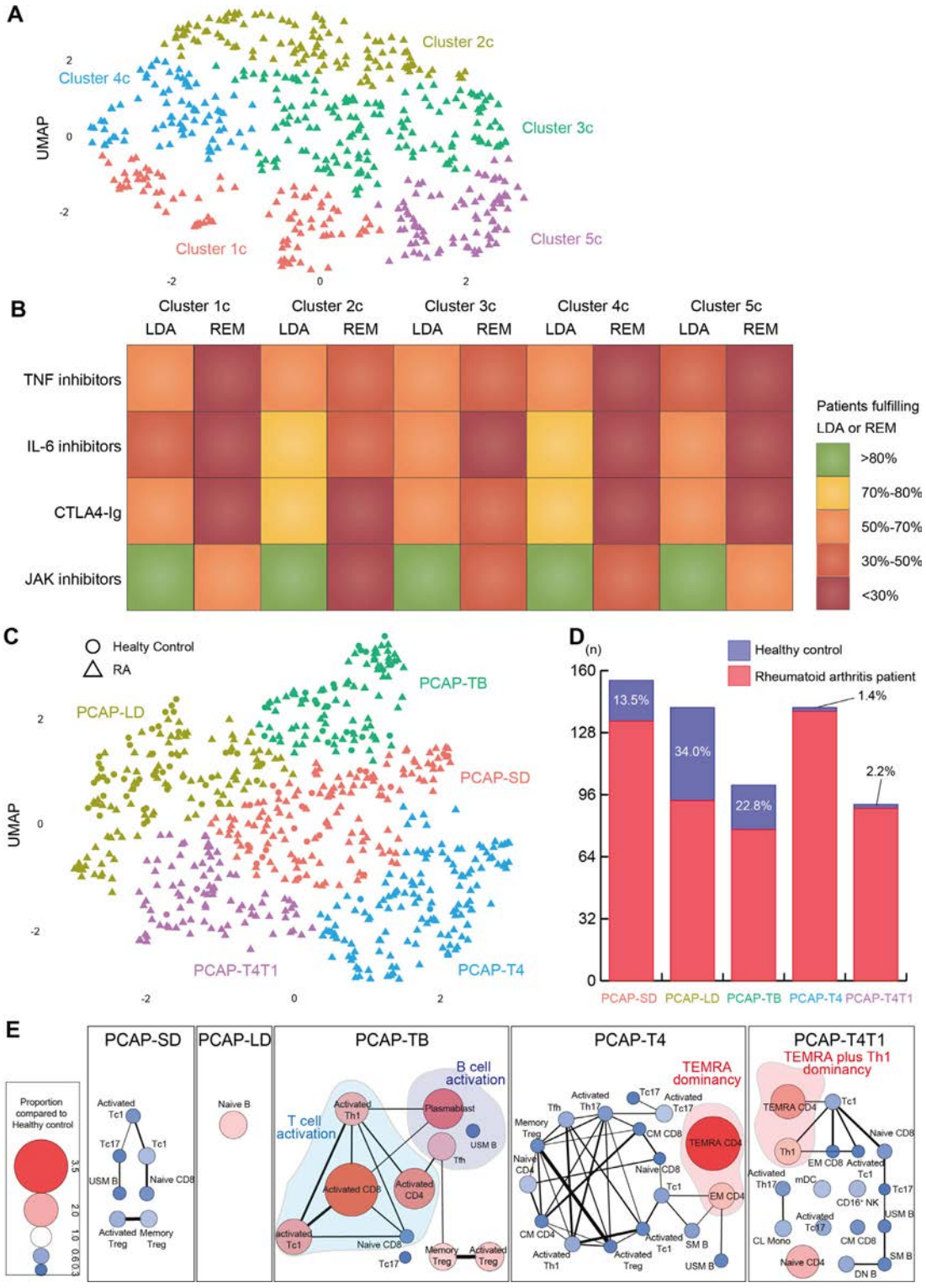

Figure 2. Subgrouping patients with RA through immunophenotyping. (A) Each cluster resulting from subgrouping based on the patients' background is visualised by UMAP. (B) Remission and low disease activity achievement rates to different therapies within each cluster based on the patients' background. (C) Each PCAP resulting from subgrouping is visualised by UMAP. (D) The count of healthy controls and patients with RA in each cluster. (E) The visualised model based on the immunophenotyping in each cluster. The colour (blue for decreases and red for increases) and size of circle indicates the ratio of each immune cell proportion in comparison with the average of healthy controls as shown in the right box. Each line shows the statistical positive correlation between immune cells. CL Mono, classical monocyte; CM, central memory; CTLA4, cytotoxic T lymphocyte-associated antigen 4; DN B, double negative B cell; EM, effector memory; IL, interleukin; JAK, Janus kinase; LDA, low disease activity; mDC, myeloid dendritic cell; NK, natural killer; PCAP-LD, peripheral blood cell abundance phenotypes-little difference; PCAP-SD, peripheral blood cell abundance phenotypes-slightly difference; PCAP-TB, peripheral blood cell abundance phenotypes T-cell and B-cell activation; RA, rheumatoid arthritis; REM, remission; SM B, class-switched memory B cell; Tc1, cytotoxic T lymphocyte 1; Tc17, cytotoxic T lymphocyte 17; TEMRA, effector memory cells re-expressing CD45RA; Tfh, T follicular helper cell; Th1, T helper 1 cell; Th17, T helper 17 cell; TNF, tumour necrosis factor; Treg, $CD4^+$ regulatory T cell; UMAP, Uniform Manifold Approximation and Projection; USM B, IgM memory B cell.

Table 1
Baseline demographic and clinical characteristics of patients with RA in each cluster

Variable	PCAP-SD (n=134)	PCAP-LD (n=93)	PCAP-TB (n=78)	PCAP-T4 (n=139)	PCAP-T4T1 (n=89)	P value
Age (years)	64.0 (12.1)	54.0 (15.2)	68.0 (12.3)	66.7 (12.6)	63.9 (13.9)	<0.0001
Sex, n (% female)	101 (75.4)	70 (75.3)	57 (73.1)	104 (74.8)	75 (84.3)	0.4244
Disease duration (month)	70.3 (88.3)	77.1 (117.7)	78.6 (111.1)	82.4 (121.3)	79.3 (110.9)	0.9059
Steinbrocker's stage, I/II/III/IV, %	31/44/17/8	38/48/5/9	30/45/8/18	32/48/12/9	27/45/16/12	0.1613
MTX use at baseline, n (%)	99 (73.9)	69 (74.2)	37 (47.4)	98 (70.5)	76 (85.4)	<0.0001
MTX dose mg/week at baseline	12.3 (4.0)	13.1 (3.4)	11.4 (3.7)	11.9 (3.7)	12.5 (3.3)	0.1539
Other csDMARDs use at baseline, n (%)	16 (11.9)	8 (8.6)	15 (19.2)	23 (16.6)	5 (5.6)	0.0336
Glucocorticoid use at baseline, n (%)	19 (14.2)	20 (21.5)	24 (30.8)	31 (22.3)	25 (28.1)	0.0392
Glucocorticoid dose mg/day at baseline	8.7 (12.6)	13.1 (17.2)	17.5 (19.4)	9.3 (13.9)	7.2 (10.8)	0.1232
28-tender joint count	7.9 (5.3)	9.0 (6.4)	10.3 (6.5)	9.3 (5.7)	8.2 (6.2)	0.0463
28-swollen joint count	7.4 (4.6)	7.7 (5.1)	9.1 (5.4)	8.4 (5.3)	8.4 (5.2)	0.1321
GH (mm)	52.9 (24.8)	50.7 (21.4)	57.5 (24.1)	53.2 (23)	51.7 (25.6)	0.2211
Pain-VAS (mm)	55.5 (25.5)	50.8 (24.4)	53.0 (28.5)	53.7 (26.2)	50.9 (27.8)	0.8383
CDAI	25.1 (10.6)	26.2 (11.4)	30.3 (12.3)	27.7 (10.7)	26.5 (12.3)	0.0137
HAQ-DI	1.2 (0.8)	1.1 (0.7)	1.5 (0.8)	1.3 (0.8)	1.3 (0.9)	0.0035
CRP (mg/dL)	2.2 (3.0)	2.0 (3.0)	3.5 (4.3)	2.3 (3.3)	2.6 (3.7)	0.0092
ESR (mm/hour)	48.5 (30.0)	40.2 (28.4)	63.1 (27.5)	51.4 (32.1)	48.6 (32.7)	<0.0001
Rheumatoid factor (U/mL)	121.5 (236.9)	171.4 (418.5)	274.5 (523.3)	207.7 (1073.4)	151.7 (315.4)	0.0111
Rheumatoid factor, positive, n (%)	109 (81.3)	68 (73.1)	62 (79.5)	112 (80.6)	65 (73.0)	0.3943
Anti-CCP antibody (U/mL)	339.8 (567.1)	270.5 (722.95)	439.6 (645.761)	442.7 (1224.9)	222.2 (363.7)	0.1367
Anti-CCP antibody, positive, n (%)	93 (69.4)	65 (69.9)	56 (71.8)	101 (72.7)	62 (69.7)	0.9747
MMP-3 (ng/mL)	224.6 (271.4)	188.7 (246.2)	290.2 (447.4)	192.6 (251.3)	257.4 (354.6)	0.0666

CCP, cyclic citrullinated peptide; CDAI, Clinical Disease Activity Index; CRP, C reactive protein; csDMARDs, conventional synthetic disease-modifying antirheumatic drugs; ESR, erythrocyte sedimentation rate; GH, growth hormone; HAQ-DI, Health Assessment Questionnaire-Disability Index; MMP-3, matrix metalloproteinase-3; MTX, methotrexate; PCAP-LD, peripheral blood cell abundance phenotypes-little difference; PCAP-SD, peripheral blood cell abundance phenotypes-slightly difference; PCAP-TB, peripheral blood cell abundance phenotypes T-cell and B-cell activation; RA, rheumatoid arthritis; VAS, Visual Analogue Scale.

achieving remission after 6 months (online supplemental table S12). Conversely, PCAP-TB stood out as the only cluster where none of the drugs resulted in a remission rate surpassing 30%, with approximately half of the patients treated with IL-6 inhibitors and CTLA4-Ig still exhibiting moderate or high disease activity after 6 months. The responsiveness trends for each of these clusters were similar when using Disease Activity Score (DAS)28 (ESR) and Boolean remission criteria. However, IL-6 inhibition reduces the inflammatory response, so for DAS28 (ESR), both IL-6 inhibitors and JAK inhibitors increased the apparent efficacy compared with the analysis with CDAI (online supplemental table S13).

In summary, although it is important to note that the relatively low usage of JAK inhibitors across all clusters and the modest utilisation of IL-6 inhibitors in the PCAP-LD cluster, JAK inhibitors were consistently linked to increased efficacy. Additionally, PCAP-LD exhibited increased effectiveness with IL-6 inhibition, PCAP-T4 with TNF inhibition and PCAP-T4T1 with CTLA4-Ig (figure 3A). Subsequently, to evaluate the variance in efficacy when preferred b/ts DMARDs were used, we divided the patients into two groups: the expected b/tsDMARDs group, where promising agents were used and the non-expected b/tsDMARDs group, where they were not used. Molecular targeted therapies with statistically higher remission or low disease activity rates in each cluster were selected as expected b/tsDMARDs, with the exception of PCAP-TB. In PCAP-TB, where no agents showed significantly higher efficacy, TNF inhibitors and JAK inhibitors, which had numerically higher rates of achieving low disease activity, were chosen for the expected b/tsDMARDs group. Consequently, 153 patients were assigned to the expected group (ie, PCAP-SD: JAK inhibitor, PCAP-LD: JAK inhibitor and IL-6 inhibitor, PCAP-TB: JAK inhibitor and TNF inhibitor, PCAP-T4: JAK inhibitor and TNF inhibitor, PCAP-T4T1: JAK inhibitor and CTLA4-Ig) and 380 to the non-expected group (online supplemental table S14). The clinical background differences between the expected b/tsDMARDs group and the non-expected b/tsDMARDs group are presented in online supplemental table S15. Patient backgrounds in the two groups were homogenised using PS-IPTW to identify the statistical differences in remission rates and the rate of achieving low disease activity after 26 weeks (online supplemental table S15). The Sankey diagram visually illustrates the transition of disease activity between the expected b/tsDMARDs group and the non-expected b/tsDMARDs group (figure 3B). The analysis revealed that the expected b/tsDMARDs group exhibited significantly higher remission rates (39.9% vs 24.6%, p=0.0004) and a higher rate of achieving low disease activity (80.8% vs 60.2%, p<0.0001) compared with the non-expected b/tsDMARDs group (online supplemental table S16).

TNF inhibitors, the efficacy of which was ambiguous in PCAP-TB, were reclassified as non-expected group and subjected to further analysis. The remission rates were 40.9% and 25.3% (expected b/tsDMARDs group vs non-expected b/tsDMARDs group, p=0.0007), respectively (online supplemental table S17). Additionally, the rates of achieving low disease activity were 81.0% and 62.5% (expected b/tsDMARDs group vs non-expected b/tsDMARDs group, p<0.0001). Similarly, when JAK inhibitors were excluded from all cases, taking into account the relatively small number of JAK inhibitor cases, the remission achievement rates were 36.8% and 24.9% for expected versus non-expected, respectively (p=0.0151, online supplemental table S18). Additionally, the rates of achieving low disease activity were 78.5% and 60.8% (p=0.0007). These results were consistent with the original findings.

To delve into the heterogeneity within these two groups and to provide a clearer visualisation of the changes over time, trajectory analysis was employed. The optimal fit for the linear model of the trajectory was cubic for both groups (online

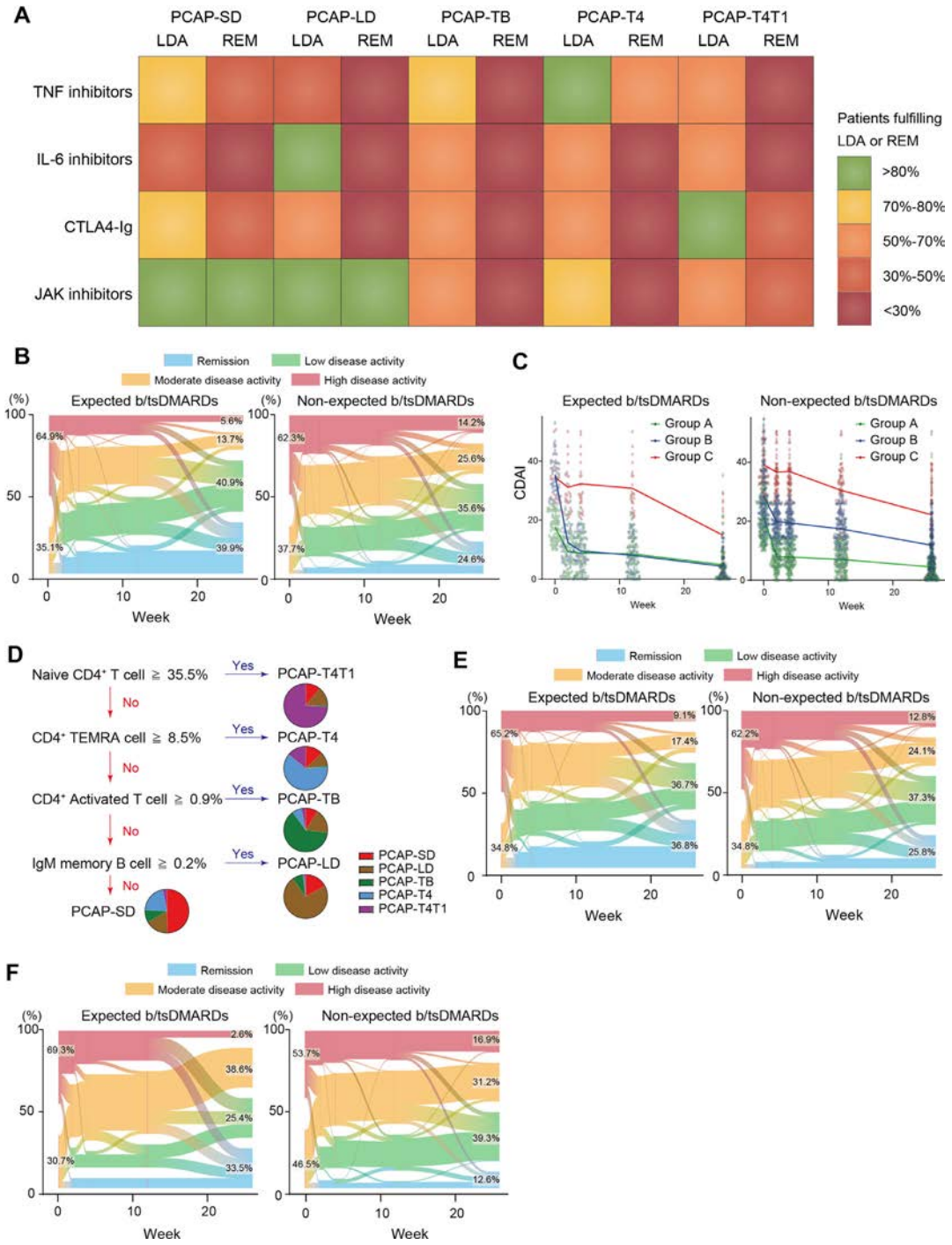

Figure 3. Effectiveness of different molecular targeted therapies within each cluster among patients with rheumatoid arthritis. (A) REM and LDA achievement rates to different therapies within each cluster. (B) Sankey diagram illustrating proportion of patients per CDAI disease activity category over time in the discovery cohort. The values displayed in the graph are calculated using PS-IPTW. However, as the data using PS-IPTW cannot be represented in a Sankey diagram, the graph is illustrated using the raw data before PS-IPTW. (C) Lines represent locally estimated scatter plot smoothing trajectories for the three patient trajectory groups. Dots depict changes in CDAI for all patients. Group A is indicated by the green line and dots, group B by the blue line and dots and group C by the red line and dots. (D) Results of decision tree analysis when each cluster is represented by a reduced set of immune cell subsets. The pie chart illustrates the percentage assigned to the original cluster. (E) Sankey diagram illustrating proportion of patients per CDAI disease activity category over time, comparing two groups according to the reduced set of immune cell subsets. The values displayed in the graph are calculated using PS-IPTW. However, as the data using PS-IPTW cannot be represented in a Sankey diagram, the graph is illustrated using the raw data before PS-IPTW. (F) Sankey diagram illustrating proportion of patients per CDAI disease activity category over time in the validation cohort. The values displayed in the graph are calculated using PS-IPTW. However, as the data using PS-IPTW cannot be represented in a Sankey diagram, the graph is illustrated using the raw data before PS-IPTW. b/tsDMARDs, biological/targeted synthetic disease-modifying antirheumatic drugs; CDAI, Clinical Disease Activity Index; CTLA4-Ig, cytotoxic T lymphocyte-associated antigen 4-Ig; IL, interleukin; JAK, Janus kinase; LDA, low disease activity; PCAP-LD, peripheral blood cell abundance phenotypes-little difference; PCAP-SD, peripheral blood cell abundance phenotypes-slightly difference; PCAP-TB, peripheral blood cell abundance phenotypes T-cell and B-cell activation; PS-IPTW, inverse probability of treatment weighting based on propensity score; REM, remission; TNF, tumour necrosis factor.

supplemental table S19 and 20). It was observed that both the expected b/tsDMARDs group and the non-expected b/tsDMARDs group exhibited three major changing patterns over time (figure 3C). Among these trajectories, the most notable difference between the two groups was observed in trajectory B. In the expected group, some patients with high disease activity showed a favourable progression after the second week, similar to trajectory A. The difference in trajectory B was identified as the most significant distinction between the expected and non-expected groups.

Furthermore, to explore the potential for clustering without using all immunophenotypes, we attempted to classify each cluster using decision tree analysis with a reduced set of immune cells. The results indicated that using only $CD4^+$-naïve T cell, $CD4^+$ TEMRA, activated $CD4^+$ and IgM memory B cell values could to some extent classify the patients into five clusters based on immunophenotype (figure 3D and online supplemental table S21). When the analysis was conducted within clusters divided solely by these four immune cell subsets, the remission achievement rate was 36.2% and 25.7% ($p=0.0159$) for expected versus non-expected, respectively (figure 3E). Additionally, the low disease activity achievement rate was 73.0% and 63.5% ($p=0.0361$), demonstrating similar trends (figure 3E). Nevertheless, the disparity in efficacy was more pronounced in clusters categorised by the complete immunophenotype than in clusters divided by only four cell populations.

At last, cluster analysis was conducted by integrating immunophenotyping with clinical background data to assess differences in the efficacy of molecular targeted therapies. Clustering facilitated the division of patients with RA into five distinct clusters, revealing more pronounced differences in response to each molecular targeted therapy compared with clustering based solely on clinical patient backgrounds (online supplemental figure S3A and B, online supplemental table 22). However, these differences in responsiveness were less pronounced than those observed when clustering by immunophenotype alone. These results suggest that differences in immunophenotype, typically less visible in routine clinical practice, are more influential than clinical background in selecting appropriate therapies.

These findings indicate that the subgrouping based on immunophenotyping exhibited varying treatment responsiveness, suggesting that the use of suitable molecular targeted therapies could result in favourable subsequent outcomes.

Validation of clustering of patients with RA to enhance treatment effectiveness

We sought to validate these findings by analysing an additional cohort of 183 patients who had not undergone treatment with molecular targeted therapies. As a validation cohort, immunophenotyping was conducted before initiating molecular target therapies. Subsequently, employing the knn method, each case in the validation cohort was allocated to a cluster by identifying three original cases ($k=3$) with phenotypes closely resembling that of each case (online supplemental figure S4). The allocated cluster was kept undisclosed from the attending physician and patient, and each patient received molecular targeted therapy chosen and administered through shared decision-making. The patients were then categorised into the expected b/tsDMARDs group ($n=38$) and non-expected b/tsDMARDs group ($n=145$) based on the molecular targeted therapy they used and the criteria applied in the discovery cohort (online supplemental table S23). The percentage of use of each molecular targeted therapy in the assigned clusters is provided in online supplemental table S24. The use of JAK inhibitors decreased significantly in the validation cohort following the results of the Oral Rheumatoid Arthritis Trial (ORAL) Surveillance study [29]. However, since JAK inhibitors originally belonged to the expected b/tsDMARDs group with high efficacy in all clusters, the validation results were not affected. Disease activity at 26 weeks was assessed after applying PS-IPTW to adjust for potential bias in patient backgrounds in both groups (online supplemental tables S25 and 26). As illustrated in figure 3F, disease activity at 26 weeks was superior in the expected b/tsDMARDs group (online supplemental table S27). Notably, the remission rate was more than twice as high in the expected b/tsDMARDs group (33.5% vs 18.2% in the non-expected b/tsDMARDs group, $p=0.0021$). The efficacy of each drug in each cluster is shown in online supplemental table S28.

In summary, the clustering based on peripheral blood immunophenotyping demonstrates the potential to optimise the efficacy of each molecular targeted therapy.

Immunophenotype after treatment

Next, we examined the immunophenotype of each cluster after treatment. Notably, in PCAP-TB, T-cell and B-cell differentiation abnormalities changed, leading to the disappearance of elevated activated T cells and plasmablasts after treatment (figures 2E and 4A). Conversely, clusters 4 and 5 showed residual elevations in $CD4^+$ TEMRA after treatment. Figure 4B displays the changes in the percentage of $CD4^+$ T-cell differentiation subsets, including $CD4^+$ TEMRA. On assessing the impact of each drug on the proportion of $CD4^+$ TEMRA, abatacept exhibited the most pronounced reduction (figure 4B). Figure 4C illustrates the percentage change in various immunocompetent cells before and after treatment. Abatacept induced a reduction in the percentage of several $CD4^+$ T cell subsets, marking a distinct alteration from other molecular targeted therapies (figure 4C). Contrastingly, the TNF inhibitor increased the percentage of cell types such as effector memory $CD8^+$ T cells and Tc17 cells, setting it apart from the other treatments (figure 4C). These findings align with previous reports that indicate an increase in peripheral blood lymphocytes following the suppression of adhesion molecules due to TNF inhibitor administration [30].

DISCUSSION

Our research highlights the considerable heterogeneity among patients with RA. Moreover, it demonstrates that immune clusters in these patients cannot be distinctly delineated using existing clinical syndromes or serum markers. Contrarily, our findings reveal that certain groups of patients with RA exhibit immunophenotypic patterns similar to those found in healthy individuals. These findings align with a recent study employing single-cell RNA sequencing of synovium, which revealed that some RA patient groups display patterns akin to those of osteoarthritis [28]. A pivotal discovery of our study is the identification of variations in the effectiveness of molecular targeted therapies across different clusters.

It is evident that the immunophenotyping is influenced by various factors. For instance, the immunophenotype was influenced by the presence or absence of glucocorticoid use and the use of MTX (online supplemental table S29 and 30). Ageing is also a factor that can impact immunophenotyping. In our study, individuals in PCAP-LD were younger than those in the other clusters. This pattern was also noted in healthy subjects, indicating that age plays a crucial role in shaping PCAP-LD (online

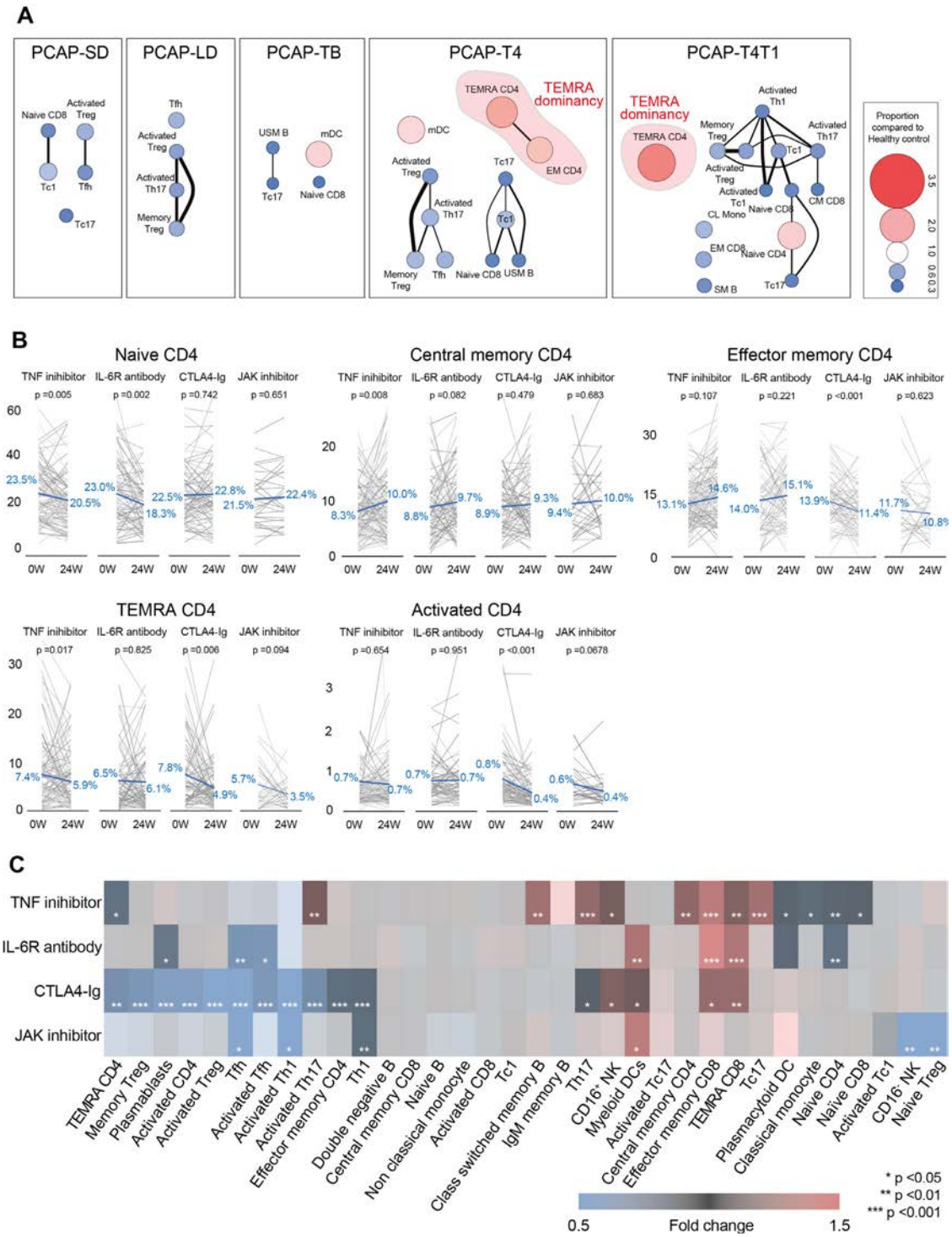

Figure 4. The alterations in immunophenotype following treatment. (A) The visualised model based on the immunophenotyping in each cluster after treatment. The colour (blue for decreases and red for increases) and size of circle indicates the ratio of each immune cell proportion in comparison withh healthy controls as shown in the right box. Each line shows the statistical positive correlation between immune cells. (B) Changes in $CD4^+$-naïve T cells, $CD4^+$ central memory T cells, $CD4^+$ effector memory T cells, $CD4^+$ TEMRA cells, activated $CD4^+$ T cells in each molecular targeted therapy. Thin lines: Individual patients, blue lines and vertical bars: mean±SD values of the whole group. The p values were calculated using a paired t-test. (C) Alterations in immune cell subsets for each specific molecularly targeted therapy are illustrated. The extent of change is depicted by colour in comparison with pretreatment values (blue for decrease and red for increase). Statistically significant changes are denoted by asterisks, while those that are not statistically significant exhibit increased colour transparency. The p values were calculated using a paired t-test. CL Mono, classical monocyte; CM, central memory; CTLA4-Ig, cytotoxic T lymphocyte-associated antigen 4-Ig; EM, effector memory; IL-6R, interleukin-6 receptor; JAK, Janus kinase; mDC, myeloid dendritic cell; NK, natural killer; PCAP-LD, peripheral blood cell abundance phenotypes-little difference; PCAP-SD, peripheral blood cell abundance phenotypes-slightly difference; PCAP-TB, peripheral blood cell abundance phenotypes T-cell and B-cell activation; SM B, class-switched memory B cell; Tc1, cytotoxic T lymphocyte 1; Tc17, cytotoxic T lymphocyte 17; TEMRA, effector memory cells re-expressing CD45RA; Tfh, T follicular helper cell; Th1, T helper 1 cell; Th17, T helper 17 cell; TNF, tumour necrosis factor; Treg, $CD4^+$ regulatory T cell; USM B, IgM memory B cell.

supplemental table S31). The healthy group in this study was younger than the patients with RA, and this could be one of the limitations in this study. However, age-matching had minimal impact on the immunophenotypic differences between healthy subjects and patients with RA (online supplemental table S32). Our study uncovered that in the selection of molecular targeted drugs, the immunophenotype, encompassing these and other environmental factors, can influence therapeutic efficacy.

To date, numerous researchers have concentrated on advancing precision medicine in the field of RA [31]. Synovial tissue has been thoroughly investigated by an international consortium employing single-cell analysis, leading to the identification of new subsets of synovial fibroblasts [16,32]. Single-cell transcriptome analysis from 70 patients with RA revealed the potential division of patients into six clusters [28]. The study identified specific clusters, such as condensed plasmablasts and elevated Tfh cells (CTAP-TB) and condensed cytotoxic $CD4^+$ T cells (CTAP-TF). These clusters may correspond to PCAP-TB and PCAP-T4/T4T1 observed in our study. One of the most notable studies in precision medicine is a synovial biopsy-driven clinical trial demonstrating that synovial analysis can guide the selection of a more effective treatment [33,34]. We anticipate that the utilisation of both synovial tissues and peripheral blood will contribute to unravelling the aetiology of RA and advancing the field of precision medicine.

Although our findings mark a promising start towards achieving precision medicine, incorporating this research into clinical workflows necessitates the development of standardised protocols and infrastructure. Additionally, future efforts will need to focus on identifying biomarkers capable of distinguishing these clusters, which is essential for advancing personalised treatment strategies.

There are several limitations to this study. First, because validating the difference in efficacy of b/tsDMARDs within each cluster would require a very large number of cases, we opted to divide and compare the expected and non-expected groups for validation purposes. Consequently, we could not validate differences in efficacy among b/tsDMARDs in each cluster. Second, there was a risk of overfitting in the discovery cohort. Additionally, the clustering in the validation cohort did not perfectly align with that of the discovery cohort, suggesting that noise from batch effects may have been unavoidable. This may be one of the limitations of using flow cytometry in the study, as it assesses limited number of protein levels. However, the validation cohort enabled us to replicate the findings of the discovery cohort. Therefore, although overfitting may have occurred, we do not deem its influence to be substantial. Furthermore, certain immunocompetent cell subsets, such as peripheral helper T cells, age-associated B cells and intermediate monocytes, were not included through immunophenotyping in this study. Among them, our study revealed a correlation between T-bet^+ $CD11c^+$ B cells and $CD27^-$ IgD^- B cells, as depicted in online supplemental figure S5.

In conclusion, this study highlights the diversity of pathogenesis that are often overlooked in RA, where both genetic predisposition and environmental factors play a role in shaping the disease. Our study provides insights into the pathogenesis of individual patients with RA and the potential for therapeutic applications based on molecular foundations.

Acknowledgments

The authors thank N Sakaguchi for the excellent technical assistance.

Contributors

SK contributed to the study design, the overall statistical analysis, the overall review and the writing of the manuscript. YM was involved in the study design and statistical analysis on clinical effectiveness in each cohort. YF contributed to the in vitro study. KI contributed to the writing of the manuscript and played a pivotal role in the data analysis. KK contributed to the in vitro study. MK was played a pivotal role in the data analysis. TN was played a pivotal role in the data analysis. TK was played a pivotal role in the data analysis. HT was involved in the overall statistical analysis on clustering and validation cohort. MU played a pivotal role in data collection. YS-K played a pivotal role in data collection. YI played a pivotal role in data collection. YTo played a pivotal role in data collection. IM was involved in the performance of the study and review of the manuscript. KH was involved in the performance of the study and review of the manuscript. SN was involved in the performance of the study. YTa participated in the study design, overall review and coordination. All authors read and approved the final manuscript. YTa is the guarantor.

Funding

This work was supported in part by KAKENHI and The JCR Grant for Promoting Research for Precision Medicine in Rheumatoid Arthritis.

Competing interests

SK has received speaking fees from Eli Lilly, GlaxoSmithKline, Bristol Myers, AbbVie, Eisai, Pfizer, AstraZeneca and also research grants from Daiichi Sankyo, AbbVie, Boehringer Ingelheim and Astellas. YM has received consulting fees from AstraZeneca, speaking fees and/or honoraria from Eli Lilly and GlaxoSmithKline. SN has received speaking fees from Bristol Myers, UCB, Astellas, AbbVie, Eisai, Pfizer and Takeda and also research grants from Mitsubishi Tanabe, Novartis and MSD. YTa has received consulting fees, speaking fees and/or honoraria from AbbVie, Daiichi Sankyo, Chugai, Takeda, Mitsubishi Tanabe, Bristol Myers, Astellas, Eisai, Janssen, Pfizer, Asahi Kasei, Eli Lilly, GlaxoSmithKline, UCB, Teijin, MSD and Santen and also research grants from Mitsubishi Tanabe, Takeda, Chugai, Astellas, Eisai, Taisho Toyama, Kyowa Kirin, AbbVie and Bristol Myers. KI, YF, KK, MK, TN, HT, MU, YS-K, YI, YTo, IM and KH have nothing to declare.

Patient and public involvement

Patients and/or the public were not involved in the design, or conduct, or reporting, or dissemination plans of this research.

Patient consent for publication

Consent obtained directly from patient(s).

Ethics approval

This study was approved by the ethics review board of the University of Occupational and Environmental Health, Japan (UOEHCRB21-103). This study was carried out in compliance with the Helsinki Declaration. Informed consent was obtained from patients.

Data availability statement

The data sets generated during and/or analysed during the current study are available from the corresponding author on reasonable request and after ethics application.

Supplementary materials

Supplementary material associated with this article can be found in the online version at doi:10.1136/ard-2024-226228.

Orcid

Satoshi Kubo: http://orcid.org/0000-0001-9693-9263
Yusuke Miyazaki: http://orcid.org/0000-0001-5692-3881
Takahiro Nishino: http://orcid.org/0000-0002-6441-7572
Masanobu Ueno: http://orcid.org/0009-0003-0212-172X
Yoshiya Tanaka: http://orcid.org/0000-0002-0807-7139

REFERENCES

[1] Collins FS, Varmus H. A new initiative on precision medicine. N Engl J Med 2015;372:793–5. doi: 10.1056/NEJMp1500523.
[2] Mirnezami R, Nicholson J, Darzi A. Preparing for precision medicine. N Engl J Med 2012;366:489–91. doi: 10.1056/NEJMp1114866.
[3] Haendel MA, Chute CG, Robinson PN. Classification, Ontology, and Precision Medicine. N Engl J Med 2018;379:1452–62. doi: 10.1056/NEJMra1615014.
[4] Kent DM, Steyerberg E, van Klaveren D. Personalized evidence based medicine: predictive approaches to heterogeneous treatment effects. BMJ 2018;363:k4245. doi: 10.1136/bmj.k4245.
[5] Miyagawa I, Kubo S, Tanaka Y. A wide perspective of targeted therapies for precision medicine in autoimmune diseases. Expert Rev Precis Med Drug Dev 2020;5:447–53. doi: 10.1080/23808993.2020.1804867.
[6] Wang M, Herbst RS, Boshoff C. Toward personalized treatment approaches for non-small-cell lung cancer. N Med 2021;27:1345–56. doi: 10.1038/s41591-021-01450-2.
[7] Herbst RS, Morgensztern D, Boshoff C. The biology and management of non-small cell lung cancer. Nat New Biol 2018;553:446–54. doi: 10.1038/nature25183.
[8] Lin CMA, Cooles FAH, Isaacs JD. Precision medicine: the precision gap in rheumatic disease. Nat Rev Rheumatol 2022;18:725–33. doi: 10.1038/s41584-022-00845-w.
[9] Fasano S, Milone A, Nicoletti GF, et al. Precision medicine in systemic lupus erythematosus. Nat Rev Rheumatol 2023;19:331–42. doi: 10.1038/s41584-023-00948-y.
[10] Toro-Domínguez D, Alarcón-Riquelme ME. Precision medicine in autoimmune diseases: fact or fiction. Rheumatol (Oxford) 2021;60:3977–85. doi: 10.1093/rheumatology/keab448.
[11] Smolen JS, Landewé RBM, Bergstra SA, et al. EULAR recommendations for the management of rheumatoid arthritis with synthetic and biological disease-modifying antirheumatic drugs: 2022 update. Ann Rheum Dis 2023;82:3–18. doi: 10.1136/ard-2022-223356.
[12] Smolen JS, Landewé R, Breedveld FC, et al. EULAR recommendations for the management of rheumatoid arthritis with synthetic and biological disease-modifying antirheumatic drugs. Ann Rheum Dis 2010;69:964–75. doi: 10.1136/ard.2009.126532.
[13] Aletaha D, Smolen JS. Diagnosis and Management of Rheumatoid Arthritis: a Review. JAMA 2018;320:1360–72. doi: 10.1001/jama.2018.13103.
[14] Pennisi E. Development cell by cell. Science 2018;362:1344–5. doi: 10.1126/science.362.6421.1344.
[15] Stuart T, Satija R. Integrative single-cell analysis. Nat Rev Genet 2019;20:257–72. doi: 10.1038/s41576-019-0093-7.
[16] Zhang F, Wei K, Slowikowski K, et al. Defining inflammatory cell states in rheumatoid arthritis joint synovial tissues by integrating single-cell transcriptomics and mass cytometry. Nat Immunol 2019;20:928–42. doi: 10.1038/s41590-019-0378-1.
[17] Yamada S, Nagafuchi Y, Wang M, et al. Immunomics analysis of rheumatoid arthritis identified precursor dendritic cells as a key cell subset of treatment resistance. Ann Rheum Dis 2023;82:809–19. doi: 10.1136/ard-2022-223645.
[18] Maecker HT, McCoy JP, Nussenblatt R. Standardizing immunophenotyping for the Human Immunology Project. Nat Rev Immunol 2012;12:191–200. doi: 10.1038/nri3158.
[19] Aletaha D, Neogi T, Silman AJ, et al. 2010 Rheumatoid arthritis classification criteria: an American College of Rheumatology/European League Against Rheumatism collaborative initiative. Arthritis & Rheum 2010;62:2569–81. doi: 10.1002/art.27584.
[20] Aletaha D, Neogi T, Silman AJ, et al. 2010 rheumatoid arthritis classification criteria: an American College of Rheumatology/European League Against Rheumatism collaborative initiative. Ann Rheum Dis 2010;69:1580–8. doi: 10.1136/ard.2010.138461.
[21] Kubo S, Nakayamada S, Yoshikawa M, et al. Peripheral Immunophenotyping Identifies Three Subgroups Based on T Cell Heterogeneity in Lupus Patients. Arthritis Rheumatol 2017;69:2029–37. doi: 10.1002/art.40180.
[22] Kubo S, Nakayamada S, Miyazaki Y, et al. Distinctive association of peripheral immune cell phenotypes with capillaroscopic microvascular patterns in systemic sclerosis. Rheumatol (Oxford) 2019;58:2273–83. doi: 10.1093/rheumatology/kez244.
[23] Kubo S, Kanda R, Nawata A, et al. Eosinophilic granulomatosis with polyangiitis exhibits T cell activation and IgG4 immune response in the tissue; comparison with IgG4-related disease. RMD Open 2022;8:8. doi: 10.1136/rmdopen-2021-002086.
[24] Kubo S, Fritz JM, Raquer-McKay HM, et al. Congenital iRHOM2 deficiency causes ADAM17 dysfunction and environmentally directed immunodysregulatory disease. Nat Immunol 2022;23:75–85. doi: 10.1038/s41590-021-01093-y.
[25] Taylor PC, Keystone EC, van der Heijde D, et al. Baricitinib versus Placebo or Adalimumab in Rheumatoid Arthritis. N Engl J Med 2017;376:652–62. doi: 10.1056/NEJMoa1608345.
[26] Rubbert-Roth A, Enejosa J, Pangan AL, et al. Trial of Upadacitinib or Abatacept in Rheumatoid Arthritis. N Engl J Med 2020;383:1511–21. doi: 10.1056/NEJMoa2008250.
[27] Fleischmann R, Pangan AL, Song I-H, et al. Upadacitinib Versus Placebo or Adalimumab in Patients With Rheumatoid Arthritis and an Inadequate Response to Methotrexate: results of a Phase III, Double-Blind, Randomized Controlled Trial. Arthritis Rheumatol 2019;71:1788–800. doi: 10.1002/art.41032.
[28] Zhang F, Jonsson AH, Nathan A, et al. Deconstruction of rheumatoid arthritis synovium defines inflammatory subtypes. Nat New Biol 2023;623:616–24. doi: 10.1038/s41586-023-06708-y.
[29] Ytterberg SR, Bhatt DL, Mikuls TR, et al. Cardiovascular and Cancer Risk with Tofacitinib in Rheumatoid Arthritis. N Engl J Med 2022;386:316–26. doi: 10.1056/NEJMoa2109927.
[30] Tak PP, Taylor PC, Breedveld FC, et al. Decrease in cellularity and expression of adhesion molecules by anti-tumor necrosis factor alpha monoclonal antibody treatment in patients with rheumatoid arthritis. Arthritis Rheum 1996;39:1077–81. doi: 10.1002/art.1780390702.
[31] Isaacs JD, Brockbank S, Pedersen AW. RA-MAP, molecular immunological landscapes in early rheumatoid arthritis and healthy vaccine recipients. Sci Data 2022;9:196. doi: 10.1038/s41597-022-01264-y.
[32] Croft AP, Campos J, Jansen K, et al. Distinct fibroblast subsets drive inflammation and damage in arthritis. Nat New Biol 2019;570:246–51. doi: 10.1038/s41586-019-1263-7.
[33] Humby F, Durez P, Buch MH, et al. Rituximab versus tocilizumab in anti-TNF inadequate responder patients with rheumatoid arthritis (R4RA): 16-week outcomes of a stratified, biopsy-driven, multicentre, open-label, phase 4 randomised controlled trial. Lancet 2021;397:305–17. doi: 10.1016/S0140-6736(20)32341-2.
[34] Rivellese F, Surace AEA, Goldmann K, et al. Rituximab versus tocilizumab in rheumatoid arthritis: synovial biopsy-based biomarker analysis of the phase 4 R4RA randomized trial. N Med 2022;28:1256–68. doi: 10.1038/s41591-022-01789-0.

Ann Rheum Dis 84 (2025) 221–231

Contents lists available at ScienceDirect

Annals of the Rheumatic Diseases

journal homepage: https://www.sciencedirect.com/journal/annals-of-the-rheumatic-diseases

Rheumatoid arthritis

Uncovering specific genetic-respiratory disease endotypes for rheumatoid arthritis risk

Vanessa L. Kronzer[1,*], Katrina A. Williamson[1], Keigo Hayashi[2], Elizabeth J. Atkinson[3], Cynthia S. Crowson[1,3], Xiaosong Wang[4], Jing Cui[5], James R. Cerhan[3], Jennifer A. Sletten[1], Gregory C. McDermott[2], Elena K. Joerns[1], Robert Vassallo[1], John M. Davis[1], Jeffrey A. Sparks[2]

[1] *Mayo Clinic, Rochester, NY, USA*
[2] *Harvard Medical School, Boston, Massachusetts, USA*
[3] *Department of Quantitative Health Sciences, Mayo Clinic, Rochester, NY, USA*
[4] *Division of Rheumatology, Inflammation, and Immunity, Brigham and Women's Hospital, Boston, Massachusetts, USA*
[5] *Department of Medicine, Harvard Medical School, Boston, Massachusetts, USA*

ARTICLE INFO

Article history:
Received 6 June 2024
Accepted 15 October 2024

Keywords:
Rheumatoid Arthritis
Polymorphism
Genetic
Pulmonary Fibrosis
Epidemiology

ABSTRACT

Objective: We aimed to identify specific genetic-respiratory disease endotypes for rheumatoid arthritis (RA) risk.

Methods: This case–control study used the Mass General Brigham (MGB) and Mayo Clinic (MC) Biobanks for discovery and replication, respectively. We matched criteria-confirmed incident RA cases to four non-RA controls on age, sex and health record history. Genetic exposures included the top 11 RA risk alleles, and a validated human leucocyte antigen (*HLA*) genetic risk score (GRS). We identified seven respiratory diseases by codes. Using logistic regression models adjusting for potential confounders, we estimated Rs with 95% CIs for the interactions between genetic and respiratory exposures for RA risk.

Results: We identified 653 RA cases and 2607 controls in MGB, and 428 incident RA cases and 1712 non-RA controls in MC (mean age 64, 69% female). Respiratory diseases were associated with an increased risk of RA (OR 1.34, 95% CI 1.05, 1.71). Six out of 11 non-*HLA* RA risk alleles interacted strongly with specific respiratory diseases for RA risk, including *NFKBIE* and sinusitis (OR 5.49, 95% CI 1.56, 19.4 MGB; 5.26, 95% CI 2.00, 13.86 MC) and *FAM167A* and acute sinusitis for seronegative RA (OR 6.00, 95% CI 2.09, 17.24 MGB; 4.90, 95% CI 1.71, 14.1 MC). The RA *HLA* GRS interacted synergistically with interstitial lung disease for RA risk (OR 5.41, 95% CI 2.71, 10.8 in MC), with *DPB1*02:01*, *DRB1*16:01* and *DRB1*04:04* best predicting RA (positive predictive value 61%).

Conclusion: Several genetic-respiratory disease interactions strongly drive RA onset. If confirmed, these novel associations may reflect RA endotypes that can facilitate individualised prevention, diagnosis and treatment.

*Correspondence to Dr. Vanessa L. Kronzer.
E-mail address: kronzer.vanessa@mayo.edu (V.L. Kronzer).
Social media: @Kronzer (V. L. Kronzer), @GregMcDermott (G. C. McDermott), @JohnDavis (J. M. Davis), @jeffsparks (J. A. Sparks)
Handling editor Josef S. Smolen.

https://doi.org/10.1136/ard-2024-226391

WHAT IS ALREADY KNOWN ON THIS TOPIC

- Several respiratory diseases are associated with rheumatoid arthritis (RA) risk, but whether they—like smoking—interact with specific RA genetic factors remains unknown.

WHAT THIS STUDY ADDS

- This case–control study from two large biobanks identified several strong gene-respiratory interactions for RA risk, including *NFKBIE* and *FAM167A* with sinusitis and human leucocyte antigen (*HLA)* with interstitial lung disease (ILD) (OR>5 in each). Among individuals with preceding ILD, a panel including *HLA DPB1*02:01, DRB1*16:01* and *DRB1*04:04* best predicted RA, including in the large group that was seronegative (sensitivity 57%).

HOW THIS STUDY MIGHT AFFECT RESEARCH, PRACTICE OR POLICY

- These findings highlight novel genetic-respiratory disease endotypes for RA, including seronegative RA. Such endotypes may lead to individualised approaches to RA prevention, diagnosis and treatment.

INTRODUCTION

Increasing evidence suggests that rheumatoid arthritis (RA) originates at mucosal surfaces such as the lungs [1]. For example, cigarette smoking increases RA risk over twofold [2]. In addition, respiratory diseases such as sinusitis were recently found to increase RA risk twofold to fivefold, [3–5] especially in the 5–10 years before RA onset and for seronegative RA [4,5]. Other mucosal sites including the gingiva [6] and gut [7] are also implicated in RA pathogenesis. In aggregate, these findings raise the question of whether RA is composed of discrete endotypes, or disease subtypes defined by distinct pathobiological mechanisms [1,8].

Several existing gene-respiratory interactions suggest that such RA endotypes may not only be defined by their mucosal origins, but also their genetic origins. For example, cigarette smoking, [9–11] textile dust [12] and occupational inhalants [13,14] all interact synergistically with the human leucocyte antigen (*HLA) DRB1* shared epitope to increase risk of anti-citrullinated peptide antibody positive RA, with ORs over 15-fold. A recent study showed that the overall RA genetic risk score (GRS) did not interact with respiratory diseases for RA risk; however, the *MUC5B* promoter variant interacted with asthma to increase seropositive (ie, rheumatoid factor (RF) and/or anti-cyclic citrullinated peptide (CCP) positive) RA risk, and the RA *HLA* GRS interacted with interstitial lung disease (ILD) to increase RA risk [15]. These findings raise the questions: (1) to what degree do other specific non-*HLA* RA risk alleles interact with respiratory diseases to drive RA risk, and (2) which *HLA* alleles underlie the interaction with ILD?

To address these two questions, we leveraged two large biobanks with rich clinical phenotyping and extensive genotyping. We aimed to (1) determine the degree to which non-*HLA* RA risk alleles interact with respiratory diseases for RA risk, and (2) identify which specific RA *HLA* risk alleles most strongly interact with ILD for RA risk. Given the strong association between respiratory diseases and seronegative RA, we hypothesised that several non-*HLA* RA risk alleles would interact with respiratory diseases for RA risk. Furthermore, we hypothesised that specific *HLA* alleles would most strongly drive the observed *HLA*-ILD interaction, which could be useful for clinical testing panels among individuals with ILD beyond RF and anti-CCP.

METHODS

Study participants and design

We performed a case–control study using data from the Mass General Brigham (MGB) Biobank for discovery and the Mayo Clinic (MC) Biobank for replication. The MGB Biobank includes over 150 000 participants recruited from 2010 to present from clinical visits at Brigham and Women's Hospital or Massachusetts General Hospital and affiliated sites in Boston, Massachusetts, of whom approximately 57 000 have current genome-wide association study (GWAS) data [16]. Their demographic characteristics were found to match the distribution of the underlying population that receives care at these hospitals [16]. The MC Biobank includes over 57 000 participants recruited from 2009 to 2016, mainly in Minnesota (77%) followed by Florida (18%) and Wisconsin (5%), of whom approximately 53 000 have GWAS data [17]. MC Biobank participants came mainly from primary care (76%) with a 21% response rate. Participants had slightly increased age, proportion of females, proportion of non-Hispanic white race and ethnicity, education, body mass index (BMI) and never smoking history compared with the underlying general population [17]. For this study, we included participants with GWAS data and at least 5 years preceding electronic health record (EHR) history to ascertain needed genetic and respiratory exposures. The index date was the date of RA diagnosis in MGB and RA criteria fulfilment in MC (or matched date for controls). This study received approval from the MGB and MC institutional review boards (#2019P000264, 17–010806), followed the STrengthening the Reporting of OBservational studies in Epidemiology guidelines, and complied with the Declaration of Helsinki.

Patient and public involvement

Patients and the public were involved in the creation of both biobanks [16,18]. They were also involved with the design and conduct of this study via presentation and discussion with the MC Biobank community advisory board.

Incident RA cases

In the MGB Biobank, we previously identified 653 incident RA cases with at least 5 years of EHR history, all confirmed to meet the 2010 American College of Rheumatology/European Alliance of Associations for Rheumatology (ACR/EULAR) criteria [15,19]. In the MC Biobank, we identified potential incident RA cases using the presence of at least two RA codes (ICD-9714.0 or 714.9 and ICD-10 M05.x, M06.x (patients with only three or fewer M06.4 codes and no other RA codes were not reviewed)) at least 30 days apart. We also included anyone with one or fewer RA codes if they had both positive anti-CCP and disease-modifying anti-rheumatic drug (DMARD) use. Inclusion criteria included age 16 years and older at index date. A rheumatologist (VLK or KAW) then determined which of these met ACR/EULAR criteria for RA and/or had convincing rheumatology physician diagnosis with DMARD use. We defined 'seropositive' RA as the presence of RF or anti-CCP, which both came from clinical testing.

Non-RA controls

In both biobanks, we matched each confirmed incident RA case to up to four non-RA controls on age (±1 year), sex and duration of EHR history (±2 years) as of index date. We required controls to have at least 5 years of EHR history, available smoking data on the biobank questionnaire and no code for any systemic rheumatic disease. In the MC Biobank, we also required no positive RF or anti-CCP, as such individuals have a high risk of later developing RA [20].

Genetic risk factors

MGB Biobank performed GWAS genotyping and imputation as previously detailed [15]. In the MC Biobank, the Regeneron Genetics Center performed genotyping. Their sequencing assay is a hybrid capture consisting of the TWIST Comprehensive Exome custom capture and the TWIST Diversity SNP Panel. The resulting 'Genotyping-by-Sequencing' assay augments standard exome capture with 'backbone' regions intended to capture common tagging variation for purposes of GWAS. Specifically, these additional backbone regions are targeted at lower depths, which then undergo substantial post-processing via GLIMPSE to boost genotyping quality based on shared information via linkage disequilibrium and population allele frequencies. They subsequently performed imputation using the TOPMed Imputation Server using the Minimac4 V.1.6.5. Imputation output was restricted to variants with an imputation R^2>0.3. *HLA* imputation was performed using the Michigan Imputation Server (V.1.7.1) using Minimac4 V.1.0.2 and the four-digit multiethnic reference panel V.2.

For this study, we a priori chose the 11 single nucleotide polymorphisms (SNPs) with the lowest p values (p<1.0e-23) for association with RA in the most recently published multi-ancestry RA GWAS, where genetic signals were generally found to be shared across ancestries [21]. These included SNPs in or near the following genes: *PTPN22, CCR6, ANKRD55, STAT4, CTLA4, NFKBIE, KCP, AFF3, ARID5B, FAM167A* and *PCAT29* [21]. We used a dominant allelic model for each SNP, where an individual was considered 'exposed' if they had one or more copies of each allele. We only examined the top 11 in this study since the power to detect interactions declines with only modest main effects, and to limit the potential for false positives from multiple comparisons. For *HLA*, we tested the 21 classical *HLA* RA alleles associated with RA (HLA-B 0801; HLA-DPB1 0201, 0202, 0401, 0402, 0501, 1601, 1901, 2301; and HLA-DRB1 0101, 0102, 0401, 0402, 0403, 0404, 0405, 0407, 0408, 0901, 1001, 1601) [22]. We identified these classical *HLA* alleles at four-digit resolution using the SNP2HLA computational strategy in MGB [23] and the IPD-IMGT/HLA V.3.54.0 database in MC.

To replicate the two significant findings from our previous study, we also calculated the RA *HLA* GRS by multiplying the number of copies of each risk allele by the natural logarithm of their published OR for RA, and then dividing into 'higher' and 'lower' risk groups based on the highest tertile in controls [15]. In addition, we ascertained the presence of the *MUC5B* promoter variant implicated in RA-ILD risk (present (TT or GT) vs absent (GG)) [24].

Respiratory disease exposures

We included seven respiratory disease exposures in this study. These included upper respiratory tract diseases such as pharyngitis (both acute and chronic), and sinusitis (both acute and chronic), along with lower respiratory tract diseases such as asthma, ILD and pneumonia/acute lower respiratory diseases. We previously validated the presence of these respiratory exposures using diagnosis codes [3]. Across all respiratory diseases, they had a mean positive predictive value (PPV) of 86% for true respiratory disease as diagnosed by a physician. We required at least one inpatient or emergency room code or at least two outpatient diagnosis codes (at least 30 days apart for chronic respiratory diseases) before the index date. The reference or 'unexposed' group included any participants not meeting the above criteria for that exposure.

Covariates

Covariates abstracted from both biobanks included matching factors age at index date (continuous), sex (male, female) and duration of EHR history prior to index date (continuous), along with biobank enrolment year, genetic similarity (in MGB 10 and in MC four principal components obtained from GWAS data), [25] self-reported education (4-year college or higher vs lower), BMI at index date (continuous) and smoking status (never, past, current). MGB also had smoking pack-years as of the biobank enrolment year (continuous). We obtained age, sex, EHR history and BMI from the EHR, and enrolment year and education from biobank enrolment data. Of note, although for reporting purposes our table of participant characteristics presented race and ethnicity categories as assessed by a combination of GWAS and self-reported survey and registration data, all interaction analyses used genetic similarity as assessed by GWAS principal components, as advocated for genetic studies [25]. In MGB, we obtained smoking status from the biobank enrolment survey. To improve accuracy in MC, we obtained smoking from the EHR as of the index date, using the biobank enrolment survey to fill in missing values.

Statistical analysis

We compared continuous variables using t-tests and Wilcoxon rank-sum tests, and categorical variables using χ^2 tests. For interaction testing, we studied the association between each genetic risk factor and respiratory disease exposure for RA using conditional logistic regression models to obtain OR with 95% CIs. Models were adjusted for age, sex, EHR history, enrolment year, genetic similarity by principal components, education, BMI, smoking status and pack-years for MGB. We reported the attributable proportion due to interaction (AP) and multiplicative OR for interaction when compared with the double unexposed reference group. In planned subgroup analyses, we repeated analyses by RA serostatus, excluding the other serostatus and their matched controls for that analysis. We used the MGB Biobank as the discovery data set. We presented and replicated only interactions with a double-exposed OR>3 AND statistically significant AP. We also presented AP p values to allow assessment of significance at various thresholds such as Bonferroni (p<0.05/288 tests = 0.00017) [26]. For any interactions that were significant in both biobanks, we performed a three-way interaction with smoking status (ever vs never) to determine whether smoking status modified the observed associations. Finally, in post hoc analyses (after verifying the *HLA*-ILD interaction replicated), we combined the top alleles that interacted with ILD in MGB into various potential genetic panels, calculating PPV and sensitivity and attempting to replicate them in the MC Biobank. Since MC had more individuals with preceding ILD, we were also able to further test them in the anti-CCP

negative subgroup. We studied this subgroup since anti-CCP has a very high (>90%) PPV for RA [27] (compared with only 25% for RF [28]), so we wanted to develop a panel that would also be useful in the anti-CCP negative population.

In MGB, 333 (10.5%) participants were missing education history, which we imputed using all case/control and covariate data [15]. In MC, 14 (1.2%) participants were missing education history and 25 (0.7%) had BMI. We used multiple imputations to fill in these missing values using the MICE package in R with five imputed data sets. Since we only attempted to replicate a small number of interactions in the MC Biobank, we considered two-sided $p<0.05$ as statistically significant. We prespecified analyses in a study protocol and performed them using SAS V.9.4 (SAS Institute, Cary, North Carolina, USA) and R V.4.2.2 (R Core Team 2022).

RESULTS

Characteristics

In MGB, we identified 653 incident RA cases and 2607 matched non-RA controls. Within the 52 801 eligible participants in the MC Biobank, we reviewed 2403 potential RA cases and 968 met the criteria as confirmed incident RA cases. Of these, 428 had at least 5 years preceding EHR history and were included in this study, along with 1712 matched non-RA controls. Thus, this study included a total of 1081 incident RA cases matched to 4319 non-RA controls (table 1). In both biobanks, RA cases had lower education and higher smoking than controls. The MC participants were slightly older, more white non-Hispanic and had more EHR and smoking history and seropositivity compared with MGB participants. In both biobanks, we verified that none of the genetic ancestry principal components were significantly different between the RA case and control groups (see figure 1).

Genetic and respiratory exposures in MC

As previously reported in MGB, [15] we started by determining the association between genetic and respiratory variables in the MC Biobank. As expected, the RA *HLA* GRS was strongly associated with RA, especially seropositive RA (table 2). The presence of any of the seven preceding respiratory diseases was associated with RA risk (OR 1.34, 95% CI 1.05, 1.71). This was especially true for asthma (OR 2.27, 95% CI 1.32, 3.91), ILD (OR 3.61, 95% CI 1.43, 9.13) and acute sinusitis (OR 2.29, 95% CI 1.17, 4.47) in seronegative RA.

Non-HLA interactions

Our first aim was to determine the interaction between non-*HLA* risk alleles and respiratory diseases for RA. In the discovery cohort (MGB), six out of 11 (55%) of the non-*HLA* alleles tested exhibited statistically significant synergistic interactions with specific respiratory diseases for RA risk, with the top 27 most significant interactions meeting the above criteria presented in table 3. Of note, results for interactions between CCR6-ILD (double-exposed OR 2.62, 95% CI 1.06, 6.49) and ANKRD55-chronic pharyngitis in seropositive RA (double-exposed OR 2.30, 95% CI 1.07, 5.00) were not included in table 3 as the OR was <3.

In the replication cohort (MC), four of the above 27 interactions replicated, as assessed by a statistically significant double-exposed OR (table 4). One of these was *NFKBIE*-sinusitis (OR 5.49, 95% CI 1.56, 19.4 MGB; 5.26, 95% CI 2.00, 13.86 MC). Of note, the sample size for the *NFKBIE* variant was small in MC, so we calculated results for all RA rather than seropositive RA. Another replicated interaction was *FAM167A*-acute sinusitis for seronegative RA (OR 6.00, 95% CI 2.09, 17.24 MGB; 4.90, 95% CI 1.71, 14.1 MC). This interaction was not significant in either biobank for seropositive RA.

Finally, the *MUC5B* promoter variant was present in 85 of 426 RA cases (20%) in MC, and it did not interact with asthma for seropositive RA risk (OR 1.16, 95% CI 0.45, 3.02 for double exposed).

HLA-*respiratory interactions*

HLA haplotype data was available for 406 RA and 1652 non-RA participants in the MC Biobank. As seen previously in MGB, the *HLA* GRS interacted synergistically with ILD for RA risk in MC (OR 5.41, 95% CI 2.71, 10.8). *HLA-DPB1*02:01* most strongly drove this association in both biobanks (OR 15.1, 95%

Table 1
Characteristics of the 1081 incident RA cases and 4319 matched non-RA controls with at least 5 years EHR history

Characteristic	MGB RA cases (n = 653)	MGB controls (n = 2607)	MC RA cases (n = 428)	MC controls (n = 1712)
Age at index, years, mean (SD)*	54 (13)	54 (12)	64 (13)	64 (13)
Female sex, n (%)*	494 (76)	1971 (76)	296 (69)	1184 (69)
EHR history at index, years, median (IQR)*	12 (9–17)	12 (8–16)	17 (12–25)	17 (12–25)
Biobank enrolment year, median (IQR)	2015 (2014–2017)	2016 (2014–2017)	2011 (2010–2013)	2011 (2010–2013)
Race and ethnicity, n (%)				
Asian	18 (3)	50 (2)	4 (0.9)	8 (0.5)
Black	49 (8)	91 (4)	2 (0.5)	7 (0.4)
Hispanic	9 (1)	20 (1)	3 (0.7)	13 (0.8)
Other	20 (3)	43 (2)	1 (0.2)	7 (0.4)
White, non-Hispanic	529 (85)	2344 (92)	418 (98)	1677 (98)
Education 4-year college or higher, n (%)†	377 (58)	1882 (72)	172 (40)	750 (44)
BMI at index, kg/m², mean (SD)	29 (7)	28 (6)	30 (6)	29 (6)
Smoking status at index, n (%)†				
Never	320 (49)	1526 (59)	193 (45)	828 (48)
Past	274 (42)	949 (36)	205 (48)	768 (45)
Current	59 (9)	132 (5)	30 (7)	116 (7)
Seropositive RA	373/641 (58)	N/A	280 (65)	N/A

* Matching factor.
† In MGB, as of biobank enrolment.
BMI, body mass index; EHR, electronic health record; GWAS, genome wide association study; kg, kilograms; m, metres; MC, Mayo Clinic; MGB, Mass General Brigham; N/A, not applicable; RA, rheumatoid arthritis.

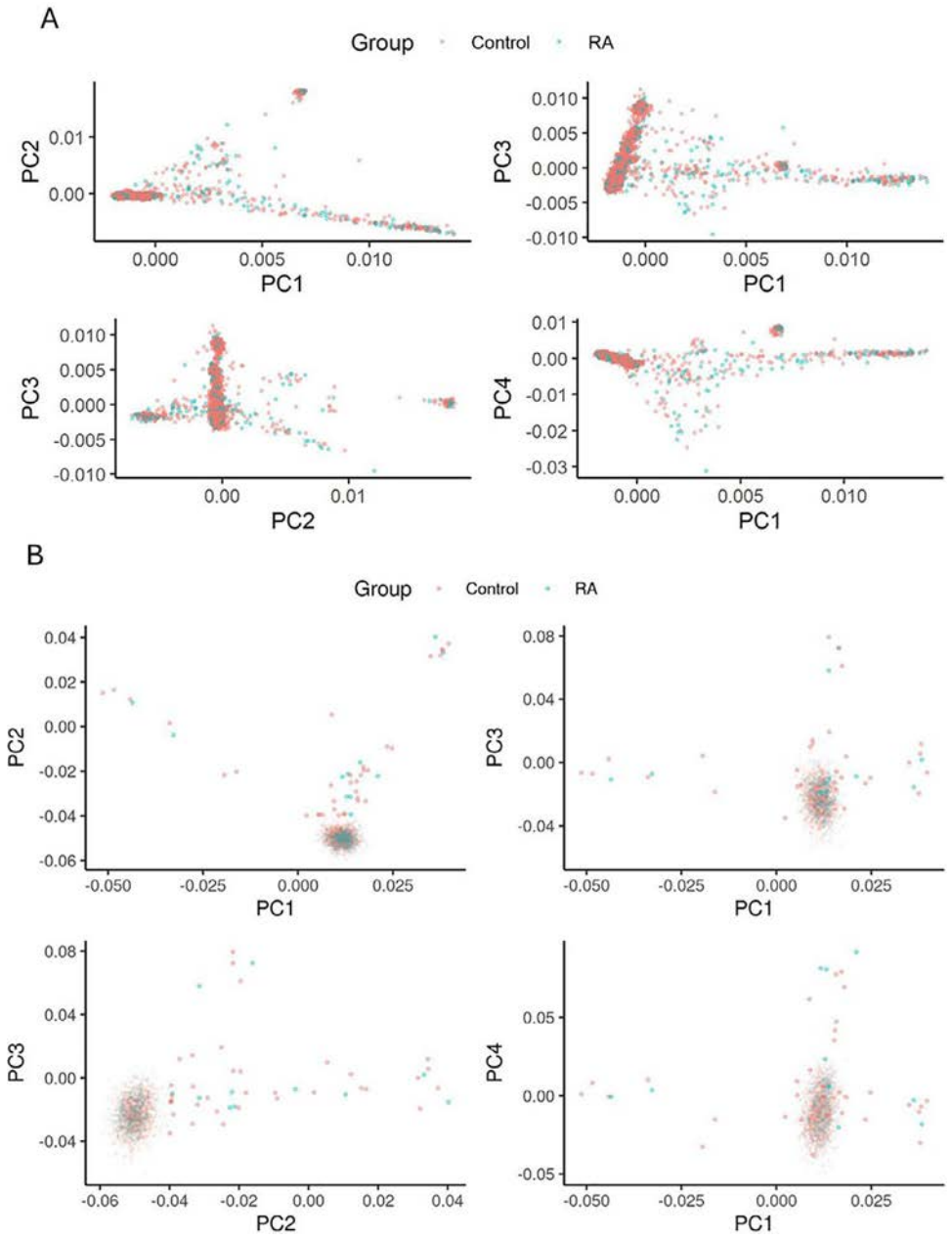

Figure 1. Overlap of genetic principal components between RA cases and controls in the Mass General Brigham (A) and Mayo Clinic (B) Biobanks. RA, rheumatoid arthritis.

CI 1.58, 144 MGB; 3.13, 95% CI 1.24, 7.87 MC, tables 3 and 4). In addition, *HLA-DRB1*16:01* interacted with ILD with high point estimates in both biobanks (OR 16.4, 95% CI 1.53, 176 MGB; OR 8.23, 95% CI 0.72, 93.9 MC). Although the sample size in the MC Biobank was too small to permit replication of several interactions, another interaction that was significant in both biobanks was *HLA-DPB1*04:02*-sinusitis for seronegative RA (OR 15.6, 95% CI 2.81, 86.4 MGB; 4.13, 95% CI 1.56, 10.9 MC). Once again, this interaction was not statistically significant for seropositive RA in either biobank. Finally, we performed three-way interaction testing with smoking for all interactions that were significant in both biobanks. None of these were statistically significant ($p<0.05$) in the same direction in both biobanks.

ILD-RA genetic panel derivation and replication

We combined the top alleles that interacted with ILD for RA risk into various potential genetic testing panels, replicating them in the MC Biobank (table 5). Overall, the panel testing *DPB1*02:01*, *DRB1*16:01* and *DRB1*04:04* performed best for predicting RA (mean PPV 61%, sensitivity 58%), compared with 66% sensitivity for seropositivity. However, 14 (48%) out of the 29 MC ILD cases that later developed RA were anti-CCP negative. In this anti-CCP negative population, the same panel (*DPB1*02:01*, *DRB1*16:01* and *DRB1*04:04*) had the highest sensitivity (57%, 95% CI 29, 82) for predicting RA (table 5).

DISCUSSION

This case–control study within two large biobanks not only confirmed previous associations between respiratory diseases and RA, but also uncovered several individual genetic-respiratory disease endotypes for RA onset including *HLA*-ILD and *NFKBIE*-sinusitis pathways. Notably, observed interactions included both non-*HLA* RA risk alleles and seronegative RA, for which relatively few associations have previously been found compared with their *HLA* and seropositive counterparts. The

Table 2
Associations between individual genetic factors and respiratory diseases for incident RA risk in the Mayo Clinic Biobank

	Number (%) or mean (SD)		Adjusted OR* (95% CI) for RA		
Exposure	RA cases (n = 428)	Controls (n = 1712)	All RA (n = 428)	Seropositive RA (n = 280)	Seronegative RA (n = 148)
Genetic factors					
RA *HLA* genetic risk score					
Highest tertile, n (%)	189/409 (46)	512/1652 (31)	**1.86 (1.47, 2.35)**	**1.94 (1.43, 2.62)**	**1.79 (1.22, 2.64)**
Continuous (SD)	1.48 (0.88)	1.18 (0.74)	**2.12 (1.62, 2.76)**	**2.46 (1.71, 3.53)**	**1.60 (1.01, 2.54)**
Respiratory tract diseases before index date*					
Any respiratory tract disease, n (%)	285 (67)	1032 (60)	**1.34 (1.05, 1.71)**	1.32 (0.97, 1.80)	1.47 (0.97, 2.22)
Asthma	57 (13)	154 (9)	**1.50 (1.07, 2.09)**	1.20 (0.77, 1.86)	**2.27 (1.32, 3.90)**
Interstitial lung disease	29 (7)	72 (4)	**1.76 (1.10, 2.83)**	1.42 (0.81, 2.50)	**3.61 (1.42, 9.13)**
Pharyngitis	91 (21)	329 (19)	1.14 (0.86, 1.53)	1.11 (0.78, 1.59)	1.25 (0.75, 2.07)
Acute pharyngitis or nasopharyngitis	75 (18)	274 (16)	1.11 (0.81, 1.53)	1.06 (0.72, 1.57)	1.27 (0.73, 2.20)
Chronic rhinitis and pharyngitis	15 (4)	44 (3)	1.33 (0.73, 2.42)	1.52 (0.74, 3.14)	0.87 (0.28, 2.71)
Pneumonia and acute lower diseases	53 (12)	166 (10)	1.25 (0.89, 1.75)	1.46 (0.98, 2.18)	0.87 (0.45, 1.69)
Sinusitis	81 (19)	244 (14)	**1.38 (1.03, 1.85)**	1.31 (0.91, 1.89)	1.57 (0.94, 2.63)
Acute sinusitis	43 (10)	123 (7)	1.44 (0.98, 2.13)	1.12 (0.69, 1.84)	**2.29 (1.17, 4.46)**
Chronic sinusitis	47 (11)	141 (8)	1.37 (0.95, 1.97)	1.47 (0.93, 2.34)	1.20 (0.65, 2.22)

* Reference group was individuals with no respiratory tract disease codes prior to index date (or assigned date for matched controls). Adjusting for age, sex, electronic health record history, biobank enrolment year, genetic similarity by principal components, education, body mass index, smoking status. Bold values are statistically significant ($p<0.05$).
HLA, human leucocyte antigen; RA, rheumatoid arthritis.

strong interaction between *HLA* and ILD for RA risk was driven primarily by three alleles: *DPB1*02:01, DRB1*16:01* and *DRB1*04:04*. In aggregate, these findings offer novel opportunities for an individualised approach to RA prevention, diagnosis and treatment using a precision or 'endotype-based' approach. For example, among patients with ILD, specific *HLA* typing could identify individuals at very elevated risk to develop RA.

The first key finding was that most non-*HLA* RA risk alleles tested interacted with a variety of specific respiratory diseases for increased RA risk. Indeed, six of the 11 non-HLA SNPs interacted with at least one respiratory disease. Several of these replicated in MC Biobank, including *NFKBIE*-sinusitis and *FAM167A*-acute sinusitis. Although upper respiratory diseases such as chronic rhinosinusitis and RA are genetically correlated, [29] such correlation would be expected to induce a negative interaction rather than the synergistic interactions we observed. These strong synergistic interactions indicate the presence of distinct RA endotypes. Such endotypes provide new opportunities for individualised RA prevention, for example, by more aggressive treatment of sinus disease in those with high-risk alleles. Future studies should determine whether such treatment is effective in preventing RA, and also whether these endotypes have distinct treatment response patterns.

The second key finding was that gene-respiratory disease interactions were just as prominent, if not more so, in seronegative RA. For example, alleles in both *FAM167A* and *HLA-DPB1*04:02* interacted with acute sinusitis for seronegative RA alone. Such results are highly interesting since previous literature on genetics in RA had observed associations mainly for seropositive RA, especially in *HLA* [9,22]. These associations with seronegative RA may explain the stronger associations observed between respiratory diseases and seronegative RA in three previous populations including the Epidemiological Investigation of RA in Sweden, [30] MGB Biobank, [4] Rochester Epidemiology Project (REP) [5] and now the MC Biobank, the large majority of whom do not overlap with the REP. Thus, this finding represents a potential breakthrough regarding the biological underpinnings of seronegative RA, a common disease which is on the rise [31] but has few established risk factors and unclear pathogenesis.

The third key finding was that *HLA* once again exhibited a strong interaction with ILD for RA risk, especially *HLA DPB1*02:01, DRB1*16:01* and *DRB1*04:04*. In fact, in the MC Biobank, the interaction between high *HLA* GRS and ILD was even stronger than previously observed in the MGB Biobank, with a fivefold increased risk of RA in persons with both exposures [15]. We suspect one reason for this stronger interaction is the longer duration and higher coverage of the EHR in the MC Biobank, [17] which may have reduced misclassification of individuals with ILD or other preceding respiratory exposures as 'unexposed', thus explaining the higher prevalence of respiratory diseases in the MC Biobank. On investigating this *HLA*-ILD interaction more closely, we found that testing three *HLA* alleles (*DPB1*02:01, DRB1*16:01* and *DRB1*04:04*) could be helpful in identifying future RA cases. A genetic panel combining these three alleles identified more than half of seronegative ILD to RA cases (sensitivity 57%). As over one-third of individuals with ILD who developed RA are seronegative, this panel represents a complementary addition to RF and anti-CCP testing for informing RA referrals and diagnosis.

Strengths of this study include the discovery and replication of interactions in two biobanks, relatively large sample sizes, manual confirmation of RA cases which is not possible in larger biobanks, respiratory disease exposure data and data on RA serostatus. There are also several important limitations. The populations in both biobanks were mostly white, non-Hispanic and differed slightly from the general population in other ways, most notably with older age and less smoking history. In addition, despite the large size of the biobanks, once restricted to RA cases with at least 5 years of EHR history, we had limited power to detect several interactions, especially in the MC Biobank. For both reasons, future studies should replicate these findings in larger databases assembled from more diverse general populations before regarding results as confirmed [32]. Because of linkage disequilibrium, *HLA* alleles are likely not completely independent from each other. We assessed respiratory diseases using diagnosis codes, though this definition had a high PPV [3]. Many of the strong interactions from MGB did not replicate in MC, including the strong associations of *PTPN22* with several respiratory diseases. This lack of replication is likely due to the

Table 3

Strongest interactions between RA risk alleles and respiratory diseases for incident RA risk in the MGB Biobank

			Adjusted* OR for RA (95% CI)				Gene-respiratory interactions	
Genetic allele§	n (%)¶	Respiratory disease	Gene−/Resp+	Gene+/Resp−	Gene+/Resp+	AP (95% CI)	AP p value	Multiplicative OR
*HLA-DPB1*02:01*	677 (26)	Interstitial lung disease	0.96 (0.36, 2.55)	1.18 (0.97, 1.45)	**15.1 (1.58, 144)**	**0.92 (0.74, 1.00)**	<0.00001	**13.2 (1.13, 155)**
*HLA-DPB1*04:02*	562 (23)	Acute sinusitis‡	1.12 (0.53, 3.95)	1.04 (0.74, 1.47)	**15.6 (2.81, 86.4)**	**0.93 (0.78, 1.00)**	<0.00001	**13.3 (1.98, 89.8)**
*HLA-DPB1*05:01*	210 (5)	Chronic pharyngitis‡	0.65 (0.27,1.53)	1.24 (0.62, 2.48)	6.34 (0.39, 105)	**0.86 (0.44, 1.00)**	0.00007	**7.89 (0.39, 158)**
*HLA-DPB1*16:01*	20 (0.8)	Acute pharyngitis‡	1.96 (1.19, 3.22)	1.95 (0.46, 8.26)	**16.9 (1.33, 214)**	**0.83 (0.36,1.00)**	0.00058	4.43 (0.23, 84.8)
		Pharyngitis‡	**1.58 (1.01, 2.45)**	1.94 (0.46, 8.21)	**16.2 (1.28, 205)**	**0.84 (0.41, 1.00)**	0.00015	5.28 (0.28, 100)
		Any respiratory disease‡	0.94 (0.70, 1.27)	1.25 (0.13, 11.9)	**4.97 (1.09, 22.7)**	**0.76 (0.09, 1.00)**	0.0268	4.23 (0.28, 64.5)
*HLA-DRB1*01:01*	360 (14)	Pharyngitis‡	1.44 (0.89, 2.34)	1.52 (0.99, 2.32)	**4.41 (1.67, 11.6)**	**0.56 (0.08, 1.00)**	0.0221	2.01 (0.64, 6.36)
*HLA-DRB1*01:02*	108 (4)	Pneumonia	1.28 (0.94, 1.74)	1.42 (0.91, 2.21)	**21.2 (2.23, 203)**	**0.92 (0.74, 1.00)**	<0.00001	**11.7 (1.17, 116)**
*HLA-DRB1*04:01*	327 (13)	Chronic pharyngitis	0.91 (0.52, 1.59)	1.81 (1.40, 2.34)	**4.10 (1.32, 12.7)**	**0.58 (0.09, 1.00)**	0.0203	2.50 (0.71, 8.81)
*HLA-DRB1*04:05*	57 (2)	Asthma†	1.19 (0.81, 1.74)	**2.97 (1.40, 6.28)**	**9.65 (1.51, 61.8)**	**0.67 (0.04, 1.00)**	0.03817	2.74 (0.37, 20.1)
		Asthma	0.95 (0.72, 1.26)	1.47 (0.81, 2.66)	**6.32 (1.59, 25.2)**	**0.77 (0.44, 1.00)**	0.00001	**4.51 (1.00, 20.4)**
*HLA-DRB1*16:01*	68 (3)	Sinusitis†	1.26 (0.80, 1.98)	**2.07 (1.05, 4.10)**	**16.4 (1.53, 176)**	**0.86 (0.51, 1.00)**	<0.00001	6.39 (0.54, 73.7)
		Chronic pharyngitis	0.96 (0.57, 1.61)	1.43 (0.84, 2.44)	**13.6 (1.20, 154)**	**0.90 (0.64, 1.00)**	<0.00001	9.88 (0.79, 124)
		Interstitial lung disease	1.26 (0.53, 3.00)	1.45 (0.85, 2.47)	10.1 (0.86, 119)	**0.83 (0.39, 1.00)**	0.00025	5.49 (0.38, 79)
		Pneumonia	1.29 (0.95, 1.74)	1.35 (0.78, 2.34)	**9.68 (1.99, 47)**	**0.83 (0.55, 1.00)**	<0.00001	**5.58 (1.03, 30.1)**
		Sinusitis	1.35 (0.99, 1.85)	1.44 (0.84, 2.47)	**8.41 (1.33, 53)**	**0.79 (0.39, 1.00)**	0.00013	4.34 (0.64, 29.6)
PTPN22 (rs2476601)	421 (16)	Interstitial lung disease†	1.33 (0.95, 1.86)	1.24 (0.90, 1.71)	**16.8 (1.73, 164)**	**0.91 (0.68, 1.00)**	<0.00001	10.3 (0.77, 136)
		Interstitial lung disease	1.05 (0.41, 2.73)	1.12 (0.88, 1.43)	**5.73 (1.24, 26.5)**	**0.79 (0.44, 1.00)**	<0.00001	4.85 (0.81, 29)
		Acute pharyngitis‡	**1.78 (1.06, 3.04)**	0.88 (0.57, 1.35)	**4.09 (1.35, 12.4)**	**0.59 (0.10, 1.00)**	0.0183	2.61 (0.75, 9.03)
		Acute sinusitis†	1.18 (0.62, 2.23)	1.25 (0.90, 1.72)	**3.74 (1.05, 13.4)**	**0.62 (0.10, 1.00)**	0.0196	2.56 (0.61, 10.7)
		Pharyngitis†	1.27 (0.85, 2.21)	0.83 (0.54, 1.29)	**3.64 (1.41, 9.41)**	**0.67 (0.31, 1.00)**	0.0003	**3.20 (1.07, 9.57)**
NFKBIE (rs28362855)	222 (9)	Acute sinusitis†	1.17 (0.63, 2.16)	1.10 (0.71, 1.69)	**5.95 (1.15, 30.7)**	**0.79 (0.41, 1.00)**	0.0001	4.64 (0.76, 28.2)
		Sinusitis†	1.15 (0.72, 1.83)	1.05 (0.67, 1.62)	**5.49 (1.56, 19.4)**	**0.78 (0.48, 1.00)**	<0.00001	**4.57 (1.12, 18.7)**
		Acute pharyngitis†	1.04 (0.62, 1.74)	1.08 (0.70, 1.67)	**4.97 (1.06, 23.3)**	**0.78 (0.40, 1.00)**	0.0001	4.44 (0.84, 23.5)
		Pharyngitis†	1.07 (0.69, 1.66)	1.06 (0.68, 1.66)	**3.93 (1.12, 13.7)**	**0.71 (0.21, 1.00)**	0.0004	3.46 (0.87, 13.8)
KCP (rs3757387)	1699 (66)	Chronic pharyngitis†	0.53 (0.14, 2.04)	**1.58 (1.18, 2.12)**	**3.35 (1.49, 7.53)**	**0.67 (0.31, 1.00)**	0.0002	4.00 (0.85, 18.9)
FAM167A (rs2736340)	1048 (40)	Acute sinusitis‡	0.99 (0.42, 2.34)	1.15 (0.85, 1.55)	**6.00 (2.09, 17.2)**	**0.81 (0.57, 1.00)**	<0.00001	**5.30 (1.38, 20.4)**

* Included interactions where the OR for gene+/Resp+ was >3 AND where AP was significant. Reference group was individuals without respiratory tract disease exposure and without genetic exposure. Adjusting for age, sex, EHR history, biobank enrolment year, genetic similarity by principal components, education, body mass index, smoking status and pack-years. Bold values are statistically significant (p<0.05).

† Outcome of seropositive RA.

‡ Outcome of seronegative RA.

§ Ordered by strength of allele's association with RA.

¶ Number (per cent) of controls with at least one copy of each allele.

AP, attributable proportion; COPD, chronic obstructive pulmonary disease; EHR, electronic health record; GRS, genetic risk score; *HLA*, human leucocyte antigen; n/a, not able to be calculated due to small sample size; RA, rheumatoid arthritis; Resp, respiratory tract exposure; SNP, single nucleotide polymorphism.

Table 4

Replication of significant gene-respiratory interactions for incident RA risk in the Mayo Clinic Biobank

			Adjusted* OR for RA (95% CI)			Gene-resftpiratory interactions	
Genetic exposure	n (%)‡	Respiratory disease	Gene−/Resp+	Gene+/Resp−	Gene+/Resp+	AP (95% CI)	Multiplicative OR
*HLA-DPB1*02:01*	399 (24)	Interstitial lung disease	1.52 (0.87, 2.66)	0.91 (0.70, 1.19)	**3.13 (1.24, 7.87)**	0.54 (−0.41, 1.00)	2.26 (0.76, 6.75)
*HLA-DPB1*04:02*	372 (23)	Acute sinusitis‡	1.82 (0.74, 4.49)	1.44 (0.93, 2.25)	**4.13 (1.56, 10.9)**	0.45 (−0.54, 1.00)	1.57 (0.43, 5.70)
*HLA-DPB1*05:01*	74 (5)	Chronic pharyngitis‡	1.43 (0.66, 3.08)	0.50 (0.20, 1.22)	n/a	n/a	n/a
*HLA-DPB1*16:01*	29 (1.8)	Acute pharyngitis‡	1.03 (0.68, 1.56)	0.49 (0.11, 2.20)	1.31 (0.13, 13.59)	0.60 (−1.00, 1.00)	2.61 (0.16, 42.57)
		Pharyngitis‡	1.10 (0.75, 1.60)	0.52 (0.12, 2.36)	1.05 (0.11, 10.0)	0.41 (−1.00, 1.00)	1.84 (0.12, 27.3)
		Any respiratory disease‡	1.35 (0.98, 1.86)	0.70 (0.08, 6.06)	0.80 (0.17, 3.71)	−0.31 (−1.00, 1.00)	0.85 (0.06, 11.5)
*HLA-DRB1*01:01*	283 (17)	Pharyngitis‡	1.35 (0.91, 2.01)	**1.62 (1.12, 2.33)**	0.65 (0.24, 1.72)	**−1.00 (−1.00, −0.48)**	**0.30 (0.10, 0.85)**
*HLA-DRB1*01:02*	23 (1.4)	Pneumonia	1.22 (0.86, 1.73)	0.82 (0.27, 2.45)	n/a	n/a	n/a
*HLA-DRB1*04:01*	272 (17)	Chronic pharyngitis	1.26 (0.59, 2.70)	**1.77 (1.35, 2.33)**	2.07 (0.68, 6.28)	0.02 (−1.00, 1.00)	0.93 (0.23, 3.68)
*HLA-DRB1*04:05*	20 (1.2)	Asthma†	**2.18 (1.24, 3.83)**	3.15 (0.69, 14.4)	n/a	n/a	n/a
		Asthma	1.49 (1.06, 2.11)	**2.22 (0.98, 5.05)**	n/a	n/a	n/a
*HLA-DRB1*16:01*	42 (2.5)	Sinusitis†	1.63 (0.97, 2.75)	0.91 (0.18, 4.45)	n/a	n/a	n/a
		Chronic pharyngitis	1.28 (0.68, 2.39)	0.67 (0.31, 1.46)	1.11 (0.67,1.83)	n/a	n/a
		Interstitial lung disease	**1.76 (1.08, 2.87)**	0.52 (0.22, 1.24)	8.23 (0.72, 93.9)	0.84 (−1.00, 1.00)	9.03 (0.68, 120)
		Pneumonia	1.23 (0.86, 1.75)	0.69 (0.30, 1.57)	0.57 (0.06, 4.93)	−0.62 (−1.00, 1.00)	0.67 (0.07, 6.84)
		Sinusitis	1.43 (1.06, 1.94)	0.78 (0.36, 1.72)	n/a	n/a	n/a
PTPN22 (rs2476601)	370 (22)	Interstitial lung disease†	1.62 (0.87, 3.04)	1.03 (0.74, 1.44)	0.90 (0.26, 3.18)	−0.84 (−1.00, 0.88)	0.54 (0.13, 2.23)
		Interstitial lung disease	1.96 (1.16, 3.31)	1.00 (0.76, 1.31)	1.21 (0.44, 3.31)	−0.61 (−1.00, 0.69)	0.62 (0.20, 1.94)
		Acute pharyngitis‡	1.01 (0.54, 1.90)	0.77 (0.46, 1.30)	2.10 (0.80, 5.54)	0.63 (-0.40,1.00)	2.69 (0.79, 9.20)
		Acute sinusitis†	1.02 (0.58, 1.77)	0.95 (0.68, 1.34)	1.59 (0.58, 4.37)	0.39 (-0.68,1.00)	1.64 (0.50, 5.31)
		Pharyngitis‡	1.03 (0.58, 1.82)	0.76 (0.44, 1.30)	1.95 (0.78, 4.86)	0.60 (−0.36, 1.00)	2.50 (0.79, 7.95)
NFKBIE (rs28362855)	109 (6)	Acute sinusitis	1.39 (0.93, 2.08)	1.25 (0.81, 1.92)	3.75 (0.99, 14.20)	0.56 (−0.77, 1.00)	2.16 (0.52, 9.03)
		Sinusitis	1.28 (0.94, 1.74)	1.09 (0.69, 1.72)	**5.26 (2.00, 13.86)**	0.74 (−0.22, 1.00)	**3.79 (1.29, 11.17)**
		Acute pharyngitis	1.08 (0.78, 1.49)	1.20 (0.76, 1.91)	2.02 (0.85, 4.81)	0.37 (−0.53, 1.00)	1.56 (0.58, 4.21)
		Pharyngitis	1.10 (0.81, 1.48)	1.15 (0.71, 1.86)	2.17 (0.99, 4.75)	0.43 (−0.38, 1.00)	1.72 (0.68, 4.35)
KCP (rs3757387)	1175 (69)	Chronic pharyngitis†	1.01 (0.26, 3.87)	1.09 (0.81, 1 .47)	2.01 (0.84, 4.83)	0.45 (−0.61, 1.00)	1.83 (0.38, 8.90)
FAM167A (rs2736340)	744 (44)	Acute sinusitis‡	1.90 (0.83, 4.38)	1.41 (0.94, 2.12)	**4.90 (1.71, 14.1)**	0.53 (−0.53, 1.00)	1.83 (0.48, 6.96)

* Reference group was individuals without respiratory tract disease exposure and without genetic exposure (eg, lowest two GRS tertiles in the GRS). Adjusting for age, sex, electronic health record history, biobank enrolment year, genetic similarity by principal components, education, body mass index and smoking status. Bold values are statistically significant ($p<0.05$).

† Outcome of seropositive RA.

‡ Outcome of seronegative RA.

§ Number (per cent) of controls with at least one copy of each allele.

AP, attributable proportion; COPD, chronic obstructive pulmonary disease; GRS, genetic risk score; *HLA*, human leucocyte antigen; n/a, not able to calculate due to small sample size; RA, rheumatoid arthritis; RERI, relative excess risk due to interaction; Resp, respiratory tract exposure.

Table 5
Performance of genetic panels for predicting RA among individuals with preceding ILD

	MGB biobank				MC biobank—full cohort			
Genetic panel	**RA case (n = 11)**	**Control (n = 20)**	**PPV (95% CI)**	**Sens (95% CI)**	**RA Case (n = 29)**	**Control (n = 72)**	**PPV (95% CI)**	**Sens (95% CI)**
*DPB1*02:01*, *DRB1*16:01* or *DRB1*04:04*	7 (64)	3 (15)	70 (35, 93)	64 (31, 89)	15 (52)	14 (19)	52 (33, 71)	52 (33, 71)
*DPB1*02:01* or *DRB1*04:04*	6 (54)	2 (10)	75 (35, 97)	55 (23, 83)	13 (45)	16 (22)	45 (26, 64)	45 (26, 64)
*DPB1*02:01* or *DRB1*16:01*	6 (54)	2 (10)	75 (35, 97)	55 (23, 83)	11 (38)	18 (25)	38 (21, 58)	38 (21, 58)
*DPB1*02:01*, *DRB1*16:01* or *PTPN22**	8 (73)	5 (25)	62 (32, 86)	73 (39, 94)	15 (52)	14 (19)	52 (33, 71)	52 (33, 71)
*DPB1*02:01* or *PTPN22**	7 (64)	4 (20)	64 (31, 89)	64 (31, 89)	13 (45)	16 (22)	45 (26, 64)	45 (26, 64)
*DRB1*16:01* or *DRB1**04:04	3 (27)	2 (10)	60 (15, 95)	27 (6, 61)	7 (24)	22 (31)	24 (10, 44)	24 (10, 44)
*DRB1*16:01* or *PTPN22**	6 (54)	4 (20)	60 (26, 88)	55 (23, 83)	7 (24)	22 (31)	24 (10, 44)	24 (10, 44)

* rs2476601.
AUC, area under curve; ILD, interstitial lung disease; MC, Mayo Clinic; MGB, Mass General Brigham; PPV, positive predictive value; RA, rheumatoid arthritis; RF, rheumatoid factor; Sens, sensitivity.

known phenomenon in genetic studies called 'the winner's curse', [33] but could also reflect the smaller sample size of the MC Biobank and/or differences between the two biobank populations. For example, the RA population in MC was older, more frequently white, more seropositive, and had a higher proportion of previous respiratory exposures. We performed 288 interaction tests in the discovery cohort, so findings replicated in both studies are more likely to be valid, though still could have occurred due to chance. Although we used medical record review to determine RA onset, some patients could have had undiagnosed RA when exposures were assessed. This, along with our respiratory exposure cut-off at the index date of RA onset, could have led to reverse causation with respiratory disease exposures. Finally, while we had many covariates available, there may be some unmeasured confounders, such as pollutants and healthcare utilisation [34].

In conclusion, we uncovered several genetic-respiratory interactions that strongly drive RA onset, including the previously understudied non-*HLA* RA risk alleles and seronegative RA. If confirmed, these novel endotypes for RA may prove useful for RA prevention, diagnosis and treatment.

Acknowledgments

We thank the Mayo Clinic Center for Individualized Medicine, Regeneron Genetics Center, as well as all the participants and researchers involved with the Mass General Brigham and Mayo Clinic Biobanks for their support.

Contributors

All authors meet all four ICMJE criteria for authorship, and all who meet the four criteria are identified as authors. There are no other contributors to the work. No one who fulfils the criteria has been excluded as an author. VLK: Conception, analysis, interpretation, drafting, final approval, guarantor. KAW: Conception, interpretation, drafting, final approval. KH: Conception, analysis, interpretation, drafting, final approval. EJA: Conception, analysis, interpretation, drafting, final approval. CSC: Conception, analysis, interpretation, drafting, final approval. XW: Analysis, interpretation, drafting, final approval. JC: Conception, analysis, interpretation, drafting, final approval. JRC: Conception, interpretation, drafting, final approval. JAS: Conception, interpretation, drafting, final approval. GCM: Interpretation, drafting, final approval. EKJ: Interpretation, drafting, final approval. RV: Conception, interpretation, drafting, final approval. JD: Conception, interpretation, drafting, final approval. JAS: Conception, analysis, interpretation, drafting, final approval.

Funding

This study was supported by the RRF Scientist Development Award (VLK, GCM), and the National Institute of Arthritis and Musculoskeletal and Skin Diseases awards NIH-P30-AR072577 (VERITY Pilot & Feasibility award to VLK) and R01 AR46849 (CSC). JAS is supported by the National Institute of Arthritis and Musculoskeletal and Skin Diseases (grant numbers R01 AR080659, R01 AR077607, P30 AR070253, and P30 AR072577), the National Heart, Lung, and Blood Institute (grant number R01 HL155522), the R Bruce and Joan M Mickey Research Scholar Fund, and the Llura Gund Award funded by the Gordon and Llura Gund Foundation.

Competing interests

EKJ has received research support from Pfizer. JD has received research support from Pfizer, licensing agreements with Girihlet and Remission Medical and intellectual property/patent licensed to NLC Health Ventures. JAS has received research support from Bristol Myers Squibb, Boehringer Ingelheim and Sonoma Biosciences. He has performed consultancy for AbbVie, Amgen, Boehringer Ingelheim, Bristol Myers Squibb, Gilead, Inova Diagnostics, Janssen, Optum, Pfizer, ReCor, Sobi and UCB. All these disclosures are unrelated to this work. The remaining authors and contributors have no competing interests to disclose.

Patient and public involvement

Patients and/or the public were involved in the design, or conduct, or reporting, or dissemination plans of this research. Refer to the Methods section for further details.

Patient consent for publication

Not applicable.

Ethics approval

This study received approval from the MGB and MC institutional review boards (#2019P000264, 17-010806). Participants gave informed consent to participate in the study before taking part.

Data availability statement

Data are available upon reasonable request. Reasonable requests for Mass General Brigham or Mayo Clinic Biobank data from qualified researchers may be directed to biobank@ partners. org or Biobank@ mayo.edu.

Orcid

Vanessa L. Kronzer: http://orcid.org/0000-0002-7489-3134
Cynthia S. Crowson: http://orcid.org/0000-0001-5847-7475
Gregory C. McDermott: http://orcid.org/0000-0002-9750-5448
John M. Davis: http://orcid.org/0000-0002-9710-8143
Jeffrey A. Sparks: http://orcid.org/0000-0002-5556-4618

REFERENCES

[1] Holers VM, Demoruelle MK, Kuhn KA, et al. Rheumatoid arthritis and the mucosal origins hypothesis: protection turns to destruction. Nat Rev Rheumatol 2018;14:542–57. doi: 10.1038/s41584-018-0070-0.
[2] Di Giuseppe D, Discacciati A, Orsini N, et al. Cigarette smoking and risk of rheumatoid arthritis: a dose-response meta-analysis. Arthritis Res Ther 2014;16:R61. doi: 10.1186/ar4498.
[3] Kronzer VL, Huang W, Zaccardelli A, et al. Association of Sinusitis and Upper Respiratory Tract Diseases With Incident Rheumatoid Arthritis: A Case-control Study. J Rheumatol 2022;49:358–64. doi: 10.3899/jrheum.210580.
[4] Kronzer VL, Huang W, Crowson CS, et al. Timing of sinusitis and other respiratory tract diseases and risk of rheumatoid arthritis. Semin Arthritis Rheum 2022;52:151937. doi: 10.1016/j.semarthrit.2021.11.008.
[5] Kronzer VL, Davis JM, Hanson AC, et al. Association between sinusitis and incident rheumatic diseases: a population-based study. RMD Open 2024;10:e003622. doi: 10.1136/rmdopen-2023-003622.
[6] Brewer RC, Lanz TV, Hale CR, et al. Oral mucosal breaks trigger anti-citrullinated bacterial and human protein antibody responses in rheumatoid arthritis. Sci Transl Med 2023;15:eabq8476. doi: 10.1126/scitranslmed.abq8476.
[7] Chriswell ME, Lefferts AR, Clay MR, et al. Clonal IgA and IgG autoantibodies from individuals at risk for rheumatoid arthritis identify an arthritogenic strain of Subdoligranulum. Sci Transl Med 2022;14:eabn5166. doi: 10.1126/scitranslmed.abn5166.
[8] Blair JPM, Bager C, Platt A, et al. Identification of pathological RA endotypes using blood-based biomarkers reflecting tissue metabolism. A retrospective and explorative analysis of two phase III RA studies. PLoS One 2019;14:e0219980. doi: 10.1371/journal.pone.0219980.
[9] Klareskog L, Stolt P, Lundberg K, et al. A new model for an etiology of rheumatoid arthritis: smoking may trigger HLA-DR (shared epitope)-restricted immune reactions to autoantigens modified by citrullination. Arthritis Rheum 2006;54:38–46. doi: 10.1002/art.21575.
[10] Too CL, Yahya A, Murad S, et al. Smoking interacts with HLA-DRB1 shared epitope in the development of anti-citrullinated protein antibody-positive rheumatoid arthritis: results from the Malaysian Epidemiological Investigation of Rheumatoid Arthritis (MyEIRA). Arthritis Res Ther 2012;14:R89. doi: 10.1186/ar3813.
[11] Lee H-S, Irigoyen P, Kern M, et al. Interaction between smoking, the shared epitope, and anti-cyclic citrullinated peptide: a mixed picture in three large North American rheumatoid arthritis cohorts. Arthritis Rheum 2007;56:1745–53. doi: 10.1002/art.22703.
[12] Too CL, Murad S, Hansson M, et al. Differences in the Spectrum of Anti-Citrullinated Protein Antibody Fine Specificities Between Malaysian and Swedish Patients With Rheumatoid Arthritis: Implications for Disease Pathogenesis. Arthritis Rheumatol 2017;69:58–69. doi: 10.1002/art.39827.
[13] Tang B, Liu Q, Ilar A, et al. Occupational inhalable agents constitute major risk factors for rheumatoid arthritis, particularly in the context of genetic predisposition and smoking. Ann Rheum Dis 2023;82:316–23. doi: 10.1136/ard-2022-223134.
[14] Ebel AV, Lutt G, Poole JA, et al. Association of Agricultural, Occupational, and Military Inhalants With Autoantibodies and Disease Features in US Veterans With Rheumatoid Arthritis. Arthritis Rheumatol 2021;73:392–400. doi: 10.1002/art.41559.
[15] Kronzer VL, Hayashi K, Crowson CS, et al. Gene-respiratory disease interactions for rheumatoid arthritis risk. Semin Arthritis Rheum 2023;63:152254. doi: 10.1016/j.semarthrit.2023.152254.
[16] Karlson EW, Boutin NT, Hoffnagle AG, et al. Building the Partners HealthCare Biobank at Partners Personalized Medicine: Informed Consent, Return of Research Results, Recruitment Lessons and Operational Considerations. J Pers Med 2016;6:2. doi: 10.3390/jpm6010002.
[17] Olson JE, Ryu E, Hathcock MA, et al. Characteristics and utilisation of the Mayo Clinic Biobank, a clinic-based prospective collection in the USA: cohort profile. BMJ Open 2019;9:e032707. doi: 10.1136/bmjopen-2019-032707.
[18] Olson JE, Ryu E, Johnson KJ, et al. The Mayo Clinic Biobank: a building block for individualized medicine. Mayo Clin Proc 2013;88:952–62. doi: 10.1016/j.mayocp.2013.06.006.
[19] Liao KP, Cai T, Gainer V, et al. Electronic medical records for discovery research in rheumatoid arthritis. Arthritis Care Res (Hoboken) 2010;62:1120–7. doi: 10.1002/acr.20184.
[20] Nielen MMJ, van Schaardenburg D, Reesink HW, et al. Specific autoantibodies precede the symptoms of rheumatoid arthritis: a study of serial measurements in blood donors. Arthritis Rheum 2004;50:380–6. doi: 10.1002/art.20018.
[21] Ishigaki K, Sakaue S, Terao C, et al. Multi-ancestry genome-wide association analyses identify novel genetic mechanisms in rheumatoid arthritis. Nat Genet 2022;54:1640–51. doi: 10.1038/s41588-022-01213-w.
[22] Raychaudhuri S, Sandor C, Stahl EA, et al. Five amino acids in three HLA proteins explain most of the association between MHC and seropositive rheumatoid arthritis. Nat Genet 2012;44:291–6. doi: 10.1038/ng.1076.
[23] Jia X, Han B, Onengut-Gumuscu S, et al. Imputing Amino Acid Polymorphisms in Human Leukocyte Antigens. PLoS ONE 2013;8:e64683. doi: 10.1371/journal.pone.0064683.
[24] Juge P-A, Lee JS, Ebstein E, et al. MUC5B Promoter Variant and Rheumatoid Arthritis with Interstitial Lung Disease. N Engl J Med 2018;379:2209–19. doi: 10.1056/NEJMoa1801562.
[25] Byun J, Han Y, Gorlov IP, et al. Ancestry inference using principal component analysis and spatial analysis: a distance-based analysis to account for population substructure. BMC Genomics 2017;18:789. doi: 10.1186/s12864-017-4166-8.
[26] Bland JM, Altman DG. Multiple significance tests: the Bonferroni method. BMJ 1995;310:170. doi: 10.1136/bmj.310.6973.170.
[27] Imran M, O'Brien S, Hamblin M, et al. AB0349 Significance of Positive Anti-Ccp Antibody and Development of Interstitial Lung Disease in Patients with and without Clinically Apparent Rheumatoid Arthritis. Ann Rheum Dis 2014;73:920. doi: 10.1136/annrheumdis-2014-eular.2620.

[28] Shmerling RH, Delbanco TL. How useful is the rheumatoid factor? An analysis of sensitivity, specificity, and predictive value. Arch Intern Med 1992;152:2417–20.
[29] Saarentaus EC, Karjalainen J, Rämö JT, et al. Inflammatory and infectious upper respiratory diseases associate with 41 genomic loci and type 2 inflammation. Nat Commun 2023;14:83. doi: 10.1038/s41467-022-33626-w.
[30] Kronzer VL, Westerlind H, Alfredsson L, et al. Respiratory Diseases as Risk Factors for Seropositive and Seronegative Rheumatoid Arthritis and in Relation to Smoking. Arthritis Rheumatol 2021;73:61–8. doi: 10.1002/art.41491.
[31] Myasoedova E, Davis J, Matteson EL, et al. Is the epidemiology of rheumatoid arthritis changing? Results from a population-based incidence study, 1985-2014. Ann Rheum Dis 2020;79:440–4. doi: 10.1136/annrheumdis-2019-216694.
[32] Denny JC, Rutter JL, Goldstein DB, et al. The "All of Us" Research Program. N Engl J Med 2019;381:668–76. doi: 10.1056/NEJMsr1809937.
[33] Xiao R, Boehnke M. Quantifying and correcting for the winner's curse in genetic association studies. Genet Epidemiol 2009;33:453–62. doi: 10.1002/gepi.20398.
[34] Zhang J, Fang X-Y, Wu J, et al. Association of Combined Exposure to Ambient Air Pollutants, Genetic Risk, and Incident Rheumatoid Arthritis: A Prospective Cohort Study in the UK Biobank. Environ Health Perspect 2023;131:37008. doi: 10.1289/EHP10710.

Ann Rheum Dis 84 (2025) 232–252

Contents lists available at ScienceDirect

Annals of the Rheumatic Diseases

journal homepage: https://www.sciencedirect.com/journal/annals-of-the-rheumatic-diseases

Rheumatoid arthritis

ITGA5^{+} synovial fibroblasts orchestrate proinflammatory niche formation by remodelling the local immune microenvironment in rheumatoid arthritis

Linli Zheng[1,2], Minghui Gu[1,2], Xiang Li[2,3], Xuantao Hu[1,2,4], Chen Chen[5,6], Yunze Kang[1,2], Baiqi Pan[1,2], Weishen Chen[1,2], Guoyan Xian[7], Xiaoyu Wu[1,2], Chengxin Li[1,2], Chao Wang[1,2], Zhiwen Li[1,2], Mingqiang Guan[8], Guanming Zhou[8], Ali Mobasheri[9,10,11], Weidong Song[5], Sui Peng[6,12,13,*], Puyi Sheng[1,2,*], Ziji Zhang[1,2,*]

[1] *Department of Joint Surgery, Sun Yat-sen University First Affiliated Hospital, Guangzhou, Guangdong, China*
[2] *Guangdong Provincial Key Laboratory of Orthopaedics and Traumatology, Sun Yat-sen University First Affiliated Hospital, Guangzhou, Guangdong, China*
[3] *Department of Spine Surgery, Sun Yat-sen University First Affiliated Hospital, Guangzhou, Guangdong, China*
[4] *Department of Spine Surgery, Sun Yat-sen University Third Affiliated Hospital, Guangzhou, Guangdong, China*
[5] *Trauma Orthopedics, Foot and Ankle Surgery, Sun Yat-sen Memorial Hostpial, Guangzhou, Guangdong, China*
[6] *Institute of Precision Medicine, Sun Yat-sen University First Affiliated Hospital, Guangzhou, Guangdong, China*
[7] *Universite de Paris, Paris, France*
[8] *Department of Orthopedics and Traumatology, Foshan Hospital of Traditional Chinese Medicine, Foshan, Guangdong, China*
[9] *Research Unit of Medical Imaging, Physics and Technology, Faculty of Medicine, University of Oulu, Oulu, Finland*
[10] *Department of Regenerative Medicine, State Research Institute Centre for Innovative Medicine, Vilnius, Lithuania*
[11] *Public Health Aspects of Musculoskeletal Health and Aging, World Health Organization Collaborating Centre, Liege, Belgium*
[12] *Clinical Trials Unit, Sun Yat-sen University First Affiliated Hospital, Guangzhou, Guangdong, China*
[13] *Department of Gastroenterology and Hepatology, Sun Yat-sen University First Affiliated Hospital, Guangzhou, Guangdong, China*

ARTICLE INFO

Article history:
Received 8 March 2024
Accepted 17 October 2024

Keywords:
arthritis
rheumatoid
autoimmunity
fibroblasts
T-lymphocytes
cytokines

ABSTRACT

Objectives: To investigate the phenotypic heterogeneity of tissue-resident synovial fibroblasts and their role in inflammatory response in rheumatoid arthritis (RA).
Methods: We used single-cell and spatial transcriptomics to profile synovial cells and spatial gene expressions of synovial tissues to identify phenotypic changes in patients with osteoarthritis, RA in sustained remission and active state. Immunohistology, multiplex immunofluorescence and flow cytometry were used to identify synovial fibroblasts subsets. Deconvolution methods further validated our findings in two cohorts (PEAC and R4RA) with treatment response. Cell coculture was used to access the potential cell-cell interactions. Adoptive transfer of synovial cells in collagen-induced arthritis (CIA) mice and bulk RNA sequencing of synovial joints further validate the cellular functions.

*Correspondence to Dr. Ziji Zhang; Professor Puyi Sheng; Professor Sui Peng.
E-mail addresses: pengsui@mail.sysu.edu.cn (S. Peng), shengpy@mail.sysu.edu.cn (P. Sheng), zhangziji@mail.sysu.edu.cn (Z. Zhang).
Handling editor Josef S. Smolen.
LZ, MG, XL, XH and CC contributed equally.

https://doi.org/10.1136/ard-2024-225778

Results: We identified a novel tissue-remodelling CD45^{-}CD31^{-}PDPN^{+}ITGA5^{+} synovial fibroblast population with unique transcriptome of POSTN, COL3A1, CCL5 and TGFB1, and enriched in immunoregulatory pathways. This subset was upregulated in active and lympho-myeloid type of RA, associated with an increased risk of multidrug resistance. Transforming growth factor (TGF)-β1 might participate in the differentiation of this subset. Moreover, ITGA5^{+} synovial fibroblasts might occur in early stage of inflammation and induce the differentiation of CXCL13^{hi}PD^{-}1^{hi} peripheral helper T cells (TPHs) from naïve CD4^{+} T cells, by secreting TGF-β1. Intra-articular injection of ITGA5^{+} synovial fibroblasts exacerbates RA development and upregulates TPHs in CIA mice.
Conclusions: We demonstrate that ITGA5^{+} synovial fibroblasts might regulate the RA progression by inducing the differentiation of CXCL13^{hi}PD^{-}1^{hi} TPHs and remodelling the proinflammatory microenvironments. Therapeutic modulation of this subpopulation could therefore be a potential treatment strategy for RA.

WHAT IS ALREADY KNOWN ON THIS TOPIC

- The CXCL13^{hi}PD^{-}1^{hi} peripheral helper T cells (TPHs) identified in previous single-cell sequencing study contributed to the pathogenesis of the inflamed joint of rheumatoid arthritis (RA).
- Notch signalling drives THY1^{+} sublining synovial fibroblast and endothelial cells crosstalk.
- Potential immune-stromal cell interaction networks were found on a global scale in the inflamed joint for RA.
- Spatial transcriptomic analysis revealed that local exposures to myeloid and T cell-derived cytokines, including tumour necrosis factor, interferon-γ and interleukin^{-}1β, drove four distinct states of synovial fibroblasts.

WHAT THIS STUDY ADDS

- The ITGA5^{+} synovial fibroblasts, identified as novel activated sublining fibroblasts, delineated a critical region for modulating the proinflammatory response, signalling to neighbouring cells, and remodelling the tissue microenvironment.
- ITGA5^{+} synovial fibroblasts upregulated in active and lympho-myeloid pathotypes of synovitis of RA and was associated with an increased risk of multidrug resistance.
- Identification of distinct differential trajectories of synovial fibroblasts and potential regulators, including transcription factors and cytokines.
- ITGA5^{+} synovial fibroblasts might occur in early stage of inflammation and induce the differentiation of CXCL13^{hi}PD^{-}1^{hi} TPHs from naïve CD4^{+} T cells, by secreting transforming growth factor-β1.

HOW THIS STUDY MIGHT AFFECT RESEARCH, PRACTICE OR POLICY

- The single-cell and spatial atlas of synovial cells deepens our understanding of RA synovial inflammation pathogenesis and reveals new opportunities for targeted therapeutic intervention on ITGA5^{+} synovial fibroblasts.

INTRODUCTION

Rheumatoid arthritis (RA) is characterised by persistent synovitis, systemic inflammation and autoantibodies [1]. The symptoms of RA are highly dynamic, with approximately 50% of patients relapsing after treatment cessation, underscoring the need to understand the mechanisms of treatment resistance [2–4]. Previous studies have shown that a low proportion of MerTK^{pos} synovial tissue macrophages (Mks) in patients in remission is associated with an increased risk of disease flare after treatment cessation [5]. The expression levels of genes associated with lymphoid aggregates and inflammatory cytokines are reduced in EULAR good-responder patients [6]. Nevertheless, the potential immunological pathways associated with resistance mechanisms and targets outside of inflammatory cytokines and immune cells have yet to be identified [7].

Fibroblasts (Fbs) play multifaceted roles in health and diseases, including defining tissue architecture, aiding the functioning and positioning of cells and promoting healing or driving inflammation and scarring [6]. In synovial tissues, Fbs supply nutrients and extracellular matrix (ECM) components and lubricate joints [8]. In RA, synovial Fbs transform into a cancer-like phenotype, thereby forming pannus, producing matrix metalloproteinases (MMPs), and mediating cartilage damage [9]. Moreover, FAPα^{+}CD90^{+} Fbs are expanded in patients with RA and drive leucocyte recruitment and activation [10,11]. The synovial lining Fbs also showed enrichment of genes downstream of interferon (IFN)-γ, tumour necrosis factor (TNF) and interleukin (IL)$^{-}$1β, which was associated with activator protein 1 activation in inflamed synovial tissue of patients with RA [12].

Recent studies have also indicated that synovial Fbs may play an important role in treating resistant and active RA. Synovial biopsy-based biomarker analysis has suggested that DKK3^{+} Fbs might be associated with refractoriness [13]. Circulating CD45^{-}CD31^{-}PDPN^{+} proinflammatory mesenchymal or PRIME cells may migrate into the synovium, contributing to RA flare after treatment cessation [14]. However, these bulk RNA sequencing (RNA–seq)–based studies limit the ability of the systemic immune microenvironment to recapitulate distinct states of the RA synovium and the potential roles and immunological pathways of specific subsets of Fbs in patients with active and resistant RA.

Recent single-cell transcriptome sequencing (scRNAseq) analyses have shown that different synovial Mk clusters may have important implications for therapies aimed at modulating inflammation or tissue repair [5]. Although great success has been achieved in depicting proinflammatory Fbs in chronic inflammation, the potential therapeutic targeting of Fbs involved in RA relapse and resistance has not been validated [15]. Moreover, an improved understanding of the architecture of the synovium from gross anatomy to single-cell and spatial gene expression levels, in parallel with evidence demonstrating how synovial Fbs are vital for inflammation and homeostasis and how dysregulated signalling of Fbs in tissue remodelling leads to chronic inflammation and tissue destruction in the RA joint, has opened new ways of thinking about the pathogenesis of RA.

RESULTS

A single-cell landscape of RA synovial tissue

To generate a cellular map of the human synovia that accounts for the dynamic changes in spatial microenvironments, synovial tissue samples were analysed via scRNA-seq and spatial transcriptomics (ST) methods (10x Genomics Visium slides and high-resolution microscopy) (figure 1A). Cell type annotation

was performed by analysing the expression levels of canonical gene markers and differentially expressed genes (DEGs).

We were able to generate a synovial map of 169 797 cells from 19 individuals, including 4 patients with OA and 15 patients with RA with distinct disease activity statuses (active RA: n = 9; remission RA: n = 6) (figure 1A). We identified seven clusters that were assigned cell identities based on their expression of known markers (figure 1B and online supplemental figure S1A). These clusters were grouped into the main cellular categories: synovial Fbs, Mks, osteoclasts, dendritic cells (DCs), mast cells, T lymphocytes, B lymphocytes, endothelial cells (ECs) and mural cells. Based on the cellular markers of unsupervised clustering, synovial cells were divided into subclusters. The distinct synovial Fb clusters included CLIC5$^+$PRG4$^+$ Fb, MMP2$^+$VCAN$^+$ Fb, MMP3$^+$VCAM1$^+$ Fb, ITGA5$^+$ Fb, HLA-DRA^{hi} Fb, DPP4$^+$PI16$^+$CD34$^+$ Fb, CSN1S1$^+$ Fb, MT1X$^+$IRX3$^+$ Fb and AMTN$^+$ Fb [11,12,16–21]. Among the synovial Mks, the C1QA^{hi} (C1QA^{hi}TIMD4$^+$ Mk, C1QA^{hi}CCL$^+$ Mk and C1QA^{hi}CCL18$^+$ Mk), IL1B$^+$ (IL1B$^+$MCL1$^+$ Mk, IL1B$^+$AREG$^+$ Mk, IL1B$^+$S100A12$^+$ Mk), CCL2$^+$SLC2A3$^+$ Mk, CXCL10$^+$IRF1$^+$ Mk and TREM2^{hi}SPP1$^+$ Mk subclusters were identified. The DC subclusters included cDC1, cDC2, LAMP3$^+$ DC and plasmacytoid DC. For T lymphocytes, CD4$^+$ subclusters, including naïve T cells, central memory T (TCM) cells, PD$^-$1^{hi} peripheral helper T cells (TPHs), PD$^-$1^{hi}CXCL13^{hi} TPHs and regulatory T (Treg) cells, CD8$^+$ subclusters, including effective memory T (TEM), GZMK$^+$ and GZMB$^+$ T cells, gamma-delta T cells, proliferating T (ProT) cells and natural killer (NK) cells were identified. Memory B cells and plasma B cells (IGG$^+$IGKC$^+$, IGG$^+$IGLC$^+$, IGA$^+$) were also included. ECs were further divided into ACKR1$^+$ and CCL2$^+$ subclusters and into arterial endothelial cells (AECs), capillary ECs and lymphatic ECs. The marker gene expression levels of each subcluster are also shown in the online supplemental figures (online supplemental figure S1A).

Subclusters of Fbs (ITGA5$^+$ Fbs), lymphocytes (PD$^-$1^{hi}CXCL13^{hi} TPH, PD$^-$1^{hi} TPH and plasma B cells) and myeloid cells (LAMP3$^+$ DC, cDC1, CCL2$^+$SLC3A2$^+$ Mk, IL1B$^+$AREG$^+$ Mk and TREM2^{hi}SPP1$^+$ Mk) were increased in active RA, whereas other subclusters of Fbs (DPP4$^+$PI16$^+$CD34$^+$ Fb, MT1X$^+$IRX3$^+$ Fbs), ECs (capillary ECs and AECs) and mast cells were upregulated in those with RA in remission (figure 1C). Moreover, the percentages of ITGA5$^+$ Fbs, cDC1s, PD-1^{hi} TPHs and PD-1^{hi} CXCL13^{hi} TPHs were positively correlated with disease activity (erythrocyte sedimentation rate (ESR), C reactive protein (CRP) and Disease Activity Score using 28 Joints (DAS28) (DAS28-ESR and DAS28-CRP)) in patients with RA (figure 1D), suggesting that these cellular subclusters may contribute to active RA. Pathology of the synovial tissues revealed that subclusters of Fbs (ITGA5$^+$ Fb, MMP3$^+$VCAM1$^+$ Fb) and lymphocytes (PD$^-$1^{hi} TPH and PD$^-$1^{hi}CXCL13^{hi} TPH) were also increased in patients with lympho-myeloid synovitis (online supplemental figure S1B), suggesting that these cells may participate in lymphocyte aggregation (online supplemental figure S1B,S1C) [22].

Identification of a novel fibroblast subcluster in rheumatoid synovium

Since subcluster analysis revealed stromal heterogeneity, we further studied the unique transcriptomes of nine distinct clusters of synovial Fbs (figure 2A). PRG4$^+$ lining Fbs and THY1$^+$ sublining Fbs were found among synovial Fbs subclusters (figure 2B, online supplemental figure S2A, S2B). CLIC5$^+$PRG4$^+$ Fbs expressed CRTAC1, TSPAN15 and CD55 and were involved in the positive regulation of cell adhesion molecule production (figure 2B and online supplemental figure S2C) [10,11,23]. MMP3$^+$VCAM1$^+$ Fbs were highly transcriptionally similar to activated lining Fbs induced by age-associated B cells with upregulated MMP3, CXCL9 and CXCL10 expressions and exhibited invasive, proinflammatory and immune-interacting phenotypes (figure 2B and online supplemental figure S2C) [24,25]. Other lining Fbs with high expression of casein alpha s1 (CSN1S1), metallothionein (MT1X, MT1G) and amelotin (AMTN) were also identified. Among the sublining Fbs, the HLA-DRA^{hi} Fb subset may be involved in the adaptive immune response by upregulating major histocompatibility complex class II molecules (figure 2B and online supplemental figure S2C). DPP4$^+$PI16$^+$CD34$^+$ Fbs were also known as ‘universal fibroblast’ and a stromal progenitor to various steady-state and pathological Fbs [16–21]. The MMP2$^+$VCAN$^+$ Fbs expressing DKK3, CXCL12 and MDK were also identified in our study (figure 2B and online supplemental figure S2C) [11,15].

Interestingly, we identified a novel activated sublining Fb subcluster (F4: ITGA5$^+$ Fb) with a distinct transcriptional profile that included high expression of genes encoding ECM (POSTN, COL3A1 and TGFBI), chemokines (CCL5), cytokines (TGFB1 and TNFSF11, also known as RANKL), stem cell growth factors (CLEC11A), fibroblast activation protein-α (FAP) and proliferative markers (MKI67 and TOP2A) (figure 2B and online supplemental figure S2D). DEG analysis further showed that in active RA, ITGA5$^+$ Fbs upregulated IFN-responsive genes (IFI6, IFI27 and ISG15) (online supplemental figure S2E). Using the Liger algorithm and cosine distance similarity analysis, we found that ITGA5$^+$ Fbs may share a partial transcriptome between the SC$^-$F3 (DKK3$^+$ sublining) and SC$^-$F2 (HLA-DRA^{hi} sublining) populations identified by Zhang *et al* (online supplemental figure S2F, S2G) [11,26,27].

Gene set enrichment analysis (GSEA) of the genes and gene ontology (GO) pathways revealed that ITGA5$^+$ Fbs were enriched in the development pathway (tendon development, bone cell development), metabolic pathways (G-6-P metabolic process, 10-formyltetrahydrofolate metabolic process, citrate metabolic process), angiogenesis (regulation of sprouting angiogenesis, positive regulation of the VEGF signalling pathway) and immune regulation (positive regulation of B-cell differentiation, T-cell extravasation) (figure 2C). SCENIC analysis predicted that the transcription factors (TFs) SRY-box transcription factor 9 (SOX9), DNA methyltransferase 1, MYC-associated zinc finger protein (MAZ) and hypoxia-inducible factor 1α (HIF1A), which are associated with Fb activation, would be upregulated in the ITGA5$^+$ subset (figure 2D) [28,29]. Co-expressions of HIF1A and SOX9 is also critical in chondrogenic precursors, which might lead to subsequent new bone formation and ankylosis in the chronic phase of RA [30,31]. Our study also suggested that ITGA5$^+$ Fbs might be the potential therapeutic target in the modulation of chondrogenesis in RA [32].

The percentages of ITGA5$^+$ subsets were significantly increased in patients with active RA (figure 2E). Moreover, these immunoregulatory and activated subclusters (F4: ITGA5$^+$ Fbs) were also significantly increased in the lymphoid-myeloid pathotype compared with the pauci-immune pathotype (figure 2F).

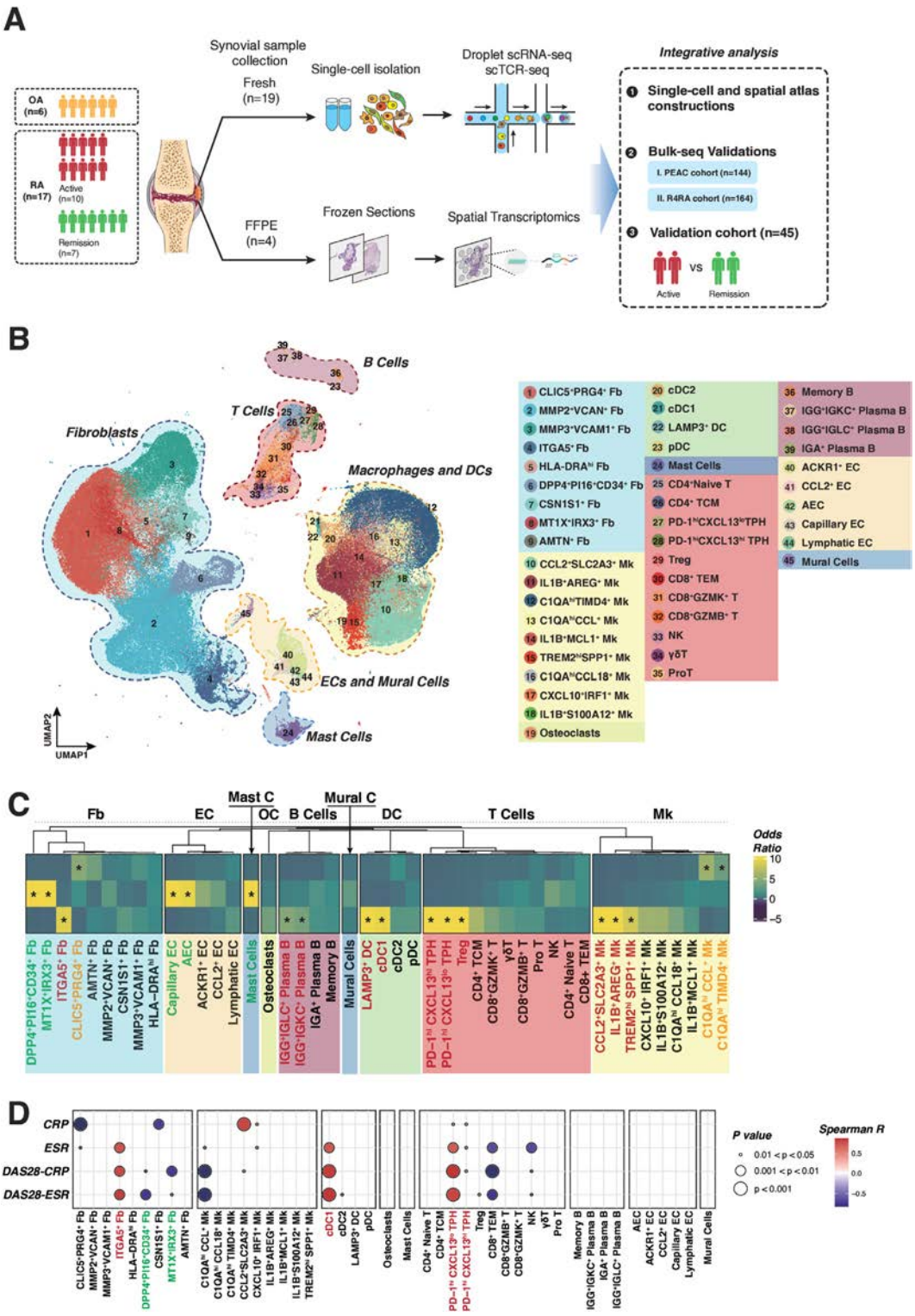

Figure 1. Single-cell atlas of synovial tissues from patients with osteoarthritis (OA) and rheumatoid arthritis (RA). (A) Study overview of patient sample processing for single-cell RNA sequencing (scRNA-seq), spatial transcriptomics (ST), pathotype evaluation and multiplex immunofluorescence (mIF) to (1) construct the single-cell and ST atlas and validate the findings; (2) evaluate distinct categories of disease-relevant signatures in a cell type-specific manner and (3) validate the applicability of the findings in the PEAC cohort, R4RA cohort and retrospective cohort. (B) Uniform manifold approximation and projection (UMAP) plots of the scRNA-seq data and relative proportions of cells from synovial tissues of patients with OA (n = 4) and RA (n = 15) according to cell type and cell subtype (number of cells: 169 797). (C) Heatmap showing the ORs of cell subtypes occurring in each tissue (synovial tissues from patients with OA (n = 4), patients with remission RA (n = 6) and patients with active RA (n = 9)). *OR >5 indicates that the cell subtype is preferentially distributed in the corresponding tissue. Hierarchical clustering based on the cosine distance is applied for rows. The name and background colour of each subcluster are in accordance with (B). EC: endothelial cells; Fb: fibroblasts; Mast C: mast cells; Mk: macrophages; Mural C: mural cells; OC: osteoclasts. (D.) Dot plot showing the Spearman's correlations of the proportions of cell subclusters in each cell type and clinical features, including the erythrocyte sedimentation rate (ESR), C- reactive protein (CRP), and Disease Activity Score using 28 Joints (DAS28) (DAS28-ESR and DAS28-CRP). 15 patients with RA patients were included. P values were corrected for multiple testing using the Benjamini–Hochberg method.

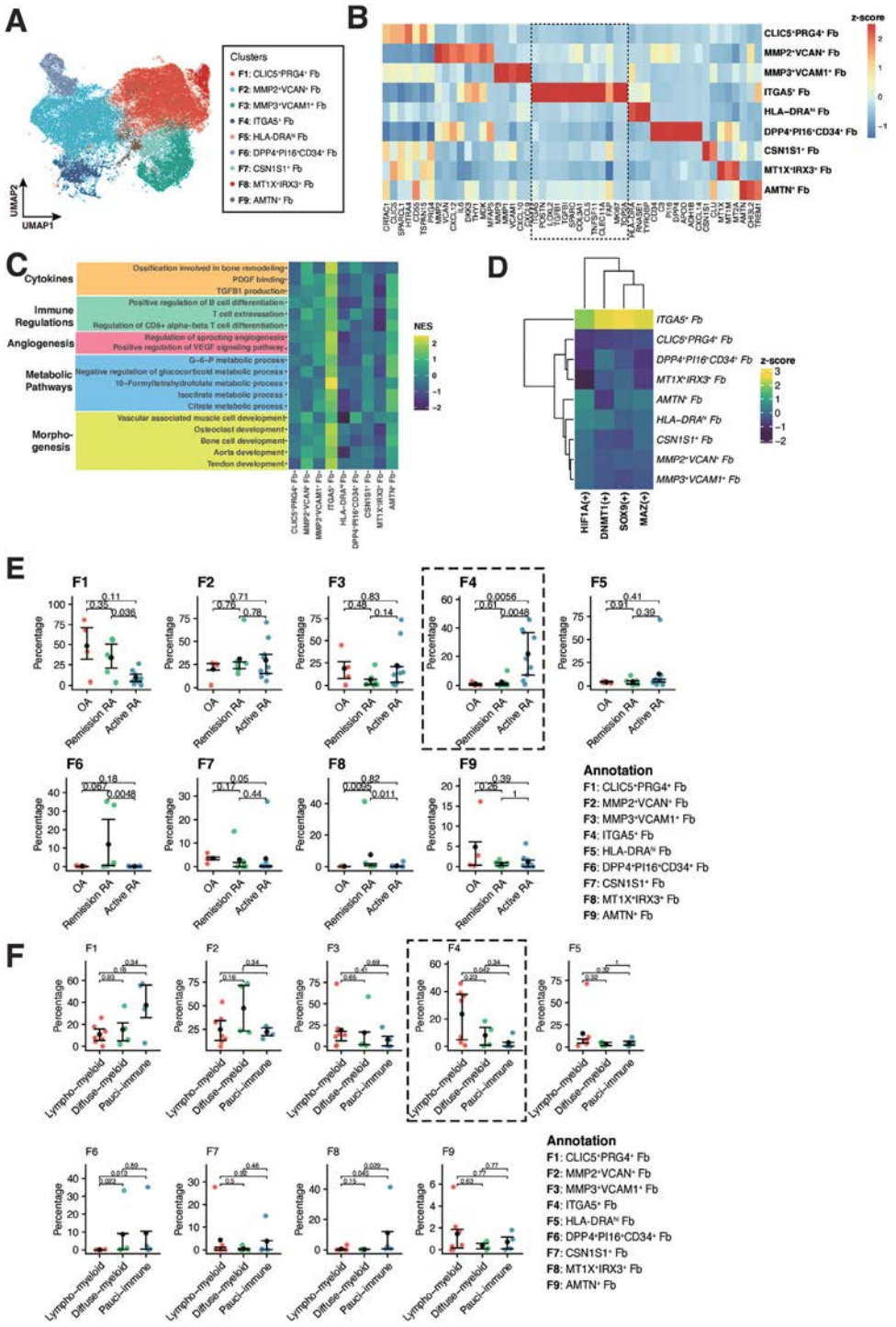

Figure 2. Distinct fibroblast clusters in synovial tissues from patients with osteoarthritis (OA), remission rheumatoid arthritis (RA) and active RA. (A) Uniform manifold approximation and projection (UMAP) visualisation of synovial fibroblast clusters. We identified nine synovial fibroblast clusters across 96 492 cells. (B) Heatmap of marker gene expression in distinct fibroblast subsets. (C) Heatmap of the gene set enrichment analysis (GSEA) results of the enriched gene ontology (GO) pathways in ITGA5$^+$ synovial fibroblasts. NES, normalised enrichment score. (D) Heatmap of single-cell regulon scores inferred by SCENIC. (E) Differential proportions of synovial fibroblast clusters across patients with OA (n = 4), remission RA (n = 6), and active RA (n = 9). Statistics: two-sided Wilcoxon test. Data are shown as mean and error bars (point: mean; upper limit: upper quartile; lower limit: lower quartile). (F) Differential proportions of synovial fibroblast clusters across the lympho-myeloid (n = 7), diffuse-myeloid (n = 4) and pauci-immune (n = 4) pathotypes of synovitis. Statistics: two-sided Wilcoxon test. Data are shown as mean and error bars (point: mean; upper limit: upper quartile; lower limit: lower quartile).

ITGA5$^+$ synovial fibroblasts may contribute to active RA

We validated our findings in our retrospective clinical cohort of synovial pathology data from patients with RA using multiple immunofluorescence staining (figure 3A, online supplemental figure S3A). The percentage of ITGA5$^+$PDPN$^+$ synovial cells was significantly greater in patients with active RA and in patients with the lympho-myeloid pathotype (figure 3A and B). The percentage of ITGA5$^+$ cells among synovial Fbs (PDPN$^+$ cells) and the percentage of ITGA5$^+$PDPN$^+$ cells among all cells

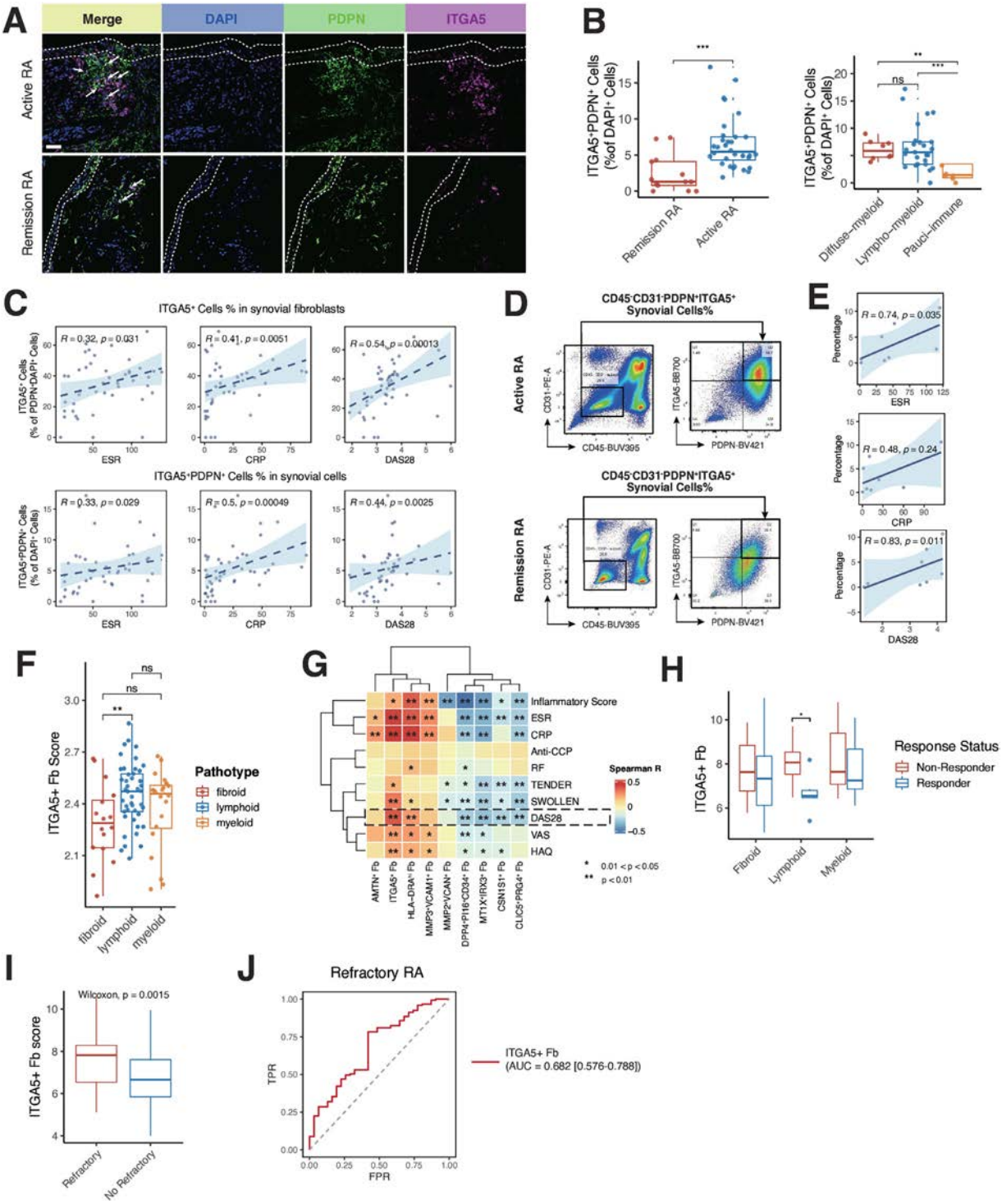

Figure 3. Identification of ITGA5$^+$ synovial fibroblasts (Fbs) and validation in large cohort datasets. (A) Immunofluorescence (IF) staining of PDPN (green) and ITGA5 (purple) to identify PDPN$^+$ITGA5$^+$ synovial Fbs in patients with active (top) and remission (bottom) RA. Arrows indicate double-positive cells. Scale bars, 50 μm. Representative images from one of three independent experiments are shown. (B) Box plots showing IF results for the percentages of PDPN$^+$ITGA5$^+$ double-positive synovial Fbs in patients with active (n = 32) and remission (n = 13) RA and in patients with the lympho-myeloid (n = 25), diffuse-myeloid (n = 8) and pauci-immune (n = 12) pathotypes. (C) Upper, two-tailed Spearman's correlation between the percentages of ITGA5$^+$ cells among PDPN$^+$DAPI$^+$ cells and the erythrocyte sedimentation rate (ESR), C reactive protein (CRP) concentration and Disease Activity Score using 28 Joints (DAS28); lower, two-tailed Spearman's correlation between the percentages of ITGA5$^+$PDPN$^+$ cells among DAPI$^+$ cells and the ESR, CRP concentration and DAS28 (n = 45). The light blue area represents the 95% CIs. (D) Representative flow cytometric gating scheme for the identification of CD45$^-$CD31$^-$PDPN$^+$ITGA5$^+$ synovial Fbs in patients with active RA (top) and remission RA (bottom). Leucocytes (CD45$^+$) and endothelial cells (CD31$^+$) were excluded from the analysis. Within the CD31$^-$CD45$^-$ gate, specific synovial Fbs (PDPN$^+$ITGA5$^+$) can be identified. (E) Two-tailed Spearman's correlation between the percentages of CD45$^-$CD31$^-$PDPN$^+$ITGA5$^+$ synovial Fbs and the CRP concentration, ESR and DAS28 (n = 8). Values represent Spearman's correlation coefficients. P values were corrected for multiple testing using Benjamini-Hochberg method. (F) Box plot showing the ITGA5$^+$ Fb score for the fibroid, lymphoid and myeloid in the PEAC cohort. (G) Heatmap of Spearman's correlation coefficients between Fb subset signature scores and clinical features in the PEAC cohort (anti-CCP, anti-cyclic citrullinated peptide antibodies; HAQ, Health Assessment Questionnaire; RF, rheumatic factor; SWOLLEN, number of swollen joints; TENDER, number of tender joints; VAS, visual analogue scale for pain). (H) Box plot showing the ITGA5$^+$ Fb score of methotrexate (MTX) treatment responders and non-responders with the fibroid,

from synovial tissue were positively correlated with disease activity (ESR, CRP concentration and DAS28) (figure 3C). The histopathology findings were also validated by flow cytometry, and the percentages of ITGA5$^+$PDPN$^+$ cells were positively correlated with disease activity (ESR and DAS28) (figure 3D and E).

Circulating CD45$^-$CD31$^-$PDPN$^+$ proinflammatory mesenchymal, or PRIME, cells have been identified in the peripheral blood before an RA flare-up and may play an important role in resistance to treatment [14]. After integrating the transcriptome of PRIME cells, we calculated the 'PRIME Cell Score' using single sample Gene Set Enrichement Analysis (ssGSEA) and found that the synovial sublining CD45$^-$CD31$^-$PDPN$^+$ITGA5$^+$ Fbs shared the most similar transcriptome to that of PRIME cells, suggesting that this subset of Fbs may migrate into peripheral blood before an RA flare-up occurs (online supplemental figure S3B,C) [33].

Next, we applied deconvolution analysis to further validate the unique transcriptome and proportions of ITGA5$^+$ Fbs in larger cohorts with bulk RNA-seq information. With respect to the PEAC cohort, we studied the associations of the scores of distinct Fb subsets with the synovial pathotype, disease activity and other clinical features, including tenderness, swelling, visual analogue scale (VAS) score, Health Assessment Questionnaire (HAQ) score and inflammatory score, using the ssGSEA method (figure 3F and G). We found that ITGA5$^+$ Fbs (F4) were significantly upregulated in the lymphoid type compared with the fibroid type (figure 3F). The homeostatic clusters PRG4$^+$CLIC5$^+$ (F1) and DPP4$^+$PI16$^+$CD34$^+$ Fb (F6) were negatively correlated with DAS28, ESR, CRP, tenderness, swelling and inflammatory scores, whereas the activated clusters MMP3$^+$VCAM1$^+$ (F2) and ITGA5$^+$ Fb (F4) were positively correlated with the above indicators (figure 3G). The ITGA5$^+$ subset had the strongest association with DAS28 (figure 3G) [22]. The signatures of the ITGA5$^+$ (F4) subset, which included POSTN, LOXL2, COL3A1, TGFB1 and CLEC11A, were also positively correlated with disease activity in the PEAC cohort (online supplemental figure S3D). The R4RA study was a stratified, biopsy-driven, multicentre, open-label, phase IV randomised controlled trial to evaluate rituximab versus tocilizumab treatment in patients with RA and an anti-TNF inadequate response [13]. By using an Microenvironment Cell Populations-counter (MCP-counter) to estimate the population abundance, ITGA5$^+$ Fbs were found to be upregulated in lymphoid-type synovial tissue from non-responder participants (figure 3H) [13,34]. The transcriptomes of ITGA5$^+$ Fbs subsets (POSTN, COL3A1, SPARC and FAP) were also upregulated in lymphoid-type and non-responder participants (online supplemental figure S3E, S3F, S3G). Moreover, the percentage of ITGA5$^+$PDPN$^+$ Fbs had predictive value for refractory RA (non-responders to both rituximab and tocilizumab) (area under the curve: 0.682 (95% CI 0.576 to 0.788)) (figure 3I and J). Taken together, these findings suggest that ITGA5$^+$ Fbs might be associated with lymphoid cells and contribute to the active state of RA, and might be the potential therapeutic targets for refractory RA.

Distinct synovial fibroblast differentiation lineages in patients with active and remission RA

Using several different computational prediction algorithms (scVelo, Slingshot and Monocle), we observed a strong and distinct cell trajectory originating from the stemness-associated DPP4$^+$PI16$^+$CD34$^+$ cluster into ITGA5$^+$ Fbs, CLIC5$^+$PRG4$^+$ Fbs and MMP3$^+$VCAM1$^+$ Fbs through the MMP2$^+$VCAN$^+$ Fb population (figure 4A and B) [16,35–38]. The DPP4$^+$PI16$^+$CD34$^+$ Fb were also known as a stromal progenitor, and our differentiation lineage implied that this Fbs precursors also gave rise to other synovial Fbs subset [16–21]. Two branch points were identified in the Monocle trajectories (T1, T2 and T3) (figure 4A). Prebranch analysis of branch point 1 showed that along the trajectory T1, gene expression levels of collagen (COL3A1, COL6A3), other ECM components (POSTN, TGFBI, SPARC, TNC), cell-cell/cell-matrix interactions (LGALS1), developmental regulation (BGN) and biogenesis of connective tissue (LOX, LOXL2) were increased, with upregulated Kyoto Encyclopedia of Genes and Genomes pathways of ECM-receptor interaction, antigen processing and presentation and TGF-β signalling pathway (figure 4C) [39–42]. The proportions of ITGA5$^+$ Fbs and synovial Fbs in patients with active RA increased along the T1 trajectory (figure 4D). To further explore the transcriptomic perturbation during the development trajectory, we integrated our Monocle trajectory with the predicted TF of synovial Fbs. Interestingly, TF associated with fibrosis (SPI1), cell proliferation and migration (KLF6) and hypoxia (HIF1A) may regulate Fb differentiation from DPP4$^+$PI16$^+$CD34$^+$ Fbs to ITGA5$^+$ Fbs (figure 4E) [43,44]. Among these TFs, KLF6(+) was the most significantly upregulated gene and was only enriched in the T1 trajectory (Spearman's r = 0.75, p<0.001) (figure 4E and F).

Prebranch analysis of branch point 2 also revealed distinct transcriptome alterations when the cells were differentiated into MMP3$^+$VCAM1$^+$ Fb (T2) and CLIC5$^+$PRG4$^+$ Fb (T3) populations, and we found that the toll-like receptor signalling pathway may participate in the T2 trajectory (cluster 4), whereas tryptophan metabolism may be involved in the T3 trajectory (online supplemental figure S4A–C). Moreover, STAT1(+) was significantly upregulated in T2, suggesting that the IFN-related pathway may be involved in F2 phenotype induction, and CUX1 (+) was upregulated in T3, indicating that cellular senescence may also contribute to T3 development (online supplemental figure S4D-E).

To evaluate the transcriptomic response to proinflammatory cytokines, we used the flow-cytometry sorted CD45$^-$CD31$^-$PDPN$^+$DPP4$^+$CD34$^+$ synovial Fbs subset from patients with RA and stimulated it with TGF$^-\beta$1, TNF$^-\alpha$, IL$^-$1β and IFN-γ (figure 4G and online supplemental figure S4F). The expression level of the chemokine CCL5 was upregulated after stimulation with proinflammatory cytokines (TGFβ1, IFN$^-\gamma$ and TNF$^-\alpha$) after 72 hours. The DPP4$^+$CD34$^+$ synovial Fbs also express TGFB1 after stimulation with IL$^-$1β and TNF$^-\alpha$, and this expression can be enhanced by TGF-β1. Moreover, TGF-β1 upregulated the expression of marker genes of ITGA5$^+$ Fbs, including ITGA5 and COL3A1, in the late stage (72 hours), and KLF6 a

lymphoid and myeloid pathotypes in the PEAC cohort. (I) Box plot showing the ITGA5$^+$ Fb score of participants who were refractory to treatment or not in the R4RA cohort. (J) Receiver operating characteristic (ROC) curve showing the predictive value of ITGA5$^+$ Fb for multidrug refractory in the R4RA cohort. TPR, true-positive rate; FPR, false-positive rate. Statistics: two-sided Wilcoxon test in (B, F, H, I); Spearman's correlation analysis in (C, E, G) and p values were corrected for multiple testing using Benjamini-Hochberg method. Data are shown as box plots in (B, F, H, I) (centre line, median; box limits, upper and lower quartiles; whiskers, maximum and minimum values) (*p<0.05, **p<0.01, ***p<0.001, ns, not significant).

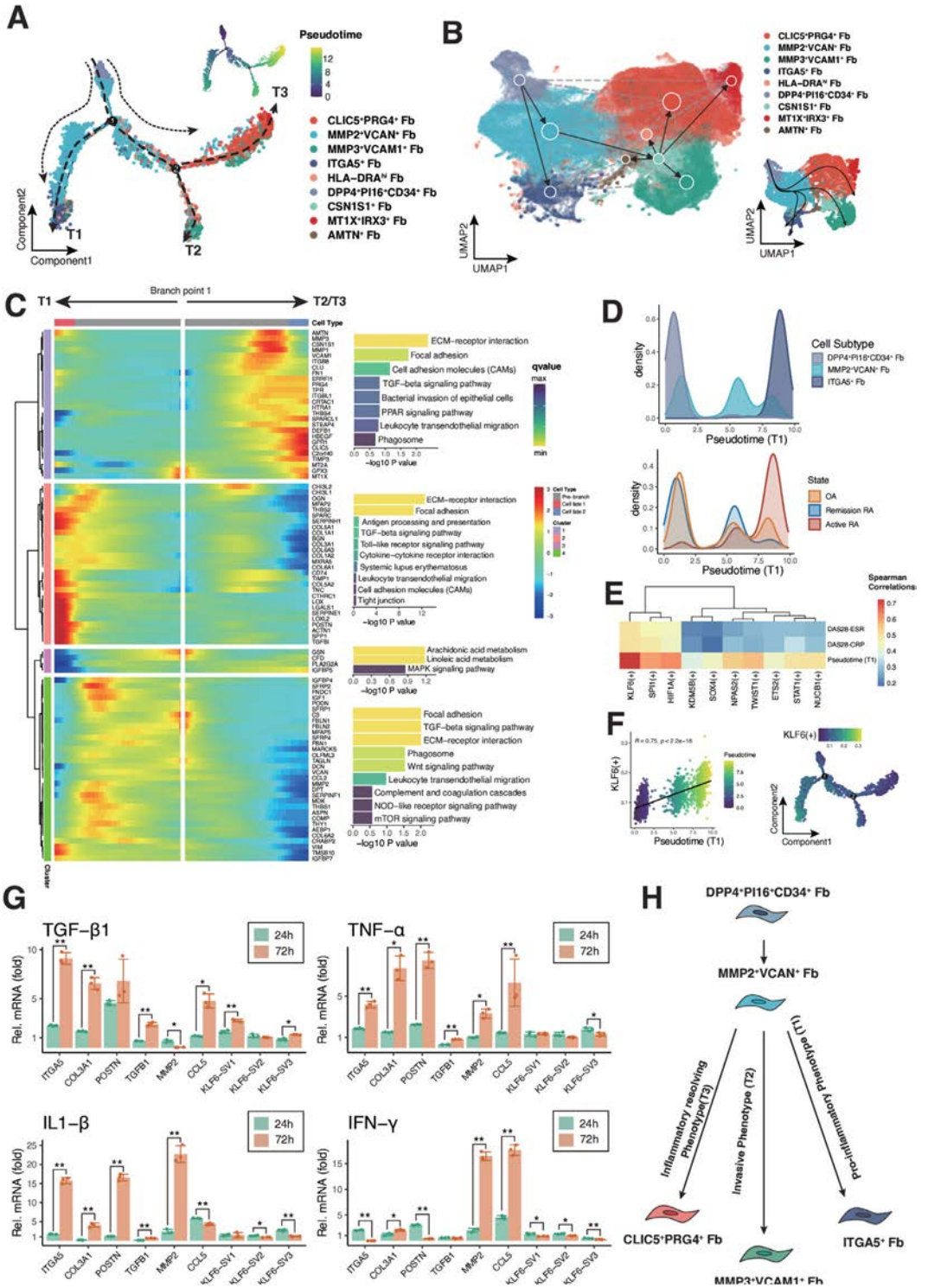

Figure 4. Dynamics of ITGA5$^+$ synovial fibroblasts (Fbs) and unique cell trajectories in human synovial Fbs. (A) Monocle trajectory of synovial Fbs of nine distinct synovial Fb subsets (trajectories T1, T2 and T3; branch points 1 and 2) (bottom) and the corresponding pseudotime lineage (top). (B) scVelo of PAGA velocity graph (left) and Slingshot (right) analyses of synovial Fbs. Arrows indicate the predicted lineage trajectories. (C) Heatmap showing the dynamic gene expression at branch point 1 on the Monocle trajectory and corresponding Kyoto Encyclopedia of Genes and Genomes pathways in each cluster. (D) Dynamic changes in the relative proportions of cell subtypes (DPP4$^+$PI16$^+$CD34$^+$ Fb, MMP2$^+$VCAN$^+$ Fb and ITGA5$^+$ Fb) and synovial Fbs from patients with osteoarthritis (OA), active rheumatoid arthritis (RA) and remission RA on the T1 trajectory. (E) Heatmap showing Spearman's correlations of predicted TF activity and trajectory T1 pseudotime, Disease Activity Score using 28 Joints (DAS28)-ESR and DAS28-C reactive protein (CRP). Values represent Spearman's correlation coefficients. (F) Two-tailed Spearman's correlation between predicted KLF6 activity and T1 pseudotime (left) and between KLF6 activity and the pseudotime lineage (right). Values represent Spearman's correlation coefficients. P values were corrected for multiple testing using Benjamini-Hochberg method. (G) Bar plot showing the relative mRNA expression levels of ITGA5, COL3A1, POSTN, TGFB1, MMP2, CCL5, KLF-SV1, KLF-SV2 and KLF after stimulation with transforming growth factor (TGF)-β1 (10 ng/mL), tumour necrosis factor (TNF)-α (20 ng/mL), interleukin (IL)$^-$1β (10 ng/mL) and interferon (IFN)-γ (10 ng/mL). The gene expression data are normalised to an untreated control in each group (n = 3). Statistics: two-sided Wilcoxon test. Data are mean±SD. Stars represent the level of statistical significance: *p<0.05, **p<0.01. (H) Scheme showing the differential trajectory of synovial fibroblasts (T1: proinflammatory; T2: invasive; T3: inflammatory resolving).

potential TF governing the regulatory process, was also significantly upregulated (figure 4G), suggesting that the positive feedback loop of TGFB1-TGFBR in ITGA5$^+$ Fbs may participate in ECM remodelling in the late stage of inflammation.

In summary, we developed a differential lineage of synovial Fbs that emerged from the DPP4$^+$PI16$^+$CD34$^+$ cluster, passed through the MMP2$^+$VCAN$^+$ cluster and ended at specialised clusters in proinflammatory trajectories (T1, T2) and an inflammatory-resolving trajectory (T3) (figure 4H). The TGF-β1 and TGF-β1 signalling pathways may be involved in the formation of ITGA5$^+$ Fbs (T1) and in tissue remodelling in rheumatoid synovia.

Interaction of ITGA5$^+$ synovial fibroblasts with CD4$^+$PD1$^+$ T cells

We mapped the landscape of the specific stromal-immune compositions of distinct states of RA synovia using correlation analysis of the specific synovial cells subsets. The proportions of ITGA5$^+$ Fbs were positively correlated with proinflammatory myeloid cells (CCL2$^+$SLC2A3$^+$ Mk, cDC1) and T lymphocytes (CD4$^+$ TCM, PD$^-$1^{hi}CXCL13^{lo} TPH, PD$^-$1^{hi} CXCL13^{hi} TPH), suggesting that the ITGA5$^+$ subset may be involved in the proinflammatory microenvironment (figure 5A).

To assess the underlying stromal-immune crosstalk mechanism in active RA, we performed intercellular differential ligand-receptor interaction analyses between ITGA5$^+$ Fb subclusters and stromal and immune cells in RA synovia using CellChat and CellPhoneDB [45]. Thereafter, we identified significant interactions that were considered to be upregulated in active RA synovial cells subclusters relative to the corresponding remission RA synovial cells subclusters. The specific upregulated interactome showed that ITGA5$^+$ Fbs may participate in osteoclast activation (TNFSF11-TNFSF11A), lymphocyte aggregation (CXCL12-CXCR4), angiogenesis (VEGFA-VEGFR1) and synovial Fb proliferation (TGFB1-TGFBR1/TGFBR2) in active RA (online supplemental figure S5A). Interestingly, Fb-T-cell interactions were significantly greater in patients with active RA than in patients with remission RA (figure 5B). The most significant interactions were ITGA5$^+$ Fb$^-$PD$^-$1^{hi}CXCL13^{lo} TPH and ITGA5$^+$ Fb$^-$PD$^-$1^{hi} CXCL13^{hi} TPH (figure 5C). Further interactome analysis revealed that CCL5$^-$CCR5, JAG1-NOTCH1, CD70$^-$CD27, TNF-TNFRSF1A and TGFB1-TGFBR3 were upregulated in active RA (figure 5D).

To systematically map the location of the cell types within the synovial lining and sublining identified by scRNA-seq and further validate the CCI at the spatial level, we used Visium ST technology and dissected the synovial microenvironment in specific niches [46]. We examined four synovial samples from four individuals with OA (n = 2) and RA (n = 2, active and remission RA, respectively). By unsupervised clustering of ST data using SpaGCN, we identified distinct clusters of synovial lining (PRG4, FN1), sublining stroma (COL1A1, DCN), perivascular niche (MCAM, VWF, PECAM1), Mk (CD68, MARCO) and lymphocyte infiltration (CD3D, IGHG4) (online supplemental figure S5B–S5E, online supplemental figure S6A) [47]. After further deconvolution using Cell2location, we found that the ITGA5$^+$ Fb subset was enriched around the lymphocyte infiltration region and was significantly correlated with PD$^-$1^{hi} CXCL13^{hi} TPHs (figure 5E and F) [48]. Integration with spatial transcriptomic data further revealed that only TGFB1$^-$TGBR3 and CCL5-CCR5, which are associated with incoming patterns of CCIs, were increased in spatial regions of PD$^-$1^{hi} CXCL13^{hi} TPH aggregations (figure 5G and H).

ITGA5$^+$ Fbs may induce the differentiation of PD$^-$1^{hi} CXCL13^{hi} TPH cells via the TGF-β1 signalling pathway

Since ITGA5$^+$ Fbs might interact with autoreactive T lymphocytes, we assumed that ITGA5$^+$ Fbs may also promote CD4$^+$ T-cell differentiation into PD$^-$1^{hi} CXCL13^{hi} TPHs. Subcluster analysis further revealed that PD$^-$1^{hi} CXCL13^{lo} TPHs and PD$^-$1^{hi} CXCL13^{hi} TPHs were significantly upregulated in synovial tissue from patients with active RA (figure 6A and B). For PD$^-$1^{hi} CXCL13^{hi} TPHs, expression levels of CXCL13, IL21 and MAF were increased, with upregulated expression of the predicted TFs FOXJ3, KLF8, sec1 and CEBPA (figure 6C, online supplemental figure S7A) [49,50]. CXCL13, when highly expressed in PD$^-$1^{hi} CXCL13^{hi} TPHs, may interact with B cells through the CXCL13-CXCR5 pathway (online supplemental figure S7B). The integration of spatial transcriptomic data revealed that PD$^-$1^{hi} CXCL13^{hi} TPHs and CXCL13-expressing cells were spatially close to memory B cells, with upregulation of the CXCL13 (online supplemental figure S7C,D).

scTCR analysis further identified the clone type of each subcluster of T cells, and PD$^-$1^{hi} CXCL13^{lo} TPHs and PD$^-$1^{hi} CXCL13^{hi} TPHs were clonally expanded in the synovial tissues of patients with active RA (figure 6D, online supplemental figure S7E). Moreover, among PD$^-$1^{hi} CXCL13^{hi} TPHs, clonally expanded cells had higher expression levels of CXCL13, PDCD1, SMAD3 and TGFBR3 (online supplemental figure S7F).

Differentiation trajectory analysis further revealed distinct trajectories from naïve CD4$^+$ T cells to PD-1^{hi} CXCL13^{hi} TPHs (T1) and Tregs (T2) (figure 6E). During T1 of the CD4$^+$ T-cell differentiation trajectory, the expression of CXCL13, HIF1A and SMAD3 increased, as did the percentage of ITGA5$^+$ Fbs (figure 6F). Moreover, after integration with SCENIC analysis for TF prediction, SMAD3, KLF6, KLF4, etc, were upregulated in the T1 trajectory (online supplemental figure S7G). Corresponding to the transcriptomic alterations, the TGF-β signalling pathway was also upregulated, suggesting that TGF-β may mediate the differentiation of CD4$^+$ naïve T cells into PD1^{hi} CXCL13^{hi} TPHs. For T2 trajectory, distinct TFs, including FOXP3, EP300 and ZNF665, were upregulated with increasing antigen processing and presentation pathway (online supplemental figure S7G,H).

Multiplex immunofluorescence (mIF) further revealed that the percentage of CD4$^+$PD$^-$1^{hi} T cells was significantly greater in synovial tissues from patients with active RA than from patients with remission RA, and CXCL13 expression was upregulated (figure 6H). Furthermore, ITGA5$^+$PDPN$^+$ Fbs were found to aggregate around the niche of CD4$^+$PD$^-$1$^+$ T cells (niche1), suggesting potential Fb-T cell interactions among these clusters (figure 6I).

To test the hypothesis that ITGA5$^+$ synovial Fb-derived TGF-β1 may stimulate T-cell differentiation into TPHs in active RA synovia, we dissolved and identified ITGA5$^+$ synovial Fbs using flow cytometry and coculture with naïve CD4$^+$ T cells/Jurkat T cells (figure 6J). Compared with CD31$^-$CD45$^-$PDPN$^+$ITGA5$^-$ synovial Fbs, ITGA5$^+$ synovial Fbs had a greater adhesion capacity to Jurkat T cells (figure 6K). After coculture with ITGA5$^+$ Fbs, the naïve CD4$^+$ T cells were differentiated into CD4$^+$PD$^-$1^{hi}CXCL13^{hi} T cells (figure 6L). Moreover, culture medium from ITGA5$^+$ Fbs also induced the differentiation of naïve CD4$^+$ T cells into CD4$^+$PD$^-$1^{hi}CXCL13^{hi} T cells, which was similar to the effect of TGF-β1 (figure 6L). Jurkat T cells were also induced to differentiate into PD$^-$1^{hi} CXCL13^{hi} T cells using the same coculture and supernatant system (online supplemental figure S7I). Adding the TGF$^-\beta$1 inhibitor (P144) to the coculture system and supernatant significantly reduced the

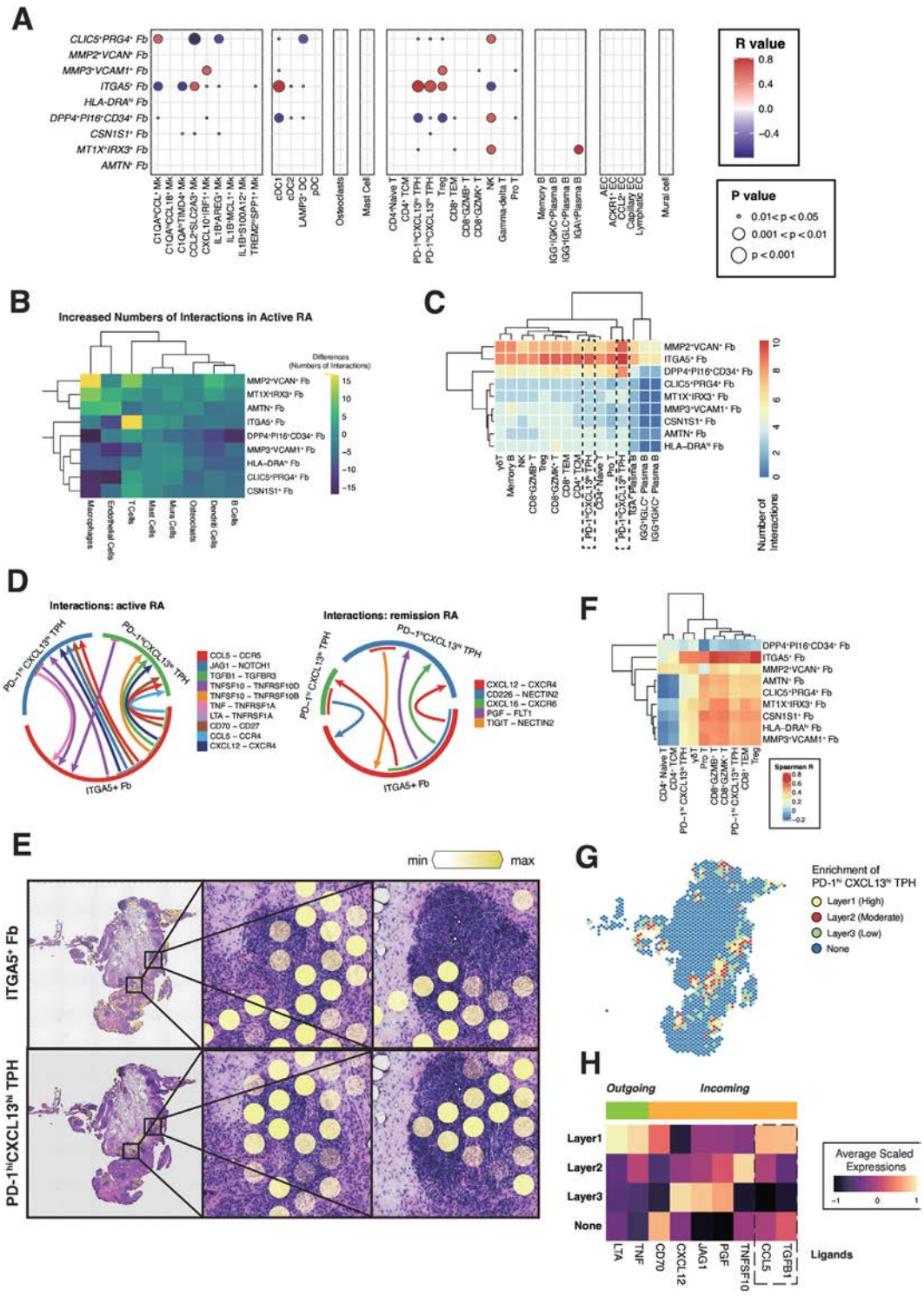

Figure 5. Dissecting the interactome of ITGA5$^+$ synovial fibroblasts (Fbs) and the increase in cell-cell interactions (CCIs) between ITGA5$^+$ Fbs and T cells in active rheumatoid arthritis (RA) synovia. (A) Dot plot showing Pearson's correlation coefficients of the percentages of cell subclusters and synovial Fb subclusters. Values represent Pearson's correlation coefficients. P values were corrected for multiple testing using Benjamini-Hochberg method. (B) Heatmap of differences in the number of CCIs in the interactome of synovial cells between patients with active and remission RA. (C) Heatmap of the CCI between subclusters of Fbs and lymphocytes in patients with active RA. (D) Circle plot of upregulated signalling between ITGA5$^+$ Fbs and PD$^-$1^{hi}CXCL13^{lo} or PD$^-$1^{hi}CXCL13^{hi} T peripheral helper cells (TPHs) in active and remission RA. (E) Spatial plot showing the spatial distributions of the predicted ITGA5$^+$ Fbs and PD$^-$1^{hi}CXCL13^{hi} TPHs in active RA synovial tissue. (F) Heatmap showing the Spearman's correlation coefficients of the spatial locations of distinct fibroblast subsets and T lymphocyte subsets. (G) Spatial plot of the gradients of PD$^-$1^{hi}CXCL13^{hi} TPH enrichment (layer 1: high; layer 2: moderate; layer 3: low). (H) Heatmap showing average scaled expression of ligands from the CCI of ITGA5$^+$ Fbs to PD$^-$1^{hi}CXCL13^{hi} TPHs in outgoing and incoming patterns.

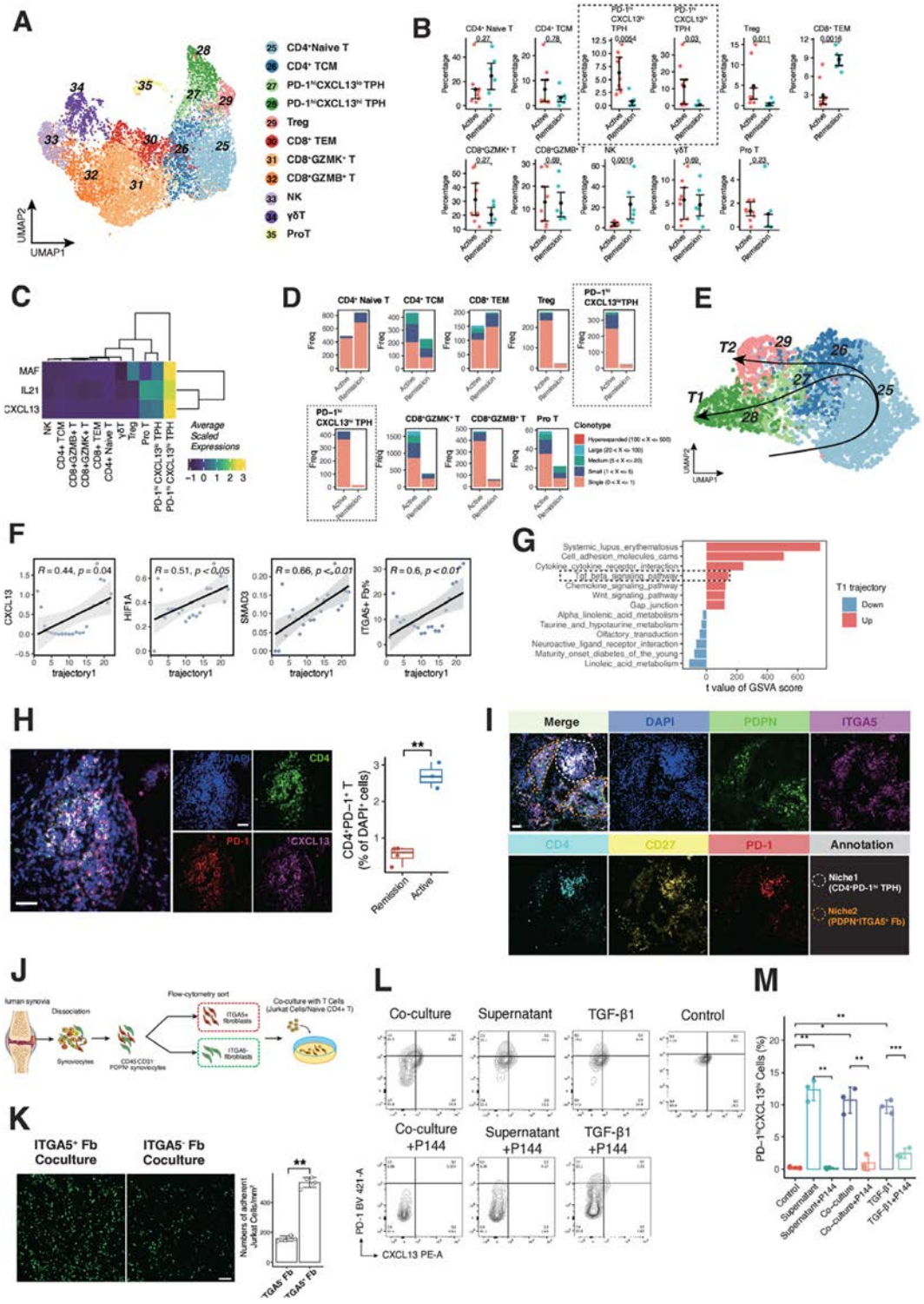

Figure 6. Distinct lymphocyte subsets in remission and active rheumatoid synovia. (A) Uniform manifold approximation and projection (UMAP) visualisation of 11 distinct T cell subsets (number of cells: 9076). (B) Differential proportions of T cell subtypes across patients with active rheumatoid arthritis (RA) (n = 9) and remission RA (n = 6) in the single-cell dataset. Statistics: two-sided Wilcoxon test. Data are shown as mean and error bars (point: mean; upper limit: upper quartile; lower limit: lower quartile). (C) Heatmap of the average scaled expression levels of IL21, CXCL13 and MAF in T cell subsets. (D) Frequency and clonotype of T cell subsets determined by single-cell T cell receptor (scTCR) analysis. (E) Slingshot analysis of the pseudotime trajectory of $CD4^+$ T cells, with distinct differential trajectories (T1: $CD4^+$ naïve T cells to $PD^-1^{hi}CXCL13^{hi}$ peripheral helper T cells (TPHs); T2: $CD4^+$ naïve T cells to regulatory T (Treg) cells). (F.) Two-tailed Spearman's correlation between the T1 pseudotime trajectory and the gene expression of CXCL13, HIF1A, SMAD3 and $ITGA5^+$ Fb%. The light grey area represents 95% CIs. (G) Upregulated and downregulated Kyoto Encyclopedia of Genes and Genomes pathways in the T1 trajectory. (H.) Left, immunofluorescence (IF) staining of CD4 (green), programmed cell death protein 1 (PD-1) (red) and CXCL13 (purple) to identify $CD4^+PD^-1^+$ T cells and CXCL13 signalling in active RA synovial tissues. Scale bars, 50 μm. Right, box plots showing IF results of the proportions of $CD4^+PD^-1^+$ double-positive T cells in active (n = 3) and remission (n = 4) RA. (I) Multiplex IF (mIF) staining of PDPN (green) and ITGA5 (purple) in $ITGA5^+PDPN^+$ synovial fibroblasts (Fbs) and of CD4 (light blue), CD27 (yellow) and PD^-1 (red) in $CD4^+PD^-1^+$ TPHs from patients with resistant RA. Scale bars, 50 μm. Representative images from one of three independent experiments are shown. The white dashed line outlines Niche1 ($CD4^+PD\text{-}1^+$ TPH), and the yellow dashed line outlines Niche2 ($ITGA5^+PDPN^+$ Fbs). (J) Scheme of coculture of synovial Fbs with T cells. Synovial tissues from patients with RA were dissociated, and $CD45^-CD31^-PDPN^+ITGA5^+$ Fbs and

differentiation of T cells (figure 6L and M). Taken together, these findings indicate that TGF-β1 derived from ITGA5$^+$ synovial Fbs could induce naïve CD4$^+$ T cells to differentiate into CD4$^+$PD$^-$1^{hi}CXCL13^{hi} T cells and maintain a sustained proinflammatory environment for lymphocyte aggregation and B cell differentiation.

ITGA5$^+$ fibroblast subsets are responsible for synovial inflammation and joint destruction in rheumatoid arthritis

Since ITGA5$^+$ synovial Fbs may induce the differentiation of naïve CD4$^+$ T cells to PD-1^{hi} CXCL13^{hi} TPHs in the proinflammatory microenvironment, we hypothesised that ITGA5$^+$ Fbs are involved in the early stage of joint inflammation and play a vital role in lymphocyte infiltration of rheumatoid synovia. To test this hypothesis, we used collagen-induced arthritis (CIA) in DBA/1 mice to study the proportions of Cd45$^-$Cd31$^-$Pdpn$^+$Itga5$^+$ synovial Fbs at the early (days 21, 28) and established (day 35) stages of joint inflammation and the corresponding phenotypes (arthritis score, bone micro-CT, pathological evaluation and gene expression) (figure 7A). Moreover, we injected flow cytometry-sorted Cd45$^-$Cd31$^-$Pdpn$^+$Itga5$^+$ and Cd45$^-$Cd31$^-$Pdpn$^+$Itga5$^-$ synovial Fbs into the synovial joints of CIA mice on day 14 to evaluate the potential role of Itga5$^+$ Fbs in joint inflammation (figure 7A).

Bone erosion, synovitis and cartilage degeneration were more severe in the late stage of joint inflammation (figure 7B). However, the proportions of Cd45$^-$Cd31$^-$Pdpn$^+$Itga5$^+$ synovial Fbs were upregulated in the early stage (days 21 and 28) (figure 7C and D). As predicted from the single-cell transcriptome analysis, the ITGA5$^+$ Fb subset exhibited an immune effector profile characterised by increased expression of chemokines and cytokines, including CCL5 and TNFSF11 as well as MMP9 and MMP13, which are involved in cartilage degradation. Using ssGSEA for deconvolution, we found that the Itga5$^+$ Fbs were positively correlated with the Mmp9, Tgfb1 and Il1b expression in mouse synovial joints (figure 7E, online supplemental figure S8A). Compared with Itga5$^-$ synovial Fbs and phosphate-buffered saline (PBS), intra-articular injection of Itga5$^+$ synovial Fbs led to more inflamed ankle joints with greater Hind paw thickness and arthritis scores (figure 7F, online supplemental figure S8B). The bone erosion score, synovitis score and percentage of destained cartilage also increased after Itga5$^+$ Fb injection (figure 7G and H, online supplemental figure S8C). Intra-articular injection of TGF-β1 also led to joint destruction, synovitis and cartilage degeneration (online supplemental figure S8D,E). Interestingly, the gene expression of Cxcl13 and the PD$^-$1^{hi} CXCL13^{hi} TPH score were significantly upregulated in the early and late stage of joint inflammation after intra-articular injection, suggesting that Itga5$^+$ Fbs might be keystones of the aggregation and differentiation of TPHs in the synovial joint in the late stage (figure 7I, online supplemental figure S8E,F). The expression of multiple cytokines that may reflect tissue remodelling (Tgfb1, Tnfsf11, Csf1, Mmp3, Mmp9, Mmp13, Adamts4, Adamts5, Vegfc and Pdgfra) was also upregulated after Itga5$^+$ Fbs injection in the late stage of synovitis (online supplemental figure S8G).

DISCUSSION

Multiple cell components and typical transcriptomic signatures may jointly maintain the complex pathophysiology of autoimmune diseases and affect disease status [51]. Here, using the integrated methods of scRNA-seq, scTCR-seq and spatial profiling of ST and mIF, we were able to fully assess the underlying cellular ecosystem and zonations that may drive distinct disease activities, pathotypes and responses to treatment in RA joints. We identified a novel subset of activated sublining Fbs (CD45$^-$CD3$^-$PDPN$^+$ITGA5$^+$) delineating a critical region for potentially modulating the proinflammatory response, signalling to neighbouring cells and remodelling the tissue microenvironment. Moreover, we propose the central involvement of TGF-β signalling in the initiation, formation and maintenance of synovial inflammation in patients with RA (online supplemental figure S9).

Integrin alpha 5 (ITGA5) was found in cancer-associated fibroblasts (CAFs) to promote invasion, proliferation and chemoresistance [52]. Integrated single-cell data and functional validation revealed the potential multifaceted functions of this terminally differentiated subset of synovial Fbs, including proangiogenic effects, proliferative effects, ECM reconstruction and immune regulation, suggesting the central role of tissue remodelling in persistent inflammation. Coordinated expression of HIF1A and SOX9 further implied that this subset might undergo differentiation into osteochondrogenic lineage in chronic phase and leads to an increased susceptibility to chronic inflammatory arthritis and subsequent new bone formation, reminiscent of ankylosis [31].

The current realistic goal of RA management is to achieve remission or low disease activity (LDA) [53]. However, the critical multicellular mechanism involved in relapsing and remitting RA, especially after disease-modifying antirheumatic drugs (DMARDs) treatment, has not been identified [14]. Fbs play key roles in regulating immune responses in individuals with disease and healthy individuals, and synovial Fbs have long been attractive therapeutic targets [54]. To date, no therapy targeting synovial Fbs has been approved [55]. One of the explanations for resistance to the currently available DMARDs, which fail to treat fibroblastic disease, is the significant role of non-immune stromal pathology [7]. Validated by the PEAC and R4RA cohorts, our analysis revealed that the ITGA5$^+$ Fb subset with a unique transcriptome may also predict multidrug resistance to DMARDs

CD45$^-$CD31$^-$PDPN$^+$ITGA5$^-$ Fbs were sorted using flow cytometry. Sorted synovial Fbs were cocultured with Jurkat T cells or CD4$^+$ naïve T cells. (K) Adhesion assay showing the increased adherence of ITGA5$^+$ synovial Fbs to Jurkat T cells (n = 5 for ITGA5$^+$ Fb coculture and ITGA5$^-$ Fb coculture group, respectively). (L) Representative flow cytometric gating scheme for the identifications of PD$^-$1$^+$CXCL13$^+$ T cells in different conditions including direct coculture with ITGA5$^+$ synovial Fbs, direct coculture adding P144 (TGF-β1 inhibitor), adding the supernatant of ITGA5$^+$ Fbs to T cell medium, adding the supernatant with P144 to T cell medium, adding TGF-β1 to T cell medium and adding TGF-β1 with P144 to T cell medium, compared with control group (n = 3 for each group, respectively). (M) Percentages of PD$^-$1^{hi}CXCL13^{hi} T cells in different coculture conditions corresponding to figure 6L (n = 3 for each group, respectively). Representative images from one of three independent experiments are shown in (H, I, K). Statistics: two-sided Wilcoxon test in (B, H, K, M). Two-tailed Spearman's correlation in (F) and p values were corrected for multiple testing using Benjamini-Hochberg method. Data are shown as mean and IQR (point: mean; upper limit: upper quartile; lower limit: lower quartile) in (B); box plots (centre line, median; box limits, upper and lower quartiles; whiskers, maximum and minimum values) in (H); mean±SD. in (K, M). *P<0.05, **p<0.01 and ***p<0.001.

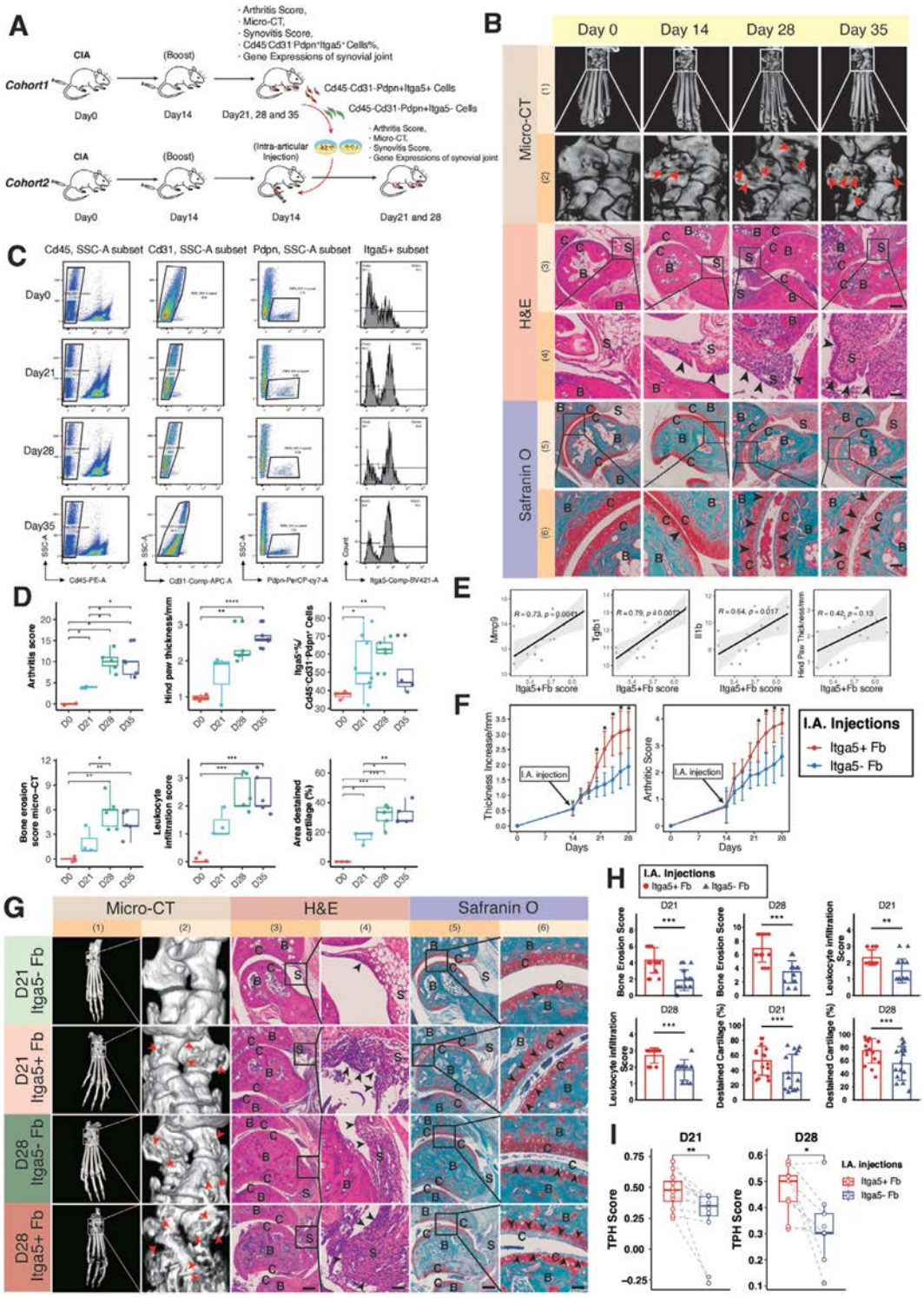

Figure 7. Itga5$^+$ synovial fibroblasts (Fbs) regulate synovial inflammation and tissue remodelling in different stages of collagen-induced arthritis (CIA). (A) Scheme of the design of the CIA mouse model to evaluate the relationships between synovitis and Itga5$^+$ Fbs (cohort 1) and adoptive transfer of mouse synovial fibroblasts to evaluate the role of Itga5$^+$ Fbs (cohort 2). (B) Representative images at days 0, 21, 28 and 35 of the micro-CT scan (1, 2), H&E staining (3, 4) and safranin O staining (5, 6) of the ankle joints of CIA mice. Scale bars (3, 5): 200 μm; scale bars (4, 6): 50 μm. (C) Representative flow cytometric gating scheme for the analysis and identification of mouse Cd45$^-$Cd31$^-$Pdpn$^+$Itga5$^+$ Fbs in the ankle joints of CIA mice at days 0, 21, 28 and 35 (n = 3 in each group). (D) Quantification of the arthritis score, hind paw thickness, Itga5$^+$ Fbs%, bone erosion, leucocyte infiltration and cartilage damage (day 0: n = 3; day 21: n = 3 (except Itga5$^+$ Fbs%: n = 7); day 28: n = 5; day 35: n = 6). (E) Two-tailed Spearman's correlation between the Itga5$^+$ Fb score and the gene expression of Mmp3, Tgfb1 and Il1b and between the Itga5$^+$ Fb score and hind paw thickness (n = 14). (F) Effect of intra-articular (I.A.) injection of Itga5$^+$ Fbs into the ankle joints of day 14 CIA mice compared with Itga5$^-$ Fbs into the contralateral joints (n = 17 for each group). (G) Representative images at days 21 and 28 of the micro-CT scan, H&E and safranin O staining of intra-articular injection of Itga5$^+$ Fbs in ankle joints of CIA mice, compared with Itga5$^-$ Fbs into the contralateral joints. Scale bars (3, 5): 200 μm; scale bars (4, 6): 50 μm. (H) Quantification of the bone erosion, leucocyte infiltration and cartilage damage of I.A. injection of Itga5$^+$ Fbs and Itga5$^-$ Fbs of CIA mice in days 21 and 28 after primary immunisation (day 21: n = 16 for each group; day 28: n = 17 for each group). (I) Quantification Pd$^-$1^{hi}Cxcl13^{hi} TPHs score from RNA-seq data of I.A. injection of Itga5$^+$ Fbs and Itga5$^-$ Fbs in ankle joints of CIA mice in day 21 and 28 after primary immunisation (day 21: n = 12 for each group; day 28: n = 9 for each group). Representative images from one of three independent experiments are shown in (B, G). Statistics: two-sided

[56]. Targeting ITGA5$^+$ Fbs might be the key to overcoming the ceiling effect of current DMARD therapies.

Our study unveiled the unique differentiation trajectories of distinct synovial Fbs subsets, and ITGA5$^+$ Fbs subsets might be induced by TGF-β1 and differentiated from DPP4$^+$PI16$^+$CD34$^+$ 'universal fibroblasts' as a stromal progenitor to various steady-state and pathological Fbs [16–21]. DPP4$^+$PI16$^+$CD34$^+$ Fbs are pivotal in the beginning of the multiple differentiation trajectories, and potentially regulated by multiple pathways and TFs into different subsets of synovial Fbs (figure 4 and online supplemental figure S4). Other distinct Fbs differentiation lineage and potential regulatory mechanism was also found in alveolar Fbs [57]. Previous study revealed that RA-specific synovial T cell-derived transforming growth factor (TGF)-β and Mk IL$^-$1β synergy in driving the transcriptional profile of FAPα^+THY1$^+$ invasive synovial Fbs [58]. Moreover, previous study also implicated that ETS1 drives polarisation towards tissue-destructive Fbs by orchestrating hitherto undescribed regulatory elements of the osteoclast differentiation factor receptor activator of nuclear factor-κB ligand (RANKL) as well as MMPs [59]. Our study also identified KLF6 as a novel target for therapeutic intervention, which might govern the perturbation of transcriptomic profile and regulate the phenotypic alterations and activations of synovial Fbs to ITGA5$^+$ Fbs [43]. As far as we known, KLF6 drives inflammatory response, promote cellular differentiation, proliferation and plasticity, and the TGFβ-KLF6 axis plays a central role in epithelial-to-mesenchymal transition (EMT) in fibrosis, which has not yet been reported in the RA [60]. Moreover, targeting DPP4$^+$PI15$^+$CD34$^+$ Fbs and modulating the differential trajectory of DPP4$^+$PI16$^+$CD34$^+$ Fbs to ITGA5$^+$ Fbs might be the potential therapeutic strategy for RA synovitis for regaining regeneration capacity and the homeostatic microenvironment [61].

We propose the central involvement of TGF-β signalling in initiating and maintaining the proinflammatory microenvironment in synovitis in addition to other mediators, such as SMAD3, HIF1A and SPI1, which are linked to cell migration, Fb activation and differentiation, hypoxia and fibrosis [62–64]. TGF-β1, secreted from the ITGA5$^+$ Fb subset, may induce the differentiation of peripheral synovial Fbs and the expression of CCL5, TGF-β1 and TNFSF11A (RANKL) at an early stage, forming spatial niches for aggregated ITGA5$^+$ synovial Fbs. Moreover, ITGA5$^+$ synovial Fbs may also promote the chemotaxis of naïve CD4$^+$ T cells via CCL5$^-$CCR4 interactions and induce the differentiation of naïve CD4$^+$ T cells into PD$^-$1^{hi} CXCL13^{hi} TPHs via TGF-β1. Other studies also point to Fbs as pivotal drivers of tertiary lymphoid structure (TLS) formation at the earliest phases of TLS establishment, preceding lymphocyte infiltration [65]. Our study revealed that ITGA5$^+$ synovial Fbs initiate lymphocyte aggregation in rheumatoid synovitis. PD$^-$1^{hi} CXCL13^{hi} TPHs, which were identified as disease exacerbation-related T cell subsets, can attract B cells through CXCL13-CXCR5 interactions and have the unique capacity to induce plasma cell differentiation through IL-21 secretion and SLAMF5 interactions both within lymphoid aggregates and more diffusely throughout the inflamed synovium [49,50]. Our findings emphasised the role of PD$^-$1^{hi}CXCL13^{hi} TPHs in RA development and revealed the upstream mechanisms involved in the local differentiation of TPHs. The close spatial interaction between ITGA5$^+$ Fbs and T cells was also validated by ST and mIF, which might be key factors driving RA progression. In the late stage of inflammation, ECM-related signatures (POSTN and COL3A1) were also significantly increased, suggesting the tissue-remodelling effect of ITGA5$^+$ Fb niches. An in vivo study further revealed that TGF-β1-expressing Itga5$^+$ synovial Fbs could lead to joint destruction and cartilage degeneration in the late stage. The TGF-β signalling pathway is also regulated by epigenetic modifications during the development of RA [66]. Previous studies have shown that the pleiotropic nature of the TGF-β signalling pathway contributes to drug resistance in tumours, [67] and TGF-β might also be the underlying mechanism and novel target of multidrug resistance in RA. Activated ITGA5$^+$ Fbs expressing TGF-β1 might also explain the relapse and flare-up of RA. Our findings may help to generate new therapeutic strategies to exploit Fb-based endogenous mechanisms involved in the resolution of synovitis.

Limitations of this study include the modest sample size in each subgroup, which may not be sufficient to precisely determine the correlation between the heterogeneity of patients with RA in the transcriptome data and patient characteristics, such as genomic alterations. However, deconvolution of multiple public transcriptome datasets and mIF staining of synovial tissues in cohort studies may further extend our findings.

In summary, our osteoarthritic and rheumatoid atlas is valuable for rheumatic disease researchers because it largely updates the RA taxonomy in human synovial tissue and explains the potential tissue-remodelling effect of PDPN$^+$ITGA5$^+$ synovial Fbs in active RA. This study provides a platform for future research that aims to deepen our understanding of rheumatoid synovial biology and to improve the management of drug-resistant RA.

METHODS

Human samples

For scRNA-seq and ST, synovial samples were prospectively collected from patients with RA (n = 17) or OA (n = 6) who had undergone total joint arthroplasty or synovial biopsy between January and December 2021. Furthermore, for functional experiments, additional RA synovial tissue samples (n = 10) were collected between March 2022 and August 2022. Each sample was evaluated by an expert pathologist, and pathotypes were identified. For each patient with RA, clinical and laboratory evaluations included the number of tender and swollen joints (28 examined), the ESR, the CRP level and the DAS28. Peripheral blood samples were tested for IgA, IgM-RF and ACPA. Patients with RA in sustained clinical remission (DAS28 <2.6 for more than 1 year) or persistent active remission (DAS28 >2.6) were selected [2,13].

Histological analysis

All synovial biopsies were obtained and paraffin-embedded at the First Affiliated Hospital of Sun Yat-sen University. Tissue sections (3–5 μm thick) were stained with H&E and for the

Wilcoxon test in (D); Spearman's correlation analysis and p values were corrected using Benjamini-Hochberg method in (E); Wilcoxon signed-rank test (F, H, I). Data are shown as box plots (centre line, median; box limits, upper and lower quartiles; whiskers, maximum and minimum values) in (D, I); mean±SD in (F, H). *P<0.05, **p<0.01, ***p<0.001, ****p<0.0001. B, bone; C, cartilage; S, synovial tissue.

immunohistochemistry (IHC) markers CD68 (Mk), CD3 (T cells), CD20 (B cells) and CD138 (plasma cells). Following IHC staining, two investigators determined the levels of $CD20^+$ B cells, $CD3^+$ T cells, $CD138^+$ plasma cells and the $CD68^+$ lining and sublining Mk sections using semi-quantitative scoring (0–4). Synovial biopsies were classified into pathotypes according to the following criteria: (1) lympho-myeloid—grades 2–3 $CD20^+$ aggregates, CD20 ≥2 and/or CD138≥ 2; (2) diffuse-myeloid—CD68SL ≥2, CD20 ≤1 and/or CD3 ≥1 and CD138 ≤2 and (3) pauci-immune-fibroid—CD68SL <2 and CD3, CD20 and CD138 <1 [56]. H&E-stained slides were also evaluated to determine the level of synovitis according to the Krenn synovitis score (0–9) [68].

Single-cell isolation of synovial tissues

After collection, fresh synovial tissues were cut into 1–2 mm^3 fragments using a sterile scalpel and transferred to a sterile universal container containing 10 mL of sterile RPMI supplemented with 100 U/mL penicillin/streptomycin and 2 mM L-glutamine. The RPMI medium also contained 1 mg/mL collagenase I (no. 17100017, Thermo Fisher) and 50 U/mL hyaluronidase (H3506, Sigma-Aldrich). The tissue pieces were incubated at 37°C and 5% CO2 in a humidified atmosphere for 15 min, after which 0.25% trypsin-EDTA (No. 252000556, Gibco) was subsequently added for 10 min with rotation on a Miltenyi MACSmix tube rotator during this incubation. After incubation, the digested mixture was filtered through a 50 mL Falcon tube using an Easy Strain 100 μM cell strainer. Complete medium (RPMI supplemented with 10% fetal calf serum) was added to the Falcon tube through the filter, after which the mixture was centrifuged at 1800 r.p.m. for 10 min at 4°C, after which the supernatant was carefully removed. Red blood cells were lysed using red blood cell lysis buffer (Miltenyi, no. 130-094-183). The cells were subsequently centrifuged at 1500 r.p.m. for 5 min at 4°C. The supernatant was removed, and the cells were aliquoted for subsequent scRNA-seq. Moreover, the residual cells were added to 1 mL of ice-cold freezing mix (Bambanker, no. 302-14681), immediately frozen at −80°C and stored in liquid nitrogen.

Spatial transcriptomics

We performed ST using the Visium Spatial Gene Expression assay (10x Genomics). In brief, human synovial samples were incubated in optimal cutting temperature compound (OCT) at 4°C for 30 min, frozen in OCT and stored at −80°C. Ten micromolar sections of synovial tissues were placed on a Visium Gateway gene expression slide and stored with desiccants at −80°C until staining and library preparation. Using a Visium Spatial Tissue Optimisation slide, we estimated that the optimal permeabilisation time was 15 min. H&E staining was performed on the Visium slides and images. Tissue sections were permeabilised immediately to capture RNA molecules on barcoded spots on the slide. Libraries were then prepared and sequenced (150 bp paired-end) on an Illumina NovaSeq 6000.

Library preparation, sequencing and data preprocessing

Single-cell suspensions were converted to barcoded scRNA-seq libraries using a Chromium Single-Cell 5' Kit (V.1) (10x Genomics) according to the manufacturer's instructions (PN-1000020, 10x Genomics), aiming for 8000–10 000 cells per library. Library quality control and quantification were performed using a 2100 Bioanalyzer Instrument (G2939BA) and a 2100 Bioanalyzer High Sensitivity DNA Kit (Agilent, 5067-4626). Libraries were sequenced on an Illumina NovaSeq 6000 sequencing platform with an average depth of 58 073 reads per cell, mapped to the human genome (build GRCh38) and demultiplexed using CellRanger pipelines (10x Genomics, V.3.1.0).

Data processing and cell clustering of individual cases

The preprocessed data from every sample were subjected to additional processing and analysis on an individual basis using RStudio (V.4.0.2) and the R package Seurat (V.4.1.0) [69]. Using SoupX software, the background signal from the UMI count data was filtered [70]. Once ribosomal genes, genes expressed in fewer than three cells and cells expressing fewer than 200 genes were eliminated, we removed low-quality cells or those with fewer than 200 unique features. Additionally, cells with unique feature counts more than three times the median value (perhaps doublets) and/or more than twice the median amount of mitochondrial genes (maybe lysed or apoptotic cells) were eliminated. Using the DoubletFinder program, we eliminated duplicate data from our datasets [71]. Next, we used the normalizeData function to normalise the data and the FindVariableFeatures function to extract highly variable features. Using the RunPCA function, normalised data were subjected to linear transformation (scaling) and principal component analysis (PCA) based on variable characteristics. Next, using the default parameters of the FindNeighbors and FindClusters functions, graph-based clustering according to the gene expression profiles was carried out. The results were subsequently evaluated using the RunUMAP and DimPlot functions as part of the non-linear dimensional reduction uniform manifold approximation and projection (UMAP) technique. Expression levels for canonical markers, such as VWF and PECAM1 for ECs, ACTA2 and MCAM for mural cells, MARCO and CD68 for synovial Mks, DCN and PRG4 for synovial Fbs and MKI67 and TOP2A, were used to identify clusters of an aggressively proliferative nature and to annotate cell clusters.

Data integration with batch effect collection

We performed SCTransform analysis for normalisation and variance stabilisation of single-cell RNA-seq data using regularised negative binomial regression [72]. Integrated data were scaled and subjected to PCA, as performed for individual datasets. We performed graph-based clustering of PCA-reduced integrated data and supervised annotation, as described in the 'Data processing and cell clustering of individual cases' section. Clusters characterised by extremely low unique feature counts (low-quality cells) were removed.

After extracting the main components of synovial cells (Fbs, ECs, Mks, T lymphocytes and B lymphocytes), we divided each component into unsupervised graph-based subclustering, scaling and PCA-based dimensional reduction. We eliminated subclusters that inconsistently exhibited high numbers of unique features and high expression of marker genes for distinct synovial cells components, which suggested that these cells might be doublets.

Tissue enrichment analysis

To characterise the tissue distribution of cell subtypes, ORs were calculated and used to indicate preferences according to the detailed method described by Zheng *et al* [73].

DEG analysis

With a minimum of 20% of the gene-expressing cells and a minimum log fold change of 0.25 in the gene expression between each cluster and other clusters, DEG analysis was carried out using the FindMarkers or FindAllMarkers tools. For DEG detection, we mainly employed the Wilcoxon rank-sum test. We also employed model-based analysis via single-cell transcriptomics (MAST) to validate the DEGs that we identified [74]. DEGs were identified as genes that, when examined using both approaches, demonstrated an adjusted p value (derived from the Bonferroni correction) of <0.05. DEG lists were created using the Wilcoxon rank-sum test. Gene set variation analysis and GSEA were used to conduct GO enrichment analysis of DEGs in specific clusters [33,75].

Trajectory analysis

We used the Slingshot (V.2.2.1), scVelo and Monocle (V.2.22.0) packages to perform trajectory analysis on combined synovial data [35–37]. The preprocess_cds function was used to preprocess the data for Monocle analysis, with a setting of 100 for the number of dimensions. The reduce_dimension and cluster_cells functions were used for dimensionality reduction and clustering, respectively. Next, we used the learn_graph function to fit a main graph inside each cluster, and the plot_cells function, along with the pseudotime colouring option, allowed us to display the cell order in pseudotime. UMAP embeddings of the Fb object were employed as the input for the Slingshot trajectory analysis [36]. The Cell Ranger output files were subjected to the read counting process velocyto.py to produce.loom files for RNA velocity, which describes the rate of gene expression change for an individual gene at a given time point based on the ratio of its spliced and unspliced messenger mRNA [35]. These files were subsequently read in R using the SeuratWrappers V.0.2.0 and Velocyto V.0.6 packages [76]. After the Fb cluster was chosen, the 'spliced', 'unspliced' and 'ambiguous' data, along with any related metadata (such as cell type annotation), were stored in an h5ad file using the technique described in the sceasy R package. The Fbs object's 'spliced', 'unspliced' and 'ambiguous' tests, together with any related metadata (such as cell type annotation), were stored as an h5ad file. The scVelo package was used in the Jupyter Notebook to read the h5ad file. Filtered and normalised data were used. The scvelo.pp.moments() command was used to calculate moments; the arguments were number of neighbours = 20 and number of pcs = 20. The scvelo.tl.velocity() command was used to estimate velocity in the default stochastic mode. Next, PAGA estimation was carried out with default settings using scvelo.tl.paga(). A combined scVelo and PAGA plot was generated using the scvelo.pl.paga() command, with $\alpha = 0.1$, min_edge_width = 2 and node_size_scale = 1.5 as options (https://scvelo.readthedocs.io/en/stable/) [35,38].

REGULON NETWORK

The R package SCENIC (V.1.1.3), which examines the coexpression of TFs and their potential target genes, was used to construct a regulon network. We used the default parameters to construct and score the gene regulatory network. Using the runCorrelation and runGENIE3 programs, a coexpression network was constructed using the raw count matrix. RcisTarget identified potential regulons based on DNA-motif analysis, while AUCell identified active gene networks. For every cell, the average normalised expression of potential target genes was used to compute the regulon activity.

Spatial transcriptomics data processing and analysis

Manual fiducial dot alignment was performed on H&E images using the Loupe browser V.5.0.1 (10x Genomics). Spaceranger V.1.2.2 (10x Genomics) was used to process FASTQ files and align H&E images, with the GRCh38 (GENCODE V.32/Ensembl 98) genome serving as a reference. Using Seurat V.4.0.1 on R, spot UMI tables and reference H&E photos were further examined. Using the SCTransform V.0.3.2 technique, the data were standardised. The SpatialFeaturePlot() tool was used to visualise spatial gene expression. The ST dots were manually placed on high-resolution H&E images for improved visibility. The RunPCA() and RunUMAP() commands were used to reduce dimensions, and an SSN technique was used for clustering. Heatmaps were generated using the doHeatmap() function, and markers were located for every cluster using the FindAllMarkers () command. Using the Cell2location program, scRNA-seq data from human synovial samples used in this investigation were combined with ST data [48].

Immunohistochemistry

After being dried and embedded in paraffin, the synovial tissues were fixed in 4% paraformaldehyde overnight. After preparing 4 μm thick slices, antigen retrieval was carried out for 10 min at 95°C in citrate buffer (pH 6.0). ZSGB-Bio (Beijing, China) carried out further staining and image scanning. Antihuman CD68 (ab201340, Abcam), antihuman CD20 (ab78237, Abcam), antihuman CD3 (ab40804, Abcam) and antihuman CD138 (ab128936, Abcam) were the primary antibodies used.

MULTIPLEX IMMUNOFLUORESCENCE

For mIF, tissue slides were deparaffinised with xylene and rehydrated through a graded series of ethanol solutions (100%, 95% and 70%). Then, the slides were subjected to microwave irradiation to induce antigen retrieval via citric acid solution for 15 min. For mIF analysis of the human samples, seven panels of primary antibodies were used, including (1) ITGA5 (1:200, ab150361, Abcam) and PDPN (1:5,000, ab236529, Abcam); (2) CD4 (1:100, ZA0508, ZSGB), PD1 (1:100,18106-1-AP, PTG) and CXCL13 (1:100, PA5-28827, Invitrogen) and (3) PDPN (1:5,000, ab236529, Abcam), ITGA5 (1:200, ab150361, Abcam), CD27 (1:100, ab131254, Abcam), PD1 (1:100,18106-1-AP, PTG) and CD4 (1:100, ZA0508, ZSGB). Following that, the slides were treated for 10 min at room temperature with secondary antibodies (1:1100 μL per slide; horseradish peroxidase (HRP)-conjugated antirabbit IgG, ZSGB, or PV-6001; or HRP-conjugated antimouse IgG, ZSGB, PV-6002). Heat-induced epitope retrieval was used to eliminate all antibodies, including primary and secondary antibodies, following each staining cycle. To perform mIF staining, the AlphaTSA Multiplex IHC Kit (AXT36100031, AlphaX) was used. After the samples were mounted in mounting media, the nuclei were counterstained with 4',6-diamidino-2-phenylindole (DAPI) for 10 min. A ZEISS AXIOSCAN 7 was used to obtain multispectral images. Using QuPath (V.0.2.0) or Halo (V.3.4; Indica Labs), the cells of interest were evaluated.

Flow cytometry and cell sorting

For ITGA5$^+$ Fb (CD45$^-$CD31$^-$PDPN$^+$ITGA5$^+$) and mesenchymal precursor cells (CD45$^-$CD31$^-$PDPN$^+$CD26(DPP4)$^+$CD34$^+$) sorting and quantification, cryopreserved cells were thawed and washed twice in cold PBS. For clumped samples, deoxyribonuclease (DNase) I (Roche, 10104159001) solution (1 mg/mL) was used to dissociate the cells. The cell suspensions were stained in PBS/1% bovine serum albumin (BSA) (stain buffer) with Fixable Viability Stain 700 (BD Biosciences, 564997) and the following antibodies for 15 min: anti-CD31-PE and anti-CD45-BUV395 (from BD Biosciences). Additional panels of antibodies included anti-PDPN-BV421, anti-ITGA5-BB700, anti-CD34-PE-Cy7 and anti-CD26-FITC from BD Biosciences. The cells were washed in cold stain buffer and passed through a 70 μm filter. The data were acquired and analysed on a BD FACS LSRFortessa X-20 or FACS Aria II using FACSDiva software. The data analysis was performed using FlowJo V.10.8.1. After correction, a set of gates for CD45, CD31, PDPN and ITGA5 or CD34 and CD26 was deployed on all the samples. The percentage of ITGA5$^+$ Fb populations among PDPN$^+$ synovial cells populations and the percentage of ITGA5$^+$PDPN$^+$ Fbs among total synovial cells were calculated for the indicated samples. The CD45$^-$CD31$^-$PDPN$^+$CD26$^+$CD34$^+$ synovial cells were also sorted from patients with RA.

PRIME cell signatures and enrichment analysis of distinct fibroblast subsets

The transcriptomic signatures of circulating CD45$^-$CD31$^-$PDPN$^+$ preinflammatory mesenchymal or PRIME cells were also aligned to our single-cell transcriptomic datasets of distinct Fb subsets [14]. Transcriptome data were downloaded from supplementary materials from the research article by Orange *et al* [14].

Analysis of candidate genes and signatures of fibroblast subsets in the PEAC cohort

The UK Health Research Authority approved the bulk RNA-seq of synovial tissues from 90 patients with RA who had not yet received therapy, as detailed earlier in the PEAC cohort (no. REC 05/Q0703/198, National Research Ethics Service Committee London) [22,77]. RNA-seq data were uploaded to ArrayExpress (accession no. E-MTAB-6141). The data are expressed as regularised log2-transformed reads. Distinct signatures from the scRNA-seq marker genes of 9 Fb subsets were enriched in the PEAC RNA-seq data, and different scores of Fb subsets were calculated using the ssGSEA method [33]. Correlation analysis (Spearman's test) was also performed for Fb signature scores and clinical features, including inflammatory score, ESR, CRP level, cyclic peptide-containing citrulline level, tenderness and swelling of the joint, DAS28, VAS score and HAQ score in the PEAC cohort. Moreover, patient responsiveness to methotrexate treatment in the PEAC cohort was recorded, and the Wilcoxon test was used for statistical assessment of signature scores when comparing responders and non-responders.

Analysis of fibroblast subset signatures and prediction of drug resistance in the R4RA cohort

In the R4RA cohort, a total of 164 patients with RA who were failing or intolerant to conventional synthetic DMARD therapy and had at least one biologic DMARD were recruited, and synovial biopsy and RNA-seq of synovial tissues were performed [13]. After a synovial biopsy, patients were randomly assigned to receive either tocilizumab or rituximab. Throughout the 48-week study treatment period, RA disease activity assessments and safety data were gathered, and patients were monitored every 4 weeks. At 16 + 6 weeks, a second optional synovial biopsy was carried out on the same joint that was collected at baseline. The comprehensive protocol (number ISRCTN97443826) was registered in the ISRCTN database [13]. Regularised log2-transformed reads were used to describe the data. Individuals who experienced medication failure with both treatments during the research were considered to be multidrug resistant or refractory. Using the software Immunedeconv, MCP counter was used to deconvolute synovial RNA-seq in the R4RA cohort [78]. For Fb subtype enrichment (ITGA5$^+$ Fb), we employed established markers from our single-cell datasets and the average expression of gene signatures derived from differential gene expression research. By using the proportions of ITGA5$^+$ Fbs via univariate logistic regression, refractory to multidrug therapy was predicted.

Real-time quantitative PCR

The recombinant cytokines were added to the medium at the following concentrations: 10 ng/mL TGF-β1 (PeproTech, 100-21), 20 ng/mL TNF-alpha (PeproTech, AF-300-01A), 10 ng/mL IL-1β (PeproTech, 200-01B) and 10 ng/mL IFN-γ (PeproTech, 300-02). Then, the cells were cultured for 48 hours. We used a SteadyPure Universal RNA Extraction Kit (AG21017, Accurate Biology, China) for the isolation of total RNA from the culture. Complementary DNA (cDNA) was reverse transcribed using Evo M-MLV RT Master Mix (AG11706, Accurate Biology, China). NovoStart SYBR qPCR SuperMix plus (E096, NovoProtein, China) was used for real-time quantitative PCR according to the manufacturer's instructions on a CFX96 Touch (Bio-Rad) (n = 3). The $2^{-\Delta\Delta CT}$ method was used to calculate the fold change in target gene expression. The sequences of primers used are listed in online supplemental table 1.

Coculture of synovial fibroblasts from patients with RA and naïve CD4$^+$ T cells

Synovial Fbs were prepared from RA synovial tissue cell suspensions as previously described. Fbs and the supernatants from four patients cultured for 48 hours were collected. CD4$^+$ T cells were isolated from the peripheral blood of healthy donors. In brief, we employed a direct negative selection approach using the EasySep Direct Human CD4$^+$ T−Cell Isolation Kit (19662, Stemcell, USA) according to the manufacturer's protocol. Primary CD4$^+$ T cells were subsequently expanded using Dynabeads Human T-Activator CD3/CD28 (11 161D, Thermo Fisher, USA) according to the manufacturer's instructions. Disitertide diammonium (DD, P144) (HY-P0118B, MedChemExpress, USA) is a peptide-based TGF-β1 inhibitor that specifically blocks the interaction between TGF-β1 and its receptor. DD was dissolved in PBS at 5 mg/mL for storage. To investigate the induction of CD4$^+$PD$^-$1^{hi} CXCL13^{hi} T cells, 2.5×10^5 CD4$^+$ T cells were seeded in 24-well plates and treated in seven different groups for 48 hours: (1) control group (PBS-treated); (2) supernatant from synovial Fbs; (3) supernatant + P144 (100 ng/mL); (4) preseeded Fbs (2.5×10^5); (5) preseeded Fbs (2.5×10^5) + P144 (100 ng/mL); (6) TGF-β1 (10 ng/mL) and (7) TGF-β1 (10 ng/mL) + P144 (100 ng/mL).

Flow cytometry analysis of human T cells

The cocultures of Fbs and T cells were disaggregated using 0.25% trypsin. All the treated T cells were collected in groups and resuspended in cold PBS. The cell suspensions were stained in PBS/1% BSA (stain buffer) with Fixable Viability Stain 700 (BD Biosciences, 564997) and the following antibodies against cell surface proteins for 15 min: anti-CD4-BV510 (562970, BD Pharmingen, USA) and anti-PDCD1-BV421 (562516, BD Pharmingen, USA). The Transcription Factor Buffer Set (562574, BD Pharmingen, USA) was used to fix and permeabilise the cells prior to intracytoplasmic protein staining according to the manufacturer's instructions. Intracytoplasmic CXCL13 was stained using an anti-CXCL13 PE (NBP2-12222PE; Novus, USA) antibody for 45 min.

The data analysis was performed using FlowJo V.10.8.1. After being corrected for compensation, a set of gates for CD4, PDCD1 and CXCL13 was applied to all the samples. The percentage of $CD4^+PD\text{-}1^{hi}CXCL13^{hi}$ T cells among the total $CD4^+$ T cells was calculated based on the gating thresholds.

Mouse models of inflammatory arthritis

Male DBA/1 mice were immunised with 100 or 200 μg of rat CII emulsified 1:1 in Freund's incomplete adjuvant (IFA) containing either *Mycobacterium tuberculosis* H37Ra (Difco; 3.33 mg/mL) or complete Freund's adjuvant (CFA; Difco, containing *Mycobacterium butyricum*, 0.5 mg/mL) for CIA. Two weeks later, the mice were boosted with 100 μg CII in IFA. Callipers were used to measure the thickness of the ankle or wrist joints, and the difference from the baseline was reported.

Cell isolation from murine joints

Cell isolation from murine joints was conducted according to protocols reported in previous studies. In brief, murine joints were dissected and digested using 1 mg/mL collagenase type IV (17104019; Gibco, USA) in RPMI 1640 supplemented with 100 U/mL penicillin and 0.1 mg/mL streptomycin for 40 min of incubation at 37°C with continuous agitation. Subsequently, the mixture was filtered using a 40 μm cell strainer, and the resulting cell suspension was subjected to further processing.

RNA-seq of mouse synovial joints

Following the manufacturer's instructions, the murine joints were dissected, and total RNA was extracted and purified using TRIzol reagent (Invitrogen, Carlsbad, California, USA). The RNA quantity and purity of each sample were measured using a NanoDrop ND-1000 (NanoDrop, Wilmington, Delaware, USA). Using denaturing agarose gel electrophoresis, the RNA integrity was verified and evaluated using a Bioanalyzer 2100 (Agilent, California, USA) with a RNA integrity number (RIN) >7.0. Using Dynabeads Oligo (dT)25-61005 (Thermo Fisher, California, USA), poly(A) RNA was purified from 1 μg of total RNA through two rounds of purification. Next, after incubating at 94°C for 5 min, the poly(A) RNA was broken down into tiny pieces using the Magnesium RNA Fragmentation Module (NEB, cat. e6150, USA). Then, using *Escherichia coli* DNA polymerase I (NEB, cat. m0209, USA), RNase H (NEB, cat. m0297, USA) and deoxyuridine triphosphate (dUTP) Solution (Thermo Fisher, cat. R0133, USA), the cleaved RNA fragments were reverse transcribed to create cDNA using SuperScript II Reverse Transcriptase (Invitrogen, cat. 1896649, USA). The blunt ends of each strand are next treated with an A-base to prepare them for ligation to the indexed adapters. To ligate the adapter to the A-tailed fragmented DNA, each adapter has a T-base overhang. The fragments were ligated to single-index or dual-index adapters, and AMPure XP beads were used to choose the desired size. Following treatment of the U-labelled second-strand DNAs with the heat-labile UDG enzyme (NEB, cat. m0280, USA), the ligated products were amplified using PCR under the following conditions: eight cycles of denaturation at 98°C for 15 s, annealing at 60°C for 15 s, extension at 72°C for 30 s and a final extension at 72°C for 5 min. For the final cDNA library, the average insert size was 300±50 bp. Finally, using the vendor-recommended methodology, we executed 2×150 bp paired-end sequencing (PE150) on an Illumina NovaSeq 6000 (LC-Bio Technologies, Hangzhou, China).

RNA-seq data analysis of the mouse synovial joint

FASTP software (https://github.com/OpenGene/fastp) was used to remove the reads that contained adaptor contamination, low-quality bases and undetermined bases with default parameters. The sequence quality was subsequently verified using FASTP. We used HISAT2 (https://ccb.jhu.edu/software/hisat2) to map reads to the reference genome of *Mus musculus* (GRCm39). The mapped reads of each sample were assembled using StringTie (https://ccb.jhu.edu/software/stringtie) with default parameters. Then, all the transcriptomes from all the samples were merged to reconstruct a comprehensive transcriptome using gffcompare (https://github.com/gpertea/gffcompare/). After the final transcriptome was generated, StringTie was used to estimate the expression levels of all the transcripts. StringTie was used to determine the expression levels of mRNAs by calculating the FPKM (FPKM = [total_exon_fragments/mapped_reads (millions)×exon_length (kB)]). The differentially expressed mRNAs were selected for a fold change >2 or <0.5 and with a parametric F-test comparing nested linear models ($p<0.05$) via the R package edgeR (https://bioconductor.org/packages/release/bioc/html/ edgeR.html).

Flow cytometry analysis of murine synovial $Cd45^-Cd31^-Pdpn^+Itga5^+$ fibroblasts

For murine $Itga5^+$ Fb ($Cd45^-Cd31Ppdn^+Itga5^+$) identification, the cell suspensions from murine synovial joints were resuspended in cold PBS.

For clumped samples, DNase I (Roche, 10104159001) solution (1 mg/mL) was used to dissociate the cells. The cell suspensions were stained in PBS/1% BSA (stain buffer) with Fixable Viability Stain 700 (564997, BD Biosciences, USA) and the following antibodies for 15 min: anti-Cd45-PE (553081, BD Biosciences, USA), anti-Cd31-APC (551262, BD Biosciences, USA), anti-Pdpn-PE-Cy7 (25-5381-82, Thermo Fisher, USA) and anti-Itga5-BV421 (740017, BD Biosciences, USA).

The data were acquired and analysed on a BD FACS LSRFortessa X-20 or FACS Aria II using FACSDiva software. The data analysis was performed using FlowJo V.10.8.1. The compensation settings were established using single-labelled UltraBeads (01-2222-42; Thermo Fisher, USA). After correction and compensation, a set of gates for Cd45, Cd31, Pdpn and Itga5 was deployed on all the samples. The percentage of $Itga5^+$ Fb populations among $Pdpn^+$ synovial cells populations and the percentage of $Itga5^+Pdpn^+$ Fbs among total synovial cells were calculated based on the gating thresholds.

Mouse tissue histology and immunofluorescence staining

Mouse legs were decalcified in 10% EDTA (pH 7.4) and preserved for 24 hours in 10% formalin solution (Sigma-Aldrich). At the First Affiliated Hospital of Sun Yat-sen University Pathology Laboratories, the samples were sectioned, fixed in paraffin and stained with H&E in accordance with the normal protocol. Cartilage was stained with safranin O according to the previously mentioned method.

Histomorphometry scoring

Images from complete joint tissue sections were subjected to H&E and safranin O analysis and cell counting following previously reported methods. A score of 0–3 was assigned to leucocyte infiltration (0, normal; 1, minimum infiltration; 2, moderate infiltration and 3, marked infiltration). Two impartial, blinded assessors completed the scoring and measurements on three distinct cutting levels and a consistent area of the ankle joint. The results are reported as the means of these measurements.

Adoptive transfer of fibroblasts

A total of 500 000 live, flow cytometry-sorted cells, specifically gated as $Cd45^{-}Cd31^{-}Pdpn^{+}Itga5^{+}$, were injected into the inflamed talotibial joint of CIA recipient mice on day 28, as soon as the animals exhibited signs of arthritis. PBS was injected into the contralateral joint.

Micro-CT analysis

The mice were euthanised via cervical dislocation after receiving pentobarbital narcosis. The hind limbs were dissected and amputated at a location 4–5 mm proximal to the ankle joint and subsequently fixed in a 4% paraformaldehyde solution. The fixed specimens were then scanned using a SkyScan-1276 (Bruker, Karlsruhe, Germany) at an isotropic voxel size of 8 μm. Images were reconstructed on the Skyscan micro-CT analysis suite. The trabecular bone volume per tissue volume (BV/TV) of the ankle joint was analysed. The periarticular bone erosions were estimated blindly using the reconstructed images as previously described. The three regions that made up the micro-CT meshes were the heel (which included the calcaneus, centrale, distal tarsals, tibulae and astroglia as well as the distal tibia and fibula), metatarsals and phalanges (which did not include the claws). The degree of erosion (0, none; 1, a few small places; 2, numerous small-medium areas; 3, multiple medium-large areas) and the extent of the affected area (0, none; 1, a few small spots; 2, pitting; 3, full-thickness holes) were assigned scores for each region. For each region, the two scores were then multiplied. Micro-CT scores from the front and hind limbs were averaged for each animal, with the exception of local deletion and intra-articular cell transfer investigations.

STATISTICAL ANALYSIS

GraphPad Prism (V.9.0) was used for the experimental data, and R (V.4.0.2), RStudio (V.4.0.2) and Python (V.3.7.4) were used for the sequencing data and matching clinical variables in the statistical analysis. For categorical variables, χ^2 tests or Fisher's exact tests were used to compare groups. For continuous variables, the Shapiro-Wilk test was employed to assess the normality of the data distribution. Where the assumption of normality was met, the independent samples t-test was used. In cases where data were not normally distributed, the Wilcoxon test was applied. For paired samples, the paired t-test was used for normally distributed difference scores, and the Wilcoxon signed-rank test was used for scores that did not follow a normal distribution. Log-rank tests were used for survival analysis. A value of $p<0.05$ was considered to indicate statistical significance. All tests were two-tailed. Multiple testing corrections were applied where appropriate, using the Benjamini-Hochberg procedure to control the false discovery rate. The sample size of the scRNA-seq libraries was not predetermined using any statistical technique. Unless specified otherwise, every experiment was carried out three or more times using biologically distinct samples.

Acknowledgments

We thank our staff at the associated institutions and departments for cooperating in the collection of the human samples. We are thankful for the bioinformatics support from LC-Bio Technologies and Gene Denovo Technology.

Contributors

LZ, MG (Minghui Gu), XH, XL and CC conceived and designed the study. LZ, CC, BP, XH and YK collected clinical samples and data. LZ and CC performed single-cell and spatial transcriptomic bioinformatic analyses. MG (Minghui Gu), PS, ZZ, MG (Mingqiang Guan), GZ and WS processed synovial biopsy and blood samples. LZ, XH, XL, CC, YK, BP, WC, GX, XW, CL and ZL performed validation experiments. SP, PS and ZZ designed and supervised the functional experiments. MG (Minghui Gu), PS and ZZ recruited patients and performed clinical evaluation. LZ, MG (Minghui Gu), XL, XH and CC wrote and revised the manuscript. AM assisted the editing of the manuscript. SP, PS and ZZ supervised the study. ZZ is the guarantor for this research.

Funding

This work was supported by the National Science Foundation of China (nos. 82201719, 81972050 and 81874014) and the Natural Science Foundation of Guangdong Province, China (no. 2022A1515012279).

Competing interests

None declared.

Patient and public involvement

Patients and/or the public were not involved in the design, or conduct, or reporting, or dissemination plans of this research.

Patient consent for publication

Consent obtained directly from patient(s).

Ethics approval

This study was approved by the Ethics Committee of the First Affiliated Hospital of Sun Yat-sen University (ICE(2021)673), and informed consent was obtained from all participants in accordance with the Declaration of Helsinki.

Data availability statement

The source data for this research are available on reasonable request. Access to any additional data can be sought by contacting the relevant authors. This work is supplied with source data. All the analysis scripts used are available on reasonable request. All the packages used are available online.

Supplemental material

Supplementary material associated with this article can be found in the online version at doi:10.1136/ard-2024-225778.

REFERENCES

[1] Smolen JS, Aletaha D, Barton A, et al. Rheumatoid arthritis. Nat Rev Dis Primers 2018;4:18001. doi: 10.1038/nrdp.2018.1.

[2] Alivernini S, Peluso G, Fedele AL, et al. Tapering and discontinuation of TNF-α blockers without disease relapse using ultrasonography as a tool to identify patients with rheumatoid arthritis in clinical and histological remission. Arthritis Res Ther 2016;18:39. doi: 10.1186/s13075-016-0927-z.

[3] Baker KF, Skelton AJ, Lendrem DW, et al. Predicting drug-free remission in rheumatoid arthritis: A prospective interventional cohort study. J Autoimmun 2019;105:102298. doi: 10.1016/j.jaut.2019.06.009.

[4] Cordisco AJ, Olave M, George MD, et al. Identifying Factors Associated With Treatment Response in Rheumatoid Arthritis Clinical Trials. ACR Open Rheumatol 2022;4:811–8. doi: 10.1002/acr2.11468.

[5] Alivernini S, MacDonald L, Elmesmari A, et al. Distinct synovial tissue macrophage subsets regulate inflammation and remission in rheumatoid arthritis. N Med 2020;26:1295–306. doi: 10.1038/s41591-020-0939-8.

[6] Humby F, Lewis M, Ramamoorthi N, et al. Synovial cellular and molecular signatures stratify clinical response to csDMARD therapy and predict radiographic progression in early rheumatoid arthritis patients. Ann Rheum Dis 2019;78:761–72. doi: 10.1136/annrheumdis-2018-214539.

[7] Buckley CD. Fibroblast cells reveal their ancestry. Nature New Biol 2021;593:511–2. doi: 10.1038/d41586-021-01204-7.

[8] Yoshitomi H. Regulation of Immune Responses and Chronic Inflammation by Fibroblast-Like Synoviocytes. Front Immunol 2019;10:1395. doi: 10.3389/fimmu.2019.01395.

[9] Orr C, Vieira-Sousa E, Boyle DL, et al. Synovial tissue research: a state-of-the-art review. Nat Rev Rheumatol 2017;13:463–75. doi: 10.1038/nrrheum.2017.115.

[10] Croft AP, Campos J, Jansen K, et al. Distinct fibroblast subsets drive inflammation and damage in arthritis. Nature New Biol 2019;570:246–51. doi: 10.1038/s41586-019-1263-7.

[11] Zhang F, Wei K, Slowikowski K, et al. Defining inflammatory cell states in rheumatoid arthritis joint synovial tissues by integrating single-cell transcriptomics and mass cytometry. Nat Immunol 2019;20:928–42. doi: 10.1038/s41590-019-0378-1.

[12] Smith MH, Gao VR, Periyakoil PK, et al. Drivers of heterogeneity in synovial fibroblasts in rheumatoid arthritis. Nat Immunol 2023;24:1200–10. doi: 10.1038/s41590-023-01527-9.

[13] Rivellese F, Surace AEA, Goldmann K, et al. Rituximab versus tocilizumab in rheumatoid arthritis: synovial biopsy-based biomarker analysis of the phase 4 R4RA randomized trial. Nat Med 2022;28:1256–68. doi: 10.1038/s41591-022-01789-0.

[14] Orange DE, Yao V, Sawicka K, et al. RNA Identification of PRIME Cells Predicting Rheumatoid Arthritis Flares. N Engl J Med 2020;383:218–28. doi: 10.1056/NEJMoa2004114.

[15] Mizoguchi F, Slowikowski K, Wei K, et al. Functionally distinct disease-associated fibroblast subsets in rheumatoid arthritis. Nat Commun 2018;9:789. doi: 10.1038/s41467-018-02892-y.

[16] Buechler MB, Pradhan RN, Krishnamurty AT, et al. Cross-tissue organization of the fibroblast lineage. Nature New Biol 2021;593:575–9. doi: 10.1038/s41586-021-03549-5.

[17] Merrick D, Sakers A, Irgebay Z, et al. Identification of a mesenchymal progenitor cell hierarchy in adipose tissue. Science 2019;364:eaav2501. doi: 10.1126/science.aav2501.

[18] Knights AJ, Farrell EC, Ellis OM, et al. Synovial fibroblasts assume distinct functional identities and secrete R-spondin 2 in osteoarthritis. Ann Rheum Dis 2023;82:272–82. doi: 10.1136/ard-2022-222773.

[19] Collins FL, Roelofs AJ, Symons RA, et al. Taxonomy of fibroblasts and progenitors in the synovial joint at single-cell resolution. Ann Rheum Dis 2023;82:428–37. doi: 10.1136/ard-2021-221682.

[20] Li J, Gui T, Yao L, et al. Synovium and infrapatellar fat pad share common mesenchymal progenitors and undergo coordinated changes in osteoarthritis. J Bone Miner Res 2024;39:161–76. doi: 10.1093/jbmr/zjad009.

[21] Tabib T, Huang M, Morse N, et al. Myofibroblast transcriptome indicates SFRP2^{hi} fibroblast progenitors in systemic sclerosis skin. Nat Commun 2021;12:4384. doi: 10.1038/s41467-021-24607-6.

[22] Buch MH, Eyre S, McGonagle D. Persistent inflammatory and non-inflammatory mechanisms in refractory rheumatoid arthritis. Nat Rev Rheumatol 2021;17:17–33. doi: 10.1038/s41584-020-00541-7.

[23] Smith MH, Gao VR, Schizas M. Heterogeneity of inflammation-associated synovial fibroblasts in rheumatoid arthritis and its drivers. bioRxiv, 2028.

[24] Qin Y, Cai M-L, Jin H-Z, et al. Age-associated B cells contribute to the pathogenesis of rheumatoid arthritis by inducing activation of fibroblast-like synoviocytes via TNF-α-mediated ERK1/2 and JAK-STAT1 pathways. Ann Rheum Dis 2022;81:1504–14. doi: 10.1136/ard-2022-222605.

[25] Korsunsky I, Wei K, Pohin M, et al. Cross-tissue, single-cell stromal atlas identifies shared pathological fibroblast phenotypes in four chronic inflammatory diseases. Med 2022;3:481–518. doi: 10.1016/j.medj.2022.05.002.

[26] Welch JD, Kozareva V, Ferreira A, et al. Single-Cell Multi-omic Integration Compares and Contrasts Features of Brain Cell Identity. Cell 2019;177:1873–87. doi: 10.1016/j.cell.2019.05.006.

[27] Garcia-Alonso L, Handfield L-F, Roberts K, et al. Mapping the temporal and spatial dynamics of the human endometrium in vivo and in vitro. Nat Genet 2021;53:1698–711. doi: 10.1038/s41588-021-00972-2.

[28] Gajjala PR, Kasam RK, Soundararajan D, et al. Dysregulated overexpression of Sox9 induces fibroblast activation in pulmonary fibrosis. JCI Insight 2021;6:20. e152503. 10.1172/jci.insight.152503.

[29] Chen X, Zhao J, Herjan T, et al. IL-17-induced HIF1α drives resistance to anti-PD-L1 via fibroblast-mediated immune exclusion. J Exp Med 2022;219:e20210693. doi: 10.1084/jem.20210693.

[30] Robins JC, Akeno N, Mukherjee A, et al. Hypoxia induces chondrocyte-specific gene expression in mesenchymal cells in association with transcriptional activation of Sox9. Bone 2005;37:313–22. doi: 10.1016/j.bone.2005.04.040.

[31] Miura Y, Ota S, Peterlin M, et al. A Subpopulation of Synovial Fibroblasts Leads to Osteochondrogenesis in a Mouse Model of Chronic Inflammatory Rheumatoid Arthritis. JBMR Plus 2019;3:e10132. doi: 10.1002/jbm4.10132.

[32] Le Rossignol S, Ketheesan N, Haleagrahara N. Redox-sensitive transcription factors play a significant role in the development of rheumatoid arthritis. Int Rev Immunol 2018;37:129–43. doi: 10.1080/08830185.2017.1363198.

[33] Subramanian A, Tamayo P, Mootha VK, et al. Gene set enrichment analysis: a knowledge-based approach for interpreting genome-wide expression profiles. Proc Natl Acad Sci U S A 2005;102:15545–50. doi: 10.1073/pnas.0506580102.

[34] Becht E, Giraldo NA, Lacroix L, et al. Estimating the population abundance of tissue-infiltrating immune and stromal cell populations using gene expression. Genome Biol 2016;17:218. doi: 10.1186/s13059-016-1070-5.

[35] Bergen V, Lange M, Peidli S, et al. Generalizing RNA velocity to transient cell states through dynamical modeling. Nat Biotechnol 2020;38:1408–14. doi: 10.1038/s41587-020-0591-3.

[36] Street K, Risso D, Fletcher RB, et al. Slingshot: cell lineage and pseudotime inference for single-cell transcriptomics. BMC Genomics 2018;19:477. doi: 10.1186/s12864-018-4772-0.

[37] Qiu X, Hill A, Packer J, et al. Single-cell mRNA quantification and differential analysis with Census. Nat Methods 2017;14:309–15. doi: 10.1038/nmeth.4150.

[38] Wolf FA, Hamey FK, Plass M, et al. PAGA: graph abstraction reconciles clustering with trajectory inference through a topology preserving map of single cells. Genome Biol 2019;20:59. doi: 10.1186/s13059-019-1663-x.

[39] You S, Yoo S-A, Choi S, et al. Identification of key regulators for the migration and invasion of rheumatoid synoviocytes through a systems approach. Proc Natl Acad Sci U S A 2014;111:550–5. doi: 10.1073/pnas.1311239111.

[40] Corona A, Blobe GC. The role of the extracellular matrix protein TGFBI in cancer. Cell Signal 2021;84:110028. doi: 10.1016/j.cellsig.2021.110028.

[41] Bhattacharyya S, Midwood KS, Varga J. Tenascin-C in fibrosis in multiple organs: Translational implications. Semin Cell Dev Biol 2022;128:130–6. doi: 10.1016/j.semcdb.2022.03.019.

[42] Carabias P, Espelt MV, Bacigalupo ML, et al. Galectin-1 confers resistance to doxorubicin in hepatocellular carcinoma cells through modulation of P-glycoprotein expression. Cell Death Dis 2022;13:79. doi: 10.1038/s41419-022-04520-6.

[43] Rane MJ, Zhao Y, Cai L. Krüppel-like factors (KLFs) in renal physiology and disease. EBioMedicine 2019;40:743–50. doi: 10.1016/j.ebiom.2019.01.021.

[44] Wohlfahrt T, Rauber S, Uebe S, et al. PU.1 controls fibroblast polarization and tissue fibrosis. Nature New Biol 2019;566:344–9. doi: 10.1038/s41586-019-0896-x.

[45] Jin S, Guerrero-Juarez CF, Zhang L, et al. Inference and analysis of cell-cell communication using CellChat. Nat Commun 2021;12:1088. doi: 10.1038/s41467-021-21246-9.

[46] Rao A, Barkley D, França GS, et al. Exploring tissue architecture using spatial transcriptomics. Nature New Biol 2021;596:211–20. doi: 10.1038/s41586-021-03634-9.
[47] Hu J, Li X, Coleman K, et al. SpaGCN: Integrating gene expression, spatial location and histology to identify spatial domains and spatially variable genes by graph convolutional network. Nat Methods 2021;18:1342–51. doi: 10.1038/s41592-021-01255-8.
[48] Kleshchevnikov V, Shmatko A, Dann E, et al. Cell2location maps fine-grained cell types in spatial transcriptomics. Nat Biotechnol 2022;40:661–71. doi: 10.1038/s41587-021-01139-4.
[49] Rao DA, Gurish MF, Marshall JL, et al. Pathologically expanded peripheral T helper cell subset drives B cells in rheumatoid arthritis. Nature New Biol 2017;542:110–4. doi: 10.1038/nature20810.
[50] Argyriou A, Wadsworth MH, Lendvai A, et al. Single cell sequencing identifies clonally expanded synovial CD4+ TPH cells expressing GPR56 in rheumatoid arthritis. Nat Commun 2022;13:4046. doi: 10.1038/s41467-022-31519-6.
[51] Nakano M, Ota M, Takeshima Y, et al. Distinct transcriptome architectures underlying lupus establishment and exacerbation. Cell 2022;185:3375–89. doi: 10.1016/j.cell.2022.07.021.
[52] Hussain A, Voisin V, Poon S, et al. Distinct fibroblast functional states drive clinical outcomes in ovarian cancer and are regulated by TCF21. J Exp Med 2020;217:e20191094. doi: 10.1084/jem.20191094.
[53] Davidson S, Coles M, Thomas T, et al. Fibroblasts as immune regulators in infection, inflammation and cancer. Nat Rev Immunol 2021;21:704–17. doi: 10.1038/s41577-021-00540-z.
[54] Davidson S, Coles M, Thomas T, et al. Fibroblasts as immune regulators in infection, inflammation and cancer. Nat Rev Immunol 2021;21:704–17. doi: 10.1038/s41577-021-00540-z.
[55] Nygaard G, Firestein GS. Restoring synovial homeostasis in rheumatoid arthritis by targeting fibroblast-like synoviocytes. Nat Rev Rheumatol 2020;16:316–33. doi: 10.1038/s41584-020-0413-5.
[56] Lliso-Ribera G, Humby F, Lewis M, et al. Synovial tissue signatures enhance clinical classification and prognostic/treatment response algorithms in early inflammatory arthritis and predict requirement for subsequent biological therapy: results from the pathobiology of early arthritis cohort (PEAC). Ann Rheum Dis 2019;78:1642–52. doi: 10.1136/annrheumdis-2019-215751.
[57] Tsukui T, Wolters PJ, Sheppard D. Alveolar fibroblast lineage orchestrates lung inflammation and fibrosis. Nature New Biol 2024;631:627–34. doi: 10.1038/s41586-024-07660-1.
[58] Floudas A, Smith CM, Tynan O, et al. Distinct stromal and immune cell interactions shape the pathogenesis of rheumatoid and psoriatic arthritis. Ann Rheum Dis 2022;81:1224–42. doi: 10.1136/annrheumdis-2021-221761.
[59] Yan M, Komatsu N, Muro R, et al. ETS1 governs pathological tissue-remodeling programs in disease-associated fibroblasts. Nat Immunol 2022;23:1330–41. doi: 10.1038/s41590-022-01285-0.
[60] Syafruddin SE, Mohtar MA, Wan Mohamad Nazarie WF, et al. Two Sides of the Same Coin: The Roles of KLF6 in Physiology and Pathophysiology. Biomolecules 2020;10:1378. doi: 10.3390/biom10101378.
[61] Yao Y, Wang C. Dedifferentiation: inspiration for devising engineering strategies for regenerative medicine. NPJ Regen Med 2020;5:14. doi: 10.1038/s41536-020-00099-8.
[62] Ong CH, Tham CL, Harith HH, et al. TGF-β-induced fibrosis: A review on the underlying mechanism and potential therapeutic strategies. Eur J Pharmacol 2021;911:174510. doi: 10.1016/j.ejphar.2021.174510.
[63] Frangogiannis NG. Transforming growth factor-β in myocardial disease. Nat Rev Cardiol 2022;19:435–55. doi: 10.1038/s41569-021-00646-w.
[64] Corcoran SE, O'Neill LAJ. HIF1α and metabolic reprogramming in inflammation. J Clin Invest 2016;126:3699–707 84431 10.1172/JCI84431.
[65] Buckley CD, Barone F, Nayar S, et al. Stromal cells in chronic inflammation and tertiary lymphoid organ formation. Annu Rev Immunol 2015;33:715–45. doi: 10.1146/annurev-immunol-032713-120252.
[66] Ham S, Bae J-B, Lee S, et al. Epigenetic analysis in rheumatoid arthritis synoviocytes. Exp Mol Med 2019;51:1–13 22 10.1038/s12276-019-0215-5.
[67] Kim B-G, Malek E, Choi SH, et al. Novel therapies emerging in oncology to target the TGF-β pathway. J Hematol Oncol 2021;14:55. doi: 10.1186/s13045-021-01053-x.
[68] Krenn V, Morawietz L, Burmester G-R, et al. Synovitis score: discrimination between chronic low-grade and high-grade synovitis. Histopathology 2006;49:358–64. doi: 10.1111/j.1365-2559.2006.02508.x.
[69] Hao Y, Hao S, Andersen-Nissen E, et al. Integrated analysis of multimodal single-cell data. Cell 2021;184:3573–87. doi: 10.1016/j.cell.2021.04.048.
[70] Young MD, Behjati S. SoupX removes ambient RNA contamination from droplet-based single-cell RNA sequencing data. Gigascience 2020;9:giaa151. doi: 10.1093/gigascience/giaa151.
[71] McGinnis CS, Murrow LM, Gartner ZJ. DoubletFinder: Doublet Detection in Single-Cell RNA Sequencing Data Using Artificial Nearest Neighbors. Cell Syst 2019;8:329–37. doi: 10.1016/j.cels.2019.03.003.
[72] Choudhary S, Satija R. Comparison and evaluation of statistical error models for scRNA-seq. Genome Biol 2022;23:27. doi: 10.1186/s13059-021-02584-9.
[73] Zheng L, Qin S, Si W, et al. Pan-cancer single-cell landscape of tumor-infiltrating T cells. Science 2021;374:abe6474. doi: 10.1126/science.abe6474.
[74] Finak G, McDavid A, Yajima M, et al. MAST: a flexible statistical framework for assessing transcriptional changes and characterizing heterogeneity in single-cell RNA sequencing data. Genome Biol 2015;16:278. doi: 10.1186/s13059-015-0844-5.
[75] Hänzelmann S, Castelo R, Guinney J. GSVA: gene set variation analysis for microarray and RNA-seq data. BMC Bioinformatics 2013;14:7. doi: 10.1186/1471-2105-14-7.
[76] La Manno G, Soldatov R, Zeisel A, et al. RNA velocity of single cells. Nature New Biol 2018;560:494–8. doi: 10.1038/s41586-018-0414-6.
[77] Lewis MJ, Barnes MR, Blighe K, et al. Molecular Portraits of Early Rheumatoid Arthritis Identify Clinical and Treatment Response Phenotypes. Cell Rep 2019;28:2455–70. doi: 10.1016/j.celrep.2019.07.091.
[78] Sturm G, Finotello F, List M. Immunedeconv: An R Package for Unified Access to Computational Methods for Estimating Immune Cell Fractions from Bulk RNA-Sequencing Data. Methods Mol Biol 2020;2120:223–32. doi: 10.1007/978-1-0716-0327-7_16.

Ann Rheum Dis 84 (2025) 253–261

Contents lists available at ScienceDirect

Annals of the Rheumatic Diseases

journal homepage: https://www.sciencedirect.com/journal/annals-of-the-rheumatic-diseases

Psoriatic arthritis

Psoriatic arthritis phenotype clusters and their association with treatment response: a real-world longitudinal cohort study from the psoriatic arthritis research consortium

Paras Karmacharya[1,*], Leslie J. Crofford[1], Daniel W. Byrne[2], Alisa Stephens-Shields[3], M. Elaine Husni[4], Jose U. Scher[5], Ethan Craig[6], Robert Fitzsimmons[7], Soumya M. Reddy[5], Marina N. Magrey[8], Jessica A. Walsh[9,#], Alexis Ogdie[10,#]

[1] *Department of Medicine, Division of Rheumatology, Vanderbilt University Medical Center, Nashville, Tennessee, USA*
[2] *Byrne Research, Maryland, Maryland, USA*
[3] *Biostatistics, Epidemiology and Informatics, University of Pennsylvania Perelman School of Medicine, Philadelphia, Pennsylvania, USA*
[4] *Cleveland Clinic, Cleveland, Ohio, USA*
[5] *New York University School of Medicine, New York, New York, USA*
[6] *Department of Medicine and Rheumatology, University of Pennsylvania, Philadelphia, Pennsylvania, USA*
[7] *Department of Dermatology, University of Pennsylvania, Philadelphia, Pennsylvania, USA*
[8] *University Hospitals, Case Western Reserve University, Cleveland, Ohio, USA*
[9] *Rheumatology, University of Utah, Salt Lake City, Utah, USA*
[10] *Department of Medicine and Rheumatology, University of Pennsylvania Perelman School of Medicine, Philadelphia, Pennsylvania, USA*

ARTICLE INFO

Article history:
Received 22 May 2024
Accepted 29 October 2024

Keywords:
psoriatic arthritis
treatment
disease activit
machine learning

ABSTRACT

Objectives: To identify phenotype clusters and their trajectories in psoriatic arthritis (PsA) and examine the association of the clusters with treatment response in a real-world setting.
Methods: In the multicentre PsA Research Consortium (PARC) study, we applied factor analysis of mixed data to reduce dimensionality and collinearity, followed by hierarchical clustering on principal components. We then evaluated the transition of PsA clusters and their response to new immunomodulatory therapy and tumour necrosis factor inhibitor (TNFi).
Results: Among 627 patients with PsA, three clusters were identified: mild PsA and psoriasis only (PsO) (Cluster 1, 47.4%), severe PsA and mild PsO (Cluster 2, 34.3%) and severe PsA and severe PsO (Cluster 3, 18.3%). Among 339 patients starting or changing, significant differences in response were observed (mean follow-up of 0.7 years, SD 0.8), with Cluster 3 showing the largest improvements in cDAPSA and PsAID. No differences were found among those starting TNFi (n = 218). cDAPSA remission and PsAID patient acceptable symptom state were achieved in 10%

*Correspondence to Dr. Paras Karmacharya.
E-mail address: paraskarmacharya@gmail.com (P. Karmacharya).
Social media: @paraskarmachary (P. Karmacharya)
Handling editor Josef S. Smolen.
JAW and AO are joint senior authors.
Co-last authors.

https://doi.org/10.1136/ard-2024-226150

and 54%, respectively. Clusters remained stable over time despite treatment changes, though some transitions occurred, notably from Cluster 3 to milder clusters.
Conclusion: Data-driven clusters with distinct therapy responses identified in this real-world study highlight the extensive heterogeneity in PsA and the central role of psoriasis and musculoskeletal severity in treatment outcomes. Concurrently, these findings underscore the need for better outcome measures, particularly for individuals with lower disease activity.

WHAT IS ALREADY KNOWN ON THIS TOPIC

• Psoriatic arthritis (PsA) is studied and managed as if it were a single disease. Current treatment recommendations focus on patientss' worst disease characteristics.

WHAT THIS STUDY ADDS

• Our real-world study identified three data-driven stable clusters, where the degree of psoriasis and PsA seem to be the most important.

HOW THIS STUDY MIGHT AFFECT RESEARCH, PRACTICE OR POLICY

• Our findings highlight the need for better outcome measures that allow us to capture important aspects of disease and validly measure disease activity. Furthermore, there is a pressing need for improved therapies targeting musculoskeletal (MSK) manifestations and a deeper understanding of expected therapeutic response.

INTRODUCTION

Despite a significant increase in treatment options for psoriatic arthritis (PsA), only about 30% of patients achieve disease remission [1]. This is, in part, because PsA is studied and managed as if it were a single disease, similar to polyarticular rheumatoid arthritis [2,3]. However, every patient with PsA is unique, presenting with their own combination of symptoms (musculoskeletal and skin) with varying severity [4]. Additionally, the severity of skin psoriasis does not necessarily correlate with joint symptoms.

The impact of PsA on patients' lives is also heterogeneous, and the extent to which each disease characteristic affects physical function, work productivity, social participation, emotional well-being and fatigue varies significantly [5]. However, current treatment recommendations primarily focus on the most severe aspects of the disease, not often capturing the heterogeneity of presentation and their diverse needs [6].

The importance of early and effective treatment in PsA in terms of improving long-term prognosis is well-recognised [7]. Yet, the current lack of biomarkers reliably predicting treatment response forces a trial-and-error approach in treatment, leading to unreliable responses, unnecessary side effects and potential progression of the disease [6]. Our previous work shows that disease characteristics such as comorbidities cluster in PsA [8], and certain clusters (eg, anxiety/depression cluster) are associated with worse outcomes [9]. Expanding this concept further to disease specific features, different clinical subgroups within PsA may respond differently to expanding classes of medications available to treat psoriatic disease. Although phenotype clusters in PsA have been described using baseline data from randomised controlled trials (RCTs) [10–12]. RCTs generally enrol a homogenous subgroup of PsA (polyarticular). Therefore, findings from the RCTs are not necessarily generalisable to realworld clinical practice, where majority of patients have oligoarticular disease. Therefore, we lack an understanding of PsA phenotype clusters in the real-world setting and how they evolve over time. Additionally, it is unclear how these clusters relate to long-term outcomes in PsA. To develop more personalised and effective treatment strategies for patients with PsA, our study aimed to: (1) identify distinct PsA phenotype clusters and their trajectories, and (2) examine the association of the clusters with treatment outcomes using a real-world cohort.

METHODS

Study design and data source

We used longitudinal data from the PsA Research Consortium (PARC), a longitudinal observational cohort from PsA-dedicated clinics at five institutions in the USA: the University of Pennsylvania, Cleveland Clinic, New York University, the University of Utah and Vanderbilt University Medical Center (NCT03378336) [13]. Data on sociodemographics, psoriasis and PsA characteristics, comorbidities, laboratory data, radiographic features, treatments, patient-reported outcomes (PROs), disease activity and impact measures were systematically collected via Research Electronic Data Capture (REDCap) at baseline and follow-up visits.

Patient population

Adults (≥18 years) meeting the Classification Criteria for PsA (CASPAR) were included from 2017 to 2023. In the second part of the study where we examined treatment response, a subset of patients with PsA starting or switching therapy with at least one follow-up visit for assessment of treatment response were identified. Within the PARC cohort, patients were enrolled and followed clinically except in a subset of patients initiating therapy, where at least one follow-up was mandatory as a part of the study. However, the study was interrupted by the COVID-19 pandemic in 2020 resulting in incomplete follow-up for patients enrolled in late 2019 and early 2020.

Exposure

Clustering variables, selected based on clinical relevance and prior research [14], included PsA and psoriasis clinical characteristics, PROs, body mass index (BMI), extra-musculoskeletal manifestations, prior biologic use and C reactive protein (CRP) levels, totaling 34 variables (online supplemental table).

Outcomes

For the cluster analysis, data-driven PsA clusters and their trajectories over the first three visits in the cohort were outcomes of interest. For the next part, the primary outcomes of interest were treatment response in these PsA clusters defined as the median changes in clinical Disease Activity of PsA (cDAPSA, range 0–154) and PsA Impact of Disease 12-item questionnaire

(PsAID12, range 0–10) from treatment start or change to follow-up visit. We chose these two measures because PsAID is based on patient experience incorporating relatively broad disease features (first provisionally endorsed PRO measure in PsA by OMERACT [15]) and cDAPSA is a composite measure with physician evaluation. Additionally, we recently showed that both PsAID and cDAPSA demonstrated good responsiveness in this real-world cohort [3].

Secondary outcomes included the proportion of patients achieving remission (cDAPSA ≤4 (remission) and patient acceptable symptom state PsAID ≤4) [16]. We also examined the proportion of patients in each cluster who achieved minimally clinically important improvement (MCII). The MCII for cDAPSA and PsAID were taken as −3.25 (−1.61 to −4.89) and −0.65 (−0.41 to −0.99) based on our prior study findings [3]. We also examined composite measures for treatment response (similar to European League Against Rheumatism response criteria for rheumatoid arthritis [17]): remission and/or MCII for cDAPSA, and patient acceptable symptom state and/or MCII for PsAID. Patients with cDAPSA <3.25 (n = 8) and PsAID <0.65 (n = 14) at baseline were excluded for the analyses including MCII because they would not be able to achieve MCII even when disease activity and function scores improve to 0 at follow-up.

Statistical analysis

Descriptive statistics (medians, percentages, etc) were used to summarise the data. Kruskal-Wallis and Fisher's exact tests were performed to examine differences in continuous and categorical variables, respectively, across the clusters. Continuous variables were standardised prior to clustering to ensure uniform weighting. Multiple Imputation by Chained Equations (MICE) was performed for missing mixed-type data using 'mice' package in R.

Since most of the important disease-specific variables for PsA were highly correlated, we first used factor analysis of mixed data (FAMD). FAMD is similar to PCA but can handle mixed data (FactoMineR package in R), unlike PCA which can only handle continuous data. We also examined the contribution of each variable for the FAMD. We then formed hierarchical clustering of the principal components derived from FAMD. The optimal number of clusters was determined using 'the tree method' which evaluates the balance between within-cluster variance reduction and between-cluster variance reduction for each level of the hierarchical clustering tree. The clusters were named based on the predominant clinical variable within the cluster and across the identified clusters.

To ascertain the stability of the clusters, sensitivity analyses were performed in the full cohort and in the subset of patients starting therapy at baseline and two subsequent follow-up visits. Sankey diagrams were used to visualise the transition of patients in the identified clusters from baseline to follow-up visits.

Statistical tests were performed to examine the differences in treatment outcomes across the three clusters. Analyses were performed using Stata V.16 (College Station, Texas: StataCorp LLC) and R V.4.0.3 (R Foundation for Statistical Computing, Vienna, Austria).

RESULTS

Among 627 enrolled participants with PsA, the mean age was 50.1 years (SD 13.7), 56.4% were female and the majority were white (92.7%). The median BMI was 28.8 (IQR 9.0), and 39.1% of patients had a history of smoking. The disease duration for psoriasis only (PsO) and PsA were 17.5 years (IQR 22.9) and 7.5 years (IQR 12.0), respectively. Elevated CRP was observed in 30.0% of patients (median CRP 4.0 mg/L, SD 9.0). Among the 627 participants, 339 started or switched to a new therapy with a follow-up visit to document treatment response (online supplemental figure 6) and of these, 218 started a tumour necrosis factor inhibitor (TNFi, online supplemental figure 7).

PsA phenotype clusters in the overall cohort (n = 627)

We identified three PsA phenotype clusters in the overall PsA cohort (n = 627, figure 1A, B): Cluster 1 (n = 297, 47.4%) was characterised by patients with significantly lower joint counts, enthesitis, dactylitis and low body surface area (BSA) involvement with psoriasis, indicating mild PsA and mild PsO. Conversely, Cluster 2 (n = 215, 34.3%) presented with severe disease activity, evidenced by high joint counts and psoriasis BSA, alongside a notable history of biological treatment (63.3%, p<0.001), suggesting severe PsA and mild PsO cluster. Cluster 3 (n = 115, 18.3%) was marked by extensive psoriasis involvement (with higher guttate, palmoplantar, inverse, genital psoriasis, nail dystrophy), and higher mean BMI and CRP levels, pointing to severe PsA and severe PsO cluster (figure 2).

Patients in Cluster 3 were significantly younger (mean age: 45.5, SD 13.0) and had a significantly lower proportion of females (46.5%) compared with clusters 1 and 2 (table 1). The clusters were not significantly different in terms of PsO or PsA symptom duration, proportion of patients having axial disease or extra-articular manifestations (uveitis and inflammatory bowel disease (online supplemental table 1). Notably, compared with Cluster 1, patients in Clusters 2 and 3 were more commonly initiating TNFi (30.7% and 29.6% vs 15.8%, p<0.01) and IL-17i (4.2% and 7.0% vs 1.4%), further supporting the severe disease phenotype in Clusters 2 and 3. Overall, these data suggest that the clusters were primarily driven by PsO and PsA severity.

Longitudinal transition of PsA clusters (n = 627)

The longitudinal analysis of PsA clusters revealed a notable stability in cluster assignments over time, particularly within Clusters 1 and 2. Specifically, 74.4% of patients in Cluster 1 (n = 252) and 50.2% of patients in Cluster 2 (n = 123) remained in their respective clusters from the first to the second visit (figure 3, online supplemental table 1).

Among the patients in Cluster 1 at the first visit, 26.6% (n = 45) transitioned to other clusters by the second visit. Of these, the majority (n = 32) moved to Cluster 2. However, most of these patients (n = 26) transitioned back to Cluster 1 by the third visit, indicating a return to their original phenotype. A smaller subset (n = 13) transitioned to Cluster 3 at the second visit, with the majority of this group (n = 8) also returning to Cluster 1 by the third visit.

For patients initially in Cluster 2, 80 transitioned to Cluster 1 by the second visit. Of these, 36 patients returned to Cluster 2 by the third visit, while 41 remained in Cluster 1. Additionally, 12 patients moved from Cluster 2 to Cluster 3 by the second visit; 10 of these patients stayed in Cluster 3 at the third visit, while 3 transitioned back to Cluster 2.

Patients initially in Cluster three showed a significant shift towards milder clusters, with 57.4% (n = 64) moving to other clusters by the second visit. Among these, 35 patients transitioned to Cluster 1, with 32 subsequently moving to Cluster two by the third visit. Of the 29 patients who moved

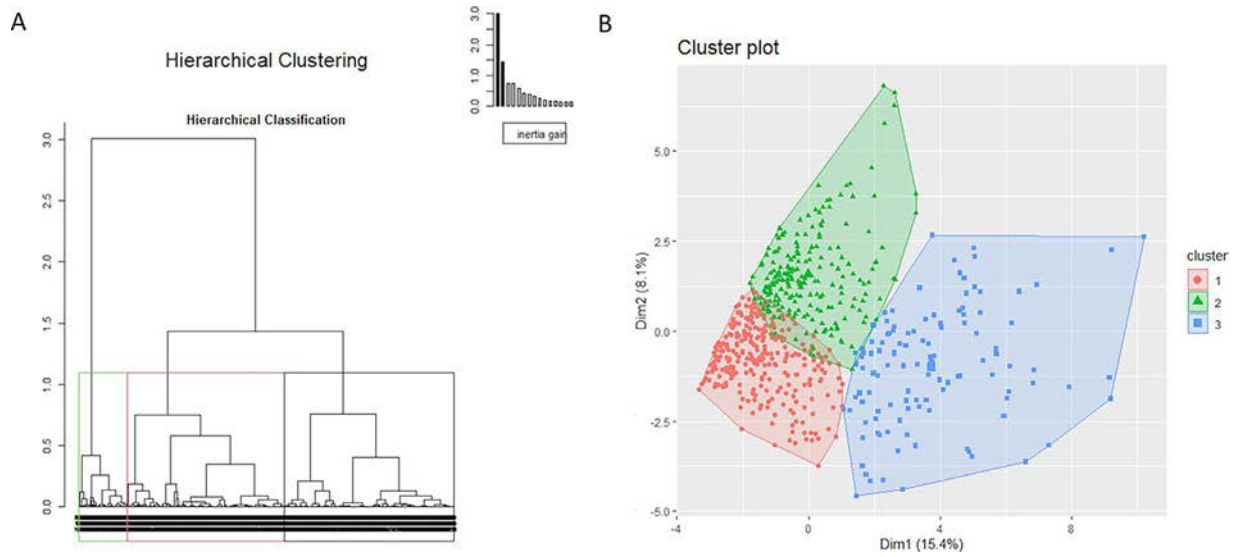

Figure 1. (A) Optimal number of clusters determined using 'the tree method', which balances within-cluster variance reduction and between-cluster variance reduction for each level of the hierarchical clustering tree. (B) Hierarchical clustering on the principal components on the principal components derived from the FAMD on baseline clinical variables. Note: FAMD was performed before clustering because most of the important disease-specific variables for PsA were highly correlated. FAMD is similar to PCA but can handle mixed data, unlike PCA which can only handle continuous data. FAMD, factor analysis of mixed data; PCA, Principal Component Analysis; PsA, psoriatic arthritis.

to Cluster two at the second visit, 23 remained in Cluster 2, while six returned to Cluster three by the third visit. This shift toward milder clusters, particularly from Cluster three to Clusters 1 and 2, may reflect effective treatment responses for psoriasis.

Sensitivity analysis of patients with complete data across all three visits (n = 335) showed similar results (online supplemental figure 2, online supplemental table 3). This observation likely reflects better treatment responses for psoriasis; however, because patients in Cluster 1 were starting with lower disease activity, floor effect may be playing a role.

Baseline characteristics of therapy starters (n = 339)

The subset of patients who started or switched to a new medication (n = 339) had similar baseline characteristics as the full cohort (n = 627, (online supplemental tables 4, 5 and 6). While the same three clusters were replicated in this subset of therapy starters, severe PsA and mild PsO (Cluster 2) constituted the majority of patients (n = 197, 58.1%) in this subset unlike in the full cohort where Cluster 1 formed the majority (47.4%). This seems plausible because we would expect those who start or change therapy to have more severe PsA. There were no differences in the percentage of patients already on or starting a particular therapy among the clusters, except Cluster 3 (n = 62), which had a higher percentage of patients starting IL-17i compared with the other clusters (22.6% vs 6.3% and 11.8% in clusters 1 and 2 respectively, p = 0.01).

Treatment response among therapy starters (n = 339)

Cluster analysis of the subgroup of patients initiating therapy (n = 339) showed the same three clusters. Among patients who started or switched to a new medication (n = 339), Cluster 3 showed significantly higher improvement in cDAPSA and PsAID scores: median cDAPSA score reduction of −6.5 (SD 19.0) and a PsAID score improvement of −1.3 (SD 3.5), compared with Cluster 2 (cDAPSA −1.5, SD 14.0 and PsAID −0.2, SD 2.4), and Cluster 1 (cDAPSA 0.3, SD 10.8 and PsAID −0.4, SD 1.9) (online supplemental figures 8, 9). Additionally, 14.5% of patients in Cluster 3 achieved remission (cDAPSA ≤4) and 27.4% reached patient acceptable symptom state (PsAID ≤4), significantly higher compared with Clusters 1 and 2. The proportion of patients achieving MCII in terms of cDAPSA and PsAID scores was also significantly higher in Cluster 3 (63.9% and 63.3%) compared with Clusters 2 (44.3% and 45.3%) and 1 (37.8% and 46.5%), respectively. Composite treatment response measure (score ≤4 and/or MCII) was significantly different among the clusters for cDAPSA but not for PsAID (table 2). Overall, these data indicate better treatment outcomes in cluster 3 with severe PsO compared with the other clusters.

Treatment response among first TNFi starters (n = 218)

While numerically greater reductions in cDAPSA and PsAID scores were noted from TNFi start to follow-up in cluster 3 compared with clusters 1 and 2, the differences were not statistically significant, likely related to the smaller number of patients in each cluster (eg, n = 37 for cluster 3). Similarly, the proportion of patients achieving cDAPSA ≤4 and PsAID ≤4 was slightly higher at follow-up compared with baseline as expected, but the difference among the clusters was not statistically significant. The proportion of patients achieving MCII for cDAPSA and PsAID scores was highest in cluster 3, at 63.9% for cDAPSA (p = 0.16) and 61.1% for PsAID (p = 0.05), indicating that TNFi starters with severe PsA and PsO are more likely to experience significant clinical improvements. Similarly, composite treatment response measures (score ≤4 and/or MCII) were not significantly different among the clusters in terms of cDAPSA or PsAID (table 3).

DISCUSSION

Our study demonstrates the heterogeneity of PsA and highlights the potential value of identifying subgroups based on distinct clinical characteristics to inform treatment decisions and

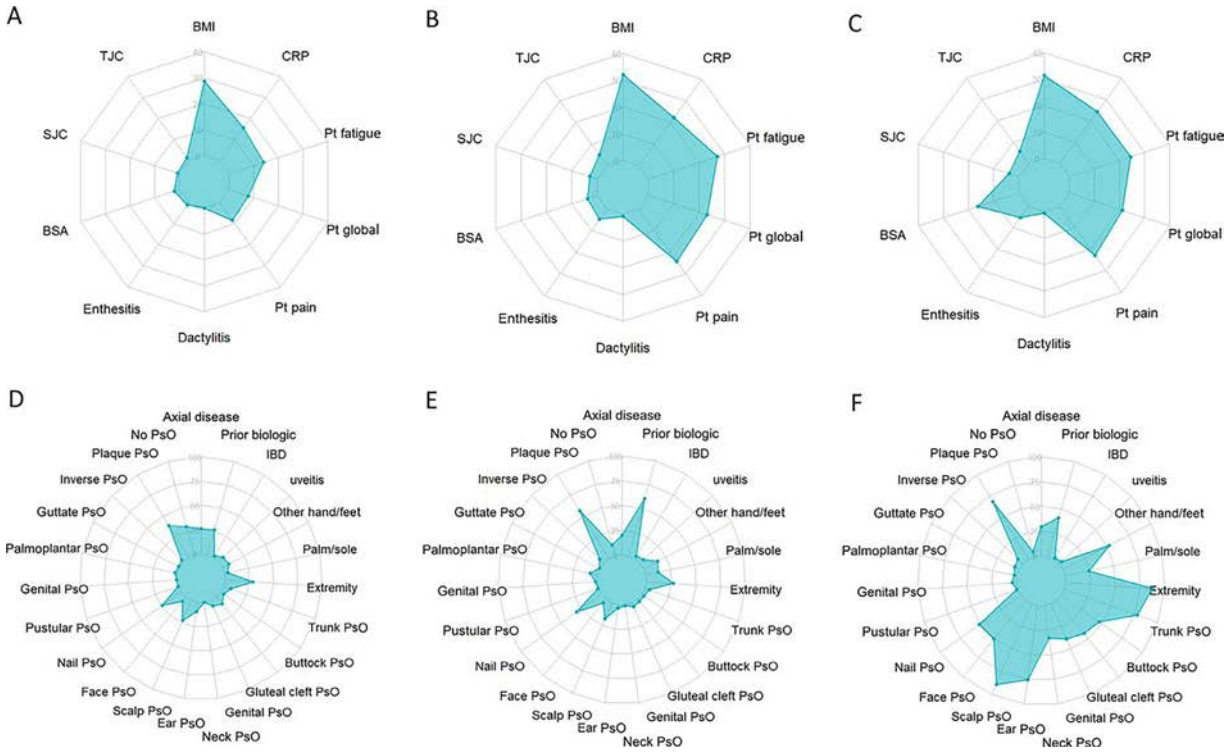

Figure 2. Radar chart comparing the three phenotypic clusters of PsA in the PARC cohort (n = 627). Panels A, B and C show a comparison of the mean values of the continuous variables across clusters 1, 2, and 3, respectively. Panels D, E and F show a comparison of the per cent prevalence of the categorical variables across clusters 1, 2, and 3, respectively. Note: the variables are not standardised for better interpretability and hence on different scales plotted from 0 (lowest at the centre) to maximum value for the variable (highest at the outside). Maximum value for the different variables is as follows: BMI 40, TJC 68, SJC 66, BSA 20, Enthesitis count 8 (Leeds enthesitis index + proximal plantar fascia), Dactylitis count 20, Pt pain 10, Pt global 10 and Pt fatigue 10. Extremity refers to PsO at upper and lower extremities. BMI, body mass index; BSA, body surface area; CRP, C reactive protein; PARC, PsA Research Consortium; PsA, psoriatic arthritis; PsO, psoriasis only; pt, patient; SJC, swollen joint count; TJC, tender joint count.

advance personalised care. Our objective was to address this goal by using semisupervised clustering methods to identify potential subgroups in this real-world population. We identified three distinct clusters based on phenotypic characteristics, primarily driven by the relative severity of PsA and psoriasis. Notably, these clusters exhibited remarkable stability across follow-up visits, although transitions between clusters were observed in some patients over time. Importantly, these clusters demonstrated significant improvements in disease activity (cDAPSA) and disease impact (PsAID) scores for the initial therapy, but not for the first TNFi initiated within the cohort. The clusters identified are thus somewhat intuitive and align with clinical practice, where treatment decisions are most often based on the severity of PsA and psoriasis.

Other studies have also investigated PsA clusters based on phenotype, although using differing variables. For instance, a single-centre study from Hungary identified seven PsA clusters based on joint distribution and psoriasis type [18]. Additionally, secondary analyses of RCT) have examined clusters defined by disease phenotypes. Unlike our study, these post-hoc analyses of RCTs found additional clusters for dactylitis, enthesitis or axial involvement [10–12]. However, differences in clusters identified in RCTs are likely related to differences in the population being studied and variables included in the clustering process. Specifically, in our real-world cohort, the prevalence and severity dactylitis and enthesitis were very low compared with the patients included in the RCTs. We also did not include specific joint involvement (eg, hands, feet) as clustering variables. While axial disease was included, the lower prevalence of patients with axial involvement in our study may have led to this not being a separate cluster. Similarly, methodological differences in clustering could have also accounted for the differences in clusters obtained. Unlike these prior studies, we performed FAMD to account for collinearity among the clinical variables followed by hierarchical clustering. We used this method to 'let the data tell us' what was important or not important so as not to first judge the most important variables a priori. In clinical practice, we use a certain clinical framework to categorise patients with PsA into different subgroups in relation to their long-term prognosis. However, often the complexity of patients with PsA and the number of variables to consider can hinder categorising patients. In the study, we considered all important clinical variables, which we included into the factor analysis and clustering. The fact that we still found PsA and PsO severity as the most important factors acknowledges how we assess and manage the disease in clinical practice.

While prior studies have not examined PsA clusters longitudinally, the stability of clusters over time in our cohort aligns with the University of Toronto PsA cohort, where most patients with oligoarticular disease maintained their disease pattern over time [19]. However, our study also observed some patients transitioning between clusters, especially for Cluster 3 with severe psoriasis and PsA, reflecting changes in disease severity, clinical manifestations and response to therapy. This stability could be leveraged in clinical practice by developing long-term management plans tailored to these stable phenotype profiles. This finding together with the difference in treatment responses across the clusters underscore the importance of considering patient phenotypes in treatment decisions. Better treatment response observed in Clusters 2 and 3 with high disease

Table 1
Baseline characteristics of patients with PsA in the PARC cohort, overall and by clusters

Baseline characteristics	Overall (n = 627)	Cluster 1 Mild PsA and mild PsO (n = 297)	Cluster 2 Severe PsA and mild PsO (n = 215)	Cluster 3 Severe PsA and severe PsO (n = 115)	P value*
Age in years, mean (SD)	50.1 (13.7)	51.1 (14.4)	51.6 (12.5)	45.5 (13.0)	<0.01
Female (%)	325 (56.4%)	144 (53.7%)	128 (66.0%)	53 (46.5%)	<0.01
Race/ethnicity					0.06
Non-Hispanic white	524 (92.7%)	252 (95.1)	175 (92.1)	97 (88.2%)	
Hispanic/non-white	41 (7.3%)	13 (4.9%)	15 (7.9%)	13 (11.8%)	
BMI, median (IQR)	28.8 (24.9, 33.9)	26.60 (24.3, 30.9)	31.04 (26.3, 36.0)	30.5 (25.8, 35.8)	<0.01
Smoking, ever (%)	219 (39.1%)	86 (32.3%)	79 (44.1%)	54 (47.0%)	<0.01
PsO symptom duration in years, median (IQR)	17.5 (8.3, 31.2)	18.59 (8.7, 32.2)	16.43 (7.4, 31.0)	19.15 (9.4, 28.2)	0.77
PsA symptom duration in years, median (IQR)	7.5 (3.5, 15.5)	8.45 (3.7, 15.0)	7.03 (3.6, 7.0)	6.21 (3.1, 15.3)	0.45
Follow-up duration in years, median (IQR)	1.7 (0.2, 4.7)	2.0 (0.3, 5.8)	1.6 (0, 4.3)	1.5 (0.2, 3.7)	0.18
CRP mg/L, median (IQR)	4.0 (1.0, 10.0)	2.0 (1.0, 6.2)	5.5 (2.0, 12.0)	5.0 (2.0, 15.0)	<0.01
Elevated CRP (%)	146 (30.0%)	46 (20.0%)	67 (40.12%)	33 (36.67%)	<0.01
Medication use, current†					
Methotexate	155 (24.7%)	66 (22.2%)	60 (27.9%)	29 (25.2%)	0.33
Apremilast	18 (2.9%)	10 (3.4%)	4 (1.9%)	4 (3.5%)	0.54
Other small molecules‡	61 (9.7%)	31 (10.4%)	18 (8.4%)	12 (10.4%)	0.71
TNFi	183 (29.2%)	99 (33.3%)	56 (26.1%)	28 (24.4%)	0.09
IL-17i	45 (7.2%)	18 (6.1%)	17 (7.9%)	10 (8.7%)	0.57
Other biologics	24 (3.8%)	7 (2.4%)	11 (5.1%)	6 (5.2%)	0.17
Medication start/change					
Methotexate	38 (6.1%)	14 (4.7%)	14 (6.5%)	10 (8.7%)	0.29
Apremilast	10 (1.6%)	4 (1.4%)	5 (2.3%)	1 (0.9%)	0.64
Other small molecules‡	24 (3.8%)	8 (2.7%)	11 (5.1%)	5 (4.4%)	0.32
TNFi	147 (23.4%)	47 (15.8%)	66 (30.7%)	34 (29.6%)	<0.01
IL-17i	21 (3.4%)	4 (1.4%)	9 (4.2%)	8 (7.0%)	0.01
Other biologics	12 (1.9%)	2 (0.7%)	7 (3.3%)	3 (2.6%)	0.06
Prior biologic use	284 (45.3%)	96 (32.3%)	136 (63.3%)	52 (45.2%)	<0.01
Uveitis	33 (5.3%)	19 (6.4%)	10 (4.7%)	4 (3.5%)	0.48
IBD	14 (2.2%)	6 (2.0%)	6 (2.8%)	2 (1.7%)	0.77
Axial disease	154 (24.6%)	77 (25.9%)	43 (20.0%)	34 (29.6%)	0.11
Tender joint count	2 (0, 7)	1 (0, 3)	5 (2, 12)	5 (2, 13)	<0.01
Swollen joint count	1 (0, 4)	0 (0, 2)	3 (0, 7)	4 (1, 9)	<0.01
BSA	0.5 (0, 2)	0.2 (0, 1)	0.6 (0.1, 2)	3 (1, 10)	<0.01
Patient-reported pain	4 (0,7)	2 (1, 3.5)	6.5 (4.5, 8)	6.5 (3.5, 8)	<0.01
Patient-reported global assessment	4 (1.5, 6)	1.5 (0.5, 3)	5.5 (4, 7)	5 (3, 7)	<0.01
BASDAI Fatigue Score	5 (3, 7)	3 (2, 5)	7 (5, 8)	6 (4, 8)	<0.01
cDAPSA (0–154), median (IQR)	14 (7, 23)	7 (3, 11)	21.5 (14.5, 28.5)	22 (13, 35.5)	<0.01
PsAID (0–10), median (IQR)	3.0 (1.4, 5.4)	1.6 (0.7, 2.5)	4.9 (3.5, 6.3)	4.9 (2.9, 7.0)	<0.01
cDAPSA ≤4§	82 (17.19%)	73 (34.27%)	4 (2.61%)	5 (4.50%)	<0.01
PsAID ≤4¶	289 (61.10%)	200 (93.46%)	47 (31.33%)	42 (38.53%)	<0.01

Other biologics include ustekinumab, IL-23 inhibitors (guselkumab and brodalumab), JAK inhibitors and abatacept.
The PARC cohort included adults (≥18 years) meeting the Classification Criteria for PsA (CASPAR) from five academic centers in the USA (2017–2023).

* P value for the difference in variables by clusters (K-Wallis for continuous and Fisher's Exact test for categorical variables).
† Patients could be on more than one therapy (eg, methotrexate and a TNFi).
‡ Other small molecules include hydroxychloroquine, leflunomide and sulfasalazine.
§ Remission.
¶ Patient acceptable symptom state.

BASDAI, Bath Ankylosing Spondylitis Disease Activity Index; BMI, body mass index; BSA, body surface area; CASPAR, Classification Criteria for PsA; cDAPSA, Clinical Disease Activity of PsA; CRP, C reactive protein; IBD, inflammatory bowel disease; IL-17i, interleukin 17 inhibitors; N, number of patients; PARC, PsA Research Consortium; PsA, psoriatic arthritis; PsAID, PsA Impact of Disease questionnaire; PsO, psoriasis only; TNFi, tumour necrosis factor inhibitors.

activity and elevated CRP observed in our cohort align with prior studies which showed that high baseline disease activity and CRP were associated with improved treatment response or persistence of TNFi in PsA [20,21]. Notably, these clusters showed better treatment response despite having a high BMI, which has been shown to be associated with worse treatment outcomes [22]. It is possible that the severity of psoriasis and PsA may play a more crucial role in determining treatment effectiveness than BMI alone. However, the difference in treatment response might also reflect limitations in our current PsA outcome measures, in particular, a floor effect for patients in cluster 1.

Interestingly, our findings indicate that a significant number of patients in Clusters 1 and 2, who were already at a patient-acceptable symptom state (PsAID ≤4), opted to initiate new therapies. This decision could reflect a misalignment between our current clinical measures and the patients' personal experience of their disease, suggesting that current measures might not fully capture the patient's quality of life or functional limitations. Consequently, the results of traditional RCTs, which often rely on these very measures, may not be generalisable to the

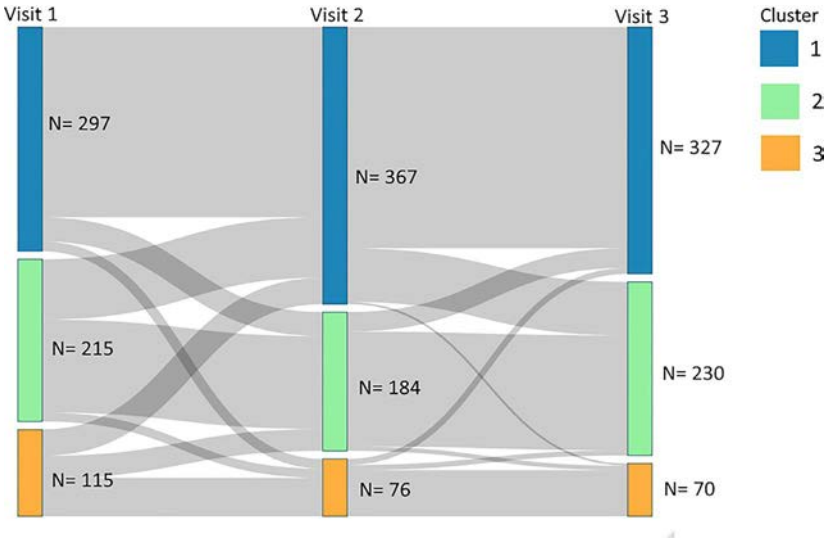

Figure 3. Transition of patients across the first three visits in the cohort showing stability of the clusters.

broader patient population with PsAseen in clinical practice, where many exhibit lower disease activity at baseline.

The lower disease activity seen in clinical practice also has relevance for interpretation of the findings of this study. The absolute scores for cDAPSA and PsAID did not differ at follow-up among the clusters and the proportion of patients achieving cDAPSA remission and PsAID patient acceptable symptom state was also similar at follow-up. However, patients in Cluster 3 started at a higher level of disease activity and had a greater improvement in the cDAPSA and PsAID scores. This demonstrates the floor effects of current measures, the challenges in measuring and interpreting disease improvement and the need for more sensitive and nuanced tools to capture the full spectrum of disease activity, particularly for those in the lower disease activity cluster. Additionally, it may prompt more detailed evaluations to understand the factors driving treatment changes despite seemingly controlled disease states in patients in the lower disease activity states.

The robustness of our identified clusters is demonstrated across different follow-ups and among patients initiating therapy, with most patients staying within their baseline cluster throughout the follow-up period. This consistency enhances the

Table 2
Disease activity and functional status measures among first therapy starters at therapy start and follow-up, overall and by clusters

Baseline characteristics	Overall (n = 339)	Cluster 1 Mild PsA and mild PsO (n = 80)	Cluster 2 Severe PsA and mild PsO (n = 197)	Cluster 3 Severe PsA and severe PsO (n = 62)	P value*
At baseline					
cDAPSA (0–154), median (IQR)	15.5 (9.5, 23)	13.0 (10.3, 19.3)	15.00 (8.5, 23.0)	22.0 (14.0, 32.0)	<0.01
PsAID (0–10), median (IQR)	3.75 (1.8, 5.75)	2.85 (1.6, 5.1)	3.55 (1.8, 5.2)	5.28 (3.3, 7.1)	<0.01
cDAPSA ≤4†	34 (10.03%)	7 (8.75%)	25 (12.69%)	2 (3.23%)	0.08
PsAID ≤4‡	183 (53.98%)	50 (62.50%)	112 (56.85%)	21 (33.87%)	<0.01
At follow-up					
cDAPSA (0–154), median (IQR)	13.00 (6.5, 20.0)	13.50 (7, 20.3)	12.00 (7.0, 19.5)	13.25 (6.0, 23.0)	0.56
PsAID (0–10), median (IQR)	3.1 (1.4, 4.8)	3.00 (1.2, 4.4)	3.15 (1.5, 4.8)	3.1 (1, 5.4)	0.64
cDAPSA ≤4†	58 (17.1%)	13 (16.3%)	34 (17.3%)	11 (17.7%)	0.98
PsAID≤4‡	219 (64.6%)	56 (70.0%)	125 (63.5%)	38 (61.3%)	0.49
cDAPSA MCII (%)*	148 (46.5%)	28 (37.8%)	81 (44.3%)	39 (63.9%)	0.01
PsAID MCII (%)*	153 (49.04%)	33 (46.48%)	82 (45.30%)	38 (63.33%)	0.05
cDAPSA ≤4 and/or cDAPSA MCII (%)*	155 (48.74%)	29 (39.19%)	87 (47.54%)	39 (63.93%)	0.02
PsAID ≤4 and/or PsAID MCII (%)*	155 (48.74%)	29 (39.19%)	87 (47.54%)	39 (63.93%)	0.02
Follow-up duration in years, median (IQR)	0.4 (0.3, 0.7)	0.4 (0.3, 0.5)	0.4 (0.3, 0.6)	0.4 (0.3, 1.1)	0.94
Difference from baseline to follow-up					
cDAPSA (0–154), median (IQR)	−2.00 (−9.5, 4.5)	0.25 (−5.25, 5.5)	−1.50 (−9.5, 4.5)	−6.50 (−17.0, 2.0)	<0.01
PsAID (0–10), median (IQR)	−0.40 (−1.8, 0.6)	−0.38 (-1.4, 0.6)	−0.20 (−1.7, 0.7)	−1.3 (−3.5, 0)	<0.01
cDAPSA ≤4 proportion change (overall)	24 (7.10%)	6 (7.50%)	9 (4.57%)	9 (14.52%)	0.03
cDAPSA >4 to cDAPSA ≤4	42 (12.39%)	8 (10.00%)	24 (12.18%)	10 (16.13%)	
cDAPSA ≤4 to cDAPSA >4	18 (5.31%)	2 (2.50%)	15 (7.61%)	1 (1.61%)	
PsAID ≤4 proportion change (overall)	36 (10.62%)	6 (7.50%)	13 (6.60%)	17 (27.42%)	<0.01
PsAID >4 to PsAID ≤4	73 (21.53%)	14 (17.50%)	37 (18.78%)	22 (35.48%)	
PsAID ≤4 to PsAID >4	37 (10.91%)	8 (10.00%)	24 (12.18%)	5 (8.06%)	

Note: cDAPSA <3.25 (n = 21) and PsAID <0.65 (n = 27) at baseline were excluded from outcomes including MCII because they would not be able to achieve MCII even when disease activity and function scores improve to 0 at follow up.

* Proportion of patients achieving minimal clinically important difference (MCII) defined as cDAPSA difference of −3.25 and PsAID difference of −0.65 from baseline to follow-up.[3]

† Remission.

‡ Patient acceptable symptom state.

cDAPSA, Clinical Disease Activity of PsA (range 0-154); f/u, follow up; MCII, minimally clinically important improvement; N, number of patients; PsA, psoriatic arthritis; PsAID, PsA Impact of Disease 12-item questionnaire (range 0–10); PsO, psoriasis.

Table 3
Disease activity and functional status measures among first TNFi starters at therapy start and follow-up, overall and by clusters

Baseline characteristics	Overall (n = 218)	Cluster 1 Mild PsA and mild PsO (n = 55)	Cluster 2 Severe PsA and mild PsO (n = 126)	Cluster 3 Severe PsA and severe PsO (n = 37)	P value*
At baseline					
cDAPSA (0–154), median (IQR)	16.3 (10.0, 24.0)	15.0 (10.0, 22.5)	16.3 (9.5, 24.0)	22.0 (13.5, 30.0)	0.14
PsAID (0–10), median (IQR)	4.0 (2.1, 5.9)	3.9 (2.2, 5.5)	3.7 (2.0, 5.8)	5.4 (2.3, 6.7)	0.10
cDAPSA ≤4†	17 (7.80%)	2 (3.64%)	14 (11.11%)	1 (2.70%)	0.17
PsAID ≤4‡	110 (50.46%)	30 (54.55%)	67 (53.17%)	13 (35.14%)	0.13
At follow-up					
cDAPSA (0–154), median (IQR)	13.0 (6.5, 20.0)	13.5 (7.0, 20.0)	12.5 (6.5, 19.5)	13 (5.0, 21.0)	0.78
PsAID (0–10), median (IQR)	3.1 (1.2, 4.4)	3.1 (1.0, 4.5)	3.1 (1.3, 4.4)	3.1 (1.0, 4.7)	0.99
cDAPSA ≤4†	37 (17.0%)	5 (9.1%)	23 (18.3%)	9 (24.3%)	0.13
PsAID ≤4‡	149 (63.9%)	39 (70.9%)	85 (67.5%)	25 (67.6%)	0.92
cDAPSA MCII (%)*	113 (51.8%)	24 (43.6%)	66 (55.5%)	23 (63.9%)	0.16
PsAID MCII (%)*	106 (52.0%)	25 (48.1%)	59 (50.9%)	22 (61.1%)	<0.05
cDAPSA ≤4 and/or cDAPSA MCII (%)*	118 (56.2%)	25 (45.5%)	70 (58.8%)	23 (63.9%)	0.16
PsAID ≤4 and/or PsAID MCII (%)*	158 (77.5%)	40 (76.9%)	89 (76.7%)	29 (80.6%)	0.95
Follow-up duration in years, mean (IQR)	0.4 (0.3, 0.6)	0.3 (0.3, 0.5)	0.4 (0.3, 0.6)	0.4 (0.3, 1.0)	0.21
Difference from baseline to follow-up					
cDAPSA (0–154), median (IQR)	−3.8 (-10.0, 2.0)	−0.5 (-10.0, 6.0)	−4.0 (-9.5, 2.0)	−8.00 (-17.0, 2.0)	0.13
PsAID (0–10), median (IQR)	−0.6 (-2.0, 0.5)	−0.5 (-1.7, 0.5)	−0.4 (-2.0, 0.5)	−1.20 (-3.1,−0.2)	0.19
cDAPSA ≤4 proportion change (overall)	20 (9.2%)	9 (5.5%)	9 (7.1%)	8 (21.6%)	0.03
cDAPSA >4 to cDAPSA ≤4	29 (13.3%)	5 (9.1%)	16 (12.7%)	8 (21.6%)	
cDAPSA ≤4 to cDAPSA >4	9 (4.1%)	2 (3.6%)	7 (5.6%)	0 (0.0%)	
PsAID ≤4 proportion change (overall)	39 (17.9%)	9 (16.4%)	18 (14.3%)	12 (32.4%)	0.04
PsAID >4 to PsAID ≤4	51 (23.4%)	12 (21.8%)	26 (20.6%)	13 (35.1%)	
PsAID ≤4 to PsAID >4	12 (5.5%)	3 (5.5%)	8 (6.4%)	1 (2.7%)	

Note: cDAPSA <3.25 (n = 8) and PsAID <0.65 (n = 14) at baseline were excluded from outcomes including MCII because they would not be able to achieve MCII even when disease activity and function scores improve to 0 at follow up.

* Proportion of patients achieving minimal clinically important difference (MCII) defined as cDAPSA difference of −3.25 and PsAID difference of −0.65 from baseline to follow- up.[3]

cDAPSA, Clinical Disease Activity of PsA (range 0–154); f/u, follow up; MCII, minimally clinically important improvement; N, number of patients; PsA, psoriatic arthritis; PsAID, PsA

Impact of Disease 12-item questionnaire (range 0–10); PsO, psoriasis.

clinical utility of our findings. However, several limitations should be considered when interpreting our results. First, our study included patients at various stages of their disease, not just those with new diagnoses. This means the initial therapy postenrolment may not represent their first-ever treatment. Next, axial involvement was determined by the Assessment of SpondyloArthritis International Society (ASAS) axial spondyloarthritis criteria, with diagnostic imaging performed at the discretion of the treating physician [23]. This could have led to missed cases of asymptomatic or mild axial disease due to selective imaging practices. We also did not incorporate the pattern of peripheral joint involvement in our clustering analysis. Our preliminary modelling revealed that including specific joint counts (eg, MCP, PIP) resulted in the clustering driven primarily by the total number of affected joints, rather than providing distinct patterns of disease. To focus on clinically meaningful distinctions and reduce redundancy in constructs, we opted to include only the total swollen and tender joint counts (online supplemental figures 4, 5). Additionally, we did not account for comorbidities such as fibromyalgia or depression, which are known to influence treatment outcomes. The lack of a specific cluster for mild PsA with severe psoriasis can potentially be due to referral biases (ie, these patients may predominantly receive care from dermatologists).

The COVID-19 pandemic caused an interruption in our study in 2020, leading to incomplete follow-up for patients enrolled in 2019 and early 2020. There is also the possibility that the greater improvement observed in cluster 3 represents regression to the mean, a limitation common to studies examining treatment effects. Lastly, the study's generalisability may be limited by a selection bias towards patients from academic centres with PsA expertise, potentially skewing the cohort towards more severe or treatment-resistant cases.

In conclusion, PsA is a highly heterogeneous disease, and our use of machine learning methods helped simplify patient categorisation by focusing on the severity of both skin and joint involvement. This categorisation was not only relevant for understanding disease subgroups but also for predicting treatment response. Clinically, this highlights the need for a holistic approach to PsA management. Patients with PsA are often followed by rheumatologists who are trained to consider primarily the musculoskeletal disease, but these results emphasise the importance of skin severity, which should be equally considered in therapy selection. In this specific study, we did not consider differential treatment response by therapy class. In a larger dataset with more patients using non-TNFi biologic therapies, a similar study could be repeated to understand the impact of therapy selection on outcomes in each cluster. This would help inform personalised medicine approaches. At the same time, our results highlight the need for better outcome measures that allow us to capture important aspects of disease and validly measure disease activity. Furthermore, there is a pressing need for improved therapies targeting MSK manifestations and a deeper understanding of expected therapeutic response.

Correction notice

This article has been corrected since it published Online First. The joint senior author statement has been added.

Acknowledgements

We thank Kat Bush, Nadia Grant and Sarah Wood for administrative support, and all the patients participating in this study. Part of this study was presented at the American College of Rheumatology Convergence meeting 2023 as an oral presentation.

Contributors

PK, LC and AO were involved in the study conception and design. PK wrote the proposal and initial draft of the manuscript. All authors were involved in the analysis and interpretation of data, and revision of the manuscript. All authors read and approved the final manuscript. PK is the overall guarantor. JW and AO co-last authors.

Funding

This work was supported by NIH/NIAMS R01 AR072363, K23AR082990 and Rheumatology Research Foundation (RRF) Scientist Development Award.

Patient and public involvement

Patients and/or the public were not involved in the design, or conduct, or reporting or dissemination plans of this research.

Patient consent for publication

Not applicable.

Ethics approval

Institutional Review Board approval was obtained at all five sites: University of Pennsylvania (PARC-819801; PARC-B-828357), Cleveland Clinic (IRB 07-623), New York University (14-00487), University of Utah (IRB_00074499) and Vanderbilt University Medical Center (IRB #211492). Patients signed a written consent form prior to enrolment in the study. Participants gave informed consent to participate in the study before taking part.

Data availability statement

Data are available upon reasonable request. Access to the complete deidentified data can be made available following approval. Requests for additional study-related data can be sent to Alexis Ogdie at alexis. ogdie@pennmedicine.upenn.edu.

Supplementary materials

Supplementary material associated with this article can be found in the online version at doi:10.1136/ard-2024-226150.

Orcid

Paras Karmacharya: http://orcid.org/0000-0003-1034-1530
Leslie J. Crofford: http://orcid.org/0000-0002-6347-5738
Jose U. Scher: http://orcid.org/0000-0002-1072-6994

REFERENCES

[1] Lubrano E, Perrotta FM, Scriffignano S, et al. Sustained Very Low Disease Activity and Remission in Psoriatic Arthritis Patients. Rheumatol Ther 2019;6:521–8.
[2] Ogdie A, Coates L. The Changing Face of Clinical Trials in Psoriatic Arthritis. Curr Rheumatol Rep 2017;19:21.
[3] Karmacharya P, Stull C, Stephens-Shields A, et al. Responsiveness and Minimum Clinically Important Difference in Patient-Reported Outcome Measures Among Patients With Psoriatic Arthritis: A Prospective Cohort Study. Arthritis Care Res (Hoboken) 2023;75:2182–9.
[4] Ritchlin CT, Colbert RA, Gladman DD. Psoriatic Arthritis. N Engl J Med 2017;376:957–70.
[5] Orbai A-M, de Wit M, Mease P, et al. International patient and physician consensus on a psoriatic arthritis core outcome set for clinical trials. Ann Rheum Dis 2017;76:673–80.
[6] Coates LC, Kavanaugh A, Mease PJ, et al. Group for Research and Assessment of Psoriasis and Psoriatic Arthritis 2015 Treatment Recommendations for Psoriatic Arthritis. Arthritis Rheumatol 2016;68:1060–71.
[7] Haroon M, Gallagher P, FitzGerald O. Diagnostic delay of more than 6 months contributes to poor radiographic and functional outcome in psoriatic arthritis. Ann Rheum Dis 2015;74:1045–50.
[8] Multimorbidity clusters in psoriatic arthritis: a population-based study. ACR Meeting Abstracts. Available: https://acrabstracts.org/abstract/multimorbidity-clusters-in-psoriatic-arthritis-a-population-based-study/[Accessed 13 Nov 2020].
[9] Karmacharya P, Crowson CS, Lennon RJ, et al. Multimorbidity phenotypes in ankylosing spondylitis and their association with disease activity and functional impairment: Data from the prospective study of outcomes in ankylosing spondylitis cohort. Semin Arthritis Rheum 2024;64:152282.
[10] Pournara E, Kormaksson M, Nash P, et al. Clinically relevant patient clusters identified by machine learning from the clinical development programme of secukinumab in psoriatic arthritis. RMD Open 2021;7:e001845.
[11] Richette P, Vis M, Ohrndorf S, et al. Identification of PsA phenotypes with machine learning analytics using data from two phase III clinical trials of guselkumab in a bionaïve population of patients with PsA. RMD Open 2023;9:e002934.
[12] Baraliakos X, Pournara E, Coates LC, et al. Patient clusters identified by machine learning from a pooled analysis of the clinical development programme of secukinumab in psoriatic arthritis, ankylosing spondylitis and psoriatic arthritis with axial manifestations. Clin Exp Rheumatol 2024;42:696–701.
[13] Wan MT, Walsh JA, Craig ET, et al. A comparison of physical function instruments in psoriatic arthritis: HAQ-DI vs MDHAQ vs PROMIS10 global physical health. Rheumatol (Oxford) 2021;60:2307–16.
[14] Luque Ramos A, Redeker I, Hoffmann F, et al. Comorbidities in Patients with Rheumatoid Arthritis and Their Association with Patient-reported Outcomes: Results of Claims Data Linked to Questionnaire Survey. J Rheumatol 2019;46:564–71.
[15] Orbai A-M, Holland R, Leung YY, et al. PsAID12 Provisionally Endorsed at OMERACT 2018 as Core Outcome Measure to Assess Psoriatic Arthritis-specific Health-related Quality of Life in Clinical Trials. J Rheumatol 2019;46:990–5.
[16] Tucker LJ, Coates LC, Helliwell PS. Assessing Disease Activity in Psoriatic Arthritis: A Literature Review. Rheumatol Ther 2019;6:23–32.
[17] van Gestel AM, Prevoo ML, van 't Hof MA, et al. Development and validation of the European League Against Rheumatism response criteria for rheumatoid arthritis. Comparison with the preliminary American College of Rheumatology and the World Health Organization/International League Against Rheumatism Criteria. Arthritis Rheum 1996;39:34–40.
[18] Koó T, Nagy Z, Seszták M, et al. Subsets in psoriatic arthritis formed by cluster analysis. Clin Rheumatol 2001;20:36–43.
[19] Gladman DD, Ye JY, Chandran V, et al. Oligoarticular vs Polyarticular Psoriatic Arthritis: A Longitudinal Study Showing Similar Characteristics. J Rheumatol 2021;48:1824–9.
[20] Scrivo R, Giardino AM, Salvarani C, et al. An observational prospective study on predictors of clinical response at six months in patients with active psoriatic arthritis treated with golimumab. Clin Exp Rheumatol 2020;38:107–14.
[21] Gratacós J, Casado E, Real J, et al. Prediction of major clinical response (ACR50) to infliximab in psoriatic arthritis refractory to methotrexate. Ann Rheum Dis 2007;66:493–7.
[22] Karmacharya P, Ogdie A, Eder L. Psoriatic arthritis and the association with cardiometabolic disease: a narrative review. Ther Adv Musculoskelet Dis 2021;13.

Ann Rheum Dis 84 (2025) 262–273

Contents lists available at ScienceDirect

Annals of the Rheumatic Diseases

journal homepage: https://www.sciencedirect.com/journal/annals-of-the-rheumatic-diseases

Systemic lupus erythematosus

Molecular basis for the disease-modifying effects of belimumab in systemic lupus erythematosus and molecular predictors of early response: blood transcriptome analysis implicates the innate immunity and DNA damage response pathways

Georgia-Savina Moysidou[1,2], Panagiotis Garantziotis[1,3], George Sentis[1], Dimitra Nikoleri[4], Nikolaos Malissovas[1], Myrto Nikoloudaki[5], Eirini-Maria Stergioti[1], Styliani Polia[5], Nikolaos Paschalidis[1], Anastasia Filia[1], Maria Grigoriou[1,6], Dionysis Nikolopoulos[1,7], Noemin Kapsala[2], Spyridon Katechis[8], Antonis Fanouriakis[9], George Bertsias[5,10], Dimitrios T. Boumpas[1,2,*]

[1] *Laboratory of Autoimmunity and Inflammation, Center of Clinical, Experimental Surgery and Translational Research, Biomedical Research Foundation of the Academy, Athens, Greece*
[2] *4th Department of Internal Medicine, Attikon University Hospital, National and Kapodistrian University Faculty of Medicine, Athens, Greece*
[3] *Department of Internal Medicine 3-Rheumatology and Immunology, Friedrich Alexander University Erlangen-Nuremberg and Universitätsklinikum Erlangen, Erlangen, Germany*
[4] *Laboratory of Auoimmunity-Inflammation, Institute of Molecular Biology and Biotechnology, Heraklion, Greece*
[5] *Rheumatology, Clinical Immunology and Allergy Department, University of Crete School of Medicine, Heraklion, Greece*
[6] *1st Department of Internal Medicine, University Hospital of Alexandroupolis, Democritus University of Thrace - Alexandropoulis Campus, Alexandroupolis, Greece*
[7] *Division of Rheumatology, Department of Medicine Solna, Karolinska Institute, Stockholm, Sweden*
[8] *4th Department of Internal Medicine, Attikon University Hospital, National and Kapodistrian University School of Medicine, Athens, Greece*
[9] *4th Department of Medicine, National and Kapodistrian University Faculty of Medicine, Athens, Greece*
[10] *Laboratory of Autoimmunity-Inflammation, Institute of Molecular Biology and Biotechnology, Heraklion, Greece*

*Correspondence to Dr. Dimitrios T. Boumpas.
E-mail address: boumpasd@uoc.gr (D.T. Boumpas).
Social media: @george_bertsias (G. Bertsias)
Handling editor Josef S. Smolen.
G-SM and PG contributed equally.
GB and DTB contributed equally.

https://doi.org/10.1136/ard-2024-226051

ARTICLE INFO

Article history:
Received 1 May 2024
Accepted 21 July 2024

Keywords:
Lupus Erythematosus
Systemic
Biological Therapies
Machine Learning

ABSTRACT

Objectives: Belimumab is a putative disease-modifying agent in systemic lupus erythematosus (SLE), yet the molecular underpinnings of its effects and the ability to predict early clinical response remain unexplored. To address these, we undertook a longitudinal, in-depth blood transcriptome study.

Methods: RNA-sequencing was performed in the blood of active SLE patients at baseline and following 6 months of belimumab treatment (n = 45 paired samples). Clinical response was determined according to the SLE Responder Index (SRI)-4 and Lupus Low Disease Activity State (LLDAS). Weighted correlation network analysis (WGCNA) was used to uncover gene module trait associations. Reversibility of SLE susceptibility and severity gene signatures was assessed. Machine learning was used to build models predictive of response.

Results: Belimumab induced widespread transcriptome changes with downregulation of pathways related to B cells, type I/II interferon, IL-6/STAT3 and neutrophil activation. These effects were more pronounced among patients with LLDAS+ compared with to SRI-4+/LLDAS− response, with amelioration of the SLE 'susceptibility' signature observed in the former group. Unsupervised analysis unveiled gene modules enriched in neutrophil degranulation, type I interferon signalling and cytokine production to correlate positively with response at 6 months. Using neural networks, a set of 50 genes (including *CCL4L2, CARD10, MMP1*5 and *KLRC2*) predicted response to belimumab with a cross-validated 84% specificity (test set). Lack of response was linked to perturbations of the cell cycle checkpoints, PI3K/ Akt/mammalian target of rapamycin and TGF-beta signalling pathways.

Conclusion: Belimumab treatment ameliorates multiple innate and adaptive immunity dysregulations of SLE and may reverse the disease signature, consistent with the drug effects on reducing activity and preventing flares. Fingerprints of innate immunity correlate with robust improvement whereas DNA damage response with less responsive disease to BAFF inhibition.

WHAT IS ALREADY KNOWN ON THIS TOPIC

- Despite lower frequencies in controlled trials, belimumab exhibits response rates of 60%–70% within the first 6–12 months in observational studies, reducing both the occurrence of systemic lupus erythematosus (SLE) flares and the progression of organ damage over time.
- The molecular basis for these disease-modifying effects and/or the ability to predict responses are not known.

WHAT THIS STUDY ADDS

- Belimumab effectively mitigates dysregulations associated with both humoral and innate immune pathways.
- Attainment of Lupus Low Disease Activity State correlates with attenuation of the SLE susceptibility signature, consistent with its ability to reduce disease activity and prevent flares.
- Distinct innate immunity signatures identify belimumab responders prior to therapy.
- A molecular index comprising 50 genes predicts robust clinical response with high specificity.
- Dysregulation in cell cycle and metabolic pathways is associated with insufficient response to treatment.

HOW THIS STUDY MIGHT AFFECT RESEARCH, PRACTICE OR POLICY

- These data substantiate the putative disease-modifying effects of belimumab in decreasing disease activity and risk of flares.
- Transcriptional signatures indicative of insufficient response to belimumab may provide insights into additional treatment strategies to further potentiate its efficacy.

INTRODUCTION

Belimumab, a recombinant, human, immunoglobulin G1 lambda (IgG1k) monoclonal antibody that binds to and antagonises soluble B-cell activating factor (BAFF) is beneficial in patients with active systemic lupus erythematosus (SLE), with response rates of 60%–70% at 6–12 months [1–4]. Importantly, belimumab has proved its disease-modifying effect [5] by reducing the rate of SLE flares, including severe flares [1,2,6–8] and organ damage accrual [7,9,10], enabling tapering of glucocorticoids with a favourable toxicity profile with low risk of infections [7–9], compared with other biological agents used in rheumatic diseases.

Belimumab primarily inhibits the survival of the B cells in the T2 stage of development but can also interfere with the activation, differentiation and isotype-switching of naive B cells, the emergence of the short-lived plasma cells, the germinal centre reactions and the differentiation of the memory B cells [11]. Notably, BAFF seems to exert broader immunomodulatory effects, extending its influence on both the T cell and innate immune cell compartments [12,13]. To this end, the molecular consequences following the inhibition of BAFF by belimumab and their connection with the drug's multifaceted clinical effects warrant further exploration.

The existing paradigm in SLE care focuses on the sustained attainment of remission or low disease activity in order to slow the accrual of organ damage, prevent relapses and improve patient-related and disease-related outcomes [14]. The 2023 update of the (European Alliance of Associations for Rheumatology (EULAR) recommendations emphasises the timely introduction of immunomodulatory agents—including biologics like belimumab—in patients who do not meet the aforementioned targets or require maintenance glucocorticoids above 5 mg/day of prednisone equivalent [15]. To fully materialise this strategy, however, it is important to stratify SLE patients according to the anticipated response to different interventions, thus enhancing the overall benefit-to-risk of available treatments. In this regard, although high disease activity (Systemic Lupus Erythematosus Disease Activity Index 2000 (SLEDAI)≥10), anti-dsDNA positivity, low serum complement, glucocorticoid treatment, high

expression of BAFF and type I interferon pathway have emerged as potential predictors of response to belimumab treatment [16,17], they have modest individual discriminatory capacity and thus, have not yet been influential to everyday clinical practice.

Here, we explored the molecular basis of the disease-modifying effects of the belimumab treatment through an in-depth transcriptome characterisation at baseline and 6 months post-treatment. Using advanced machine learning classifiers, we developed a gene panel capable of predicting therapeutic response to the agent. Finally, we have defined the transcriptional landscape of insufficient response to be used towards strategies to further enhance the drug's efficacy.

METHODS

Study population

SLE patients were recruited from two rheumatology hospital departments (Attikon University Hospital and University Hospital of Heraklion) with dedicated Lupus clinics. All patients fulfilled the Systemic Lupus International Collaborating Clinics (SLICC) [18] and/or the 2019 EULAR/American College of Rheumatology classification criteria for SLE [19]. Belimumab was initiated (standard approved dose of intravenous 10 mg/kg or subcutaneous 200 mg/week) due to active disease and according to the current standard of care. Active SLE was defined as the presence of clinical (ie, excluding serology) SLEDAI-2K≥6 [20] and/or Physician Global assessment (PGA) ≥1.5 [21]. Blood specimens were obtained at baseline and 6 months following belimumab treatment and stored at −80°C until processing.

Outcomes, sample size and statistical analysis

Clinical response was defined according to the SLE Responder Index (SRI-4) response [22] and the Lupus Low Disease Activity State (LLDAS) [23]. Based on the reported and our own experience [2] and assuming ≥40% LLDAS and ≥80% retention rate at 6 months, we included 71 patients (n≥20 in the response and insufficient response subsets) to ensure sufficient statistical power for group-wise transcriptome comparisons. Continuous data are reported as mean (SD) values. Between-group comparisons were performed with the non-parametric Mann-Whitney U test and logistic regression; paired-sampled statistics were performed with paired t-test (p values <0.05 (two tailed)).

Isolation of total RNA, library preparation and mRNA sequencing

Total RNA extraction was carried out using the Qiagen RNeasy kit. RNA quality was evaluated using the Agilent Bio Analyser and the mRNA libraries were prepared using the Illumina stranded TruSeq kit. mRNA sequencing was performed on the Illumina NextSeq 500 at the Greek Genome Center of the Biomedical Research Foundation of the Academy of Athens and on the Illumina HiSeq4000 at the Department of Genetic Medicine and Development, University of Geneva Medical School.

Computational analysis of the gene expression data

Quality of sequencing was assessed using the FastQC [24]. The raw reads were aligned against the human reference genome (GRCh38.p12) by the STAR 2.6 algorithm [25]. Gene quantification was performed by HTSeq [26] using Gencode V.29 annotation. Raw read counts were adjusted for batch effects using combat [27]. Differential expression analysis was conducted using the DESeq2 R package [28]. Statistical significance was set at nominal $p<0.05$. Enrichment analysis was performed using the gProfiler [29], the Gene Set Variation Analysis (GSVA) and the Gene Set Enrichment Analysis (GSEA) [30]. Weighted gene coexpression network analysis was performed using the R package WGCNA [31]. We used a previously defined SLE 'susceptibility' signature, comprising the intersection of differentially expressed genes (DEGs) identified in comparisons between healthy individuals and patients with active SLE, as well as between healthy individuals and patients with inactive SLE, excluding DEGs identified in the active vs inactive SLE comparison (online supplemental table S4) [32]. As SLE 'severity' signature (online supplemental table S5), we employed the DEGs resulting from the comparison of patients with active lupus nephritis versus those with activity from other organs, as described previously [26]. Protein−protein interaction networks were generated using the STRINGdb R package [33] and the visualisation was performed by using ggraph. The deconvolution analysis was performed using the CIBERSORTx tool [34].

Machine learning

The mRNA-sequencing dataset of the baseline samples was randomly split into training (70%) and test (30%) sets. Normalisation of the raw read counts using DESeq2 and z-scaling was

Table 1
Demographics, clinical characteristics and treatment at baseline (n = 58)

Female, n (%)	56 (96.6)
Age (years), mean (SD)	46.7 (13.4)
Disease duration at belimumab initiation (years), mean (range)	5.9 (0−30)
White, n (%)	58 (100)
Previous treatments, n (%)	
Hydroxychloroquine	7 (12.1)
Methotrexate	10 (17.2)
Azathioprine	11 (19)
Mycophenolate mofetil	17 (29.3)
Cyclophosphamide	9 (15.5)
Concomitant treatment, n (%)	
Hydroxychloroquine	51 (87.9)
Methotrexate	23 (39.7)
Azathioprine	9 (15.5)
Mycophenolate mofetil	13 (22.4)
SLEDAI2K*, mean (SD)	8.2 (2.8)
SLEDAI2K* ≥10, n (%)	17 (29.3)
PGA, mean (SD)	1.7 (0.3)
Corticosteroids use, n (%)	37 (63.8)
Corticosteroids >7.5 mg†/day, n (%)	13 (22.4)
Active arthritis‡, n (%)	56 (96.6)
Active rash‡, n (%)	32 (55.2)
Anti-dsDNA, n (%)	14 (24.1)
Low C3 or C4, n (%)	16 (27.6)
Proteinuria‡, n (%)	8 (13.8)
Haematuria‡, n (%)	4 (6.9)
Active hair loss‡, n (%)	16 (27.6)
Ulcers‡, n (%)	15 (25.9)
Leucopenia‡, n (%)	3 (5.2)

Data are presented as number (percentage), mean (SD or range); anti-ds DNA, antidouble-stranded DNA; PGA, physician global assessment; SLEDAI-2K, Systemic Lupus Erythematosus Disease Activity Index 2000.

* The SLEDAI-2K is a 24-item weighted score of lupus activity ranging from 0 to 105.

† Prednisolone equivalent.

‡ Based on the SLEDAI-2K definitions.

performed for the training and the test sets, separately. Leveraging the DEGs identified through the baseline comparison of LLDAS and/or SRI-4 responders versus insufficient responders ($p<0.05$) in the training set, a recursive feature elimination filtering process using random forest (fivefold cross-validation) was applied to eliminate noise and retain the smallest set of genes that best predict the response to belimumab treatment in the training set. Next, five predictive models using *caret* [35] were fit (twofold cross-validation) to identify the best classifier model. The best model based on accuracy was validated in the test set. Accuracy, sensitivity, specificity and area under the curve, following the receiver operating curve analysis, were determined in the test set.

RESULTS

Patients' characteristics and clinical response to belimumab

A total of 71 patients were enrolled. Specimens were either unavailable or the extracted RNA did not meet quality control standards for 13 patients at baseline and 14 patients at M6, respectively. At baseline (n = 58), 96.6% of the patients were women with a mean (SD) age of 46.7 (13.4) years and a mean disease duration (range) of 5.9 (0–30) years. Detailed clinical characteristics are shown in table 1. Mean (SD) SLEDAI-2K and PGA were 8.2 (2.8) and 1.7 (0.3), respectively, with inflammatory synovitis and rash being the most frequent manifestations. Following 6 months of treatment with belimumab, disease activity was significantly lowered (SLEDAI-2K: 4.4 (2.4), $p<0.001$; PGA: 1 (0.6), $p<0.001$) followed by a reduction in the daily dose of glucocorticoids ($p = 0.05$). Accordingly, SRI-4, LLDAS and SRI-4 and/or LLDAS were achieved by n = 31 (53.4%), n = 31 (53.4%) and n = 36 (62.1%) patients, respectively.

Treatment with belimumab ameliorates transcriptional perturbations linked to humoral and innate immunity

To explore the molecular basis underlying the putative disease-modifying effects of belimumab, we compared the blood transcriptome in the entire population of SLE patients at baseline and 6 months following treatment initiation. Computational analysis was conducted on paired samples from 45 patients (online supplemental table S1). Differential expression analysis unveiled a total of 1121 DEGs at 6 months versus baseline ($p<0.05$) (figure 1A). Belimumab treatment induced a statistically significant suppression of pathways related to B-cell mediated responses, type I and II interferon and IL-6/STAT3 signalling pathways, and neutrophil activation coupled with an upregulation of the IL2/STAT5 signalling pathway (figure 1B). Computational estimation of the blood immune cell abundancies with the CIBERSORTx tool revealed a significant reduction in the neutrophil populations along with an expansion of the CD8 + T cell compartment at 6 months post-treatment initiation (figure 1C). Collectively, these data suggest that in addition to B-cell/humoral responses, the effect of belimumab may also encompass inflammatory and innate immunity pathways relevant to SLE disease.

Major clinical improvement under belimumab treatment correlates with distinct molecular changes

Next, we examined changes in the blood transcriptome of SLE patients according to their clinical response to belimumab at 6 months versus baseline (figure 2A). We focused on low disease activity defined by LLDAS, which has been associated with the prevention of organ damage and other favourable outcomes. Comparing the transcriptional profiles of patients who achieved LLDAS with or without SRI-4 response at 6 months versus baseline (55.6% in the subset of patients with second blood sample), yielded 1253 DEGs ($p<0.05$). Attaining LLDAS was associated with a statistically significant downregulation of pathways related to type I and II interferon signalling, complement activation, IL-6 pathway and B-cell mediated responses (figure 2B). We also found a significant reduction in NK cell population 6 months post-treatment initiation in LLDAS responders compared to baseline (online supplemental figure S1A).

Analysis of transcriptional changes among SLE patients who experienced SRI-4—but not LLDAS—response, revealed less profound downregulation of the B-cell gene signatures, which was also accompanied by upregulation of the IL-6 signalling pathway 6 months after treatment initiation (figure 2B). No statistically significant differences were identified in the proportion of molecularly profiled blood immune cell subsets between SRI-4^+/LLDAS$^-$ responders at 6 months compared with baseline (online supplemental figure S1B).

Next, we were interested to examine the impact of belimumab treatment on the previously defined SLE disease 'susceptibility' and 'severity' gene signatures [32]. Out of the 2726 genes included in the 'susceptibility' signature, 2612 were identified in our dataset. LLDAS response was accompanied by a significant downregulation of the SLE 'susceptibility' signature ($p = 0.02$) (figure 2C). Of the 136 genes comprising the 'severity' signature, 130 were detected in our dataset. While statistical significance was not achieved, a tendency ($p = 0.130$) towards amelioration of this signature was observed in patients who achieved LLDAS (figure 2C). Of note, the attainment of SRI-4 did not result in a reversal of either signature (figure 2C).

Innate immunity signatures distinguish belimumab responders prior to initiation of treatment

Molecular stratification of patients according to their response to various treatments holds the potential to facilitate personalised care in individuals with SLE. To this end, the baseline blood transcriptome in SLE patients who responded to therapy (ie, attainment of SRI-4 and/or LLDAS) was compared against that of counterparts who did not, revealing a total of 1610 DEGs ($p<0.05$) (figure 3A). Pathways related to neutrophil activation, type I interferon and pattern recognition receptor signalling were significantly enriched among these DEGs (figure 3B). To corroborate these results, we employed an unsupervised, coexpression analysis to explore the relationship of baseline transcriptional signatures with clinical response (ie, SRI-4 or LLDAS) following 6 months of belimumab treatment. WGCNA identified twelve modules of coexpressed transcripts, designated by different colours (figure 3C). The yellow, purple and green modules positively correlated with LLDAS (but not SRI-4) attainment at 6 months. Enrichment analysis of these modules revealed a profound dysregulation of pathways implicated with neutrophil degranulation, type I interferon signalling and cytokine production, respectively (figure 3D–F). Of note, key interferon inducible genes including IFIT1, IFI27, IFI44, IFI44L, ISG15, HERC5, OAS1, OAS3, SERPING1 and RSAD2 [36] along with S100A12, a calcium-binding S100 protein whose levels are correlated with SLE disease activity and response to treatment with rituximab [37] were upregulated in LLDAS responders (figure 3D–F). In agreement with the differential gene expression analysis presented in figure 2, only the pink module

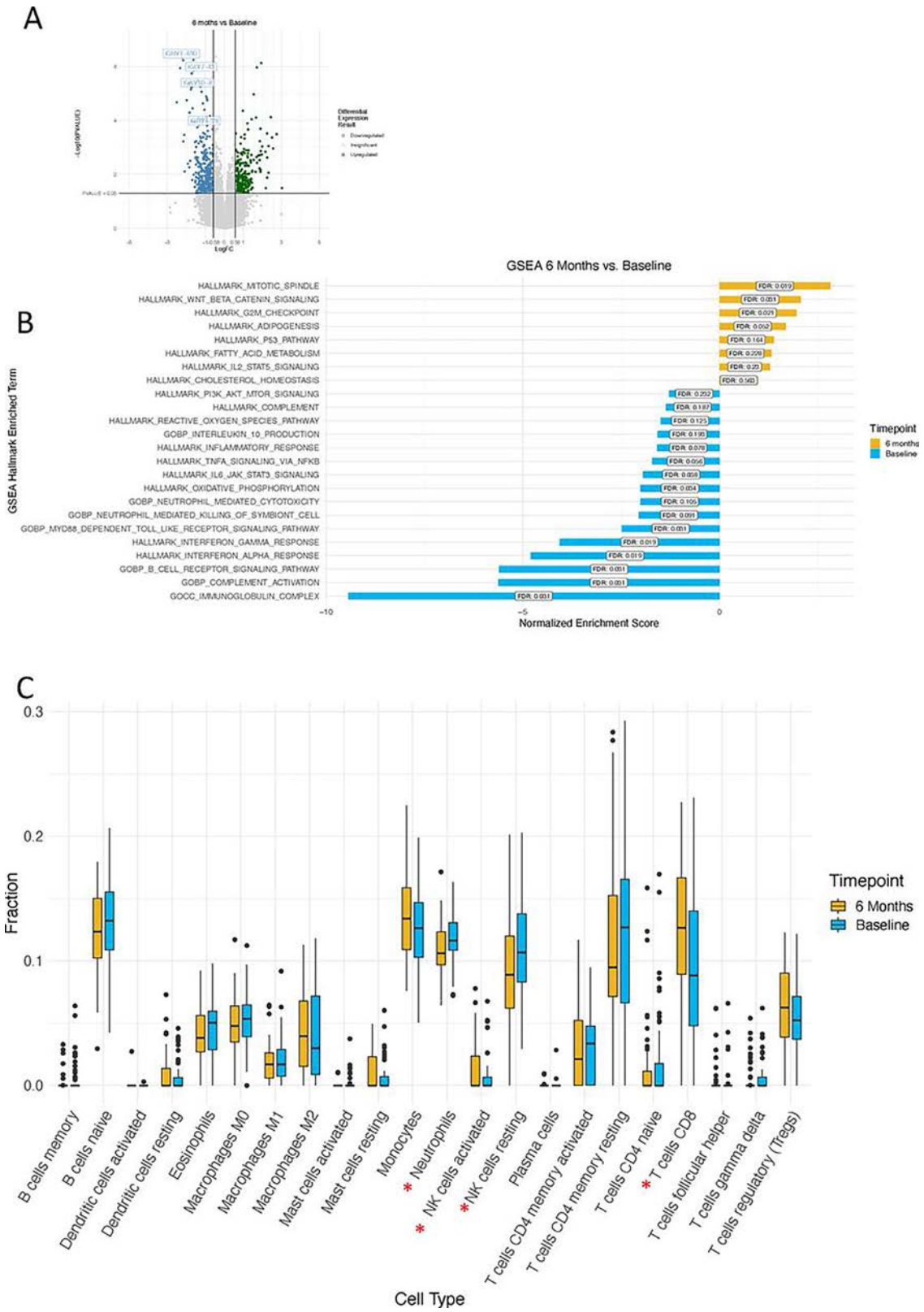

Figure 1. Longitudinal effect of belimumab on the blood transcriptome of SLE patients. (A) Volcano plot highlighting the differentially expressed genes in patients who received belimumab at 6 months (left) versus baseline (right). Upregulated DEGs are coloured green, and downregulated DEGs are coloured blue. DEGs not reaching the significance thresholds (|log2FC|>0.58 and p<0.05) are shown in grey. (B) Bar plot demonstrating the results of GSEA in patients who received belimumab at 6 months versus baseline. Belimumab elicited a statistically significant (FDR<0.1) suppression of pathways linked to B cell-mediated responses, type I and II interferon signalling, IL-6/STAT3 signalling pathways, and neutrophil activation 6 months post-treatment initiation. (C) Deconvolution analysis using CIBERSORTx showing the estimated proportions of different immune cell subsets in patients treated with belimumab at 6 months versus baseline. Mann-Whitney U test *p<0.05. DEGs, differentially expressed genes; FDR, false discovery rate; GSEA, gene set enrichment analysis; SLE, systemic lupus erythematosus.

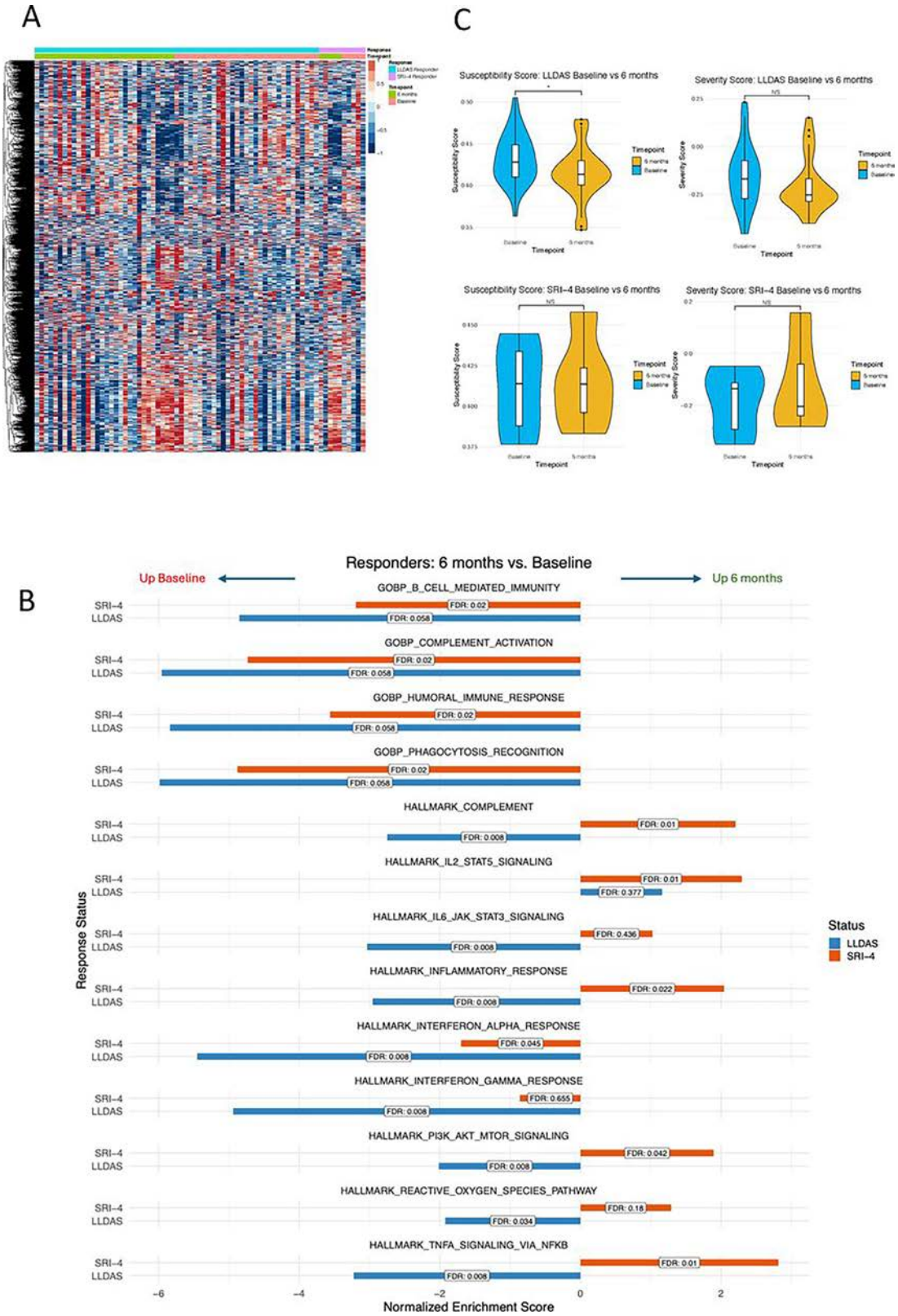

Figure 2. Effect of belimumab on the whole blood transcriptome. (A) The heatmap displaying log-transformed normalised gene counts of patients who attained LLDAS with or without SRI-4 response, and those who achieved SRI-4 but not LLDAS at 6 months and at baseline. The top annotation bar indicates patient response status: LLDAS responders with or without SRI-4 ('LLDAS Responder', blue) and SRI-4 responders but not LLDAS ('SRI-4 Responder', purple). The second annotation bar shows the sample collection timepoint: baseline (green) or 6 months (pink). (B) Bar plots showing the GSEA results based on expression profiles from two comparisons: (1) patients who attained LLDAS with or without SRI-4 at 6 months versus baseline and (2) patients who achieved SRI-4 but not LLDAS at 6 months versus baseline. A positive normalised enrichment score (NES) indicates upregulation of the examined pathway at 6 months compared with baseline, while a negative NES indicates upregulation at baseline compared with 6 months. Achieving LLDAS was linked to a downregulation (FDR<0.1) of pathways related to type I and II interferon signalling, complement activation, the IL-6 production and B-cell mediated response. SLE patients who experienced an SRI-4 response but did not attain LLDAS exhibited less pronounced down-regulation of B-cell gene signatures. (C) GSVA-based estimation of the 'susceptibility' and 'severity' scores using the logarithm of counts per million reads as input, in patients who achieved LLDAS with or without SRI-4 response and those who achieved SRI-4 but not the LLDAS response target at 6 months versus baseline. Mann-Whitney U test *p<0.05. FDR, false discovery rate; GSEA, gene set enrichment analysis; GSVA, gene set variation analysis; LLDAS, Lupus Low Disease Activity State; SLE, systemic lupus erythematosus; SRI, SLE Responder Index.

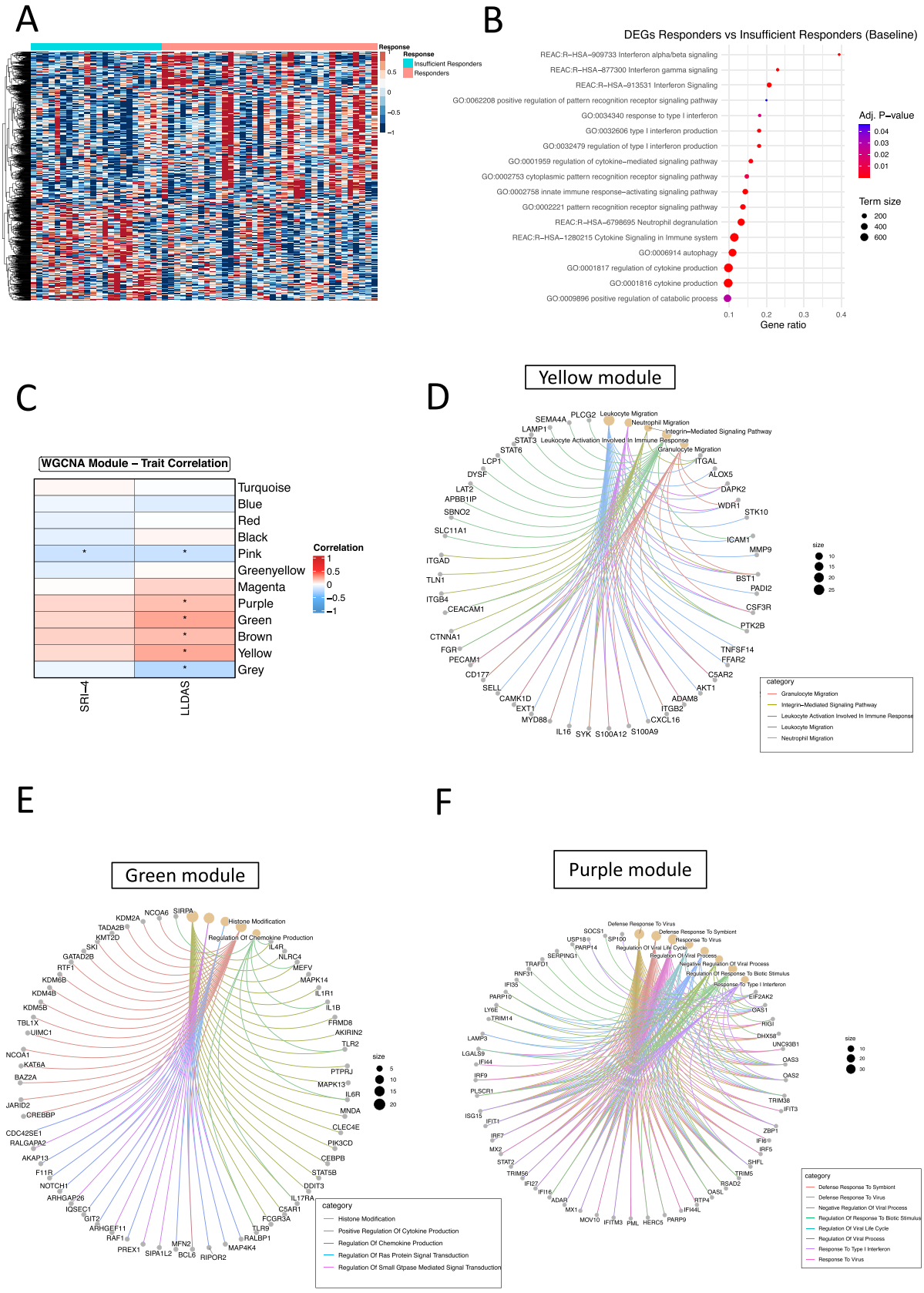

Figure 3. Transcriptional signatures versus insufficient responders prior to initiation of treatment. (A) Heatmap demonstrating the statistically significant DEGs ($p<0.05$) derived from the comparison of patients who attained LLDAS and/or SRI-4 response versus insufficient responders at baseline. (B) Dotplot showing the functional enrichment analysis results of the DEGs yielded from the comparison of LLDAS and/or SRI-4 responders versus insufficient responders at baseline. (C) Heatmap of the module–trait relationships, depicting correlation between the WGCNA derived-module eigengene and the attainment of LLDAS and SRI-4 response 6 months post-treatment initiation. The degree of correlation is illustrated with the colour legend. The green, purple, yellow and brown modules positively correlated with the attainment of LLDAS 6 months post-treatment initiation ($p<0.05$). The pink and grey modules significantly ($p<0.05$) correlated with failure to attain LLDAS. (D–F) Gene-concept networks demonstrating the linkages between genes and biological processes, enriched in the green, purple and yellow modules. *p-value<0.05. DEGs, differentially expressed genes; LLDAS, Lupus Low Disease Activity State; SLE, systemic lupus erythematosus; SRI, SLE Responder Index.

demonstrated significant correlation with SRI-4 response (figure 3C), indicating that innate immunity signatures at baseline may predict robust clinical response to treatment. The proportion of the molecularly profiled blood immune cell subsets did not exhibit any significant differences between the two groups at baseline (online supplemental figure S2A).

A molecular index to predict robust clinical response to belimumab

Previously, high disease activity, active lupus serology and use of glucocorticoids have been associated with enhanced clinical improvement following treatment with belimumab [16,17]. Motivated by our findings indicating an association between blood molecular modules and clinical outcomes, we sought to devise a gene panel capable of forecasting response—specifically, the achievement of SRI-4 and/or LLDAS—6 months after initiating belimumab treatment. To accomplish this, we applied machine-learning techniques to baseline gene expression profiles. Gene expression profiles obtained from the comparison of responders versus insufficient responders ($p<0.05$) in the training set were used in the recursive feature elimination feature selection algorithm under fivefold cross-validation, which determined a panel of 50 genes as the smallest set of genes that best predicted clinical response. Subsequently, multiple predictive models were fitted (twofold cross-validation) and the best model distinguishing patients according to their response status was a neural network model with 69% accuracy (95% CI 0.41% to 0.89%), 60% sensitivity and 84% specificity in the test set (online supplemental figure S3A,B). Notably, the selected gene set (online supplemental table S3) included genes with putative roles in regulation of immune responses including *CCL4L2*, recognised for its involvement in orchestrating immune cell migration [38], as well as the *CARD10*, which encodes a molecular scaffold, essential for the activation of the NF-κB and c-Jun N-terminal kinase pathways [39]. Our model underscored the significance of the extracellular matrix remodelling-related gene *MMP1*5 [40], and the *KLRC2*, which is linked to natural killer cell responses [41].

Dysregulation in cell cycle and metabolism shapes the transcriptional landscape of insufficient response to belimumab treatment

To delineate the transcriptional signature of insufficient response to belimumab, we performed GSEA using as input the DEGs obtained from the baseline comparison of patients who achieved LLDAS and/or SRI-4 response versus those who did not. Gene signatures associated with cell cycle checkpoints, PI3K/Akt/mammalian target of rapamycin (mTOR) pathway, oxidative phosphorylation and TGF-beta signalling were upregulated in patients exhibiting inadequate response to belimumab (figure 4A). To gain further insights, we determined a '*resistant disease*' gene signature by comparing the gene expression profiles of insufficient responders at baseline and 6 months following treatment. GSEA revealed heightened activation of pathways related to lipid and protein metabolic processes in the patients with lack of response at 6 months compared with baseline (online supplemental figure S4C).

Leveraging our WGCNA analysis, we detected two modules of coexpressed transcripts (pink, grey) which significantly, negatively correlated with LLDAS response to belimumab (figure 3C). In line with the GSEA findings, gene ontologies related to DNA damage were overrepresented in the pink and grey modules (online supplemental figure S4B). No statistically significant changes were observed in the expression of these modules in insufficient responders at 6 months compared with baseline, suggesting that belimumab might not affect these potential underlying resistant disease mechanisms (online supplemental figure S4D). To identify potential key molecular drivers of belimumab insufficient response, protein–protein interaction networks—inferred using the genes included in the pink and grey modules—were created (figure 4B, C). Topological analysis of the constructed network uncovered a high degree of interconnectivity of genes primarily associated with cell cycle checkpoint, apoptosis regulation and DNA damage response (DDR), including *CCNB2, CCNB1, BIRC5* and *DDB1* [42–45].

DISCUSSION

Our study provides a comprehensive, longitudinal profiling of the whole blood transcriptome of SLE patients, providing novel insights into the molecular processes underlying the diverse treatment response to belimumab. Pending further clinical validations, our approach suggests transcriptional signatures related to innate immunity and DDR mechanisms as potential transcriptional biomarkers of response to belimumab treatment (figure 5).

Belimumab in combination with background SLE therapy is associated with significant reduction in critical contributors of organ damage, including disease activity and risk of new flares [46,47]. Importantly, in our study, treatment with belimumab had a disease-modifying effect in all SLE patients, including insufficient responders, by inducing statistically significant suppression of type I and II interferon signalling pathways, correlated with SLE disease activity [36,48], coupled with an upregulation of the IL2/STAT5 signalling. This finding is in alignment with a previous study supporting that treatment with belimumab can restore Treg/Th17 balance in SLE patients with uncontrolled disease activity [49] suggesting that belimumab holds the potential to rectify the SLE-related immune aberrations, thereby imparting a protective effect against disease flares.

The treat-to-target strategy is extensively employed in the management of chronic conditions, including inflammatory arthritis [50]. In SLE, Definition of Remission in SLE [51] and LLDAS [23] have emerged as widely accepted treatment targets [15]. Observational studies have demonstrated that achieving these targets is associated with favourable outcomes, including reduced damage accrual [14,52], fewer flares, glucocorticoid therapy withdrawal, improved quality of life [53], improved mortality rates [54] and reduced healthcare costs [55]. Disease activity though does not always reflect the molecular portrait of patients. We have previously provided evidence for the existence of a 'susceptibility' signature, which persists even in the absence of disease activity following treatment [32]. Here, we demonstrated that achieving LLDAS was associated with a more robust downregulation of inflammatory pathways compared with SRI-4 response attainment. This was accompanied by a statistically significant improvement in the SLE 'susceptibility' gene signature and a trend towards decreasing the SLE 'severity' signature, suggesting that LLDAS may be associated with a more effective reversal of biological processes related to SLE pathogenesis. Our data are in accordance with recent data from the PRECISESADS project whereby LLDAS/remission was associated with reversal of biological processes related to SLE pathogenesis and specific clinical manifestations [56].

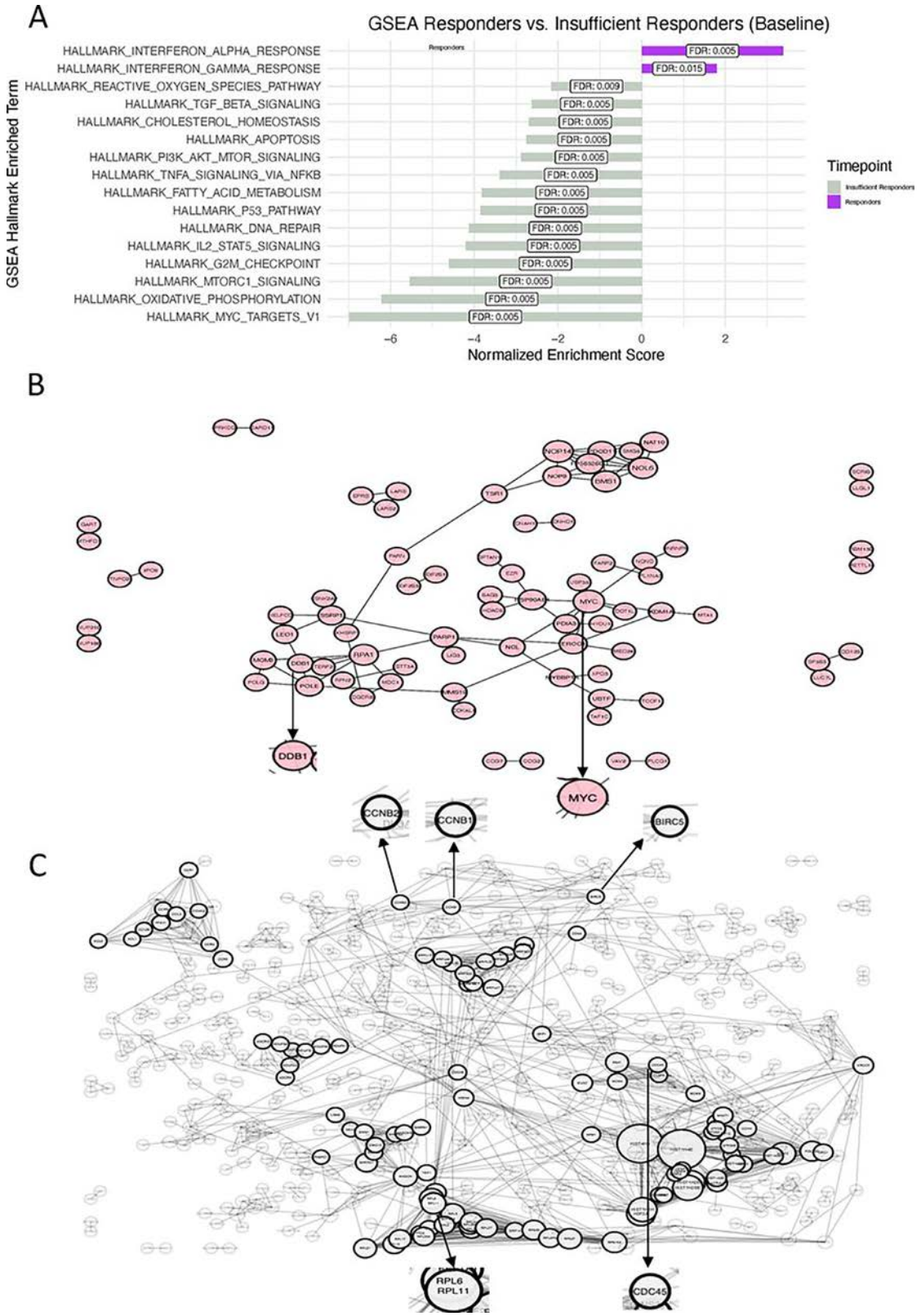

Figure 4. Gene expression signatures related to insufficient response to belimumab. (A) Bar plot demonstrating the results of GSEA in patients who achieved LLDAS and/or SRI-4 response versus insufficient responders at baseline. Processes upregulated in insufficient responders showed negative NES (grey bar plot). Transcriptome of insufficient responders at baseline was characterised by upregulation of pathways related to cell cycle checkpoints and oxidative phosphorylation compared with responders. (B, C) Protein–protein interaction networks using as input the genes included in the pink (B) and grey (C) modules. NES: GSEA, gene set enrichment analysis; LLDAS, Lupus Low Disease Activity State; NES, Normalised Enrichment Score; SLE, systemic lupus erythematosus; SRI, SLE Responder Index.

SLE is a notoriously heterogeneous disease. To this end, employing molecular taxonomy approaches might impact the benefits of drug treatment, through facilitating tailored treatment recommendations [57]. In the TULIP-2 trial, the presence of an elevated type I interferon was associated with higher effect sizes of response to anifrolumab [58]. In the same context, a tubular fibrotic gene expression signature has emerged as a potential indicator of poor response to therapeutic interventions

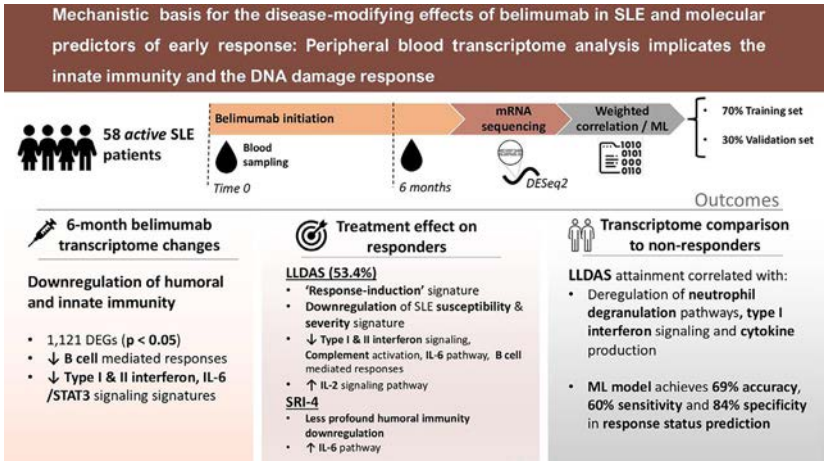

Figure 5. Belimumab effectively normalises transcriptional dysregulations in humoral and innate immune pathways. Achieving LLDAS with belimumab is associated with a reduction in the SLE 'susceptibility' signature and potentially in the 'severity' signature, in line with its ability to decrease disease activity and prevent flares. Dysregulation in cell cycle and metabolic pathways may contribute to insufficient responses to belimumab treatment. A molecular index of 50 genes enables prediction of robust clinical response to belimumab with high specificity. DEGs, differentially expressed genes; LLDAS, Lupus Low Disease Activity State; SLE, systemic lupus erythematosus; SRI, SLE Responder Index.

in lupus nephritis [59]. In our study, blood transcriptional signatures related to neutrophil degranulation and type I interferon signalling, prior to initiation of treatment, discriminated responders from insufficient responders, in alignment with a post hoc meta-analysis of the BLISS trials demonstrating a tendency towards improved response to add-on intravenous belimumab 10 mg/kg in patients with high baseline BLyS protein and IFN-1 mRNA levels [17]. To further investigate the predictive value of deep molecular profiling in predicting response to belimumab treatment, we applied diverse machine learning algorithms, culminating in the selection of a transcriptome model proven effective at predicting insufficient treatment response with the specificity of 84%.

Impaired DDR is not confined to tumourigenesis or increased susceptibility to viral infections but also has been implicated in autoimmunity [60,61]. Activation of the DDR pathways, indicative of increased DNA damage, combined by enrichment of signatures related to G2/M checkpoint—implying a transient cell cycle arrest—was associated with insufficient response to belimumab treatment at baseline. Substantial evidence points to increased DNA damage in SLE, with the genome integrity being constantly challenged by a diverse range of both intrinsic and extrinsic factors [62]. Endogenous sources of DNA damage include excessive production of reactive oxygen species, mainly generated as by-products of oxidative phosphorylation in the mitochon drial electron transport chain [63]. SLE adaptive and innate immune cells exhibit mitochondrial dysfunction, with oxidative stress leading to the extrusion of mitochondrial DNA from the mitochondria into the cytoplasm [64]. Along the same lines, persistent mitochondrial hyperpolarisation activates the mTOR, a sensor of mitochondrial transmembrane potential, inducing alterations in endocytic recycling of CD3ζ and T cell lineage specification in SLE [65]. Accordingly, it would be tempting to speculate that the enrichment of oxidative phosphorylation, mTOR and DDR pathways, observed in patients with inadequate response to belimumab treatment may signify increased DNA damage resulting from oxidative stress linked to mitochondrial impairment and redox dysregulation.

Dysregulated lipid metabolism has been strongly implicated in SLE at both systemic and cellular levels, with cardiovascular disease emerging as a well-recognised complication of SLE [66]. Altered lipid rafts have been described in the context of dysfunctional B and T cell signalling in SLE [67,68]. Moreover, eicosanoids, which are produced following phospholipase A2-mediated release of arachidonic acid, play a pivotal role in driving inflammation in autoimmune rheumatic diseases [69]. Insufficient response to treatment was associated with upregulation of pathways related to lipid biosynthesis, including arachidonic acid metabolism. Together, these findings might suggest that disturbed immunometabolism may represent a critical, BAFF-independent, potentially druggable contributor to resistant disease.

Certain limitations of our study deserve acknowledgement. First, our findings are based on a longitudinal profiling of the whole blood transcriptome, which may not fully capture tissue-specific molecular alterations. A lack of a control arm on 'standard of care' is an additional caveat as modulation of gene transcripts could be affected by conventional agents as well as by belimumab. Moreover, while our machine learning approach demonstrated significant specificity in predicting treatment response, further validation on a larger sample size is warranted to establish the robustness and generalisability of the identified transcriptional biomarkers.

In conclusion, our study has yielded novel insights into the molecular mechanisms driving the putative disease-modifying effects of belimumab treatment, providing additional insights for the development of biomarkers for treatment response while at the same time providing additional credence to the beneficial effects of this biological in improving patient care and clinical outcomes.

Correction notice

This article has been corrected since it published Online First. Footnotes from table 1 have been amended.

Acknowledgements

We thank Dr. Ioannis Vatsellas from the Greek Genome Center, BRFAA for the next-generation sequencing service.

Contributors

G-SM and PG followed patients, collected samples, performed experiments, analysed data, generated figures and wrote the manuscript. DNikoleri, E-MS and NM evaluated patients, performed sample preparation for cell isolation and RNA-seq experiment. PG, GS and AFilia performed bioinformatics analysis of the transcriptional data. G-SM, MN, SP, GB, AFanouriakis and DTB performed clinical evaluation of SLE individuals, provided human samples and critically edited the manuscript. DTB, GB

and AFilia conceived, revised and oversaw the study and the writing. All authors reviewed and approved the manuscript. DTB is the guarantor.

Funding

This work was supported by an ERC advanced grant (LUPUS-CARE grant agreement number 742390), to DTB, an investigator initiated research grant from GSK (grant agreement number 213662) to DTB and GB and by the Deutsche Forschungsgemeinschaft (DFG, German Research Foundation) through the Clinician Scientist Program NOTICE (grant number 493624887) to PG. Computational time granted from the National Infrastructures for Research and Technology S.A. (GRNET S.A.) in the National HPC facility—ARIS—under project ID pr014012_taskp-PRECISION_-SLE.

Competing interests

None declared.

Patient and public involvement

Patients and/or the public were not involved in the design, or conduct, or reporting, or dissemination plans of this research.

Patient consent for publication

Consent obtained directly from patient(s).

Ethics approval

This study involves human participants and was approved by Ethics Committee of the 'Attikon' University Hospital of Athens and University Hospital of Heraklion (299/3-6-2020 and 38/14-11-18, respectively). Participants gave informed consent to participate in the study before taking part.

Data availability statement

Data are available on reasonable request.

Supplementary materials

Supplementary material associated with this article can be found in the online version at doi:10.1136/ard-2024-226051.

REFERENCES

[1] Doria A, Stohl W, Schwarting A, et al. Hypocomplementemic Patients With Systemic Lupus Erythematosus. Arthritis Rheumatol 2018;70:1256–64.
[2] Fanouriakis A, Adamichou C, Koutsoviti S, et al. Low disease activity-irrespective of serologic status at baseline-associated with reduction of corticosteroid dose and number of flares in patients with systemic lupus erythematosus treated with belimumab: A real-life observational study. Semin Arthritis Rheum 2018;48:467–74.
[3] Guerreiro Castro S, Isenberg DA. Belimumab in systemic lupus erythematosus (SLE): evidence-to-date and clinical usefulness. Ther Adv Musculoskelet Dis 2017;9:75–85.
[4] Trentin F, Gatto M, Zen M, et al. Effectiveness, Tolerability, and Safety of Belimumab in Patients with Refractory SLE: a Review of Observational Clinical-Practice-Based Studies. Clin Rev Allergy Immunol 2018;54:331–43.
[5] van Vollenhoven R, Askanase AD, Bomback AS, et al. Conceptual framework for defining disease modification in systemic lupus erythematosus: a call for formal criteria. Lupus Sci Med 2022;9:e000634.
[6] Furie RA, Wallace DJ, Aranow C, et al. Long-Term Safety and Efficacy of Belimumab in Patients With Systemic Lupus Erythematosus: A Continuation of a Seventy-Six-Week Phase III Parent Study in the United States. Arthritis Rheumatol 2018;70:868–77.
[7] Iaccarino L, Bettio S, Reggia R, et al. Effects of Belimumab on Flare Rate and Expected Damage Progression in Patients With Active Systemic Lupus Erythematosus. *Arthritis Care Res (Hoboken)* 2017;69:115–23.
[8] Wallace DJ, Ginzler EM, Merrill JT, et al. Safety and Efficacy of Belimumab Plus Standard Therapy for Up to Thirteen Years in Patients With Systemic Lupus Erythematosus. Arthritis Rheumatol 2019;71:1125–34.
[9] Bruce IN, Urowitz M, van Vollenhoven R. Long-term organ damage accrual and safety in patients with SLE treated with belimumab plus standard of care. Lupus (Los Angel) 2016;25:699–709.
[10] Urowitz MB, Ohsfeldt RL, Wielage RC, et al. Organ damage in patients treated with belimumab versus standard of care: a propensity score-matched comparative analysis. Ann Rheum Dis 2019;78:372–9.
[11] Sanz I. Connective tissue diseases: targeting B cells in SLE: good news at last!. Nat Rev Rheumatol 2011;7:255–6.
[12] Chang SK, Arendt BK, Darce JR. A role for BLyS in the activation of innate immune cells. Blood 2006;108:2687–94.
[13] Maeda S, Hashimoto H, Maeda T, et al. High-dimensional analysis of T-cell profiling variations following belimumab treatment in systemic lupus erythematosus. Lupus Sci Med 2023;10:e000976.
[14] Pitsigavdaki S, Nikoloudaki M, Garantziotis P, et al. Pragmatic targets for moderate/severe SLE and their implications for clinical care and trial design: sustained DORIS or LLDAS for at least 6 months is sufficient while their attainment for at least 24 months ensures high specificity for damage-free progression. Ann Rheum Dis 2024;83:464–74.
[15] Fanouriakis A, Kostopoulou M, Andersen J. EULAR recommendations for the management of systemic lupus erythematosus: 2023 update. Ann Rheum Dis 2024;83:15–29.
[16] van Vollenhoven RF, Petri MA, Cervera R, et al. Belimumab in the treatment of systemic lupus erythematosus: high disease activity predictors of response. Ann Rheum Dis 2012;71:1343–9.
[17] Wilkinson C, Henderson RB, Jones-Leone AR, et al. The role of baseline BLyS levels and type 1 interferon-inducible gene signature status in determining belimumab response in systemic lupus erythematosus: a post hoc meta-analysis. Arthritis Res Ther 2020;22:102.
[18] Petri M, Orbai A-M, Alarcón GS, et al. Derivation and validation of the Systemic Lupus International Collaborating Clinics classification criteria for systemic lupus erythematosus. Arthritis Rheum 2012;64:2677–86.
[19] Aringer M, Costenbader K, Daikh D, et al. 2019 European League Against Rheumatism/American College of Rheumatology Classification Criteria for Systemic Lupus Erythematosus. Arthritis Rheumatol 2019;71:1400–12.
[20] Gladman DD, Ibañez D, Urowitz MB. Systemic lupus erythematosus disease activity index 2000. J Rheumatol 2002;29:288–91.
[21] Petri M, Genovese M, Engle E, et al. Definition, incidence, and clinical description of flare in systemic lupus erythematosus. A prospective cohort study. Arthritis & Rheum 1991;34:937–44.
[22] Furie RA, Petri MA, Wallace DJ, et al. Novel evidence-based systemic lupus erythematosus responder index. Arthritis Rheum 2009;61:1143–51.
[23] Franklyn K, Lau CS, Navarra SV, et al. Definition and initial validation of a Lupus Low Disease Activity State (LLDAS). Ann Rheum Dis 2016;75:1615–21.
[24] Andrews S. FastQC: a quality control tool for high throughput sequence data. 2010. Available: http://www.bioinformatics.babraham.ac.uk/projects/fastqc
[25] Dobin A, Davis CA, Schlesinger F, et al. STAR: ultrafast universal RNA-seq aligner. Bioinformatics 2013;29:15–21.
[26] Anders S, Pyl PT, Huber W. HTSeq—a Python framework to work with high-throughput sequencing data. Bioinformatics 2015;31:166–9.
[27] Johnson WE, Li C, Rabinovic A. Adjusting batch effects in microarray expression data using empirical Bayes methods. Biostatistics 2007;8:118–27.
[28] Love MI, Huber W, Anders S. Moderated estimation of fold change and dispersion for RNA-seq data with DESeq2. Genome Biol 2014;15:550.
[29] Reimand J, Kull M, Peterson H, et al. g:Profiler—a web-based toolset for functional profiling of gene lists from large-scale experiments. Nucleic Acids Res 2007;35:W193–200.
[30] Subramanian A, Tamayo P, Mootha VK, et al. Gene set enrichment analysis: a knowledge-based approach for interpreting genome-wide expression profiles. Proc Natl Acad Sci U S A 2005;102:15545–50.
[31] Langfelder P, Horvath S. WGCNA: an R package for weighted correlation network analysis. BMC Bioinformatics 2008;9:559.
[32] Panousis NI, Bertsias GK, Ongen H, et al. Combined genetic and transcriptome analysis of patients with SLE: distinct, targetable signatures for susceptibility and severity. Ann Rheum Dis 2019;78:1079–89.
[33] Szklarczyk D, Gable AL, Nastou KC, et al. The STRING database in 2021: customizable protein−protein networks, and functional characterization of user-uploaded gene/measurement sets. Nucleic Acids Res 2021;49:D605–12.

[34] Newman AM, Steen CB, Liu CL, et al. Determining cell type abundance and expression from bulk tissues with digital cytometry. Nat Biotechnol 2019;37:773–82.
[35] Kuhn M. Building predictive models in R using the caret package. J Stat Softw 2008;28:1–26.
[36] Chasset F, Mathian A, Dorgham K, et al. Serum interferon-α levels and IFN type I-stimulated genes score perform equally to assess systemic lupus erythematosus disease activity. Ann Rheum Dis 2022;81:901–3.
[37] Davies JC, Midgley A, Carlsson E, et al. Urine and serum S100A8/A9 and S100A12 associate with active lupus nephritis and may predict response to rituximab treatment. RMD Open 2020;6:e001257.
[38] Pedrosa E, Carretero-Iglesia L, Boada A, et al. CCL4L polymorphisms and CCL4/CCL4L serum levels are associated with psoriasis severity. J Invest Dermatol 2011;131:1830–7.
[39] Blonska M, Lin X. NF-κB signaling pathways regulated by CARMA family of scaffold proteins. Cell Res 2011;21:55–70.
[40] Lee HS, Kim WJ. The Role of Matrix Metalloproteinase in Inflammation with a Focus on Infectious Diseases. IJMS 2022;23:10546.
[41] Vietzen H, Zoufaly A, Traugott M, et al. Deletion of the NKG2C receptor encoding KLRC2 gene and HLA-E variants are risk factors for severe COVID-19. Genet Med 2021;23:963–7.
[42] Liu Q, Yuan Y, Shang X, et al. Cyclin B2 impairs the p53 signaling in nasopharyngeal carcinoma. BMC Cancer 2024;24:25.
[43] Zhang H, Zhang X, Li X, et al. Effect of CCNB1 silencing on cell cycle, senescence, and apoptosis through the p53 signaling pathway in pancreatic cancer. J Cell Physiol 2019;234:619–31.
[44] Li F, Ambrosini G, Chu EY, et al. Control of apoptosis and mitotic spindle checkpoint by survivin. Nat New Biol 1998;396:580–4.
[45] Iovine B, Iannella ML, Bevilacqua MA. Damage-specific DNA binding protein 1 (DDB1): a protein with a wide range of functions. Int J Biochem Cell Biol 2011;43:1664–7.
[46] Nikoloudaki M, Nikolopoulos D, Koutsoviti S, et al. Clinical response trajectories and drug persistence in systemic lupus erythematosus patients on belimumab treatment: A real-life, multicentre observational study. Front Immunol 2022;13:1074044.
[47] Urowitz MB, Aranow C, Asukai Y, et al. Impact of Belimumab on Organ Damage in Systemic Lupus Erythematosus. Arthritis Care Res (Hoboken) 2022;74:1822–8.
[48] Petri M, Fu W, Ranger A, et al. Association between changes in gene signatures expression and disease activity among patients with systemic lupus erythematosus. BMC Med Genomics 2019;12:4.
[49] Prete M, Leone P, Frassanito MA, et al. Belimumab restores Treg/Th17 balance in patients with refractory systemic lupus erythematosus. *Lupus (Los Angel)* 2018;27:1926–35.
[50] Smolen JS. Treat to Target in Rheumatology: A Historical Account on Occasion of the 10th Anniversary. Rheum Dis Clin North Am 2019;45:477–85.
[51] van Vollenhoven R, Voskuyl A, Bertsias G, et al. A framework for remission in SLE: consensus findings from a large international task force on definitions of remission in SLE (DORIS). Ann Rheum Dis 2017;76:554–61.
[52] Petri M, Magder LS. Comparison of Remission and Lupus Low Disease Activity State in Damage Prevention in a United States Systemic Lupus Erythematosus Cohort. Arthritis Rheumatol 2018;70:1790–5.
[53] Ríos-Garcés R, Espinosa G, van Vollenhoven R, et al. Treat-to-target in systemic lupus erythematosus: Where are we? Eur J Intern Med 2020;74:29–34.
[54] Sharma C, Raymond W, Eilertsen G, et al. Association of Achieving Lupus Low Disease Activity State Fifty Percent of the Time With Both Reduced Damage Accrual and Mortality in Patients With Systemic Lupus Erythematosus. Arthritis Care Res (Hoboken) 2020;72:447–51.
[55] Yeo AL, Koelmeyer R, Kandane-Rathnayake R. Lupus Low Disease Activity State and Reduced Direct Health Care Costs in Patients With Systemic Lupus Erythematosus. Arthritis Care Res (Hoboken) 2020;72:1289–95.
[56] Parodis I, Lindblom J, Barturen G, et al. Molecular characterisation of lupus low disease activity state (LLDAS) and DORIS remission by whole-blood transcriptome-based pathways in a pan-European systemic lupus erythematosus cohort. Ann Rheum Dis 2024;83:889–900.
[57] Garantziotis P, Nikolakis D, Doumas S, et al. Molecular Taxonomy of Systemic Lupus Erythematosus Through Data-Driven Patient Stratification: Molecular Endotypes and Cluster-Tailored Drugs. Front Immunol 2022;13:860726.
[58] Morand EF, Furie R, Tanaka Y, et al. Trial of Anifrolumab in Active Systemic Lupus Erythematosus. N Engl J Med 2020;382:211–21.
[59] Der E, Suryawanshi H, Morozov P, et al. Tubular cell and keratinocyte single-cell transcriptomics applied to lupus nephritis reveal type I IFN and fibrosis relevant pathways. Nat Immunol 2019;20:915–27.
[60] Manolakou T, Verginis P, Boumpas DT. DNA Damage Response in the Adaptive Arm of the Immune System: Implications for Autoimmunity. Int J Mol Sci 2021;22:5842.
[61] Manolakou T, Nikolopoulos D, Gkikas D. ATR-mediated DNA damage responses underlie aberrant B cell activity in systemic lupus erythematosus. Sci Adv 2022;8:eabo5840.
[62] Mireles-Canales MP, González-Chávez SA, Quiñonez-Flores CM, et al. DNA Damage and Deficiencies in the Mechanisms of Its Repair: Implications in the Pathogenesis of Systemic Lupus Erythematosus. J Immunol Res 2018;2018:8214379.
[63] Cucchi D, Gibson A, Martin SA. The emerging relationship between metabolism and DNA repair. Cell Cycle 2021;20:943–59.
[64] Zhao L, Hu X, Xiao F, et al. Mitochondrial impairment and repair in the pathogenesis of systemic lupus erythematosus. Front Immunol 2022;13:929520.
[65] Perl A. Oxidative stress in the pathology and treatment of systemic lupus erythematosus. Nat Rev Rheumatol 2013;9:674–86.
[66] Robinson GA, Wilkinson MGL, Wincup C. The Role of Immunometabolism in the Pathogenesis of Systemic Lupus Erythematosus. Front Immunol 2022;12:806560.
[67] Jury EC, Kabouridis PS, Flores-Borja F, et al. Altered lipid raft–associated signaling and ganglioside expression in T lymphocytes from patients with systemic lupus erythematosus. J Clin Invest 2004;113:1176–87.
[68] Flores-Borja F, Kabouridis PS, Jury EC, et al. Altered lipid raft-associated proximal signaling and translocation of CD45 tyrosine phosphatase in B lymphocytes from patients with systemic lupus erythematosus. Arthritis Rheum 2007;56:291–302.
[69] Robinson G, Pineda-Torra I, Ciurtin C, et al. Lipid metabolism in autoimmune rheumatic disease: implications for modern and conventional therapies. J Clin Invest 2022;132:e148552.

Ann Rheum Dis 84 (2025) 274–283

Contents lists available at ScienceDirect

Annals of the Rheumatic Diseases

journal homepage: https://www.sciencedirect.com/journal/annals-of-the-rheumatic-diseases

Systemic lupus erythematosus

Evaluation and prediction of relapse risk in stable systemic lupus erythematosus patients after glucocorticoid withdrawal (PRESS): an open-label, multicentre, non-inferiority, randomised controlled study in China

Yunyun Fei[1,2,3], Lidan Zhao[1,3], Lijun Wu[4], Xiaoxia Zuo[5], Rongli Li[1], Jiaomei Cheng[5], Hui Luo[5], Xue Wu[4], Li Sun[6], Jingjing Xu[7], Yingxuan Zhu[8], Yang Wang[8], Zhu Chen[6], Xiaomei Li[6], Xiaofei Wang[7], Xuan Zhang[9,*], PRESS study team

[1] *Department of Rheumatology and Clinical Immunology, Peking Union Medical College Hospital, Chinese Academy of Medical Sciences & Peking Union Medical College, Beijing, China*
[2] *Department of Heath Medicine, Peking Union Medical College Hospital, Beijing, China*
[3] *National Clinical Research Center for Dermatologic and Immunologic Diseases (NCRC-DID), Beijing, China*
[4] *Department of Rheumatology and Immunology, People's Hospital of Xinjiang Uygur Autonomous Region, Urumqi, Xinjiang, China*
[5] *Department of Rheumatology and Immunology, Xiangya Hospital Central South University, Changsha, Hunan, China*
[6] *Department of Rheumatology and Immunology, The First Affiliated Hospital of USTC, Division of Life Sciences and Medicine, University of Science and Technology of China, Hefei, Anhui, China*
[7] *Department of Rheumatology and Clinical Immunology, Shengjing Hospital of China Medical University, Shenyang, Liaoning, China*
[8] *Medical Research and Biometrics Centre, Chinese Academy of Medical Sciences & Peking Union Medical College Fuwai Hospital, Xicheng, Beijing, China*
[9] *Department of Rheumatology, Beijing Hospital, National Centre of Gerontology, Institute of Geriatric Medicine, Clinical Immunology Centre, Chinese Academy of Medical Sciences, Beijing, China*

ARTICLE INFO

Article history:
Received 16 March 2024
Accepted 23 October 2024

Keywords:
Lupus Erythematosus
Systemic
Glucocorticoids
Hydroxychloroquin

ABSTRACT

Objectives: To explore the relapse rate after glucocorticoid (GC) withdrawal with or without hydroxychloroquine (HCQ) maintenance in sustained clinically inactive systemic lupus erythematosus (SLE).

Methods: The PRESS trial is a multicentre, 33-week, open-label, three-arm, non-inferiority designed, randomised controlled trial. SLE patients with sustained clinically inactive disease who maintained on low-dose GC plus HCQ therapy were screened and qualified patients were randomly assigned to three groups: drug-free group (both GC and HCQ withdrew); HCQ group (discontinued GC but maintained HCQ); dual maintenance group (both GC and HCQ

*Correspondence to Dr. Xuan Zhang.
E-mail address: zhangx@bjhmoh.cn (X. Zhang).
Handling editor Josef S. Smolen.
YF, LZ, LW and XZ contributed equally.
YF, LZ, LW and XZ are joint first authors.

https://doi.org/10.1136/ard-2024-225826

continued). The primary endpoint was to compare the proportion of patients experiencing a relapse as defined by the Safety of Estrogens in Lupus Erythematosus National Assessment-Systemic Lupus Erythematosus Disease Activity Index flare index by 33 weeks. Two parallel non-inferiority analyses were performed (drug-free group vs dual maintenance group and HCQ group vs dual maintenance group).

Results: From 3 November 2016 to 13 August 2021, 333 participants complied with the protocol after randomisation were analysed. The relapse rates in the three groups were 26.1%, 11.2% and 4.7%, respectively. Compared with dual maintenance group, drug-free group failed to achieve non-inferiority significance (relapse rate difference 21.4%; 95% CI 12.3% to 30.5%; Pnon-inferiority = 0.238), whereas HCQ group achieved non-inferiority (relapse rate difference 6.5%; 95% CI −0.5% to 13.5%; Pnon-inferiority = 0.034). HCQ group also exhibited fewer relapses than drug-free group (p = 0.006). Adverse events were similar among all three groups.

Conclusions: GC withdrawal may be feasible in sustained clinically inactive SLE patients. HCQ maintenance can exert a protective role in preventing disease relapse after GC withdrawal.

Trial registration number NCT02842814.

WHAT IS ALREADY KNOWN ON THIS TOPIC

• Prolonged exposure to glucocorticoids, even at low dosages, is associated with increased accumulated disease damage. Although European Alliance of Associations for Rheumatology recommendations suggest to taper glucocorticoid to 5 mg/day prednisone for maintenance in individuals with stable systemic lupus erythematosus (SLE) disease and if possible, withdrawing, no consolidated evidence is available as to answer when and who can withdraw glucocorticoid after achieving the goal of remission or low lupus disease activity state, and dispute regarding the optimal glucocorticoid-sparing strategy in clinical practice warranted effort for more solid evidence.

WHAT THIS STUDY ADDS

• Over two-thirds of sustained clinically inactive SLE patients could enjoy glucocorticoid-free or even drug-free safely in an 8-month follow-up period. Continuous hydroxychloroquine may substitute for glucocorticoid as an effective maintenance strategy.

HOW THIS STUDY MIGHT AFFECT RESEARCH, PRACTICE OR POLICY

• This prospective randomised non-inferiority study revealed the feasibility of glucocorticoid withdrawal in sustained inactive SLE patients and indicated continuous hydroxychloroquine being an effective substitute maintenance strategy to prevent relapses. Potential risk factors for disease relapse were explored and awaited further investigations.

INTRODUCTION

Systemic lupus erythematosus (SLE) is becoming a big burden globally with the prevalence estimated to be 43.7 (15.87 to 108.92) per 100 000 persons and the affected population reaching 3.41 million [1]. Asian SLE patients are reported to suffer from a more active and severe disease, higher organ damage accrual and higher mortality and morbidity than Caucasian counterparts [2].

SLE is a clinically heterogeneous chronic autoimmune disease affecting multiple organs, which can be well controlled but seldom cured. Relapses of SLE are frequently observed and a wide range of relapse rates have been reported in literature from 8% to 45% [3–7]. Glucocorticoids (GCs) remain pivotal in the treatment of SLE and play a critical role in inducing remission in active patients. GCs have long been considered a key player in the successive maintenance therapy after remission induction, which is intended to achieve the goal of sustained remission or low lupus disease activity state (LLDAS) by preventing relapse. Currently, there are lacking of predictive factors for disease relapse, and low-dose GC therapy is usually maintained in sustained inactive SLE patients for many years or even lifelong. As well known, prolonged exposure to GCs could introduce a lot of unwanted side effects and disabling comorbidities such as atherosclerosis, osteoporotic fractures, diabetes, cataract, etc [8–13], leading to impaired quality of life and cumulative damage. It was reported that withdrawal of unnecessary GC therapy can help reduce both renal and extrarenal damage accrual in SLE patients [14]. The European Alliance of Associations for Rheumatology (EULAR) recommended tapering GCs to 5 mg/day prednisone (or equivalent) for maintenance in individuals with stable disease and, if possible, withdrawing these drugs [15]. However, due to the heterogeneity of SLE, it is unclear how to, when to and who can withdraw GC maintenance after achieving remission.

Hydroxychloroquine (HCQ) is an essential treatment for SLE that help control disease activity and prevent disease relapse. HCQ has less side effects than GCs and is recommended to be used in all lupus patients without contraindications [15,16]. Long-term HCQ therapy seems beneficial in combating GC-related metabolic disturbances and its potential in reducing disease relapse and damage accrual in lupus patients has been documented [17–21]. Therefore, it is also important to clarify whether HCQ could replace GCs as an alternative maintenance regimen for SLE patients who were in sustained remission or LLDAS.

To investigate the relapse risk after GCs withdrawal in stable SLE patients with sustained remission or LLDAS and to identify who can remain stable after GCs withdrawal, as well as to examine the protective role of HCQ in preventing disease relapse, we conducted this multicentre, open-label, non-inferiority design, randomised controlled clinical trial. With the assumptions that GCs were not indispensable for preventing disease relapse in patients achieving sustained remission/LLDAS, and HCQ alone was efficacious to maintain remission/LLDAS after GC withdrawal, a non-inferiority design was adopted.

METHODS

Study design and patients

This study is an open-label, multicentre, non-inferiority, investigator-initiated, randomised controlled study. The study design was discussed among 10 rheumatologists along with biometrics specialists and was registered on ClinicalTrials.gov with

the identifier NCT02842814 on 3 June 2016. The trial protocol is provided in online supplemental appendix.

Five geographically representative tertiary rheumatology centres across China, including Peking Union Medical College Hospital (Central), The First Affiliated Hospital of USTC (also known as Anhui Provincial Hospital)(East), People's Hospital of Xinjiang Uygur Autonomous Region (West), Shengjing Hospital (North) and Xiangya Hospital (South), participated in this trial.

Patient recruitment started in November 2016 according to the following inclusion/exclusion criteria. The inclusion criteria were as follows: subjects fulfilled the Systemic Lupus International Collaborating Clinic revision of the American College of Rheumatology Classification Criteria for SLE (SLICC-2012) [22]; age 18–60 years; disease was sustained inactive ≥1 year, defined as SELENA-SLEDAI (the Safety of Estrogens in Lupus Erythematosus National Assessment-Systemic Lupus Erythematosus Disease Activity Index) continued to be no higher than 3 and previous system impairment had been relieved and stabilised with no newly occurred organ lesions attributed to SLE; anti-double strand DNA (anti-dsDNA) was negative by immunofluorescence measurement and ≤200 IU/mL by ELISA method (reference: <100 IU/mL); serum complement 3 (C3)≥ 0.5 × lower limit of the normal range, and C3 fluctuation was less than 10% within the last year; 24 hour urine protein ≤0.5 g; prednisone (or equivalent) ≤7.5 mg/day for more than 6 months; no immunosuppressants other than HCQ, including cyclosporine A, mycophenolate mofetil, cyclophosphamide, tacrolimus, leflunomide, methotrexate, had been used within the last 6 months; no previous use of biological agents, including rituximab, belimumab and telitacicept; no severe organ involvement, including lupus encephalopathy, diffused alveolar haemorrhage, thrombotic thrombocytopaenia purpura, rapid progressive glomerulonephritis, severe thrombocytopaenia, severe haemolytic anaemia, myocardial involvement, myelitis or severe peripheral neuropathy, in the last 2 years.

The exclusion criteria were as follows: pregnancy or breast feeding or planning for pregnancy; currently scheduled surgery or had a surgery within the past 6 months; current infections; history of malignancy; severe organ dysfunction or other complications; inability to follow-up; unwilling to be enrolled and psoriasis, porphyria, arrhythmia or eye diseases that contraindicate HCQ usage.

If all inclusion criteria and none of the exclusion criteria were met, patients were considered eligible for the study. Informed consent was obtained from all the enrolled subjects. Participants were allowed to withdraw consent anytime during the study. However, those withdrew consent in the first week after randomisation were not included in the final analysis.

Randomisation and interventions

Randomisation was performed by an independent third party who was masked from the subjects' clinical situations and the detail of interventions. By using a computer-generated randomisation code, enrolled patients were assigned in a 1:1:1 ratio to the three arms: drug-free group, HCQ group and dual maintenance group. The detailed information of intervention corresponding to each group was unmasked to the rheumatologists who were responsible for the participants' recruitment and follow-up but were blinded to the staff responsible for the randomisation. Drug-free group stopped their HCQ treatment and reduced their GC dosage to discontinuation; HCQ group reduced their GC dosage to discontinuation while maintaining their HCQ dosage; dual maintenance group continued their GC and HCQ dosages without change. In both drug-free and HCQ group, GC was tapered and stopped in 4 weeks with a reduction of one-fourth of the baseline dosage each week. In this open-label trial, both the patients and the research physicians were aware of the grouping information after randomisation, and the research physicians were responsible for supervising the participants to implement corresponding interventions. All the five centres conducted randomisation via the same randomisation code table. Calcium tablets and/or vitamin D were permitted during the study. For cases complicated with antiphospholipid syndrome or with the presence of antiphospholipid antibodies, aspirin or anticoagulants were allowed to take as needed.

Procedures

The patients were followed up regularly. Disease activity and relevant laboratory indices were monitored at baseline and each following visit. The on-site follow-up visits were set at 5, 9, 21 and 33 weeks (online supplemental figure and protocol) with one telephone follow-up during 1–4 weeks to ascertain the compliance to study scheme. Disease relapse was evaluated by the modified SFI (SELENA-SLEDAI flare index) [23,24] and the British Isles Lupus Activity Group (BILAG) scoring system [25], and disease damage was assessed by SDI (the SLICC/American College of Rheumatology Damage Index) [26]. Physician global assessment (PGA) was recorded as well at each visit. Patients were informed to contact their physicians once they felt any discomfort suggestive of SLE disease relapse. Once relapse was confirmed during the follow-up visit, the endpoint event was considered and the patient received appropriate treatment without limitations from the study. Also, the modified management should be taken into the consideration in the relapse severity evaluations. Patients were asked for contraception during the whole trial. In case unintended pregnancy occurred, subjects were asked to withdraw from the trial for safety considerations.

Endpoint and outcomes

The primary endpoint was the percentage of subjects who experienced a relapse as evaluated by SFI during the study. The secondary endpoints included the following: the percentage of subjects with a SELENA-SLEDAI score <4 points; mean change in PGA; the percentage of subjects with at least one B in any of the domains evaluated with BILAG scoring and the percentage of subjects experiencing a severe relapse or a mild/moderate relapse according to the SFI and BILAG scoring systems.

The outcomes were evaluated by at least two rheumatologists in each centre. Endpoint events and adverse effects were evaluated at each visit until the end of 33 weeks. Imputation for the relapse condition of those who dropped out during the follow-up was implemented based on the baseline-observation-carried-forward (BOCF) strategy, WOCF (worst observation carried forward) method was applied as sensitivity analysis.

Patient and public involvement

Patients or the public were not involved in the design, or conduct, or reporting, or dissemination plans of our research.

Statistical analysis

The sample-size calculation was based on the following assumptions: SLE patients with sustained clinically inactive

disease and low-dose GC plus HCQ maintenance had a relapse rate of 15%. Those taking HCQ alone and drug-free patients had a similar relapse risk after GC withdrawal by 33 weeks. Two parallel non-inferiority tests of drug-free group versus dual maintenance group and HCQ group versus dual maintenance group were conducted. A difference of 15% in the proportion of relapse was set as the non-inferiority margin, based on the wide range of relapse rate reported previously in stable SLE patients [3–7]. Considering multiplicity, the significance level was adjusted to one-sided 0.025. The sample size of 89 in each group would provide a power of 80%. As three arms were arranged and a dropout rate of 20% was considered, the sample size of each group needed to be 111.

All analyses were performed on an intention-to-treat (ITT) basis. Categorical data are expressed as numbers (%), and quantitative parameters are presented as mean±SD or median (quartiles), alternatively, according to the data distribution. For the primary endpoint, the Newcombe hybrid score interval method was applied to analyse the difference in relapse rates between groups. The difference in the relapse rate in two parallel non-inferiority tests and the corresponding 95% CI were calculated. Furthermore, time to relapse was shown with a Kaplan-Meier survival curve. Differences in secondary endpoints between the drug-free group versus the dual maintenance group, and the HCQ group versus the dual maintenance group were examined using Student's t-tests or Mann-Whitney U tests for continuous data and χ^2 tests or Fisher's exact tests for categorical data.

The results of subgroup analyses regarding clinical features were presented using forest plots. The p values of the Breslow-Day test were used as an indication of interaction between subgroup factors and treatment groups. The potential factors associated with relapse were explored by logistic regression.

All tests were conducted as one-sided tests, with $p<0.025$ defined as the statistical significance level, and were performed using SAS V.9.4 software.

RESULTS

From 3 November 2016 to 13 August 2021, a total of 466 patients were screened, and 352 patients fulfilling the inclusion criteria were randomised. There were 117, 118 and 117 patients assigned to drug-free group, HCQ group and dual maintenance group, respectively. 19 patients (6, 2 and 11 patients in drug-free group, HCQ group and dual maintenance group, respectively) withdrew consent right after randomisation (figure 1). Finally, 111, 116 and 106 patients were included in the modified ITT analysis, among whom 188 cases were in remission according to the DORIS definition. The average age of modified ITT participants was 37.35±10.34 years. Female patients were predominant with the gender ratio of F:M being 21.2:1. During the follow-up, 8, 7 and 10 patients dropped out from drug-free group, HCQ group and dual maintenance group, respectively (figure 1). The baseline data of the participants were comparable among the three groups which are presented in table 1. The mean HCQ dosage during follow-up was comparable between HCQ group and dual maintenance group (0.22±0.08 g/day vs 0.23±0.09 g/day). The mean prednisone (or equivalent) dosage was 4.02±1.98 mg/day in dual maintenance group.

Primary endpoint

In the modified ITT analysis, the relapse rates of the three groups (drug-free group, HCQ group and dual maintenance group) during the 33 weeks of study duration evaluated by SFI were 26.1%, 11.2% and 4.7%, respectively (figure 2). Between the two parallel non-inferiority analyses (drug-free group vs dual maintenance group, HCQ group vs dual maintenance group), drug-free group failed to achieve non-inferiority significance in relapse rate (rate difference 21.4%; 95% CI 12.3% to 30.5%; $P_{\text{non-inferiority}} = 0.238$), thus reject the first non-inferiority hypothesis, whereas HCQ group successfully achieved non-inferiority in comparison with dual maintenance group in the

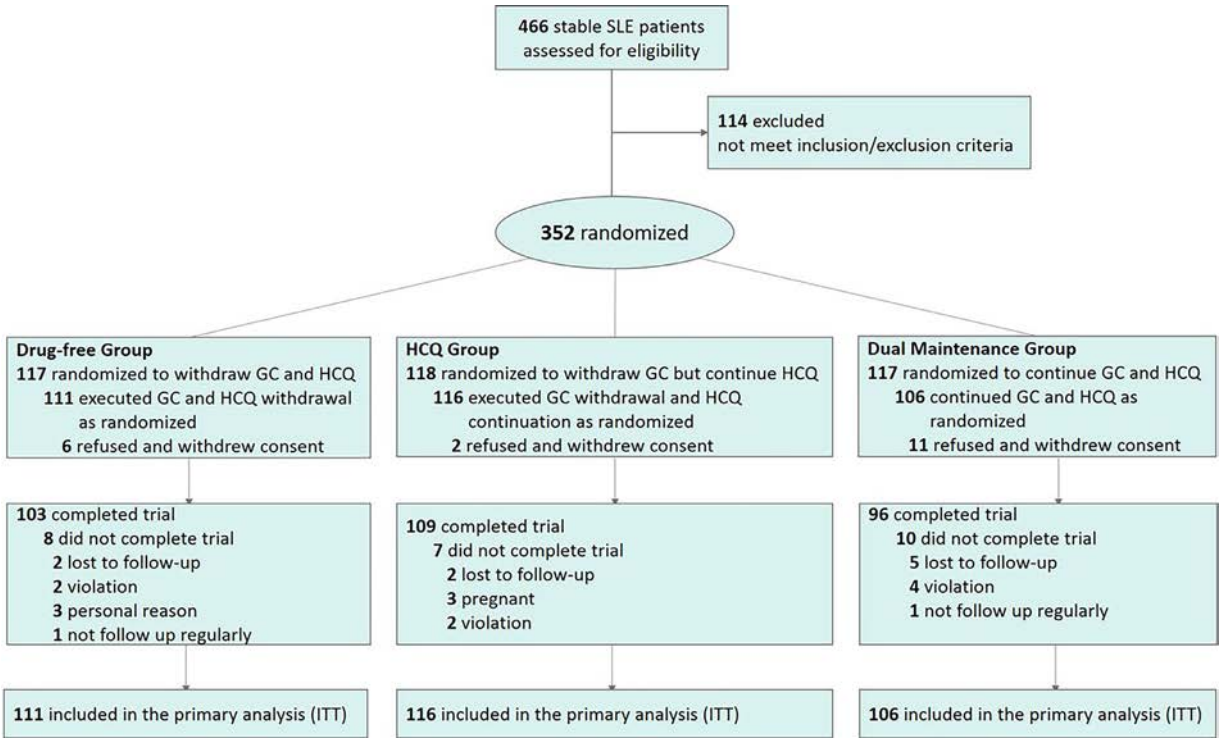

Figure 1. Study flow diagram. GC, glucocorticoids; HCQ, hydroxychloroquine; ITT, intention-to-treat analysis; SLE, systemic lupus erythematosus.

Table 1
Baseline demographic and clinical characteristics of different groups

	Drug-free group (n = 111)	HCQ group (n = 116)	Dual maintenance group (n = 106)
Sex (female:male)	104:7	113:3	101:5
Average onset age (mean±SD, years)	35.3±10.1	34.7±10.3	34.4±10.7
Disease duration at enrolment (mean±SD, years)	8.0±5.6	7.2±4.5	7.4±4.5
SELENA-SLEDAI at enrolment (median, IQR)	0 (0, 2.0)	0 (0, 2.0)	0 (0, 2.0)
SELENA-SLEDAI at enrolment (mean±SD)	0.67±0.94	0.56±0.93	0.58±0.91
SELENA-SLEDAI at diagnosis (median, IQR)	9.0 (7.0, 11.0)	9.0 (6.0, 11.5)	9.0 (7.0, 12.0)
SELENA-SLEDAI at diagnosis (mean±SD)	9.86±4.14	9.16±3.93	10.37±5.01
GC dose at enrolment (mean±SD, mg)	4.37±1.98	4.06±1.97	4.13±2.01
Low-dose GC maintenance time (mean±SD, months)*	47.07±34.77	38.67±25.99	41.55±30.80
DORIS remission at enrolment (%)	57 (53.3)	72 (62.6)	59 (56.2)
History of Relapse (%)	21 (18.9)	26 (22.4)	23 (21.7)
System involvement and serological positivity in history			
Renal involvement (%)	49 (44.1)	44 (37.9)	42 (39.6)
Central nervous system involvement (%)	8 (7.2)	5 (4.3)	9 (8.5)
Haematological involvement (%)	62 (55.9)	54 (46.6)	57 (53.8)
Arthritis (%)	51 (45.9)	64 (55.2)	53 (50.0)
Rashes or mucosal ulceration (%)	77 (69.4)	80 (69.0)	78 (73.6)
Gastrointestinal tract involvement (%)	4 (3.6)	4 (3.4)	2 (1.9)
Hypocomplementaemia (%)	90 (81.1)	93 (80.2)	79 (74.5)
Anti-dsDNA positivity (%)	69 (62.2)	61 (52.6)	54 (50.9)
Antiphospholipid positivity† (%)	6/105 (5.7)	9/108 (8.4)	2/102 (2.0)
Anti-ribosomal P positivity‡ (%)	29 (26.1)	28/115 (24.3)	25 (24.0)

* Low-dose GC maintenance time: The maintaining time of prednisone (or equivalent) ≤7.5 mg/day and no use of DMARDs (disease-modifying anti-rheumatic drugs) other than HCQ.
† Percentage was calculated among those with available information, the number of whom was presented below diagonal as /n.
‡ Percentage was calculated among those with available information, the number of whom was presented below diagonal as /n. Were there no /n, information of the variables was intact and available from all members (n in the table header) of the corresponding groups.
dsDNA, double-strand DNA; GC, glucocorticoid; HCQ, hydroxychloroquine; SELENA-SLEDAI, the Safety of Estrogens in Lupus Erythematosus National Assessment-Systemic Lupus ErythematosusDisease Activity Index.

relapse rate and accepted the second non-inferiority hypothesis (rate difference 6.5%; 95% CI −0.5% to 13.5%; $P_{non\text{-}inferiority} = 0.034$). Maintenance of HCQ therapy (HCQ group) showed a significantly reduced relapse rate compared with drug-free group ($p = 0.006$). The patients who dropped out during the follow-up were assessed as having no relapse at 33 weeks. Sensitivity analysis by imputation of missing data using WOCF strategy consistently supported the non-inferiority conclusion, with the current main analysis being more conservative.

Secondary endpoint

The percentages of subjects with a SELENA-SLEDAI score <4 points throughout the trial were 78.4%, 90.5% and 98.1% in drug-free group, HCQ group and dual maintenance group, respectively. The proportion of patients experiencing a relapse at 33 weeks measured by the BILAG index was similar to that recorded by the SFI. In evaluations of the severity of relapse, mild/moderate relapses were more frequently observed (23.4%, 7.8% and 3.8% in drug-free group, HCQ group and dual maintenance group by SFI, respectively), and severe relapses were scarce (2.7%, 2.6% and 0.9% in drug-free group, HCQ group and dual maintenance group by SFI, respectively), and there was no significant difference in severe relapse among the three groups (table 2). Mild/moderate relapses evaluated by SFI were more common in drug-free group than in dual maintenance group but were non-inferior in HCQ group as compared with those in dual maintenance group. Similarly, when measured by BILAG, more mild relapses were observed in drug-free group than dual maintenance group, but no significant difference was observed between HCQ group and dual maintenance group. Moderate relapses were found of no significant difference in the two parallel comparisons. As for SDI, two patients in HCQ group had SDI increase, one presenting with acute myocardial infarction, and the other with cerebral infarction that occurred during follow-up (table 2).

Relapse events

A total of 47 relapse events were observed. Precisely, there were 29 cases of relapse in drug-free group, including 10 patients presenting with rash or mucosal ulcers, 7 with lupus nephritis, 5 with arthritis, 3 with leucopenia, 3 with thrombocytopaenia and 1 with liver dysfunction. The 13 relapse cases in HCQ group included 5 patients presenting with leucopenia, 2 with nephritis, 1 with cutaneous manifestations, 1 with cerebral infarction, 1 with arthritis, 1 with myositis, 1 with thrombocytopaenia and 1 with leucopenia and cutaneous manifestations. The five relapse cases in dual maintenance group included one patient with thrombocytopaenia, two with rash and mucosal ulcers, one with arthritis and one with scleritis. As regarding the relapse events, leucopenia accounted for the most in relapses of HCQ group (6, 5.2%), while mucocutaneous lesions (10, 9%) and nephritis (7, 6.3%) were more frequently observed in relapse of drug-free group (table 2). Nephritis relapse was defined by urine test of appearance/reappearance of urine protein over 0.5 g/24 hours or haematuria. Among the nine cases with nephritis relapse, three were new-onset.

Subgroup analysis

To preliminarily explore if there were some potential features at baseline could help predict patients' relapse outcome later on under different treatment strategies, we classified patients based on their baseline clinical features and historical laboratory indices. Interaction between subgroup factors and treatment strategies was investigated but with no significant

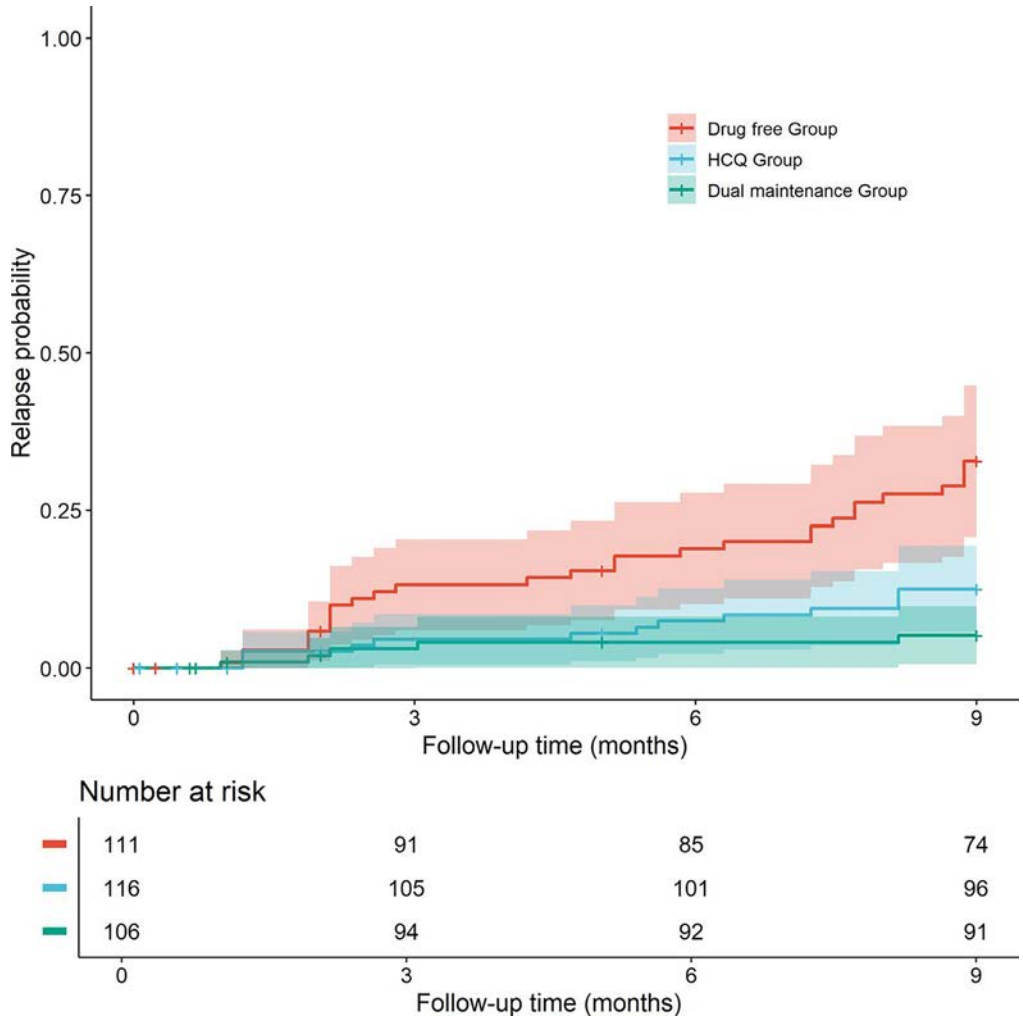

Figure 2. The Kaplan-Meier survival curve showing the proportion of systemic lupus erythematosus patients of the three groups experiencing a relapse over study period. HCQ, hydroxychloroquine.

Table 2

Primary and secondary endpoints in two parallel non-inferiority analyses at 33 weeks

	Drug-free group vs dual maintenance group (N = 111:106)	P value	HCQ group vs dual maintenance group (N = 116:106)	P value
Cumulative relapse (%)	29 (26.1): 5 (4.7)	0.238 for non-inferiority	13 (11.2): 5 (4.7)	0.034 for non-inferiority
Median relapse time points (months)	4.7±3.0: 3.0±2.8	0.335	3.4±2.7: 3.0±2.8	0.997
Relapse by SFI (%)	29 (26.1): 5 (4.7)	**<0.001**	13 (11.2): 5 (4.7)	0.077
Mild/moderate relapse (%)	26 (23.4): 4 (3.8)	**<0.001**	10 (7.8): 4 (3.8)	0.207
Severe relapse (%)	3 (2.7): 1 (0.9)	0.622	3 (2.6):1 (0.9)	0.623
Relapse by BILAG index (%)	29 (26.1): 5 (4.7)	**<0.001**	13 (11.2): 5 (4.7)	0.077
Mild relapse (%)	21 (18.9): 4 (3.8)	**<0.001**	7 (6.0): 4 (3.8)	0.438
Moderate relapse (%)	2 (1.8): 0 (0.0)	0.498	3 (2.6): 0 (0.0)	0.248
Severe relapse (%)	6 (5.4): 1 (0.9)	0.120	3 (2.6): 1 (0.9)	0.623
Moderate/severe (%)	8 (7.2): 1 (0.9)	**0.036**	6 (5.2): 1 (0.9)	0.122
Patients experiencing an increase in the SDI (%)	0 (0.0): 0 (0.0)	–	2 (1.7): 0 (0.0)	0.499
Mean change in PGA				
PGA≥1 and <2.5 (%)	24 (21.6): 4 (3.8)	**<0.001**	10 (8.6): 4 (3.8)	0.138
PGA≥2.5 (%)	2 (1.8): 1 (0.9)	1.000	2 (1.7): 1 (0.9)	1.000
Relapse organs				
Nephritis (%)	7 (6.3): 0 (0)	**0.014**	2 (1.7): 0 (0)	0.499
Central nervous system (%)	0 (0): 0 (0)	–	1 (0.9): 0 (0)	1.000
Leucopenia (%)	3 (2.7): 0 (0)	0.247	6 (5.2): 0 (0)	**0.030**
Thrombocytopaenia (%)	1 (0.9): 1 (0.9)	1.000	1 (0.9): 1 (0.9)	1.000
Skin/mucosa (%)	10 (9.0): 2 (1.9)	**0.022**	2 (1.7): 2 (1.9)	1.000
Arthritis (%)	5 (4.5): 1 (0.9)	0.213	1 (0.9): 1 (0.9)	1.000
Myositis (%)	0 (0): 0 (0)	–	1 (0.9): 0 (0)	1.000
Digestive system (%)	1 (0.9): 0 (0)	1.000	0 (0): 0 (0)	–

p value < 0.05 was shown in bold.

BILAG, British Isles Lupus Activity Group scoring system; HCQ, hydroxychloroquine; PGA, physician global assessment; SDI, Systemic Lupus International Collaborating Clinics/ American College of Rheumatology Damage Index; SELENA-SLEDAI, the Safety of Estrogens in Lupus Erythematosus National Assessment - Systemic Lupus Erythematosus Disease Activity Index; SFI, SELENA-SLEDAI flare index.

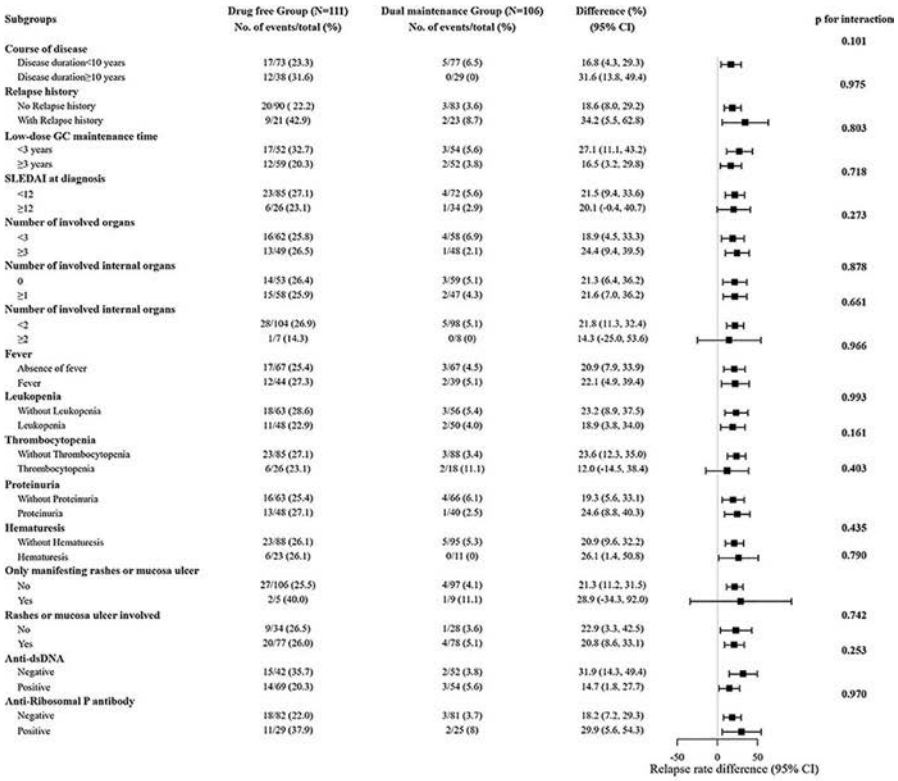

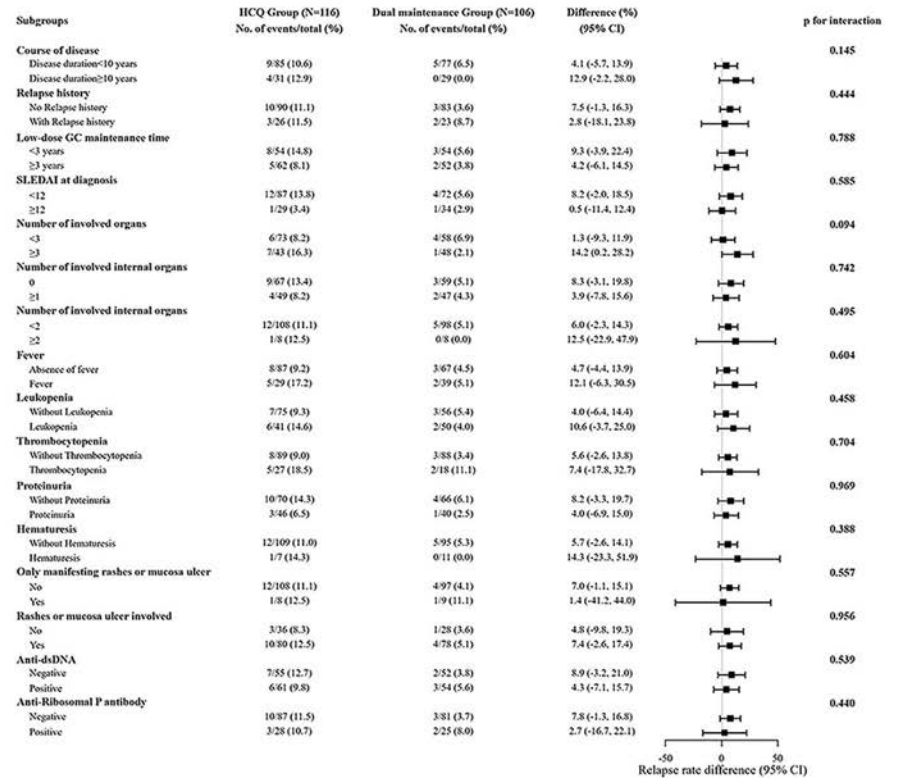

Figure 3. Forest plot of relapse in subgroups analysis with factors at baseline. (A) Forest plot of comparison of relapse with subgroup factors at baseline between drug-free group and dual maintenance Group. (B) Forest plot of comparison of relapse with subgroup factors at baseline between HCQ group and dual maintenance group. Breslow-Day test was used for subgroup analysis and p values were presented to indicate the interaction between subgroup factors and treatment groups. GC, glucocorticoid; HCQ, hydroxychloroquine; SELENA-SLEDAI, the Safety of Estrogens in Lupus Erythematosus National Assessment-Systemic Lupus Erythematosus Disease Activity Index.

findings (figure 3A,B). Not surprisingly, patients who previously manifested mainly with skin/mucosal lesions shared similar relapse rate between HCQ group and dual maintenance group (12.5% and 11.1%).

Risk factors for relapse

Potential risk factors for recurrence were also explored by using logistic regression analysis (online supplemental table).

The results showed that GC dosage at enrolment (>5 mg/day vs ≤5 mg/day, OR 2.86; 95% CI 1.12 to 7.30) was a potential risk factor for relapse. In addition, a history of fever (OR 2.25; 95% CI 1.00 to 5.02) or early age of disease onset (OR 0.95; 95% CI 0.90 to 0.99) might be potential predictive factors for recurrence. No correlation was found between relapse and other serological indices, such as anti-dsDNA antibody positivity and titres, antiphospholipid antibody profiles, Coomb's test positivity and hypocomplementaemia at disease onset. In terms of organ

involvement, nephritis, ccentral nervous system or haematological system involvement in history was not a risk factor for recurrence.

Adverse events

During the study period, there were no deaths, no new-onset diabetes, no severe infections and no ocular fundus abnormalities or other relapse-unrelated adverse events that necessitated hospitalisation or the discontinuation of HCQ or GC treatment in all groups with only one exception in HCQ group. A 59-year-old female SLE patient who had an acute myocardial infarction during follow-up was diagnosed with coronary atherosclerotic heart disease by coronary angiography and improved after receiving coronary artery bypass grafting. Twenty-five (7.1%) patients dropped out, mainly due to 'loss to follow-up' (9, 2.6%) and 'protocol violation' (8, 2.3%). Three pregnancies, two unregular follow-up and three 'personal reasons unwilling to disclose' led to the other eight dropouts.

DISCUSSION

SLE typically has a relapsing-remitting course and low-dose GC therapy is usually maintained for a long time in fear of disease relapses after the goal of remission or LLDAS has been achieved. It is suggested approximately 20%–30% of SLE patients undergo disease relapse after GC withdrawal [27,28] and that maintenance of 5 mg/d prednisone can effectively prevent relapse in most inactive SLE patients [29]. However, it is also reported that discontinuation of low-dose GC might be feasible and safe in clinically quiescent SLE [19,30]. To stop or not to stop GC in SLE patients with sustained inactive disease remains a clinical dilemma. To stop GC might render patients to the danger of disease relapse, whereas long-time GC intake, despite of low dosage, may bring a lot of unendurable side effects. On the other hand, HCQ monotherapy might be a reasonable alternative maintenance strategy [31]. To date, the optimal approach to stop GC use in SLE patients remains unclear and whether HCQ could be a substitute for GC to prevent disease relapse in clinically quiescent SLE patients awaits clarification. To answer these, we conducted this prospective randomised non-inferiority investigator-initiated RCT.

In this study, we observed that withdrawal of both GC and HCQ in sustained, clinical inactive SLE patients led to an increased relapse as compared with dual maintenance group, whereas continuous use of HCQ could exert a protective role in preventing disease relapse. Similar relapse rates (27% in GC withdraw group vs 7% in maintenance group) were reported in a recent single-centre GC withdraw study with a smaller sample size and allowance of immunosuppressants continuation [29].

Approximately one-fourth of subjects in its GC-withdraw group also had at least one immunosuppressant (such as methotrexate, azathioprine or mycophenolate mofetil) in use and its relapse rate was higher than our HCQ group [29]. In our study, based on the varied relapse rates reported previously [28], which may be explained by different treatment in use and different follow-up duration but also can be attributed to the heterogenicity of patients and the complexity of the disease, the non-inferiority margin of relapse rate increase was set at 15%, which was consistent with the previous study [29]. Few patients had severe relapse and no significant difference was found in severe relapse between the GC withdrawal and GC maintenance groups. The most common relapsed manifestation in drug-free group was mucocutaneous lesions and nephritis, while nephritis was less observed in HCQ Group, indicating that continuous use of HCQ may help prevent relapse as well as kidney involvement.

To identify those candidate patients suitable for and can benefit from GC withdrawal, future studies with larger samples and homogenised interventions are expected. In the current study, subgroup analysis was performed and non-prespecified potential predictors for relapse were explored. We found that SLE patients with a history of only mucocutaneous manifestations were less likely to relapse using HCQ as maintenance after GC withdrawal.

Serological indicators, such as historical positivity of anti-dsDNA antibody and its titres, and hypocomplementaemia, were not demonstrated to be suggestive of subsequent relapse after GC withdrawal.

In conclusion, GC withdrawal may be feasible in sustained clinically inactive SLE patients, and HCQ maintenance can exert a protective role in preventing disease relapse after GC withdrawal. Importantly, drug-free strategy was not recommended for all clinical inactive SLE patients because of the unacceptably high risk of relapse, whereas on the other hand, over 70% of lupus patients remained relapse-free after withdrawal of both GC and HCQ, signifying the importance of singling-out these patients to stop unnecessary long-term use of GC and HCQ and to avoid unwanted side effects. A history of only mucocutaneous involvement may safely stop GC while continuing HCQ as the maintenance, which warrants future verification.

Nonetheless, there are some limitations in our study. First, it had a fairly short follow-up period for capturing early relapse events. Continuous follow-up of this cohort is ongoing and we hope further data can be provided in the future. Second, the sample size may not have been sufficient for subgroup analysis due to the heterogeneity of SLE. Third, this is not a multiethnic study with Chinese Han population predominantly enrolled, thus the conclusion must be cautiously extrapolated to other ethnicities. Fourth, the imputation method of BOCF used in the main analysis could not fully circumvent the risk of bias. However, the sensitivity analysis with imputing missing data in the other direction using the WOCF method proved the result's robustness. Notably, dual maintenance group, which was supposed to have the lowest relapse rate among the three groups, had a slightly higher drop-out rate, thus assessing all drop-outs as having no relapse provided a more conservative and strict estimation to our hypothesis. In addition, we presumed that patients who were lost to follow had no relapse based on the experience from clinical practice that it is very common for SLE patients to skip scheduled visits when they are feeling well especially in the era of COVID-19 pandemic, which can also be deduced from a higher rate of lost to follow occurred in dual maintenance group.

Finally, the exploration of clinical parameters in predicting relapse risk was not prespecified, thus needs further verification. Future studies should include a larger sample size as well as a longer follow-up time, and the potential predictors found in this study need to be verified in a newly recruited cohort along with new biomarkers investigation.

Contributors

XZuo, LZ, LW, XZhang, XL and XWu were responsible for the conception and design of the study. XZuo, YF, LZ, LW, XZhang, XL, XWang, HL and ZC led study recruitment and evaluation at each visit. RL, JC, XWu, LS and JX were responsible for coordination and data arrangement. YF, YZ and YW were responsible for data analysis and had access to the whole study data. YF and

LZ drafted the manuscript and XZhang provided critical review of the manuscript. YZ and YW were responsible for production of the figures. XZuo is the guarantor. All authors contributed to interpretation of the data and agreed to submit the manuscript.

Funding

This study was supported by the National Natural Science Foundation of China (82230060, 81788101, 82271856, 82071840), the Key R&D plan of the Ministry of Science and Technology (2022YFC3602000), Chinese Academy of Medical Science Innovation Fund (CIFMS 2020-I2M-C & T-A-002, 2021-1-I2M-017, 2021-1-I2M-047) and the National High-Level Hospital Clinical Research Funding (2022-PUMCH-C-039, 2022-PUMCH-B-013, 2022-PUMCH-A-108, BJ-2022-116).

Competing interests

None declared.

Patient and public involvement

Patients and/or the public were not involved in the design, or conduct, or reporting, or dissemination plans of this research.

Patient consent for publication

Consent obtained directly from patient(s).

Ethics approval

This study involves human participants and ethics approval for this study was obtained from the ethics committees of all five centres (Peking Union Medical College Hospital, Anhui Provincial Hospital, People's Hospital of Xinjiang Uygur Autonomous Region, Shengjing Hospital, and Xiangya Hospital) (ethics approval ID: ZS-906, 2016-024, 16-28-DZX, 2016PS009K, 201603545). Participants gave informed consent before taking part.

Data availability statement

Data are available on reasonable request. We intend to make data collected for the study, including anonymised individual participant data and a data dictionary defining each field in the set, available to others. Related documents will be available, including the trial protocol and the statistical analysis plan. These data will be available with the publication of our main manuscript and all secondary projects as outlined in our trial protocol on receipt of a letter of intention detailing the study hypothesis and statistical analysis plan. The steering committee of this trial will discuss all requests and decide based on the scientific rigourness of the proposal whether data sharing is appropriate. All applicants are asked to sign a data access agreement. Please send the request to the principal investigator of this trial.

Supplementary materials

Supplementary material associated with this article can be found in the online version at doi:10.1136/ard-2024-225826.

REFERENCES

[1] Tian J, Zhang D, Yao X, et al. Global epidemiology of systemic lupus erythematosus: a comprehensive systematic analysis and modelling study. Ann Rheum Dis 2023;82:351–6.
[2] Li R, Sun J, Ren L-M, et al. Epidemiology of eight common rheumatic diseases in China: a large-scale cross-sectional survey in Beijing. *Rheumatology (Oxford)* 2012;51:721–9.
[3] Illei GG, Takada K, Parkin D, et al. Renal flares are common in patients with severe proliferative lupus nephritis treated with pulse immunosuppressive therapy: long-term followup of a cohort of 145 patients participating in randomized controlled studies. Arthritis Rheum 2002;46:995–1002.
[4] Sprangers B, Monahan M, Appel GB. Diagnosis and treatment of lupus nephritis flares–an update. Nat Rev Nephrol 2012;8:709–17.
[5] Inês L, Duarte C, Silva RS, et al. Identification of clinical predictors of flare in systemic lupus erythematosus patients: a 24-month prospective cohort study. *Rheumatology (Oxford)* 2014;53:85–9.
[6] Conti F, Ceccarelli F, Perricone C, et al. Flare, persistently active disease, and serologically active clinically quiescent disease in systemic lupus erythematosus: a 2-year follow-up study. PLoS One 2012;7:e45934.
[7] Laustrup H, Voss A, Green A, et al. SLE disease patterns in a Danish population-based lupus cohort: an 8-year prospective study. *Lupus (Los Angel)* 2010;19:239–46.
[8] Mosca M, Tani C, Carli L, et al. Glucocorticoids in systemic lupus erythematosus. Clin Exp Rheumatol 2011;29:S126–9.
[9] Zonana-Nacach A, Barr SG, Magder LS, et al. Damage in systemic lupus erythematosus and its association with corticosteroids. Arthritis Rheum 2000;43:1801–8.
[10] Tani C, Elefante E, Signorini V, et al. Glucocorticoid withdrawal in systemic lupus erythematosus: are remission and low disease activity reliable starting points for stopping treatment? A real-life experience. RMD Open 2019;5:e000916.
[11] Ward MM. Premature morbidity from cardiovascular and cerebrovascular diseases in women with systemic lupus erythematosus. Arthritis Rheum 1999;42:338–46.
[12] Karp I, Abrahamowicz M, Fortin PR, et al. Recent corticosteroid use and recent disease activity: independent determinants of coronary heart disease risk factors in systemic lupus erythematosus? Arthritis Rheum 2008;59:169–75.
[13] Bultink IEM, Lems WF, Kostense PJ, et al. Prevalence of and risk factors for low bone mineral density and vertebral fractures in patients with systemic lupus erythematosus. Arthritis Rheum 2005;52:2044–50.
[14] Moroni G, Longhi S, Giglio E, et al. What happens after complete withdrawal of therapy in patients with lupus nephritis. Clin Exp Rheumatol 2013;31:S75–81.
[15] Fanouriakis A, Kostopoulou M, Andersen J, et al. EULAR recommendations for the management of systemic lupus erythematosus: 2023 update. Ann Rheum Dis 2024;83:15–29.
[16] Fanouriakis A, Kostopoulou M, Alunno A, et al. 2019 update of the EULAR recommendations for the management of systemic lupus erythematosus. Ann Rheum Dis 2019;78:736–45.
[17] Almeida-Brasil CC, Hanly JG, Urowitz M, et al. Flares after hydroxychloroquine reduction or discontinuation: results from the Systemic Lupus International Collaborating Clinics (SLICC) inception cohort. Ann Rheum Dis 2022;81:370–8.
[18] Canadian Hydroxychloroquine Study Group. A Randomized Study of the Effect of Withdrawing Hydroxychloroquine Sulfate in Systemic Lupus Erythematosus. N Engl J Med 1991;324:150–4.
[19] Ji L, Xie W, Fasano S, et al. Risk factors of flare in patients with systemic lupus erythematosus after glucocorticoids withdrawal. A systematic review and meta-analysis. Lupus Sci Med 2022;9:e000603.
[20] Fasano S, Coscia MA, Pierro L, et al. Which patients with systemic lupus erythematosus in remission can withdraw low dose steroids? Results from a single inception cohort study. *Lupus (Los Angel)* 2021;30:991–7.
[21] Bruce IN, O'Keeffe AG, Farewell V, et al. Factors associated with damage accrual in patients with systemic lupus erythematosus: results from the Systemic Lupus International Collaborating Clinics (SLICC) Inception Cohort. Ann Rheum Dis 2015;74:1706–13.
[22] Petri M, Orbai A-M, Alarcón GS, et al. Derivation and validation of the Systemic Lupus International Collaborating Clinics classification criteria for systemic lupus erythematosus. Arthritis Rheum 2012;64:2677–86.
[23] Buyon JP, Petri MA, Kim MY, et al. The effect of combined estrogen and progesterone hormone replacement therapy on disease activity in systemic lupus erythematosus: a randomized trial. Ann Intern Med 2005;142:953–62.
[24] Petri M, Buyon J, Kim M. Classification and definition of major flares in SLE clinical trials. *Lupus (Los Angel)* 1999;8:685–91.
[25] Yee C-S, Farewell V, Isenberg DA, et al. British Isles Lupus Assessment Group 2004 index is valid for assessment of disease activity in systemic lupus erythematosus. Arthritis Rheum 2007;56:4113–9.

[26] Gladman DD, Goldsmith CH, Urowitz MB, et al. The Systemic Lupus International Collaborating Clinics/American College of Rheumatology (SLICC/ACR) Damage Index for Systemic Lupus Erythematosus International Comparison. J Rheumatol 2000;27:373–6.
[27] Goswami RP, Sit H, Ghosh P, et al. Steroid-free remission in lupus: myth or reality; an observational study from a tertiary referral centre. Clin Rheumatol 2019;38:1089–97.
[28] Ji L, Xie W, Zhang Z. Low-dose glucocorticoids should be withdrawn or continued in systemic lupus erythematosus? A systematic review and meta-analysis on risk of flare and damage accrual. *Rheumatology (Oxford)* 2021;60:5517–26.
[29] Mathian A, Pha M, Haroche J, et al. Withdrawal of low-dose prednisone in SLE patients with a clinically quiescent disease for more than 1 year: a randomised clinical trial. Ann Rheum Dis 2020;79:339–46.
[30] Tselios K, Gladman DD, Su J, et al. Gradual Glucocorticosteroid Withdrawal Is Safe in Clinically Quiescent Systemic Lupus Erythematosus. ACR Open Rheumatol 2021;3:550–7.
[31] Hanaoka H, Iida H, Kiyokawa T, et al. Glucocorticoid, immunosuppressant, hydroxychloroquine monotherapy, or no therapy for maintenance treatment in systemic lupus erythematosus without major organ manifestations. Clin Rheumatol 2019;38:2785–91.

Ann Rheum Dis 84 (2025) 284–293

Contents lists available at ScienceDirect

Annals of the Rheumatic Diseases

journal homepage: https://www.sciencedirect.com/journal/annals-of-the-rheumatic-diseases

Systemic lupus erythematosus

Pharmacodynamics of the $S1P_1$ receptor modulator cenerimod in a phase 2b randomised clinical trial in patients with moderate to severe SLE

Madeleine Suffiotti[1], Pijus Brazauskas[1], Marcel Peter Keller[1], Ouali Berkani[2], Gustavo Seifer[2], Peter Cornelisse[1], Mark Joseph Murphy[1], Daniel Stefan Strasser[1,*]

[1] *Idorsia Pharmaceuticals Ltd, Allschwil, Switzerland*
[2] *Viatris, Allschwil, Switzerland*

ARTICLE INFO

Article history:
Received 14 August 2024
Accepted 15 October 2024

Keywords:
Lupus Erythematosus
Systemic
Autoimmune Diseases
Antibodies
B-Lymphocytes

ABSTRACT

Background: Systemic lupus erythematosus (SLE) is a complex autoimmune disease characterised by autoreactive T and B lymphocytes. Sphingosine-1- phosphate (S1P) is involved in lymphocyte egress from peripheral lymphoid organs into the circulation. In phase 2a clinical trial, the potent, selective $S1P_1$ receptor modulator cenerimod reduced circulating antibody-secreting cells and interferon (IFN)-associated biomarkers.

Objectives: Pharmacodynamic effects of 2 and 4 mg cenerimod were evaluated in the phase 2b clinical trial (CARE) in moderate to severe patients with SLE (NCT03742037).

Methods: Blood samples were collected at baseline and after 6 months of treatment with cenerimod or placebo from CARE. The gene expression signatures for type 1 interferon (IFN-1), IFN-γ and plasma cells were used to assess dose-dependent pharmacodynamic effects of cenerimod. Cell-type deconvolution was performed to estimate cell abundance.

Results: Cenerimod 4 mg reduced IFN-associated protein and gene signature biomarkers after 6 months compared with placebo. A larger decrease of IFN proteins was evident in IFN-1 high patients compared with IFN-1 low patients. The median IFN-1 score in the IFN-1 high patients was reduced after 6 months of cenerimod 4 mg and the transition from IFN-1 low to high status compared with placebo was prevented. Cenerimod 4 mg exhibited a larger effect size on the pharmacodynamic biomarkers IFN-1, IFN-γ and plasma cells compared with cenerimod 2 mg.

Conclusions: This study further characterised the mechanism of action of cenerimod in patients with SLE and substantiated the scientific rationale for cenerimod 4 mg in the phase 3 clinical trials in moderate to severe SLE (OPUS-1/–2).

INTRODUCTION

Systemic lupus erythematosus (SLE) is a complex autoimmune disease characterised by the aberrant activity of the immune system and includes lymphocyte activation, autoantibody production, activation of inflammatory cytokine pathways and improper clearance of apoptotic cells with consequent immune complex deposition. This collective dysfunction results in the breakdown of tolerance and further drives tissue damage, leading to a vicious cycle and subsequent worsening of this heterogeneous disease [1].

*Correspondence to Dr. Daniel Stefan Strasser.
E-mail address: daniel.stefan.strasser@gmail.com (D.S. Strasser).
Handling editor Josef S. Smolen

https://doi.org/10.1136/ard-2024-226547

WHAT IS ALREADY KNOWN ON THIS TOPIC

- Systemic lupus erythematosus (SLE) represents a molecularly heterogeneous disease with a known involvement of type 1 interferon (IFN-1) and plasma cells.
- Previous results from a phase 2a clinical trial showed that cenerimod 4 mg reduced circulating antibody-secreting cells and IFN-associated biomarker proteins after 12 weeks of treatment.

WHAT THIS STUDY ADDS

- In the phase 2b clinical trial (CARE, NCT03742037) cenerimod 4 mg significantly reduced IFN-γ-associated proteins in addition to IFN-1 protein and gene expression signature biomarkers after 6 months of treatment when compared to placebo, with an overall larger effect size in the IFN-1 high patients.
- Cenerimod 4 mg prevented the transition of patients from an IFN-1 low to an IFN-1 high gene expression signature when compared with placebo.
- Treatment with cenerimod 4 mg resulted in a larger effect size on pharmacodynamic biomarkers IFN-1, IFN-γ, plasma cell signature and deconvoluted T and B cell subsets when compared with cenerimod 2 mg and placebo.
- The reduction observed in IFN-α and IFN-γ- related plasma protein levels was stronger in the IFN-1 high population, supporting a stronger clinical response observed in the IFN-1 high population.

HOW THIS STUDY MIGHT AFFECT RESEARCH, PRACTICE OR POLICY

- The data support the scientific rationale for the choice of cenerimod 4 mg and the inclusion of IFN-1 as a stratification biomarker in phase 3 clinical trials in patients with moderate to severe SLE (OPUS-1 and OPUS-2).

T lymphocytes drive pathogenesis and organ damage through cytokine secretion [2] and play a supportive role in activating and proliferating B lymphocytes, thus facilitating the maturation of autoantibody-producing B lymphocytes [3]. Concomitant to the activation of lymphocyte popula- tions, SLE is also characterised by dysregulation of pro-inflammatory cytokines that has hallmarks of a chronic interferon (IFN)-driven immune response [4,5].

Type 1 IFN (IFN-1) has previously been used in clinical trials [6] as a stratification biomarker for patients with SLE based on IFN-1 status (high vs low) because of its association with disease activity, flares and inflammation [7,8]. In particular, patients with IFN-1 high status have earlier disease onset and this status is more frequently associated with Asian and Afro-American ethnicity and indicators of increased disease activity such as anti-dsDNA, C3, C4, proteinuria, arthritis and skin disease manifestations [8]. The role of further IFNs including IFN-γ is underexplored as biomarkers in SLE although the role of IFN-γ has been impli- cated in SLE [9].

Sphingosine-1-phosphate (S1P) is the driving chemoattractant for lymphocyte egress out of peripheral lymphoid organs into circulation via S1P1 receptor engagement on B and T lymphocytes [10], making the S1P1 receptor an attractive therapeutic target for SLE.

Cenerimod is an orally active, highly selective S1P1 receptor modulator, previously shown to reduce blood lymphocytes, antibody-secreting cells and IFN-associated biomarkers in patients with SLE in a 12-week phase 2a clinical trial (NCT02472795) [11]. Moreover, in the phase 2b clinical trial NCT03742037 (CARE), cenerimod reduced the disease activity score compared with placebo in patients with SLE with high IFN-1 baseline levels [12].

Here, a substudy of CARE is presented, reporting exploratory analysis of whole blood transcriptomics of patients with SLE at baseline and after 6 months of treatment with either placebo, cenerimod 2 mg or 4 mg.

First, the pharmacodynamic effect of cenerimod reducing both IFN-1 and IFN-γ-driven inflammation in patients with SLE is described. Second, the larger pharmacodynamic effects of cenerimod 4 mg compared with 2 mg are shown on a priori defined IFN-1, IFN-γ, and plasma cell gene expression signatures. This study further supports the selection of the 4 mg dose for the phase 3 clinical trials OPUS-1 and OPUS-2 (NCT05648500, NCT05672576).

METHODS

CARE substudy

This retrospective sub-study used data and samples from the CARE clinical trial (NCT03742037). The study was approved by the Independent Ethics Committee or Institutional Review Board of each participating centre and the trial was conducted in compliance with the Declaration of Helsinki and GCP according to the International Conference on Harmonization.

In a double-blind placebo-controlled trial, adults with moderate or severe SLE were randomised to once per day, oral cenerimod (0.5/1/2/4 mg) or placebo, stratifying by oral corticosteroid dose and disease activity. In the present substudy, blood samples collected at baseline and after 6 months of treatment with either placebo, cenerimod 2 mg or 4 mg were analysed.

Exploratory biomarkers including both plasma protein (measured with immunological assays) and gene expression (measured by qPCR) were quantified in 138 patients with available samples at both baseline and 6 months. Among the 138 patients, 66 received cenerimod 4 mg and 72 received placebo. A total of 221 patients were analysed by RNA-sequencing (gene expression); among these patients, 75 received cenerimod 2 mg, 70 received cenerimod 4 mg and 77 received placebo. The number of patients per group might slightly vary when measure- ments from different technologies and/or associated clinical data (e.g., IFN-1 status) were integrated.

Disease score

The clinical severity was assessed as SLEDAI-2K score, modified to exclude leucopenia (mSLEDAI-2K) due to the mechanism of action of cenerimod.

Plasma protein measurements

Blood samples were collected in EDTA blood collection tubes to prepare plasma samples, which were kept frozen at −80°C until further analysis of protein biomarkers. CXCL10 was measured using a human CXCL10 V-plex kit from Mesoscale Discovery (MSD). IFN-γ was measured in using a human V-plex kit from MSD. CXCL9 was measured using a human R-plex kit from MSD. IL12p70 was measured using human S-plex singleplex kit from MSD. IFN-α was measured using commercial ELISA kits from PBL assay science. Galectin-9 was measured using commercial ELISA kits from RnD Systems. All MSD assays were acquired on a Sector imager from MSD. All ELISA plates were acquired on

a Spectramax reader from Molecular Device. Raw data were analysed using SoftmaxPro to derive the biomarker concentration.

Blood collection

Blood samples were collected in PaxGene Blood RNA Tubes (762165, BD Biosciences) according to manufacturer's instructions.

For the IFN-1 high/low status, the 4-gene IFN-1 test measures the RNA expression levels of four Interferon Stimulated Genes (ISGs) (HERC5, IFI27, IFIT1 and RSAD2) to the expression levels of three housekeeping normaliser genes (ACTB, GAPDH and TFRC).

Gene expression measurements

Gene expression (including IFN-β, IFN-γ, inflammatory gene signatures and IFN-1-related genes to determine IFN-1 status) was measured by DxTerity Diagnostics (Rancho Dominguez, California), using the DxTerity Modular Immune Profile (MIP) test. This commercially available test uses chemical ligation-dependent probe amplification for gene expression. This test also includes a relative quantita- tive analysis performed using capillary electrophoresis.

The MIP test quantifies the expression of specific genes that are linked to 12 predefined modules. PAXgene RNA Stabilized Blood was used for performing sample testing and analysis as described by [13] with minor changes to the protocol.

The IFN-1 score was calculated based on the expression of 10 genes (IFIT1, HERC5, IFI27, RSAD2, EIF2AK2, IFI44, IFI44L, IFI6, ISG15, MX1). Normalised expression values of each respective response gene were calculated per the following function:

$$\text{Normalized Expression gene}_i = \log_2(\text{height gene}_i) - \text{mean}(\log_2(\text{height normalizer gene}_i))$$

The height of each amplicon fragment's peak is determined by the capillary electrophoresis instrument (ABI 3500xL Dx). This height is directly proportional to the abundance of each gene in the sample. The DxTerity 4-gene IFN-1 signature score was calculated by averaging the normalised expression values of the four ISGs.2 The IFN-1 signature score cut-off of −0.5 between IFN high and low was determined based on measurement of 281 healthy human blood samples and placing the cut-off at two SDs (95th percentile) above the mean healthy IFN-1 score (−0.5). This cut-off falls within the trough of the observed bimodal distribution of IFN-1 scores for this and other cohorts of SLE samples where this methodology was used.

RNA extraction for sequencing

Blood was stored at −80°C before RNA extraction. RNA was extracted using PAXgene Blood RNA Kit (762174, Qiagen) according to manufacturer's instructions.

Library construction and sequencing

RNAseq libraries were prepared using TruSeq Stranded Total RNA Library Prep Globin Kit (20020613, Illumina). Briefly, 700 ng total RNA was used as a starting material. RNAseq libraries were prepared using Biomek FX (Beckman Coulter) and Bravo NGS workstation (Agilent Technologies). Final library concentration and size were estimated using Qubit V.3.0 (Invitrogen) and Fragment Analyzer (Agilent Technologies) instruments, respectively. All the libraries were spiked with 1% PhiX and sequenced on Illumina Novaseq6000 (Illumina) using NovaSeq 6000 S4 Reagent V.1.5 200 cycles Kit (20028313, Illumina) according to manufacturer's instructions. A minimum of 50 million 100 bp paired-end reads were generated per sample.

BIOINFORMATICS ANALYSIS

Sequencing data processing

Sequencing reads were processed using Nextflow (V.21.10.6) nf-core RNAseq pipeline V.3.3 [14]. STAR (V.2.6.1d) was used to align reads to human genome version GRCh38_98 and gene expression count tables were generated using Salmon (V.1.4.0) [15]. Raw counts were normalised using variance stabilising transformation (vst function from DESeq2 package).

Gene signatures

To evaluate dose-dependent molecular changes we used gene signatures summarised into z-scores.

IFN-1 status classification model

To build the binary classification model, the glmnet package in R. The use of an elastic net penalisation allowed to identify additional genes to discriminate IFN-1 high and low patients. Samples were randomly split into train/test sets (80/20). The models were evaluated in terms of mean squared error (MSE):

$$MSE = \frac{1}{n}\sum_{i=1}^{n}(Y_i - \hat{Y}_i)^2,$$

where Yi are the observed values and $\hat{Y}i$ are the predicted values.

The final model (including 88 genes) was selected based on the lambda.min value. Additional performance metrics were calcu- lated using the confusionMatrix function from caret package. Gene set enrichment analysis was performed using the MSigDB hallmark signatures (msigdb package in R).

Cell-type deconvolution

Cell-type deconvolution was performed using the immunedeconv package in R [16] on bulk RNA-sequencing data. The xCell [17] method was used to deconvolute immune cell subpopulations, while EPIC (estimating the proportion of immune and cancer cells) [18] method was used to deconvolute main cell populations.

Statistical analysis

Statistical analyses were conducted using R software V.4.1.2 (The R Foundation for Statistical Computing). Plasma protein and gene expression levels (but not gene expression scores) were log10 and log2-transformed for statistical testing, respectively. The 95% CIs around the mean were calculated as follows:

$$\text{CI } 95\% = \text{mean} \pm t\left(\frac{st.dev}{\sqrt{n}}\right),$$

where t is 0.975 for a two-tailed test. The 95% CIs around the median were calculated using the wilcox.test function with exact method.

The changes from baseline were calculated as the difference between month 6 and baseline levels ($\Delta M6\ bs$).

For visualisation purposes and avoiding extreme values to flatten the boxplots, changes from baseline were transformed as follows:

$$\log_{10}(|\Delta_{M6-bs}|) * sgn(\Delta_{M6-bs})$$

Intergroup differences (i.e., treatment groups, placebo vs cenerimod 4 mg) in plasma protein levels or gene expression scores were tested using linear regression models. Differences in plasma protein levels and gene expression scores between time points (i.e., baseline vs month 6) were tested using mixed effects models with a subject random effect (lmer function).

Patient and public involvement

Patients and/or the public were not involved in the design, conduct, reporting or dissemination plans of this research.

RESULTS

Patient populations and baseline characteristics

Baseline IFN-1 gene expression score was used to stratify patients into IFN-1 high or IFN-1 low populations. Table 1 shows the patients randomised in each arm of the trial versus samples analysed in each set of assays (immunoassays, qPCR, gene expression) and online supplemental table 1 summarises the mean and median levels of IFN-1 and IFN-γ gene expression score, and IFN-α and IFN-γ plasma protein levels at baseline for each treatment group.

The distribution of patient IFN-1 high and IFN-1 low populations was similar in placebo and cenerimod 2 mg, while exhibited a higher percentage of patients with IFN-1 low in the cenerimod 4 mg cohort. However, baseline IFN-1 score mean levels were comparable across treatment groups.

The IFN-1 gene expression score at baseline displayed a bimodal distribution (figure 1a), where −0.5 represents the cut-off value based on healthy subject gene expression levels as described in the Methods section. The comparison of baseline IFN-1 gene expression score values with IFN-α protein levels showed a strong significant correlation (R = 0.78, p<0.001) (figure 1b), demonstrating that gene expression values highly reflect the detected protein levels in plasma from patients with SLE.

Cenerimod decreases IFN-associated biomarkers in patients with SLE

To investigate the pharmacodynamic effects of cenerimod in patients with SLE in CARE, exploratory biomarkers were selected based on a previous phase 2a clinical trial that showed the reduction of IFN-associated protein levels (NCT02472795) [11].

In CARE, IFN-α protein levels in plasma (p = 0.024, figure 2a) and IFN-1 gene signature score (p<0.001, online supplementary figure 2b) were significantly reduced in cenerimod 4 mg treated patients from baseline to month 6, while no difference was observed in placebo-treated patients.

We investigated whether additional inflammation biomarkers beyond IFN-α were elevated in patients with SLE at baseline and consequently might be decreased by cenerimod. We measured both plasma protein levels and gene signatures of IFN-γ-related biomarkers. IFN-β, IFN-γ, and inflammation gene expression scores were upregulated in blood of IFN-1 high patients when compared with IFN-1 low patients (figure 2b). In addition, IFN-γ, IL12p70, CXCL9 and CXCL10 protein plasma levels were also higher in IFN-1 high patients (figure 2c). There was no association of IFN-1 high or IFN-1 low and disease activity as measured by mSLEDAI-2k (figure 2b,c).

Focusing on the IFN-1 high SLE patient population, we evaluated whether cenerimod modulated the previously mentioned molecules from the IFN-1 and IFN-γ pathways by analysing changes from baseline of both plasma protein and gene expression scores in cenerimod 4 mg compared with placebo. We observed that IFN-γ, IFN-β, and the inflammation gene expression scores were significantly decreased (p<0.001) in cenerimod 4 mg treated patients compared with placebo (figure 2d). In addition, IFN-γ (p = 0.004), IL12p70 (p = 0.008) and CXCL9 (p = 0.022) protein levels were significantly reduced in cenerimod 4 mg treated patients compared with placebo (figure 2e).

Subsequently, we investigated whether cenerimod modulated the IFN-1 score after 6 months of treatment to an equal extent in both the IFN-1 high and IFN-1 low SLE populations. When comparing the change from baseline in IFN-1 gene expression score, we observed a significant score reduction after 6 months of cenerimod 4 mg treatment compared with placebo in both IFN-1 low (p<0.001) and IFN-1 high (p<0.001) patients (figure 3a).

However, the treatment effect on the IFN-1 score in IFN-1 high patients showed that the distribution and median values decreased from baseline (median = 1.2) to month 6 (median = 0.7) in the IFN-1 high population (figure 3b). While in the IFN-1 low popu- lation, the distribution and the median at baseline (median = −2.9) and month 6 (median = −3.1) remained similar. Importantly, we observed a larger effect size in terms of median change from baseline for IFN-α protein and related biomarkers in IFN-1 high patients compared with IFN-1 low patients (figure 3c). Further- more, we evaluated patient transitions from IFN-1 high to IFN-1 low and vice versa. Three out of 37 placebo-treated patients changed from low to high, one out of 35 changed from high to low. Cenerimod 4 mg prevented any transition from low to high and one patient out of 28 changed from high to low (figure 3d).

To determine whether other genes in addition to IFN-1-related genes were associated with the separation of IFN-1 high and low patient populations at baseline, we built a binary clas- sification model with an elastic-net penalty on RNA-sequencing gene expression data obtained from whole blood of patients with SLE in CARE (see the Methods section). The final

Table 1
Summary of patients randomised and analysed using gene expression and plasma protein levels of IFN-1 and IFN-γ.

Treatment	Number of patients randomised per arm	Number of patients analysed using qPCR	Number of patients analysed using RNA- sequence	Number of patients analysed using PP levels
Placebo	86	72	77	72
Cenerimod 2 mg	**86**	Not measured	75	Not measured
Cenerimod 4 mg	84	66	**70**	**66**

IFN, interferon; PP, plasma protein; qPCR, quantitative PCR.

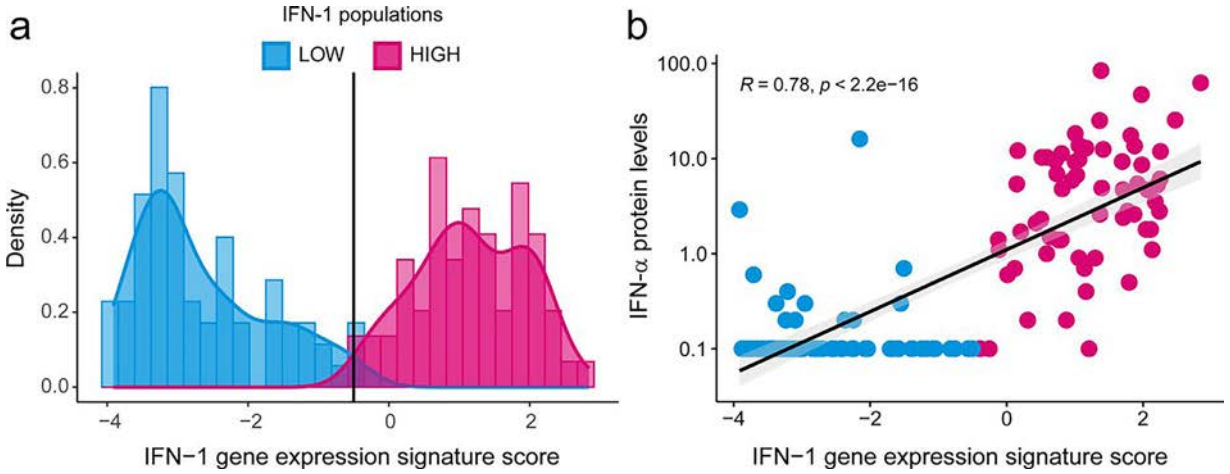

Figure 1. IFN-1 signature score distribution and correlation with IFN-α plasma levels. (a) Bimodal distribution of the baseline IFN-1 signature score in all patients randomised to placebo (n = 80) and cenerimod 4 mg (n = 79) in the CARE study. The black vertical line indicates the −0.5 cut-off for stratifying patients into IFN-1 high (pink) or IFN-1 low (blue). (b) IFN-α plasma protein levels significantly correlate with the IFN-1 gene expression signature score at baseline. Pearson correlation coefficient (R). CARE, phase 2b clinical trial; IFN, interferon.

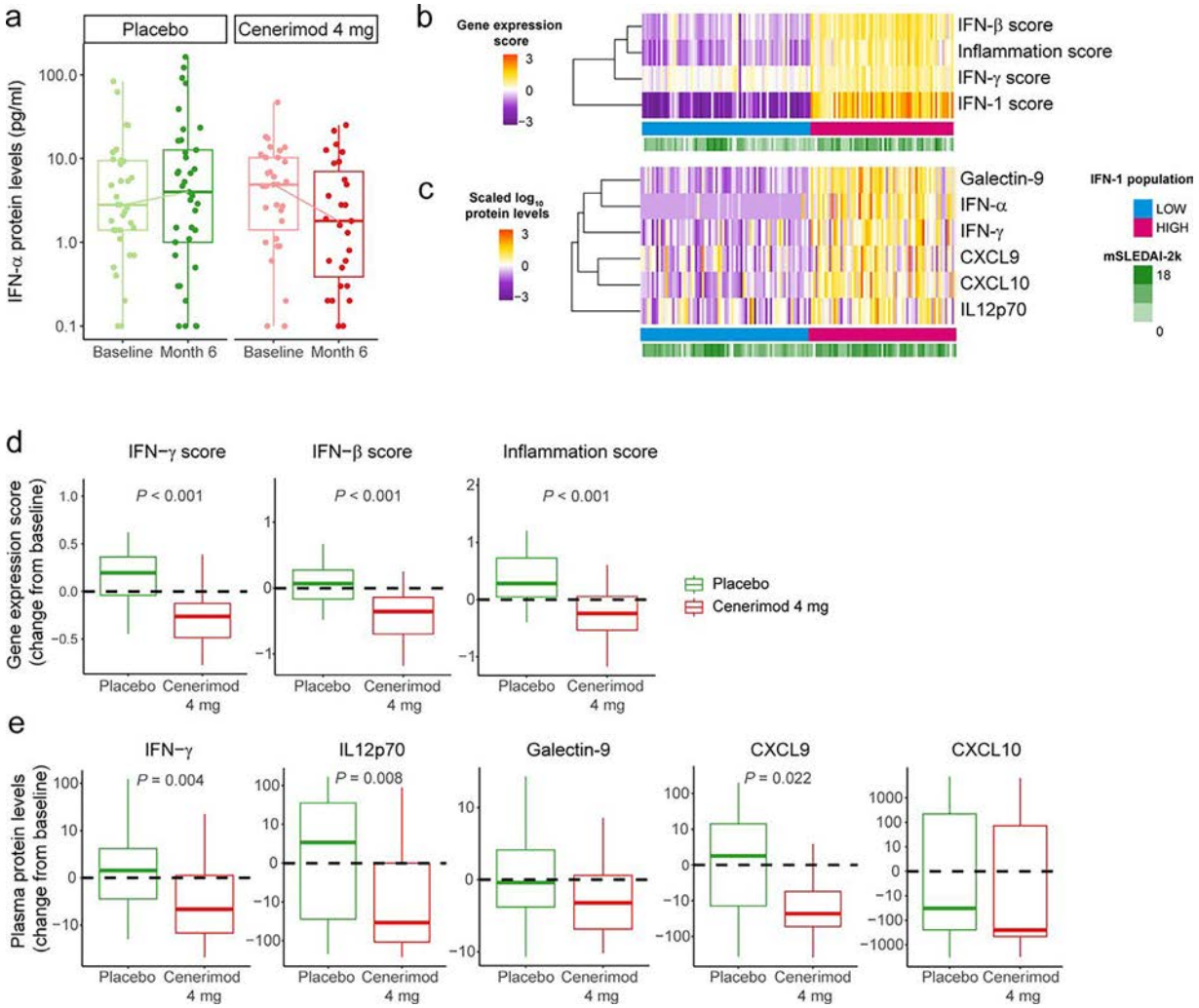

Figure 2. Cenerimod 4 mg reduces IFN-1 and IFN-γ-associated biomarkers in patients with SLE after 6 months of treatment. (a) Boxplots of IFN-α plasma levels in patients with SLE after 6 months of placebo (green) or cenerimod 4 mg (red) treatment. Dots indicate individual patients. Significance between baseline and month 6 were tested using linear mixed-effects models. (b-c) Heatmaps of type 1 and IFN-γ biomarkers in patients with SLE with IFN-1 high and low status at baseline depicting (b) gene expression scores and (c) normalised plasma protein levels. Green colour scale shows disease score (mSLEDAI-2k). IFN-1 low patients are indicated by the blue horizontal bar, and IFN-1 high by the pink horizontal bar. (d-e) Boxplots showing change from baseline in placebo (green) and cenerimod 4 mg (red) treatment groups in IFN-1 high patients (d) gene expression scores and (e) plasma protein levels. Differences between treatment groups were tested using linear regression models. P values are not adjusted for multiple testing. IFN, interferon; SLE, systemic lupus erythematosus.

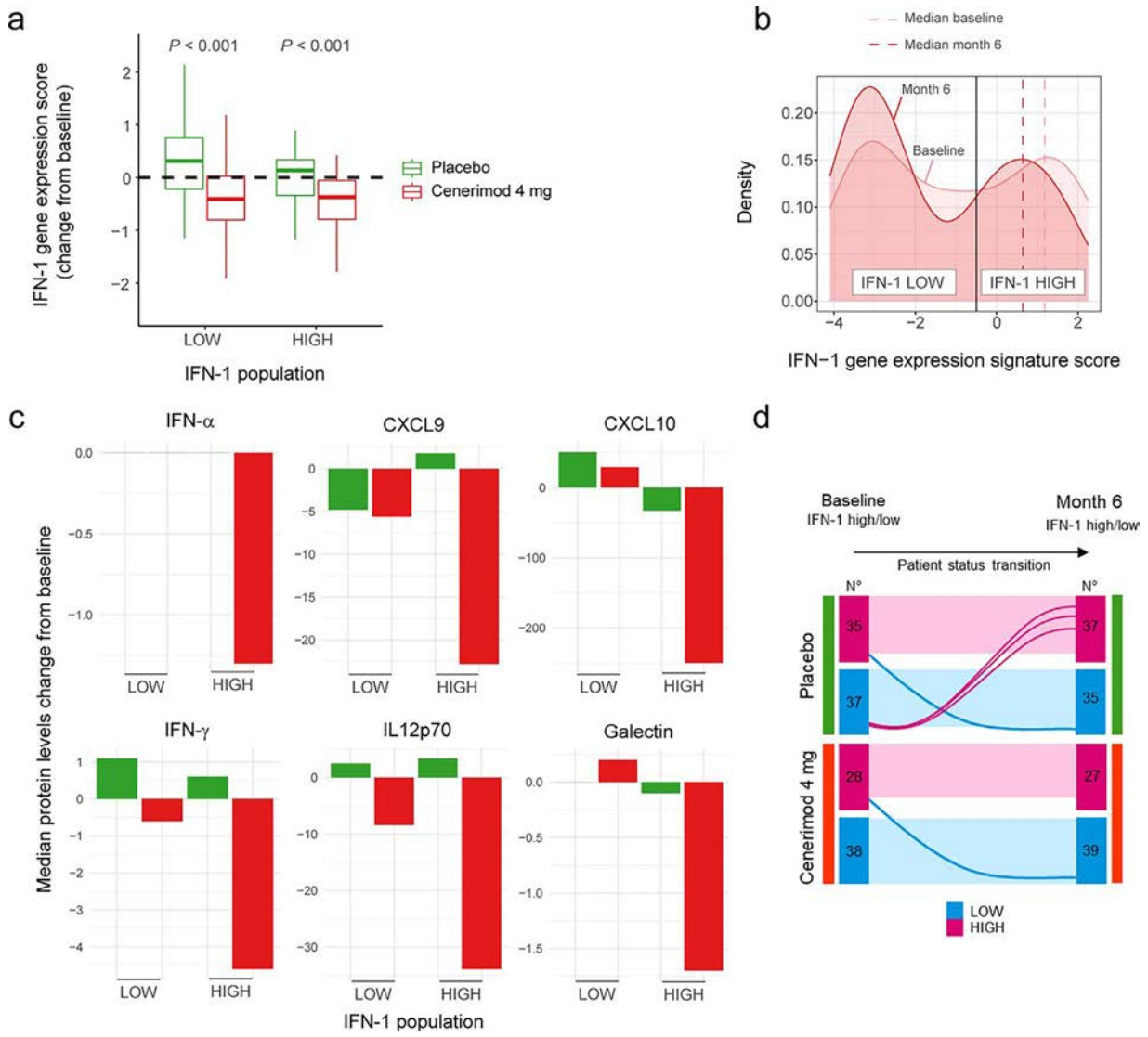

Figure 3. Cenerimod 4 mg demonstrates strong reduction of IFN-α and IFN-γ-associated proteins in IFN-1 high population while IFN-1 gene expression is reduced in all patients. (a) Boxplots of IFN-1 gene expression score (change from baseline). Significance between placebo (green) and cenerimod 4 mg (red) was tested using linear regression models. (b) IFN-1 gene expression signature score distribution from patients treated with cenerimod 4 mg at baseline (light red) and at 6 months (red). The dashed vertical lines show the median IFN-1 signature score of IFN-1 high patients at baseline (light red) and 6 months (red). The black vertical line (−0.5) represents the cut-off value between IFN-1 high and IFN-1 low. (c) Bar plots of plasma proteins depicting median change from baseline comparing size effects in IFN-1 high and low populations for placebo (green) and cenerimod 4 mg (red). (d) Graphic representation of IFN-1 high and low changes from baseline to month 6 in placebo and cenerimod 4 mg treated patients. IFN-1 low patients are shown in blue, IFN-1 high patients in pink. Lines show status transitions for individual patients. IFN, interferon.

model included 88 genes with 100% specificity and 91% sensitivity (online supplemental figure 1a,b). In addition to the expected IFN-1-related genes, IFN-γ-related as well as non-long coding genes were selected by the model for the classification of IFN-1 high and IFN-1 low patients, which was further confirmed by the gene set enrichment analysis (online supplemental figure 1c). Overall, these results demonstrated that IFN-1 stratification has a prominent IFN-γ component, supporting the observed decrease of both IFN-1 and IFN-γ-associated biomarkers after 6 months of cenerimod 4 mg treatment.

Cenerimod dose-dependently reduced gene signatures associated with inflammation

To identify additional molecular pharmacodynamic changes potentially associated with cenerimod 4 mg, the clinical efficacious dose, we compared whole blood gene expression signatures (summarised into z-scores) of patients with SLE who received cenerimod 2 mg or 4 mg to determine dose-dependent differences.

RNA-sequencing data of IFN-1 gene expression was in agreement with the data generated by qPCR, showing strong positive correlation (R = 0.97, p<0.001, online supplemental figure 2a) and a comparable significant decrease of the IFN-1 gene expression signature score (p<0.001) after 6 months of cenerimod 4 mg treatment, while no significant reduction was observed in either the placebo or 2 mg cenerimod treatment groups. The cenerimod 4 mg reduction of IFN-1 gene expression score was comparable in IFN-1 high and IFN-1 low patient populations (online supplemental figure 3) as previously shown in qPCR data (figure 3a).

In addition to the IFN-1 signature, we evaluated two additional pathway gene signatures associated with cenerimod mechanism of action (MoA); plasma cells (online supplemental

table 2) [19] and IFN-γ (online supplemental table 3). We observed a dose-dependent decrease of the plasma cell gene expression score, and the decrease was significantly more prominent in cenerimod 4 mg compared with 2 mg treatment (p = 0.018). The IFN-γ score was significantly reduced after treatment with cener- imod 4 mg (p<0.001), in contrast to placebo and cenerimod 2 mg that showed no significant changes after 6 months of treatment (figure 4a). The overall effect size for each of the signature scores in terms of mean change from baseline was higher in cenerimod 4 mg for IFN-1, plasma cells and IFN-γ compared with cener- imod 2 mg for IFN-1, plasma cells and IFN-γ, or placebo (online supplemental figure 4).

The correlation analysis of the IFN-1 gene expression score with IFN-γ or plasma cell score showed a stronger positive association of with IFN-γ in the IFN-1 high population ($R = 0.63$, p<0.001) compared with the IFN-1 low population ($R = 0.38$, p<0.001). The correlations with plasma cells were less strong in both IFN-1 high (R = 0.29, p = 0.003) and low populations (R = 0.21, p = 0.024) (figure 4b).

The comparison of treatment effect on the average gene expression scores with baseline levels demonstrated that the strongest reduction of IFN-1, IFN-γ and plasma cell signatures was observed in cenerimod 4 mg, followed by cenerimod 2 mg treatment. The placebo treatment group profile was very similar to baseline levels (figure 4c).

Taken together, the data showed a stronger dose-dependent reduction of pathways associated with SLE with 4 mg dose of cenerimod treatment.

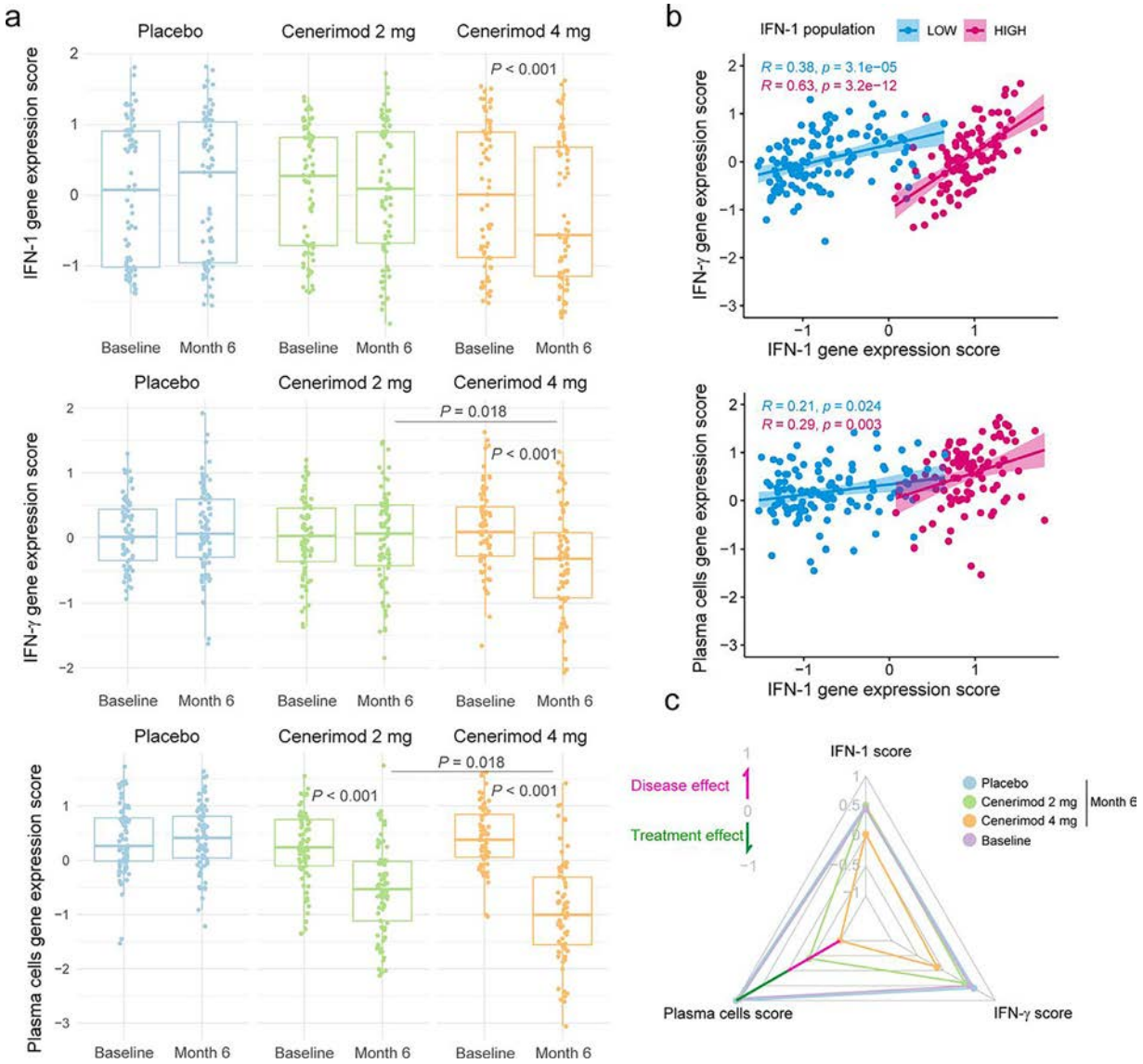

Figure 4. Dose-dependent reduction of cenerimod mechanism-related pathways in whole blood RNA-sequencing data. (a) Boxplots of IFN-1, plasma cells and IFN-γ gene expression signature score changes after 6 months of placebo (blue), cenerimod 2 mg (green) and cenerimod 4 mg (orange) treatment. Linear mixed effect models were used to test differences between baseline and month 6 in each treatment group. Linear models were used to test differences between treatment groups at a given time point. P values were adjusted for multiple testing using the Benjamini-Hochberg (false discovery rate FDR) method. (b) Correlations of IFN-1 signature score with IFN-γ and plasma cell signature score in IFN-1 high (pink) and IFN-1 low (blue) populations. Pearson correlation coefficient (R). P values were obtained using correlation tests. (c) Average gene expression score profiles summarising overall trends at baseline (purple) compared with placebo (blue), cenerimod 2 mg (green) and cenerimod 4 mg (orange) treatment.

Values greater than 0 suggest a trend toward disease-like phenotype (close to baseline profile), while values lower than 0 suggest a reduction of the molecular disease-like phenotype (treatment effect). IFN, interferon.

Cenerimod-induced dose-dependent reductions in immune cell subpopulations

The overall total lymphocyte counts and the deconvolution of main cell populations in blood (see the Methods section) showed no significant difference between cenerimod 2 mg and 4 mg, although the total lymphocyte population as a whole was signifi- cantly reduced by both doses compared with placebo (figure 5a, online supplemental figure 5a,b).

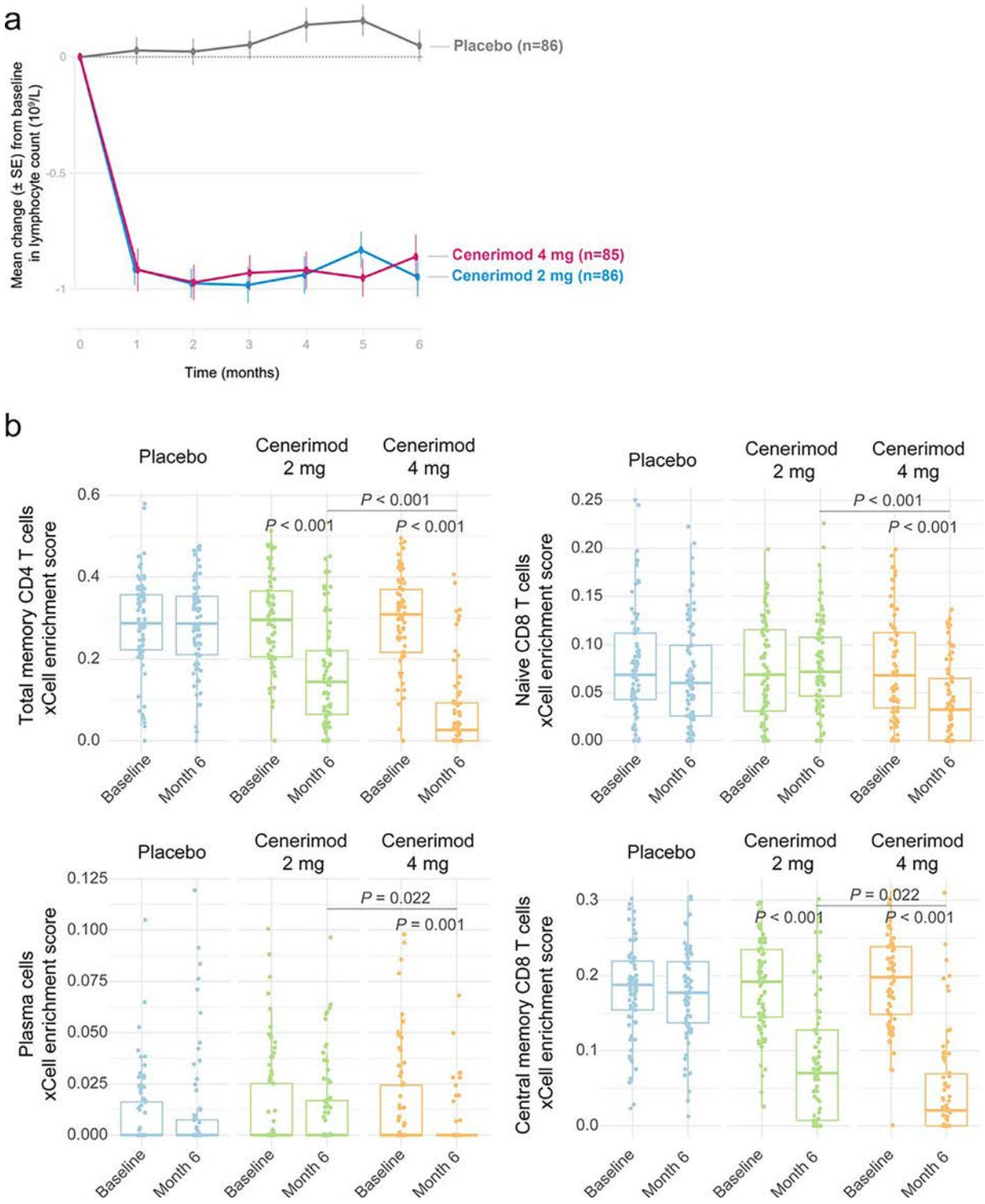

Figure 5. Dose-dependent reduction of whole blood RNA-sequencing deconvoluted cell types after 6 months of placebo, cenerimod 2 mg and cenerimod 4 mg treatment. (a) Total lymphocyte counts in blood depicted as mean change to baseline for placebo, cenerimod 2 mg and cenerimod 4 mg treatments up to 6 months. (b) Boxplots of deconvoluted immune cell sub-populations (xCell enrichment score) at baseline and after 6 months of treatment. Linear mixed effect models were used to test differences between baseline and month 6 in each treatment group. Linear models were used to test differences between treatment groups at a given time point. P values were adjusted for multiple testing using the Benjamini-Hochberg (false discovery rate FDR) method. IFN, interferon.

The objective was to determine immune cell subpopulations that were dose-dependently reduced by cenerimod, consequently we investigated cell subpopulations that were strongly decreased with cenerimod 4 mg compared with cenerimod 2 mg. To estimate immune cell-type abundance from the whole blood transcriptome, cell-type deconvolution was performed using the xCell method, which allows for a high granularity in immune cell population identification (see the Methods section). Inter- estingly, we identified different T and B cell subpopulations that showed a dose-dependent reduction after 6 months of cener- imod treatment. A significant reduction when comparing cener- imod 2 mg and cenerimod 4 mg at month 6 was observed in the following subsets: total memory CD4 T cells ($p<0.001$), naïve CD8 T cells ($p<0.001$), central memory CD8 T cells ($p=0.022$) and plasma cells ($p=0.022$) (figure 5b).

DISCUSSION AND CONCLUSIONS

The clinical manifestations in patients with SLE are highly diverse, reflecting the underlying heterogeneity of molecular disease drivers. The IFN-1 pathway represents a recognized disease driver, associated with occurrence of nephritis, and musculoskeletal and mucocutaneous manifestations [20].

The efficacy of drug candidates targeting specific pathways can be affected by molecular heterogeneity that is not necessarily reflected in clinical patient characteristics and disease activity. Hence, in clinical trials with patients with SLE, the IFN-1 gene expression score is assessed to inves- tigate response rates in molecular endotypes. In the CARE clinical trial, 50% of patients were IFN-1 high, which under- represents the IFN-1 high population in comparison to other clinical trials where 62%–83% of the total cohorts were reported to be IFN-1 high [6,21–25]. The importance of under- standing the molecular phenotype of patients is highlighted in CARE, where clinical response was found to be stronger in IFN-1 high patients [26]. This is further emphasised by the lack of association between the IFN-1 endotype and disease activity, as observed with SLE-DAI-2K in this study. This underscores the importance of stratifying the SLE popula- tion by IFN-1 high gene expression score across treatment groups in future clinical trials with cenerimod.

Cenerimod 4 mg treatment reduced the IFN-1 gene expression score in blood in both IFN-1 high and IFN-1 low patients. Importantly, the reduction observed in IFN-α and IFN-γ-related plasma protein levels was considerably stronger in the IFN-1 high population, supporting the stronger clinical response observed in the IFN-1 high population.

In addition, cenerimod 4 mg appeared to prevent transition from IFN-1 low to IFN-1 high. It has been previously reported that the IFN-1 status is stable over time (transition of 13% over 2 years, [8]) that is in line with the transitions observed in placebo treatment group (6% over 6 months). This may be clinically rele- vant as the IFN-1 high gene expression score is associated with an increased risk of developing, for example lupus nephritis [13]. Therefore, longer studies are required to elucidate and evaluate the potential of cenerimod in IFN-1 low patients.

The investigation of patient baseline characteristics demonstrated an association of IFN-1 gene expression score with the IFN-γ pathway, providing further evidence of the molecular complexity underpinning the pathology of SLE. The prominent role of IFN-1 has been well documented and measuring IFN-1 has potential clinical value [27,28]. In contrast, the role of IFN-γ in SLE pathology has been less explored but shows increasing relevance [29]. Importantly, cenerimod 4 mg reduced the IFN-γ gene expression score as well as the plasma cell signature pathways after 6 months of treatment. In addition, the overall larger effect size in IFN-α and IFN-γ protein levels reduction in IFN-1 high patients might explain the larger clinical effect observed with 4 mg cenerimod in the CARE study [26]. In particular, cenerimod 4 mg showed a larger clinical effect on resolution of alopecia and arthritis and reduction of mucosal ulcers in the IFN-1 high popula- tion [26]. Taken together, these data provide evidence of cener- imod pharmacodynamics relevant to the amelioration of SLE pathology beyond the inhibition of lymphocyte egress.

This study showed that the clinically efficacious dose of cenerimod 4 mg significantly and more markedly reduced the three inflammatory components (IFN-1, IFN-γ and plasma cells) that are part of the MoA of cenerimod, in comparison to the 2 mg dose. This dose dependency was further corrob- orated in subsets of immune cells implicated in the patho- genesis of SLE [30,31]. Particularly, the dose–response effect on plasma cells observed by cell-type deconvolution analysis is noteworthy and was further supported by the plasma cell signature score. This observation confirmed the finding in the phase 2a clinical trial with cenerimod in patients with SLE, where it was shown by flow cytometry that the 4 mg dose induced a more extensive reduction of antibody- secreting cells compared with the 2 mg dose [11].

In conclusion, this study describes the pharmacodynamics of cenerimod involved in reducing several important pro- inflammatory pathways in SLE pathology beyond lympho- cyte reduction. Importantly, it supports the scientific rationale for the choice of cenerimod 4 mg and the inclusion of IFN-1 as a stratification biomarker in the phase 3 clinical trials in patients with moderate to severe SLE (OPUS-1 and OPUS-2).

Acknowledgements

Virginie Sippel and Bérengère Renault for protein and gene expression biomarker quantification. Aaron Hart for the processing of RNA- sequencing and computational infrastructure. Medical writing assistance was provided by Anne Sayers.

Contributors

MS: conceptualisation, data curation, formal analysis, writing — original draft, writing—review and editing. PB, MJM: conceptualisation, data curation, formal analysis, methodology, writing—review and editing. MPK, OB, GS: review and editing. PC: data curation, formal analysis, methodology, writing—review and editing. MJM: conceptualisation, data curation, formal analysis, methodology, writing—review and editing. DS: conceptualisation, data curation, formal analysis, investigation, methodology, writing—review and editing. DS is the guarantor of the study. All authors had full access to all the data in the study. All authors were responsible for the decision to submit the article.

Funding

This study was funded by Idorsia Pharmaceuticals Ltd.

Competing interests

MS, MPK: employee of Idorsia and holds stocks in Idorsia Pharmaceuticals Ltd. PB: employee of Idorsia Pharmaceuticals Ltd. OB: employee of Viatris, holds stocks in Idorsia Pharmaceuticals Ltd. GS: employee of Viatris. PC: employee of Idorsia and

holds stocks in Idorsia Pharmaceuticals Ltd. Participant in Advisory Board Meetings for Idorsia Pharmaceuticals Ltd. MJM, DS: employee of Idorsia and holds stocks in Idorsia Pharmaceuticals Ltd. Holds Cenerimod patent on SLE pertaining to IFN and other biomarkers.

Patient and public involvement

Patients and/or the public were not involved in the design, or conduct, or reporting, or dissemination plans of this research.

Patient consent for publication

Not applicable.

Ethics approval

The results are part of a phase 2b clinical trial (CARE, NCT03742037) that involved human participants and was approved by IES/IRBs (details of IES/IRBs are provided as a separate attachment.) Participants gave informed consent to participate in the study before taking part.

Data availability statement

Data are available upon reasonable request. Upon substantial request, the data shall be shared and shall be provided by the corresponding author.

Supplementary materials

Supplementary material associated with this article can be found in the online version at doi:10.1136/ard-2024-226547.

Orcid

Marcel Peter Keller: http://orcid.org/0000-0002-9692-662X
Mark Joseph Murphy: http://orcid.org/0000-0002-9735-7887

REFERENCES

[1] Tsokos GC, Lo MS, Costa Reis P, et al. New insights into the immunopathogenesis of systemic lupus erythematosus. Nat Rev Rheumatol 2016;12:716–30.
[2] Comte D, Karampetsou MP, Tsokos GC. T cells as a therapeutic target in SLE. *Lupus (Los Angel)* 2015;24:351–63.
[3] Rahman A, Isenberg DA. Systemic lupus erythematosus. N Engl J Med 2008;358:929–39.
[4] Baechler EC, Batliwalla FM, Karypis G, et al. Interferon-inducible gene expression signature in peripheral blood cells of patients with severe lupus. Proc Natl Acad Sci U S A 2003;100:2610–5.
[5] Ohl K, Tenbrock K. Inflammatory cytokines in systemic lupus erythematosus. J Biomed Biotechnol 2011;2011:432595.
[6] Morand EF, Furie R, Tanaka Y, et al. Trial of Anifrolumab in Active Systemic Lupus Erythematosus. N Engl J Med 2020;382:211–21.
[7] Shobha V, Mohan A, Malini AV, et al. Identification and stratification of systemic lupus erythematosus patients into two transcriptionally distinct clusters based on IFN-I signature. *Lupus (Los Angel)* 2021;30:762–74.
[8] Northcott M, Jones S, Koelmeyer R, et al. Type 1 interferon status in systemic lupus erythematosus: a longitudinal analysis. Lupus Sci Med 2022;9:e000625.
[9] Munroe ME, Lu R, Zhao YD, et al. Altered type II interferon precedes autoantibody accrual and elevated type I interferon activity prior to systemic lupus erythematosus classification. Ann Rheum Dis 2016;75:2014–21.
[10] Chiba K, Matsuyuki H, Maeda Y, et al. Role of sphingosine 1-phosphate receptor type 1 in lymphocyte egress from secondary lymphoid tissues and thymus. Cell Mol Immunol 2006;3:11–9.
[11] Strasser DS, Froidevaux S, Sippel V, et al. Preclinical to clinical translation of cenerimod, a novel S1P1 receptor modulator, in systemic lupus erythematosus. RMD Open 2020;6:e001261.
[12] Efficacy and Safety of Cenerimod in Patients with Moderate to Severe Systemic Lupus Erythematosus (SLE): A Multicenter, Randomized, Parallel-Group, Double-Blind, Placebo-Controlled, Dose-Finding Phase 2b Trial. ACR Convergence 2022.
[13] Kim CH, Abedi M, Liu Y, et al. A novel technology for multiplex gene expression analysis directly from whole blood samples stabilized at ambient temperature using an RNA-stabilizing buffer. J Mol Diagn 2015;17:118–27.
[14] Ewels PA, Peltzer A, Fillinger S, et al. The nf-core framework for community-curated bioinformatics pipelines. Nat Biotechnol 2020;38:276–8.
[15] Patro R, Duggal G, Love MI, et al. Salmon provides fast and bias-aware quantification of transcript expression. Nat Methods 2017;14:417–9.
[16] Sturm G, Finotello F, List M. Immunedeconv: An R Package for Unified Access to Computational Methods for Estimating Immune Cell Fractions from Bulk RNA- Sequencing Data. Methods Mol Biol 2020;2120:223–32.
[17] Aran D, Hu Z, Butte AJ. xCell: digitally portraying the tissue cellular heterogeneity landscape. Genome Biol 2017;18:220.
[18] Racle J, de Jonge K, Baumgaertner P, et al. Simultaneous enumeration of cancer and immune cell types from bulk tumor gene expression data. Elife 2017;6:e26476.
[19] Streicher K, Morehouse CA, Groves CJ, et al. The plasma cell signature in autoimmune disease. Arthritis Rheumatol 2014;66:173–84.
[20] Oke V, Gunnarsson I, Dorschner J, et al. High levels of circulating interferons type I, type II and type III associate with distinct clinical features of active systemic lupus erythematosus. Arthritis Res Ther 2019;21:107.
[21] Wilkinson C, Henderson RB, Jones-Leone AR, et al. The role of baseline BLyS levels and type 1 interferon-inducible gene signature status in determining belimumab response in systemic lupus erythematosus: a post hoc meta-analysis. Arthritis Res Ther 2020;22:102.
[22] Merrill JT, Werth VP, Furie R, et al. Phase 2 Trial of Iberdomide in Systemic Lupus Erythematosus. N Engl J Med 2022;386:1034–45.
[23] Furie R, Khamashta M, Merrill JT, et al. Anifrolumab, an Anti-Interferon-α Receptor Monoclonal Antibody, in Moderate-to-Severe Systemic Lupus Erythematosus. Arthritis Rheumatol 2017;69:376–86.
[24] Furie RA, Morand EF, Bruce IN, et al. Type I interferon inhibitor anifrolumab in active systemic lupus erythematosus (TULIP-1): a randomised, controlled, phase 3 trial. Lancet Rheumatol 2019;1:e208–19.
[25] Vital EM, Merrill JT, Morand EF, et al. Anifrolumab efficacy and safety by type I interferon gene signature and clinical subgroups in patients with SLE: post hoc analysis of pooled data from two phase III trials. Ann Rheum Dis 2022;81:951–61.
[26] Efficacy of cenerimod in patients with high ifn-1 gene expression signature and high anti-dsdna antibody levels: post-hoc analysis from a phase 2 study. EULAR; 2023.
[27] Banchereau J, Pascual V. Type I interferon in systemic lupus erythematosus and other autoimmune diseases. Immunity 2006;25:383–92.
[28] Rodríguez-Carrio J, Burska A, Conaghan PG, et al. Association between type I interferon pathway activation and clinical outcomes in rheumatic and musculoskeletal diseases: a systematic literature review informing EULAR points to consider. RMD Open 2023;9:e002864.
[29] Liu W, Zhang S, Wang J. IFN-γ, should not be ignored in SLE. Front Immunol 2022;13:954706.
[30] Chen PM, Tsokos GC. The role of CD8+ T-cell systemic lupus erythematosus pathogenesis: an update. Curr Opin Rheumatol 2021;33:586–91.
[31] Yap DYH, Chan TM. B Cell Abnormalities in Systemic Lupus Erythematosus and Lupus Nephritis-Role in Pathogenesis and Effect of Immunosuppressive Treatments. Int J Mol Sci 2019;20:6231.

Ann Rheum Dis 84 (2025) 294–306

Contents lists available at ScienceDirect

Annals of the Rheumatic Diseases

journal homepage: https://www.sciencedirect.com/journal/annals-of-the-rheumatic-diseases

Systemic sclerosis

Human hypofunctional *NCF1* variants promote pulmonary fibrosis in the bleomycin-induced mouse model and patients with systemic sclerosis via expansion of SPP1^{+} monocytes-derived macrophages

Xinran Yuan[1,2], Xiaodong Qin[3], Kenji Takemoto[1], Jian Zhao[1], Matthew Sanderson[1], Xue Xu[1], Yu Zhang[1], Kristi L. Helke[4], Bethany Jacobs Wolf[5], Joel M. Guthridge[6], Judith A. James[6], Xiaodong Zhou[7], Shervin Assassi[7], Carol Feghali-Bostwick[1], Dandan Wang[2], Lingyun Sun[2,*], Betty P. Tsao[1,*]

[1] *Division of Rheumatology and Immunology, Department of Medicine, Medical University of South Carolina, Charleston, South Carolina, USA*
[2] *Department of Rheumatology and Immunology, Nanjing University Medical School Affiliated Nanjing Drum Tower Hospital, Nanjing, Jiangsu, China*
[3] *Department of Orthopedic Surgery, Nanjing University Medical School Affiliated Nanjing Drum Tower Hospital, Nanjing, China*
[4] *Department of Comparative Medicine, Medical University of South Carolina, Charleston, South Carolina, USA*
[5] *Department of Public Health Sciences, Medical University of South Carolina, Charleston, South Carolina, USA*
[6] *Arthritis and Clinical Immunology, Oklahoma Medical Research Foundation, Oklahoma City, Oklahoma, USA*
[7] *Division of Rheumatology, The University of Texas Health Science Center at Houston, Houston, Texas, USA*

ARTICLE INFO

Article history:
Received 28 April 2024
Accepted 26 August 2024

Keywords:
Scleroderma
Systemic
Pulmonary Fibrosis
Polymorphism
Genetic

ABSTRACT

Objective: We assessed the role of a systemic lupus erythematosus causal hypofunctional variant, neutrophil cytosolic factor 1 (*NCF1)*-p.Arg90His (p.R90H) substitution, in systemic sclerosis (SSc).

Methods: Association of *NCF1*-H90 with SSc was performed in case–control cohorts, bleomycin (BLM)-treated *Ncf1*-R90 C57BL/6 wildtype and *Ncf1*-H90 knock-in (KI) littermates. Peripheral blood mononuclear cell (PBMC) subsets were analysed by cytometry by time-of-flight.

Results: The *NCF1*-H90 allele is associated with risk for diffuse cutaneous SSc (dcSSc) in Chinese and European Americans, and lung fibrosis in Chinese patients with SSc (OR = 2.09, p = 7.96E−10). Low copy number of *NCF1* associated with lung fibrosis in European Americans (OR = 4.33, p = 2.60E−2). BLM-treated KI mice demonstrated increased pulmonary fibrosis, exhibiting activated type I interferon signature, elevated *Spp1*, *Ccl2, Arg1, Timp1* and *Il6* expression, enriched macrophage scores in lung tissues. In a longitudinal observation cohort, homozygous H90 patients with SSc at baseline had increased anti-nuclear antibody titres, anti-topoisomerase antibody seropositivity and anti-centromere antibody seronegativity, increased incidence of lung fibrosis and Gender-Age-lung Physiology index, elevated modified Rodnan Skin Score (mRSS) and elevated plasma osteopontin (OPN, SPP1), CCL2, ARG1, TIMP-1 and

*Correspondence to Dr. Betty P. Tsao; Professor Lingyun Sun.
E-mail addresses: lingyunsun@nju.edu.cn (L. Sun), tsaob@musc.edu (B.P. Tsao).
Social media: @ShervinAssassi (S. Assassi)
Handling editor Josef S. Smolen.
XY, XQ and KT contributed equally.

https://doi.org/10.1136/ard-2024-226034

IL-6. These H90 patients with SSc sustained elevated mRSS during follow-up years with decreased survival. The 0, 1 and 2 copies of H90 carriage in SSc PBMCs exhibited dose-dependent increases in profibrotic $CD14^+CD68^+CD11b^+Tim3^+$monocytes. Elevated OPN, CCL2 and ARG1 in $CD68^+CD11b^+$monocyte-derived macrophages from H90 patients were decreased after co-culturing with anti-CCL2 antibody.

Conclusion: Low *NCF1* activity increases the risk for the development of dcSSc and lung fibrosis via expanding profibrotic $SPP1^+$MoMs in a CCL2-dependent manner, contributing to the severity of lung fibrosis in both BLM-treated mice and patients with SSc.

WHAT IS ALREADY KNOWN ON THIS TOPIC

- The hypofunctional p.Arg90His (p.R90H, rs201802880) substitution encoded in neutrophil cytosolic factor 1 (*NCF1*), resulting in reduced NADPH oxidase 2 activity and induced type I interferon (IFN-I) signature, strongly associates with risk of multiple autoimmune diseases.

WHAT THIS STUDY ADDS

- The hypofunctional *NCF1*-H90 variant is strongly associated with diffuse cutaneous systemic sclerosis and lung fibrosis in Chinese and European Americans. The H90 variant was dose-dependently associated with increased skin thickness, lung fibrosis and mortality in a longitudinal Chinese cohort.
- The C57BL/6 (B6) mouse with a KI H90 variant in the *Ncf1* locus demonstrated severe pulmonary fibrosis and IFN-I signature on bleomycin treatment. The H90.B6 knock-in mice exhibited elevated expression of *Spp1*, *Ccl2, Arg1, Timp1* and *Il6*, along with increased macrophage cell-type score in lung tissues.
- Patients with systemic sclerosis (SSc) carrying two copies of the *NCF1*-H90 variant demonstrated increased $CD14^+CD68^+CD11b^+Tim3^+$monocytes/macrophages in peripheral blood mononuclear cells (PBMCs). The monocyte-derived macrophages from H90 patients exhibited more profibrotic, with higher expression of osteopontin in a CCL2-dependent manner.

HOW THIS STUDY MIGHT AFFECT RESEARCH, PRACTICE OR POLICY

- Patients with SSc carrying the hypofunctional *NCF1* variants have an increased risk for active disease course and lung fibrosis, and the CCL2-SPP1-ARG1 axis is a potential therapeutic target for these patients.

INTRODUCTION

Systemic sclerosis (SSc), characterised by excess deposition of extracellular matrix in the skin and internal organs, is often associated with interstitial lung disease (ILD) [1]. While the disease mechanisms are completely unknown, the genetic contribution of over 30 SSc-associated risk loci has been identified in large-scale association studies [2–4]. We previously identified a hypofunctional variant (p.R90H) in neutrophil cytosolic factor 1 (*NCF1)*, encoding a regulatory subunit of phagocyte NADPH oxidase 2 (NOX2), associated with robust risk of multiple autoimmune diseases including systemic lupus erythematosus (SLE), primary Sjögren's syndrome (pSS) and rheumatoid arthritis (RA) [5]. Additionally, decreased copy numbers of *NCF1* predisposed to SLE [5]. The hypofunctional H90-*NCF1* is an established causal variant of SLE, affecting efferocytosis efficiency in macrophages [6] and endosomal toll-like receptor (TLR)-signalling in plasmacytoid dendritic cells (pDC) [7,8] and B cells resulting in breaks of immune tolerance and increased humoral immune responses to nucleic-acid containing antigens [9]. Considering the pleiotropic effects of this variant and upregulated interferon (IFN)-I signature commonly observed in patients affected with SSc, SLE and pSS [10,11], we hypothesised that the *NCF1*-H90 variant contributes to the susceptibility of SSc. SSc is classified into limited cutaneous (lcSSc) and diffuse cutaneous (dcSSc) [12] based on the extent of skin involvement. Patients affected with dcSSc tend to have rapid progression of multiple organ involvement and an early incidence of ILD—a leading cause of death in SSc [13,14]. A commonly used animal model of pulmonary fibrosis is a 1-week bleomycin (BLM) infusion by osmotic minipump in C57BL/6 mice [15]. Here we explored the functional consequences of the *NCF1*-H90 variant in the development of disease manifestations in patients affected with SSc and in BLM-treated H90.B6 knock-in (KI) mice.

RESULTS

Association of hypofunctional NCF1*-H90 variant with SSc risks with stronger association in patients with dcSSc or lung fibrosis*

In 529 patients with SSc and 3020 controls, we observed association of H90 allele of *NCF1* with SSc in Chinese patients (OR = 1.93, p = 5.97E−12), in which more robust association signals were observed with the dcSSc subset (OR = 2.25, p = 4.25E−11) and with lung fibrosis (OR = 2.09, p = 7.96E−10). Another variant, the GTGT sequence within exon 2 of *NCF1,* distinguishes a functional *NCF1* gene from its neighbouring *NCF1B* and *NCF1C* pseudogenes containing a GT deletion (ΔGT), resulting in copy number variations (CNVs) [5]. Because the CNVs were found in <2% of East Asians and their impact on association analyses of *NCF1*-H90 in Asian data sets was expected to be negligible [5], Chinese subjects were not assessed for the CNVs. However, >15% of European Americans (EA) exhibit CNVs of this locus [5], hence we assessed CNVs in EA and genotyped the H90 variant only in subjects carrying normal copy numbers of *NCF1*. In EA, we confirmed the association between the *NCF1*-H90 variant and dcSSc (OR = 2.48, p = 2.02E−3), between low CNV (one copy number of functional *NCF1*) and dcSSc (OR = 21.3, p = 1.71E−8), and between low CNV and lung fibrosis (OR = 4.33, p = 2.60E−2) (table 1). While high CNVs (two copies of *NCF1* and one or two copies of GTGT-containing *NCF1B* and *NCF1C*) protected against dcSSc in EA (OR = 0.35, p = 9.78E−5) (table 1). These findings supported that abnormally low activity of NOX2, due to the hypofunctional *NCF1*-H90 variant [6], predisposed to SSc, especially in patient subsets affected with either dcSSc or lung fibrosis.

Increased pulmonary fibrosis and IFN-I scores in BLM-treated H90.B6 KI mice

To explore the link between the *NCF1*-H90 variant and the development of SSc-associated lung disease, we used an established BLM mouse model [15,16] and delivered graded dozes of BLM (0, 50, 75, 100 U/kg) via osmotic minipumps to H90.B6 KI

Table 1
Association of *NCF1* variant with SSc in different ancestry groups

			Subject		MAF %				
SNP	Ancestry	Subtype	Case	Control	Case	Control	OR	(95% Cl)	P value
rs201802880 (p.Arg90His, A/G)	Chinese	Total	332	2089	28.3	16.8	1.93	(1.60 to 2.32)	5.97E−12
		lcSSc	108	2089	26.4	16.8	1.79	(1.30 to 2.45)	3.14E−04
		dcSSc	170	2089	31.8	16.8	2.25	(1.77 to 2.87)	4.25E−11
		Lung	189	2089	29.9	16.8	2.09	(1.65 to 2.64)	7.96E−10
	European American	dcSSc	193	931	4.9	2.2	2.48	(1.39 to 4.42)	2.02E−03
			Subject		MAF %				
CNV	Ancestry	Subtype	Case	Control	Case	Control	OR	(95% Cl)	P value
1*	European American	dcSSc	14	3	3.1	0.1	21.3	(6.10 to 74.6)	1.71E−08
3† and 4‡			13	184	2.9	8.2	0.35	(0.20 to 0.63)	9.78E−05
2§			197	931					
			Presence	Absence	Presence	Absence			
1*		Lung	11	3	5.2	1.3	4.33	(1.19 to 15.8)	2.60E−02
3† and 4‡			6	7	2.9	2.9	1.06	(0.35 to 3.21)	1.00
2§			88	109					

A total of 332 Chinese patients and 197 European American patients were enrolled, and 4 European American patients were excluded after quality control of the genotyping results. 54 Chinese patients with SSc were excluded due to incomplete clinical information in the subset analysis.
CNV, copy number variation; dcSSc, diffuse cutaneous systemic sclerosis; lcSSc, limited cutaneous systemic sclerosis; lung, case with lung fibrosis identified by chest X-ray and/or CT/high-resolution CT; MAF, minor allele frequency; NCF1, neutrophil cytosolic factor 1; SNP, single nucleotide polymorphism; SSc, systemic sclerosis.
* One copy of functional *NCF1*.
† Two copies of functional *NCF1* and one copy of GTGT-containing *NCF1B* or *NCF1C*.
‡ Two copies of functional *NCF1* and two copies of GTGT-containing *NCF1B* or *NCF1C*.
§ Two copies of functional *NCF1* (wild type).

mice and R90.B6 wildtype (WT) littermates. Given that male B6 mice developed robust fibrosis in response to BLM treatment compared with B6 females [15,17], we used male mice first for a dose-finding experiment to study genetic effects then verified the optimum BLM dose in female mice. Compared with phosphate buffer saline (PBS)-treated mice, BLM-treated littermates exhibited a dose-dependent increase of collagen deposition in lungs (Masson's Trichrome-staining) (figure 1A) and lung fibrosis (Ashcroft score) (figure 1B left). Given significantly increased Ashcroft scores observed only in 100 U/kg BLM-treated male KI mice, we treated female KI and WT littermates with 100 U/kg BLM and confirmed significantly increased Ashcroft scores in H90.B6 KI female mice compared with their WT littermates (figure 1B left).

We next tested the effect of the *Ncf1*-H90 variant on lung transcriptome in the BLM-induced SSc model. We measured transcript levels of fibrosis-related genes (*Col1a1*, *Col1a2*, *Fn* and *Ctgf*) and IFN-I-stimulated genes (*Irf7*, *Ifit44*, *Mx1*, *Isg15*, *Oas1*), summarised them as fibrosis score and IFN-I score for each mouse lung sample, respectively [18,19]. The fibrosis score and its related-gene levels increased dose-dependently in BLM-treated male mice. Both male and female 100 U/kg BLM-treated KI mice exhibited elevated fibrosis scores compared with their respective sex-matched WT littermates (figure 1B middle and online supplemental figure 1A). Additionally, H90.B6 KI mice had elevated IFN scores in the lungs of BLM-treated male (75, 100 U/kg) and female (100 U/kg) mice compared with their WT littermates (figure 1B right and online supplemental figure 1B). Positive correlations between Ashcroft scores with either fibrosis scores or IFN-I scores were observed in both male and female mice (figure 1C). Collectively, these data showed the R to H substitution of *Ncf1* enhanced BLM-induced lung fibrosis in both sexes, and the extent of pulmonary fibrosis correlated with upregulated transcripts related to fibrosis and IFN-I pathways. We detected no measurable anti-nuclear antibody (ANA) activity in KI and WT mice treated with 100 U/kg BLM or PBS (online supplemental figure 2).

To further understand additional pathways underlying lung fibrosis, we performed pathway analysis of 770 fibrosis-related genes (NanoString) in lung tissues from experimental mice. Unsupervised hierarchical clustering of the 51 pathway scores segregated the data into eight groups based on differential gene expression levels (figure 1D). Group 1 only contained PBS-treated WT and KI mice with the lowest Ashcroft score, while Group 8 contained male mice treated with the highest dose of 100 U/kg BLM (60% KI and 20% WT) and with 75 U/kg BLM (20% KI) exhibiting the highest Ashcroft score (figure 1E). Lung samples from the female mice treated with 100 U/kg BLM were found in Groups 3 and 4 (figure 1E). An overall increase in Ashcroft scores was positively correlated with grouping from 1 to 8, and Ashcroft scores of Groups 3, 4 and 8 were significantly upregulated compared with Group 1 (figure 1E). The most upregulated profibrotic pathways we observed in the highest Ashcroft score Group 8 had a higher representation of KI mice in BLM-treated lungs compared with a higher representation of WT mice in PBS-treated lungs.

Elevated expression of Spp1 *and increased macrophage cell-type score in lung tissues of H90.B6 KI mice*

Given that 100 U/kg BLM-treated KI mice of both sexes exhibited elevated Ashcroft scores compared with their similarly treated sex-matched WT littermates, we asked which genes and pathways were differentially expressed (DE) among the 770 fibrosis-related genes and 51 pathways. While transcript levels of 23 genes were significantly increased in the KI group (figure 2A left and online supplemental table 2), levels of 74 genes were significantly increased and 7 genes were significantly decreased in male mice (figure 2A right and online supplemental table 3). Among DE genes, five upregulated genes (*Timp1*, *Ccl2*, *Il6*, *Arg1* and *Spp1*) exhibited both genotype and sex difference. As for DE

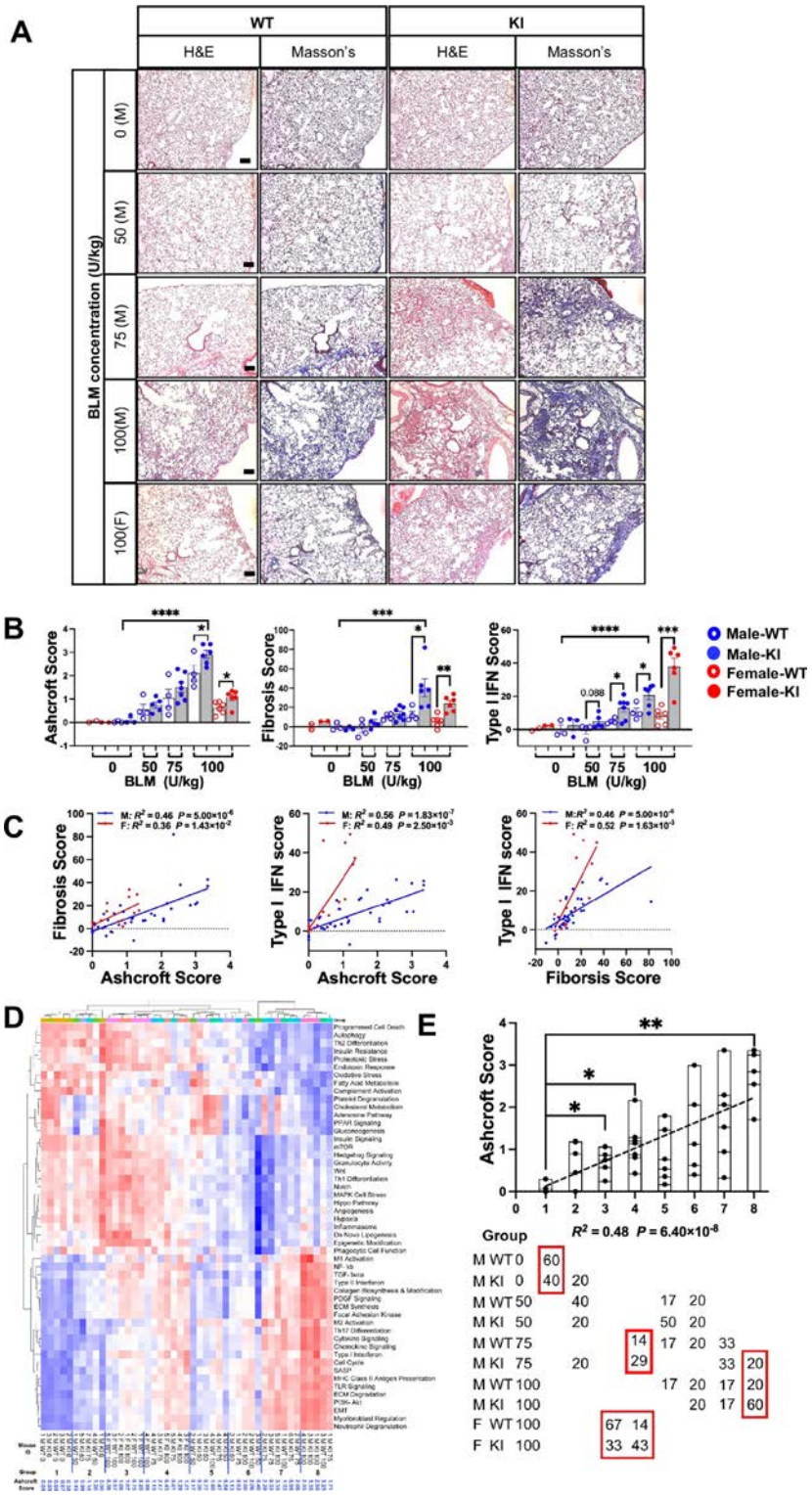

Figure 1. Increased pulmonary fibrosis and type I IFN score in BLM-treated H90.B6 KI mice. (A) Representative images of no or varying amount of BLM-treated left lung tissues of WT and KI littermates on day 28 stained with H&E or with Masson's trichrome. Intense blue Masson's staining indicated the presence of collagen. Scale bar: 100 μm. (B) Left: quantification of fibrosis of lung tissues using Ashcroft score by a blinded pathologist. Middle and right: expression levels of fibrosis-related genes (*Col1a1*, *Col1a2*, *Fn* and *Ctgf*) and type I IFN-inducible genes (*Irf7*, *Ifit44*, *Mx1*, *Isg15* and *Oas1*) in lung tissues were measured using real-time PCR and summarised as fibrosis scores and type I IFN scores, respectively. (C) Pearson correlations among Ashcroft score, fibrosis score and type I IFN score. (D) Unsupervised hierarchical clustering of 51 pathways derived from nCounter Fibrosis Panel (NanoString Technologies) visualised as eight distinct groups based on similar expression patterns. Ashcroft score of each mouse treated with graded dose of BLM were depicted below the heatmap. (E) Ashcroft score analysis among the eight groups (upper part). Percentage of WT/KI and male/female mice number in groups treated with different BLM dosage or PBS (lower part). *p<0.05, **p<0.01, ***p<0.001, ****p<0.0001, p values between WT and KI were determined using two-tailed Student's t-test, p values among more than two groups were determined using one-way analysis of variance. The correlation was calculated by linear regression test. BLM, bleomycin; F, female; IFN, interferon; KI, knock-in; M, male; PBS, phosphate buffer saline; WT, wildtype.

pathways, a total of 14 pathways exhibited both genotype and sex difference (figure 2B and online supplemental figure 3). We further investigated the connection between DE pathways and genes based on the NanoString annotation database. Epithelial-mesenchymal transition (EMT), a reported pathway of lung fibrosis, contains the pathway hallmark genes *Spp1* and *Timp1* in KI mice [20–22]. The other three upregulated genes, *Ccl2, Il6* and *Arg1,* exhibiting both sex and genotype effects, were in pathways involved in cytokine, M2 activation and neutrophil degranulation (figure 2C). Recognising that ARG1 and SPP1 could be profibrotic markers of macrophages (termed as SPP1$^+$ macrophage) in lung fibrosis [23,24], and signalling of CCL2/CCR2 in monocytes/macrophages could promote lung fibrosis [25], we assessed relative cell-type scores of lung tissues between KI mice and WT littermates, which showed increased macrophages and decreased B cells from KI group compared with those from WT group in both male and female mice treated with 100 U/kg BLM (figure 2D and online supplemental figure 4). Additionally, exhausted CD8$^+$ T cells were significantly increased in the male KI group (online supplemental figure 4). The increased macrophages cell-type score in KI was consistent with the DE gene results (*Ccl2*, *Arg1* and *Spp1* increased in KI) and DE pathway results (EMT and M2 activation upregulated in KI), suggesting the SPP1$^+$ monocytes/macrophages might be pivotal in the development of severe lung fibrosis observed in H90.B6 KI mice.

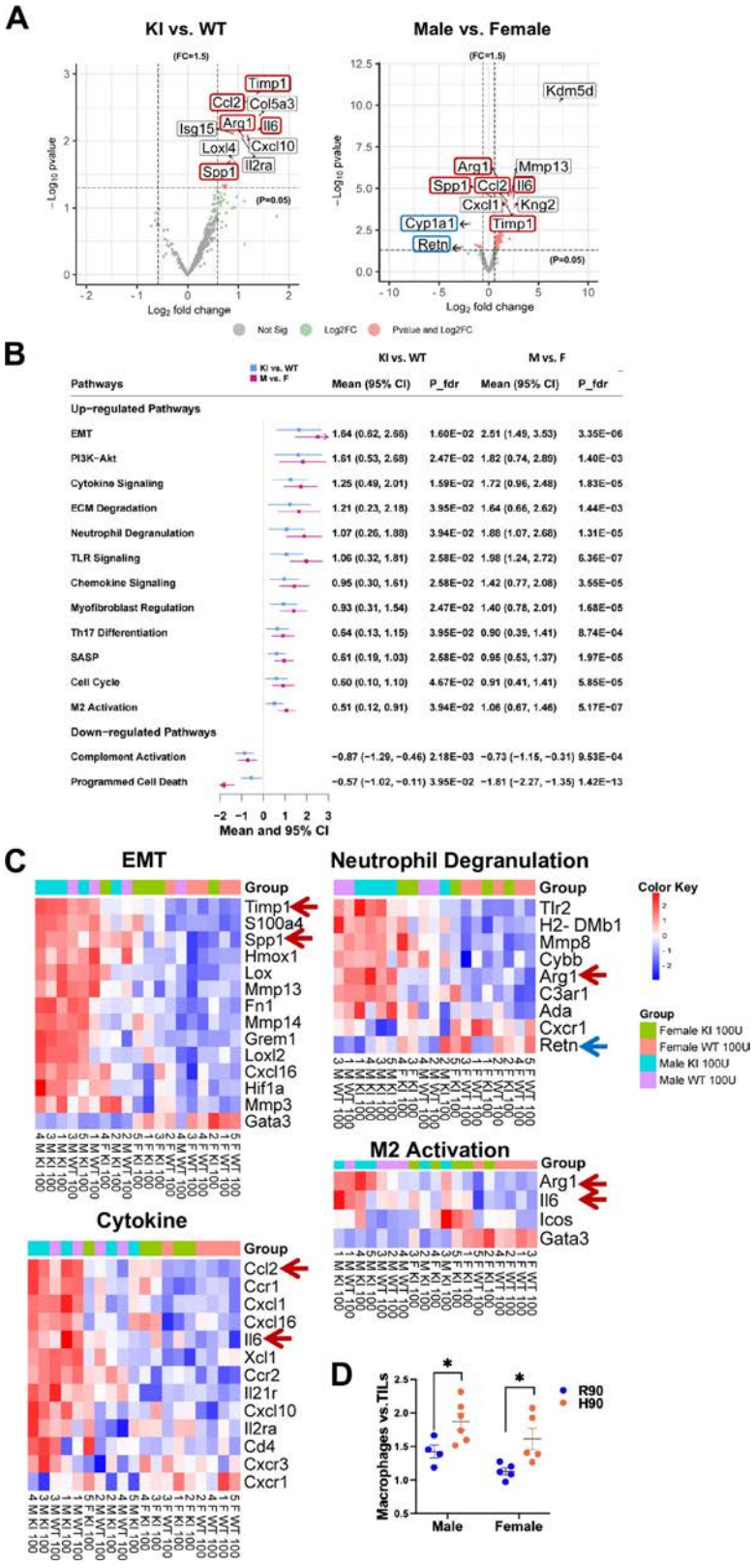

Figure 2. Increased expression of five genes and elevated macrophage cell type score in H90.B6 KI mice lung tissue by NanoString fibrosis panel. (A) Differentially expressed genes of 100 U/kg of bleomycin-treated H90.B6 KI mice compared with their WT littermates (left part) and male compared with female mice (right part). (B) Differential pathway scores between KI/WT mice (genotype difference) and male/female mice (sex difference) exhibiting 12 upregulated and 2 downregulated pathways. (C) Unsupervised hierarchical clustering of differentially expressed genes (either have genotype difference or sex difference) in pathways of EMT, cytokine. Neutrophil degranulation and M2 activation. (D) Relative cell-type scores for macrophages between KI mice and WT littermates. *p<0.05, p values between WT and KI littermates were determined using two-tailed Student's t-test. The differentially expressed pathway was analysed using a linear regression model and Benjamini-Hochberg false discovery rate correction. Results were shown as mean±SEM. ECM, extracellular matrix; EMT, epithelial-to-mesenchymal transition; FC, fold change; KI, knock-in; SASP, senescence-associated secretory phenotype; TGF, transforming growth factor; TILs, tissue infiltrating lymphocytes; TLR, toll-like receptor; WT, wildtype.

Increased risk of dcSSc and pulmonary fibrosis in a longitudinal cohort of patients with SSc carrying the NCF1*-H90 variant*

To determine if our findings in H90.B6 KI mice could be confirmed in patients with SSc, we assessed the relationship between carriage of *NCF1*-H90 variant and clinical characteristics of patients with SSc in an independent, longitudinal observation cohort of 92 Chinese patients with SSc (table 2 and online supplemental table 4). Among them, 47 were homozygous for *NCF1*-R90 (51.1%), 37 were *NCF1*-90R/H (40.2%) and 8 were homozygous for *NCF1*-H90 (8.7%). The minor allele frequency (MAF) of the H90 variant was 28.8%, which was consistent with the 28.3% depicted in table 1. The baseline demographics and clinical manifestations at diagnosis are depicted in table 2.

No genotype-associated difference in age at diagnosis was observed (figure 3A) with a female/male ratio of 4.2:1 for R90,

Table 2
Patients baseline demographics, treatment and autoantibody

		R90 (n = 47)	90R/H (n = 37)	H90 (n = 8)
Age (yrs)		52.0 (18.0–71.0)	48.0 (18.0–67.0)	50.5 (22.0–70.0)
Gender (F/M)		38/9	32/5	7/1
Disease duration (yrs)		7.4 (0.5–21.0)	7.0 (1.0–21.0)	6.9 (1.0–16.0)
SSc type (dcSSc/lcSSc)		25/22	25/12	7/1
Treatment				
MMF (%)		12 (25.5)	7 (18.9)	3 (37.5)
CTX (%)		19 (40.4)	24 (64.9)	7 (87.5)
HCQ (%)		17 (36.2)	20 (54.1)	6 (75.0)
MTX (%)		2 (4.3)	4 (10.8)	0 (0.0)
Pred (%)		44 (93.6)	36 (97.3)	8 (100.0)
ANA titre				
Low	1:100 (%)	25 (53.2%)	12 (32.4%)	1 (12.5%)
	1:320 (%)	6 (12.8%)	3 (8.1%)	1 (12.5%)
	1:640 (%)	5 (10.6%)	4 (10.8%)	0 (0.0%)
High	1:1000 (%)	10 (21.3%)	11 (29.7%)	3 (37.5%)
	1:3200 (%)	1 (2.1%)	7 (18.9%)	3 (37.5%)
ACA^+ (%)		18 (38.3)	6 (16.2)	0 (0.0)
ATA^+ (%)		7 (14.9)	13 (35.1)	6 (75.0)

ACA, anti-centromere antibody; ANA, anti-nuclear antibody; ATA, anti-topoisomerase antibody; CTX, cyclophosphamide; dcSSc, diffused cutaneous SSc; F, female; HCQ, hydroxychloroquine; high ANA titre, ≥1:1000 ; lcSSc, limited cutaneous SSc; low ANA titre, <1:1000; M, male; MMF, mycophenolate mofetil; MTX, methotrexate; Pred, prednisone; SSc, systemic sclerosis; yrs, years.

6.4:1 for 90R/H and 7.0:1 for H90 genotype patients (table 2). The MAF was 34.2% in dcSSc (n = 57) and 20.0% in lcSSc (n = 35). Given the increasing frequency of dcSSc observed in R90, 90R/H and H90 genotype groups, H90 variant carriers were more likely to develop diffuse cutaneous involvement (figure 3B). High-resolution CT (HRCT) imaging showed increasing frequencies of lung fibrosis in R90, 90R/H and H90 patients (figure 3C). With respect to autoantibody profiles, the H90 patient group exhibited elevated ANA titres, increased anti-topoisomerase antibody (ATA) seropositivity and decreased anti-centromere antibody seropositivity compared with the R90 group (figure 3D). The extent of skin fibrosis assessed using the modified Rodnan Skin Score (mRSS) was significantly higher in the H90 group than either the 90R/H group or the R90 group at baseline (figure 3E), which remained the highest during years of follow-up visits (figure 3F). Importantly, H90 patients had a much larger Gender-Age-lung Physiology (GAP) index (calculated by gender, age, forced vital capacity and diffusion capacity of the lung for carbon monoxide) compared with either 90R/H patients or R90 patients at baseline (figure 3G). Figure 3H depicts HRCT lung images from a typical patient of each genotype group representing the mean value of the GAP index. The 0, 1 or 2 copies of H90 carriage dose-dependently associated with elevated mRSS and GAP index, indicating the contribution of the *NCF1*-H90 variant in disease severity and lung damage of patients with SSc. While the overall survival rate of these 92 patients was 85.9% (79/92) during an average 5.4-year period, survival rate was 62.5% (5/8) in the H90 group, 83.8% (31/37) in the 90R/H group and 91.5% (43/47) in the R90 group, respectively, indicating H90 carriage in patients with SSc is associated with shorter survival (figure 3I). Compared with the R90 group, survival rate analysis in different subgroups showed a significantly decreased in the H90 group in patients with high ANA titre and dcSSc, but no difference with the H90 group in either ATA-positive patients or patients with lung fibrosis (online supplemental figure 5). Hence, the H90 carriage in patients with SSc appeared to promote ATA seropositivity and lung fibrosis, resulting in a shortened survival.

Elevated $CD14^+CD68^+CD11b^+Tim3^+$ monocytes in PBMCs from NCF1-*H90 patients with SSc*

To further explore the *NCF1*-H90 variant involvement in SSc disease progression, we comprehensively profiled peripheral blood mononuclear cells (PBMCs) from sex-matched and age-matched seven healthy controls (HCs) and 14 patients with SSc from the three groups of genotypes collected at their follow-up visits using cytometry by time-of-flight (CyTOF). The demographics and clinical manifestations of these subjects at the time of blood draw are depicted in online supplemental table 5. The incidence of lung fibrosis was 33.3%, 80.0% and 100.0% for R90, 90R/H and H90 group, respectively. Similarly, the H90 group had significantly higher mRSS (38.33±6.66) and GAP index (4.00±1.73) than the R90 or 90R/H group.

Based on expression levels of lineage-associated markers, PBMCs were partitioned into 38 cell clusters (online supplemental table 6) visualised on a t-distributed stochastic neighbour embedding map (figure 4A), which were annotated into 10 major immune cell lineages: $CD4^+$ T cells, $CD8^+$ T cells, double negative T (DNT) cells, double positive T (DPT) cells, natural killer T (NKT) cells, monocytes, B cells, natural killer cells, dendritic cells and stem cells. While the cell-type composition in PBMCs varied substantially among the five groups, the frequency of monocytes was significantly increased in H90 patients compared with either R90 patients or HC-R90 subjects and exhibited an H90 dose-dependent increase in patients with SSc (figure 4B, online supplemental figure 6 and 7). Moreover, cluster 37 (defined as $CD14^+CD68^+CD11b^+Tim3^+$ monocytes) were significantly increased in the SSc-H90 group compared with the other four groups (figure 4C), exhibiting an H90 dose-dependent increase in both percentage and absolute number of $CD14^+CD68^+CD11b^+Tim3^+$ monocytes. The percentage of $CD14^+CD68^+CD11b^+Tim3^+$ monocytes was positively correlated with mRSS and GAP index, indicating their profibrotic property (figure 4C). The lack of difference between the HC-R90 and HC-90R/H groups provided the rationale to combine them

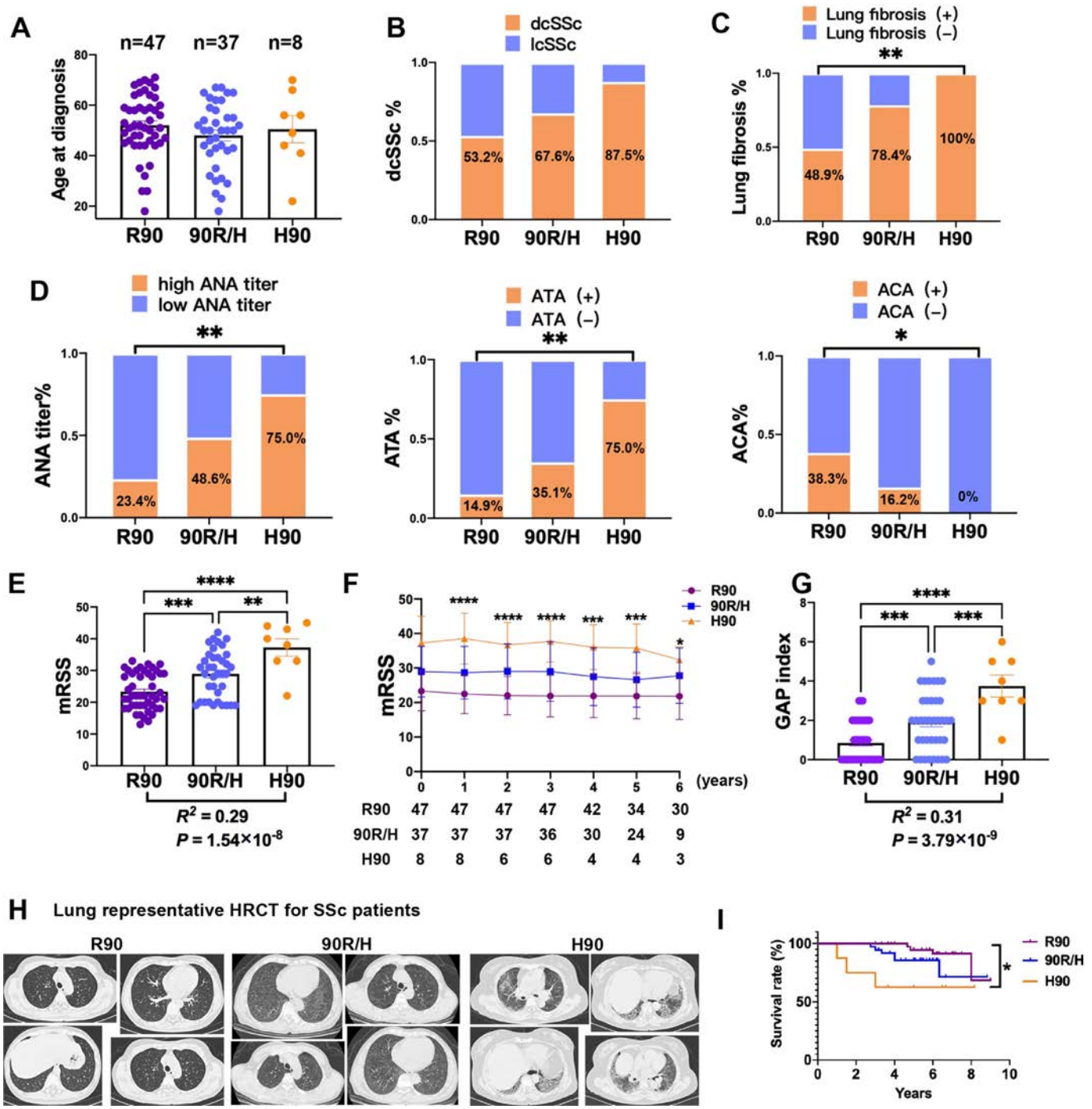

Figure 3. Dose-dependent association of *NCF1*-H90 variant with increased skin thickness, lung fibrosis and mortality in Chinese patients with SSc. (A–D) The age at diagnosis, SSc subtype (dcSSc or lcSSc), proportions of lung fibrosis identified by HRCT and autoantibody profiles of consecutive patients with SSc enrolled in a longitudinal observational cohort stratified by genotypes. High ANA titre was defined as ≥1:1000. (E) A dose-dependent association of *NCF1*-H90 variant with elevated mRSS of patients at enrolment. (F) Elevated mRSS of *NCF1*-H90 patients with SSc during follow-up visits. The decreased numbers of patients in yearly follow-up visits stratified by genotypes, were due to either mortality or limited duration of follow-up. (G) The presence and the extent of lung fibrosis were evaluated using GAP index (rang from 0 to 8, including sex, age, FVC and DL_{CO}). A dose-dependent association of *NCF1*-H90 variant with elevated GAP index of patients at enrolment that the GAP index was recorded as 0 for patients with SSc without lung fibrosis. (H) Representative HRCT images including upper lobes, middle lobes and lower lobes from one patient of each genotype group representing the mean value of GAP index. (I) Kaplan-Meier survival curve of these 92 patients with SSc. *p<0.05, **p<0.01, ***p<0.001, ****p<0.0001, p values among the three groups were determined using Fisher's exact test for categorical variables or using one-way analysis of variance with Bonferroni's multiple-comparison test for continuous variables. The association of H90 copy numbers with mRSS or GAP index was calculated by linear regression test. Results were shown as mean±SEM. ACA, anti-centromere antibody; ANA, anti-nuclear antibody; ATA, anti-topoisomerase antibody; dcSSc, diffuse cutaneous SSc; DL_{CO}, diffusion capacity of lung for carbon monoxide; FVC, forced vital capacity; GAP, Gender-Age-lung Physiology; HRCT, high-resolution CT; H90, homozygous for *NCF1*-H90; lcSSc, limited cutaneous SSc; ILD, interstitial lung disease; mRSS, modified Rodnan Skin Score; *NCF1*, neutrophil cytosolic factor 1; ns, no significance; R90, homozygous for *NCF1*-R90; SSc, systemic sclerosis; 90R/H, heterozygous for *NCF1*-90R/H.

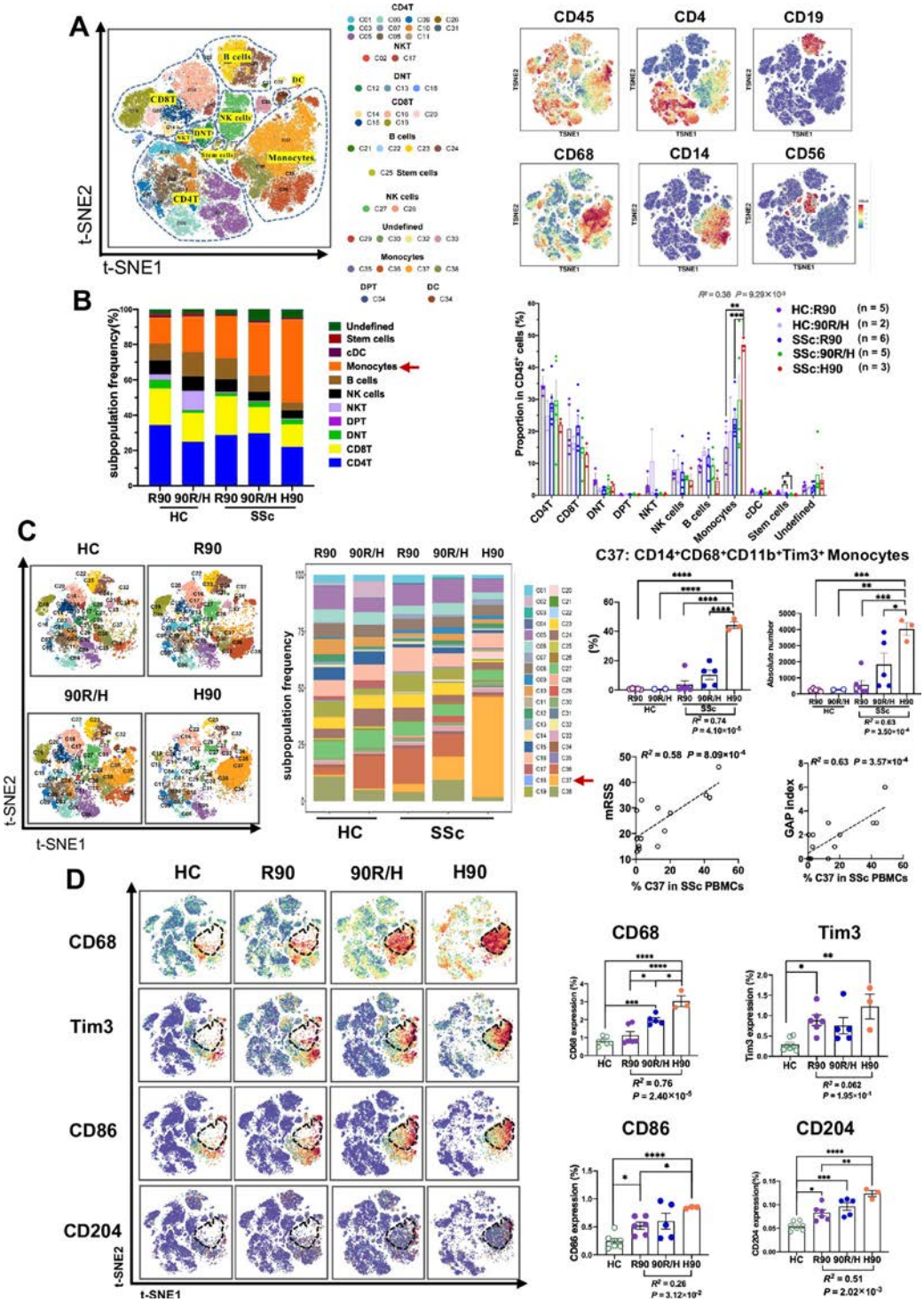

Figure 4. Dose-dependent effects of neutrophil cytosolic factor 1-H90 variant in increased $CD14^+CD68^+CD11b^+Tim3^+$ monocytes in PBMCs of patients with SSc. (A) Left: t-SNE plot of the CyTOF data of $CD45^+$ cells from PBMCs of 14 patients with SSc and 7 age-matched and sex-matched HCs. A total of 38 clusters were identified and annotated into a specific immune cell type according to the known marker expression. Right: t-SNE plot of all $CD45^+$ cells coloured by the expression levels of CD45, CD4, CD19, CD68, CD14 and CD56. (B) Frequency of 10 main types of immune cells in PBMCs of SSc-R90 (n = 6), SSc-90R/H (n = 5), SSc-H90 (n = 3), HC-R90 (n = 5) and HC-90R/H (n = 2). (C) Left: t-SNE plot of all $CD45^+$ cells from PBMCs of R90, 90R/H, H90 patients and HCs. Middle: proportions of 38 cell clusters in the five groups. Right: proportions and numbers of cluster 37 ($CD14^+CD68^+CD11b^+Tim3^+$ monocytes) associated with H90 copy numbers, mRSS and GAP index. (D) Elevated expression levels of CD68, Tim3, CD86 and CD204 in patients with SSc were associated with copy numbers of the H90 variant. *p<0.05, **p<0.01, ***p<0.001, ****p<0.0001, p values among the four groups were determined using one-way analysis of variance with Bonferroni's multiple-comparison test. The association of H90 copy numbers with the percentage of monocytes, percentage and number of C37 or expression of cell markers was calculated by linear regression test. The correlation was calculated by linear regression test. Results were shown as mean±SEM. cDC, conventional dendritic cell; CyTOF, cytometry by time-of-flight; DC, dendritic cell; DNT, double negative T cell; DPT, double positive T cell; GAP, Gender-Age-lung Physiology; HC, healthy control; mRSS, modified Rodnan Skin Score; NK, natural killer; NKT, natural killer T cell; PBMC, peripheral blood mononuclear cell; SSc, systemic sclerosis; t-SNE, t-distributed stochastic neighbour embedding.

in subsequent analyses. Additionally, the frequency of $CD8^+CD3^+CCR5^+CD28^+CXCR3^+CD31^+$ T cells (cluster 15) and $CD69^+CD34^+CCR4^+CXCR3^+CD31^+$ stem cells (cluster 25) were remarkedly decreased in the PBMCs of patients with SSc compared with those from HCs (online supplemental figure 7).

When we analysed the expression of 42 markers in each cluster, expression levels of CD68, Tim3, CD86 and CD204 were significantly higher in the H90 patient group than in the HC group. Moreover, there was an H90 dose-dependent increase in the expression of CD68, CD86 and CD204 in patients with SSc, which were all cell markers for macrophages (figure 4D). The lack of H90-dose-dependency of Tim3 could be contributed to its expression in clusters 34 and 36 in addition to cluster 37. These CyTOF findings indicated the expanded monocyte/macrophages in PBMCs might contribute to lung fibrosis in H90 patients.

CCL2-dependent elevated levels of osteopontin, CCL2 and ARG1 in monocyte-derived macrophages from H90 patients

To explore the functional consequences of the elevated monocyte subset and its underlying mechanism of regulation, we further collected peripheral blood from three H90 patients, six R90 patients and seven HCs to obtain plasma, PBMCs and monocyte-derived macrophages (MoMs). The plasma levels of CCL2, osteopontin (OPN encoded by *SPP1*), ARG1, TIMP-1 and IL-6 in H90 patients were significantly elevated than in either R90 patients or HCs, which was consistent with previous results that H90.B6 KI mice showed higher expression of *Ccl2*, *Spp1*, *Arg1*, *Timp1* and *Il6* at the transcript level (figure 5A). No significant difference in OPN, CCL2, ARG1, TIMP-1 and IL-6 plasma level was found among the three genotype groups in newly recruited 20 HCs (figure 5A and online supplemental figure 8A), indicating the increased expression of these five genes in the H90 group during the disease state.

Next, the monocytes in PBMCs were compared between R90 and H90 patients. Similar to the CyTOF results, both the percentage and absolute number of $CD14^+CD68^+CD11b^+Tim3^+$ monocytes were significantly larger in the H90 group than in the R90 group (online supplemental figure 9A). Moreover, expression levels of CD11b, CD204, CD86 and Tim3 in $CD14^+$ monocytes were significantly higher in H90 patients (online supplemental figure 9B). Further, $CD68^+CD11b^+$ MoMs were cultured from $CD14^+$ monocytes isolated from PBMCs (figure 5B), and the expression of OPN was significantly increased in MoMs from H90 patients than R90 patients, which significantly correlated with mRSS and GAP index (figure 5C). For the OPN^+ MoMs, surface expressions of CD204, Tim3, CD163, CD206, but not CD86, were significantly elevated in the H90 group (figure 5D) and the supernatant levels of active TGFβ1, TIMP-1 and IL-6 were significantly elevated in the H90 group (online supplemental figure 8B). The addition of monoclonal anti-human MCP-1/CCL2 antibody, but not the control antibody, suppressed not only elevated levels of CCL2 but also OPN and ARG1 in the culture system of H90 MoMs compared with those of R90 MoMs (figure 5E–G), indicating a critical role of the chemokine CCL2 in regulating activation of $SPP1^+$ macrophages. However, TGF-β1, TIMP-1 and IL-6 were not suppressed after anti-CCL2 treatment (online supplemental figure 8B).

DISCUSSION

Here, we showed the hypofunctional H90 *NCF1* allele is one of the strongest common causal risk variants for SSc, by using the BLM-treated H90.B6 mouse model for both in vivo and in vitro studies, and by confirming mechanistic findings from mice to patients with SSc (figure 6). We confirmed the previously reported association between the *NCF1*-H90 variant and SSc in Japanese [26] using Chinese and EA population, and observed more robust association signals in patients affected with either lung fibrosis or dcSSc.

As lung biopsies are seldom performed in patients with SSc, to investigate the relationship between *NCF1*-H90 and lung fibrosis, we explored murine lung tissues by using a widely accepted BLM-induced fibrosis model by comparing R90.B6 WT to their H90.B6 KI littermates. Several studies have shown that BLM delivery by osmotic minipump in B6 mice had similarity to human SSc-ILD [16,27]. The male B6 mice receiving BLM via the pump model, showed a dose-dependent increase in lung fibrosis [15], which was consistent with our findings that BLM resulted in lung fibrosis in a dose-dependent manner and 100 U/kg was the strongest dosage (figure 1B). Using the *Ncf1*-H90 genetically engineered B6 mice, we observed significantly enhanced lung fibrosis and IFN-I signature in KI mice compared with WT mice of both sexes. The association of the *NCF1*-H90 variant and IFN-I signature has been reported in patients with autoimmune diseases such as SLE and RA [28,29], as well as in the H90.B6 KI mouse model showing lupus-like features induced by pristane [6]. Also, Taroni *et al* identified a common pathogenic signature related to an 'innate immune-fibrotic axis' that included IFN-I and alternatively activated profibrotic macrophages in multiple SSc tissues including lung, skin and PBMCs [30]. We showed the genetic effect of the *Ncf1*-H90 variant amplified the impact of the IFN-I signature and the immune-fibrotic axis in lung fibrosis induced by BLM treatment.

We detected elevated levels of *Spp1, Arg1, Ccl2, Timp1 and Il6* in lung tissues from KI mice compared with those from WT mice using NanoString. SPP1/OPN is considered to be a marker of profibrotic macrophages in idiopathic pulmonary fibrosis (IPF) [31] and is upregulated in patients with SSc-ILD [32,33]. An important role of SPP1 in SSc-ILD is supported by the discovery of a profibrotic macrophage population marked by expression of SPP1, FN1 and ARG1 (termed $SPP1^+$ macrophages) that drives a CXCL4-dependent myofibroblast activation in fibrosis [24]. Lung fibroblast migration could be promoted by monocytes via OPN secretion, and the process could be amplified by IL-6 [34]. Moreover, the elevated serum OPN and the IL-6 responsive plasma cell signature, could predict lung function deterioration in SSc-ILD patients [34,35]. In our study, the plasma levels of OPN and IL-6 were higher in patients with SSc than HC, particularly in patients carrying the H90 variant, whose lung fibrosis was more severe with a higher GAP index. Additionally, *Spp1* was one of the top three DE genes in the EMT pathway, which was the most upregulated pathway in KI mice (figure 2B, C). The transcriptional activation of the EMT pathway is shown in SSc-ILD using single-cell RNA sequencing (scRNA-seq) [36], and the $SPP1^+$ macrophages could induce EMT of alveolar epithelial cells, resulting in pulmonary fibrosis [37].

The top DE gene in the cytokine pathway, *Ccl2* (figure 2C), was another important marker associated with SSc, especially for patients with lung fibrosis, dcSSc at early stages or ATA^+ SSc [38,39]. High circulating CCL2 levels predict ILD progression and poorer survival in SSc [40]. Conversely, after mycophenolate mofetil treatment, the expression of CCL2 and the number of macrophages in skin biopsies decrease [41]. In our study, CCL2 plasma level was significantly increased in H90 patients, who had higher mRSS and ATA seropositivity with poor survival. Another DE gene *Arg1* is a profibrotic marker of

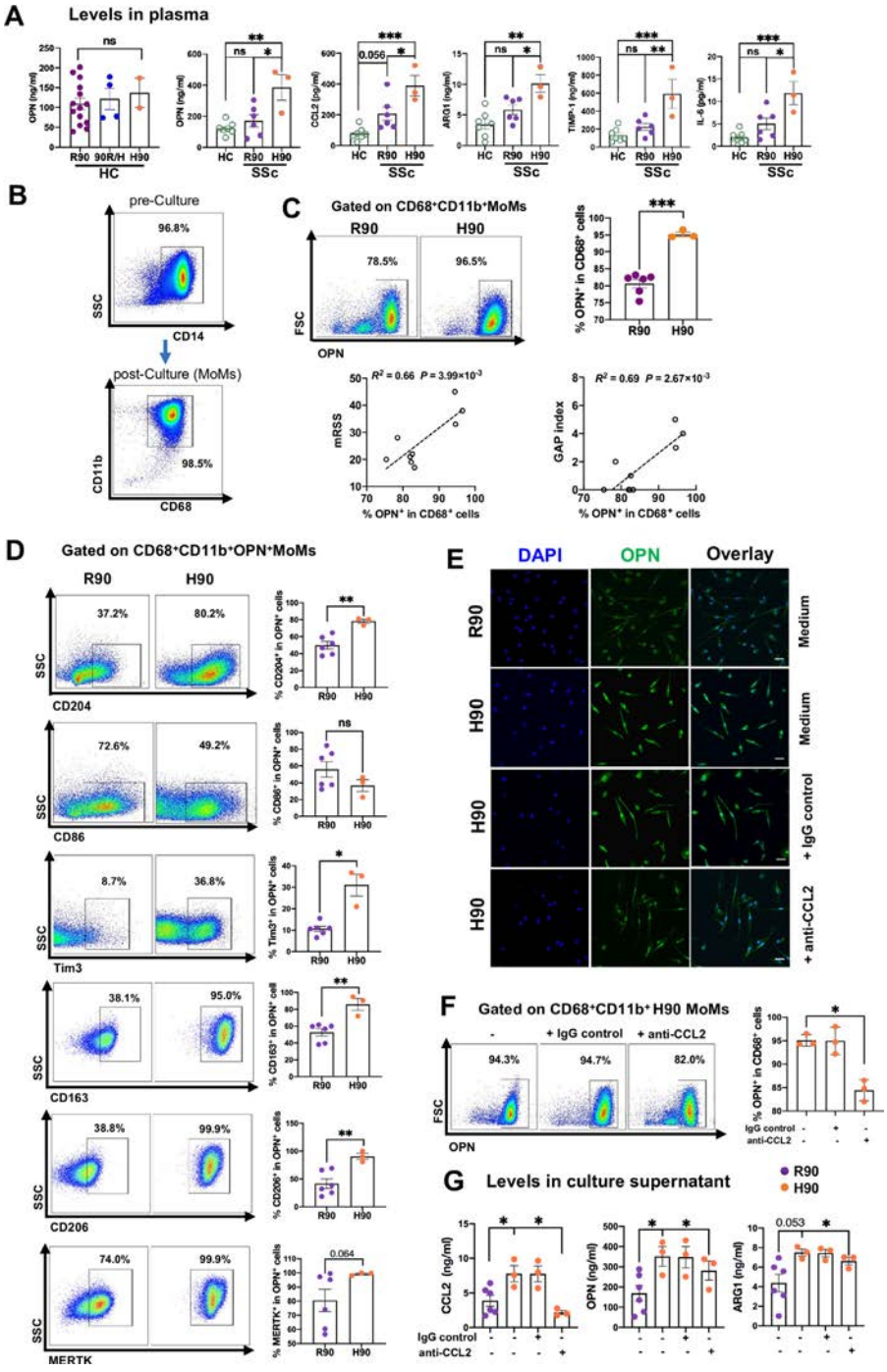

Figure 5. Monocyte-derived macrophages from PBMCs of *NCF1*-H90 patients with SSc exhibited elevated expression of OPN in a CCL2-dependent manner. (A) Elevated plasma levels of OPN, CCL2, ARG1, TIMP-1 and IL-6 from H90 patients (n = 3) compared with those from either R90 patients (n = 6) or HC (n = 7) from the subjects enrolled in the cytometry by time-of-flight study. An additional 20 HCs stratified by genotypes exhibited no significant difference in OPN plasma levels. (B) The $CD68^+CD11b^+$ MoMs (lower) differentiated from $CD14^+$ monocytes (upper) cultured in DMEM supplemented with M-CSF. (C) Levels of OPN in MoMs from R90 and H90 patients with SSc correlated with mRSS and Gender-Age-lung Physiology index. (D) Expression levels of CD204, CD86, Tim3, CD163, CD206 and MERTK in OPN^+ MoMs of R90 and H90 patients. (E,F) The expression level of OPN in MoMs was remarkedly higher in H90 patients than R90 by both flow cytometry and immunofluorescence, which was decreased in MoMs co-cultured with anti-human CCL2 antibody but not with anti-human IgG control. Bar: 100 μm; green, OPN; blue, DAPI. (G) Elevated culture supernatant levels of CCL2, OPN and ARG1 in H90 MoMs were significantly decreased with the addition of anti-human CCL2 antibody. *p<0.05, **p<0.01, ***p<0.001, ****p<0.0001, p values among three groups were determined using one-way ANOVA with Bonferroni's multiple-comparison test. P values between R90 and H90 were determined using two-tailed Student's t-test, p values among anti-CCL2 group, IgG control group and non-anti-CCL2 group were determined using one-way repeated measures ANOVA. The correlation was calculated by linear regression test. Results were shown as mean±SEM. ANOVA, analysis of variance; DAPI, 4′,6-diamidino-2-phenylin-dole; DMEM, Dulbecco's Modified Eagle Medium; HC, healthy control; H90, subjects with *NCF1*-H90; M-CSF, macrophage colony-stimulating factor; MoMs, monocyte-derived macrophages; mRSS, modified Rodnan Skin Score; *NCF1*, neutrophil cytosolic factor 1; ns, no significance; OPN, osteopontin; PBMC, peripheral blood mononuclear cell; R90, subjects with *NCF1*-R90; SSc, systemic sclerosis; 90R/H, subjects with *NCF1*-90R/H.

macrophages, activated by $Ly6C^+$ monocytes, which plays roles in lung fibrosis [23].

After anti-CCL2 treatment, the increased secretion of CCL2, OPN and ARG1, but not TIMP-1 and IL-6, in MoMs from H90 patients were suppressed, hence there was a correlation among CCL2, OPN and ARG1, which was partially investigated in previous studies. In synovial fluids of psoriatic arthritis, the transcripts for *SPP1* and *CCL2* were most highly upregulated by monocytes/macrophages and both proteins were elevated [42]. In a human monocyte cell line, *SPP1* knockdown in macrophages decreased secretion of ARG1 [43]. In our study, we further extended the effect of the *NCF1*-H90 variant in amplifying the CCL2-SPP1-ARG1 axis in monocytes/macrophages in the pathogenesis of lung fibrosis in patients with SSc, suggesting that targeting this axis might be efficacious in preventing the progression of lung fibrosis.

Timp1 was the top DE gene in our KI mice, playing a pivotal role in maintaining extracellular matrix homeostasis and has been implicated as a key non-invasive diagnostic and prognostic marker for lung fibrosis [44]. The profibrotic TIMP-1 production by monocytes was upregulated in SSc compared with RA or HC, and was mediated by TLR8 [45]. Moreover, elevated serum TIMP-1 in SSc associated with the disease severity [46]. In our study, we also observed plasma and culture supernatant levels of TIMP-1 were significantly elevated in H90 group than R90 group of patients with SSc (figure 5A and online supplemental figure 8B). While the role of TIMP-1 in SSc has been clearly demonstrated, whether elevated circulating levels of TIMP-1 associated with SLE, lupus nephritis and/or disease activity have yielded inconsistent findings [47−49], which could be attributed to disease heterogeneity and/or small sample sizes of each study. While the

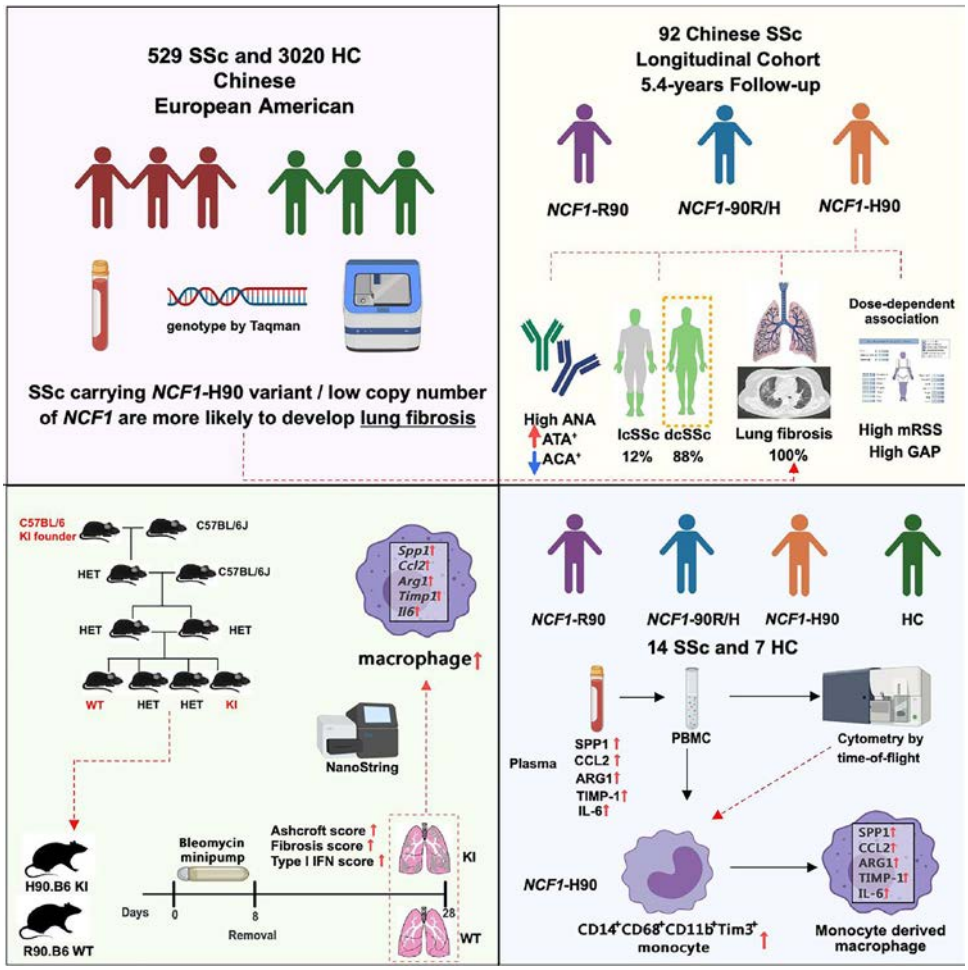

Figure 6. Overview of the experimental workflow our experiments could be summarised into four parts: (1). The *NCF1*-H90 allele is one of the strongest common risk variants for dcSSc and lung fibrosis in a case–control association study; (2). The increased lung fibrosis in the BLM-treated H90.B6 mouse model confirms *Ncf1*-H90 is a causal risk variant. Differential expression of BLM-treated lung tissues from R90.B6 versus H90.B6 and males versus female mice revealed elevated genes, pathways and infiltrating leucocytes associated with lung fibrosis; (3). The genetic effect of *NCF1*-H90 in promoting high ANA titres, seropositivity of ATA, seronegativity of ACA, dcSSc, lung fibrosis and high disease activity is confirmed in a longitudinal observation cohort of Chinese patients with SSc; (4). CyTOF cell subset analysis of SSc PBMCs identifies a profibrotic monocyte subset that MoM cultures verify the profibrotic SPP1$^+$ MoMs contributes to lung fibrosis. ACA, anti-centromere antibody; ANA, anti-nuclear antibody; ATA, anti-topoisomerase antibody; BLM, bleomycin; CyTOF, cytometry by time-of-flight; dcSSc, diffuse cutaneous SSc; GAP, Gender-Age-lung Physiology; HC, healthy control; HET, heterozygote; IFN, interferon; KI, knock-in; lcSSc, limited cutaneous SSc; MoM, monocyte-derived macrophage; mRSS, modified Rodnan Skin Score; *NCF1*, neutrophil cytosolic factor 1; PBMC, peripheral blood mononuclear cell; SSc, systemic sclerosis; WT, wildtype.

H90 risk variant predisposed to both SSc and SLE, TIMP-1 might impact the disease pathogenesis differently.

We observed an increased macrophage cell-type score in lung tissues of H90.B6 KI mice (figure 2D). Monocytes/macrophages have been implicated in the pathogenesis of SSc, especially in lung involvement [50,51]. Multiple immune cell types are affected by the H90 variant, including pDCs [7], macrophages [6], B cells [9] and T cells [52] in SLE, SSc and RA. Given that SSc has a shared genetic basis and IFN-I signature with SLE, and the induced IFN-I signature by the H90 variant is found in both the two diseases [6,28], the risk allele might be involved in SSc and SLE both through macrophages by elevated IFN-I signature produced mainly by pDCs and neutrophils. In renal biopsies from patients with lupus nephritis, CD163$^+$ M2-like macrophages are the dominant subpopulation and M2a subpopulations were associated with disease progression [53]. The current study showed elevated transcripts of five genes (*Spp1*, *Ccl2*, *Arg1*, *Timp1* and *Il6*) and macrophage infiltration in the lung tissues of BLM-treated H90 KI mice. The protein products of these five genes were elevated in plasma samples of H90 patients with SSc. The MoMs from H90 patients also had increased secretion of these five gene products, and had increased expression of CD163, CD204 and CD206 (M2 markers) (figure 5D, G and online supplemental figure 8B). Taken together, M2-like macrophage infiltration into tissue damage sites appeared to be a common theme in both SLE and SSc, in which the H90 risk variant enhanced the disease manifestations.

Limitations of this study include the following: (1) The principal components analysis could not be performed to correct for population admixture due to our candidate gene approach. However, we established a mice model to confirm the strong association between the H90 variant and SSc development. (2) The lack of availability of lung biopsy samples from SSc-ILD precluded studies of genetic effects on lung transcriptome of patients with or without H90 variant carriage. To this end, we explored DE genes in lung tissues using a murine BLM-induced fibrosis model based on H90 KI mice, and the results of mice lung transcriptome was consistent with the CyTOF results of PBMCs from patients with SSc. (3) The skin lesions in BLM-treated mice was unable to assess, because the skin fibrosis peaked in the early phase of the model (10 days) while the lung fibrosis was increased in the late phase (28 days) [15]. Our

primary focus is to assess genotype effects on lung fibrosis, we sacrificed the mice at day 28 post-BLM treatment and observed no significant change in dermal thickness between BLM-treated and PBS-treated mice. We would assess the genetic effects of the H90 variant on skin fibrosis in future work. (4) We were unable to isolate sufficient numbers of the newly CyTOF-defined $CD14^+CD68^+CD11b^+Tim3^+$ monocytes from SSc PBMCs to differentiate into MoMs to establish their direct relationship. However, the dose-dependent increase in the total number of monocytes from the H90 group, which had a higher GAP index and mRSS (figure 4B) and the positive correlation of proportions of the newly defined monocyte subset with GAP index and mRSS (figure 4C) inferred a relationship between the $CD14^+CD68^+CD11b^+Tim3^+$ monocytes and the profibrotic $SPP1^+$ MoMs cultured from total monocytes isolated from SSc PBMCs.

In summary, the hypofunctional *NCF1*-H90 variant was associated with susceptibility to SSc, especially for dcSSc with lung fibrosis. H90 patients had an abnormally increased monocyte subset in peripheral blood, which could differentiate into profibrotic $SPP1^+$ macrophages in a CCL2-dependent manner. The CCL2-SPP1-ARG1 axis is a potential therapeutic target in SSc, particularly in the patients with dcSSc carrying the H90 variant.

Correction notice

This article has been corrected since it published Online First. A corresponding author has been added.

Acknowledgments

We thank Professor Xiaodong Han for her help in the study design, Dr Ziyi Jin, Yujiao Wang, Xiaojun Tang and Shu Liu for their excellent technical assistance and all the patients and healthy controls for kindly participating in this research.

Contributors

BPT, LS and CF-B designed the study. SA, XZ and XX provided the DNA samples of patients with systemic sclerosis (SSc). XY, KT, YZ and MS conducted the animal experiments. KLH provided histology assessment of mouse lung tissues. JZ performed genotyping and association studies. XY and XQ performed the longitudinal study of patients with SSc. XY, XQ and DW performed the cytometry by time-of-flight and in vitro experiments for patients with SSc. XY, XQ and BJW analysed data and performed statistical analyses. BPT, XY and XQ drafted the manuscript. All authors edited and reviewed the manuscript. BPT is responsible for the overall content as guarantor.

Funding

This work was supported by the National Scleroderma Foundation (grant to BPT), NIH R21 AR081933-01A1 (grant to BPT), MUSC COMETS-PPG (grant to BPT) and NIH/NIAMS R01 AR081280 (grant to SA).

Competing interests

None declared.

Patient and public involvement

Patients and/or the public were not involved in the design, or conduct, or reporting, or dissemination plans of this research.

Patient consent for publication

Not applicable.

Ethics approval

Humans participants were recruited with informed consents approved by the Ethics Committee of the Affiliated Drum Tower Hospital of Nanjing University Medical School (No. 2009004), Medical University of South Carolina IRB (Pro00049290), University of Texas Health Science Center at Houston IRB (HSC-MS-08-0578), University of California, Los Angeles IRB(10-001489) and Oklahoma Medical Research Foundation (95-12 and 06-12). Participants gave informed consent to participate in the study before taking part.

Data availability statement

All data relevant to the study are included in the article or uploaded as supplementary information.

Supplemental material

Supplementary material associated with this article can be found in the online version at doi:10.1136/ard-2024-226034.

Orcid

Xinran Yuan: http://orcid.org/0009-0008-3132-9200
Xiaodong Qin: http://orcid.org/0000-0001-7655-2635
Judith A. James: http://orcid.org/0000-0002-9574-7355
Shervin Assassi: http://orcid.org/0000-0002-8059-9978
Carol Feghali-Bostwick: http://orcid.org/0000-0002-6750-6407
Lingyun Sun: http://orcid.org/0000-0002-8563-2036
Betty P. Tsao: http://orcid.org/0000-0001-7938-5975

REFERENCES

[1] Tsou PS, Sawalha AH. Unfolding the pathogenesis of scleroderma through genomics and epigenomics. J Autoimmun 2017;83:73–94. doi: 10.1016/j.jaut.2017.05.004.
[2] López-Isac E, Acosta-Herrera M, Kerick M, et al. GWAS for systemic sclerosis identifies multiple risk loci and highlights fibrotic and vasculopathy pathways. Nat Commun 2019;10:4955. doi: 10.1038/s41467-019-12760-y.
[3] López-Isac E, Campillo-Davo D, Bossini-Castillo L, et al. Influence of TYK2 in systemic sclerosis susceptibility: a new locus in the IL-12 pathway. Ann Rheum Dis 2016;75:1521–6. doi: 10.1136/annrheumdis-2015-208154.
[4] Radstake TRDJ, Gorlova O, Rueda B, et al. Genome-wide association study of systemic sclerosis identifies CD247 as a new susceptibility locus. Nat Genet 2010;42:426–9. doi: 10.1038/ng.565.
[5] Zhao J, Ma J, Deng Y, et al. A missense variant in NCF1 is associated with susceptibility to multiple autoimmune diseases. Nat Genet 2017;49:433–7. doi: 10.1038/ng.3782.
[6] Geng L, Zhao J, Deng Y, et al. Human SLE variant NCF1-R90H promotes kidney damage and murine lupus through enhanced Tfh2 responses induced by defective efferocytosis of macrophages. Ann Rheum Dis 2022;81:255–67. doi: 10.1136/annrheumdis-2021-220793.
[7] Meng Y, Ma J, Yao C, et al. The NCF1 variant p.R90H aggravates autoimmunity by facilitating the activation of plasmacytoid dendritic cells. J Clin Invest 2022;132:e153619. doi: 10.1172/JCI153619.

[8] Luo H, Urbonaviciute V, Saei AA, et al. NCF1-dependent production of ROS protects against lupus by regulating plasmacytoid dendritic cell development and functions. JCI Insight 2023;8:e164875. doi: 10.1172/jci.insight.164875.
[9] Liu S, Lagos J, Shumlak NM, et al. NADPH oxidase exerts a B cell-intrinsic contribution to lupus risk by modulating endosomal TLR signals. J Exp Med 2024;221:e20230774. doi: 10.1084/jem.20230774.
[10] Brkic Z, van Bon L, Cossu M, et al. The interferon type I signature is present in systemic sclerosis before overt fibrosis and might contribute to its pathogenesis through high BAFF gene expression and high collagen synthesis. Ann Rheum Dis 2016;75:1567–73. doi: 10.1136/annrheumdis-2015-207392.
[11] Muskardin TLW, Niewold TB. Type I interferon in rheumatic diseases. Nat Rev Rheumatol 2018;14:214–28. doi: 10.1038/nrrheum.2018.31.
[12] LeRoy EC, Black C, Fleischmajer R, et al. Scleroderma (systemic sclerosis): classification, subsets and pathogenesis. J Rheumatol 1988;15:202–5.
[13] Elhai M, Meune C, Boubaya M, et al. Mapping and predicting mortality from systemic sclerosis. Ann Rheum Dis 2017;76:1897–905. doi: 10.1136/annrheumdis-2017-211448.
[14] Steen VD, Medsger TA. Changes in causes of death in systemic sclerosis, 1972-2002. Ann Rheum Dis 2007;66:940–4. doi: 10.1136/ard.2006.066068.
[15] Watanabe T, Nishimoto T, Mlakar L, et al. Optimization of a murine and human tissue model to recapitulate dermal and pulmonary features of systemic sclerosis. PLoS One 2017;12:e0179917. doi: 10.1371/journal.pone.0179917.
[16] Lee R, Reese C, Bonner M, et al. Bleomycin delivery by osmotic minipump: similarity to human scleroderma interstitial lung disease. Am J Physiol Lung Cell Mol Physiol 2014;306:L736–48. doi: 10.1152/ajplung.00210.2013.
[17] Marangoni RG, Varga J, Tourtellotte WG. Animal models of scleroderma: recent progress. Curr Opin Rheumatol 2016;28:561–70. doi: 10.1097/BOR.0000000000000331.
[18] Feng X, Wu H, Grossman JM, et al. Association of increased interferon-inducible gene expression with disease activity and lupus nephritis in patients with systemic lupus erythematosus. Arthritis Rheum 2006;54:2951–62. doi: 10.1002/art.22044.
[19] Hübner R-H, Gitter W, El Mokhtari NE, et al. Standardized quantification of pulmonary fibrosis in histological samples. Biotechniques 2008;44:507–11. doi: 10.2144/000112729.
[20] Dong B, Wu C, Huang L, et al. Macrophage-Related SPP1 as a Potential Biomarker for Early Lymph Node Metastasis in Lung Adenocarcinoma. Front Cell Dev Biol 2021;9:739358. doi: 10.3389/fcell.2021.739358.
[21] Cabrera-Benítez NE, Parotto M, Post M, et al. Mechanical stress induces lung fibrosis by epithelial-mesenchymal transition. Crit Care Med 2012;40:510–7. doi: 10.1097/CCM.0b013e31822f09d7.
[22] D'Angelo RC, Liu X-W, Najy AJ, et al. TIMP-1 via TWIST1 induces EMT phenotypes in human breast epithelial cells. Mol Cancer Res 2014;12:1324–33. doi: 10.1158/1541-7786.MCR-14-0105.
[23] Gibbons MA, MacKinnon AC, Ramachandran P, et al. Ly6Chi monocytes direct alternatively activated profibrotic macrophage regulation of lung fibrosis. Am J Respir Crit Care Med 2011;184:569–81. doi: 10.1164/rccm.201010-1719OC.
[24] Hoeft K, Schaefer GJL, Kim H, et al. Platelet-instructed SPP1^{+} macrophages drive myofibroblast activation in fibrosis in a CXCL4-dependent manner. Cell Rep 2023;42:112131. doi: 10.1016/j.celrep.2023.112131.
[25] Osterholzer JJ, Olszewski MA, Murdock BJ, et al. Implicating exudate macrophages and Ly-6C(high) monocytes in CCR2-dependent lung fibrosis following gene-targeted alveolar injury. J Immunol 2013;190:3447–57. doi: 10.4049/jimmunol.1200604.
[26] Yokoyama N, Kawasaki A, Matsushita T, et al. Association of NCF1 polymorphism with systemic lupus erythematosus and systemic sclerosis but not with ANCA-associated vasculitis in a Japanese population. Sci Rep 2019;9:16366. doi: 10.1038/s41598-019-52920-0.
[27] Liang M, Lv J, Zou L, et al. A modified murine model of systemic sclerosis: bleomycin given by pump infusion induced skin and pulmonary inflammation and fibrosis. Lab Invest 2015;95:342–50. doi: 10.1038/labinvest.2014.145.
[28] Linge P, Arve S, Olsson LM, et al. NCF1-339 polymorphism is associated with altered formation of neutrophil extracellular traps, high serum interferon activity and antiphospholipid syndrome in systemic lupus erythematosus. Ann Rheum Dis 2020;79:254–61. doi: 10.1136/annrheumdis-2019-215820.
[29] Olsson LM, Johansson ÅC, Gullstrand B, et al. A single nucleotide polymorphism in the NCF1 gene leading to reduced oxidative burst is associated with systemic lupus erythematosus. Ann Rheum Dis 2017;76:1607–13. doi: 10.1136/annrheumdis-2017-211287.
[30] Taroni JN, Greene CS, Martyanov V, et al. A novel multi-network approach reveals tissue-specific cellular modulators of fibrosis in systemic sclerosis. Genome Med 2017;9:27. doi: 10.1186/s13073-017-0417-1.
[31] Morse C, Tabib T, Sembrat J, et al. Proliferating SPP1/MERTK-expressing macrophages in idiopathic pulmonary fibrosis. Eur Respir J 2019;54:1802441. doi: 10.1183/13993003.02441-2018.
[32] Christmann RB, Sampaio-Barros P, Stifano G, et al. Association of Interferon- and transforming growth factor β-regulated genes and macrophage activation with systemic sclerosis-related progressive lung fibrosis. Arthritis Rheumatol 2014;66:714–25. doi: 10.1002/art.38288.
[33] Kamiya M, Carter H, Espindola MS, et al. Immune mechanisms in fibrotic interstitial lung disease. Cell 2024;187:3506–30. doi: 10.1016/j.cell.2024.05.015.
[34] Gao X, Jia G, Guttman A, et al. Osteopontin Links Myeloid Activation and Disease Progression in Systemic Sclerosis. Cell Rep Med 2020;1:100140. doi: 10.1016/j.xcrm.2020.100140.
[35] Jia G, Ramalingam TR, Heiden JV, et al. An interleukin 6 responsive plasma cell signature is associated with disease progression in systemic sclerosis interstitial lung disease. i Sci 2023;26:108133. doi: 10.1016/j.isci.2023.108133.
[36] Valenzi E, Tabib T, Papazoglou A, et al. Disparate Interferon Signaling and Shared Aberrant Basaloid Cells in Single-Cell Profiling of Idiopathic Pulmonary Fibrosis and Systemic Sclerosis-Associated Interstitial Lung Disease. Front Immunol 2021;12:595811. doi: 10.3389/fimmu.2021.595811.
[37] Ji J, Zheng S, Liu Y, et al. Increased expression of OPN contributes to idiopathic pulmonary fibrosis and indicates a poor prognosis. J Transl Med 2023;21:640. doi: 10.1186/s12967-023-04279-0.
[38] Carulli MT, Handler C, Coghlan JG, et al. Can CCL2 serum levels be used in risk stratification or to monitor treatment response in systemic sclerosis? Ann Rheum Dis 2008;67:105–9. doi: 10.1136/ard.2006.067967.
[39] Bandinelli F, Del Rosso A, Gabrielli A, et al. CCL2, CCL3 and CCL5 chemokines in systemic sclerosis: the correlation with SSc clinical features and the effect of prostaglandin E1 treatment. Clin Exp Rheumatol 2012;30:S44–9.
[40] Wu M, Baron M, Pedroza C, et al. CCL2 in the Circulation Predicts Long-Term Progression of Interstitial Lung Disease in Patients With Early Systemic Sclerosis: Data From Two Independent Cohorts. Arthritis Rheumatol 2017;69:1871–8. doi: 10.1002/art.40171.
[41] Hinchcliff M, Toledo DM, Taroni JN, et al. Mycophenolate Mofetil Treatment of Systemic Sclerosis Reduces Myeloid Cell Numbers and Attenuates the Inflammatory Gene Signature in Skin. J Invest Dermatol 2018;138:1301–10. doi: 10.1016/j.jid.2018.01.006.
[42] Yager N, Cole S, Lledo Lara A, et al. Ex vivo mass cytometry analysis reveals a profound myeloid proinflammatory signature in psoriatic arthritis synovial fluid. Ann Rheum Dis 2021;80:1559–67. doi: 10.1136/annrheumdis-2021-220280.
[43] Zhang Y, Du W, Chen Z, et al. Upregulation of PD-L1 by SPP1 mediates macrophage polarization and facilitates immune escape in lung adenocarcinoma. Exp Cell Res 2017;359:449–57. doi: 10.1016/j.yexcr.2017.08.028.
[44] Almuntashiri S, Alhumaid A, Zhu Y, et al. TIMP-1 and its potential diagnostic and prognostic value in pulmonary diseases. Chin Med J Pulm Crit Care Med 2023;1:67–76. doi: 10.1016/j.pccm.2023.05.002.
[45] Ciechomska M, Huigens CA, Hügle T, et al. Toll-like receptor-mediated, enhanced production of profibrotic TIMP-1 in monocytes from patients with systemic sclerosis: role of serum factors. Ann Rheum Dis 2013;72:1382–9. doi: 10.1136/annrheumdis-2012-201958.
[46] Toubi E, Kessel A, Grushko G, et al. The association of serum matrix metalloproteinases and their tissue inhibitor levels with scleroderma disease severity. Clin Exp Rheumatol 2002;20:221–4.
[47] Lesiak A, Narbutt J, Sysa-Jedrzejowska A, et al. Effect of chloroquine phosphate treatment on serum MMP-9 and TIMP-1 levels in patients with systemic lupus erythematosus. Lupus (Los Angel) 2010;19:683–8. doi: 10.1177/0961203309356455.
[48] Jiang Z, Sui T, Wang B. Relationships between MMP-2, MMP-9, TIMP-1 and TIMP-2 levels and their pathogenesis in patients with lupus nephritis. Rheumatol Int 2010;30:1219–26. doi: 10.1007/s00296-009-1135-9.
[49] Vira HJ, Pradhan VD, Umare VD, et al. Expression of the matrix metalloproteinases MMP-2 and MMP-9 and their inhibitors TIMP-1 and TIMP-2 in systemic lupus erythematosus patients. Neth J Med 2020;78:261–8.
[50] Moreno-Moral A, Bagnati M, Koturan S, et al. Changes in macrophage transcriptome associate with systemic sclerosis and mediate GSDMA contribution to disease risk. Ann Rheum Dis 2018;77:596–601. doi: 10.1136/annrheumdis-2017-212454.
[51] Trombetta AC, Soldano S, Contini P, et al. A circulating cell population showing both M1 and M2 monocyte/macrophage surface markers characterizes systemic sclerosis patients with lung involvement. Respir Res 2018;19:186. doi: 10.1186/s12931-018-0891-z.
[52] Li Q, Zhong J, Luo H, et al. Two major genes associated with autoimmune arthritis, Ncf1 and Fcgr2b, additively protect mice by strengthening T cell tolerance. Cell Mol Life Sci 2022;79:482. doi: 10.1007/s00018-022-04501-0.
[53] Olmes G, Büttner-Herold M, Ferrazzi F, et al. CD163+ M2c-like macrophages predominate in renal biopsies from patients with lupus nephritis. Arthritis Res Ther 2016;18:90. doi: 10.1186/s13075-016-0989-y.

Ann Rheum Dis 84 (2025) 307–318

Contents lists available at ScienceDirect

Annals of the Rheumatic Diseases

journal homepage: https://www.sciencedirect.com/journal/annals-of-the-rheumatic-diseases

Myositis

Precise identification and tracking of HMGCR-reactive CD4 + T cells in the target tissue of patients with anti-HMGCR immune-mediated necrotising myopathy

Eleni Tiniakou[1,*], Alex Girgis[1,2], Tiara Siafei[1], Jemima Albayda[1], Brittany Adler[1], Julie J. Paik[1], Christopher A. Mecoli[1], Alison Rebman[1], Mark J. Soloski[1], Lisa Christopher-Stine[1], Kellie N. Smith[3], Antony Rosen[1], Andrew Lee Mammen[1,4,5], Erika Darrah[1]

[1] *Division of Rheumatology, Johns Hopkins University, School of Medicine, Baltimore, MD, USA*
[2] *Department of Biomedical Engineering, The Johns Hopkins University School of Medicine, Baltimore, Maryland, USA*
[3] *Department of Oncology and the Bloomberg-Kimmel Institute for Cancer Immunotherapy and Sidney Kimmel Comprehensive Cancer Center, The Johns Hopkins University School of Medicine, Baltimore, Maryland, USA*
[4] *NIAMS/NIH, Bethesda, Maryland, USA*
[5] *Division of Neurology, Johns Hopkins University, School of Medicine, Baltimore, MS, USA*

ARTICLE INFO

Article history:
Received 27 February 2024
Accepted 18 September 2024

Keywords:
Polymyositis
T-Lymphocytes
Autoimmunity

ABSTRACT

Background: Anti-3-hydroxy-3-methylglutaryl coenzyme A reductase (HMGCR)-positive immune-mediated necrotising myopathy (IMNM) is characterised by the presence of IgG autoantibodies against HMGCR and a strong association with specific HLA-DR alleles. Although these findings implicate HMGCR-specific $CD4^+$T-cells in the disease's pathogenesis, no such cells have been described. In this study, we aimed to identify and characterise HMGCR-reactive $CD4^+$T-cells and assess their presence in affected muscle tissue from patients with anti-HMGCR + IMNM.

Methods: Peripheral blood mononuclear cells from patients with anti-HMGCR + IMNM (n = 10) and dermatomyositis (DM; n = 10) were stimulated with HMGCR protein and peptides identified using a natural antigen processing assay (NAPA; n = 6). $CD4^+$T-cell activation was assessed by CD154 upregulation via flow cytometry. T-cell receptor β(TCR) sequencing was performed on paired HMGCR-reactive T-cells and muscle biopsy tissue (n = 5).

Results: $CD4^+$T-cell responses to HMGCR protein were higher in patients with anti-HMGCR + IMNM compared with DM (median 0.06 vs 0.00, p = 0.0059). These responses were enriched in Th1-Th17 cells, and when present, they positively correlated with anti-HMGCR antibody levels ($r^2 = 0.89$, p = 0.0012). NAPA revealed convergent presentation of seven HMGCR core peptides, with substantial overlap in the peptide repertoires between patients. These HMGCR peptides elicited robust $CD4^+$T-cell responses, with 9/10 anti-HMGCR + IMNM patients responding to at least one peptide, compared with 1/10 DM (p = 0.0003). Analysis of HMGCR-reactive TCRs β yielded antigen-reactive motifs that were enriched in muscle biopsies (projection score 0.03 vs 0.63, p = 0.007).

*Correspondence to Dr. Eleni Tiniakou.
E-mail address: etiniak1@jhmi.edu (E. Tiniakou).
Social media: @EleniTiniakou (E. Tiniakou)
Handling editor Josef S. Smolen.
ALM and ED contributed equally.

https://doi.org/10.1136/ard-2024-225732

Conclusion: HMGCR-antigen-reactive CD4$^+$ T-cells are present in the circulation and target tissue of patients with anti-HMGCR + IMNM, suggesting an active role for these cells in the pathogenesis of anti-HMGCR + IMNM.

WHAT IS ALREADY KNOWN ON THIS TOPIC

- Anti-3-hydroxy-3-methylglutaryl coenzyme A reductase (HMGCR) + immune-mediated necrotising myopathy (IMNM) has the strongest MHC class II association among all rheumatic diseases.

WHAT THIS STUDY ADDS

- Patients with anti-HMGCR + IMNM possess HMGCR-reactive CD4$^+$ T cells, which are skewed towards a Th1-17 phenotype.
- The T cell β chain repertoire in the affected muscle of patients with anti-HMGCR + IMNM exhibits strong similarities across patients and is enriched in HMGCR-reactive CD4 + T cells.

HOW THIS STUDY MIGHT AFFECT RESEARCH, PRACTICE OR POLICY

- The existence of anti-HMGCR reactive CD4 + T cells in the target tissue suggests their potential involvement in the pathogenesis of anti-HMGCR + IMMM. This finding may lead to the development of antigen-specific monitoring tools and innovative therapeutic interventions for patients with anti-HMGCR + IMMM.

INTRODUCTION

Anti-3-hydroxy-3-methylglutaryl coenzyme A reductase (HMGCR)-positive immune-mediated necrotising myopathy (anti-HMGCR + IMNM) is a subtype of idiopathic inflammatory myopathy (IIM) characterised by severe muscle weakness, highly elevated creatine phosphokinase (CPK), and muscle biopsies showing significant myofiber necrosis and sparse inflammatory infiltrates, with minimal extramuscular manifestations [1]. The defining characteristic of this disease is the presence of IgG autoantibodies targeting HMGCR [2,3]. An additional noteworthy feature of anti-HMGCR + IMNM is the striking association with a specific HLA class II allele, *HLA-DRB1**11:01, which has the highest HLA association observed among all rheumatic diseases [4]. This association has been replicated in diverse, international cohorts and has an OR of 2.52–56.5 for anti-HMGCR + IMNM, depending on the study [5–10]. Moreover, the *HLA-DRB1**07:01 has been linked with the disease in a small study of children with anti-HMGCR + IMNM [11]. Although the presence of anti-HMGCR IgG and the robust association with specific major histocompatibility complex (MHC) class II alleles strongly implicate HMGCR-specific CD4$^+$ T helper cells in disease pathogenesis, such cells have never been described.

*HLA-DRB1**11:01 and *HLA-DRB1**07:01 are MHC class II alleles, which encode for HLA-DR molecules present on antigen-presenting cells (APCs). APCs' role is to phagocytose and process any encountered antigen into peptides, which are then loaded onto the HLA-DR molecules and transported to the surface. CD4$^+$ T cells recognise these peptide/HLA-DR complexes and can facilitate antibody secretion by B cells recognising the same antigen. HLA alleles are theorised to present epitopes recognised by T cells, and studying the peptide-HLA interface can provide novel insights into disease mechanisms [12–15]. In anti-HMGCR + IMNM, HMGCR-specific CD4$^+$ T cells would provide help to HMGCR-specific B cells for the production of anti-HMGCR autoantibodies pathognomonic for this disease. Despite the importance of this step in the initiation of HMGCR-specific humoral response and potential contribution to muscle inflammation, HMGCR antigen natural processing and recognition of its epitopes by CD4$^+$ T cells have not been studied.

Here, our aim was to identify anti-HMGCR reactive CD4$^+$ T cells, outline the repertoire of HMGCR CD4$^+$ T cell epitopes consequent of the natural processing of HMGCR protein by patient-derived APCs, and track HMGCR-reactive T cells in the target tissue of patients, namely the muscle. Defining the repertoire of HMGCR CD4$^+$ T cell epitopes and their corresponding TCRs is a crucial step in understanding disease mechanisms in patients with anti-HMGCR + IMNM and provides a basis for the future development of HMGCR-specific research and therapeutic tools.

MATERIALS AND METHODS

Detailed methods are provided in online supplemental methods.

RESULTS

Patients with anti-HMGCR + IMNM possess HMGCR-reactive CD4$^+$ T cells

We initially sought to define whether HMGCR-reactive CD4$^+$ T cells were present in patients with anti-HMGCR + IMNM. To achieve this, we randomly selected patients with newly or previously diagnosed anti-HMGCR + IMNM (n = 10) who were evaluated for clinical care and consented for our longitudinal myositis cohort and stimulated their peripheral blood mononuclear cells (PBMCs) with HMGCR protein. CD4$^+$ T cell activation was then evaluated by measuring surface expression of the early activation marker CD154 by flow cytometry [15,16]. To determine specificity of the responses for anti-HMGCR + IMNM, we also stimulated PBMCs from randomly selected patients with dermatomyositis (DM) (n = 10) from our longitudinal myositis cohort as disease controls. Please see online supplemental tables 1–3 for clinical characteristics and HLA typing. We observed significantly higher CD4$^+$ T cell responses to HMGCR protein in patients with anti-HMGCR + IMNM compared with those with DM (median 0.06% vs 0.00% CD154$^+$ CD4$^+$ T cells, p = 0.0059) (figure 1A). Importantly, no significant differences were observed between the two groups in their response to CEFT (a positive control pool of peptides derived from infectious antigens) (online supplemental file 1A), or an irrelevant peptide from POLR3, employed as negative control (online supplemental file 1B).

Since the production of class-switched antibodies relies on assistance from CD4$^+$ T cells, we next examined whether the magnitude of the T cell response to HMGCR correlated with the levels of anti-HMGCR antibodies. Two of the patients did not respond to the HMGCR molecule but still had measurable autoantibody titre (online supplemental figure 2). We observed a positive correlation between anti-HMGCR antibody levels and the percentage of CD154$^+$ CD4$^+$ T cells, in eight patients with a detectable T cell response ($r^2 = 0.8934$, p = 0.0012) (figure 1B). While anti-HMGCR antibody titres were found to correlate with proximal muscle weakness and elevated CPK in our previous large cohort study [17], neither anti-HMGCR antibody levels

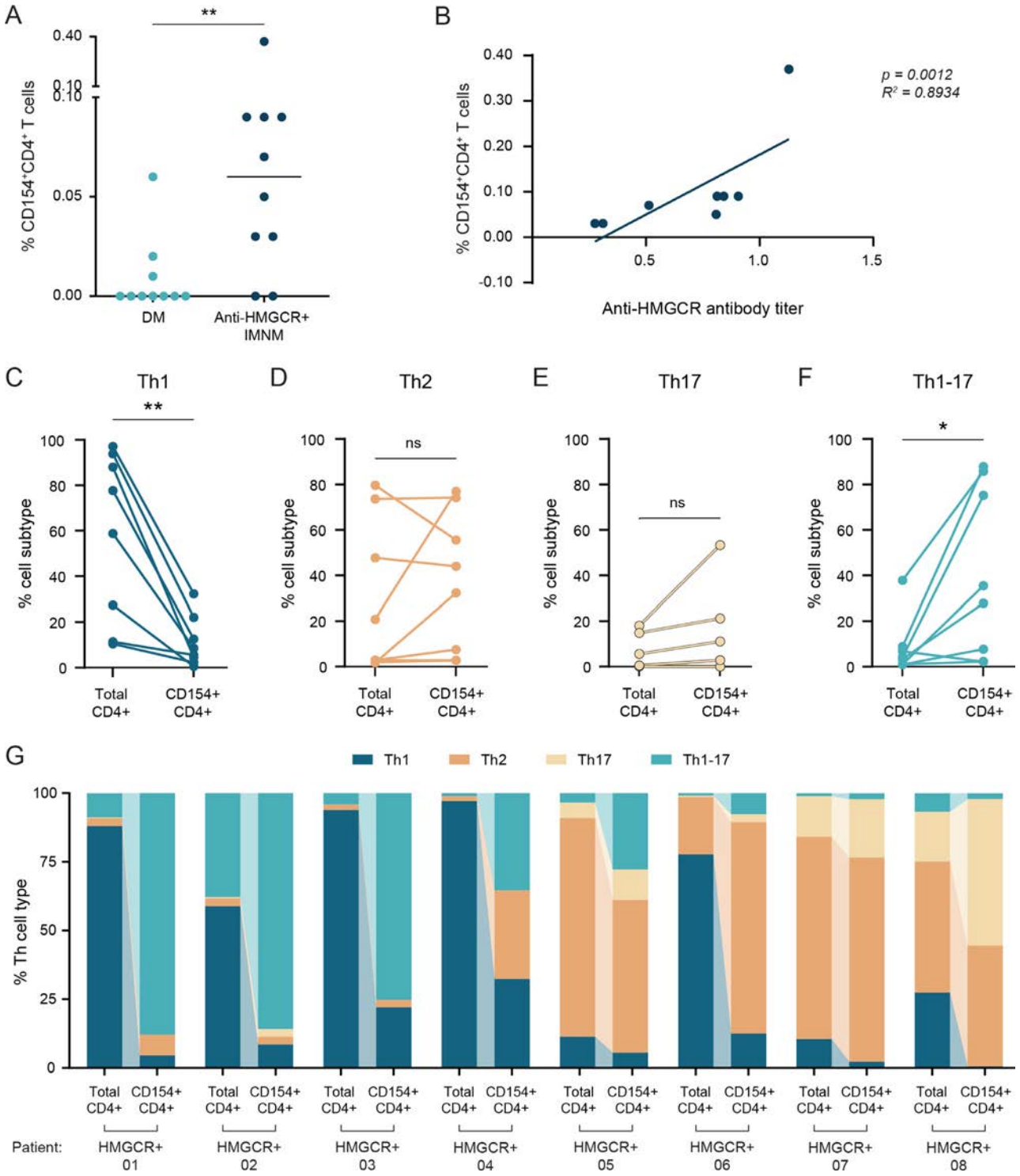

Figure 1. HMGCR-reactive CD4$^+$ T cells in patients with anti-HMGCR + IMNM correlate with the anti-HMGCR antibody titre and are preferentially Th1/17 subtype. (A) %CD154$^+$CD4$^+$ T cell responses over background plotted for 10 patients with anti-HMGCR + IMNM and 10 patients with DM. (B) The %CD154$^+$CD4$^+$ T cells in each anti-HMGCR + IMNM patient with a detectable T cell response (n = 8) was plotted against the level of anti-HMGCR antibodies measured in paired serum and analysed using a Spearman's r test. (C–G) Distribution of CD4$^+$ T helper subsets in the total CD4$^+$ or the CD154$^+$CD4$^+$ T cell population. * = p<0.05, ** = p <0.01. DM, dermatomyositis; HMGCR, hydroxy-3-methylglutaryl coenzyme A reductase; IMNM, immune-mediated necrotising myopathy.

nor T cell responses correlated with CPK or muscle strength (anti-HMGCR titre vs CPK, p = 0.63; anti-HMGCR titre vs strength, p = 0.52; CPK vs strength, p = 0.52, T cells vs CPK, p = 0.15; T cells vs strength, p = 0.12), likely owing to the small sample size.

We next characterised the phenotype of the CD154$^+$ CD4$^+$ T helper cells, using a combination of surface markers that have been shown to discriminate between Th1 (CCR6–, CCR4–, CXCR3+), Th2 (CCR6–, CCR4+, CXCR3–), Th17 (CCR6+, CCR4+, CXCR3–) and Th1/17 (CCR6+, CCR4–, CXCR3+) cells [18]. Although there was significant heterogeneity in the distribution of Th subtypes among patients within the total CD4$^+$ T cell population, when we compared with the total CD4$^+$ T cell population in each patient, HMGCR-reactive CD4$^+$ T cells preferentially exhibited a Th1/17 (p = 0.0234) phenotype and were less likely to be Th1 only (p = 0.0078) (figure 1C–G).

Given the strong association of anti-HMGCR + IMNM with specific *HLA-DRB1* alleles [4,6−8,11], we next performed immunogenetic analysis to determine whether the CD4$^+$ T cell responses to HMGCR were linked to specific HLA variants. In our study group, 60% (6/10) of individuals with anti-HMGCR + IMNM harboured one or more *HLA-DRB1*11:01* alleles and none possessed the *HLA-DRB1*07:01* variant (online supplemental table 3). This is consistent with the literature showing that, while these alleles are associated with anti-HMGCR + IMNM, they are not required for the development of anti-HMGCR antibodies or the disease [4]. The magnitude of the CD4$^+$ T cell response to HMGCR was also not significantly higher in patients with *HLA-DRB1*11:01* compared with those who were negative for this allele (median 0.09 vs 0.03, p = 0.1429) (online supplemental figure 3A). To further verify that these responses were specific for the disease status and not the HLA allele, we screened five healthy controls carrying *HLA-DRB1*11:01*. Indeed, the response to HMGCR protein was disease specific and was not observed in the healthy controls with the same *DRB1*11:01* allele (median 0.09 vs 0.00, p = 0.0498) (online supplemental figure 3B). Together, these data revealed that HMGCR-reactive CD4$^+$ T cells are present in and specific for anti-HMGCR + IMNM.

Precise definition of the HMGCR-reactive CD4$^+$ T cell epitope repertoire in anti-HMGCR + IMNM using natural antigen processing assay

To define the landscape of HMGCR peptides that could be presented on HLA-DR molecules to autoreactive CD4$^+$ T cells in anti-HMGCR + IMNM, we studied the processing and presentation of HMGCR protein by monocyte-derived dendritic cells (mo-DCs) from individuals with anti-HMGCR + IMNM who had different combinations of disease-associated and non-associated HLA-DRB1 variants using natural antigen processing assay (NAPA), as previously described [15]. Six individuals were studied including two individuals who were heterozygous for *HLA-DRB1*11:01* (one of whom also carried *HLA-DRB1*07:01*), one individual heterozygous for *HLA-DRB1*07:01* and three individuals who developed anti-HMGCR + IMNM but did not carry a known risk allele (figure 2A). Using this approach, we identified more than 300 naturally processed HMGCR peptides ranging from 12 to 22 amino acids in length (median length 15 amino acids), which clustered into nested sets, features typical of naturally presented HLA-DR peptides (figure 2A and online supplemental material).

Remarkably, and consistent with our previous study in patients with systemic sclerosis [15], the HMGCR peptides presented by these diverse HLA molecules originated from only seven distinct domains of the protein, with common peptides presented between immunogenetically distinct individuals (figure 2A). Each patient presented peptides from 1 to 5 distinct regions of the HMGCR protein (median 3 regions), and 5 out of the 7 regions were presented by at least 2 patients. Analysis of the location of the peptides within the quaternary structure of the HMGCR tetramer revealed that, although peptides 1 (394-412 aa), 2 (406-427 aa) and 3 (417-435 aa) could not be visualised due to limitations of the crystal structure available for HMGCR, peptides 5 (625-637), 6 (653-673) and 7 (745-759), presented by 2−3 patients, clustered together at the monomer interfaces of the HMGCR tetramer (figure 2B). This is in contrast to HMGCR peptide 4 (463-480 aa), which was presented by five out of six patients and was located in a distant, solvent-exposed structural portion of the HMGCR monomer that connects the C-terminal catalytic domain to the N-terminal transmembrane portion of HMGCR and is part of a α-helix/β-strand/α helix conformation. Interestingly, the two sites for the NADP(+) molecules of the enzyme are located within peptides 5 (625-637) and 6 (653-673). Given the significant overlap in HMGCR naturally presented peptides among patients with diverse *HLA-DRB1* alleles, we hypothesised that it could be due to (1) the presentation of a common set of HMGCR peptides by a shared motif in the binding groove of the different HLA molecules and (2) an inherent ability of HMGCR peptides to be promiscuously presented by diverse HLA pockets. To define the relative contribution of these two factors to HMGCR peptide presentation, we performed amino acid sequence alignment of the HLA-DRβ chains in these patients and used the β chain of the HLA-DR*11:01 variant as a reference [19]. Interestingly, HLA-DRB1*11:01 and *07:01, which have been associated with anti-HMGCR + IMNM in adults and children respectively, have the most dissimilar peptide binding grooves of our study patients. While the *HLA-DRB1*11:01* allele encodes an EYSTSE motif at positions 9−14 of the peptide binding groove, *HLA-DRB1*07:01* encodes for the distinct WQGKYK motif at this position. Of the other HLA molecules found in our study patients, 4 (DRB1*08:01, *08:03, *11:04 and *13:02) had peptide binding grooves similar to HLA-DRB1*11:01 (group 1 alleles), while the HLA-DRB1*15:01 and *01:01 variants were more similar to *07:01 (group 2 alleles) (figure 3A). Importantly, four patients in our study carried an allele belonging to each group, and two carried two group 1 alleles, which together could support the presentation of a common set of HMGCR peptides.

Using the NetMHCII algorithm, we next examined the predicted binding affinity of the naturally presented peptides for each of the HLA-DR combinations present in our study patients (figure 3B). HMGCR peptide 4 (463-480 aa), which was presented by five out of the six patients, was predicted to bind with high affinity to all the HLA-DR variants. Interestingly, this promiscuous binding was predicted to be achieved by the peptide possessing two different sets of anchor residues, which would enable binding in different registers to the various HLA-DR molecules (LVNAKHIPA and IQLVNAKHI). Peptides 2 (406-427 aa), 6 (653-673 aa) and 7 (645-759 aa), which were presented by two to three patients each, were also predicted to use different registers to bind, although the predicted affinity for the majority of HLA molecules present in our study population was low. Peptides 1 (394-412 aa), 3 (417-435 aa) and 5 (625-637 aa), which were presented by one or two patients, were predicted to bind using the same register and with high affinity with one of the two possible HLA molecules present in each patient. Together, these data reveal a core set of HMGCR peptides commonly presented by diverse HLA-DR variants present in patients with anti-HMGCR + IMNM, through a combination of promiscuous binding and shared features of the HLA-DR peptide binding groove.

To define whether the naturally presented HMGCR peptides identified using NAPA were capable of driving CD4$^+$ T cell responses, we synthesised seven representative peptides that were inclusive of the amino acids in each nested set (online supplemental table 5). The putative HMGCR epitopes ranged from 13 to 22 amino acids in length and were used to stimulate PBMCs from the same individuals stimulated with whole HMGCR protein in figure 1 (ie, 10 randomly selected patients with anti-HMGCR + IMNM, 10 randomly selected patients with DM as disease controls). CD4$^+$ T cell activation, as measured by CD154 surface expression, was observed in response to at least one HMGCR peptide in 90% (9/10) of patients with anti-

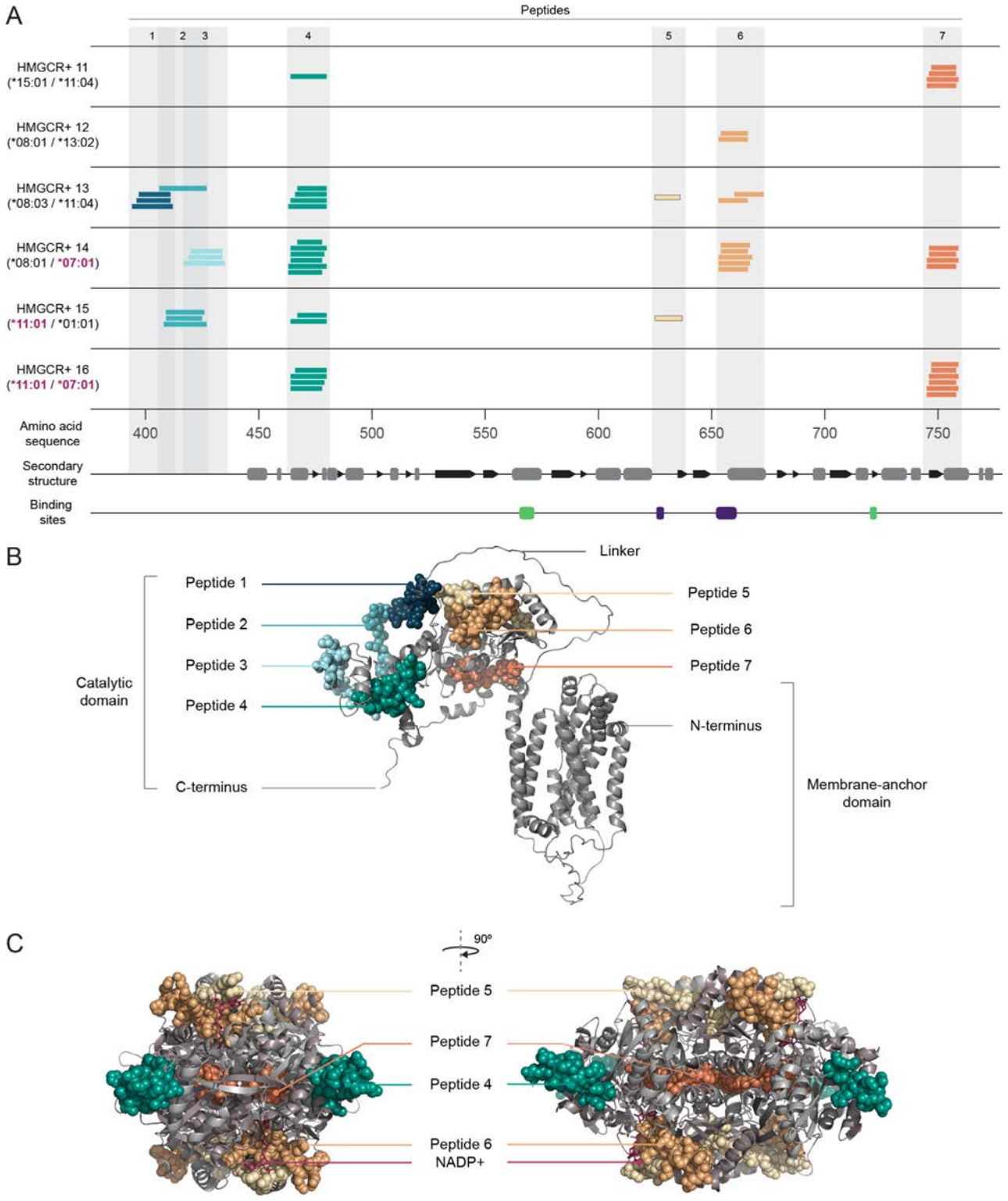

Figure 2. NAPA of monocyte-derived dendritic cells from patients with anti-HMGCR + IMNM reveals a shared set of naturally processed HMGCR peptides. (A) The location of the naturally processed and presented HMGCR peptides from six patients with anti-HMGCR + IMNM is depicted within the linear amino acid sequence of the linker and C-terminal part of the HMGCR protein. The secondary structure is denoted with β-strands represented by arrows and α-helices by ovals. The binding sites for CoA (green squares) and NADP(+) (purple squares) are indicated. (B) and (C) PyMOL structures of the HMGCR monomer predicted by Alpha-Fold AI system (P04035) and HMGCR tetramer (1DQA), respectively. The location of the naturally presented HMGCR peptides is denoted with different colours within the structures. HMGCR, hydroxy-3-methylglutaryl coenzyme A reductase; IMNM, immune-mediated necrotising myopathy; NAPA, natural antigen processing assay.

HMGCR + IMNM, compared with 40% (4/10) of patients with DM ($p = 0.019$). In addition, patients with anti-HMGCR + IMNM responded to more epitopes than the DM (median 1 vs 0; $p = 0.016$) (figure 4A).

Patients with anti-HMGCR + IMNM responded to a significantly higher total number of HMGCR peptides (24/70, 34.29%) compared with DM (5/70, 7.14%) patients ($p = 0.0001$), and they had a higher total percentage of HMGCR-reactive $CD4^+$ T cells (median 0.035% vs 0%, $p<0.0001$) (figure 4B). Focusing on each peptide individually, all peptides, except for peptides 5 and 6, were able to stimulate a significantly higher proportion of $CD4^+$ T cells from patients with anti-

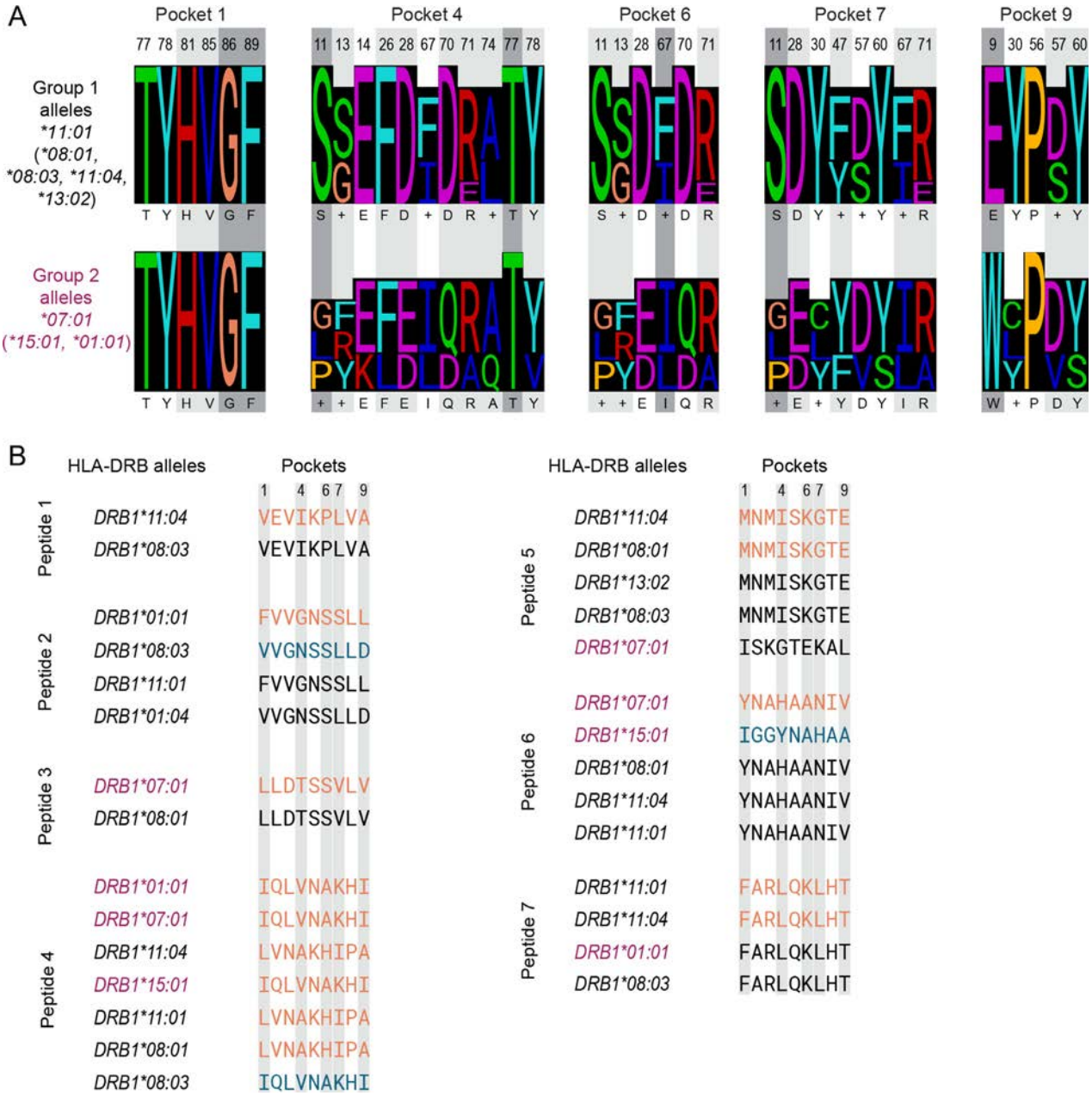

Figure 3. Characteristics of the HLA binding pockets of the patients with anti-HMGCR + IMNM of the NAPA assay, and their respective presenting HMGCR peptides. (A) Consensus amino acid sequence of the peptide contact residues for each binding pocket for group 1 and group 2 alleles. Group 1 encompasses alleles encoding sequences resembling HLA-DRB1*11:01, while group 2 includes alleles encoding sequences akin to HLA-DRB1*07:01. Various tones of grey indicate the importance of individual amino acid residues within the peptide binding pocket, with the deepest shade signifying the highest significance. (B) The anticipated binding core sequences of HMGCR peptides 1–7 for each presenting HLA allele are aligned based on the anchor binding sites to the HLA pockets. Peptides predicted to bind with an affinity of <150 nM are highlighted in orange, while those with an affinity of <500 nM are indicated in blue. The HLA alleles linked to HMGCR + IMNM are identified in purple. HMGCR, hydroxy-3-methylglutaryl coenzyme A reductase; IMNM, immune-mediated necrotising myopathy.

HMGCR + IMNM compared with patients with DM (figure 4C). These data reveal that patients with anti-HMGCR + IMNM mount robust $CD4^+$ T cell responses to a core set of naturally presented HMGCR epitopes.

HMGCR-reactive T cells are present in the target muscle tissue of patients with anti-HMGCR + IMNM

Given our discovery of a common set of HMGCR epitopes recognised by $CD4^+$ T cells in different patients with anti-HMGCR + IMNM, we hypothesised that HMGCR-reactive $CD4^+$ T cells might play a role in disease pathogenesis and may thus be present in the muscle tissue of patients with anti-HMGCR + IMNM. To explore this, we obtained matched PBMCs and muscle biopsy samples from five patients with anti-HMGCR + IMNM (online supplemental table 4). HMGCR-reactive TCRs β chains were first defined by stimulating PBMCs with the individual HMGCR epitopes identified by NAPA and performing TCR β sequencing on the combined bulk sorted $CD154^+$ $CD4^+$ T cells. In parallel, we performed TCRβ sequencing on the matched muscle biopsies of all five individuals to assess TCRβ enrichment in the muscle and on PBMCs from four of the individuals to determine circulating TCRβ frequencies. cytomegalovirus (CMV)-reactive $CD154^+$ $CD4^+$ T cells from the same patients were used to define non-specific TCRs and peripheral blood TCRs β from 45 healthy controls were included as a comparator group.

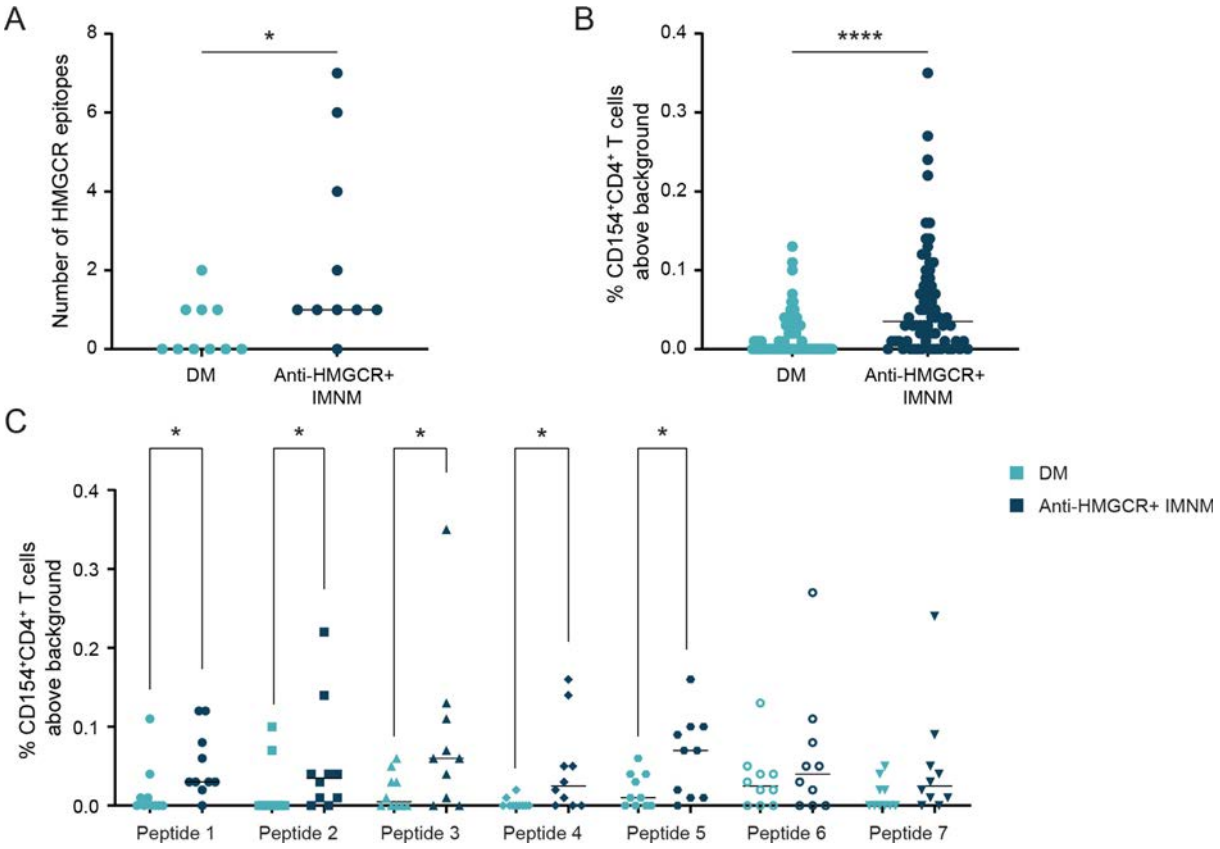

Figure 4. CD4 + T cells responses to naturally presented HMGCR peptides. (A) The number of HMGCR epitopes that eliciti a T cell response in patients with DM and those with anti-HMGCR + IMNM. (B and C) %CD154 + CD4 + T cell responses above background in patients with DM and anti-HMGCR + IMNM presented cumulatively cumulatively for all HMGCR peptides per patient, as well as individually for each peptide. * = p< 0.05, **** = p= or < 0.00001. HMGCR, hydroxy-3-methylglutaryl coenzyme A reductase; IMNM, immune-mediated necrotising myopathy.

Despite the clinical observation that muscle biopsies from anti-HMGCR + IMNM patients generally lack significant inflammatory infiltrates [2,3,20–22], we identified a total of 8849 TCR β sequences with an average of 1450 productive TCRs (range 311-2574) per patient muscle biopsy (table 1). To broadly characterise the TCR β repertoires, the repertoire dissimilarity index (RDI) and Morisita overlap index were first employed as two distinct methods to estimate repertoire similarity among samples. Anti-HMGCR + IMNM muscle biopsies had a lower intragroup RDI and higher Morisita overlap index than the peripheral repertoires of anti-HMGCR + IMNM individuals or healthy controls (figure 5A). These findings demonstrate a high degree of similarity among muscle biopsy repertories between patients, implying that muscle biopsies repertoires are not a random subsampling of the peripheral blood but are rather indicative of a shared antigen-specific immune response. This is also consistent with Shannon's equitability index, a measure of repertoire clonality, which was greater in biopsies than peripheral blood (0.044 vs 0.019, p = 0.023 (online supplemental figure 4). Among over six thousand clonotypes identified in muscle, 7.5% (475/6318) were identified in more than one biopsy, while 2.7% (173/6,318) were identified in more than two of the five biopsies (figure 5B). The number of sequences in common between individual biopsies ranged from 21 to 283 (figure 5C). The overlap coefficient, a normalised measure of sequence overlap, correlated closely with the number of common sequences (figure 5C). TCRβ analysis of the CD154 + CD4 + T cells isolated from the PBMCs of the five individuals with anti-HMGCR + IMNM following stimulation with HMGCR peptides identified productive TCRs β (table 1). Since 19 of these sequences were also found in the CMV stimulation condition, they were excluded from further analysis (online supplemental material). We next examined whether the HMGCR-reactive T cells identified from stimulation of peripheral blood were found within muscle biopsies. Muscle biopsies from these individuals contained an average of 4 (range 0–7) HMGCR-reactive TCRs β, corresponding to 0.32% of all productive TCRβ sequences. This exceeds the frequency of HMGCR-reactive TCRs β identified in the periphery (0.32% vs 0.024%, p = 0.086, online supplemental figure 5). Interestingly, HMGCR-reactive TCRs β in the muscle included those found in the respective patient's stimulated PBMCs as well as HMGCR-reactive TCRs identified in other individuals (figure 5D). Additionally, two clonotypes appeared in the HMGCR-reactive TCRβ population of two different individuals. These findings demonstrate the likely existence of public anti-HMGCR clonotypes and their presence in the muscle of anti-HMGCR + IMNM individuals.

To define a broader set of motifs reactive to HMGCR-reactive TCRs β, we applied the TCR clustering algorithm GIANA to compare all HMGCR-reactive TCRs β identified in stimulated PBMCs to the unsorted peripheral TCRs present in matched PBMCs. Among 2×10^5 clusters generated by GIANA, 118 were enriched for HMGCR-reactive TCRs β relative to the unsorted peripheral repertoire (adjusted p<0.05). (online supplemental material). TRBV and CDR3 motifs describing these clusters were generated using Clustal Omega [23]. Six motifs were excluded from further analysis due to overlap with anti-CMV motifs identified through a parallel analysis for CMV-reactive TCRs β. Hierarchical clustering further classified the 112 remaining HMGCR-reactive motifs into 8 groups (figure 6A). Motif group 1 was notable for conserved glycines across multiple residues, while motif group 8 comprised only 1 sequence of 21 amino acids found in subject

Table 1
Summary characteristics of paired peripheral blood and muscle TCRs β from patients with anti-HMGCR + IMNM

	# Productive TCRs β				
Patient ID	Total muscle biopsy	Total blood	Sorted CD154 + CD4 + HMGCR-reactive	Sorted CD154 + CD4 + CMV-reactive	Biopsy to PBMC interval (years)
HMGCR + 17	382	533 721	64	208	12
HMGCR + 18	2574	421 678	107	32	8
HMGCR + 19	311	799 897	95	54	2
HMGCR + 20	2411	N/A	64	107	4
HMGCR + 21	1570	1 091 791	77	161	6
Total	7248	2 847 087	407	562	
Mean	1450	569 417	81	112	

CMV, cytomegalovirus; HMGCR, hydroxy-3-methylglutaryl coenzyme A reductase; IMNM, immune-mediated necrotising myopathy; N/A, not available; PMBC, peripheral blood mononuclear cells; TCR, T cell receptor.

HMGCR + 19 (figure 6B). The motif groups identified may relate to the structure and binding of conserved antigens and revealed relatively conserved TRBV sequences with more variable CDR3 regions.

We then investigated if any of the TCRβ or consensus motifs we identified have been described as having any other reactivity. Comparing the clonotypes and motifs identified in our data, against all sequences annotated in VDJDb [24], we found a number of matches with annotated sequences (online supplemental table 6). First, a number of apparently antiviral sequences against CMV, Epstein-Barr virus and influenza A were identified both in the biopsies of patients with anti-HMGCR + IMNM, peripheral blood of patients with anti-HMGCR + IMNM and healthy controls, and in antigen-reactive CD4 + CD154 + T cell

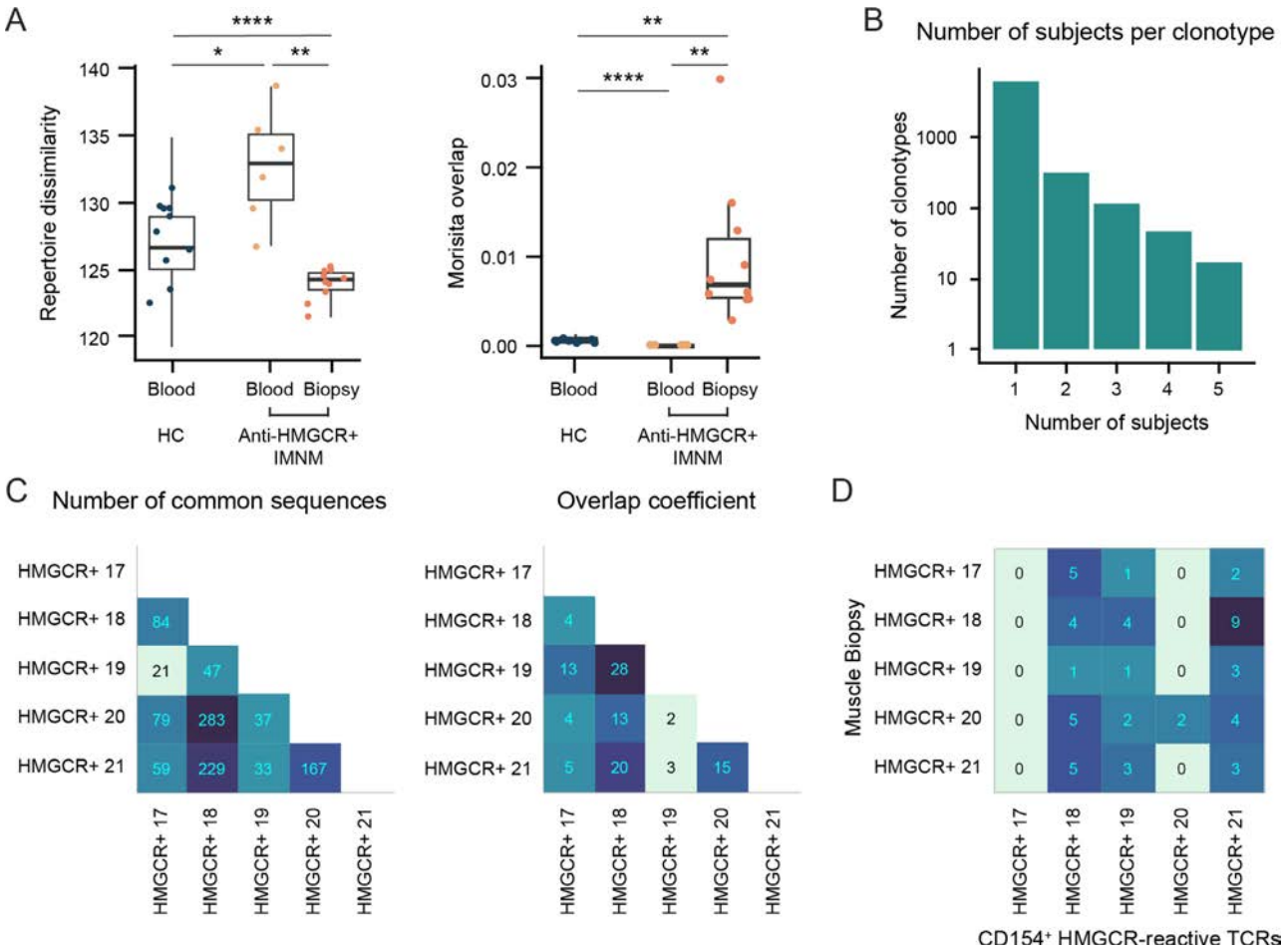

Figure 5. TCR β chain repertoire of muscle biopsies of patients with anti-HMGCR + IMNM. (A) Repertoire dissimilarity and Morisita overlap of the TCR β chain repertoire among healthy controls (n = 45) and matched peripheral blood (n = 4) and muscle biopsies (n = 5) from patients with anti-HMGCR + IMNM. (B) The count of common TCR β clonotypes is plotted against the number of muscle biopsies that is present. (C) The number and overlap coefficient (%) of TCR β sequences that shared between each pair of muscle biopsies. (D) Common HMGCR-reactive TCR β sequences among each pair of muscle biopsies. * = p,0.05, ** = p <0.01, **** = p<0.0001. HMGCR, hydroxy-3-methylglutaryl coenzyme A reductase; IMNM, immune-mediated necrotising myopathy; TCR β, T-cell receptor β.

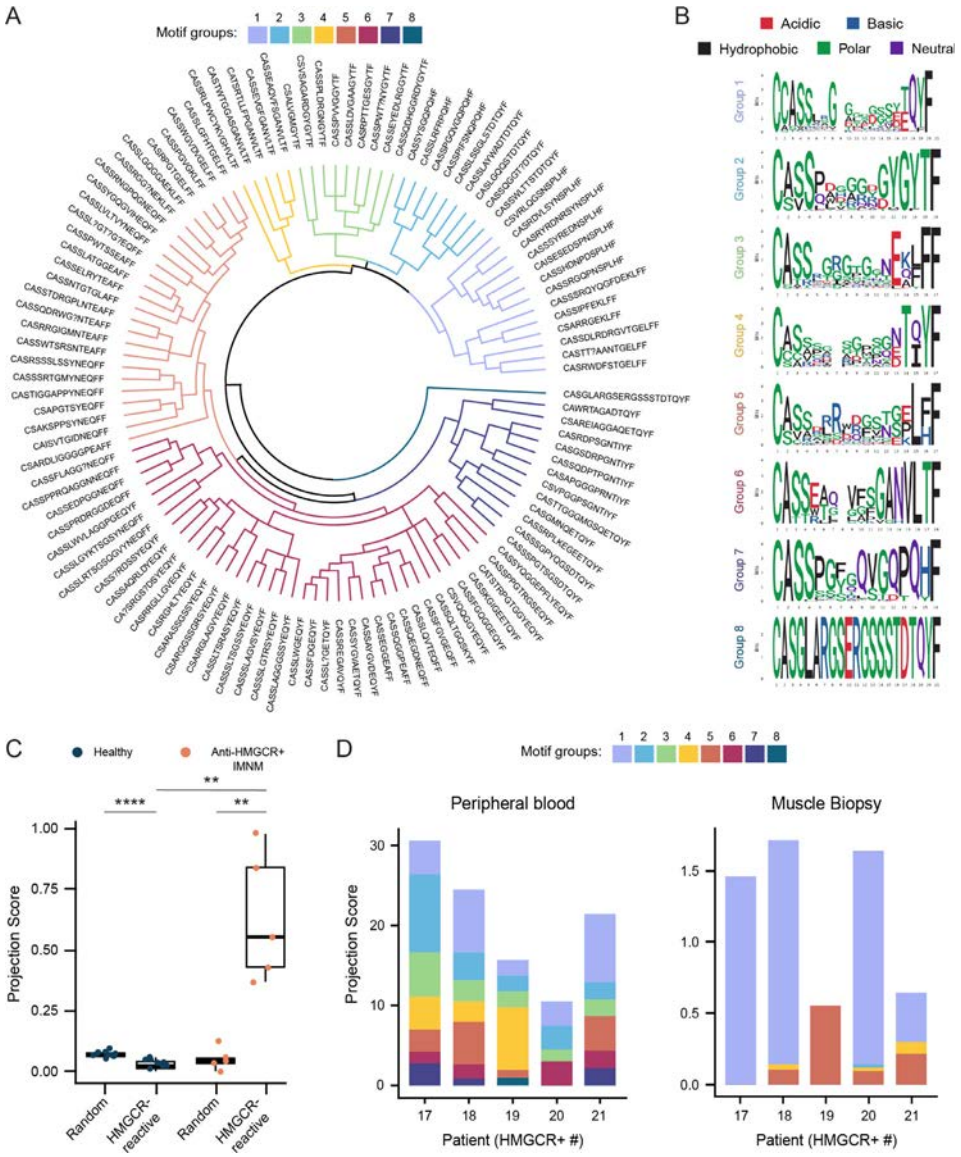

Figure 6. HMGCR-reactive TCRβ motifs are shared among patients with anti-HMGCR + IMNM (A) Plot wheel representing the hierarchical clustering of 112 HMGCR-reactive motifs into 8 groups. (B) Consensus sequence alignment of the eight groups of HMGCR-reactive motifs. (C) Projection score of randomly selected TCRβ motifs and HMGCR-reactive TCRβ motifs among healthy controls (blue dots) and patients with anti-HMGCR + IMNM. (D) Projection score and distribution of the different HMGCR-reactive TCRβ motifs for each of the patients in the periphery and the muscle biopsy. Different motifs are denoted with different colours. ** = p< 0.01, ****p<0.00001. HMGCR, hydroxy-3-methylglutaryl coenzyme A reductase; IMNM, immune-mediated necrotising myopathy; TCR β, T-cell receptor β.

sorted populations. This includes some TCRβs against irrelevant antigens highly unlikely to have been encountered by subjects, including yellow fever virus, and multiple dengue virus types. Additional TCRβs were identified against antigens impossible to have been encountered, including Simian immunodeficiency virus, synthetic peptides (that do not exist in vivo) and SARS-CoV-2 virus (our samples were obtained years before the SARS-CoV-2 pandemic). This likely indicates that although we identify individual TCRβ sequences as reactive for a given epitope, they may not be exclusive for only that one epitope.

In contrast, when we then compared the antigen-reactive motif groups (anti-HMGCR and anti-CMV) TCRβ sequences, none of 112 anti-HMGCR motifs were found in VDJDb (ie, they were unique to our anti-HMGCR + IMNM patients), and 1 of 118 anti-CMV motifs mapped to a TCRβ catalogued in VDJDb as CMV-reactive (online supplemental table 7). This suggests that, despite the presence of apparently polyreactive or viral-reactive clonotypes in our CD4 + CD154 + datasets, the conserved motifs that are overexpressed in these populations through sequence clustering are more specific to their respective antigen reactivities than any individual TCRβ in the CD4 + CD154 + repertoire.

To estimate the prevalence of anti-HMGCR motifs in muscle biopsies, the eight motif groups described above were then projected onto TCRβ chain repertoires from anti-HMGCR + INMN muscle biopsies and the peripheral blood TCRβ chain repertoires of healthy controls. HMGCR-reactive motifs appeared more frequently in muscle biopsies of anti-HMGCR + IMNM individuals compared with randomly selected motifs (projection score 0.633 vs 0.028 vs, p = 0.007). This trend was not observed when the same motifs were projected onto healthy control peripheral blood β chain repertoires, which were significantly depleted for HMGCR motifs relative to randomly selected motifs (projection score 0.072 vs 0.028, $p<1\times10^{-15}$) (figure 6C). Further assessment of these groups demonstrated a skewed representation within muscle biopsies. While most motif groups were represented across the HMGCR-reactive TCRβ chain repertoires in the peripheral blood of the five subjects tested, paired muscle biopsies predominantly expressed TCRs β belonging to only

motif groups 1 and 5 (figure 5D). Collectively, these results indicate that HMGCR-reactive TCRs β chains are enriched in target muscle tissue of anti-HMGCR + INMN individuals, suggesting a targeted and active role in the disease process.

DISCUSSION

The objective of this study was to assess the presence of $CD4^+$ T cells targeting the autoantigen HMGCR in the peripheral blood and muscle of individuals affected by anti-HMGCR + IMNM. The identification of HMGCR-reactive $CD4^+$ T cells, which are polarised towards a Th1-17 phenotype, represents a vital initial step in untangling the various immune elements that coordinate to initiate and sustain an immune response directed against the muscle tissue of these patients. Subsequently, by using NAPA, we examined the processing and presentation of the autoantigen and discovered a core set of seven HMGCR-derived peptides. These were presented by patients' APCs irrespective of their HLA-DR subtype and corresponded to $CD4^+$ T cell epitopes recognised by immunogenetically diverse anti-HMGCR + IMNM patients. Using the specificity offered by TCRβ sequencing, HMGCR-reactive $CD4^+$ T cells were then tracked back to the target muscle tissue of patients with anti-HMGCR + IMNM and were found to be shared among multiple individuals. Taken together, these findings provide novel and insightful perspectives into the underlying pathogenetic mechanisms of anti-HMGCR + IMNM.

Anti-HMGCR + IMNM exhibits a strong association with *HLA-DRB1*11:01* in adults, with an OR of 24.5 for white and 56.5 for black patients [4], a risk that surpasses any other known HLA-DRB1 association in rheumatic diseases. This finding, coupled with the presence of IgG autoantibodies against HMGCR, strongly suggested the presence of HMGCR-reactive $CD4^+$ T cells that aid B cell antibody class switching, but none had been described. Our study marks the first documentation of the existence of such T cells. Furthermore, we found that their frequency was positively correlated with anti-HMGCR antibody titre, indicating a direct relationship between the antigen-specific T and B cells in this disease. Anti-HMGCR antibodies are hypothesised to be directly pathogenic, supported by various lines of investigation, as their titre is linked to disease activity [17] and passive transfer of these antibodies in a mouse model resulted in myofiber necrosis and muscle weakness [14]. However, antibody-targeted therapies such as plasmapheresis are not universally effective treatment for anti-HMGCR + IMNM. In addition, a trial of a complement component 5 inhibitor was unsuccessful [25] despite the hypothesised role of anti-HMGCR antibodies in driving the complement deposition observed in the muscle biopsies from these patients [22]. This clinical evidence suggests that targeting anti-HMGCR antibodies is not sufficient to control disease in most patients and that targeting or manipulating HMGCR-reactive $CD4^+$ T cells might provide additional therapeutic benefit.

Analysis of the helper T cell subtype of the whole $CD4^+$ T cell compartment showed great heterogeneity among patients, and we did not find any association with immunosuppressive treatment or disease activity (data are not shown), although this is limited by the small number of patients. Despite that, we identified a predominant overrepresentation of Th1/Th17 lineage $CD4^+$ T cells in response to HMGCR stimulation compared with the whole $CD4^+$ T cell compartment across patients. These cells are notably distinct from Th1 cells. Th1/Th17 cells primarily secrete IL-17 and IFN-γ and have been observed in various autoimmune diseases, such as multiple sclerosis, lupus, rheumatoid arthritis and inflammatory bowel disease [26]. These cells can assist in antibody production by B cells, lack cytotoxic function, and are relatively resistant to T cell regulatory mediated suppression, which could explain their role in autoimmunity. In the context of IIMs, it is noteworthy that IL-17 and IFN-γ levels are elevated in individuals with muscle disease and that these levels correlate with disease duration and muscle weakness [27–29]. Interestingly, the ratio of IFNγ to IL17 was inversely associated with response to intravenous immunoglobulin (IVIG) [30], and anti-HMGCR + IMNM has been shown to be responsive to IVIG therapy [17,31]. Thus, our future endeavours need to focus in HMGCR-reactive T cell function, and how these factors correlate with disease characteristics and treatment responses.

Despite the strong association of *HLA-DRB1*11:01* with anti-HMGCR + IMNM, no significant correlation has been established between this immunogenetic risk factor and disease characteristics such as CK levels, autoantibody titres, or age at disease onset [4]. Our results support these findings, as the presence of this HLA allele did not distinguish any patients. Remarkably, even patients lacking this risk allele develop the disease, possess a similar repertoire of naturally presented HMGCR peptides and HMGCR-reactive T cells against the same epitopes. This suggests that while the presence of the HLA allele confers a higher risk of initiating the disease, once triggered, the disease progresses in a similar fashion. This is similar to what we have seen in anti-topoisomerase I + systemic sclerosis [15], in which patients without risk alleles can still develop the disease and possess a similar antigen-reactive T cell repertoire.

Following the identification of a shared repertoire of HMGCR peptides presented by mo-DCs from patients with anti-HMGCR + IMNM and confirming these peptides as epitopes for HMGCR-reactive $CD4^+$ T cells, our objective was to determine whether they were present within the disease target tissue, that is, skeletal muscle. While paired TCRs β chains between muscle and blood in IMNM have been documented in a small number of patients with IMNM in previous studies [32,33], antigen specificity of these TCRs β was not determined. Despite one of the key features of anti-HMGCR + IMNM being a lack of cellular infiltration into the muscle biopsy on histological evaluation [2,3,21,22], we were able to detect numerous TCRs β, including HMGCR-reactive $CD4^+$ T cells, within the muscle tissue of these patients. Analysis of the muscle-infiltrating cells revealed two important observations. The first was the existence of shared TCRβ sequences in the muscle biopsies of different patients with the same disease. The presence of public TCRs within the context of a particular condition has been documented in infectious diseases, autoimmune disease mouse models, and various types of malignancies, although identifying common target antigens has not been the focus in most of these studies [34–36]. In our study, the T cell population detected in muscle biopsies between patients was more similar to each other than the peripheral blood T cell repertoires between the same patients. Taken together, the unexpected convergence of TCRs from T cells present in the muscle implies a shared pathogenic mechanism, along with a common source of antigenic stimulation. The second observation was that HMGCR-reactive $CD4^+$ T cells were enriched in the muscle relative to the peripheral blood, implying that HMGCR is a common antigen in the disease. Nevertheless, these cells comprise a small proportion of the total infiltrating T cell population. An average of 0.32% of TCRs β in the muscle biopsy were exact matches to T cells known to be reactive to the seven defined HMGCR peptides, and an average of 0.63% of biopsy TCRs β contained homologous HMGCR-reactive motifs identified through sequence analysis. The antigen specificity of

the remaining T cell pool is unknown. A proportion of these T cells may recognise additional epitopes within the HMGCR protein since full-length HMGCR protein containing the N-terminus and transmembrane domains could not be synthesised, or other undiscovered protein autoantigens targeted in anti-HMGCR + IMNM. Moreover, while we positively identified CD4 + anti-HMGCR T cells, we did not study CD8 + T cells, which are also known to be present in the muscle [21] and not distinguishable from CD4 + T cells by TCR sequencing.

Focusing on HMGCR-reactive $CD4^+$ T cells against any of the seven HMGCR epitopes, we identified eight distinct families of TCR motifs enriched within the HMGCR-reactive T cells. These families were more likely to be found in the muscle biopsies of patients than non-specific sequences, suggesting that the presence of HMGCR-reactive T cells in muscle tissue of anti-HMGCR + IMNM patients is not a random occurrence. Moreover, while all motif groups were represented in the peripheral anti-HMGCR CD4 + T cells of multiple patients, motif groups 1 and 5 comprised the majority of anti-HMGCR TCRs β in the muscle. Several factors may explain this phenomenon. First, motifs 1 and 5 may play a more critical role in disease pathogenesis, leading to their higher abundance in muscle biopsies and could be the effector cell that triggers tissue injury. Additionally, the temporal gap between the collection of the biopsy and peripheral blood samples, which ranged from 2 to 12 years, might account for the distribution differences, as the other motifs present in the peripheral HMGCR-reactive beta chain repertoire may represent epitope spreading over time. Unfortunately, due to the limited number of antigen-reactive T cells, we had to combine the CD154 + T cells against all seven HMGCR epitopes for TCRβ analysis. Therefore, we were unable to distinguish which epitopes were recognised by which TCRβ motifs. It is also important to note that since we only have information about the beta chain, we cannot reconstruct these TCRs. Moreover, we did not consider other factors that could potentially affect HMGCR processing and presentation, such as statins. These are limitations that we intend to investigate.

In conclusion, we identified HMGCR-reactive T cells in both the peripheral blood and target muscle tissue of patients with anti-HMGCR + IMMM. A common set of HMGCR-reactive CD4 + T cell epitopes of T cells was defined, with shared TCRs β among diverse patients, revealing novel insights into disease pathogenesis. Along with the finding that these T cells infiltrate the target tissue, this study could lead to design of antigen-specific monitoring tools and targeted immunotherapies for patients with anti-HMGCR + IMMM.

Acknowledgments

We thank Mekha A. Thomas, PhD for artistic review and construction of the final figures. We want to thank Marta Escarra Senmarti, PhD for assistance with cell sorting. We want to thank David Hines for processing the blood samples. We thank the research coordinators and rheumatology fellows of the Johns Hopkins Myositis Center for their support in obtaining the patient samples and data; the patients of the Johns Hopkins Myositis Center who participated in this study.

Contributors

Study conception and design: ET, ED, ALM, AR and KNS. Performance of experiments: ET and TS. Acquisition of samples and data: ET, JA, BA, JP, CAM, AR, MJS, LC-S and ALM. Analysis and interpretation of data: ET, ED, AAG. Guarantor for the study: ET. All authors meet the criteria for authorship and have contributed to and approved the final version of this manuscript for submission.

Funding

This work was supported by the Rheumatology Research Foundation (to ET), the Jerome L. Greene Foundation (to ET and MA), the Dr. Peter and Carmen Lucia Buck Fund (to ET), the Huayi and Suiling Zhang Discovery Fund (to LC-S), the Steven and Alexandra Cohen Foundation (to AR and MJS) and the NIH (grants K08-AR0777732 to ET, K23-AR075898 to CAM, K23-AR073927 to JJP, P30-AR070254 for the Bayview Immunomics Core facility and the Intramural Research Program of NIAMS to ALM).

Disclaimer

The content of this study is solely the responsibility of the authors and does not necessarily represent the official views of the National Institutes of Health.

Competing interests

LC-S, AR and ALM have a patent for the anti-HMGCR antibody assay. ALM does not receive any compensation for this. ED is currently a paid employee of AstraZeneca.

Patient and public involvement

Patients and/or the public were not involved in the design, or conduct, or reporting, or dissemination plans of this research.

Patient consent for publication

Not applicable.

Ethics approval

This study involves human participants and has been approved by the Institutional review Board of Johns Hopkins University (study number: CIR00100834). All patients provided informed consent before participating in the study.

Data availability statement

Data are available in a public, open access repository. Data are available on reasonable request. All code, including data preprocessing and analysis steps, will be published on GitHub, DOI 10.5281/zenodo.10365789 [37]. [dataset] E. Tiniakou, A. Girgis, et al. Data from: Precise identification and tracking of HMGCRreactive CD4+ T cells in the target tissue of patients with anti-HMGCR immune mediated necrotizing myopathy. (2024). https://doi.org/10.5281/ZENODO.10365788. Deposited 31 May 2024.

Supplementary materials

Supplementary material associated with this article can be found in the online version at doi:10.1136/ard-2024-225732.

Orcid

Eleni Tiniakou: http://orcid.org/0000-0003-4749-870X
Julie J. Paik: http://orcid.org/0000-0001-8436-1601

Christopher A. Mecoli: http://orcid.org/0000-0002-1429-8392
Andrew Lee Mammen: http://orcid.org/0000-0003-3732-3252
Erika Darrah: http://orcid.org/0000-0003-1119-0279

REFERENCES

[1] Allenbach Y, Mammen AL, Benveniste O, et al. 224th ENMC International Workshop:: Clinico-sero-pathological classification of immune-mediated necrotizing myopathies Zandvoort, The Netherlands, 14-16 October 2016. Neuromuscul Disord 2018;28:87–99. doi: 10.1016/j.nmd.2017.09.016.
[2] Christopher-Stine L, Casciola-Rosen LA, Hong G, et al. A novel autoantibody recognizing 200-kd and 100-kd proteins is associated with an immune-mediated necrotizing myopathy. Arthritis Rheum 2010;62:2757–66. doi: 10.1002/art.27572.
[3] Mammen AL, Chung T, Christopher-Stine L, et al. Autoantibodies against 3-hydroxy-3-methylglutaryl-coenzyme A reductase in patients with statin-associated autoimmune myopathy. Arthritis Rheum 2011;63:713–21. doi: 10.1002/art.30156.
[4] Mammen AL, Gaudet D, Brisson D, et al. Increased frequency of DRB1*11:01 in anti-hydroxymethylglutaryl-coenzyme A reductase-associated autoimmune myopathy. Arthritis Care Res (Hoboken) 2012;64:1233–7. doi: 10.1002/acr.21671.
[5] Tiniakou E. Statin-Associated Autoimmune Myopathy: Current Perspectives. Ther Clin Risk Manag 2020;16:483–92. doi: 10.2147/TCRM.S197941.
[6] Rothwell S, Chinoy H, Lamb JA, et al. Focused HLA analysis in Caucasians with myositis identifies significant associations with autoantibody subgroups. Ann Rheum Dis 2019;78:996–1002. doi: 10.1136/annrheumdis-2019-215046.
[7] Ohnuki Y, Suzuki S, Shiina T, et al. HLA-DRB1 alleles in immune-mediated necrotizing myopathy. Neurology (ECronicon) 2016;87:1954–5. doi: 10.1212/WNL.0000000000003160.
[8] Limaye V, Bundell C, Hollingsworth P, et al. Clinical and genetic associations of autoantibodies to 3-hydroxy-3-methyl-glutaryl-coenzyme a reductase in patients with immune-mediated myositis and necrotizing myopathy. Muscle Nerve 2015;52:196–203. doi: 10.1002/mus.24541.
[9] Prieto-Peña D, Ocejo-Vinyals JG, Mazariegos-Cano J, et al. Epidemiological and genetic features of anti-3-hydroxy-3-methylglutaryl-CoA reductase necrotizing myopathy: Single-center experience and literature review. Eur J Intern Med 2022;101:86–92. doi: 10.1016/j.ejim.2022.04.017.
[10] Woolley M, Stebbings S, Highton J. Statin-associated immune-mediated necrotising myopathy: a New Zealand case series showing possible overrepresentation in Pacific Islanders. Intern Med J 2018;48:32–6. doi: 10.1111/imj.13575.
[11] Kishi T, Rider LG, Pak K, et al. Association of Anti-3-Hydroxy-3-Methylglutaryl-Coenzyme A Reductase Autoantibodies With DRB1*07:01 and Severe Myositis in Juvenile Myositis Patients. Arthritis Care Res (Hoboken) 2017;69:1088–94. doi: 10.1002/acr.23113.
[12] Mohan JF, Levisetti MG, Calderon B, et al. Unique autoreactive T cells recognize insulin peptides generated within the islets of Langerhans in autoimmune diabetes. Nat Immunol 2010;11:350–4. doi: 10.1038/ni.1850.
[13] Arouche-Delaperche L, Allenbach Y, Amelin D, et al. Pathogenic role of anti-signal recognition protein and anti-3-Hydroxy-3-methylglutaryl-CoA reductase antibodies in necrotizing myopathies: Myofiber atrophy and impairment of muscle regeneration in necrotizing autoimmune myopathies. Ann Neurol 2017;81:538–48. doi: 10.1002/ana.24902.
[14] Bergua C, Chiavelli H, Allenbach Y, et al. In vivo pathogenicity of IgG from patients with anti-SRP or anti-HMGCR autoantibodies in immune-mediated necrotising myopathy. Ann Rheum Dis 2019;78:131–9. doi: 10.1136/annrheumdis-2018-213518.
[15] Tiniakou E, Fava A, McMahan ZH, et al. Definition of Naturally Processed Peptides Reveals Convergent Presentation of Autoantigenic Topoisomerase I Epitopes in Scleroderma. Arthritis Rheumatol 2020;72:1375–84. doi: 10.1002/art.41248.
[16] Chattopadhyay PK, Yu J, Roederer M. A live-cell assay to detect antigen-specific CD4+ T cells with diverse cytokine profiles. Nat Med 2005;11:1113–7. doi: 10.1038/nm1293.
[17] Tiniakou E, Pinal-Fernandez I, Lloyd TE, et al. More severe disease and slower recovery in younger patients with anti-3-hydroxy-3-methylglutaryl-coenzyme A reductase-associated autoimmune myopathy. Rheumatology (Oxford) 2017;56:787–94. doi: 10.1093/rheumatology/kew470.
[18] Acosta-Rodriguez EV, Rivino L, Geginat J, et al. Surface phenotype and antigenic specificity of human interleukin 17-producing T helper memory cells. Nat Immunol 2007;8:639–46. doi: 10.1038/ni1467.
[19] Rapin N, Hoof I, Lund O, et al. MHC motif viewer. Immunogenetics 2008;60:759–65. doi: 10.1007/s00251-008-0330-2.
[20] Hoogendijk JE, Amato AA, Lecky BR, et al. 119th ENMC international workshop: Trial design in adult idiopathic inflammatory myopathies, with the exception of inclusion body myositis, 10–12 October 2003, Naarden, The Netherlands. Neuromuscul Disord 2004;14:337–45. doi: 10.1016/j.nmd.2004.02.006.
[21] Chung T, Christopher-Stine L, Paik JJ, et al. The composition of cellular infiltrates in anti-HMG-CoA reductase-associated myopathy. Muscle Nerve 2015;52:189–95. doi: 10.1002/mus.24642.
[22] Allenbach Y, Arouche-Delaperche L, Preusse C, et al. Necrosis in anti-SRP+ and anti-HMGCR+ myopathies: Role of autoantibodies and complement. Neurology (ECronicon) 2018;90:e507–17. doi: 10.1212/WNL.0000000000004923.
[23] Bodenhofer U, Bonatesta E, Horejš-Kainrath C, et al. msa: an R package for multiple sequence alignment. Bioinformatics 2015;31:3997–9. doi: 10.1093/bioinformatics/btv494.
[24] Shugay M, Bagaev DV, Zvyagin IV, et al. VDJdb: a curated database of T-cell receptor sequences with known antigen specificity. Nucleic Acids Res 2018;46:D419–27. doi: 10.1093/nar/gkx760.
[25] Mammen AL, Amato AA, Dimachkie MM, et al. Zilucoplan in immune-mediated necrotising myopathy: a phase 2, randomised, double-blind, placebo-controlled, multicentre trial. Lancet Rheumatol 2023;5:e67–76. doi: 10.1016/s2665-9913(23)00003-6.
[26] Kamali AN, Noorbakhsh SM, Hamedifar H, et al. A role for Th1-like Th17 cells in the pathogenesis of inflammatory and autoimmune disorders. Mol Immunol 2019;105:107–15. doi: 10.1016/j.molimm.2018.11.015.
[27] Patel J, Ravishankar A, Maddukuri S, et al. Identification of Similarities Between Skin Lesions in Patients With Antisynthetase Syndrome and Skin Lesions in Patients With Dermatomyositis by Highly Multiplexed Imaging Mass Cytometry. Arthritis Rheumatol 2022;74:882–91. doi: 10.1002/art.42050.
[28] Chevrel G, Page G, Granet C, et al. Interleukin-17 increases the effects of IL-1 beta on muscle cells: arguments for the role of T cells in the pathogenesis of myositis. J Neuroimmunol 2003;137:125–33. doi: 10.1016/s0165-5728(03)00032-8.
[29] Notarnicola A, Lapadula G, Natuzzi D, et al. Correlation between serum levels of IL-15 and IL-17 in patients with idiopathic inflammatory myopathies. Scand J Rheumatol 2015;44:224–8. doi: 10.3109/03009742.2014.956141.
[30] Tournadre A, Porcherot M, Chérin P, et al. Th1 and Th17 balance in inflammatory myopathies: interaction with dendritic cells and possible link with response to high-dose immunoglobulins. Cytokine 2009;46:297–301. doi: 10.1016/j.cyto.2009.02.013.
[31] Mammen AL, Tiniakou E. Intravenous Immune Globulin for Statin-Triggered Autoimmune Myopathy. N Engl J Med 2015;373:1680–2. doi: 10.1056/NEJMc1506163.
[32] Argyriou A, Horuluoglu B, Galindo-Feria AS, et al. Single-cell profiling of muscle-infiltrating T cells in idiopathic inflammatory myopathies. EMBO Mol Med 2023;15:e17240. doi: 10.15252/emmm.202217240.
[33] Anang DC, Walter HAW, Lim J, et al. TCRβ clones in muscle tissue share structural features in patients with idiopathic inflammatory myopathy and are associated with disease activity. Front Immunol 2023;14:1279055. doi: 10.3389/fimmu.2023.1279055.
[34] Marrero I, Aguilera C, Hamm DE, et al. High-throughput sequencing reveals restricted TCR Vβ usage and public TCRβ clonotypes among pancreatic lymph node memory CD4(+) T cells and their involvement in autoimmune diabetes. Mol Immunol 2016;74:82–95. doi: 10.1016/j.molimm.2016.04.013.
[35] Zhao Y, Nguyen P, Vogel P, et al. Autoimmune susceptibility imposed by public TCRβ chains. Sci Rep 2016;6:37543. doi: 10.1038/srep37543.
[36] Zhao Y, Nguyen P, Ma J, et al. Preferential Use of Public TCR during Autoimmune Encephalomyelitis. J Immunol 2016;196:4905–14. doi: 10.4049/jimmunol.1501029.
[37] Girgis A. DarrahLab/2023_Tiniakou-et-al_HMGCR-Tcells: code and data initialization. 2024.

Ann Rheum Dis 84 (2025) 319–328

Contents lists available at ScienceDirect

Annals of the Rheumatic Diseases

journal homepage: https://www.sciencedirect.com/journal/annals-of-the-rheumatic-diseases

Vasculitis

Real-life use of the PEXIVAS reduced-dose glucocorticoid regimen in granulomatosis with polyangiitis and microscopic polyangiitis

Sophie Nagle[1,2], Yann Nguyen[3,4], Mary-Jane Guerry[5], Thomas Quemeneur[5], Dimitri Titeca-Beauport[6], Thomas Crépin[7], Rafik Mesbah[8], Idris Boudhabhay[9], Grégory Pugnet[10,11], Céline Lebas[12], Antoine Néel[13], Alexandre Karras[14,15], Eric Hachulla[16], Juliette Woessner[17], Vincent Pestre[17], Raphaël Borie[18], Stephane Vinzio[19], Jean-Baptiste Gouin[20], Sara Melboucy-Belkhir[21], Roderau Outh[22], Benjamin Subran[23], Mathieu Gerfaud-Valentin[24], Sebastien Humbert[25], Philippe Kerschen[26], Yurdagul Uzunhan[27,28], Tiphaine Goulenok[29], Maxime Beydon[30], Nathalie Costedoat-Chalumeau[31], Xavier Puechal[32], Benjamin Terrier[33,34,*]

[1] *Intensive Care Unit, Avicenne Hospital, APHP, Bobigny, France*
[2] *National Referral Centre for Rare Autoimmune and Systemic Diseases, Department of Internal Medicine, Hôpital Cochin, APHP, Paris, Île-de-France, France*
[3] *Centre de Recherche en Epidémiologie et Statistiques (CRESS), Unité Inserm 1153, Université Paris Cité, Paris, France*
[4] *Internal Medicine, Department of Internal Medicine, Beaujon Hospital, AP-HP. Nord, Université Paris Cité, Clichy, France*
[5] *Department of Nephrology, Internal and Vascular Medicine, CH de Valenciennes, Valenciennes, France*
[6] *Department of Nephrology, Dialysis and Transplantation, University Hospital Centre Amiens-Picardie, Amiens, Hauts-de-France, France*
[7] *Department of Nephrology, Dialysis and Renal Transplantation, Amiens-Picardy University Hospital, Amiens, Hauts-de-France, France*
[8] *Department of Nephrology, Boulogne-sur-Mer Hospital Center, Boulogne-sur-Mer, Hauts-de-France, France*
[9] *Department of Nephrology and Transplantation, Necker University Hospital, AP-HP. Centre - Université Paris Cité, Paris, France*
[10] *INSERM UMR1027, Toulouse, France*
[11] *Department of Internal Medicine and Clinical Immunology, CHU Toulouse, Toulouse, France*
[12] *Department of Nephrology, Valenciennes Hospital, Valenciennes, France*
[13] *Department of Internal Medicine, Hôpital Hôtel-Dieu, Nantes, France*
[14] *Department of Nephrology, Hopital Europeen Georges Pompidou, Paris, Île-de-France, France*
[15] *Universite Paris Descartes, Paris, France*
[16] *Department of Internal Medicine and Clinical Immunology, CHU Lille, Centre de Référence des Maladies Autoimmunes Systémiques Rares Du Nord et Nord-Ouest de France, Lille, France*
[17] *Department of Internal Medicine, Hospital Centre Avignon, Avignon, Provence- Alpes-Côte d'Azur, France*
[18] *Department of Pneumology A, Hôpital Bichat Claude-Bernard, Paris, Île-de-France, France*
[19] *Department of Internal Medicine, Groupe Hospitalier Mutualiste de Grenoble, Grenoble, Rhône-Alpes, France*

*Correspondence to Dr. Benjamin Terrier.
E-mail address: benjamin.terrier@aphp.fr (B. Terrier).

Handling editor Josef S. Smolen.

This study was presented on plenary session, in ACR (American College of Rheumatology) Convergence meeting, in San Diego, California, in November 2023. The abstract of this study was published online on this occasion: abstract number: 0725; https://acrabstracts.org/abstract/real-life-use-of-the-pexivas-reduced-dose-glucocorticoidregimen-in-granulomatosis-with-polyangiitis-and-microscopic-polyangiitis/

https://doi.org/10.1136/ard-2024-226339

[20] Department of Nephrology, Bretagne Atlantique Hospital, Vannes, France
[21] Department of Internal Medicine, Saint-Quentin Hospital, Saint-Quentin, France
[22] Service de médecine interne et générale, Perpignan Hospital Centre, Perpignan, France
[23] Department of Internal Medicine, La Croix Saint-Simon Hospital, Paris, France
[24] Department of Internal Medicine, Centre Hospitalier Saint Joseph Saint Luc, Lyon, Rhône-Alpes, France
[25] Department of Internal Medicine, Centre Hospitalier Universitaire de Besancon, Besancon, Bourgogne-Franche-Comté, France
[26] Department of Neurology, Luxembourg Hospital Center, Luxembourg, Luxembourg
[27] Department of Pneumology, Hospital Avicenne, Bobigny, France
[28] Université Sorbonne Paris Nord, Villetaneuse, Île-de-France, France
[29] Department of Internal Medicine, Hospital Bichat - Claude-Bernard, Paris, Île-de-France, France
[30] Internal medecine, Beaujon Hospital, AP-HP Nord, Clichy, France
[31] APHP, Centre de Reference Maladies Auto-immunes et Systémiques Rares, Service de Médecine Interne, Hôpital Cochin, Paris, Île-de-France, France
[32] National Referral Center for Rare Systemic Autoimmune Diseases, Hospital Cochin, Paris, Île-de-France, France
[33] Department of Internal Medicine, Hospital Cochin, AP-HP, Paris, France
[34] Université Paris Cité, Paris, France

ARTICLE INFO

Article history:
Received 28 June 2024
Accepted 23 October 2024

Keywords:
Granulomatosis with polyangiitis
Glucocorticoids
Cyclophosphamide
Systemic vasculitis
Rituximab

ABSTRACT

Background: The PEXIVAS (Plasma exchange and glucocorticoids in severe antineutrophil cytoplasmic antibody (ANCA)-associated vasculitis) trial showed that a reduced-dose glucocorticoid regimen (redGC) was non-inferior to a standard-dose regimen (standGC) with respect to death or end-stage kidney disease (ESKD) in patients with ANCA-associated vasculitis (AAV). However, the primary endpoint did not include disease progression or relapse, cyclophosphamide was the main induction therapy and rituximab (RTX)-treated patients tended to have a higher risk of death or ESKD with redGC. We aimed to evaluate the real-world use of redGC.

Methods: We conducted a retrospective, multicentre study comparing PEXIVAS redGC with standGC in patients with AAV. The primary composite outcome was the occurrence of death, ESKD, AAV progression before remission or relapse within the 12 months following induction. Inverse probability of treatment weighting was used to correct for baseline imbalance between groups. Factors associated with the occurrence of the primary outcome were estimated.

Results: A total of 234 patients were included. The primary composite outcome occurred in 42/126 (33%) patients with redGC versus 20/108 (19%) with standGC. In unweighted multivariable analysis and in weighted analysis, redGC was independently associated with the primary outcome but not with death or ESKD. Among redGC-treated patients, those with serum creatinine>300 µmol/L were more likely to achieve the primary outcome. RTX-treated patients who received redGC were more likely to experience death or ESKD and to achieve the primary outcome.

Conclusion: In this study of patients with AAV primarily treated with RTX, redGC was associated with an increased risk of the primary outcome consisting of death, ESKD, AAV progression before remission or relapse.

INTRODUCTION

Glucocorticoids (GCs) in combination with rituximab (RTX) or cyclophosphamide (CYC) are the cornerstone of treatment for patients with severe antineutrophil cytoplasmic antibodies (ANCA)-associated vasculitis (AAV) including granulomatosis with polyangiitis (GPA) and microscopic polyangiitis (MPA) [1–3]. However, GCs have both beneficial and harmful effects. A meta-analysis showed that a shorter duration of GCs was associated with a higher number of relapses than a longer duration [4,5]. GCs are also associated with numerous adverse effects including serious and sometimes fatal infections, highlighting the importance of reducing the cumulative dose of GCs whenever possible [6–11].

The PEXIVAS (Plasma exchange and glucocorticoids in severe antineutrophil cytoplasmic antibody (ANCA)-associated vasculitis) trial compared a reduced-dose GC regimen (redGC) with a standard-dose GC regimen (standGC) in patients with severe GPA and MPA [12]. This randomised trial showed that a redGC was non-inferior to a standGC with respect to death or end-stage kidney disease (ESKD) and the rate of serious infections at one year was significantly lower with the redGC. This redGC is now the recommended regimen for induction of remission in international guidelines [1–3]. As a reminder, during the first 6 months, for an average weight of 65 kg, the cumulative dose during the first 6 months was 3920 mg for the standGC arm (with a start at 60 mg/day of prednisone and a tapering step at 5 mg/day of prednisone at 6 months) and 2240 mg for the reduced-dose arm in the PEXIVAS trial (with a start at 30 mg/day of prednisone and a tapering step at 5 mg/day of prednisone at 4 months). However, in the PEXIVAS trial, the primary endpoint did not include disease progression or relapse and CYC was the most used induction therapy which is not generalisable to current practice in many centres. In addition, in the subgroup analysis of patients treated with RTX as induction therapy, there was a trend towards a lower risk of death or ESKD if they received standGC compared with redGC. Progression of AAV before achieving remission or minor or major relapses, even if they do not lead to death or ESKD, are also important factors to consider when tapering GCs. Therefore, we

WHAT IS ALREADY KNOWN ON THIS TOPIC

- The PEXIVAS (Plasma exchange and glucocorticoids in severe antineutrophil cytoplasmic antibody (ANCA)-associated vasculitis) trial showed that a reduced-dose glucocorticoid regimen (redGC) was non- inferior to a standard-dose regimen (standGC) with respect to death or end-stage kidney disease (ESKD) in patients with severe granulomatosis with polyangiitis (GPA) or microscopic polyangiitis (MPA).

WHAT THIS STUDY ADDS

- This is the first real-life observational multicentre study comparing PEXIVAS redGC with standGC in 234 patients with severe GPA or MPA. In unweighted univariable, multivariable analysis and weighted analysis, redGC was independently associated with the occurrence of our composite primary outcome consisting of death, ESKD, ANCA-vasculitis progression before remission or relapse within the 12 months following induction; but not with death or ESKD.
- Among redGC-treated patients, those with serum creatinine>300 µmol/L were more likely to achieve the primary outcome. Rituximab (RTX)-treated patients who received redGC were more likely to experience death or ESKD and to achieve the primary outcome.

HOW THIS STUDY MIGHT AFFECT RESEARCH, PRACTICE OR POLICY

- We suggest an increased vigilance when using the redGC regimen, especially in the two subgroups of patients at higher risk of failure, that is, those receiving RTX as induction therapy and those with a baseline serum creatinine greater than 300 µmol/L.

aimed to evaluate the redGC in a population of unselected patients with severe GPA and MPA in a real-world setting.

PATIENTS AND METHODS

Patients

We conducted a retrospective, multicentre descriptive study in 19 university and general hospitals in France and Luxembourg between 1 January 2018 and 6 November 2022. Inclusion criteria were: (1) patients older than 15 years; (2) diagnosis of new or relapsing GPA or MPA according to the 2022 American College of Rheumatology/European Alliance of Associations for Rheumatology classification criteria [13,14]; (3) severe disease threatening their vital or functional prognosis and requiring induction treatment with either RTX or CYC according to the French guidelines; (4) patients receiving either a redGC according to the PEXIVAS trial or a standGC according to the PEXIVAS trial [12], the CORTAGE trial [15] or French guidelines [16]; (5) patients with GPA or MPA flare with start of treatment until 6 May 2022 (to have a 6-month follow-up). Exclusion criteria were: (1) a diagnosis of vasculitis other than GPA or MPA, (2) both RTX and CYC-based induction therapy, (3) GC regimen with a cumulative dose lower than the redGC; (4) GC regimen not following a specific regimen, (5) insufficient data on GC regimen; (6) concomitant treatment with avacopan.

Outcomes

All outcomes were assessed in the 12 months following induction treatment. The primary composite outcome included minor relapse, major relapse, progression before achieving remission, occurrence of ESKD requiring dialysis for>12 weeks and/or kidney transplantation and death within the 12 months following induction treatment whichever event occurred first.

Relapse was defined as the recurrence or new onset of disease after remission due to active vasculitis. The definitions of minor and major relapse were the same as those used in the PEXIVAS study [12]. Minor relapse was defined as the occurrence of a relapse after remission that did not involve a vital organ and did not compromise functional prognosis and major relapse was defined as the occurrence of a relapse after remission that involved a vital organ or compromised functional prognosis. Progression before achieving remission was defined by the need to change GCs or immunosuppressive therapy and therefore included refractory forms. Remission was defined as the absence of disease activity (Birmingham Vasculitis Activity Score (BVAS) (version 3) = 0).

Secondary outcomes included the occurrence of death, the occurrence of death or ESKD (which was the primary outcome in the PEXIVAS study) [12], the occurrence of relapse (major or minor), progression before achieving remission, remission and the occurrence of serious infections (defined as an infection requiring hospitalisation or leading to death).

Data collection

We collected patient characteristics and their treatments using a standardised case report form. GC dose (in prednisone equivalent, in mg/day) was collected at the start of induction treatment and then at 1, 2, 3, 4, 5, 6, 9, 12, 18 and 24 months after the start of treatment.

GC regimen

Two groups of patients were created according to the GC regimen: (1) the redGC used in the PEXIVAS study [12], (2) the standGC, including the standard dose from the PEXIVAS study [12], the standard dose from the CORTAGE study [15] (for a weight of 60 kgs: start with prednisone 60 mg/day, 20 mg/day at 3 months, 9 mg/day at 12 months, 4 mg/day at 18 months and 0 mg/day at 24 months) or the standard dose recommended by the French guidelines [16] before the publication of the PEXIVAS study (initial prednisone dose of 1 mg/kg/day, then tapering to prednisone 15–20 mg/day at 3 months, 10 mg/day at 6 months and 5 mg/day at 12 months).

Statistical analysis

Descriptive analyses were presented as number (percentage) for categorical variables and median (IQR) or mean (SD) for continuous variables. We compared baseline patient characteristics according to the GC regimen (redGC or standGC) by Student's t-tests or Wilcoxon rank sum tests for continuous variables and Pearson's χ^2 tests or Fisher's exact test for categorical variables, as appropriate.

Regarding baseline variables, there was no missing value, thus no imputation had been performed for subsequent analyses.

We first analysed the entire study population. The association between the GC regimen and the primary composite outcome was assessed by survival analysis. We first assessed associations using unweighted, univariable and multivariable Cox proportional hazard models, adjusted for potential confounders. Patients contributed person-time from the start of treatment induction until the date of the occurrence of the composite

outcome, death, loss to follow-up or the 12-month visit, whichever occurred first. The variables retained in multivariable analyses were age, subtype of AAV (GPA or MPA), history of AAV relapse, induction therapy (RTX or not) and clinical variables associated with the outcomes in univariable analyses. In an initial sensitivity analysis, we analysed each component of the primary outcome separately and also the time until remission in both groups.

Second, to address differences in baseline characteristics between treatment groups, an inverse probability of treatment weighting (IPTW) method was applied. Patients treated with redGC were weighted by 1/PS and those treated with standGC were weighted by 1/(1−PS) where PS represents the propensity score or the likelihood of a patient receiving redGC based on their baseline characteristics. The propensity score was calculated using logistic regression incorporating covariates chosen through a non-parsimonious approach to account for potential confounders and proxy variables for unknown or unmeasured confounders. The model included the following covariates: sex, age, AAV subtype (GPA or MPA), relapsing disease, general symptoms, articular and/or muscular involvement, skin, ENT (ear, nose and throat), lung, gastrointestinal, peripheral nervous system, central nervous system, or cardiac involvement, creatinine level>300 µmol/L, lung nodules, orbitary mass, subglottic stenosis, induction treatment, plasma exchange, BVAS, Five Factor Score (FFS) and methylprednisolone pulses.

To evaluate how well IPTW balanced the treatment groups, standardised differences between groups were calculated before and after weighting. A standardised difference of less than 10% was considered an indicator of successful balance and guided the construction of the propensity score. The overlap of propensity score distributions between groups was also visually assessed.

Afterwards, we similarly assessed the associations between the GC regimen and each outcome in the weighted pseudopopulation using univariable Cox proportional hazards models.

We also performed a prespecified subgroup analysis in patients who received RTX for induction therapy. Finally, we performed survival analyses among patients receiving a redGC in order to identify variables associated with the risk of failure of the redGC. A p value of less than 0.05 was considered statistically significant. We performed all analyses with R V.3.6.1 (R Foundation for Statistical Computing, Vienna, Austria).

Ethics

Informed consent was not required as patients were managed according to standard procedures and data were collected and analysed retrospectively.

RESULTS

Study population

From 318 patients with severe GPA or MPA with at least 6 months of follow-up, we excluded 84 patients because they met our exclusion criteria. The flow chart is shown in online supplemental figure S1. Finally, 234 patients from 19 centres (18 centres in France and 1 centre in Luxembourg including 3 nephrology centres and 16 internal medicine centres) were included in the study: 108 received a standGC and 126 received a redGC according to PEXIVAS. The number of patients according to each GC regimen and each centre is presented in online supplemental table S4. GC regimens were well balanced among nephrology departments and among internal medicine departments (p=0.217).

The median follow-up was 25 months. Baseline patient characteristics according to the GC regimen are shown in table 1. Half of the patients were women with a mean age of 61 years. 40% had a MPA and 60% had a GPA. MPO and PR3-ANCA were both present in approximately half of the patients. The mean BVAS was 17 and 25% of patients had relapsing disease. Renal involvement was present in 70% of patients and was severe: mean serum creatinine was 232 µmol/L and serum creatinine was >300 µmol/L in 59 patients (25.2% of all patients). 72% of patients received methylprednisolone pulses, 71% received RTX as induction therapy and 29% received CYC as induction therapy.

After 6 months, the median (IQR) cumulative doses of GC were 4646 (3966−5381) mg in the standGC group versus 2520 (2235−2895) mg in the redGC group (p<0.001) (table 1). Online supplemental figure S2 illustrates the mean prednisone dose received in the two GC regimens.

Primary outcome

The primary endpoint was met in 62/234 (26.5%) patients during the first year including 42/126 (33.3%) of patients receiving the redGC versus 20/108 (18.5%) of patients receiving the standGC (p=0.01) (table 2). The individual components of the primary composite outcome are shown in table 2.

The Kaplan-Meier survival curve comparing the occurrence of the primary outcome at 12 months in patients treated with the redGC and patients treated with standGC is shown in figure 1A.

In unweighted univariate analysis, the redGC was associated with a higher occurrence of the primary outcome compared to the standGC (HR 1.99; 95% CI 1.17 to 3.38) (table 3). In unweighted multivariable analysis, after adjustment for age, AAV subtype, relapsing disease, serum creatinine, use of methylprednisolone pulses, RTX induction, plasma exchanges and pulmonary nodules, the redGC was significantly associated with the occurrence of the primary outcome (HR 2.20; 95% CI 1.23 to 3.94) (table 3).

The overlap of propensity score distributions by GC regimen before and after IPTW is shown graphically (online supplemental figure S3) with the distribution of standardised differences of main baseline variables before and after IPTW (online supplemental figure S4).

In the inverse probability treatment weighted analysis, the composite primary outcome at 1 year was reached for 19.9% and 31.1% in the standGC and redGC groups, respectively. RedGC was significantly associated with the occurrence of the primary outcome (HR 2.03; 95% CI 1.08 to 3.83) (table 3 and figure 1B) compared to standGC.

Secondary outcomes

Death or ESKD

Death or ESKD occurred in 27/234 (12%) of patients during the first year of follow-up including 19/126 (15%) of patients receiving the redGC versus 8/108 (7.4%) of patients receiving the standGC. The survivals without death or ESKD according to the two GC regimens in the full population and the weighted pseudopopulation are shown in figure 2. In unweighted multivariable analysis, the redGC was not significantly associated with an increased risk of death or ESKD (HR 2.28; 95% CI 0.92 to 5.64) (table 3). After IPTW, death or ESKD occurred in 7.4%

Table 1
Baseline characteristics of the patients (N = 234)

Characteristic	N	Overall, N = 234*	Standard-dose GC regimen N = 108	Reduced-dose GC regimen N = 126	P value
Sex	234				0.3†
Male		120/234 (51)	51/108 (47)	69/126 (55)	
Female		114/234 (49)	57/108 (53)	57/126 (45)	
Age (years)	234	64 (51–73)	62 (49–73)	66 (51–73)	0.5†
Age≥65 years	234	109/234 (47)	46/108 (43)	63/126 (50)	0.3†
AAV Type	234				0.001†
GPA		141/234 (60)	77/108 (71)	64/126 (51)	
MPA		93/234 (40)	31/108 (29)	62/126 (49)	
ANCA positivity	234	228/234 (97)	107/108 (99)	121/126 (96)	0.2‡
MPO	234	106/234 (45)	42/108 (39)	64/126 (51)	0.068†
PR3	228	120/228 (53)	63/107 (59)	57/121 (47)	0.076†
BVAS 2003	234	15 (12–21)	16 (12–21)	15 (12–21)	>0.9§
Five-Factor Score	234				0.10†
0		45/234 (19)	26/108 (24)	19/126 (15)	
1		62/234 (26)	31/108 (29)	31/126 (25)	
≥2		127/234 (54)	51/108 (47)	76/126 (60)	
Relapsing disease	234	59/234 (25)	23/108 (21)	36/126 (29)	0.2†
Vasculitis manifestations					
General symptoms	234	168/234 (72)	80/108 (74)	88/126 (70)	0.5†
Fever	234	59/234 (25)	34/108 (31)	25/126 (20)	0.041†
Asthenia	234	131/234 (56)	59/108 (55)	72/126 (57)	0.7†
Weight Loss	234	66/234 (28)	28/108 (26)	38/126 (30)	0.5†
Articular/muscular involvement	234	98/234 (42)	51/108 (47)	47/126 (37)	0.13†
Skin	234	42/234 (18)	19/108 (18)	23/126 (18)	0.9†
Ear, nose and throat	234	104/234 (44)	59/108 (55)	45/126 (36)	0.004†
Subglottic stenosis	234	9/234 (3.8)	7/108 (6.5)	2/126 (1.6)	0.085‡
Eyes	234	37/234 (16)	23/108 (21)	14/126 (11)	0.033†
Orbital mass	234	5/234 (2.1)	4/108 (3.7)	1/126 (0.8)	0.2‡
Pulmonary involvement	234	113/234 (48)	54/108 (50)	59/126 (47)	0.6†
Lung nodules	234	53/234 (23)	25/108 (23)	28/126 (22)	0.9†
Alveolar haemorrhage	234	63/234 (27)	29/108 (27)	34/126 (27)	>0.9†
Acute respiratory failure	234	8/234 (3.4)	4/108 (3.7)	4/126 (3.2)	>0.9‡
Gastrointestinal tract	234	9/234 (3.8)	7/108 (6.5)	2/126 (1.6)	0.085‡
Peripheral nervous system	234	33/234 (14)	15/108 (14)	18/126 (14)	>0.9†
Central nervous system	234	18/234 (7.7)	14/108 (13)	4/126 (3.2)	0.005†
Cardiac	234	9/234 (3.8)	6/108 (5.6)	3/126 (2.4)	0.3‡
Kidney	234	164/234 (70)	68/108 (63)	96/126 (76)	0.028†
Laboratory features					
Creatinine	234	134 (71–303)	114 (65–291)	178 (80–318)	0.065§
Creatinine≥300 µmol/L	234	59/234 (25)	24/108 (22)	35/126 (28)	0.3†
Creatinine≥500 µmol/L	234	23/234 (9.8)	12/108 (11)	11/126 (8.7)	0.5†
Induction therapy					
High-dose methylprednisolone	234	169/234 (72)	76/108 (70)	93/126 (74)	0.6†
CYC (induction)¶	234	70/234 (30)	30/108 (28)	40/126 (32)	0.5†
RTX (induction)¶	234	174/234 (74)	84/108 (78)	90/126 (71)	0.3†
Plasma exchange	233	40/233 (17)	27/108 (25)	13/125 (10)	0.003†
Dialysis	234	20/234 (8.5)	12/108 (11)	8/126 (6.3)	0.2†
Remission achievement	233	227/233 (97)	106/108 (98)	121/125 (97)	0.7*
Maintenance therapy					
Rituximab	226	208/226 (92)	101/105 (96)	107/121 (88)	0.032†
Cumulative dose of GC (gram)					
After 6 months	211	3225 (2460–4646)	4646 (3966–5381)	2520 (2235–2895)	<0.001†
After 12 months	196	4474 (3270–6015)	5835 (4973–6926)	3360 (3135–3943)	<0.001†

Data are presented as median (IQR) for continuous variables and count (per cent) for categorical variables.
* n/N (%); median (IQR).
† Pearson's χ^2 test.
‡ Fisher's exact test.
§ Wilcoxon rank sum test.
¶ One patient died before receiving RTX or CYC.
AAV, antineutrophil cytoplasmic antibody-associated vasculitis; ANCA, antineutrophil cytoplasmic antibody; BVAS, Birmingham Vasculitis Activity Score version 3; CYC, cyclophosphamide; GC, glucocorticoids; GPA, granulomatosis with polyangiitis; MPA, microscopic polyangiitis; RTX, rituximab.

in the standGC group and 13.2% in the redGC group in the pseudopopulation. RedGC was not associated with the risk of death or ESKD (HR 1.73; 95% CI 0.70 to 4.24).

Progression before achieving remission, relapse and remission

In unweighted, adjusted and weighted analyses, redGC was not associated with the risk of progression before achieving remission at 1 year, or with the risk of major or minor relapse, or the risk of remission (table 3).

We describe in online supplemental table S6 the characteristics of the 25 patients having progression before achieving remission at 1 year and how the progression was managed. There was only one death directly related to the disease progression (4%). These progressions before achieving remission were

Table 2
Primary and secondary outcomes at 12 months (N = 234)

Characteristic	N	Overall, N = 234*	Standard-dose GC regimen N = 108	Reduced-dose GC regimen N = 126	P value
Composite primary outcome	234	62/234 (26.5)	20/108 (18.5)	42/126 (33.3)	0.010†
Outcome contributing to the primary outcome	*62*				*0.2*†
Progression before achieving remission		*23/62 (37)*	*6/20 (30)*	*17/42 (40)*	
Minor relapse		*11/62 (18)*	*4/20 (20)*	*7/42 (17)*	
Major relapse		*5/62 (8.1)*	*4/20 (20)*	*1/42 (2.4)*	
ESKD		*12/62 (19)*	*4/20 (20)*	*8/42 (19)*	
Death		*11/62 (18)*	*2/20 (10)*	*9/42 (21)*	
Progression before achieving remission	234	25/234 (11)	8/108 (7.4)	17/126 (13)	0.2†
Minor relapse	234	14/234 (6.0)	4/108 (3.7)	10/126 (7.9)	0.2†
Major relapse	234	6/234 (2.6)	5/108 (4.6)	1/126 (0.8)	0.10†
Death or ESKD	234	27/234 (12)	8/108 (7.4)	19/126 (15)	0.067†
Death	234	14/234 (6.0)	4/108 (3.7)	10/126 (7.9)	0.2†
ESKD	234	15/234 (6.4)	5/108 (4.6)	10/126 (7.9)	0.3†
Remission	228	221/228 (97)	103/105 (98)	118/123 (96)	0.5†
Severe infections	234	43/234 (18)	17/108 (16)	26/126 (21)	0.427†

* n/N (%).
† Pearson's χ^2 test.
ESKD, end-stage kidney disease; GC, glucocorticoids.

mostly severe events as 40% required highdose methylprednisolone, 36% required a modification of immunosuppressive/immunomodulator therapy and 8% required surgery.

Remission was achieved in 221/228 patients with available data (97%) including 103/105 (98%) in the standGC group and 118/123 (96%) in the redGC group (table 1). The cumulative incidence of remission according to the GC regimen is shown in online supplemental figure S5.

Severe infections

There was no significant difference in serious infections at 1 year between the redGC and the standGC (20.6% vs 15.7%, p = 0.427) (table 2).

Subgroup analysis

Patients receiving the redGC

In the subgroup of patients receiving the redGC, serum creatinine greater than 300 µmol/L was associated with a higher rate of occurrence of the primary endpoint (adjusted HR 3.02; 95% CI 1.28 to 7.11) (online supplemental table S1).

Patients treated with RTX induction therapy

In the subgroup of patients treated with RTX as induction therapy, patients receiving the redGC were more likely to meet the primary outcome in univariable (HR 2.22; 95% CI 1.12 to 4.40) and multivariable analysis (aHR 2.36; 95% CI 1.18 to 4.71) compared with standGC (online supplemental table S2). In this subgroup, patients receiving the redGC (aHR 3.45; 95% CI 1.07 to 11.17) and those with serum creatinine greater than 300 µmol/L (aHR 9.26; 95% CI 2.84 to 30.17) were also significantly more likely to experience death or ESKD in multivariable analysis (online supplemental table S3).

DISCUSSION

The present study of the real-life use of the PEXIVAS redGC in GPA and MPA suggests that redGC is associated with a higher

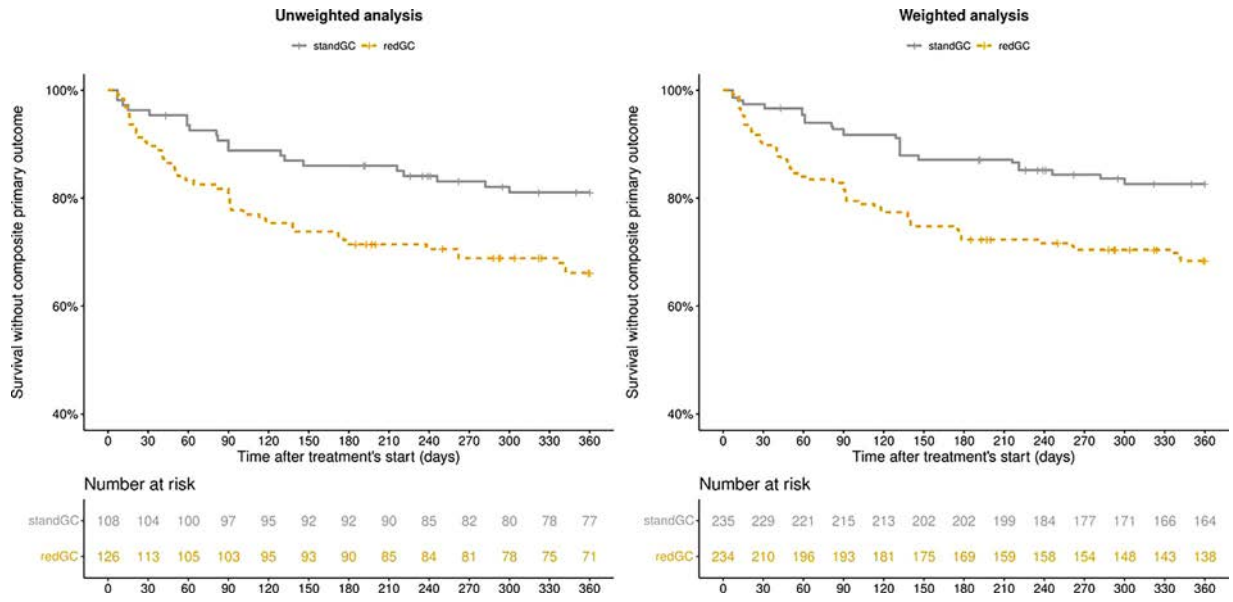

Figure 1. Kaplan-Meier survival curves comparing the occurrence of the primary endpoint at 12 months between patients who received the reduced-dose GC regimen (redGC) and the standard-dose regimen (standGC) during the first year of follow-up. Panel **A** shows the survival curve for the entire study population and Panel **B** shows the survival curve for patients after inverse probability treatment weighting.

Table 3
Associations between glucocorticoid regimen and the composite primary outcome: death or end-stage kidney disease, progression before remission, relapses and remission in the 12-month period following treatment initiation (N = 234)

		Treatment group, %			
Outcome	Analysis	Standard-dose GC regimen N = 10	Reduced-dose GC regimen N = 126	HR (95% CI)	P value
Composite primary outcome	Unweighted	18.5	33.3	**1.99 (1.17 to 3.38)**	**0.012**
	Adjusted*	NA	NA	**2.20 (1.23 to 3.94)**	**0.008**
	Weighted	19.9	31.1	**2.03 (1.08 to 3.83)**	**0.028**
Death or ESKD	Unweighted	7.4	15	2.09 (0.92 to 4.78)	0.08
	Adjusted*	NA	NA	2.28 (0.92 to 5.64)	0.08
	Weighted	7.8	11.4	1.73 (0.70 to 4.24)	0.2
Progression before achieving remission	Unweighted	7.4	13	1.69 (0.75 to 3.79)	0.203
	Adjusted*	NA	NA	2.16 (0.94 to 4.92)	0.068
	Weighted	7.4	13.2	2.18 (0.90 to 5.28)	0.086
Minor or major relapse	Unweighted	7.4	8.7	1.26 (0.51 to 3.13)	0.621
	Adjusted*	NA	NA	1.47 (0.57 to 3.80)	0.428
	Weighted	9.8	9.3	1.17 (0.39 to 3.46)	0.8
Remission†	Unweighted	98	96	1.04 (0.80 to 1.36)	0.748
	Adjusted*	NA	NA	0.97 (0.72 to 1.30)	0.692
	Weighted	96.8	114	1.01 (0.75 to 1.37)	>0.9

Bold values represent significant values.

* Covariates in the adjusted analysis were age, ANCA-associated vasculitis type (MPA), relapsing disease, serum creatinine, high-dose methylprednisolone use, rituximab induction, plasma exchanges, pulmonary nodules.

† Analyses were performed on 228 patients due to missing data for 6 patients.

ANCA, antineutrophil cytoplasmic antibody; ESKD, end-stage kidney disease; GC, glucocorticoids; MPA, microscopic polyangiitis.

risk of the composite primary outcome consisting of death, ESKD, minor or major relapse or AAV progression before remission compared with the standGC. Each component of this composite outcome was numerically higher in the redGC compared with the standGC, except for major relapse. It seems that the higher risk of occurrence of the primary outcome was mostly driven by the events of AAV progression before remission which were mainly severe events leading to the addition of immunosuppressive therapy and/or a substantial increase of GCs. However, as in the PEXIVAS study [12], there was no association between the use of the redGC and death or ESKD in our study. Moreover, a post hoc analysis of the PEXIVAS study [17] found that the GC regimen did not significantly change the risk of relapse (sub-HR 0.93–0.94; 95% CI 0.67 to 1.35).

We identified two subgroups of patients at risk of failure that require caution when using the redGC, that is, patients treated with RTX as induction therapy and patients with serum creatinine greater than 300 µmol/L. However, in the absence of renal histological data, it is difficult to know if these patients with severe kidney injury had fibrotic kidney lesions which do not respond to treatments anyway. In PEXIVAS trial, in the subgroup analysis of patients treated with RTX as induction therapy, there was a trend towards a higher risk of death or ESKD if they received redGC compared with standGC. Our study confirms

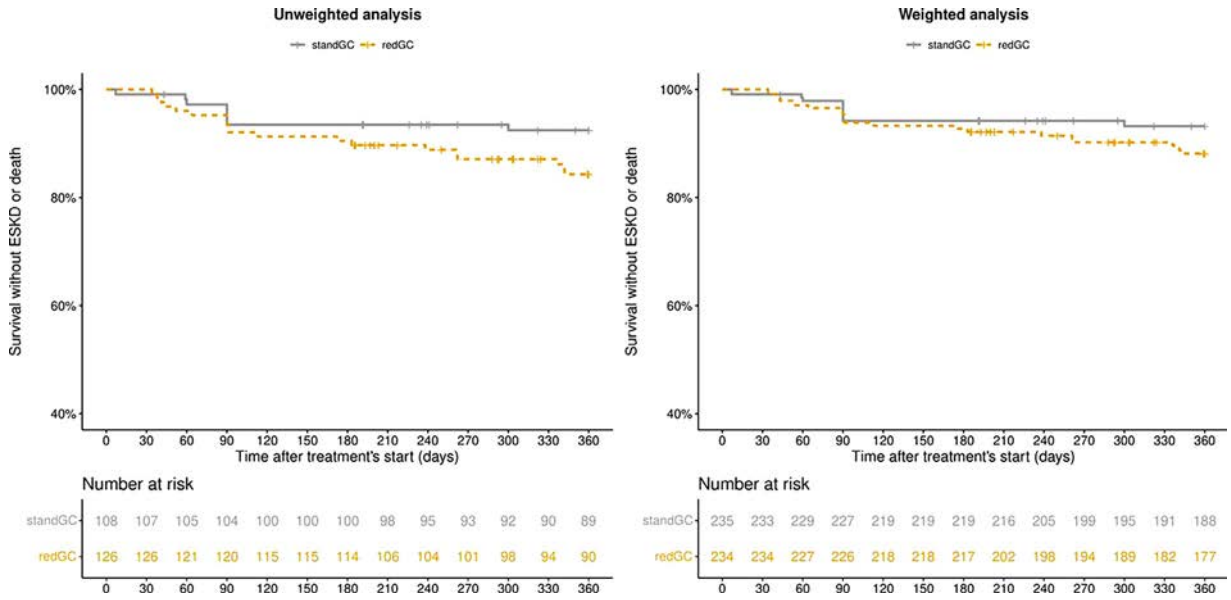

Figure 2. Kaplan-Meier survival curve comparing occurrence of death or end-stage kidney disease at 12 months of patients treated with reduced-dose GC regimen (redGC) and patients treated with standard-dose GC regimen (standGC) during the first year of follow-up. Panel **A** shows the survival curve for the entire study population and Panel **B** shows the survival curve for patients after inverse probability treatment weighting. ESKD, end-stage kidney disease.

this trend since we found a significantly higher risk of death or ESKD with the redGC compared with the standGC in the subgroup of patients treated with RTX induction therapy (which corresponded to 71% of patients).

Our data represent the only real-world experience with the redGC since the publication of the PEXIVAS study. It is not disputed that the level of evidence provided by the PEXIVAS study, the largest randomised controlled trial in the field of vasculitis, is much higher than our retrospective and real-life study. However, the discrepancies between PEXIVAS results and our results can be explained by some factors that seem important to discuss and integrate in the current management of AAV. First, the population enrolled in our study is significantly different from the severe population enrolled in the PEXIVAS study [12]. The PEXIVAS study enrolled patients with severe GPA or MPA characterised by either severe renal involvement with a glomerular filtration rate less than 50 mL/min/1.73 m² and/or intra-alveolar haemorrhage. In our study, patients had severe GPA or MPA according to French guidelines, meaning that the disease threatened their vital or functional prognosis and required induction treatment with either RTX or CYC. As a result, approximately one-quarter of our patients had neither renal involvement nor intra-alveolar haemorrhage and death or ESKD at 1 year was twice as low in our study population as in the PEXIVAS population, 11.1% versus 22.0%, respectively. Also, in contrast to PEXIVAS study, patients with comorbidities contraindicating the use of GCs, RTX or CYC were included in our study. Second, it is important to note that, in contrast to the PEXIVAS trial [12] in which only 15% of patients received RTX as induction therapy, 71% of our patients received such an induction regimen. This difference can be attributed to differences in patient severity and, most importantly, to changes in practice between the PEXIVAS inclusion period (ie, 2010–2016) and our inclusion period (2018–2022). Third, during the maintenance phase, 89% of patients in our study received RTX whereas patients in the PEXIVAS study received only azathioprine as maintenance therapy which also reflects the change in practice between our two studies. Fourth, only 17% of patients in our study received plasma exchange compared with 50% of patients in the PEXIVAS study.

The results of our study also contrast with those of the LoVAS trial [18] primarily due to differences in primary outcomes. While LoVAS focused on remission at 6 months, our primary composite outcome included death, ESKD, progression before remission and relapse. The LoVAS trial [18] found non-inferiority of a highly reduced GC regimen compared with a standard regimen in terms of remission at 6 months and we found similar results in our study given that redGC was not associated with the risk of remission. Yet, in our study, redGC was significantly associated with the risk of occurrence of our primary outcome in all our analyses (unweighted, adjusted and weighted analyses). Also, LoVAS trial had some limitations including a shorter follow-up period and a different patient population (80% of patients with MPA and exclusion of patients with severe glomerulonephritis and alveolar haemorrhage requiring oxygen therapy>2 L/min).

Considering the available data on the use of this redGC, our study has several strengths. It is the first study on the real-world use of the redGC and we included in the analysis not only death or ESKD but also other outcomes that are particularly useful in daily practice (ie, progression before achieving remission, relapse, serious infections at 1 year) in patients with severe GPA or MPA. Our study was conducted in many different centres and included a large number of patients treated according to current practice with high use of RTX induction and maintenance therapy and minimal use of plasma exchange which explains why our results are helpful and complementary to those of the PEXIVAS study. The GC regimen administered in both groups (redGC and standGC) appropriately corresponded to the expected dose based on their respective groups. In addition, we performed a thorough statistical analysis and confirmed our results through sensitivity analyses including a weighted analysis to ensure comparability. Clinically relevant criteria associated with mortality and/or relapse including age, AAV subtype, history of vasculitis relapse and baseline creatinine levels were used as adjustment factors in our multivariable analysis [19–21]. This approach avoids relying solely on factors that were statistically associated with the primary outcome in the univariable analysis. Finally, our study has significant external validity because several of our findings are consistent with those reported in the literature. We observed an association between the outcome of death or ESKD and factors known to influence mortality or ESKD such as age, MPA subtype and elevated serum creatinine [22–24]. Also, we found no association between death or ESKD and the redGC as in the PEXIVAS study [12].

Our study has also some limitations. First, it is a retrospective study with inherent limitations and we chose a composite outcome in order to increase the power of our study which also has its limits. Given that this is not a randomised clinical trial, results could be driven by an unintentional patient selection bias. Second, although there were some significant differences in baseline characteristics between redGC and standGC, it is unlikely that these differences had a significant impact on our primary outcome. For example, PR3-ANCA positivity which is known to be associated with a higher incidence of relapse [19,20] was more prevalent in the standGC group; yet, the standGC group was not at higher risk of experiencing a relapse. In addition, the redGC group received plasma exchange less frequently than the standGC group (10% vs 25%, respectively). The effect of plasma exchange on renal function remains controversial [3,25,26] and this imbalance between the two groups affected only a small number of patients. However, these factors were adjusted for in the multivariable unweighted analysis and weighted analysis. There were no other statistically significant differences between the two groups for collected factors known or suspected to be associated with death, ESKD, disease progression or relapse. Yet, it is important to note that we had no data concerning patient's comorbidities which could be potential confounders for death or ESKD or for the choice of the GC regimen. Third, a quarter of the patients in our study did not receive pulses of methylprednisolone prior to oral GCs unlike all the patients enrolled in the PEXIVAS study. Fourth, the standGC showed heterogeneity in GC regimens and the minimum follow-up was only 6 months. Caution is warranted when interpreting long-term results even though the median follow-up was 25 months. To be as close as possible to the PEXIVAS study, we restricted our outcomes to 12 months in our primary analysis. Fifth, no significant difference in severe infections was observed between the two groups in contrast to the findings of the PEXIVAS study where the reduced-dose group had fewer infections compared with the standard-dose group. This discrepancy may be explained by a potential selection bias as clinicians might have been more likely to prescribe the reduced GC regimen to patients perceived to be at higher risk of infection. In addition, the lack of kidney histological data is a notable gap that limits a comprehensive understanding of renal outcomes [22,27] but this is also the case in the PEXIVAS trial. Finally, subgroup analyses may have been hampered by a lack of statistical power.

In conclusion, in a real-life setting in patients with severe GPA or MPA, the redGC regimen was significantly associated with an increased risk of occurence of the composite primary outcome consisting of death, ESKD, AAV progression before remission or relapse compared with patients receiving a standGC regimen but not with an increased risk of death or ESKD, or the occurrence of serious infections. Therefore, our data suggest increased vigilance when using the redGC regimen, especially in the two subgroups of patients at higher risk of failure, that is, those receiving RTX as induction therapy and those with a baseline serum creatinine greater than 300 µmol/L.

Contributors

Concept and design: BT, SN, XP. Acquisition, analysis or interpretation of data: all authors. Drafting of the manuscript: SN, BT. Statistical analysis: YN, MB. Critical revision of the manuscript: all authors. Supervision: BT. Guarantor: BT.

Funding

The authors have not declared a specific grant for this research from any funding agency in the public, commercial or not-for-profit sectors.

Competing interests

None declared.

Patient and public involvement

Patients and/or the public were not involved in the design, or conduct, or reporting, or dissemination plans of this research.

Patient consent for publication

Not applicable.

Ethics approval

This study involves human participants and was approved by Comité Local d'Ethique pour les Publications de l'hôpital Cochin (decision CLEP N°: AAA-2022-08050). It is an observational retrospective study, so there is no need for an informed consent in France. This study was approved by an ethical committee and every patient was in a hospital involved in research and therefore patients were informed with the hospital chart that their data may be used anonymously for research purposes.

Data availability statement

Data are available upon reasonable request. Please send your request by email to benjamin.terrier@aphp.fr or sophie.nagle@aphp.fr.

Supplementary materials

Supplementary material associated with this article can be found in the online version at doi:10.1136/ard-2024-226339.

Orcid

Sophie Nagle: http://orcid.org/0000-0002-5859-5524
Yann Nguyen: http://orcid.org/0000-0002-0866-3824
Raphaël Borie: http://orcid.org/0000-0002-9906-0024
Maxime Beydon: http://orcid.org/0000-0003-4924-093X
Xavier Puechal: http://orcid.org/0000-0003-3573-9203
Benjamin Terrier: http://orcid.org/0000-0001-6612-7336

REFERENCES

[1] Hellmich B, Sanchez-Alamo B, Schirmer JH, et al. EULAR recommendations for the management of ANCA-associated vasculitis: 2022 update. Ann Rheum Dis 2024;83:30–47.
[2] Floege J, Jayne DRW, Sanders J-SF, et al. KDIGO 2024 Clinical Practice Guideline for the Management of Antineutrophil Cytoplasmic Antibody (ANCA)–Associated Vasculitis. Kidney Int 2024;105:S71–116.
[3] Chung SA, Langford CA, Maz M, et al. 2021 American College of Rheumatology/Vasculitis Foundation Guideline for the Management of Antineutrophil Cytoplasmic Antibody–Associated Vasculitis. Arthritis Care & Research 2021;73:1088–105.
[4] Walsh M, Merkel PA, Mahr A, et al. Effects of duration of glucocorticoid therapy on relapse rate in antineutrophil cytoplasmic antibody–associated vasculitis: A meta-analysis. Arthritis Care & Research 2010;62:1166–73.
[5] Miloslavsky EM, Niles JL, Wallace ZS, et al. Reducing glucocorticoid duration in ANCA-associated vasculitis: A pilot trial. Semin Arthritis Rheum 2018;48:288–92.
[6] Yao TC, Huang YW, Chang SM, et al. Association Between Oral Corticosteroid Bursts and Severe Adverse Events: A Nationwide Population-Based Cohort Study. Ann Intern Med 2020;173:325–30.
[7] Huscher D, Thiele K, Gromnica-Ihle E, et al. Dose-related patterns of glucocorticoid-induced side effects. Ann Rheum Dis 2009;68:1119–24.
[8] Waki D, Nishimura K, Tokumasu H, et al. Initial high-dose corticosteroids and renal impairment are risk factors for early severe infections in elderly patients with antineutrophil cytoplasmic autoantibody-associated vasculitis: A retrospective observational study. *Medicine (Baltimore)* 2020;99:e19173.
[9] Saag KG, Koehnke R, Caldwell JR, et al. Low dose long-term corticosteroid therapy in rheumatoid arthritis: An analysis of serious adverse events. Am J Med 1994;96:115–23.
[10] Curtis JR, Westfall AO, Allison J, et al. Population-based assessment of adverse events associated with long-term glucocorticoid use. Arthritis & Rheumatism 2006;55:420–6.
[11] Da Silva JAP, Jacobs JWG, Kirwan JR, et al. Safety of low dose glucocorticoid treatment in rheumatoid arthritis: published evidence and prospective trial data. Ann Rheum Dis 2006;65:285–93.
[12] Walsh M, Merkel PA, Peh C-A, et al. Plasma Exchange and Glucocorticoids in Severe ANCA-Associated Vasculitis. N Engl J Med 2020;382:622–31.
[13] Robson JC, Grayson PC, Ponte C, et al. 2022 American College of Rheumatology/European Alliance of Associations for Rheumatology Classification Criteria for Granulomatosis With Polyangiitis. Arthritis & Rheumatology 2022;74:393–9.
[14] Suppiah R, Robson JC, Grayson PC, et al. 2022 American College of Rheumatology/European Alliance of Associations for Rheumatology Classification Criteria for Microscopic Polyangiitis. Arthritis & Rheumatology 2022;74:400–6.
[15] Pagnoux C, Quéméneur T, Ninet J, et al. Treatment of systemic necrotizing vasculitides in patients aged sixty-five years or older: results of a multicenter, open-label, randomized controlled trial of corticosteroid and cyclophosphamide-based induction therapy. Arthritis Rheumatol 2015;67:1117–27.
[16] Terrier B, Charles P, Aumaître O, et al. ANCA-associated vasculitides: Recommendations of the French Vasculitis Study Group on the use of immunosuppressants and biotherapies for remission induction and maintenance. Presse Med 2020;49:104031.
[17] Junek ML, Merkel PA, Vilayur E, et al. Risk of Relapse of Antineutrophil Cytoplasmic Antibody–Associated Vasculitis in a Randomized Controlled Trial of Plasma Exchange and Glucocorticoids. Arthritis & Rheumatology 2024;76:1431–8.
[18] Furuta S, Nakagomi D, Kobayashi Y, et al. Effect of Reduced-Dose vs High-Dose Glucocorticoids Added to Rituximab on Remission Induction in ANCA-Associated Vasculitis: A Randomized Clinical Trial. JAMA 2021;325:2178–87.
[19] Morgan MD, Szeto M, Walsh M, et al. Negative anti-neutrophil cytoplasm antibody at switch to maintenance therapy is associated with a reduced risk of relapse. Arthritis Res Ther 2017;19:129.

[20] Charles P, Perrodeau É, Samson M, et al. Long-Term Rituximab Use to Maintain Remission of Antineutrophil Cytoplasmic Antibody-Associated Vasculitis: A Randomized Trial. Ann Intern Med 2020;173:179–87.
[21] Terrier B, Pagnoux C, Perrodeau É, et al. Long-term efficacy of remission-maintenance regimens for ANCA-associated vasculitides. Ann Rheum Dis 2018;77:1150–6.
[22] Brix SR, Noriega M, Tennstedt P, et al. Development and validation of a renal risk score in ANCA-associated glomerulonephritis. Kidney Int 2018;94:1177–88.
[23] Berti A, Cornec D, Crowson CS, et al. The Epidemiology of Antineutrophil Cytoplasmic Autoantibody-Associated Vasculitis in Olmsted County, Minnesota: A Twenty-Year US Population-Based Study. Arthritis Rheumatol 2017;69:2338–50.
[24] Nguyen Y, Pagnoux C, Karras A, et al. Microscopic polyangiitis: Clinical characteristics and long-term outcomes of 378 patients from the French Vasculitis Study Group Registry. J Autoimmun 2020;112:102467.
[25] Walsh M, Collister D, Zeng L, et al. The effects of plasma exchange in patients with ANCA-associated vasculitis: an updated systematic review and meta-analysis. BMJ 2022;376:e064604.
[26] Zeng L, Walsh M, Guyatt GH, et al. Plasma exchange and glucocorticoid dosing for patients with ANCA-associated vasculitis: a clinical practice guideline. BMJ 2022;376:e064597.
[27] Nezam D, Porcher R, Grolleau F, et al. Kidney Histopathology Can Predict Kidney Function in ANCA-Associated Vasculitides with Acute Kidney Injury Treated with Plasma Exchanges. J Am Soc Nephrol 2022;33:628–37.

Ann Rheum Dis 84 (2025) 329–340

Contents lists available at ScienceDirect

Annals of the Rheumatic Diseases

journal homepage: https://www.sciencedirect.com/journal/annals-of-the-rheumatic-diseases

Vasculitis

Age, anticoagulants, hypertension and cardiovascular genetic traits predict cranial ischaemic complications in patients with giant cell arteritis

Natalie J.M. Chaddock[1], Charlotte J. Harden[1,2], Louise Sorensen[1,3], Hannah R. Mathieson[1,3], Michal Zulcinski[1,3], Catherine A. Lawson[4], Eoin O'Sullivan[5], Susan P. Mollan[6,7], Javier Martin[8], Sarah L. Mackie[1,3], Mark M. Iles[1,3], Ann W. Morgan[1,2,3,*], UK GCA Consortium

[1] *School of Medicine and Leeds Institute for Data Analytics, University of Leeds, Leeds, UK*
[2] *NIHR Leeds Medicines and In Vitro Diagnostics Co-operative, Leeds Teaching Hospitals NHS Trust, Leeds, UK*
[3] *NIHR Leeds Biomedical Research Centre, Leeds Teaching Hospitals NHS Trust, Leeds, UK*
[4] *Harrogate District Hospital, Harrogate, UK*
[5] *Ophthalmology, King's College Hospital NHS, London, UK*
[6] *Ophthalmology, University Hospitals Birmingham, Birmingham, UK*
[7] *Neurometabolism, Institute of Metabolism and Systems Research, University of Birmingham, Birmingham, UK*
[8] *Institute of Parasitology and Biomedicine, López-Neyra, IPBLN, CSIC, Granada, Spain*

ARTICLE INFO

Article history:
Received 10 January 2024
Accepted 28 August 2024

Keywords:
Giant Cell Arteritis
Cardiovascular Disease
Polymorphism
Genetics

ABSTRACT

Objectives: This project aimed to determine whether cranial ischaemic complications at the presentation of giant cell arteritis (GCA) were associated with pre-existing cardiovascular (CV) risk factors, CV disease or genetic risk of CV-related traits.

Methods: 1946 GCA patients with clinicodemographic data at GCA presentation were included. Associations between pre-existing CV-related traits (including Polygenic Risk Scores (PRS) for CV traits) and cranial ischaemic complications were tested. A model for cranial ischaemic complications was optimised using an elastic net approach. Positional gene mapping of associated PRS was performed to improve biological understanding.

Results: In a sample of 1946 GCA patients (median age = 71, 68.7% female), 17% had cranial ischaemic complications at presentation. In univariable analyses, 10 variables were associated with complications (likelihood-ratio test $p \leq 0.05$). In multivariable analysis, the two variables with the strongest effects, with or without PRS in the model, were anticoagulant therapy (adjusted OR (95% CI) = 0.21 (0.05 to 0.62), $p = 4.95 \times 10^{-3}$) and age (adjusted OR (95% CI) = 1.60 (0.73 to 3.66), $p = 2.52 \times 10^{-3}$, for ≥80 years versus <60 years). In sensitivity analyses omitting anticoagulant therapy from multivariable analysis, age and hypertension were associated with cranial ischaemic complications at presentation (hypertension: adjusted OR (95% CI) = 1.35 (1.03 to 1.75), p = 0.03). Positional gene mapping of an associated transient ischaemic attack PRS identified *TEK*, *CD96* and *MROH9* loci.

Conclusion: Age and hypertension were risk factors for cranial ischaemic complications at GCA presentation, but in this dataset, anticoagulation appeared protective. Positional gene mapping suggested a role for immune and coagulation-related pathways in the pathogenesis of complications. Further studies are needed before implementation in clinical practice.

*Correspondence to Professor Ann W. Morgan.
E-mail address: a.w.morgan@leeds.ac.uk (A.W. Morgan).
Social media: @Sarah_L_Mackie (S. L. Mackie)
Handling editor Josef S. Smolen.

https://doi.org/10.1136/ard-2024-225515

WHAT IS ALREADY KNOWN ON THIS TOPIC

- Age and cardiovascular risk factors have been suggested as risk factors for cranial ischaemic complications of giant cell arteritis (GCA), such as visual loss or stroke.

WHAT THIS STUDY ADDS

- This study confirms that age and prior hypertension are associated with cranial ischaemic complications of GCA. Anticoagulant therapy appears to be protective; this is a novel finding. Interrogation of an associated transient ischaemic attack polygenic risk score also revealed a genetic basis of risk through influence on immune and coagulation pathways.

HOW THIS STUDY MIGHT AFFECT RESEARCH, PRACTICE OR POLICY

- This finding indicates the need for further evaluation of therapies that target thrombosis pathways in GCA, ultimately requiring testing in randomised controlled trials.

INTRODUCTION

Giant cell arteritis (GCA) is the most common primary systemic vasculitis affecting older people and without prompt treatment may result in irreversible visual loss [1]. Patients with GCA may present with systemic symptoms, such as fever, malaise and weight loss; cranial symptoms, such as headache, scalp tenderness, jaw or tongue claudication, with or without cranial ischaemic complications such as vision loss or stroke; symptoms relating to large-vessel involvement, such as limb claudication or critical limb ischaemia; or symptoms of polymyalgia rheumatica (proximal limb-girdle pain and stiffness). GCA is diagnosed following an assessment of these symptoms, clinical signs, laboratory markers of inflammation, temporal artery biopsy (TAB) and/or imaging of relevant vascular territories [2]. High-dose glucocorticoid therapy must be initiated promptly; higher doses are recommended for those with ischaemic complications. On subsequent tapering of glucocorticoids, relapse occurs in about half of all patients with GCA. Relapse is treated with high-dose glucocorticoids if there are ischaemic manifestations and by smaller dose escalations otherwise, along with glucocorticoid-sparing therapies [2,3].

A history of ischaemic manifestations at GCA diagnosis is linked with risk of subsequent visual loss [4]. We reasoned that identification of risk factors for ischaemic manifestations at GCA presentation might identify a subset of patients who may benefit from more intensive monitoring and potentially adjunctive treatments.

Various prior studies suggested that cranial ischaemic complications in GCA are associated with age [5] and prior cardiovascular (CV) risk factors, including atherosclerosis [6], stroke, peripheral vascular disease [7], hypertension [6] and socioeconomic status [8]. Ischaemic complications are less common in those with high levels of acute phase markers, erythrocyte sedimentation rate and C reactive protein [9]. Data are conflicting on whether antiplatelet/anticoagulant therapy may protect against ischaemic complications in GCA [10–13]. However, all these studies have been relatively small (less than 500 cases).

Larger population studies have demonstrated an excess risk of CV disease (CVD), hypertension and diabetes following a diagnosis of GCA [14–16], where dose-dependent associations have been demonstrated with glucocorticoid use [17]. However, vascular inflammation is also proatherogenic and disentangling the effects of age, lifestyle influences and medication from CV-related risk factors can be challenging. One approach to this is to examine ischaemic complications at presentation and the relationship between genetic predisposition to CV risk factors, using a Polygenic Risk Score (PRS) approach. A PRS estimates an individual's genetic propensity to a trait by enumerating the number of risk alleles they carry across multiple loci, weighted by the effect sizes of each estimated from a genome-wide association study (GWAS) [18]. Testing for such associations could provide evidence for the role of pre-existing or predisposed CV risk factors and ischaemic manifestations of GCA and could identify novel pathogenic mechanisms underlying both disorders.

Previous candidate gene studies have identified strong associations between GCA susceptibility and genes of the major histocompatibility complex (MHC) [19,20], as well as associations in genes related to vascular function [21] and cytokines [22]. A GWAS identified associations of GCA susceptibility with *HLA-DRB1* and *HLA-DQA1* in the HLA class II, *HLA-B* in the HLA class I, as well as loci in the region of *PLG* and *P4HA2* [23].

In this study, we aimed to identify associations between pre-existing CV risk factors, CVD or genetic risk of CV-related traits and cranial ischaemic complications at GCA presentation. We then constructed PRS for CV-related risk factors, tested these for association with ischaemic complications and evaluated the performance of these PRS alongside non-genetic risk factors. Finally, we used positional gene mapping to highlight the pathogenic mechanisms underlying PRS loci.

METHODS

Data source/study population

This study used individual-level clinicodemographic and genetic data from the UKGCA Consortium and UK Biobank. For details of both cohorts, and information about the genotyping, quality control and imputation of UKGCA genetic data, see online supplemental methods.

Study outcomes

The primary outcome was cranial ischaemic complications at presentation of GCA, including ocular and non-ocular complications. Secondary outcomes were a transient cranial ischaemic features composite (including ocular and non-ocular ischaemic features) and a composite of extracranial ischaemic manifestations, comprising extracranial ischaemic features (arm and leg claudication secondary to GCA) and/or extracranial ischaemic complications (fixed vascular stenosis to a limb secondary to GCA). For further details of outcome definitions, see online supplemental methods, table 1.

Patients with both cranial ischaemic complications and transient cranial ischaemic features recorded were retained in the primary cohort and removed from both the case and reference cohorts of the secondary (transient) outcome, in order to ensure mutual exclusivity. Individuals with both cranial ischaemic complications and extracranial ischaemic manifestations were not removed from the secondary (extracranial) outcome cohort, to prevent substantial losses in sample size (N = 203 with both outcomes vs N = 59 with solely secondary outcome).

Risk factors studied were pre-existing CVDs, CV risk factors, CV medication and CV-related trait PRS. Definitions of these risk factors may be found in online supplemental methods.

Using PRSice V.2.3.3 [24], PRSs were calculated for CVDs and CV risk factors using effect sizes from publicly available GWAS summary statistics or GWAS performed in white European UK Biobank data using linear or logistic regression in PLINK V.1.9 [25]. More details of this approach, as well as a full list of traits for which PRSs were calculated and their respective data sources, may be found in online supplemental methods, table 2.

Statistical analyses

We first described the clinical and sociodemographic characteristics of the UKGCA Consortium sample, including different classification/diagnostic criteria and subcohorts with ischaemic complications, and/or transient ischaemic features. Data were described with either number (N) and percentage (%), or median (MD) and lower IQR and upper IQR (Q1–Q3), unless otherwise stated.

Correlations between investigated risk factors were assessed using the Pearson correlation coefficient, R^2. One variable from any pair with $R^2 \geq 0.8$ was removed from further analyses.

Statistical analyses were performed in R V.3.6.2 to model the risk of cranial ischaemic complications in GCA using logistic regression. To reduce the number of df in our models, all non-binary risk factors (including PRS) were modelled as continuous variables.

Univariable analyses were first performed to test for associations between cranial ischaemic complications in GCA and clinical and sociodemographic variables.

Sensitivity analyses were then performed, removing individuals with either of the secondary outcomes (transient cranial ischaemic features or extracranial ischaemic manifestations) from the primary reference cohort, and re-evaluating univariable associations with cranial ischaemic complications.

Traits with a likelihood ratio (LR) test $p \leq 0.1$ in univariable regression were added to an elastic net regression model ($\alpha = 0.50$; $\lambda = 6.43 \times 10^{-3}$) to perform variable selection and reduce the number of redundant variables. Every variable was missing in some samples so the LR test p value threshold was chosen both to avoid possible bias by imputing these and to minimise sample loss in the elastic net regression. Variables retained using this technique were included in a complete-case multivariable logistic regression to assess effect sizes of risk factors.

Univariable associations between PRS and the primary outcome were tested; those PRS with LR test $p \leq 0.1$ were added to the clinical and sociodemographic model optimised using elastic net and logistic regression, in order to avoid substantial data losses due to the complete case approach used in subsequent analyses. Elastic net regression was used for variable selection, and effect estimates for the final clinical, sociodemographic and genetic model were retrieved with multivariate regression.

Finally, the resulting model was tested for association with the secondary outcomes (transient cranial ischaemic features and extracranial ischaemic manifestations) in logistic regression.

Trait PRS with an LR test $p \leq 0.05$ in univariable regression were further interrogated by positional mapping of genetic loci within the PRS. Genetic loci within 10 kb of a gene, or with known functional consequences (including exonic, splicing, intronic, 3'untranslated region (UTR) and 5' UTR single nucleotide polymorphisms (SNPs)) were mapped using Ensembl build 85 (V.11) [26] and ANNOVAR [27]. Furthermore, StringDB [28] network analysis was performed using proteins encoded by positionally mapped genes, and compared with proteins mapped by previous work [23,29].

Patient and public involvement

Patients and the public were not involved in the original design of the UKGCA Consortium, which commenced in 2005. However, the study has subsequently been discussed with patients with lived experience with GCA through the MRC TARGET Programme Management Board that includes three patient partners.

RESULTS

A total of 1946 UKGCA Consortium patients (94.8% (N = 1844/1946) with genetic data) were included in the analyses. The sample size for each of the analyses presented is provided to highlight missing clinical data. 99.2% (N = 1863/1878) were 'white European' (online supplemental methods) and 68.7% (N = 1331/1938) were female (table 1). The median age at diagnosis was 71 (IQR = 66–77) years. 93.0% (N = 1324/1424) fulfilled the 1990 American College of Rheumatology (ACR) classification criteria for GCA after imputation of ESR using CRP where necessary and 94.9% (N = 1583/1669) fulfilled 2022 ACR/European Alliance of Associations for Rheumatology (EULAR) classification criteria for GCA (see online supplemental methods). 69.2% (N = 992/1434) had a diagnosis of GCA confirmed by TAB and/or diagnostic vascular imaging (online supplemental table 3). No notable differences in demographic variables were observed between the overall cohort and any diagnostic category (table 1, online supplemental table 3), although a disproportionately high number of individuals (28.9%; 389/1346) fell within the UK population's 'least deprived' index of multiple deprivation 2019 quintile (online supplemental results).

Of 1946 UKGCA individuals in this study, 17.0% (N = 327/1925) had cranial ischaemic complications, 59.3% (N = 951/1604) had transient cranial ischaemic features, and 12.5% (N = 203/1630) had extracranial ischaemic manifestations (table 2). No differences in the prevalence of ischaemic manifestations were observed between the different diagnostic groups (online supplemental results, table 4) and subsequent analyses were performed on the total GCA cohort.

Of the cohort with cranial ischaemic complications (primary outcome), 15.6% (N = 43/275) also had symptoms suggestive of extracranial ischaemic features, and 2.2% (N = 6/300) had extracranial ischaemic complications (table 3). 26.9% (N = 80/298) of the cohort with cranial ischaemic complications reported PMR symptoms, with 63.8% of these (N = 51/80) reporting an onset of PMR symptoms before their GCA symptoms began. Further descriptions of cohorts in this work are summarised in online supplemental results, table 4–9.

Prior to the testing of univariable associations with the primary outcome, pairwise Pearson correlations were estimated between variables. No trait pairs were found to be strongly correlated (Pearson $R^2 \geq 0.80$) and all were retained in the analyses. A few traits had a correlation $R^2 \geq 0.45$, including hyperlipidaemia and cholesterol-lowering medication ($R^2 = 0.50$, $p = 3.44 \times 10^{-80}$), and atrial fibrillation (AF) and anticoagulant therapy ($R^2 = 0.49$, $p = 4.75 \times 10^{-66}$). More details of these correlations may be found in online supplemental table 10.

In univariable analyses, risk factors with associations with cranial ischaemic complications in GCA with an LR test $p < 0.05$ (table 4, online supplemental results, tables 11–13) included:

Table 1

Patient demographics at presentation: total GCA cohort; those fulfilling imputed 1990 ACR classification criteria; confirmed diagnosis by temporal artery biopsy or vascular imaging

	Total cohort (N = 1946)	Fulfilling imputed 1990 ACR classification criteria (N* = 1324/1424)	Diagnosis confirmed by biopsy/imaging (N* = 992/1434)
Age at diagnosis (years), median (IQR)	71 (66–77)	71 (66–77)	73 (68–78)
Female sex	1331/1938 (68.7%)	892/1320 (67.6%)	663/992 (66.8%)
Ethnicity			
EUR	1863/1878 (99.2%)	1273/1287 (98.9%)	954/963 (99.1%)
AFR	2/1878 (0.1%)	2/1287 (0.2%)	1/963 (0.1%)
SAS	13/1878 (0.7%)	12/1287 (0.9%)	8/963 (0.8%)
EAS	0/1878 (0%)	0/1287 (0%)	0/963 (0%)
Family history of GCA	26/947 (2.8%)	21/758 (2.8%)	11/448 (2.5%)
Family history of PMR	42/939 (4.5%)	34/751 (4.5%)	18/444 (4.1%)
BMI (kg/m^2)			
<18.5	21/937 (2.2%)	15/756 (2.0%)	13/454 (2.9%)
18.5 to <25	383/937 (40.9%)	312/756 (41.3%)	221/454 (48.7%)
25 to <30	354/937 (37.8%)	284/756 (37.6%)	160/454 (35.2%)
≥30 kg/m^2	179/937 (19.1%)	145/756 (19.2%)	60/454 (13.2%)
Smoking tobacco (ever)	809/1568 (51.6%)	660/1267 (52.1%)	413/795 (52.0%)
Smoking tobacco at GCA diagnosis	208/1563 (13.3%)	172/1263 (13.6%)	125/792 (15.8%)
Alcohol units/week	5 (0 to 7)	5 (0 to 7)	5 (0 to 7)
Alcohol ≥14 units/week	110/1147 (9.59%)	96/920 (10.4%)	58/565 (10.3%)
Index of Multiple Deprivation 2019 (quintiles)			
1 (most deprived)	270/1346 (20.1%)	187/885 (21.1%)	143/706 (20.3%)
2	269/1346 (20.0%)	176/885 (19.9%)	146/706 (20.7%)
3	269/1346 (20.0%)	173/885 (19.6%)	130/706 (18.4%)
4	269/1346 (20.0%)	182/885 (20.6%)	143/706 (20.3%)
5 (least deprived)	269/1346 (20.0%)	167/885 (18.9%)	144/706 (20.4%)

*Sample size varied in different analyses due to missing clinical data. The N in this column reflects the individuals included in the various analyses.

ACR, American College of Rheumatology; AFR, African; BMI, body mass index; CV, cardiovascular disease; EAS, east Asian; EUR, white European (European/American); GCA, giant cell arteritis; N, sample number; PMR, polymyalgia rheumatica; IQR, interquartile range; SAS, South Asian.

Table 2

Patient demographics at presentation, categorised according to presence and type of ischaemic manifestations

	Cranial ischaemic complications (N† = 327/1925)	Transient cranial ischaemic features* (N† = 951/1604)	Extracranial ischaemic manifestations (N† = 203/1630)	No ischaemic manifestations (N† = 514/1944)
	MD (Q1–Q3) or N (%)			
Age at diagnosis (years)	72 (68–78)	71 (66–77)	69 (64–74)	71 (65–76)
Sex (female)	216/325 (66.5%)	675/948 (71.2%)	141/200 (70.5%)	351/513 (68.4%)
Ethnicity				
EUR	313/317 (98.7%)	909/915 (99.3%)	195/197 (98%)	501/504 (99.4%)
AFR	1/317 (0.3%)	1/915 (0.1%)	1/197 (0.5%)	0/504 (0%)
SAS	3/317 (1.0%)	5/915 (0.6%)	1/197 (0.5%)	3/504 (0.6%)
EAS	0/317 (0%)	0/915 (0%)	0/197 (0%)	0/504 (0%)
Family history of GCA	3/177 (1.7%)	10/389 (2.6%)	2/125 (1.6%)	12/336 (3.6%)
Family history of PMR	10/178 (5.6%)	20/387 (5.2%)	6/124 (4.8%)	11/328 (3.4%)
BMI (kg/m^2)				
<18.5	2/169 (1.2%)	8/384 (2.1%)	3/116 (2.6%)	8/333 (2.4%)
18.5 to <25	68/169 (40.2%)	173/384 (45.1%)	47/116 (40.5%)	123/333 (36.9%)
25 to <30	63/169 (37.3%)	131/384 (34.1%)	47/116 (40.5%)	136/333 (40.8%)
≥30 kg/m^2	36/169 (21.3%)	72/384 (18.8%)	19/116 (16.4%)	66/333 (19.8%)
Smoking tobacco (ever)	165/311 (53.1%)	368/700 (52.6%)	97/195 (49.7%)	227/460 (49.4%)
Smoking tobacco at GCA diagnosis	41/311 (13.2%)	91/700 (13%)	24/194 (12.4%)	62/456 (13.6%)
Alcohol units/week	4 (0 to 6)	5 (0 to 7)	4 (0 to 6)	5 (0 to 7)
Alcohol ≥14 units/week	21/218 (9.6%)	51/492 (10.4%)	14/149 (9.4%)	33/379 (8.7%)
Index of Multiple Deprivation 2019 (quintiles)				
1 (most deprived)	45/209 (21.5%)	137/678 (20.2%)	35/169 (20.7%)	63/353 (17.9%)
2	43/209 (20.6%)	132/678 (19.5%)	34/169 (20.1%)	73/353 (20.7%)
3	34/209 (16.3%)	141/678 (20.8%)	38/169 (22.5%)	78/353 (22.1%)
4	50/209 (23.9%)	139/678 (20.5%)	39/169 (23.1%)	61/353 (17.3%)
5 (least deprived)	37/209 (17.7%)	129/678 (19.0%)	23/169 (13.6%)	78/353 (22.1%)

AFR, African; BMI, body mass index; CV, cardiovascular; EAS, east Asian; EUR, white European (European/American); GCA, giant cell arteritis; MD, median; N, sample number; PMR, polymyalgia rheumatica; Q, quartile; SAS, South Asian.

* Omitting individuals with cranial ischaemic complications.

† Sample size varied in different analyses due to missing clinical data. The N in this column reflects the individuals included in the various analyses.

Table 3
Patient clinical characteristics at presentation: cranial ischaemic complications; transient cranial ischaemic features; extra-cranial ischaemic manifestations

	Cranial ischaemic complications	Transient cranial ischaemic features*	Extracranial ischaemic manifestations	No ischaemic features
	(N† = 327/1925) MD (Q1–Q3) or N (%)	(N† = 951/1604)	(N† = 203/1630)	(N† = 514/1944)
GCA symptoms to steroids duration (days)	44 (4–58)	49 (7–61)	69 (13–92)	39 (7–50)
Cranial ischaemic manifestations‡				
Cranial ischaemic complications	327/327 (100.0%)	0/938 (0%)	49/201 (24.4%)	0/514 (0%)
Ocular complications	297/327 (90.8%)	0/942 (0%)	38/199 (19.1%)	0/510 (0%)
Non-ocular cranial complications	42/295 (14.2%)	0/948 (0%)	14/181 (7.7%)	0/439 (0%)
Transient cranial ischaemic features*	0/325 (0%)	951/951 (100%)	93/154 (60.4%)	0/514 (0%)
Ocular ischaemic features*	0/327 (0%)	423/942 (44.9%)	40/199 (20.1%)	0/510 (0%)
Non-ocular cranial ischaemic features*	0/321 (0%)	768/948 (81%)	78/153 (51%)	0/504 (0%)
Extracranial ischaemic manifestations				
Extracranial ischaemic features§	43/275 (15.6%)	92/598 (15.4%)	192/203 (94.6%)	0/435 (0%)
Extracranial ischaemic complications¶	6/300 (2.2%)	1/746 (0.2%)	11/203 (5.4%)	0/514 (0%)
PMR and polymyalgic symptoms**	80/298 (26.9%)	263/666 (35.4%)	87/188 (46.3%)	143/437 (32.7%)
Before GCA	51/80 (63.8%)	146/236 (61.9%)	57/87 (65.5%)	104/143 (72.7%)
At GCA presentation	21/80 (26.3%)	90/236 (38.1%)	30/87 (34.5%)	39/143 (27.3%)
Systemic inflammatory response				
Weight loss/kg	0.7 (−1.0 to 4.0)	0.3 (−2.0 to 3.4)	−0.2 (−3.9 to 4.8)	−0.08 (−2.15 to 3.0)
Weight loss≥4 kg	81/154 (52.6%)	151/327 (46.2%)	62/119 (52.1%)	104/279 (37.3%)
ESR mm/hour	58 (32–86)	64 (36–93)	59.9 (33–88)	61 (34–87)
CRP mg/L	67 (13–107)	75 (20–109)	73 (19–110)	67 (17–96)
Platelet count, $\times 10^9$/L	369 (274–447)	398 (302–468)	390 (291–456)	368 (278–439)

CRP, C reactive protein; ESR, erythrocyte sedimentation rate; GCA, giant cell arteritis; MD, median; PMR, polymyalgia rheumatica; Q, quartile.
* Omitting individuals with cranial ischaemic complications.
† Sample size varied in different analyses due to missing clinical data. The N in this column reflects the individuals included in the various analyses.
‡ Cranial ischaemic manifestations at GCA presentation. (A) Transient cranial ischaemic features. Ocular ischaemic features: transient diplopia; transient double vision/absence of ocular motility; transient field defect; transient reduced acuity; transient vision loss. Non-ocular cranial ischaemic features: jaw claudication; tongue claudication; transient ischaemic attack at presentation considered secondary to GCA. (B) Cranial ischaemic complications. Ocular complications: Anterior ischaemic optic neuropathy; branch retinal artery occlusion; cilioretinal artery occlusion; cranial nerve palsy (III, IV or V); central retinal artery occlusion; posterior ischaemic optic neuropathy; relative afferent pupillary defect; irreversible visual loss; irreversible visual field defect; irreversible ocular motility; irreversible diplopia. Non-ocular cranial complications: Scalp necrosis; tongue necrosis; cerebrovascular accident at presentation considered secondary to GCA.
§ Extracranial ischaemic features: arm claudication; leg claudication.
¶ Extracranial ischaemic complications: fixed vascular stenosis to limb at presentation, secondary to GCA.
** PMR and polymyalgic symptoms: Polymyalgic symptoms and/or a formal PMR diagnosis were recorded at the time of initial GCA diagnosis. Where PMR was diagnosed and treated with medium-dose glucocorticoids (eg, 10–20 mg prednisolone) prior to developing symptoms of GCA we classified these cases as having PMR prior to GCA, whereas untreated symptoms at GCA presentation were recorded as occurring at GCA presentation.

age at GCA diagnosis (OR 1.54, 95% CI 0.87 to 2.74, $p = 2.00\times10^{-3}$, for the highest (≥80 years) vs lowest (<60 years) decade), PMR symptoms at GCA diagnosis (OR (95% CI) = 0.73 (0.56 to 0.95), p = 0.02), and weight loss ≥4 kg (OR (95% CI) = 1.54 (1.08 to 2.19), p = 0.08). The CVD composite (OR (95% CI) = 1.68 (1.27 to 2.22), $p < 1.00\times10^{-3}$), hypertension (OR (95% CI) = 1.59 (1.24 to 2.05), $p < 1\times10^{-3}$), hyperlipidaemia (OR (95% CI) = 1.5 (1.15 to 1.96), $p = 3.00\times10^{-3}$), cholesterol-lowering medication pre-GCA (OR (95% CI) = 1.38 (1.03 to 1.84), p = 0.03) and antiplatelet therapy pre-GCA (OR (95% CI) = 1.42 (1.02 to 1.99), p = 0.04) were also each associated with cranial ischaemic complications in GCA.

An additional two risk factors had an LR p<0.1: platelet count (OR (95% CI) = 0.61 (0.41 to 0.91), p = 0.06, for the highest vs lowest quintile) and anticoagulant therapy pre-GCA (OR (95% CI) = 0.5 (0.22 to 1.10), p = 0.06). 29/435 (6.7%) presenting without any ischaemic features were on anticoagulant therapy, whereas only 7/280 (2.5%) GCA patients presenting with cranial ischaemic complications were on anticoagulant therapy (online supplemental table 6).

Sensitivity analyses were performed whereby individuals with transient cranial ischaemic features or extracranial ischaemic manifestations were removed from the primary reference cohort, and univariable analyses were re-evaluated, excluding up to N = 997 reference subjects. Several risk factors remained associated with cranial ischaemic complications in GCA at LR p<0.05 (table 4). These included age at GCA diagnosis (OR (95% CI) = 1.62 (0.85 to 3.09), $p < 1.00\times10^{-3}$, for the highest (≥80 years) vs lowest (<60 years) decade), weight loss ≥4 kg (OR (95% CI) = 1.85 (1.24 to 2.75), $p = 2.00\times10^{-3}$), the CVD composite (OR (95% CI) = 1.42 (1.01 to 2.00), p = 0.04), hypertension (OR (95% CI) = 1.54 (1.16 to 2.05), $p = 3.00\times10^{-3}$), antiplatelet therapy (OR (95% C) = 1.48 (1.00 to 2.20), p = 0.05) and anticoagulant therapy (OR (95% CI) = 0.38 (0.16 to 0.87), p = 0.01).

Elastic net regression was performed on risk factors with an LR p<0.1 (n = 13) to remove redundant or highly correlated variables from the model and to perform variable selection. The weight loss (≥4 kg) variable was omitted from regression due to low sample numbers with non-missing data (N samples with non-missing data for weight loss variable = 681). Full details of model optimisation, including alpha and lambda selection, and variable weights as determined by elastic net regression (online supplemental table 14), are described in online supplemental results. The 11 variables prioritised by elastic net regression were tested in multivariable regression (sample N = 789), adjusted for clinical and sociodemographic risk factors (table 5). This revealed two statistically significant associations with

Table 4
Univariable associations with cranial ischaemic complications with likelihood ratio p≤0.1

	Primary univariable associations			Sensitivity analyses*		
Trait	OR (95% CIs)	P value†	DF	OR (95%CIs)	P value†	DF
Age at GCA diagnosis‡		2.00×10^{-3}	1899		8.17×10^{-4}	909
<60 years	1.00			1.00		
60 to <70 years	0.99 (0.57 to 1.71)			0.95 (0.52 to 1.74)		
70 to <80 years	1.43 (0.84 to 2.43)			1.63 (0.91 to 2.92)		
≥80 years	1.54 (0.87 to 2.74)			1.66 (0.87 to 3.17)		
PMR symptoms	0.73 (0.56 to 0.95)	0.02	1529	0.86 (0.64 to 1.17)	0.33	789
Weight loss (≥4 kg)	1.54 (1.08 to 2.19)	0.02	797	1.85 (1.24 to 2.75)	2.00×10^{-3}	437
ESR quintiles (mm/hour)‡		0.09	1200		0.57	654
<29	1.00			1.00		
29 to <49	0.57 (0.36 to 0.91)			0.60 (0.36 to 1.00)		
49 to <69	1.08 (0.71 to 1.64)			1.29 (0.80 to 2.08)		
69 to <96	0.69 (0.44 to 1.08)			0.76 (0.46 to 1.26)		
≥96	0.67 (0.43 to 1.04)			0.82 (0.50 to 1.34)		
Platelet count quintiles ($\times10^9$/L)‡		0.06	1507		0.69	770
<271	1.00			1.00		
271 to <334.8	0.65 (0.44 to 0.96)			0.78 (0.50 to 1.22)		
334.8 to <396	0.67 (0.45 to 0.99)			0.81 (0.52 to 1.27)		
396 to <485	0.89 (0.61 to 1.29)			1.20 (0.78 to 1.84)		
≥485	0.61 (0.41 to 0.91)			0.90 (0.57 to 1.42)		
CVD composite	1.68 (1.27 to 2.22)	$<1\times10^{-3}$	1924	1.52 (1.11 to 2.10)	0.01	930
TIA/CVA	1.64 (1.06 to 2.52)	0.03	1550	1.78 (1.06 to 2.99)	0.03	801
Hyperlipidaemia	1.50 (1.15 to 1.96)	3.00×10^{-3}	1545	1.62 (1.19 to 2.21)	2.00×10^{-3}	810
Hypertension	1.59 (1.24 to 2.05)	$<1.00\times10^{-3}$	1616	1.53 (1.15 to 2.03)	4.00×10^{-3}	827
Antiplatelet therapy	1.42 (1.02 to 1.99)	0.04	1321	1.48 (1.00 to 2.2)	0.05	682
Anticoagulant therapy	0.50 (0.22 to 1.10)	0.06	1398	0.38 (0.16 to 0.87)	0.01	733
Cholesterol-lowering medication	1.38 (1.03 to 1.84)	0.03	1316	1.38 (0.99 to 1.93)	0.06	678
Platelet count PRS quintiles‡		0.09	1843		0.17	891
1 (lowest)	1.00			1.00		
2	0.83 (0.57 to 1.21)			0.69 (0.45 to 1.06)		
3	0.69 (0.47 to 1.03)			1.03 (0.68 to 1.56)		
4	1.06 (0.73 to 1.54)			0.80 (0.53 to 1.21)		
5 (highest)	1.02 (0.70 to 1.48)			0.69 (0.45 to 1.06)		
TIA PRS quintiles‡		0.027	1842		0.098	891
1 (lowest)	1			1		
2	0.98 (0.66 to 1.47)			0.75 (0.48 to 1.17)		
3	1.25 (0.85 to 1.85)			1.03 (0.66 to 1.62)		
4	0.97 (0.64 to 1.45)			0.78 (0.49 to 1.24)		
5 (highest)	1.37 (0.93 to 2)			1.22 (0.79 to 1.90)		

CVA, cerebrovascular attack; CVD, cardiovascular disease; DF, degrees of freedom; ESR, erythrocyte sedimentation rate; GCA, giant cell arteritis; PMR, polymyalgia rheumatica; PRS, Polygenic Risk Score; TIA, transient ischaemic attack.
* Sensitivity analyses include a reference group with no ischaemic features.
† P value from likelihood ratio test.
‡ Analyses performed using continuous variables, quantile/group ORs presented for interpretation purposes.

cranial ischaemic complications in GCA: age at GCA diagnosis (adjusted OR (95% CI) = 1.85 (0.84 to 4.32), $p = 2.81\times10^{-3}$, for the highest (≥80 years) vs lowest (<60 years) decade) and anticoagulant therapy prior to GCA (adjusted OR (95% CI) = 0.18 (0.04 to 0.53), $p = 1.09\times10^{-3}$).

To assess associations between CVDs/CV risk factors and cranial ischaemic complications in GCA without the confounding influence of age, PRS for these traits were tested for association with GCA in univariable analyses (online supplemental table 15), revealing one PRS with an LR p<0.05 (table 4), a transient ischaemic attack (TIA) PRS (OR (95% CI) = 1.37 (0.93 to 2.00), p = 0.03, for the highest compared with the lowest PRS quintile) and one PRS with an LR p<0.1, a platelet count PRS (OR (95%I) = 1.02 (0.70 to 1.48), p = 0.09).

PRSs with an LR p<0.10 were added to the clinical and sociodemographic model, elastic net regression was performed for variable selection (online supplemental table 16), and multivariable regression was performed on the final clinical, sociodemographic and genetic model (N = 812). The two variables associated with cranial ischaemic complications prior to the addition of PRS remained significant and retained similar effect sizes compared with the model without PRS (table 5): age at GCA diagnosis (adjusted OR (95% CI) = 1.60 (0.73 to 3.66), $p = 2.52\times10^{-3}$, for the highest (≥80 years) vs lowest (<60 years) decade) and anticoagulant therapy pre-GCA (adjusted OR (95% CI) = 0.21 (0.05 to 0.62), $p = 4.95\times10^{-3}$). Both of these variables remained strongly associated with cranial ischaemic complications in women, but not men, in sex-stratified analyses (online supplemental table 17), as well as in analyses performed using solely patients who fulfilled the 2022 ACR/EULAR classification criteria (online supplemental table 18). Of note, the platelet count PRS was also strongly associated with the outcome in this analysis (AOR (95% CI) = 0.41 (0.22 to 0.73), p = 0.04), suggesting a potentially protective role of increased heritable platelet levels in cranial ischaemic complications.

Details of associations with secondary outcomes may be found in online supplemental table 19. Briefly, no variables had an association with transient cranial ischaemic complications at LR p<0.05. Associations were found between extracranial ischaemic manifestations and PMR symptoms at GCA diagnosis

Table 5
Multivariable associations with cranial ischaemic complications in GCA at presentation (complete case approach), following variable selection with elastic net regression

	Model including clinical and sociodemographic variables		Model including clinical, sociodemographic and PRS variables	
Trait	OR (95% CIs)	P value*	OR (95% CIs)	P value*
Age at diagnosis†		2.81×10^{-3}		2.52×10^{-3}
<60 years	1.00		1.00	
60 to <70 years	0.70 (0.34 to 1.55)		0.58 (0.28 to 1.25)	
70 to <80 years	1.21 (0.60 to 2.62)		1.06 (0.54 to 2.23)	
≥80 years	1.85 (0.84 to 4.32)		1.60 (0.73 to 3.66)	
PMR	0.76 (0.52 to 1.10)	0.13	0.80 (0.55 to 1.16)	0.26
ESR quintiles (mm/hour)†		0.29		0.24
<29	1.00		1.00	
29 to <49	0.54 (0.29 to 1.00)		0.49 (0.27 to 0.90)	
49 to <69	1.30 (0.73 to 2.31)		1.13 (0.66 to 1.95)	
69 to <96	0.69 (0.37 to 1.27)		0.62 (0.34 to 1.10)	
≥96	0.69 (0.37 to 1.29)		0.63 (0.36 to 1.11)	
Platelet count quintiles ($\times10^9$/L)†		0.70	NA‡	
<271	1.00			
271 to <334.8	0.61 (0.35 to 1.08)			
334.8 to <396	0.56 (0.30 to 1.04)			
396 to <485	0.93 (0.52 to 1.66)			
≥485	0.63 (0.34 to 1.17)			
CVD composite	1.41 (0.81 to 2.41)	0.23	1.13 (0.65 to 1.93)	0.72
TIA/CVA	1.20 (0.57 to 2.52)	0.72	1.34 (0.62 to 2.82)	0.50
Hyperlipidaemia	1.61 (1.02 to 2.54)	0.11	1.44 (0.90 to 2.26)	0.33
Hypertension	1.47 (1.01 to 2.14)	0.07	1.34 (0.93 to 1.95)	0.11
Antiplatelet therapy	1.19 (0.70 to 1.98)	0.66	1.25 (0.73 to 2.10)	0.43
Anticoagulant therapy	0.18 (0.04 to 0.53)	1.09×10^{-3}	0.21 (0.05 to 0.62)	4.95×10^{-3}
Cholesterol-lowering therapy	0.60 (0.36 to 0.98)	0.14	0.68 (0.41 to 1.12)	0.24
Platelet count PRS quintiles†	NA			0.11
1			1	
2			0.55 (0.31 to 0.94)	
3			1.03 (0.6 to 1.75)	
4			0.69 (0.41 to 1.17)	
5			0.45 (0.25 to 0.81)	
TIA PRS quintiles†	NA			0.13
1			1	
2			0.99 (0.55 to 1.76)	
3			1.21 (0.67 to 2.19)	
4			1.05 (0.59 to 1.87)	
5			1.29 (0.74 to 2.26)	

CVA, cerebrovascular accident; CVD, cardiovascular disease; ESR, erythrocyte sedimentation rate; GCA, giant cell arteritis; NA, not available; PMR, polymyalgia rheumatica; PRS, Polygenic Risk Score; TIA, transient ischaemic attack.
* P value from likelihood ratio test.
† Analyses performed using continuous variables, quantile/group ORs presented for interpretation purposes.
‡ Platelet count was not retained by elastic net regression for this round of analyses, see online supplemental results.

(adjusted OR (95% CI) = 1.99 (1.21 to 3.29), p = 0.01) and the CVD composite (adjusted OR (95% CI) = 2.39 (1.17 to 4.75), $p = 5.2\times10^{-3}$).

Positional mapping of the TIA PRS using Ensembl V.11 [26] and ANNOVAR [27] revealed 17 mapped loci (16 protein-coding genes), including the *MROH9, CD96, IBTK, CLTA, TEK* and *KLB* genes (figure 1).

Sensitivity analysis

A sensitivity analysis was performed on the clinical and sociodemographic multivariable model, omitting the 'anticoagulant use prior to GCA' variable and reperforming elastic net regression for variable selection. Following this, three variables remained in the multivariable model (complete case N = 1429), of which two were statistically significant (table 6): age at diagnosis (adjusted OR (95% CI) = 1.03 (1.01 to 1.04), $p = 4.15\times10^{-3}$) and hypertension (adjusted OR (95% CI) = 1.35 (1.03 to 1.75), p = 0.03). When PRSs were added to the sensitivity analysis model (omitting the anticoagulant use prior to GCA variable) and elastic net was performed (complete case N = 1545), three variables remained in the model including age at diagnosis (adjusted OR (95% CI) = 1.25 (0.69 to 2.34), p = 0.01, for the highest (≥80 years) vs lowest (<60 years) decade), hypertension (adjusted OR (95% CI) = 1.53 (1.18 to 1.98), $p = 1.17\times10^{-3}$) and platelet count PRS (adjusted OR (95% CI) = 0.63 (0.42 to 0.93), p = 0.10).

DISCUSSION

Using the largest cohort of well-characterised GCA patients recruited from secondary care to date (N = 1946), the univariable analysis identified 10 variables significantly associated with cranial ischaemic complications at GCA presentation. The large sample size permitted multivariable analysis, which identified that advanced age was a risk factor and anticoagulant therapy protective, following adjustment for all the other included variables. If anticoagulant therapy was removed from the multivariable model, age and hypertension remained in the model as significantly associated with cranial ischaemic complications. Positional gene mapping of an associated TIA PRS revealed loci in genes related to immune and coagulation pathways.

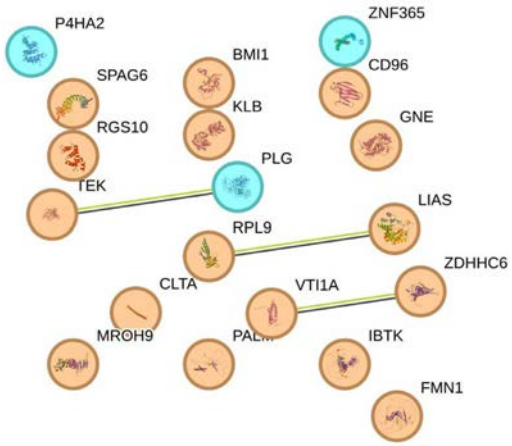

Figure 1. StringDB[28] network analysis using proteins (nodes) encoded by positionally mapped genes of TIA PRS loci (orange nodes) and proteins encoded by positionally mapped loci from previous work (blue nodes).[23,29] Edges of this network represent protein-protein links found by StringDB via text mining (green edges) and coexpression (black edges). BMI1, BMI1 Proto-Oncogene, Polycomb Ring Finger; CD96, Cluster of Differentiation 96; CLTA, Clathrin Light Chain A; FMN1, Formin 1; GNE, Glucosamine (UDP-N-Acetyl)−2-Epimerase/N-Acetylmannosamine Kinase; IBTK, Inhibitor Of Bruton Tyrosine Kinase; KLB, Beta-Klotho; LIAS, Lipoic Acid Synthetase; MROH9, Maestro Heat Like Repeat Family Member 9; PALM, Paralemmin; PLG, Plasminogen; P4HA2, Prolyl 4-Hydroxylase Subunit Alpha 2; RGS10, Regulator of G Protein Signalling 10; RPL9, Ribosomal Protein L9; SPAG6, Sperm Associated Antigen 6; TEK, Tyrosine Kinase; VTI1A, Vesicle Transport Through Interaction With T-SNAREs 1A; ZDHHC6, Zinc Finger DHHC-Type Containing 6; ZNF365, Zinc Finger Protein 365.

The present work confirms the association of cranial ischaemic complications with increasing age [3,5] and additionally identifies a potential protective effect of anticoagulant use, but not antiplatelet use, prior to GCA diagnosis. The use of antiplatelet drugs was strongly associated with age in our study and larger studies are required to disentangle any potential beneficial effects of antiplatelet medication from the effects of age. Small studies initially suggested a protective effect of antiplatelet/anticoagulant) therapy against ischaemic events in GCA [11,12] but meta-analysis failed to confirm this clearly [10]. Currently, due to the lack of randomised controlled trial data, neither antiplatelet nor anticoagulant therapy is universally recommended for patients with GCA [2]. As expected, anticoagulant use was correlated with AF. The lack of association of AF with ischaemic complications in univariable analyses, and clinical implausibility of a protective effect of AF against ischaemic manifestations, makes this an unlikely source of confounding. Nor does confounding by other CV risk factors appear likely. It is difficult to entirely control for confounding by indication: it is possible that an unmeasured confounder (such as prothrombotic tendency reflected in the history of thromboembolic disease) may be influencing results. Nonetheless, the effect size observed in this study in relation to anticoagulation is striking and suggests that further exploration is warranted to determine whether there may be a direct beneficial effect of anticoagulation in GCA.

Inflammation-induced thrombosis is widely recognised in the vasculitides [30]. While thrombosis is infrequently observed in the temporal arteries in GCA, it is unclear whether thrombosis occurs in the smaller vessels supplying the eye. GCA is associated with venous thromboembolism, particularly during active disease [31]. A number of small studies have reported antiphospholipid antibodies (lupus anticoagulant and IgG anti-cardiolipin, β2-glycoprotein I and prothrombin antibodies) in up to 48% of GCA cases [32–34]. In one study, there was a suggestion that two or more antiphospholipid antibodies were associated with visual manifestations [34], but this requires confirmation. Genetic associations with *PLG* have been demonstrated [23,29]. *PLG* encodes plasminogen, the precursor of plasmin, which lyses fibrin clots as well as inactivating coagulation factors (thereby acting as an anticoagulant) [35,36]. A recent report suggests that overproduction of reactive oxygen species by peripheral blood leucocytes in GCA results in the oxidation of fibrinogen [37]; this, in turn, causes a striking impairment of fibrinogen function such that it becomes less susceptible to fibrinolysis by plasmin; this functional impairment was reversed in vitro by tocilizumab. Taken together with the present findings, this provides a plausible mechanism linking immune and thrombotic pathways in GCA, providing new perspectives on therapy.

Further studies are now required to explore the role of thrombosis in cranial ischaemic manifestations, to determine whether

Table 6
Associations with cranial ischaemic complications in GCA at presentation, adjusted for sociodemographic, clinical and genetic factors, following variable selection with elastic net regression

Trait	Model including clinical and sociodemographic variables		Model including clinical, sociodemographic and PRS variables	
	OR (95% CI)	P value*	OR (95%CI)	P value*
Age at GCA diagnosis†		4.15×10^{-3}		0.01
<60 years	1.00		1.00	
60 to <70 years	0.83 (0.48 to 1.49)		0.85 (0.49 to 1.53)	
70 to <80 years	1.25 (0.74 to 2.22)		1.29 (0.77 to 2.29)	
≥80 years	1.33 (0.73 to 2.49)		1.25 (0.69 to 2.34)	
PMR	0.78 (0.59 to 1.02)	0.07	NA	
Hypertension	1.35 (1.03 to 1.75)	0.03	1.53 (1.18 to 1.98)	1.17×10^{-3}
Platelet count PRS Quintiles†	NA			0.10
1			1.00	
2			0.59 (0.39 to 0.88)	
3			0.88 (0.60 to 1.29)	
4			0.70 (0.47 to 1.03)	
5			0.63 (0.42 to 0.93)	

Sensitivity analysis omitting anticoagulant use prior to GCA.
CVD, cardiovascular disease; GCA, giant cell arteritis; NA, not available; PMR, polymyalgia rheumatica; PRS, Polygenic Risk Score.
* P value from likelihood ratio test.
† Analyses performed using continuous variables, quantile/group ORs presented for interpretation purposes.

short-term anticoagulant therapy in combination with glucocorticoid use could reduce the risk of complications in high-risk GCA patients. Patients presenting with visual symptoms, particularly those with monocular blindness or amaurosis fugax, are at elevated risk of further visual loss shortly after GCA diagnosis [38]. This is illustrated by an orbital MRI study that showed that 38% of patients with unilateral visual symptoms had MRI abnormalities of the contralateral eye [39], illustrating a potential window of opportunity to prevent bilateral blindness.

Given the relatively small number of patients taking an anticoagulant prior to GCA diagnosis, we sought to determine if other risk factors may also be relevant for those not using anticoagulants. These secondary analyses revealed the importance of both age and hypertension in fully adjusted models. An association between severe ischaemic complications and hypertension was observed in previous studies [6,40]. While involvement of the renal arteries is traditionally viewed to be a more typical feature of Takayasu arteritis, imaging studies have shown up to 16% of patients with large vessel GCA have evidence of renal artery involvement [41].

To gain further mechanistic insight, a PRS constructed for TIA had a statistically significant association (LR $p<0.05$) with cranial ischaemic complications in univariate analyses, yet the strength of this association was reduced following adjustment for clinical, sociodemographic and genetic risk factors. Positional mapping of this PRS with Ensembl [26] and ANNOVAR [27] revealed genetic variants localised to 16 protein-coding genes in the genome. These loci included *TEK*, which encodes the angiopoietin-1 receptor (TIE2), known to be elevated in GCA [42]. TIE2 is instrumental in cell surface interactions at the vascular wall and is implicated in haemostasis pathways shared with plasminogen [23,43]. Plasminogen is thought to act in multiple haemostasis pathways: first in platelet activation, signalling and aggregation, a cascade in which the procoagulant properties of platelets (which contain angiogenesis stimulators and inhibitors) are enhanced and thrombus formation occurs [44], and second in the dissolution of fibrin clots, which includes tissue remodelling, cell migration and inflammation [36]. The presence of GCA susceptibility and GCA outcome associations in genes which encode proteins implicated in these haemostasis-related and coagulation-related pathways further supports the potential importance of these pathways in GCA pathogenesis.

Limitations

While the size of this GCA cohort (N = 1946) is the largest with detailed clinical characterisation reported to date, the use of a complete case design in this work and the interrogation of disease subsets reduces the number of samples, cutting statistical power. Another limitation is that this cohort was primarily Caucasian. Although the prevalence of GCA is high in northern European countries, many reports confirm that GCA can occur in non-Caucasian individuals. The lack of representation of non-Caucasian populations in this work therefore limits the application of findings from the study to individuals from other ethnic groups. This is particularly prudent for PRS associations found in this work, since patterns of linkage disequilibrium vary across ethnicities and SNP associations found for one population may not be relevant to another. It is also important to note that PRS may include some genetic variants that are not genuine predictors of the outcome for which the PRS is optimised (eg, TIA). However, optimal PRS tend to yield sufficient true associations to outweigh those included due to stochastic variation, meaning that over-representation of biological pathways in PRS should still be indicative of possible functional relevance.

Covariates included in multivariable analyses must be chosen carefully when looking for evidence of causal relationships, to avoid overadjustment [45]. For example, hypertension influences both AF and anticoagulant prescribing decisions; therefore, if seeking to investigate the causal role of hypertension, adjustment for anticoagulant therapy might distort estimates of the causal effect of hypertension on cranial ischaemic complications in GCA and reduce power to detect association, especially if anticoagulant therapy has its own direct effect on the outcome. The sensitivity analyses omitting anticoagulant therapy in part address this limitation.

Finally, current GCA guidelines advise the use of at least one diagnostic test (eg, TAB or imaging) to confirm GCA, in order to avoid misdiagnosis of non-arteritic anterior ischaemic optic neuropathy (AION) (which constitutes approximately 95% of all AION) as arteritic-AION [2,46]. Given that 30.8% of this cohort, presenting over three decades, did not have a confirmatory diagnostic test, it is possible that some individuals in this cohort were misdiagnosed with GCA. A number of sensitivity analyses were performed, including analyses of biopsy or imaging-confirmed GCA.

CONCLUSION

This work identified risk factors associated with cranial ischaemic complications in GCA, which included age at diagnosis, hypertension and a potentially protective role of anticoagulant therapy in severe complications in GCA. It must be emphasised that, since unmeasured confounding could not be ruled out, these findings are not sufficient yet to change clinical practice; further research, such as randomised controlled trials. Positional gene mapping of an associated TIA PRS also highlighted genetic loci related to immune and coagulation pathways. Together, these results suggest a need for further interrogation of the role of thrombosis in GCA, and to elucidate whether anticoagulant therapy alongside glucocorticoids might be beneficial in patients with GCA, especially those with transient or monocular visual involvement, or other high-risk subsets.

Acknowledgments

We thank all patients who participated in this study. All UK GCA Consortium group members contributed to patient and data collection and were integral to the delivery of this project. A list of group members can be found in online supplemental appendix 1, available online. In addition, we thank Dr Mar Pujades Rodriguez for her invaluable advice on the design of the case report form.

Collaborators

UK GCA Consortium: Louise Sorensen, School of Medicine, University of Leeds, Leeds UK (Lubna Haroon Raashid, Steve Martin, James I Robinson); Chapel Allerton Hospital, Chapeltown Road, Leeds, LS7 4SA, UK (Ann Morgan, Sarah Mackie, Oliver Wordsworth, Isobel Whitwell, Jessica Brock); Pinderfields General Hospital, Aberford Road, Wakefield, WF1 4DG, UK (Victoria Douglas, Chamila Hettiarachchi, Jacqui Bartholomew); Dewsbury District and General Hospital, Halifax Road, Dewsbury, WF13 4HS, UK (Stephen Jarrett, Gayle Smithson); York Hospital, Wigginton Road, York, YO31 8HE, UK (Michael

Green, Pearl Clark Brown); Harrogate District Hospital, Lancaster Park Rd, Harrogate, HG2 7SX, UK (Cathy Lawson, Esther Gordon); Ipswich Hospital, Heath Road, Ipswich, IP4 5PD, UK (Suzanne Lane, Rebecca Francis); Southend Hospital, Prittlewell Chase, Westcliff-on-Sea, Essex, SS0 0RY, UK (Bhaskar Dasgupta, Bridgett Masunda, Jo Calver); Hull Royal Infirmary, Anlaby Road, Hull, HU3 2JZ, UK (Yusuf Patel, Charlotte Thompson, Louise Gregory); Croydon University Hospital, 530 London Road, Croydon, Surrey, CR7 7YE, UK (Sarah Levy); Haywood Hospital, High Lane, Burslem, Staffordshire, ST6 7AG, UK (Ajit Menon, Amy Thompson, Lisa Dyche, Michael Martin); Royal Surrey County Hospital, Egerton Road, Guildford, GU2 7XX, UK (Charles Li); Queen's Hospital, Belvedere Road, Burton-on-Trent, DE13 0RB, UK (Ramasharan Laxminarayan, Louise Wilcox, Ralph de Guzman); Freeman Hospital, Freeman Road, High Heaton, Newcastle upon Tyne, Tyne and Wear, NE7 7DN, UK (John Isaacs, Alice Lorenzi, Gary Reynolds, Ross Farley, Helain Hinchcliffe-Hume); Barnsley Hospital, Gawber Road, Barnsley, S75 2EP, UK (Victoria Bejarano, Susan Hope); Northampton General Hospital, Cliftonville, Northampton, NN1 5BD, UK (Pradip Nandi, Lynne Stockham, Catherine Wilde, Donna Durrant); Frimley Park Hospital, Portsmouth Road, Camberley, GU16 7UJ, UK (Mark Lloyd); Doncaster Royal Infirmary, Armthorpe Road, Doncaster, DN2 5LT, UK (Chee-Seng Ye, Rob Stevens); Chelsea and Westminster Hospital, Fulham Road, London, SW10 9NH, UK (Amjad Jilani); Great Western Hospital, Marlborough Road, Swindon, SN3 6BB, UK (David Collins, Suzannah Pegler, Ali Rivett, Liz Price); Royal National Hospital for Rheumatic Diseases, Upper Borough Walls, Bath, Avon, BA1 1RL, UK (Neil McHugh, Sarah Skeoch, Diana O'Kane, Sue Kirkwood); Gateshead Queen Elizabeth Hospital, Queen Elizabeth Avenue, Gateshead, NE9 6SX, UK (Saravanan Vadivelu, Susan Pugmire); Airedale General Hospital, Skipton Road, Keighley, BD20 6TB, UK (Shabina Sultan, Emma Dooks, Lisa Armstrong); Warrington Hospital, Lovely Lane, Warrington, Cheshire, WA5 1QG, UK (Hala Sadik); Basildon University Hospital, Nethermayne, Basildon, SS16 5NL, UK (Anupama Nandagudi, Tolu Abioye, Angelo Ramos, Steph Gumus); St George's Hospital, Blackshaw Road, London, SW17 0QT, UK (Nidhi Sofat, Abiola Harrison, Abi Seward); Queen Elizabeth Hospital, Mindelsohn Way, Birmingham, B15 2TH, UK (Susan Mollan, Ray Rahan, Helen Hawkins); Royal Preston Hospital, Sharoe Green Lane, Preston, PR2 9HT, UK (Hedley Emsley, Anna Bhargava, Vicki Fleming, Marianne Hare, Sonia Raj); Arrowe Park Hospital, Arrowe Park Road, Birkenhead, CH49 5PE, UK (Emmanuel George, Nicola Allen, Karl Hunter); King's College Hospital, Denmark Hill, London, SE5 9RS, UK (Eoin O'Sullivan, Georgina Bird); Stoke Mandeville Hospital, Mandeville Road, Aylesbury, HP21 8AL, UK (Malgorzata Magliano, Katarina Manzo, Bobbie Sanghera); Royal Cornwall Hospital, Treliske, Truro, TR1 3LJ, UK (David Hutchinson, Fiona Hammonds), Peterborough City Hospital, Bretton Gate, Peterborough, PE3 9GZ, UK (Poonam Sharma, Richard Cooper, Graeme McLintock); Scarborough Hospital, Woodlands Drive, Scarborough, YO12 6QL, UK (Zaid S. Al-Saffar, Mike Green, Kerry Elliott, Tania Neale, Janine Mallinson); Queen's Medical Centre, Derby Road, Nottingham, NG7 2UH, UK (Peter Lanyon, Marie-Josephe Pradere); Addenbrooke's Hospital, Hills Road, Cambridge, CB2 0QQ, UK (Natasha Jordan, Ei Phyu Htut, Thelma Mushapaidzi, Donna Abercrombie, Sam Wright, Jane Rowlands); Norfolk and Norwich University Hospital, Colney Lane, Norwich, NR4 7UY, UK (Chetan Mukhtyar, James Kennedy); James Paget Hospital, Lowestoft Road, Great Yarmouth, NR31 6LA, UK (Damodar Makkuni, Elva Wilhelmsen); The Queen Elizabeth Hospital, Gayton Road, King's Lynn, PE30 4ET, UK (Michael Kouroupis); West Suffolk Hospital, Hardwick Lane, Bury St Edmunds, IP33 2QZ, UK (Shweta Bhagat, Lily John); Ashford and St. Peter's Hospitals, London Road, Ashford, TW15 3AA, UK (Rod Hughes, Margaret Walsh, Marie Buckley); Torbay Hospital, Newton Road, Torquay, TQ2 7AA, UK (Kirsten Mackay, Tracey Camden-Woodley, Joan Redome, Kirsty Pearce); Lister Hospital, Coreys Mill Lane, Stevenage, SG1 4AB, UK (Thiraupathy Marianayagam, Carina Cruz, Elizabeth Warner); North Tyneside General Hospital, Rake Lane, North Shields, NE29 8NH, UK (Ishmael Atchia, Claire Walker, Karen Black, Stacey Duffy); Royal Lancaster Infirmary/Westmorland General Hospital, Ashton Road, Lancaster, LA1 4RP, UK (Marwan Bukhari, Lynda Fothergill, Rebecca Jefferey, Jackie Toomey); Royal Glamorgan Hospital, Ynysmaerdy, Pontyclun, CF72 8XR, UK (Ceril Rhys Dillon, Carla Pothecary, Lauren Green); Warwick Hospital, Lakin Road, Warwick, CV34 5BW, UK (Tracey Toms, Linda Maher); West Middlesex Hospital, Twickenham Road, Isleworth, TW7 6AF, UK (Diana Davis, Amrinder Sayan, Mini Thankachen); Royal Devon and Exeter Hospital, Barrack Road, Exeter, EX2 5DW, UK (Mahdi Abusalameh, Jessica Record); Birmingham Heartlands Hospital, Bordesley Green, Birmingham, B9 5SS, UK (Asad Khan, Sam Stafford); Royal Derby Hospital, Uttoxeter Road, Derby, DE22 3NE, UK (Azza Hussein, Clare Williams, Alison Fletcher, Laura Johson, Richard Burnett); Aintree University Hospital, Lower Lane, Liverpool, L9 7AL, UK (Robert Moots, Helen Frankland); University Hospital Wishaw, Netherton Street, Wishaw, ML2 0DP, UK (James Dale, Karen Black, Kirsten Moar, Carol Hollas); Manchester Royal Infirmary, Oxford, Manchester, M13 9WL, UK (Ben Parker, Derek Ridings, Sandhya Eapen, Sindhu John); Bristol Royal Infirmary, Upper Maudlin Street, Bristol, BS2 8HW, UK (Jo Robson, Lucy Belle Guthrie, Rose Fyfe, Moira Tait); Christchurch Hospital, Fairmile Road, Christchurch, BH23 2JX, UK (Jonathan Marks, Emma Gunter, Rochelle Hernandez); Ninewells Hospital & Medical School, James Arrott Drive, Dundee, DD2 1SG, UK (Smita Bhat, Paul Johnston); Poole Hospital, Longfleet Road, Poole, BH15 2JB, UK (Muhammad Khurshid, Charlotte Barclay); Countess of Chester Hospital, Liverpool Road, Chester, CH2 1UL, UK (Deepti Kapur, Helen Jeffrey, Anna Hughes, Lauren Slack); Nevill Hall Hospital, Brecon Road, Abergavenny, NP7 7EG, UK (Eleri Thomas, Anna Royon, Angela Hall); Derriford Hospital, Derriford Road, Plymouth, PL6 8DH, UK (Jon King, Sindi Nyathi); University College Hospital, Euston Road, London, NW1 2BU, UK (Vanessa Morris, Madhura Castelino, Ellie Hawkins, Linda Tomson); Royal Free Hospital, Pond Street, London, NW3 2QY, UK (Animesh Singh, Annalyn Nunag, Stella O'Connor); Darlington Memorial Hospital, Hollyhurst Road, Darlington, DL3 6HX, UK (Nathan Rushby, Nicola Hewitson); Leicester Royal Infirmary, Infirmary Square, Leicester, LE1 WW, UK (Kenny O'Sunmboye, Adam Lewszuk, Louise Boyles); Royal Alexandra Hospital/Vale of Leven Hospital/Inverclyde Royal Hospital, Great Western Road, Glasgow, G12 0XH, UK (Martin Perry); Royal Hampshire County Hospital, Romsey Road, Winchester, SO22 5DG, UK (Emma Williams, Christine Graver, Emmanuel Defever); Salford Royal Hospital, Stott Lane, Salford, M6 8HD, UK (Sanjeet Kamanth, Dominic Kay, Joe Ogor, Louise Winter); Minerva Health Centre, Lowthorpe Rd, Preston PR1 6SB, UK (Sarah Horton, Gillian Welch, Kath Hollinshead); Hammersmith Hospital, Du Cane Road, London, W12 0HS, UK (James Peters, Julius Labao, Andrea Dmello); St Helens Hospital, Marshalls Cross Rd, Saint Helens WA9 3DA, UK (Julie Dawson, Denise Graham); Queen Elizabeth the Queen Mother Hospital, Ramsgate Rd, Margate CT9 4AN, UK (Denise De Lord, Jo Deery, Tracy Hazelton).

Contributors

NJMC was responsible for the analysis planning, data collection, verification, data analysis, data interpretation and manuscript writing of analyses in this work. CJH, LS and HRM contributed to the data collection and verification in this work. MMI contributed to the quality control of genetic data in this work. AWM (guarantor) and MMI contributed to the study conception, design, data interpretation and drafting of this work and all authors contributed to the critical revision of the article and approved the final submitted version. CJH, LS and HRM are joint second authors.

Funding

This work was supported in part by the MRC 'Treatment According to Response in Giant cEll arTeritis' (TARGET) Partnership award, MRC DiMen award, NIHR Leeds Biomedical Research Centre (NIHR203331) and Leeds Cares. The MRC TARGET Partnership award supported the salaries of AWM, CJH and LS. SLM was initially funded by an NIHR Clinician Scientist Fellowship award, AWM, LS, MMI and SLM were supported by the NIHR Leeds Biomedical Research Centre, AWM and CJH were supported by the NIHR Leeds MedTech and In Vitro Diagnostic Co-operative, HRM was supported by Leeds Hospital Charitable Foundation, NJMC was supported by an MRC DiMeN PhD studentship and MZ was supported by the HELICAL European Union Horizon 2020 International Training Network. AWM is additionally supported through an NIHR Senior Investigator award.

Disclaimer

The views expressed in this article are those of the authors and not necessarily those of the NIHR, the NIHR Leeds Biomedical Research Centre, the National Health Service or the UK Department of Health and Social Care.

Competing interests

None declared.

Patient and public involvement

Patients and/or the public were not involved in the design, or conduct, or reporting, or dissemination plans of this research.

Patient consent for publication

Not applicable.

Ethics approval

This study involves human participants and was approved by Yorkshire and the Humber Leeds West Research Ethics Committee (05/Q1108/28). Participants gave informed consent to participate in the study before taking part.

Data availability statement

Data are available on reasonable request. Data access requests should be directed to the corresponding author. UK Biobank data may be accessed by completing an application at https://www.ukbiobank.ac.uk/. Generated PRS is available on request.

Supplementary materials

Supplementary material associated with this article can be found in the online version at doi:10.1136/ard-2024-225515.

Orcid

Mark M. Iles: http://orcid.org/0000-0002-2603-6509

REFERENCES

[1] Weyand CM, Goronzy JJ. Clinical practice. Giant-cell arteritis and polymyalgia rheumatica. N Engl J Med 2014;371:50–7. doi: 10.1056/NEJMcp1214825.
[2] Mackie SL, Dejaco C, Appenzeller S, et al. British Society for Rheumatology guideline on diagnosis and treatment of giant cell arteritis. Rheumatology (Oxford) 2020;59:e1–23. doi: 10.1093/rheumatology/kez672.
[3] Pugh D, Karabayas M, Basu N, et al. Large-vessel vasculitis. Nat Rev Dis Primers 2022;7:93. doi: 10.1038/s41572-021-00327-5.
[4] Vodopivec I, Rizzo JF. Ophthalmic manifestations of giant cell arteritis. Rheumatol (Oxford) 2018;57:ii63–72. doi: 10.1093/rheumatology/kex428.
[5] Monti S, Milanesi A, Klersy C, et al. Age at diagnosis influences the clinical phenotype, treatment strategies and outcomes in patients with giant cell arteritis: results from the observational GCAGE study on a large cohort of 1004 patients. Ann Rheum Dis 2023;82:1098–106. doi: 10.1136/ard-2023-223895.
[6] Salvarani C, Bella CD, Cimino L, et al. Risk factors for severe cranial ischaemic events in an Italian population-based cohort of patients with giant cell arteritis. Rheumatology (Sunnyvale) 2009;48:250–3. doi: 10.1093/rheumatology/ken465.
[7] Yates M, MacGregor AJ, Robson J, et al. The association of vascular risk factors with visual loss in giant cell arteritis. Rheumatology (Sunnyvale) 2017;56:kew397. doi: 10.1093/rheumatology/kew397.
[8] Mackie SL, Dasgupta B, Hordon L, et al. Ischaemic manifestations in giant cell arteritis are associated with area level socio-economic deprivation, but not cardiovascular risk factors. Rheumatology (Oxford) 2011;50:2014–22. doi: 10.1093/rheumatology/ker265.
[9] Gonzalez-Gay MA, Lopez-Diaz MJ, Barros S, et al. Giant cell arteritis: laboratory tests at the time of diagnosis in a series of 240 patients. Medicine (Balt) 2005;84:277–90. doi: 10.1097/01.md.0000180043.19285.54.
[10] Martínez-Taboada VM, López-Hoyos M, Narvaez J, et al. Effect of antiplatelet/anticoagulant therapy on severe ischemic complications in patients with giant cell arteritis: A cumulative meta-analysis. Autoimmun Rev 2014;13:788–94. doi: 10.1016/j.autrev.2014.02.006.
[11] Nesher G, Berkun Y, Mates M, et al. Low–dose aspirin and prevention of cranial ischemic complications in giant cell arteritis. Arthritis & Rheum 2004;50:1332–7. doi: 10.1002/art.20171.
[12] Lee MS, Smith SD, Galor A, et al. Antiplatelet and anticoagulant therapy in patients with giant cell arteritis. Arthritis & Rheum 2006;54:3306–9. doi: 10.1002/art.22141.
[13] Narváez J, Bernad B, Gómez-Vaquero C, et al. Impact of antiplatelet therapy in the development of severe ischemic complications and in the outcome of patients with giant cell arteritis. Clin Exp Rheumatol 2008;26:S57–62.
[14] Ray JG, Mamdani MM, Geerts WH. Giant cell arteritis and cardiovascular disease in older adults. Heart 2005;91:324–8. doi: 10.1136/hrt.2004.037481.
[15] Amiri N, De Vera M, Choi HK, et al. Increased risk of cardiovascular disease in giant cell arteritis: a general population–based study. Rheumatology (Sunnyvale) 2016;55:33–40. doi: 10.1093/rheumatology/kev262.
[16] Pujades-Rodriguez M, Duyx B, Thomas SL, et al. Associations between polymyalgia rheumatica and giant cell arteritis and 12 cardiovascular diseases. Heart 2016;102:383–9. doi: 10.1136/heartjnl-2015-308514.
[17] Pujades-Rodriguez M, Morgan AW, Cubbon RM, et al. Dose-dependent oral glucocorticoid cardiovascular risks in people with immune-mediated inflammatory diseases: A population-based cohort study. PLoS Med 2020;17:e1003432. doi: 10.1371/journal.pmed.1003432.
[18] International Schizophrenia Consortium, Purcell SM, Wray NR, et al. Common polygenic variation contributes to risk of schizophrenia and bipolar disorder. Nat New Biol 2009;460:748–52. doi: 10.1038/nature08185.
[19] Combe B, Sany J, Le Quellec A, et al. Distribution of HLA-DRB1 alleles of patients with polymyalgia rheumatica and giant cell arteritis in a Mediterranean population. J Rheumatol 1998;25:94–8.

[20] Jacobsen S, Baslund B, Madsen HO, et al. Mannose-binding lectin variant alleles and HLA-DR4 alleles are associated with giant cell arteritis. J Rheumatol 2002;29:2148–53.
[21] Amoli MM, Garcia-Porrua C, Llorca J, et al. Endothelial nitric oxide synthase haplotype associations in biopsy-proven giant cell arteritis. J Rheumatol 2003;30:2019–22.
[22] Rueda B, Roibas B, Martin J, et al. Influence of interleukin 10 promoter polymorphisms in susceptibility to giant cell arteritis in Northwestern Spain. J Rheumatol 2007;34:1535–9.
[23] Carmona FD, Vaglio A, Mackie SL, et al. A Genome-wide Association Study Identifies Risk Alleles in Plasminogen and P4HA2 Associated with Giant Cell Arteritis. Am J Hum Genet 2017;100:64–74. doi: 10.1016/j.ajhg.2016.11.013.
[24] Choi SW, O'Reilly PF. PRSice-2: Polygenic Risk Score software for biobank-scale data. Gigascience 2019;8:giz082. doi: 10.1093/gigascience/giz082.
[25] Chang CC, Chow CC, Tellier LC, et al. Second-generation PLINK: rising to the challenge of larger and richer datasets. Gigascience 2015;4:7. doi: 10.1186/s13742-015-0047-8.
[26] Cunningham F, Allen JE, Allen J, et al. Ensembl 2022. Nucleic Acids Res 2022;50:D988–95. doi: 10.1093/nar/gkab1049.
[27] Wang K, Li M, Hakonarson H. ANNOVAR: functional annotation of genetic variants from high-throughput sequencing data. Nucleic Acids Res 2010;38:e164. doi: 10.1093/nar/gkq603.
[28] Szklarczyk D, Kirsch R, Koutrouli M, et al. The STRING database in 2023: protein-protein association networks and functional enrichment analyses for any sequenced genome of interest. Nucleic Acids Res 2023;51:D638–46. doi: 10.1093/nar/gkac1000.
[29] Ortiz-Fernández L, Carmona EG, Kerick M, et al. Identification of new risk loci shared across systemic vasculitides points towards potential target genes for drug repurposing. Ann Rheum Dis 2023;82:837–47. doi: 10.1136/ard-2022-223697.
[30] Emmi G, Silvestri E, Squatrito D, et al. Thrombosis in vasculitis: from pathogenesis to treatment. Thrombosis J 2015;13. doi: 10.1186/s12959-015-0047-z.
[31] Unizony S, Lu N, Tomasson G, et al. Temporal Trends of Venous Thromboembolism Risk Before and After Diagnosis of Giant Cell Arteritis. Arthritis Rheumatol 2017;69:176–84. doi: 10.1002/art.39847.
[32] Manna R, Latteri M, Cristiano G, et al. Anticardiolipin antibodies in giant cell arteritis and polymyalgia rheumatica: a study of 40 cases. Rheumatol (Sunnyvale) 1998;37:208–10. doi: 10.1093/rheumatology/37.2.208.
[33] Espinosa G, Tàssies D, Font J, et al. Antiphospholipid antibodies and thrombophilic factors in giant cell arteritis. Semin Arthritis Rheum 2001;31:12–20. doi: 10.1053/sarh.2001.23499.
[34] Hocevar A, Jese R, Rotar Z, et al. AB0552 Antiphospholipid antibodies in giant cell arteritis. Ann Rheum Dis 2017:1243–4. doi: 10.1136/annrheumdis-2017-eular.2508.
[35] Hoover-Plow J. Does plasmin have anticoagulant activity? Vasc Health Risk Manag 2010;6:199–205. doi: 10.2147/vhrm.s9358.
[36] Chapman HA. Plasminogen activators, integrins, and the coordinated regulation of cell adhesion and migration. Curr Opin Cell Biol 1997;9:714–24. doi: 10.1016/s0955-0674(97)80126-3.
[37] Bettiol A, Argento FR, Fini E, et al. ROS-driven structural and functional fibrinogen modifications are reverted by interleukin-6 inhibition in Giant Cell Arteritis. Thromb Res 2023;230:1–10. doi: 10.1016/j.thromres.2023.08.011.
[38] Bilton EJ, Mollan SP. Giant cell arteritis: reviewing the advancing diagnostics and management. Eye (Lond) 2023;37:2365–73. doi: 10.1038/s41433-023-02433-y.
[39] Guggenberger KV, Pavlou A, Cao Q, et al. Orbital magnetic resonance imaging of ocular giant cell arteritis: a systematic review and individual participant data meta-analysis. Eur Radiol 2023;33.
[40] Gonzalez-Gay MA, Piñeiro A, Gomez-Gigirey A, et al. Influence of Traditional Risk Factors of Atherosclerosis in the Development of Severe Ischemic Complications in Giant Cell Arteritis. Medicine (Baltimore) 2004;83:342–7. doi: 10.1097/01.md.0000145369.25558.b5.
[41] Grayson PC, Maksimowicz-McKinnon K, Clark TM, et al. Distribution of arterial lesions in Takayasu's arteritis and giant cell arteritis. Ann Rheum Dis 2012;71:1329–34. doi: 10.1136/annrheumdis-2011-200795.
[42] van Sleen Y, Boots AMH, Abdulahad WH, et al. High angiopoietin-2 levels associate with arterial inflammation and long-term glucocorticoid requirement in polymyalgia rheumatica. Rheumatology (Oxford) 2020;59:176–84. doi: 10.1093/rheumatology/kez261.
[43] Ward NL, Dumont DJ. The angiopoietins and Tie2/Tek: adding to the complexity of cardiovascular development. Seminars in Cell & Developmental Biology 2002;13:19–27. doi: 10.1006/scdb.2001.0288.
[44] Italiano JE, Richardson JL, Patel-Hett S, et al. Angiogenesis is regulated by a novel mechanism: pro- and antiangiogenic proteins are organized into separate platelet α granules and differentially released. Blood 2008;111:1227–33. doi: 10.1182/blood-2007-09-113837.
[45] Westreich D, Greenland S. The table 2 fallacy: presenting and interpreting confounder and modifier coefficients. Am J Epidemiol 2013;177:292–8. doi: 10.1093/aje/kws412.
[46] Atkins EJ, Bruce BB, Newman NJ, et al. Treatment of nonarteritic anterior ischemic optic neuropathy. Surv Ophthalmol 2010;55:47–63. doi: 10.1016/j.survophthal.2009.06.008.

Ann Rheum Dis 84 (2025) 341–350

Contents lists available at ScienceDirect

Annals of the Rheumatic Diseases

journal homepage: https://www.sciencedirect.com/journal/annals-of-the-rheumatic-diseases

Osteoarthritis

Vascular occlusion for optimising the functional improvement in patients with knee osteoarthritis: a randomised controlled trial

Ewoud Jacobs[1,*], Lenka Stroobant[2], Jan Victor[2], Dirk Elewaut[3,4], Thomas Tampere[2], Steven Wallaert[5], Erik Witvrouw[1], Joke Schuermans[1], Evi Wezenbeek[1,6]

[1] *Department of Rehabilitation Sciences, Ghent University Faculty of Medicine and Health Sciences, Ghent, Belgium*
[2] *Department of Orthopaedic Surgery, University Hospital Ghent, Ghent, Belgium*
[3] *Department of Rheumatology, University Hospital Ghent, Ghent, Belgium*
[4] *Unit for Molecular Immunology and Inflammation, VIB Center for Inflammation Research, Ghent University, Ghent, Belgium*
[5] *Department of Biostatistics, Ghent University, Ghent, Belgium*
[6] *Department of Rehabilitation Sciences and Physiotherapy, University of Antwerp, Antwerp, Belgium*

ARTICLE INFO

Article history:
Received 14 August 2024
Accepted 18 October 2024

Keywords:
Osteoarthritis
Knee
Physical Therapy Modalities
Rehabilitation
Orthopedic Procedures

ABSTRACT

Objectives: Knee osteoarthritis (KOA) is a leading cause of global disability with conventional exercise yielding only modest improvements. Here we aimed to investigate the benefits of integrating blood flow restriction (BFR) into traditional exercise programmes to enhance treatment outcomes.
Methods: The Vascular Occlusion for optimizing the Functional Improvement in patients with Knee Osteoarthritis randomised controlled trial enrolled 120 patients with KOA at Ghent University Hospital, randomly assigning them to either a traditional exercise programme or a BFR-enhanced programme over 24 sessions in 12 weeks. Assessments were conducted at baseline, 6 weeks, 12 weeks and 3 months postintervention using linear mixed models with Dunn-Sidak corrections for multiple comparisons. Primary outcome was the Knee injury and Osteoarthritis Outcome Score (KOOS) questionnaire at 3 months follow-up with knee strength, Pain Catastrophizing Scale questionnaire and functional tests as secondary outcomes. Analysis followed an intention-to-treat approach (NCT04996680).
Results: The BFR group showed greater improvements in KOOS pain subscale (effect size (ES) $=0.58$; $p=0.0009$), quadriceps strength (ES $=0.81$; $p<0.0001$) and functional tests compared with the control group at 12 weeks. At 3 months follow-up, the BFR group continued to exhibit superior improvements in KOOS pain (ES $=0.55$; $p=0.0008$), symptoms (ES $=0.59$; $p=0.0004$) and quality of life (QoL) (ES $=0.66$; $p=0.0001$) with sustained benefits in secondary outcomes. Drop-out rates were similar in both groups.
Conclusion: Incorporating BFR into traditional exercise programmes significantly enhances short-term and long-term outcomes for patients with KOA demonstrating persistent improvements in pain, symptoms, QoL and functional measures compared with conventional exercise alone. These findings suggest that BFR can provide the metabolic stimulus needed to achieve muscle strength and functional gains with lower mechanical loads. Reduced pain and increased strength support a more active lifestyle, potentially maintaining muscle mass, functionality and QoL even beyond the supervised intervention period.
Trial registration number: NCT04996680.

*Correspondence to Ewoud Jacobs.
E-mail address: ewoud.jacobs@ugent.be (E. Jacobs).
Handling editor Josef S. Smolen

https://doi.org/10.1136/ard-2024-226579

WHAT IS ALREADY KNOWN ON THIS TOPIC

- Knee osteoarthritis (KOA) is a leading cause of global disability with exercise therapy being a primary non-pharmacological treatment recommended by European Alliance of Associations for Rheumatology guidelines.
- Traditional exercise regimens for KOA typically result in only small to moderate short-term improvements in pain and function.
- Limited research exists on the addition of blood flow restriction (BFR) to traditional exercise programmes for KOA with previous studies showing controversial results and lacking long-term follow-up.

WHAT THIS STUDY ADDS

- This study is the first large-scale randomised controlled trial to investigate the lasting effects of adding BFR to traditional exercise programmes for KOA.
- The study found that incorporating BFR led to significantly better outcomes with moderate to large effect sizes for pain, muscle strength and functionality after 12 weeks compared with standard exercise alone.
- Notably, these improvements persisted and even enhanced at 3 months follow-up unlike the standard exercise group which required continuous training to maintain benefits.

HOW THIS STUDY MIGHT AFFECT RESEARCH, PRACTICE OR POLICY

- The findings suggest that adding BFR to exercise therapy for KOA could offer a more effective and sustainable approach to improving patient outcomes, potentially influencing clinical guidelines and treatment strategies.
- The study highlights the potential of BFR to enable lower mechanical loads during exercise, reducing the risk of joint overloading in patients with KOA while still achieving significant strength and functional gains.
- This research could lead to a shift in rehabilitation practices, emphasising the incorporation of BFR to optimise long-term benefits in KOA management.

INTRODUCTION

Osteoarthritis (OA) is a highly prevalent and debilitating whole-joint disease estimated to affect 595 million individuals worldwide in 2020 which is a staggering increase of 132.2% since 1990 [1]. For the knee, the most commonly affected joint within OA, the prevalence is estimated around 23% in people aged over 40 which is expected to increase 74.9% by 2050 due to ageing, obesity and the lack of disease-modifying OA drugs [1,2]. Previously considered merely an age-related consequence, OA is now understood to result from a complex interaction between patient-related, biological and societal factors involving cartilage, subchondral bone and synovium [3]. Furthermore, this degenerative process inflicts a significant burden in terms of pain, stiffness and disability, thereby often requiring (para)medical interventions and the need for prosthetic joint replacement for the most severe cases [4].

While total knee arthroplasty (TKA) is a common and effective treatment for KOA, especially in the elderly with typically higher Kellgren-Lawrence scores, it is found less suitable for younger, more active patients [5]. As the decision for TKA strongly depends on the patients' remaining functionality, quality of life (QoL) and structural degradation, surgery is often not the preferred method of treatment at the onset of KOA [6,7]. Nevertheless, a significant amount of time is often spent with a diminished QoL meanwhile aiming to maintain a certain level of physical activity, although accompanied by pain, discomfort and even potential mental difficulties [8]. To tackle these problems, both EULAR (European Alliance of Associations for Rheumatology) and AAOS (American Academy of Orthopaedic Surgeons) guidelines clearly recommend conservative therapy comprising of tailored exercise therapy with adequate dosage and progression [9,10]. Indeed, due to its significant correlation with function, lower limb strength training, specifically targeting the M. quadriceps remains crucial for the QoL of patients with KOA [11,12]. By improving both muscle mass and strength of the M. quadriceps, the stability of the knee joint increases while also improving shock absorbing capabilities, thus decreasing levels of pain and discomfort. When combined with weight loss and a healthy lifestyle, this reduces work abstinence while postponing primary TKA's and preventing revision TKA's, thus simultaneously reducing the economic burden [13–15]. However, limitations arise from structural degradation and clinical symptoms restricting patients to low-intensity exercises, thus limiting the results of the treatment, particularly in the medium to long-term follow-up [16].

Recently, blood flow restriction (BFR) has emerged as an addition to traditional low-intensity exercise therapy and a potential substitute for high-load strength training. Originating in bodybuilding, BFR is now widely used in sports medicine to enhance muscle mass and strength in athletes who cannot tolerate high loads such as after a fracture or anterior cruciate ligament (ACL) surgery [17]. BFR involves applying a tourniquet or cuff around the proximal aspect of the affected limb causing partial arterial and full venous occlusion. This induces localised hypoxia and the accumulation of metabolites, mimicking the effects of high-load resistance training without the need for heavy loads. By significantly increasing the metabolic stimulus, BFR allows for much lower mechanical loads compared with the 70% of one repetition maximum (1RM) recommended by the American College of Sports Medicine for strength increments [18]. Consequently, BFR might offer a suitable and more effective strength training method for patients with KOA whose degenerated joints do not tolerate high-intensity exercises well.

Therefore, this randomised controlled trial (RCT) aimed to assess the functional results (both short-term and sustained) of BFR in a large sample of KOA. This evaluation covered muscle strength, functionality in daily activities (ADL), QoL, pain and other symptoms such as knee stiffness and swelling both post 12-week therapy (short-term) and at a 3-month follow-up (sustained).

METHODS

Study design

This parallel RCT was conducted at the Centre for Sports Medicine at the Ghent University Hospital. The study took place between July 2021 and February 2024 with recruitment ending in September 2023. The study was preregistered at ClinicalTrials.gov and reported according to Consolidated Standards of Reporting Trials and template for intervention description and replication guidelines. Data collection and randomisation were done using Research Electronic Data Capture (REDCap V.13.7.30).

Participants

A total of 196 participants, aged 30−80 with knee osteoarthritis (KOA) classified as Kellgren-Lawrence grade 1−4, were recruited through referral of orthopaedic surgeons. Eligible patients were of any ethnicity and gender, aged 30−80 years, presented with clinical symptoms such as pain and loss of function, had radiographic evidence of KOA and were able to consent and were willing to comply with the study protocol. Patients were considered non-eligible for surgery by the orthopaedic surgeon due to the early onset of the disease or their preference to postpone surgery. Patients were not eligible if they presented with cardiovascular, metabolic or neuromuscular diseases, injuries impacting lower limb function except for KOA, pregnancy, body mass index (BMI) >30, knee infiltrations in the last 12 months or had a history of venous thromboembolism. If participants were eligible, the first assessment and physiotherapy session were scheduled and an informed consent was signed in accordance with the Declaration of Helsinki.

Randomisation and masking

Eligible participants were randomly assigned in a 1:1 ratio stratified by gender (female, male, X) and affected leg (right, left, both) with computer-generated blocks of sizes 6−10. The randomisation sequence was generated by a biostatistician. Allocation was concealed in password-protected software (REDCap, V.13.7.30) and only visible to the trial coordinator. After randomisation, the trial coordinator revealed patient allocation to the treating physiotherapists as they provided exercise sessions for both trial groups to ensure treatment quality was similar across groups. Intervention adherence and fidelity were monitored by the trial coordinator and treating physiotherapists. The study was single-blinded with the outcome assessor being blinded from randomisation whereas masking of participants and treating physiotherapists was not possible due to the nature of the intervention. However, patients were masked to trial hypotheses and instructed not to discuss the intervention-related aspects with the outcome assessor. Outcome assessment was done at baseline, 6 weeks, 12 weeks and at 3 months follow-up by a physiotherapist who administered the strength measurement and functional tests but was otherwise not involved in the data processing. The questionnaires were self-administered by the patients. Patients were randomised between a control group receiving traditional low-intensity exercise therapy (CON) and an experimental group which received the same low-intensity exercise therapy but with additional BFR (BFRT) by means of pressurised cuffs.

Procedures

Both groups completed a 12-week resistance training programme with two times a week sessions supervised by experienced physiotherapists with BFR education [11,19]. Each session began with a 10 min cycling warm-up at 1.5 W/kg and ended with a 10 min cool-down at 1.2 W/kg. The programme included five lower limb exercises focusing on quadriceps strengthening through leg press and leg extension exercises [20,21]. Both legs were trained separately to avoid compensation by the non-affected leg. Repetition schemes varied with quadriceps exercises progressing to failure in the final set. To maximise training results and minimise dropout rates, participants in both groups underwent exercise regimens customised to their individual capacities and pain levels which was revised on a weekly basis, a widely employed practice in clinical settings. Besides aligning with established clinical norms where high load is not feasible in the treatment of patients with KOA, this methodology also prioritised participant safety and adherence. A complete overview of the exercise protocol can be found in the online supplemental file 1, p.17.

In the BFR group, a pressurised tourniquet at 60% limb occlusion pressure (LOP) was applied during quadriceps exercises, except in the first 2 weeks where it was only used during the leg press for familiarisation [21−23]. The LOP, determined by blood pressure (BP), limb circumference and cuff width was measured using validated SmartCuffs PRO (cuff width 10.16 cm). The cuff was deflated between quadriceps exercises. Other lower limb exercises were identical in both groups without BFR. The trial coordinator monitored adherence and fidelity.

Assessments were conducted at baseline, 6 weeks, 12 weeks and 24 weeks with the latter being the primary endpoint. Postrehabilitation, patients were allowed to resume their daily activities independently reflecting typical discharge practices in real-world settings.

Outcome measures

Primary and secondary outcomes were analysed as mean differences between groups at baseline, 6 weeks, 12 weeks and 3 months follow-up focusing on the added value of BFR compared with conventional physiotherapy. The primary outcome measure was the Knee Osteoarthritis Outcome Score (KOOS) at 3 months follow-up which is a validated 42-item questionnaire assessing five domains: pain, symptoms, daily activities, sports and QoL scored on a 0−100 scale [24].

Secondary outcomes included muscle strength, pain catastrophising and functional performance with the primary time point also at 3 months follow-up. Muscle strength of the quadriceps and hamstrings was measured using a hand-held dynamometer [25]. Each muscle was tested three times with average results. Pain catastrophising was assessed using the 13-item Pain Catastrophizing Scale which measures rumination, magnification and helplessness with a maximum score of 52 [26].

A functional test battery evaluated participants' abilities in daily activities. The stair climb test measured the time to ascend and descend 11 steps [27]. The 30-second chair stand test assessed leg strength and endurance by counting the number of chair rises within 30 s [27]. The 30-second knee bend test evaluated lower limb strength and coordination through unipodal squats [28]. Walking speed and endurance were measured by the 6-minute walk test (6MWT) [27,29] and the 40 m fast-pace walk test [27] which recorded the distance covered and speed over 40 m.

Adverse events

Adverse events were defined as unintended or detrimental effects related to the exercise protocol prohibiting participants from continuing with the exercise [30].

Patient and public involvement

No participants were directly involved in designing the research question or in conducting the research. However, participants were asked for advice on interpretation of the adverse events experienced.

Statistical analysis

The sample size was a priori determined to be 60 per group. Assuming an expected standardised effect size of 0.83, [31] a significance level of 0.05 and equal allocation, the power for the primary analyses was calculated to be at least 93%. Descriptive statistics were calculated using means and SD for continuous variables and numbers and percentages for categorical variables. Effect sizes are reported as the interaction coefficient divided by the SD of the differences between baseline and time point. For the comparative analyses, linear mixed models were fitted with treatment group, time point (categorical), the interaction between treatment group and time point, gender, affected side and pretreatment level of activity as fixed effects and a random intercept per patient. Analysis followed an intention-to-treat approach. The difference between treatment groups in mean change from baseline at 6 weeks, 12 weeks and follow-up (24 weeks) was assessed by the interaction terms (three hypothesis tests) with 24 weeks being the primary endpoint. The primary outcome variable (KOOS) consists of 5 scales and thus a total of 5×3 = 15 hypothesis tests were planned. To control the family-wise error rate (FWER) at 5%, Dunn-Sidak correction for 15 comparisons was made by setting the individual significance level for each test at $1-(1-0.05)^{(1/15)} \approx 0.0019$. For the secondary outcome measures at 6, 12 and 24 weeks, 9×3 = 27 hypothesis tests were planned if at least one null hypothesis of the primary analysis could be rejected. To control the FWER at 5% in the secondary analysis, Dunn-Sidak correction for 27 comparisons was made by setting the individual significance level for each test at $1-(1-0.05)^{(1/27)} \approx 0.0034$. Reported p values are uncorrected and CIs are at the corrected 95% confidence level for both the primary and secondary endpoints. Model assumptions were graphically checked. In case of possible violations, ad hoc sensitivity analyses were performed and reported to check the robustness of the results. Sensitivity analyses consisted of using a different conditional distribution (beta instead of Gaussian) accounting for heteroscedasticity or leaving out possibly influential observations. The analyses were performed with R version V.4.3.3 (R Core Team 2004) and statistical package for Social Sciences V.28 (SPSS V.28 IBM) [32].

RESULTS

Between 12 July 2021 and 25 September 2023, 120 participants were enrolled from 196 patients screened (figure 1). No important differences in baseline characteristics were present (table 1). Of the 120 patients, 9 (7.5%) did not complete the assessment at 6 weeks (BFR: n = 3, CON: n = 6), 17 (14.2%) did not complete the 12-week assessment (BFR: n = 11, CON: n = 6) and 33 (27.5%) patients did not complete the 3-month follow-up (BFR: n = 16, CON: n = 17).

Adverse events

In the control group, six patients (10%) and in the BFR group, four patients (6.7%) dropped out due to pain. Six patients (CON: n = 2, BFR: n = 4) dropped out of the study after a mutual decision with the orthopaedic surgeon to perform knee surgery. Five out of these six patients had grade 4 KOA according to the KL scale. In the BFR group, one patient developed a deep venous thrombosis (DVT). A comprehensive overview of all medical and non-medical dropouts (CON: n = 9, BFR: n = 8) can be found in online supplemental appendix p. 16.

For both primary and secondary outcome measures, the difference between the two arms in mean change from baseline at 6, 12 and 24 weeks was assessed by group × time interaction terms.

Primary outcome measure

After 6 weeks of exercise therapy with or without BFR, no statistically meaningful differences between groups were found for any of the KOOS-subscales. After completing the 12-week intervention, change from baseline was greater in the BFR group compared with the control group for the KOOS-pain subscale (8.8 (1.0 to 16.6), ES = 0.58, p = 0.0009). No statistically relevant differences from baseline between groups were found for subscale symptoms, ADL, sport or QoL at 12 weeks. At 3 months follow-up, change from baseline in mean KOOS-pain score was considerably different between groups at 3 months follow-up (9.4 (1.2 to 17.7), ES = 0.55, p = 0.0008) with the BFR group having better KOOS-pain score evolution. For KOOS-subscales symptoms and QoL at 3 months follow-up, greater improvements in mean change from baseline were found in favour of the BFR group (9.0 (1.6 to 16.5), ES = 0.59, p = 0.0004) and (13.2 (3.6 to 22.9), ES = 0.66, p = 0.0001) respectively. For KOOS-subscales ADL and sport, no meaningful differences were found between BFR and CON at 3 months follow-up. KOOS-subscales pain, other symptoms and QoL are visualised in figure 2. A complete overview of KOOS-subscales can be found in table 2.

Secondary outcome measures

For mean normalised quadriceps strength, greater improvement in mean difference from baseline between arms at 6, 12 and 24 weeks was found in favour of the BFR group (6 weeks: 0.72 N/kg (0.1 to 1.3), ES = 0.77, p = 0.0002, 12 weeks: 1.12 N/kg (0.5 to 1.7), ES = 0.81, p<0.0001, 24 weeks: 0.95 N/kg (0.3 to 1.6), ES = 0.71, p<0.0001). No significant differences were found for the normalised mean hamstring strength at any time point. (figure 3)

In terms of functional tests, change from baseline in the mean number of repetitions during the knee bend test was greater in the BFR group at 12 weeks (4.5 reps (0.6 to 8.4), ES = 0.56, p = 0.0004) and at 24 weeks follow-up (5.2 reps (1.1 to 9.3), ES = 0.63, p = 0.0001), compared with the CON group. The mean change from baseline in amount of repetitions from sit to stand during the 30 s chair to stand test significantly differed between groups both at 12 weeks (3.6 reps (1.2 to 6.0), ES = 0.69, p<0.0001) and 24 weeks (4.7 reps (2.2 to 7.3), ES = 0.78, p<0.0001) in favour of the BFR group. For the 6MWT, mean changes from baseline were greater in the BFR group at 6 weeks (44 m (7 to 81), ES = 0.71, p = 0.0002) 12 weeks (62 m, (24 to 100), ES = 0.74, p<0.0001) and 24 weeks (57 m (17 to 97), ES = 0.75, p<0.0001) compared with the CON group. For the 40 m fast pace walk test, mean changes from baseline were significantly different between arms at 24 weeks (−2.3 s, (−4.1 to −0.4), ES = −0.65, p = 0.0001), again in favour of the BFR group. A complete overview of secondary outcomes can be found in table 2.

DISCUSSION

To our knowledge, our study is the first to explore the long-term effects of a BFR intervention compared with a control group receiving traditional exercise therapy alone. Following a 12-week regimen, significantly better improvements were

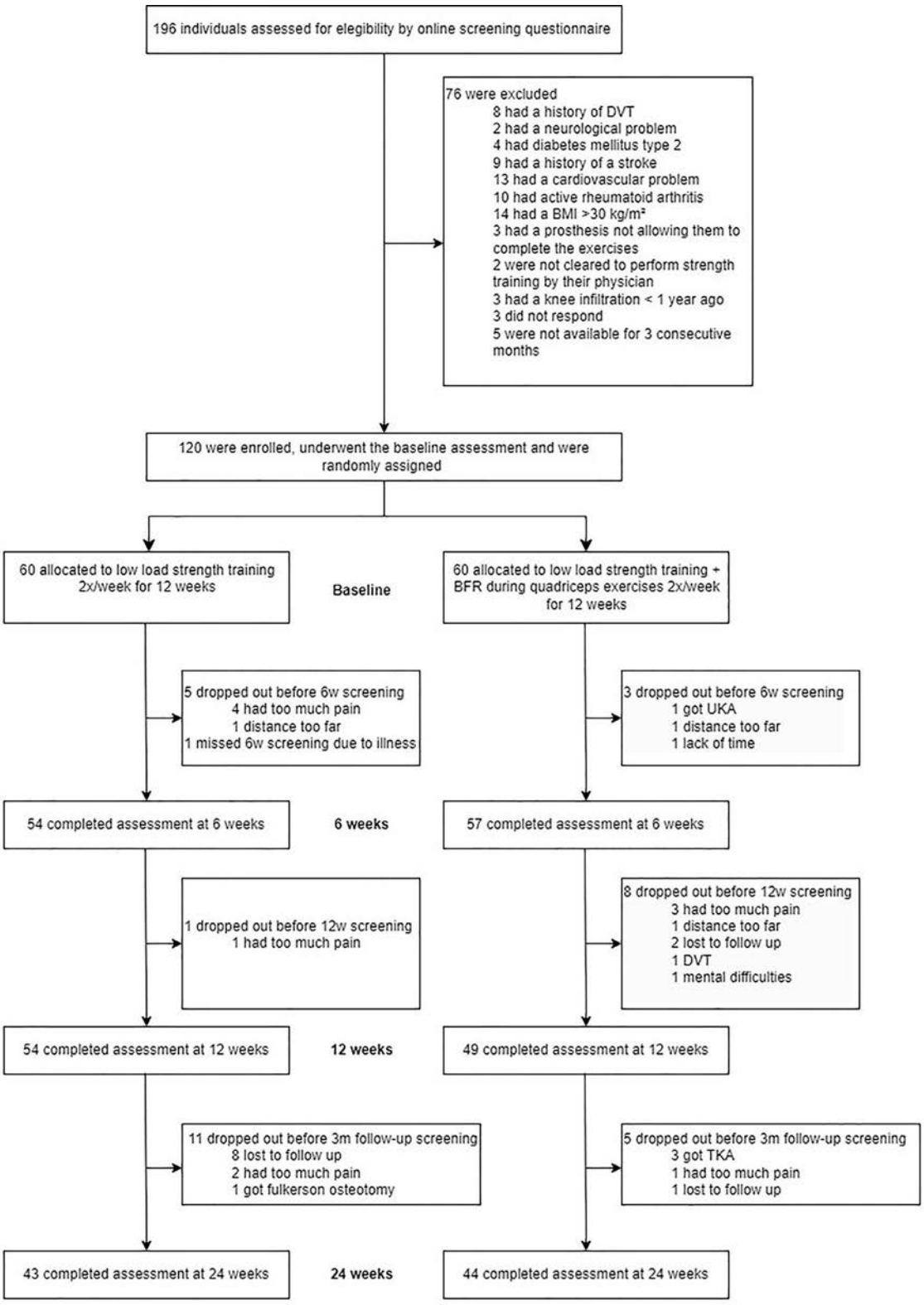

Figure 1. Participant flowchart. BFR, blood flow restriction; BMI, body mass index; DVT, deep venous thrombosis; TKA, total knee arthroplasty; UKA, unicompartmental knee arthroplasty.

observed in pain reduction, quadriceps strength and functional capacity in the BFR group as assessed by various functional tests. Notably, these improvements in pain alleviation, symptom mitigation and QoL enhancement persisted at 3 months follow-up as evaluated through the KOOS questionnaire. Furthermore, our results demonstrate sustained improvements in quadriceps strength and functional performance at follow-up in the BFR group compared with the control group. These findings are particularly noteworthy given the mixed evidence regarding the efficacy of BFR in short-term outcomes and the lack of data on its long-term effectiveness.

When comparing the results of this study with conventional exercise therapy without BFR, it appears that the addition of BFR leads to moderate to large improvements in pain, strength and physical functioning compared with conservative exercise alone [33–35]. High–quality evidence from 44 trials (3537

Table 1
Patient demographics

	BFR (n = 60)	Control (n = 60)
Age (years)	58 (9)	57 (11)
Height (cm)	171 (9)	171 (9)
Weight (kg)	75 (13)	71 (13)
BMI (kg/m²)	25.5 (3.4)	24.4 (3.2)
Sex		
Male	14 (23)	19 (32)
Female	46 (77)	41 (68)
Affected knee		
Both	27 (45)	29 (48)
Left	17 (28)	16 (27)
Right	16 (27)	15 (25)
Dominant leg		
Left	13 (22)	8 (13)
Right	47 (78)	52 (87)
Degree of knee OA*		
2	22 (37)	25 (42)
3	29 (48)	27 (45)
4	9 (15)	8 (13)
NPRS pretrial (0–10)	3.05 (1.64)	3.48 (1.68)
Pre-intervention activity (0–100)	45 (19)	42 (20)
Mean limb occlusion pressure (mm Hg)	131 (15)	/

Mean (SD) or n (%)
*According to the KL-scale.
BFR, blood flow restriction; BMI, body mass index; KL, Kellgren-Lawrence; NPRS, numeric pain rating scale; OA, osteoarthritis.

participants) indicates that exercise therapy reduced pain (standardised mean difference (SMD) −0.49) immediately after treatment [35]. In these studies, pain was estimated at 44 points on a 0–100 point scale in the control group; by adding exercise, pain was reduced by an equivalent of 12 points. Notably, our results demonstrate that adding BFR leads to even greater reductions in pain at 12 weeks with an additional 9.4-point improvement on a similar 0–100 scale compared with traditional exercise therapy [35]. Interestingly, these improvements in pain persist at the 3-month follow-up showing a sustained moderate effect size (SMD = 0.55) and a mean difference of 9.4 points compared with conservative exercise therapy alone. In contrast, Fransen *et al* reviewed 11 studies with 2–6 months post-treatment data on 1468 participants showing that conventional exercise produced only small persisting effects for knee pain [35].

Additionally, evidence from 13 studies (1073 participants) indicated that exercise improves QoL (SMD = 0.28) immediately post-treatment. In comparison, our study found that BFR added to exercise therapy resulted in a greater improvement in QoL at 12 weeks (SMD = 0.42). More importantly, our findings show that these benefits persist and even further improve at 3 months with a moderate to good effect size (SMD = 0.66).

Similarly, our results show that BFR has a large effect on strength consistent with the findings of Ferraz *et al* [11]. While a slight decrease in quadriceps strength is observed at 3 months follow-up, the BFR group still demonstrates a nearly one newton per kg bodyweight advantage over the control group which received standard exercise therapy alone. While speculative, a plausible hypothesis could suggest that individuals undergoing a traditional exercise programme supplemented with BFR may experience notable enhancements in strength while reporting minimal discomfort in the knee joint. This instils confidence in their knees, improves their functional capacities and motivates them to remain active and maintain their progress postintervention. In contrast, limited gains were achieved by the control group with smaller improvements in terms of pain, muscle strength, functionality and subsequent QoL.

These findings contrast with those of Wang *et al* who reported no significant benefits of BFR compared with conventional resistance training for pain, strength and physical function. However, their systematic review and meta-analysis included studies with considerable heterogeneity in intervention duration (4–12 weeks), occlusion pressures and sample sizes (34–48 patients) which may explain the differing outcomes [36]. In contrast, our results align with Hu *et al* and the systematic review and meta-analysis by Hughes *et al*, both of which concluded that BFR training provides a more effective approach compared with low-intensity exercise therapy and is a more tolerable alternative to high-intensity exercise therapy [37].

Based on the recent evidence and results of this study, it seems that the addition of BFR in a traditional exercise programme might offer a solution to optimise training effects in

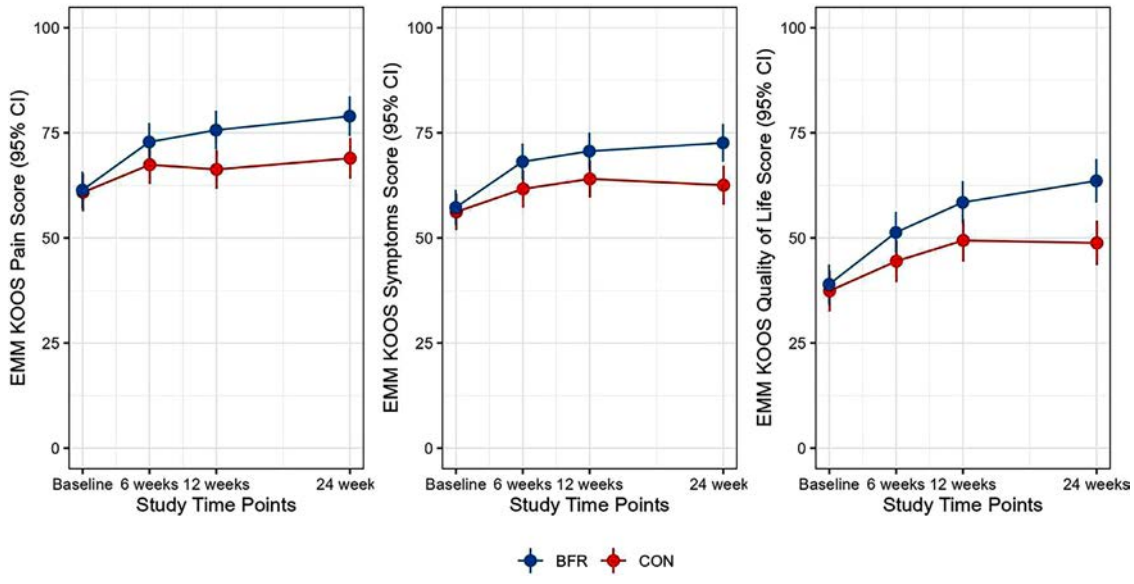

Figure 2. KOOS estimated marginal means for subscales pain, other symptoms and QoL. BFR, blood flow restriction; CON, control group receiving traditional low intensity exercise therapy; EMM, estimated marginal means; KOOS, Knee injury and Osteoarthritis Outcome Score; QoL, quality of life.

Table 2
Primary and secondary outcome measures

	Difference in change between groups (baseline to 6 weeks)			Difference in change between groups (baseline to 12 weeks)			Difference in change between groups (baseline to 24 weeks)		
	Mean difference (95% CI)	P value	Effect size	Mean difference (95% CI)	P value	Effect size	Mean difference (95% CI)	P value	Effect size
Primary outcomes*									
KOOS—pain	4.88 (−2.72 to 12.47)	0.0593	0.35	8.81 (1.02 to 16.60)	0.0009	0.58	9.44 (1.23 to 17.66)	0.0008	0.55
KOOS—other symptoms	5.43 (−1.48 to 12.34)	0.0218	0.42	5.54 (−1.54 to 12.63)	0.0218	0.39	9.03 (1.55 to 16.51)	0.0004	0.59
KOOS—ADL	1.31 (−6.39 to 9.02)	0.6163	0.10	6.59 (−1.31 to 14.49)	0.0144	0.41	6.95 (−1.38 to 15.28)	0.0144	0.42
KOOS—sport	2.96 (−10.72 to 16.64)	0.5237	0.14	5.89 (−8.19 to 19.96)	0.2184	0.23	7.49 (−7.05 to 22.04)	0.1296	0.32
KOOS—QoL	5.29 (−3.63 to 14.20)	0.0817	0.33	7.50 (−1.64 to 16.64)	0.0161	0.42	13.23 (3.59 to 22.87)	0.0001	0.66
Secondary outcomes*									
Mean quadriceps strength (N/kg)	0.72 (0.13 to 1.30)	0.0002	0.77	1.12 (0.52 to 1.73)	<0.0001	0.81	0.95 (0.31 to 1.59)	<0.0001	0.71
Mean hamstring strength (N/kg)	0.16 (−0.10 to 0.42)	0.0605	0.32	0.14 (−0.12 to 0.41)	0.0931	0.34	0.17 (−0.12 to 0.45)	0.0669	0.35
PCS—total	−0.07 (−4.95 to 4.81)	0.9644	−0.01	−0.60 (−5.59 to 4.40)	0.7090	−0.07	−2.98 (−8.25 to 2.29)	0.0780	−0.30
30-second knee bend test	1.74 (−2.05 to 5.53)	0.1519	0.27	4.49 (0.59 to 8.38)	0.0004	0.56	5.19 (1.06 to 9.32)	0.0001	0.63
30-second chair to stand test	2.19 (−0.14 to 4.53)	0.0035	0.59	3.56 (1.16 to 5.97)	<0.0001	0.69	4.73 (2.19 to 7.28)	<0.0001	0.78
6 MWT	44.11 (7.35 to 80.86)	0.0002	0.71	61.83 (24.03 to 99.63)	<0.0001	0.74	56.90 (16.87 to 96.92)	<0.0001	0.75
40 m FPWT	−1.14 (−2.83 to 0.56)	0.0362	−0.33	−1.70 (−3.45 to −0.04)	0.0024	−0.62	−2.28 (−4.12 to −0.43)	<0.0001	−0.65
SCT—up	−0.36 (−1.04 to 0.33)	0.1040	−0.26	−0.45 (−1.16 to 0.25)	0.0449	−0.32	−0.54 (−1.28 to 0.20)	0.0241	−0.46
SCT—down	−0.54 (−1.29 to 0.22)	0.0267	−0.31	−0.42 (−1.20 to 0.36)	0.0928	−0.33	−0.44 (−1.26 to 0.38)	0.0952	−0.36

Data are adjusted for baseline level of outcome, time, gender, affected knee and multiple measurements per participant. Effect sizes are reported as the interaction coefficient divided by the SD of the differences between baseline and time point.
Muscle strength normalised for body weight (N/kg).
*Post hoc sensitivity analysis with beta distribution was performed for all variables to account for possible heteroscedasticity with only the 40 m FPWT showing different levels of significance at 12 weeks. An overview of the sensitivity analysis results for both primary and secondary outcome measures is provided in online supplemental file 1.
ADL, activities of daily living; KOOS, Knee Osteoarthritis Outcome Score (0−100, higher scores indicating better outcome); 40 m FPWT, 40 m fast-pace walk test (in seconds, lower values indicating higher speed); 6 MWT, 6-minute walk test (in meter); PCS, Pain Catastrophizing Scale (0−52; lower scores indicating better outcome); QoL, quality of life; SCT up and down, stair climb test up and down (in seconds, lower values indicating higher speed) .

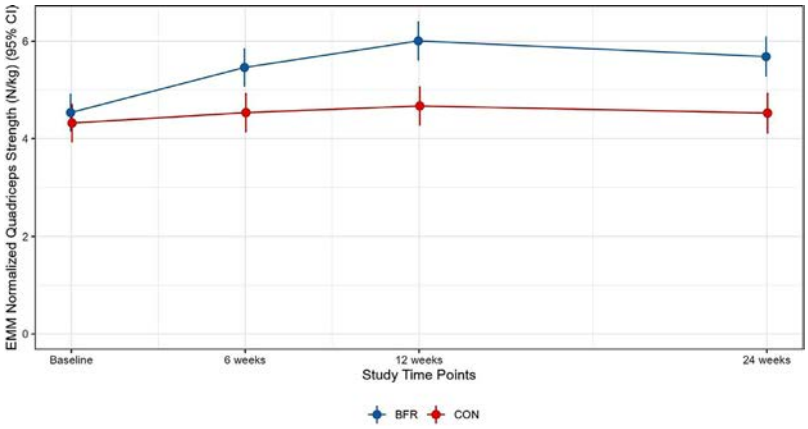

Figure 3. Estimated marginal means for normalised quadriceps strength (N/kg). BFR, blood flow restriction; CON, control group receiving traditional low intensity exercise therapy; EMM, estimated marginal means.

contrast to high loads which are often recommended [18,38]. While heavy strength training has shown excellent results in terms of muscle characteristics, it also implies substantial loading of the degenerated intra-articular and periarticular structures making its implementation in OA-associated exercise therapy less suited. Due to qualitative cartilage degeneration and volume reduction, patients often lack sufficient local joint load-bearing capacity leading to limited shock absorption and heightened sensitivity in and around the knee joint(s). This scenario can significantly exacerbate patient frustration and induce a more sedentary lifestyle and even mental health issues, especially in cases where surgery is not yet suitable as an alternative [8]. Consequently, therapists frequently opt for traditional low-intensity exercise therapy alone which may not deliver optimal results.

However, this negative vicious cycle might be reversed through traditional low intensity exercise therapy complemented with BFR. Using a personalised LOP, the arterial inflow is reduced while fully occluding the venous outflow thereby creating localised hypoxia and simultaneously enhancing the accumulation of metabolites such as lactate, hydrogen ions, inorganic and dihydrogen phosphate [39,40]. This metabolic stress has been suggested to be a primary factor responsible for anabolic/anticatabolic muscle adaptations by activating numerous other mechanisms such as increased type II muscle fibre recruitment, mechanotransduction, cell swelling, muscle damage as well as satellite cell activation [19,38,39,41]. Important to note is that although these mechanisms might all induce anabolic muscle adaptations separately, it is assumed they contribute to a complex network altogether mediating a positive muscle protein synthesis. These physiological responses lead to substantial enhancements in muscle mass and strength along with improved physical function despite the relatively low training intensities (<50% of 1RM) typically used during BFR training [42].

Given the small sample sizes, heterogeneity in methods and conflicting evidence regarding the effectiveness of BFR in patients with KOA, this study focused on individuals with KOA who did not have severe comorbidities. This approach was chosen to minimise confounding factors and ensure a clearer understanding of the additional effects of BFR, both in the short term and after 3 months. Nonetheless, this sample does not represent the entire KOA population. Future studies should aim to include patients with comorbidities to generalise the findings to a larger population, especially since BFR appears safe when used according to evidence-based guidelines. Nakajima *et al* for example reported low rates of serious adverse events with BFR: 0.055% for DVT and 0.008% each for pulmonary embolism and rhabdomyolysis [43]. Furthermore, research on blood coagulation factors after BFR training in elderly individuals has not shown adverse effects even in those with ischaemic heart disease [44−47]. Nonetheless, this study did observe one serious adverse event. One patient in the BFR group developed a DVT after the 12th session despite showing no signs of redness or swelling. Ultrasound confirmed the presence of DVT alongside elevated D-dimer levels (1930 ng/mL). The patient was treated with antithrombotic medication and recovered without complications. While it is difficult to attribute DVT to a single factor (eg, BFR training, immobilisation, contraceptives), future studies and practitioners should thoroughly assess for potential risk factors (ie, through questionnaires) as indicated in previous literature [22,48]. Additionally, an in-depth anamnesis based on the questionnaire is recommended to make sure all risk factors are mapped out. In the case of the DVT reported in our study, the patient failed to mention she was on contraceptive medication and that she experienced a similar cramp-like feeling in her calf after immobilisation for an ankle fracture in 2021. Although existing literature indicates a very low risk of thrombotic events associated with BFR [30,49,50], this case underscores the need for a comprehensive screening process which should include questionnaires and an in-depth anamnesis.

This study has limitations. Due to the nature of the intervention, it was difficult to blind patients or physiotherapists from the intervention. However, the latter were not involved in the data analysis and patients were blinded from the study hypothesis. Furthermore, the generalisability of this study is limited to patients with KOA with a BMI<30 and without other severe comorbidities such as cardiovascular, neurological or metabolic conditions (eg, chronic hypertension >160 mm Hg systolic BP, stroke or type 2 diabetes). Given the high prevalence of obesity and comorbidities in the broader KOA population, future studies should include patients with KOA with higher BMI's (not suffering from systemic disorders making BFR training a relative contraindication) as well to enhance the applicability of these findings. Additionally, the monocentric study design may have contributed to challenges in maintaining the sham condition as participants could compare experiences with others at the same facility.

Nonetheless, based on the findings of this study, it can be concluded that incorporating BFR training in low intensity exercise therapy optimises training results and yields positive outcomes at 12 weeks with continued improvement observed up to 3 months postintervention. Given the limited tolerance for high-intensity exercise therapy and the suboptimal results from low-

intensity exercise, BFR training serves as a viable alternative to high-intensity exercise mitigating excessive loading on degenerated knee joints.

Acknowledgments

We would like to express our sincere gratitude to the physiotherapists at the Centre for Sports Medicine for their dedication and effort during the rehabilitation process. We also extend our thanks to the orthopaedic surgeons for their frequent referrals and to the patients for their participation in this study.

Contributors

JV, EWi, JS, EWe and EJ conceptualised the study. SW performed the formal analysis and visualisation and was responsible for data curation. EJ, JS, EWi and EWe wrote the original draft. All authors reviewed and edited the manuscript. EWi, JV and EWe supervised the study. EJ is guarantor of the study.

Funding

This research was funded by the Fonds voor Wetenschappelijk Onderzoek Vlaanderen (FWO); grant number T001620N. The funding source had no involvement in the study design, interpretation, writing or publication of the manuscript.

Competing interests

None declared.

Patient and public involvement

Patients and/or the public were not involved in the design, or conduct, or reporting, or dissemination plans of this research.

Patient consent for publication

Not applicable.

Ethics approval

The study was approved by the ethics committee of Ghent University Hospital (approval no. BC-09925). Participants gave informed consent to participate in the study before taking part.

Data availability statement

Data are available upon reasonable request. Requests for data sharing from appropriate researchers and entities will be considered on a case-by-case basis. Interested parties should contact EJ.

Supplementary materials

Supplementary material associated with this article can be found in the online version at doi:10.1136/ard-2024-226579.

Orcid

Ewoud Jacobs: http://orcid.org/0000-0002-4658-0552
Dirk Elewaut: http://orcid.org/0000-0002-7468-974X

REFERENCES

[1] GBD 2021 Osteoarthritis Collaborators. Global, regional, and national burden of osteoarthritis, 1990-2020 and projections to 2050: a systematic analysis for the Global Burden of Disease Study 2021. Lancet Rheumatol 2023;5:e508–22. doi: 10.1016/S2665-9913(23)00163-7.
[2] Cui A, Li H, Wang D, et al. Global, regional prevalence, incidence and risk factors of knee osteoarthritis in population-based studies. EClinMed 2020;29−30:100587. doi: 10.1016/j.eclinm.2020.100587.
[3] Bijlsma JWJ, Berenbaum F, Lafeber F. Osteoarthritis: an update with relevance for clinical practice. Lancet 2011;377:2115–26. doi: 10.1016/S0140-6736(11)60243-2.
[4] Litwic A, Edwards MH, Dennison EM, et al. Epidemiology and burden of osteoarthritis. Br Med Bull 2013;105:185–99. doi: 10.1093/bmb/lds038.
[5] Aggarwal VK, Goyal N, Deirmengian G, et al. Revision total knee arthroplasty in the young patient: is there trouble on the horizon? J Bone Joint Surg Am 2014;96:536–42. doi: 10.2106/JBJS.M.00131.
[6] Vince KG. You can do arthroplasty in a young patient, but. . .: Commentary on articles by John P. Meehan, MD, et al.: "Younger age is associated with a higher risk of early periprosthetic joint infection and aseptic mechanical failure after total knee arthroplasty," and Vinay K. Aggarwal, et al.: "Revision total knee arthroplasty in the young patient: is there trouble on the horizon?". J Bone Joint Surg Am 2014;96:e58. doi: 10.2106/JBJS.M.01596.
[7] Carr AJ, Robertsson O, Graves S, et al. Knee replacement. Lancet 2012;379:1331–40. doi: 10.1016/S0140-6736(11)60752-6.
[8] Stubbs B, Aluko Y, Myint PK, et al. Prevalence of depressive symptoms and anxiety in osteoarthritis: a systematic review and meta-analysis. Age Ageing 2016;45:228–35. doi: 10.1093/ageing/afw001.
[9] Moseng T, Vliet Vlieland TPM, Battista S, et al. EULAR recommendations for the non-pharmacological core management of hip and knee osteoarthritis: 2023 update. Ann Rheum Dis 2024;83:730–40. doi: 10.1136/ard-2023-225041.
[10] Brophy RH, Fillingham YA. AAOS Clinical Practice Guideline Summary: Management of Osteoarthritis of the Knee (Nonarthroplasty), Third Edition. J Am Acad Orthop Surg 2022;30:e721–9. doi: 10.5435/JAAOS-D-21-01233.
[11] Ferraz RB, Gualano B, Rodrigues R, et al. Benefits of Resistance Training with Blood Flow Restriction in Knee Osteoarthritis. Med Sci Sports Exerc 2018;50:897–905. doi: 10.1249/MSS.0000000000001530.
[12] Skou ST, Roos EM. Physical therapy for patients with knee and hip osteoarthritis: supervised, active treatment is current best practice. Clin Exp Rheumatol 2019;37(Suppl 120):112–7.
[13] Bannuru RR, Osani MC, Vaysbrot EE, et al. OARSI guidelines for the non-surgical management of knee, hip, and polyarticular osteoarthritis. Osteoarthr Cartil 2019;27:1578–89. doi: 10.1016/j.joca.2019.06.011.
[14] Sharma L. Osteoarthritis of the Knee. N Engl J Med 2021;384:51–9. doi: 10.1056/NEJMcp1903768.
[15] Kolasinski SL, Neogi T, Hochberg MC, et al. 2019 American College of Rheumatology/Arthritis Foundation Guideline for the Management of Osteoarthritis of the Hand, Hip, and Knee. Arthritis Care Res (Hoboken) 2020;72:149–62. doi: 10.1002/acr.24131.
[16] Holden MA, Hattle M, Runhaar J, et al. Moderators of the effect of therapeutic exercise for knee and hip osteoarthritis: a systematic review and individual participant data meta-analysis. Lancet Rheumatol 2023;5:e386–400. doi: 10.1016/S2665-9913(23)00122-4.
[17] Jack RA, Lambert BS, Hedt CA, et al. Blood Flow Restriction Therapy Preserves Lower Extremity Bone and Muscle Mass After ACL Reconstruction. Sports Health 2023;15:361–71. doi: 10.1177/19417381221101006.
[18] American College of Sports M. American College of Sports Medicine position stand. Progression models in resistance training for healthy adults. Med Sci Sports Exerc Mar 2009;41:687–708. doi: 10.1249/MSS.0b013e3181915670.
[19] Patterson SD, Hughes L, Warmington S, et al. Blood Flow Restriction Exercise: Considerations of Methodology, Application, and Safety. Front Physiol 2019;10:533. doi: 10.3389/fphys.2019.00533.
[20] Bryk FF, Dos Reis AC, Fingerhut D, et al. Exercises with partial vascular occlusion in patients with knee osteoarthritis: a randomized clinical trial. Knee Surg Sports Traumatol Arthrosc 2016;24:1580–6. doi: 10.1007/s00167-016-4064-7.
[21] Cerqueira MS, de Brito Vieira WH. Effects of blood flow restriction exercise with very low load and low volume in patients with knee osteoarthritis: protocol for a randomized trial. Trials 2019;20:135. doi: 10.1186/s13063-019-3238-2.
[22] Nicholas R, Kyle K, Mikhail CS, et al. Perceived Barriers to Blood Flow Restriction Training. Front Physiol 2021. doi: 10.3389/fresc.2021.697082.
[23] Ilett MJ, Rantalainen T, Keske MA, et al. The Effects of Restriction Pressures on the Acute Responses to Blood Flow Restriction Exercise. Front Physiol 2019;10:1018. doi: 10.3389/fphys.2019.01018.

[24] Roos EM, Toksvig-Larsen S. Knee injury and Osteoarthritis Outcome Score (KOOS) - validation and comparison to the WOMAC in total knee replacement. Health Qual Life Outcomes 2003;1:17. doi: 10.1186/1477-7525-1-17.
[25] Chopp-Hurley JN, Wiebenga EG, Gatti AA, et al. Investigating the Test-Retest Reliability and Validity of Hand-Held Dynamometry for Measuring Knee Strength in Older Women with Knee Osteoarthritis. Physiother Can 2019;71:231–8. doi: 10.3138/ptc-2018-0051.
[26] Ong WJ, Kwan YH, Lim ZY, et al. Measurement properties of Pain Catastrophizing Scale in patients with knee osteoarthritis. Clin Rheumatol 2021;40:295–301. doi: 10.1007/s10067-020-05163-8.
[27] Bennell K, Dobson F, Hinman R. Measures of physical performance assessments: Self-Paced Walk Test (SPWT), Stair Climb Test (SCT), Six-Minute Walk Test (6MWT), Chair Stand Test (CST), Timed Up & Go (TUG), Sock Test, Lift and Carry Test (LCT), and Car Task. Arthritis Care Res (Hoboken) 2011;63(Suppl 11):S350–70. doi: 10.1002/acr.20538.
[28] Bremander AB, Dahl LL, Roos EM. Validity and reliability of functional performance tests in meniscectomized patients with or without knee osteoarthritis. Scand J Med Sci Sports 2007;17:120–7. doi: 10.1111/j.1600-0838.2006.00544.x.
[29] Millar SC, Bennett K, Rickman M, et al. Retention of kinematic patterns during a 6-minute walk test in people with knee osteoarthritis. Gait Posture 2023;101:106–13. doi: 10.1016/j.gaitpost.2023.02.004.
[30] Minniti MC, Statkevich AP, Kelly RL, et al. The Safety of Blood Flow Restriction Training as a Therapeutic Intervention for Patients With Musculoskeletal Disorders: A Systematic Review. Am J Sports Med 2020;48:1773–85. doi: 10.1177/0363546519882652.
[31] Collins NJ, Misra D, Felson DT, et al. Measures of knee function: International Knee Documentation Committee (IKDC) Subjective Knee Evaluation Form, Knee Injury and Osteoarthritis Outcome Score (KOOS), Knee Injury and Osteoarthritis Outcome Score Physical Function Short Form (KOOS-PS), Knee Outcome Survey Activities of Daily Living Scale (KOS-ADL), Lysholm Knee Scoring Scale, Oxford Knee Score (OKS), Western Ontario and McMaster Universities Osteoarthritis Index (WOMAC), Activity Rating Scale (ARS), and Tegner Activity Score (TAS). Arthritis Care Res (Hoboken) 2011;63(Suppl 11):S208–28. doi: 10.1002/acr.20632.
[32] R: a language and environment for statistical computing. R foundation for statistical computing, vienna, austria. 2024. Available: https://www.R-project.org.
[33] Wang T-J, Lee S-C, Liang S-Y, et al. Comparing the efficacy of aquatic exercises and land-based exercises for patients with knee osteoarthritis. J Clin Nurs 2011;20:2609–22. doi: 10.1111/j.1365-2702.2010.03675.x.
[34] da Silva FS, de Melo FES, do Amaral MMG, et al. Efficacy of simple integrated group rehabilitation program for patients with knee osteoarthritis: Single-blind randomized controlled trial. J Rehabil Res Dev 2015;52:309–22. doi: 10.1682/JRRD.2014.08.0199.
[35] Fransen M, McConnell S, Harmer AR, et al. Exercise for osteoarthritis of the knee. Cochrane Database Syst Rev 2015;1:CD004376. doi: 10.1002/14651858.CD004376.pub3.
[36] Wang H, Chen Y, Cheng L, et al. Efficacy and Safety of Blood Flow Restriction Training in Patients With Knee Osteoarthritis: A Systematic Review and Meta−Analysis. Arthritis Care Res (Hoboken) 2022;74:89–98. doi: 10.1002/acr.24787.
[37] Hu C, Zhu B, Wang Y, et al. Effectiveness of blood flow restriction versus traditional weight-bearing training in rehabilitation of knee osteoarthritis patients with MASLD: a multicenter randomized controlled trial. Front Endocrinol (Lausanne) 2023;14:1220758. doi: 10.3389/fendo.2023.1220758.
[38] Hughes L, Paton B, Rosenblatt B, et al. Blood flow restriction training in clinical musculoskeletal rehabilitation: a systematic review and meta-analysis. Br J Sports Med 2017;51:1003–11. doi: 10.1136/bjsports-2016-097071.
[39] Pearson SJ, Hussain SR. A review on the mechanisms of blood-flow restriction resistance training-induced muscle hypertrophy. Sports Med 2015;45:187–200. doi: 10.1007/s40279-014-0264-9.
[40] Freitas EDS, Karabulut M, Bemben MG. The Evolution of Blood Flow Restricted Exercise. Front Physiol 2021;12:747759. doi: 10.3389/fphys.2021.747759.
[41] Loenneke JP, Fahs CA, Wilson JM, et al. Blood flow restriction: the metabolite/volume threshold theory. Med Hypotheses 2011;77:748–52. doi: 10.1016/j.mehy.2011.07.029.
[42] Jacobs E, Rolnick N, Wezenbeek E, et al. Investigating the autoregulation of applied blood flow restriction training pressures in healthy, physically active adults: an intervention study evaluating acute training responses and safety. Br J Sports Med 2023;57:914–20. doi: 10.1136/bjsports-2022-106069.
[43] Nakajima T, Iida H, Kurano M, et al. Hemodynamic responses to simulated weightlessness of 24-h head-down bed rest and KAATSU blood flow restriction. Eur J Appl Physiol 2008;104:727–37. doi: 10.1007/s00421-008-0834-3.
[44] Fry CS, Glynn EL, Drummond MJ, et al. Blood flow restriction exercise stimulates mTORC1 signaling and muscle protein synthesis in older men. J Appl Physiol 2010;108:1199–209. doi: 10.1152/japplphysiol.01266.2009.
[45] Yasuda T, Fukumura K, Iida H, et al. Effects of detraining after blood flow-restricted low-load elastic band training on muscle size and arterial stiffness in older women. Springerplus 2015;4:348. doi: 10.1186/s40064-015-1132-2.
[46] Yasuda T, Fukumura K, Uchida Y, et al. Effects of Low-Load, Elastic Band Resistance Training Combined With Blood Flow Restriction on Muscle Size and Arterial Stiffness in Older Adults. J Gerontol A Biol Sci Med Sci 2015;70:950–8. doi: 10.1093/gerona/glu084.
[47] Madarame H, Kurano M, Takano H, et al. Effects of low-intensity resistance exercise with blood flow restriction on coagulation system in healthy subjects. Clin Physiol Funct Imaging 2010;30:210–3. doi: 10.1111/j.1475-097X.2010.00927.x.
[48] Nascimento D da C, Rolnick N, Neto IV de S, et al. A Useful Blood Flow Restriction Training Risk Stratification for Exercise and Rehabilitation. Front Physiol 2022;13:808622. doi: 10.3389/fphys.2022.808622.
[49] Bond CW, Hackney KJ, Brown SL, et al. Blood Flow Restriction Resistance Exercise as a Rehabilitation Modality Following Orthopaedic Surgery: A Review of Venous Thromboembolism Risk. J Orthop Sports Phys Ther 2019;49:17–27. doi: 10.2519/jospt.2019.8375.
[50] Nakajima T, Kurano M, Iida H, et al. Use and safety of KAATSU training: Results of a national survey. Int J KAATSU Ttaining Res 2006;2:5–13. doi: 10.3806/ijktr.2.5.

Ann Rheum Dis 84 (2025) 351–367

Contents lists available at ScienceDirect

Annals of the Rheumatic Diseases

journal homepage: https://www.sciencedirect.com/journal/annals-of-the-rheumatic-diseases

Osteoarthritis

Cell and transcriptomic diversity of infrapatellar fat pad during knee osteoarthritis

Hayley Peters[1,2,3], Pratibha Potla[1,3], Jason S. Rockel[1,3], Teodora Tockovska[1,4], Chiara Pastrello[1,3], Igor Jurisica[1,3,5], Keemo Delos Santos[1,3], Shabana Vohra[1,3], Noah Fine[1,3], Starlee Lively[1,3], Kim Perry[1,3], Nikita Looby[1,3,6], Sheng Han Li[2,3,6], Vinod Chandran[1,2,3,6,7], Katrina Hueniken[1,3], Paramvir Kaur[1,3], Anthony V. Perruccio[1,3,8,9], Nizar N. Mahomed[1,3,8], Raja Rampersaud[1,3,8], Khalid Syed[1,3,8], Eric Gracey[10,11], Roman Krawetz[12], Matthew B. Buechler[13], Rajiv Gandhi[1,2,3,8], Mohit Kapoor[1,2,3,8,*]

[1] *Division of Orthopaedics, Osteoarthritis Research Program, Schroeder Arthritis Institute, University Health Network, Toronto, Ontario, Canada*

[2] *Department of Laboratory Medicine and Pathobiology, University of Toronto, Toronto, Ontario, Canada*

[3] *Krembil Research Institute, University Health Network, Toronto, Ontario, Canada*

[4] *Bioinformatics and HPC Core, Princess Margaret Cancer Research Tower, University Health Network, Toronto, Ontario, Canada*

[5] *Departments of Medical Biophysics and Computer Science, and Faculty of Dentistry, University of Toronto, Toronto, Ontario, Canada*

[6] *Division of Rheumatology, Psoriatic Arthritis Research Program, Schroeder Arthritis Institute, University Health Network, Toronto, Ontario, Canada*

[7] *Institute of Medical Science, University of Toronto, Toronto, Ontario, Canada*

[8] *Department of Surgery, University of Toronto, Toronto, Ontario, Canada*

[9] *Institute of Health Policy, Management and Evaluation, Dalla Lana School of Public Health, University of Toronto, Toronto, Ontario, Canada*

[10] *Molecular Immunology and Inflammation Unit, VIB Centre for Inflammation Research, Ghent University, Ghent, Belgium*

[11] *Department of Rheumatology, University Hospital Ghent, Ghent, Belgium*

[12] *McCaig Institute for Bone and Joint Health, University of Calgary, Calgary, Alberta, Canada*

[13] *Department of Immunology, University of Toronto, Toronto, Ontario, Canada*

ARTICLE INFO

Article history:
Received 5 April 2024
Accepted 19 September 2024

Keywords:
Osteoarthritis
Knee
Arthritis
Fibroblasts
Risk Factors

ABSTRACT

Objectives: In this study, we employ a multiomic approach to identify major cell types and subsets, and their transcriptomic profiles within the infrapatellar fat pad (IFP), and to determine differences in the IFP based on knee osteoarthritis (KOA), sex and obesity status.

Methods: Single-nucleus RNA sequencing of 82 924 nuclei from 21 IFPs (n = 6 healthy control and n = 15 KOA donors), spatial transcriptomics and bioinformatic analyses were used to identify contributions of the IFP to KOA. We mapped cell subclusters from other white adipose tissues using publicly available literature. The diversity of fibroblasts within the IFP was investigated by bioinformatic analyses, comparing by KOA, sex and obesity status. Metabolomics was used to further explore differences in fibroblasts by obesity status.

Results: We identified multiple subclusters of fibroblasts, macrophages, adipocytes and endothelial cells with unique transcriptomic profiles. Using spatial transcriptomics, we resolved

*Correspondence to Professor Mohit Kapoor.

E-mail address: mkapoor@uhnresearch.ca (M. Kapoor).

Handling editor Josef S. Smolen.

https://doi.org/10.1136/ard-2024-225928

distributions of cell types and their transcriptomic profiles and computationally identified putative cell–cell communication networks. Furthermore, we identified transcriptomic differences in fibroblasts from KOA versus healthy control donor IFPs, female versus male KOA-IFPs and obese versus normal body mass index (BMI) KOA-IFPs. Finally, using metabolomics, we defined differences in metabolite levels in supernatants of naïve, profibrotic stimuli-treated and proinflammatory stimuli-treated fibroblasts from obese compared to normal BMI KOA-IFPs.
Conclusions: Overall, by employing a multiomic approach, this study provides the first comprehensive map of the cellular and transcriptomic diversity of human IFP and identifies IFP fibroblasts as key cells contributing to transcriptomic and metabolic differences related to KOA disease, sex or obesity.

WHAT IS ALREADY KNOWN ON THIS TOPIC

- Previous studies suggest that the infrapatellar fat pad (IFP) is a source of tissue repair cells and contributes to knee osteoarthritis (KOA) through inflammation, fibrosis and pain; however, the exact cell composition and transcriptomic diversity of the IFP based on KOA, sex and obesity status is largely unknown.

WHAT THIS STUDY ADDS

- With this study, we present a cellular and transcriptomic map of the major cell populations and their subsets within the human IFP.
- We spatially locate all identified major cell types, as well as fibroblast subtypes and transcriptomic profiles.
- We uncover putative cell–cell communications between fibroblasts and all other major cell types.
- We compare transcriptomic profiles of IFP fibroblasts from KOA versus healthy control, female versus male KOA and obese versus normal body mass index (BMI) KOA, highlighting differences across all groups. Metabolomics uncovered potential alterations in metabolites measured from supernatants of fibroblast cultures isolated from obese compared to normal BMI KOA-IFPs.

HOW THIS STUDY MIGHT AFFECT RESEARCH, PRACTICE OR POLICY

- Discovering how the IFP contributes to KOA pathogenesis in relation to OA disease, sex and obesity, we reveal potential cellular and molecular targets for future intervention that may be related to future precision medicine approaches to KOA.

INTRODUCTION

Osteoarthritis (OA) is a progressive disease that diminishes the quality of life of those afflicted. The number of cases globally has increased by 132% since 1990 [1]. In adults aged 45 years and older, 30% have detectable knee (K)OA, the majority being women [2]. As knee osteoarthritis (KOA) progresses, severe pain and reduced mobility are primary symptoms. Primary (non-traumatic) KOA is associated with degradation of articular cartilage, chondrocyte loss and subchondral bone remodelling [3]. In addition, elevated joint cytokine levels increase angiogenesis and inflammation of the synovium and fat pads [3]. There is growing interest in the contribution of soft tissues to KOA pathogenesis; however, few studies have focused on understanding the infrapatellar fat pad (IFP).

The IFP is the largest fat pad within the knee, located posterior to the inferior pole of the patella, anterior to the tibia and between the anterior horns of the meniscus and femur [4]. Composed of white fibrous adipose tissue, the presently known functions of the IFP are to aid with shock absorption and support the joint structure [4] and may contain cells involved in tissue repair [5]. However, its biological and pathological functions are not well characterised. The IFP is highly vascularised, becoming inflamed during KOA, leading to fibrosis and structural changes, potentially contributing to significant pain [6]. A recent study identified some cell types in combined IFP and synovial tissue, showing that apolipoprotein from fibroblasts and macrophages imparts a cartilage-destructive effect [7]. To our knowledge, no study has focused on understanding the complex diversity of the cellular composition and their transcriptomic profiles exclusively in the IFP.

Obesity [body mass index (BMI) ≥30 kg/m^2] is one of the strongest risk factors for developing KOA [2]. Obese individuals demonstrate chronic, low-grade, systemic inflammation and increased mechanical stress on knee joints, consequentially increasing proinflammatory adipokines and cytokines that promote KOA [8]. Females are also at increased risk of KOA, and typically present with more severe pain and functional limitations compared to males [9]. In a preclinical model of idiopathic KOA, removal of the IFP led to decreased cartilage degeneration within female compared to male guinea pigs [10]. However, how obesity status and sex impact the IFP during KOA pathogenesis is not fully understood.

In this study, we used single-nucleus RNA sequencing (snRNA-seq), spatial transcriptomics and advanced bioinformatic methods to identify cell types and subclusters within IFPs from patient-matched samples, creating a comprehensive cell and transcriptomic map of the IFP. We determined that the IFP contains multiple cell types with specific cell subclusters, each having a unique transcriptomic profile and spatial distribution. We have performed pseudotime trajectory analysis, revealing a fibroblast population expressing universal markers that can putatively differentiate into both other fibroblast subclusters as well as adipocytes. Cell–cell communication analysis revealed putative signalling patterns across all major cell types. We demonstrated differences in the transcriptomes of fibroblasts from IFPs of KOA versus healthy control donors, females versus males with KOA and obese BMI (30–40 kg/m^2) versus normal BMI (18.5–24.9 kg/m^2) with KOA, suggesting putative mechanisms by which fibroblasts may contribute to KOA pathogenesis. Finally, targeted metabolomics revealed that metabolite levels in culture supernatants were modified in fibroblasts from obese compared to normal BMI KOA-IFPs and were further altered by profibrotic and proinflammatory stimuli. Overall, we provide a comprehensive map of the cellular and transcriptomic diversity of the human IFP, with considerations for KOA, sex and obesity status.

METHODS

Full detailed materials and methods are available in online supplemental information.

RESULTS

Cellular composition of the IFP

IFPs from 21 study participants (6 healthy control and 15 KOA) were analysed using snRNA-seq and bioinformatic analyses to identify cell types [11] (figure 1A; online supplemental figure 1,2,3A, online supplemental table 1). A total of 82 924 nuclei were sequenced and, after filtering, 73 808 nuclei were analysed. Eight cell types were identified based on canonical markers: fibroblasts, adipocytes, macrophages, endothelial cells, dendritic cells, smooth muscle cells, lymphocytes and mast cells (figure 1B–D; online supplemental figure 3A). The major cell populations contributing to the IFP (>10% of nuclei analysed) were fibroblasts (44.35%), macrophages (19.44%), adipocytes (16.41%) and endothelial cells (12.12%) (figure 1C,D).

Cell subclusters and transcriptomic profiles of the IFP

We next aimed to determine cell subclusters of each major cell type identified within the IFP (n = 21) [11]. Subclustering fibroblasts determined five subclusters, with proportions ranging from 30.32% (subcluster 0) to 9.63% (subcluster 4) (total nuclei: 32 862, resolution 0.2) (figure 1E; online supplemental figure 3B). Unique transcriptomic profiles for each fibroblast subcluster were generated by identifying differentially expressed genes (DEGs) in one subcluster as compared to others. These unique profiles ranged from 225 genes (subcluster 2) to 43 genes (subcluster 3) [q<0.05, log2 fold change (FC) ≥0.5, min.pct≥0.25] (online supplemental figure 4; online supplemental table 2A). The top five genes for each fibroblast subcluster, based on decreasing Log2FC, included subcluster 0: FBN1, PXDNL, PIEZO2, GUCY1A2 and PTGIS; subcluster 1: ABCA10, KCND2, ABCA6, ABCA8 and ABCA9; subcluster 2: CRTAC1, CLIC5, PRG4, FN1 and SEMA3A; subcluster 3: GPAM, FABP4, F13A1, FTL and FTH1 and subcluster 4: MGAT4C, GRIP1, BTBD11, IGF1 and C1GALT1 (figure 1F, online supplemental figure 3C; online supplemental table 2A). We then used flow cytometry to identify the major fibroblast subclusters at the protein level using an additional n = 12 IFP samples (online supplemental figure 5A). Our flow cytometry panel included CD26/DPP4, CD10/MME/CALLA and HLA-C, cell surface proteins that we identified as key markers for the three major fibroblast subclusters, subcluster 0, subcluster 1 and subcluster 2, respectively (online supplemental figure 5B). These markers were assessed on fibroblasts (PDPN + CD45−), revealing subcluster 0 and subcluster 1 populations to be the most prevalent (online supplemental figure 5C,D), as we observed in our snRNA-seq dataset.

Next, pseudotime trajectory analysis using SCORPIUS V.1.0.9 [12] showed a clear transition of fibroblast subclusters from subcluster 0 to subcluster 2, through subclusters 3, 1 and 4 (figure 1G). We identified genes that predicted the ordering of fibroblast subclusters along pseudotime, ranked by importance scores. There were distinct changes in module expression profiles, corresponding to transcriptomic profiles of fibroblast subclusters (figure 1G). Additionally, top markers of subcluster 0 (FBN1), subcluster 1 (ABCA10), subcluster 2 (CRTAC1) and subcluster 4 (MGAT4C) showed peak expression in respective subclusters along pseudotime (figure 1G). Fibroblasts expressing DPP4, PI16 and CD34 have previously been characterised as universal fibroblasts able to differentiate into more specialised fibroblast subtypes [13]. In our dataset, these markers were highly expressed in subcluster 0, suggesting that it may act as precursors for other fibroblast subclusters we identified (figure 1G; online supplemental figure 6).

Using a similar bioinformatic strategy, we uncovered four subclusters of macrophages within the IFP, with proportions ranging from 49.85% (subcluster 0) to 8.06% (subcluster 3) (total nuclei: 14 351, resolution 0.1) (figure 2A, online supplemental figure 7A). Each macrophage subcluster had unique transcriptomic profiles spanning from 232 genes (subcluster 1) to 74 genes (subcluster 3) (online supplemental figure 8; online supplemental table 2B). The top five genes for each macrophage subcluster based on decreasing log2FC (q<0.05, Log2FC≥0.5, min.pct≥0.25) included subcluster 0: P2RY14, MAN1A1, FGF13, DSCAML1 and PID1; subcluster 1: FN1, TPRG1, KCNQ3, PDE3A and FMNL2; subcluster 2: TTN, STAB1, AHNAK, RBM25 and PRRC2C; subcluster 3: NOVA1, ADH1B, DLC1, FBN1 and NEGR1 (figure 2B; online supplemental figure 7B; online supplemental table 2B).

Subclustering of adipocytes identified four subclusters, with proportions ranging from 72.97% (subcluster 0) to 2.25% (subcluster 3) (total nuclei: 12 111, resolution 0.08) (figure 2C; online supplemental figure 9A). All adipocyte subclusters had unique transcriptomic markers, ranging from 160 genes (subcluster 2) to 89 genes (subcluster 0) (online supplemental figure 10; online supplemental table 2C). The top five genes for each subcluster based on decreasing log2FC (q<0.05, log2FC≥0.5, min.pct≥0.25) included subcluster 0: CLSTN2, WDPCP, PDE11A, ESR2 and LEPR; subcluster 1: CCDC200, SCD, TEX14, PDE4D and F13A1; subcluster 2: ITGBL1, ANO5, GPC6, STK32A and SEMA3C; subcluster 3: ATP1B3, CMSS1, PGAP1, PHLDB2 and CTH (figure 2D; online supplemental figure 9B; online supplemental table 2C). Pseudotime trajectory analysis of both adipocytes and fibroblasts together demonstrated a bidirectional differentiation pattern. Fibroblast subcluster 0 showed the greatest expression of universal fibroblast markers DPP4, PI16 and CD34, as described within fibroblast trajectory alone (figure 1G). This fibroblast population showed a trajectory towards adipocyte subcluster 1, through subclusters 3 and 0, terminating in subcluster 2, a more differentiated adipocyte population expressing PPARG and ADIPOQ (online supplemental figure 11). Fibroblast subcluster 3 was located between fibroblast subcluster 0 and all adipocyte subclusters within the trajectory suggesting that fibroblast subcluster 3 may contain a population of preadipocyte cells which further differentiates into specialised adipocyte populations (online supplemental figure 11). Additionally, fibroblasts expressing universal markers could also differentiate into more specialised fibroblasts, as demonstrated through CD55 and PDGFRA expression (online supplemental figure 11). This suggests that more differentiated adipocytes and fibroblasts can be derived from fibroblasts that express universal fibroblast markers.

Finally, we identified five endothelial cell subclusters within the IFP, with proportions ranging from 40% (subcluster 0) to 4.22% (subcluster 4) (total nuclei: 8944, resolution 0.05) (figure 2E; online supplemental figure 12A). Each endothelial cell subcluster had unique transcriptomic markers, ranging from 225 genes (subcluster 3) to 153 genes (subcluster 0) (online supplemental figure 13; online supplemental table 2D). The top five genes for each endothelial cell subcluster based on decreasing log2FC (q<0.05, log2FC≥0.5, min.pct≥0.25) included subcluster 0: CADM2, BTNL9, CD36, KIAA1217 and PPARG; subcluster 1: PLCXD3, TLL1, GPM6A, ZNF521 and MYRIP; subcluster 2: NR4A1, UBC, ZFP36, DEPP1 and ACTA2; subcluster 3: NKAIN2, SULF1, ARL15, PCSK5 and TOX; subcluster 4: NOVA1, ABI3BP, DCN, DCLK1 and BICC1 (figure 2F; online supplemental figure 12B; online supplemental table 2D).

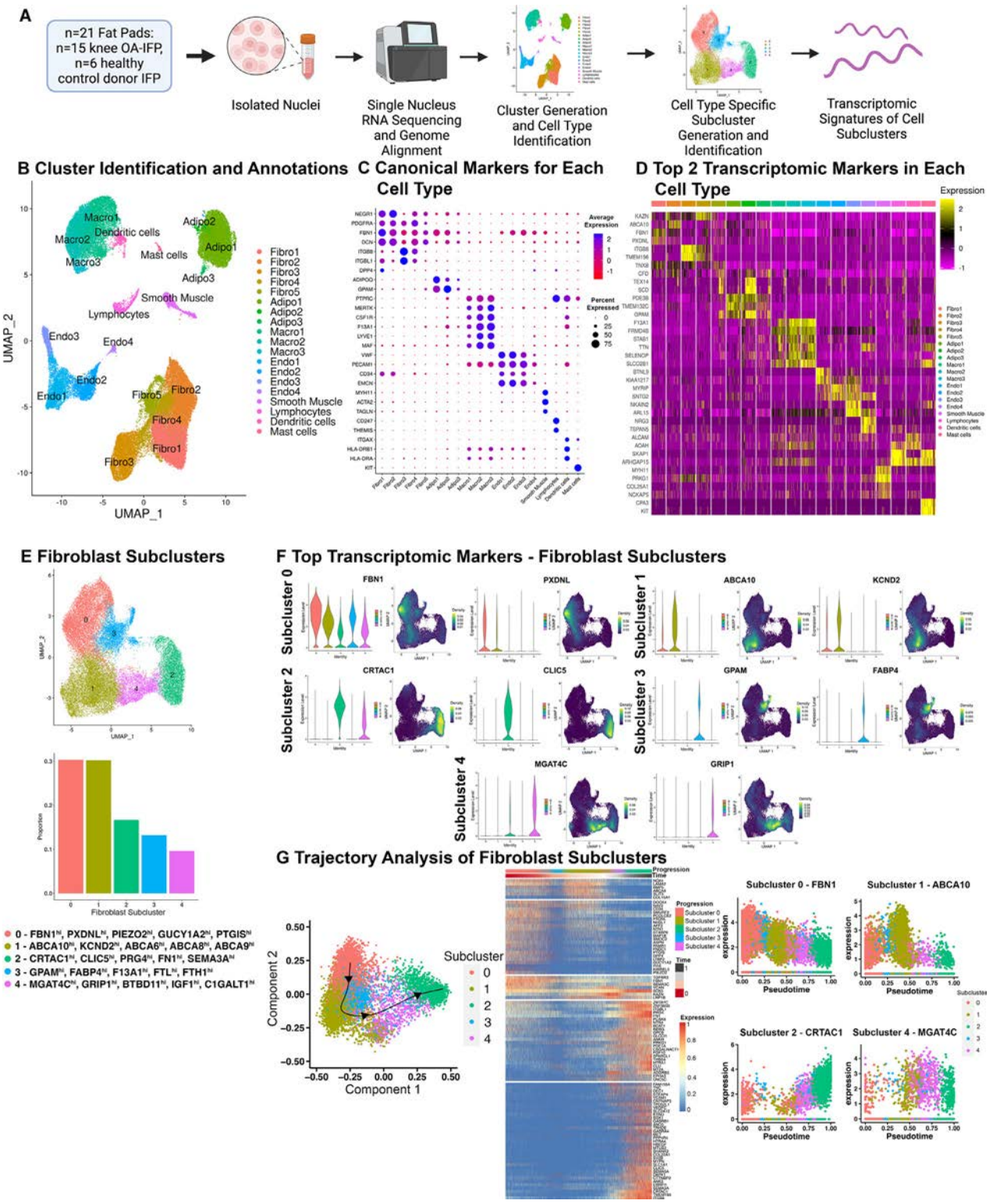

Figure 1. Infrapatellar fat pad (IFP) cell populations and fibroblast subclusters identified by single-nucleus RNA sequencing (n = 21). (A) Schematic workflow to identify cell types and subclusters within human IFPs (created with BioRender.com). (B) Uniform manifold approximation and projection (UMAP) of clusters identified in IFPs. (C) Dot plot with the average and percent population expression of canonical markers for each cell population. (D) Heatmap displaying expression of the top two differentially expressed genes (DEGs) within each cell population. (E) UMAP of fibroblast subclusters and bar plot depicting fibroblast proportion of each subcluster. Top five unique DEGs defining each subcluster are indicated. (F) Violin and density plots displaying the expression of the top two unique DEGs within each fibroblast subcluster. Density plots display expression density ranging from dark purple (low) to yellow (high). (G) Two-dimensional plot showing inferred trajectory across pseudotime of integrated fibroblast subclusters using SCORPIUS. Heatmap demonstrating the change in average scaled expression of the top 94 important genes defining fibroblast subcluster trajectory across pseudotime (q<0.05). Genes in the heatmap are clustered into four modules, each representing a set of genes expressed at different time points of the trajectory. Jitter plots depict the expression of the top marker gene for distinct subclusters across pseudotime (see online supplemental figures 2–4, online supplemental figure 6 and online supplemental table 2A).

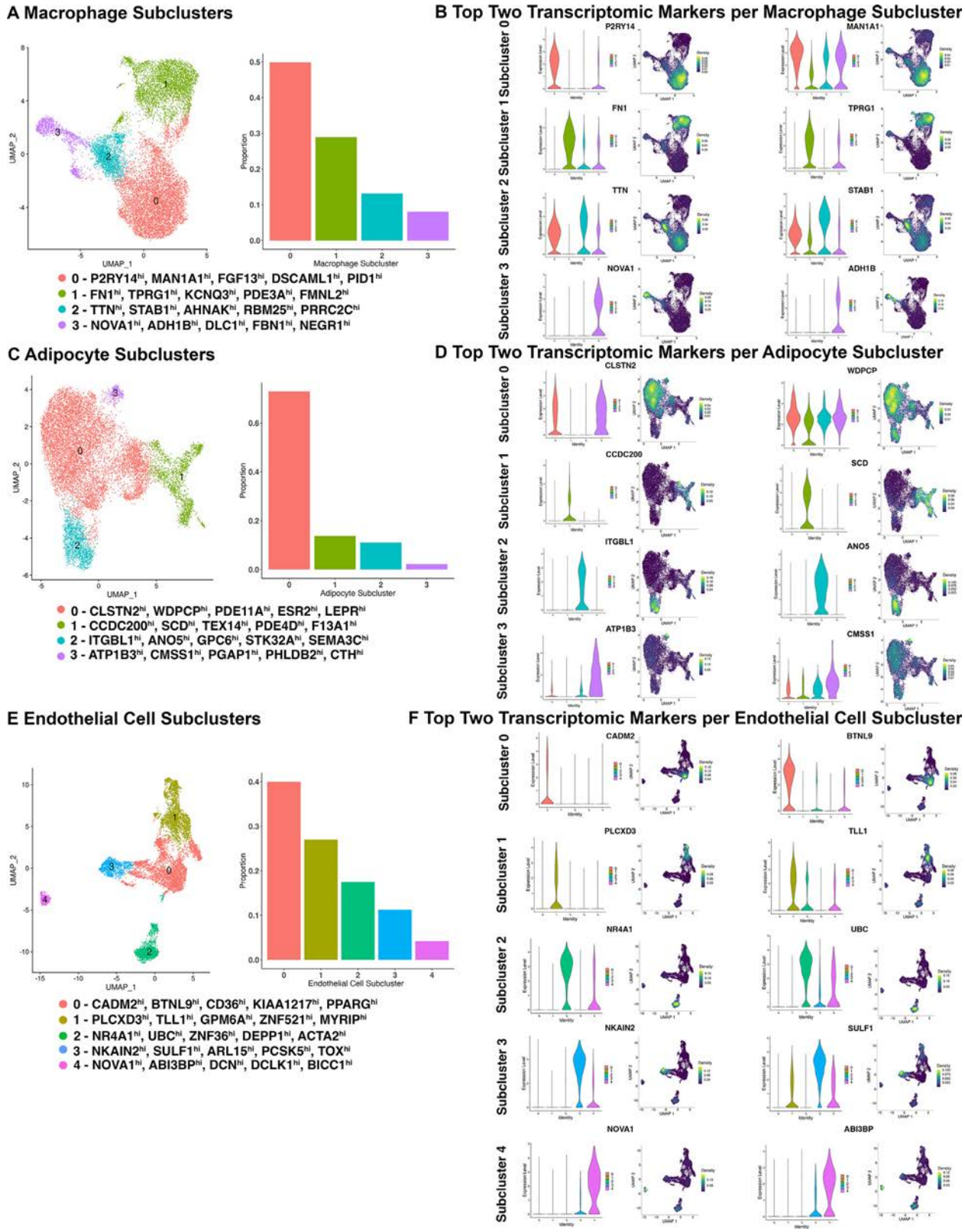

Figure 2. Macrophage, adipocyte and endothelial cell subclusters in infrapatellar fat pad identified by single-nucleus RNA sequencing (n = 21). (A, C, E) UMAPs and bar plots depicting cell type subclusters and their respective proportions. Top five DEGs within each cluster are indicated. (B, D, F) Violin plots and density plots depicting the expression of the top two unique transcriptomic markers within each macrophage, adipocyte and endothelial cell subcluster. Density plots present the expression density from dark purple (low) to yellow (high) (see online supplemental figures 7–13, online supplemental table 2B–D). DEGs, differentially expressed genes; UMAP, uniform manifold approximation and projection.

Using previously published datasets, we determined that fibroblast subclusters within the IFP mapped to fibroblast populations identified from other adipose tissues (online supplemental figure 14A) [7,13−16]. In combined IFP and synovial tissue, four fibroblast subsets were uncovered [7], consistent with that determined using IFP only in our study (online supplemental figure 14A). Fibroblasts identified can also be referred to as preadipocytes, adipocyte stem and progenitor cells and mesenchymal stromal cells as they mapped to populations using this nomenclature [7,13−16]. In addition, we mapped macrophage, adipocyte and endothelial cell subclusters we identified using reported white adipose tissue markers (online supplemental figure 14 B−D) [13].

Spatial profiling of major cell types, fibroblast subclusters and transcriptomic profiles of the KOA-IFP

After revealing major cell types, subtypes and their transcriptomic profiles within the IFP, we sought to resolve their spatial distribution using spatial transcriptomics (figure 3A). We analysed n = 12 KOA-IFPs patient-matched to tissues analysed by snRNA-seq using Visium CytAssist spatial transcriptomics [17] (online supplemental table 1). Spatial data were clustered and annotated independently from snRNA-seq data. We confirmed that fibroblasts, macrophages, adipocytes and endothelial cells were the major cell populations within IFPs, with fibroblasts distributed across the IFP alongside all other major cell types (Figure 3B; online supplemental figure 15A).

Fibroblasts from spatial transcriptomic data were deconvoluted using fibroblast subcluster annotations derived from snRNA-seq data. Each fibroblast subcluster was visualised in areas independently identified as fibroblasts by spatial transcriptomics (figure 3C). Subsequently, we spatially resolved the transcriptomic profiles of identified fibroblast subclusters through coexpression of the top 10 genes of each subcluster (figure 3D). We also visualised one of the top DEGs of each fibroblast subcluster including: subcluster 0: FBN1; subcluster 1: COL15A1; subcluster 2: CRTAC1; subcluster 3: FABP4; subcluster 4: ENAH (figure 1F; figure 3E; online supplemental figure 3C,15B).

Neighbourhood analysis using hoodscanR [18] identified the probability of colocalisation of all cell types within the KOA-IFP. In five potential neighbourhoods, we found unique neighbourhoods containing all cell populations (figure 3F; online supplemental figure 16). Based on probabilities, adipocytes and endothelial cells were most likely to be found across all neighbourhoods (figure 3F). All fibroblast subclusters had a probability of being found across all neighbourhoods, with subcluster 1 likely being the dominant fibroblast subcluster within most neighbourhoods (figure 3F). Fibroblast subclusters 0 and 1 were likely the most dominant fibroblast subcluster within neighbourhood 4 (figure 3F). While we have identified five distinct neighbourhoods where all fibroblast subclusters reside, at this point, we are unable to specifically identify which anatomical features individual neighbourhoods are associated with. Overall, these data suggest that fibroblast subclusters are distributed across the IFP alongside adipocytes, endothelial cells and macrophages, with the potential to communicate.

Cell−cell communications within the KOA-IFP

Since fibroblasts had the largest proportion of nuclei, and all major cell types were spatially organised proximal to fibroblasts across IFPs, we investigated putative communications that occur between fibroblasts and all other major cell types within our snRNA-seq data. Using CellChat V.2.0 [19], we identified major ligand-receptor cell signalling pathways, with macrophages, adipocytes and endothelial cells as 'sender' cells expressing ligands and fibroblasts as 'receiver' cells expressing receptors. Multiple cell communications to fibroblasts were identified, with the highest proportion of ligand-receptor pairs originating from adipocytes and the highest proportion of interactions occurring with fibroblast CD44 and ITGAV/ITGB8 receptors (figure 4A; online supplemental table 3).

Additional investigations uncovered outgoing signalling patterns from all major cell types, without defining 'receivers' or 'senders'. Regardless of directionality, fibroblasts, macrophages, adipocytes and endothelial cells had unique outgoing signalling patterns composed of multiple signalling pathways (figure 4B) suggesting intercommunication through multiple outgoing signals including collagen, PECAM1, PDGF and ANGPTL, which are known to stimulate regeneration and repair, extracellular matrix (ECM) deposition and angiogenesis [20−23].

Since the collagen signalling pathway had the highest proportion of signalling going towards fibroblasts across all cell types, we spatially plotted the connectivity of this signalling network (figure 4C; online supplemental figure 17A). Furthermore, we were also able to spatially colocalise the COL4A2-CD44 ligand-receptor pair, which had one of the highest proportions of signalling within the collagen signalling pathway (figure 4A, C; online supplemental figure 17B).

We next analysed cell−cell communications within KOA-IFPs versus healthy control donor IFPs. Macrophages had a higher proportion of signalling towards fibroblasts within KOA-IFPs compared to healthy control donor IFPs (online supplemental figure 18A). Furthermore, KOA-IFPs had a higher proportion of upregulated communication interactions across all cell type pairings, compared to healthy control donor IFPs (figure 4D). The CD44 and ITGAV/ITGB8 receptors were involved in most upregulated and downregulated signals within KOA-IFPs and healthy control donor IFPs (figure 4D). Regardless of directionality, all major cell types had some unique outgoing signalling patterns based on OA status, with a larger number of signalling interactions identified within KOA-IFPs (online supplemental figure 18B).

Transcriptomic differences in fibroblasts within the IFP based on KOA status

Since signalling to fibroblasts appeared modified in KOA-IFPs compared to healthy control donor IFPs, we investigated differences in cell composition and transcriptomic signatures based on KOA status. Fibroblasts, having the highest proportion of cells contributing to the IFP, were selected for subsequent analysis. Bioinformatic investigations of snRNA-seq data determined alterations in fibroblast subclusters within KOA-IFPs (n = 15) compared to healthy control donor IFPs (n = 6) (online supplemental table 1). We found all fibroblast subclusters within individual KOA-IFPs and healthy control donor IFPs (figure 5A). However, subcluster 3 had a higher proportion of nuclei contributed from healthy control donor IFPs compared to KOA-IFPs ($q = 0.032$, multiple unpaired t-tests with false discovery rate (FDR) correction; figure 5B). Additionally, 38 DEGs (20 upregulated, 18 downregulated) were identified within KOA-IFPs versus healthy control donor IFPs, with the top five upregulated genes: FN1, ZNF385B, PRG4, ANKH and KAZN, and the top five downregulated genes: JUN, ABCA1, VIM, GSN and SAMD4A (figure 5C; online supplemental table 4A). The top five

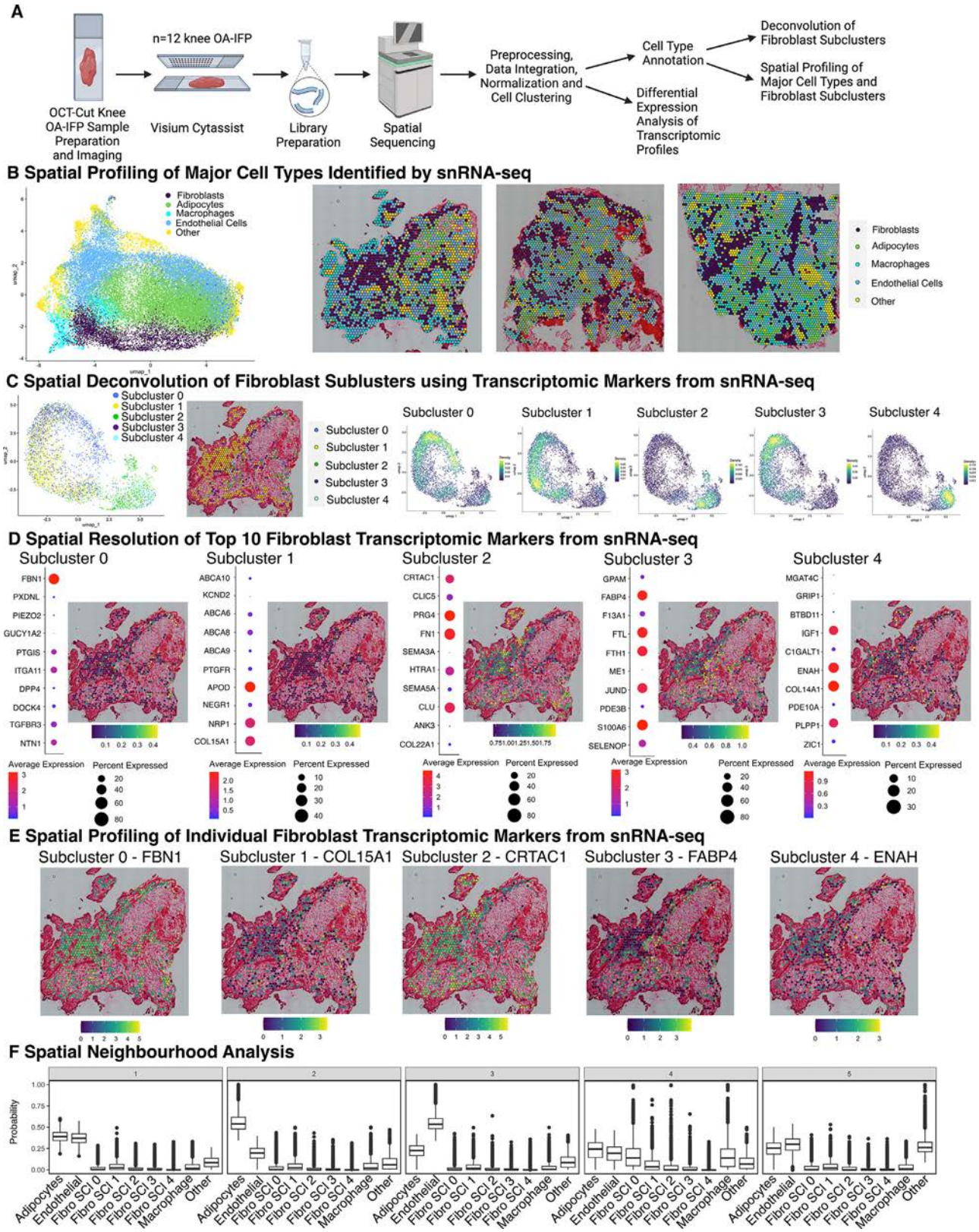

Figure 3. Spatial profiling of major cell types identified by snRNA-seq data. (A) Schematic workflow to spatially resolve cell types within IFPs using spatial sequencing (created with BioRender.com). (B) UMAP (left) of spatial sequencing data of n = 12 knee osteoarthritis (KOA)-IFP. Spatial resolution of cell populations identified using spatial sequencing across multiple IFPs (right). (C) UMAP (left) of spatial deconvolution of fibroblast subclusters across n = 12 IFPs using snRNA-seq. Spatial resolution of deconvolved fibroblast subclusters within a representative IFP sample (middle). Density plots (right) displaying the module scores of the average gene expression of the top 10 transcriptomic markers of each deconvolved fibroblast subcluster. Module scores within density plots range from yellow (high) to dark purple (low). (D) Dot plots show the average expression of the top 10 transcriptomic markers within each fibroblast subcluster, from blue (low average expression) to red (high average expression). Spatial plots show the resolution of the module scores of coexpression for the top 10 transcriptomic markers of each fibroblast subcluster within a representative IFP, from blue (low module score) to yellow (high module score). (E) Spatial resolution of individual transcriptomic markers for each fibroblast subcluster include subcluster 0—FBN1 (DEG 1), subcluster 1—COL15A1 (DEG 10), subcluster 2—CRTAC1 (DEG 1), subcluster 3—FABP4 (DEG 2), subcluster 4—ENAH (DEG 5). (F) Bar plot showing the probability of each fibroblast subcluster and major cell types residing within a neighbourhood (see online supplemental figures 15,16). DEG, differentialy expressed gene; IFP, infrapatellar fat pad; snRNA-seq, single-nucleus RNA sequencing; UMAP, uniform manifold approximation and projection.

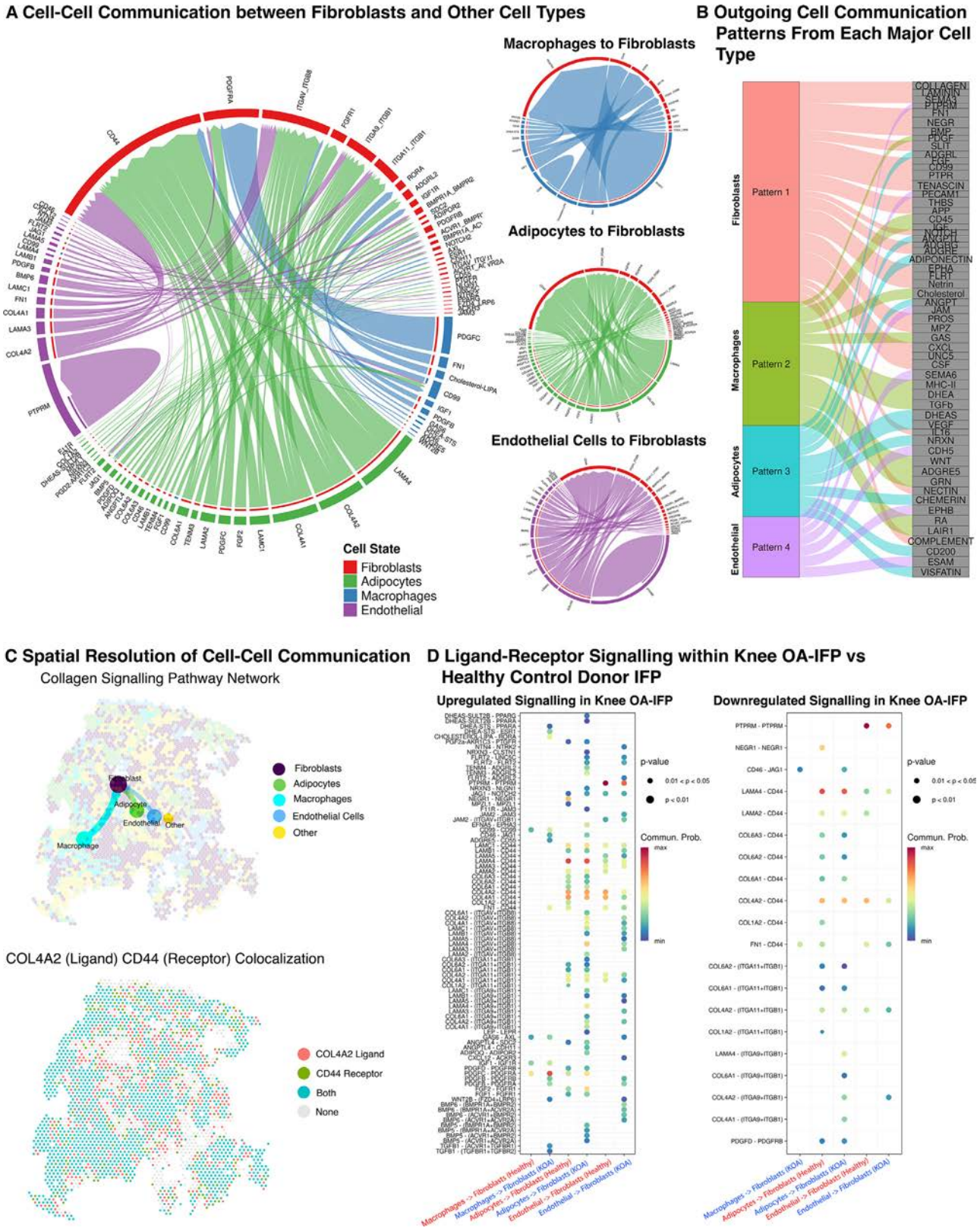

Figure 4. Putative cell–cell communication patterns between fibroblasts and major cell types. (A) Chord diagram (left) showing putative cell–cell communication between fibroblasts and other identified major cell types using snRNA-seq data from n = 21 IFP samples. Fibroblasts are the 'receiver' cell type, expressing receptors and all other cell types are the 'sender' cells, expressing ligands. Individual chord diagrams (right) showing cell–cell communication between fibroblasts and other individual cell types. (B) River plot displays putative outgoing signalling patterns from each identified cell type. (C) Spatial plot showing putative collagen signalling between four major cell types along with another spatial plot displaying the expression of the COL4A2-CD44 ligand-receptor pair in a representative sample. (D) Bubble plots displaying putative upregulated (left) and downregulated (right) signalling interactions between fibroblasts expressing receptors and other major cell types expressing ligands within KOA-IFPs compared to healthy control donor IFPs (see online supplemental table 3, online supplemental figures 17,18). IFP, infrapatellar fat pad; KOA, knee osteoarthritis; snRNA-seq, single nucleus RNA sequencing.

upregulated genes were highly expressed within subclusters 2 and 4 while the top five downregulated genes were highly expressed within subclusters 0, 1 and 3 (online supplemental figure 19). As downregulated and upregulated genes were localised to fibroblast clusters consistent with universal fibroblasts and the terminal fibroblast subclusters, respectively (figure 1G; online supplemental file 6), these results suggest that KOA-IFP fibroblasts have the expression profile of a more terminal differentiation state.

We next used pathDIP analysis (pathDIP V.5, https://ophid.utoronto.ca/pathDIP)[24] to identify enriched pathways associated with DEGs in KOA-IFPs compared to healthy control donor IFPs (figure 5D,E; online supplemental table 4B,C). Network analysis revealed connections between DEGs and enriched pathways from KOA-IFPs versus healthy control donor-IFPs, and putative interactions between transcription factors (Figure 5F). Of note, transcription factors SOX5 and CUX1 were upregulated in KOA-IFPs compared to healthy control donor IFPs while JUN and RBPJ were downregulated, with putative interactions between JUN and CUX1, SOX5 and JUN, and RBPJ and CUX1 (figure 5C,F). This suggests that transcription factor interactions may regulate fibroblast gene expression in KOA compared to healthy IFP.

Sex-based transcriptomic differences in fibroblasts within the KOA-IFP

To understand how sex influences fibroblasts within KOA-IFPs, we performed bioinformatic analyses of snRNA-seq data of female (n = 8) compared to male (n = 7) KOA-IFPs (online supplemental table 1). We observed no significant differences in the presence or proportions of fibroblast subclusters ($q<0.05$, multiple unpaired t-tests with FDR correction; figure 6A,B; online supplemental figure 20). However, we identified differences in transcriptomic profiles of fibroblasts within female versus male KOA-IFPs (figure 6C). We determined 105 DEGs: 35 upregulated and 70 downregulated. The top five upregulated genes include CLU, HTRA1, PRG4, TMEM196 and FN1 and the top five downregulated genes include UTY, USP9Y, LAMA2, AFF3 and NAV3 (figure 6C; online supplemental table 5A).

We used clusterProfiler [25] and pathDIP [24] to perform Gene Ontology biological process and pathway enrichment analysis, identifying processes and pathways associated with DEGs of female versus male KOA-IFPs (figure 6D,E; online supplemental table 5B–E). Network analysis determined connections between DEGs and associated biological processes and pathways, with putative interactions between transcription factors (figure 6F). Notably, transcription factors SOX5, FOXP2 and CREB5 were upregulated within female versus male KOA-IFPs, while ZEB1, BCL6, ZBTB16, EBF2 and RBPJ were downregulated, with putative interactions between transcription factor pairs ZBTB16 and BCL6, and ZEB1 and BCL6 (figure 6C,F), suggesting transcriptional gene regulation by transcription factor interactions in males.

Transcriptomic differences of fibroblasts within the KOA-IFP based on obesity status

To discern how obesity status influences fibroblasts of KOA-IFPs, we performed bioinformatic analysis of snRNA-seq data comparing fibroblast subclusters within obese (n = 8; BMI 30–40 kg/m^2) versus normal BMI KOA-IFPs (n = 7; BMI 18.5–24.9 kg/m^2) (online supplemental table 1). We found no significant differences in the presence or proportions of fibroblast subclusters between normal and obese BMI KOA-IFPs ($q<0.05$, multiple unpaired t-tests with FDR correction) (figure 7A,B; online supplemental figure 21). However, 21 DEGs were identified; 10 upregulated, 11 downregulated (figure 7C; online supplemental table 6A). Upregulated genes from obese versus normal BMI KOA-IFPs included: HMCN1, LHFPL6, ABCA6, PRRX1, ABCA8, ITGA11, DST, STARD9, SRRM2 and FBLN1, while downregulated genes included PRG4, CLU, FN1, ITGB8, FKBP5, UGP2, TIMP3, GPC6, ZBTB16, ITM2B and CREB5 (figure 7C; online supplemental table 6A).

We spatially resolved the 10 upregulated DEGs in obese compared to normal BMI KOA-IFPs using spatial transcriptomics (n = 12; n = 6 normal and n = 6 obese BMI KOA-IFPs). All 10 upregulated genes identified in snRNA-seq data were also upregulated within spatial sequencing data based on log2FC (figure 7D; online supplemental table 6B). Interestingly, DST has a higher percent expression within snRNA-seq while FBLN1 has higher percent expression within spatial data (figure 7D). Of the 10 upregulated genes, ITGA11, STARD9 and ABCA6 were significantly upregulated in spatial transcriptomic analyses ($q<0.05$; figure 7D; online supplemental table 6B).

We used clusterProfiler [25] and pathDIP [24] to perform Gene Ontology biological process and pathway enrichment analysis and identified enriched biological processes and pathways associated with DEGs in obese compared to normal BMI KOA-IFPs (figure 7E,F; online supplemental table 6C-F). Network analysis determined connections between DEGs and enriched biological processes and pathways, with putative interactions between transcription factors (figure 7G). Of note, the transcription factor PRRX1 was upregulated in obese versus normal BMI KOA-IFPs while ZBTB16 and CREB5 were downregulated, with a putative link between PRRX1 and ZBTB16 (figure 7C,G), suggesting transcription factor interactions may mediate transcriptional changes related to obesity status. We also identified enriched pathways related to metabolic functions, including lipid transport and carbohydrate metabolism (figure 7G).

Differences in metabolite levels of fibroblasts isolated from obese and normal BMI KOA-IFPs

Since metabolic dysregulation is a key element of obesity, and transcriptional differences in fibroblasts by obesity status had enriched pathways linked to metabolism, we sought to elucidate if alterations in supernatant metabolite levels of cultured fibroblasts from obese (n = 5) compared to normal BMI KOA-IFPs (n = 5) existed using targeted metabolomics (figure 8A). Overall, 445 metabolites were detected with 5 metabolites found at significantly different levels ($p<0.05$) from obese versus normal BMI KOA-IFPs, including upregulated: triglycerides (TG) (54:2) and TG (50:2), C18:2 (linoleic acid) and choline; downregulated: homoarginine (figure 8B; online supplemental table 7A). Using pathDIP [24], we found that differentially secreted metabolites from KOA-IFP fibroblasts by obesity status were annotated to metabolism-related pathways, including lipid metabolism, with enriched pathways associated with molecular transport (figure 8E; online supplemental figure 22).

Transforming growth factor β (TGF-β) can be found within KOA synovial fluid and is a key mediator involved in fibroblast activation and joint fibrosis [26,27]. Furthermore, tumour necrosis factor α (TNF-α) is also found in KOA synovial fluid and is involved in promoting inflammatory responses in synovial fibroblasts [28,29]. To mimic the fibrotic and inflammatory response in IFP fibroblasts, we stimulated cells with TGF-β or TNF-α, respectively. We then investigated how metabolite levels

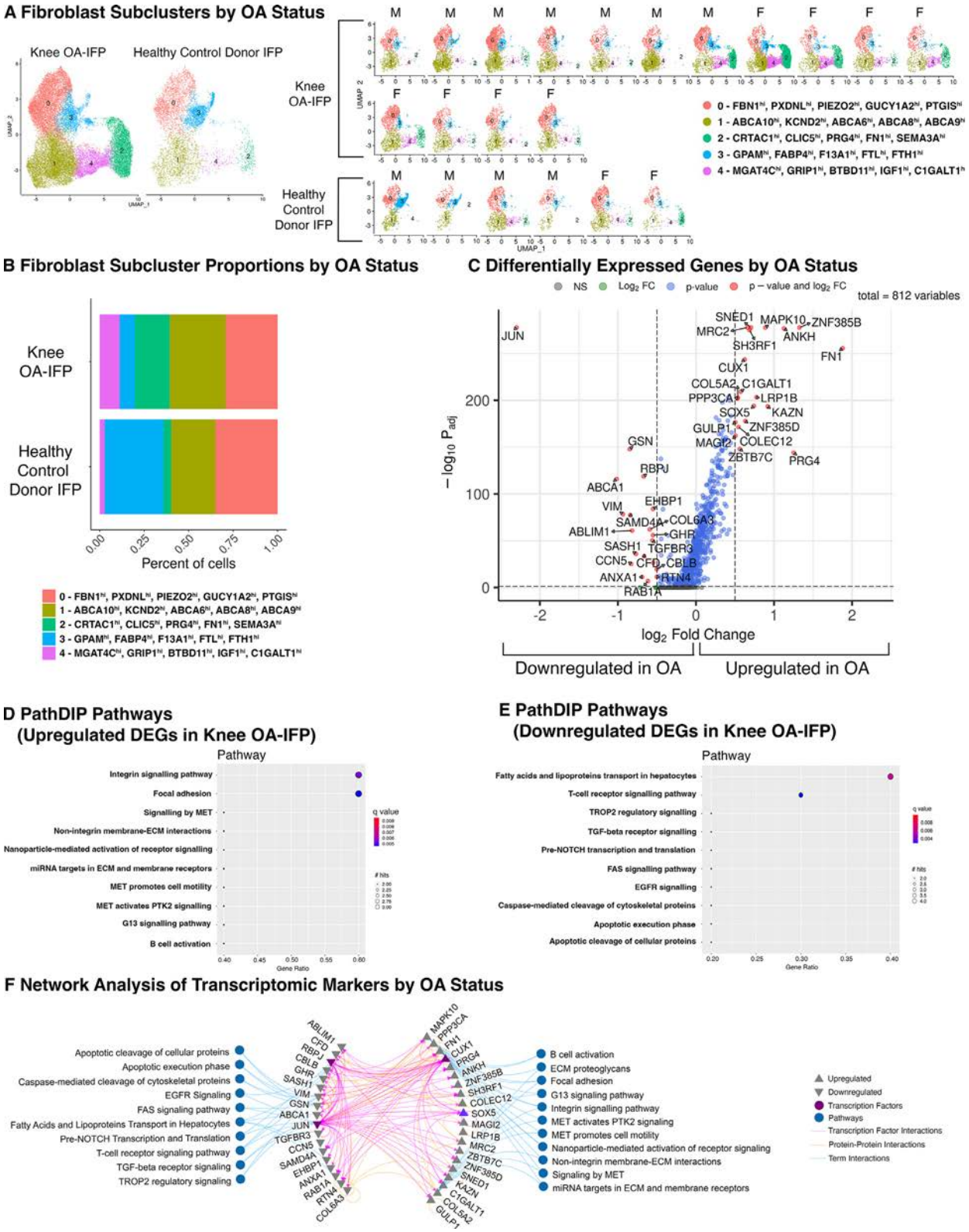

Figure 5. Differences in IFP fibroblast subclusters based on OA status. (A) UMAPs of fibroblast subclusters within n = 21 IFPs split by disease state (n = 15 KOA-IFPs, n = 6 healthy control donor IFPs). UMAPs of fibroblast subclusters within each of the n = 21 IFPs. 15 IFPs (top) have KOA while 6 (bottom) are healthy control donor IFPs. (B) Stacked bar plot displaying the proportion of fibroblast subclusters within KOA-IFPs compared to healthy control donor IFPs. Fibroblast subcluster 3 had significantly more nuclei contributed from healthy control donor IFPs compared to KOA-IFPs ($q = 0.032$). Fibroblast subcluster proportions were analysed by arcsin-transformation of the absolute proportions across all samples and performing multiple unpaired t-tests with false discovery rate (FDR) correction using the Benjamini, Krieger and Yekutieli two stage step up method. Top five DEGs within each cluster are indicated. (C) Volcano plot showing the log2 fold change (FC) of DEGs in KOA-IFPs compared to healthy control donor IFPs. DEGs were defined by a minimum of 50% of nuclei expressing a marker, genes with a log2FC>0.5, $q<0.05$ are upregulated while genes with a log2FC<−0.5, $q<0.05$ are downregulated. (D) Enriched PathDIP pathways associated with the upregulated DEGs from KOA-IFPs compared to healthy control donor IFPs. (E) Enriched PathDIP pathways associated with the downregulated DEGs from KOA-IFPs compared to healthy control donor IFPs. (F) Interaction network showing protein−protein interactions and transcription factor-gene interactions with enriched pathDIP pathways linked to DEGs (see online supplemental table 4A-C and online supplemental figure 19). DEGs, differentially expressed gene; IFP, infrapatellar fat pad; KOA, knee osteoarthritis; UMAP, uniform manifold approximation and projection.

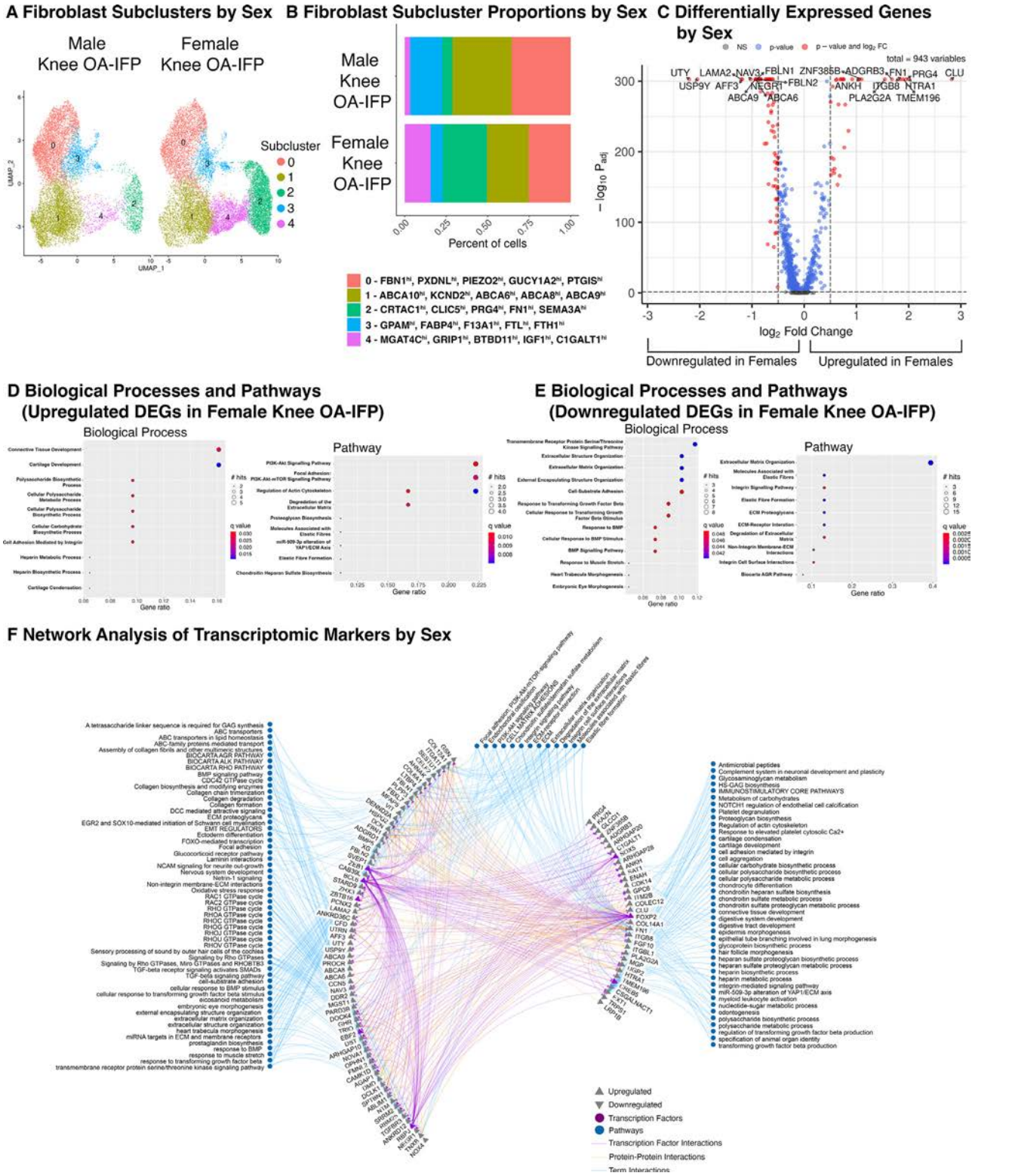

Figure 6. Differences in KOA-IFP fibroblast subclusters based on sex. (A) UMAPs of fibroblast subclusters within n = 15 KOA-IFPs split by sex (n = 8 female KOA-IFPs, n = 7 male KOA-IFPs). (B) Stacked bar plot displaying the proportion of fibroblast subclusters within female KOA-IFPs compared to male KOA-IFPs. No significant differences were found in proportions of nuclei contributed to subclusters from KOA-IFPs from female versus male study participants ($q<0.05$). Fibroblast subcluster proportions were analysed by arcsin-transformation of the absolute proportions across all samples and performing multiple unpaired t-tests with FDR correction using the Benjamini, Krieger and Yekutieli two stage step up method. Top five DEGs within each cluster are indicated. (C) Volcano plot showing the log2 fold change (FC) of DEGs in female KOA-IFP samples compared to male KOA-IFP samples. DEGs were defined by a minimum of 50% of nuclei expressing a marker, genes with a log2FC>0.5, $q<0.05$ are upregulated while genes with a log2FC<−0.5, $q<0.05$ are downregulated. (D) Gene Ontology (GO) biological processes and pathDIP pathways enriched in the upregulated genes of female compared to male KOA-IFPs. (E) GO biological processes and pathDIP pathways enriched for the downregulated genes within female compared to male KOA-IFPs. (F) Interaction network showing protein−protein interactions and transcription factor−gene interactions with enriched biological processes or pathDIP pathways linked to DEGs (see online supplemental figure 20 and online supplemental file 5A-E). DEGs, differentially expressed genes; FDR, false discovery rate; KOA, knee osteoarthritis; IFP, infrapatellar fat pad; UMAP, uniform manifold approximation and projection.

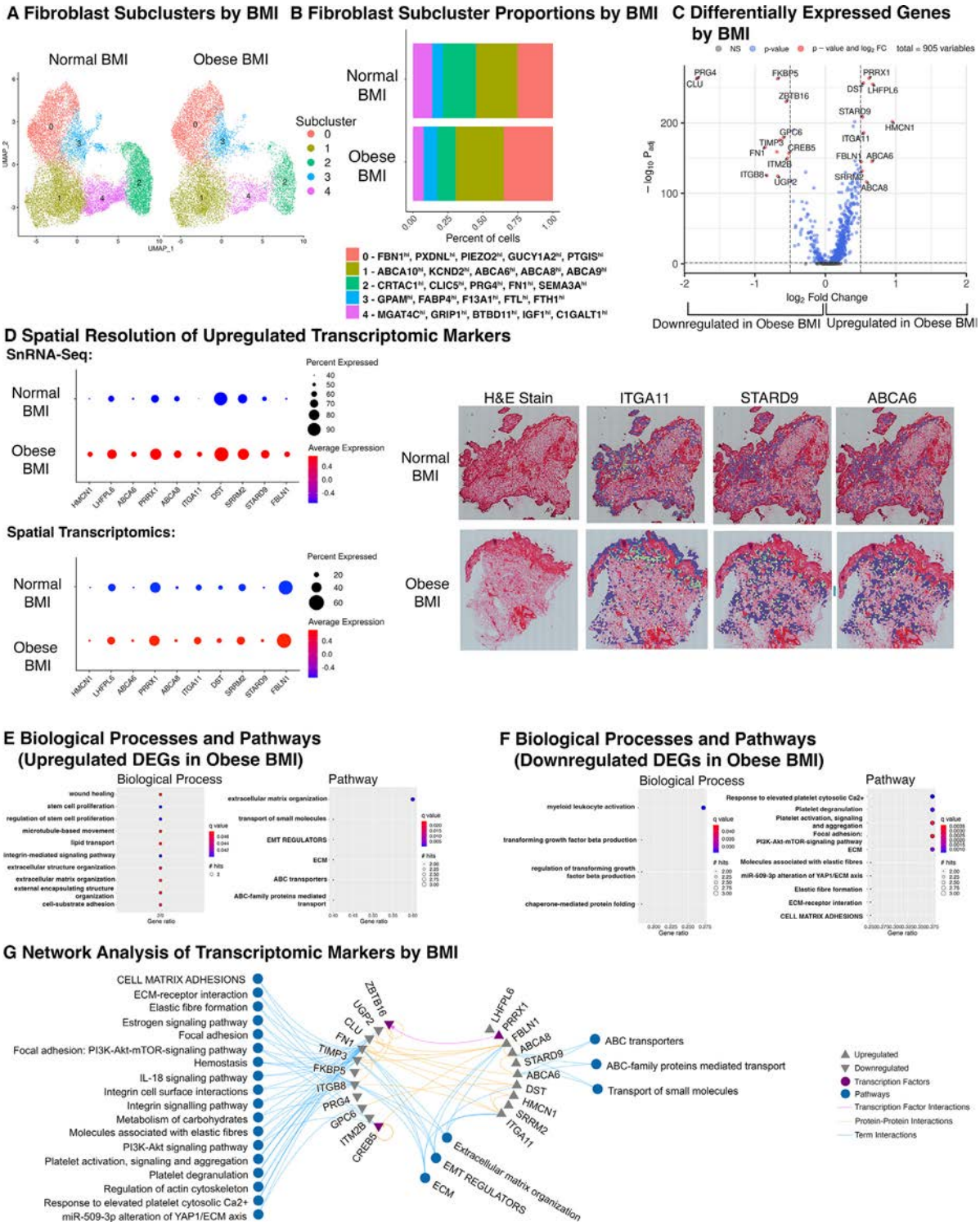

Figure 7. Differences in KOA-IFP fibroblast subclusters based on obesity status. (A) UMAPs of fibroblast subclusters within n = 15 KOA-IFPs, split by obesity status (n = 7 normal BMI KOA-IFPs (18.5–25 kg/m^2), n = 8 obese BMI KOA-IFPs (30–40 kg/m^2)). (B) Stacked bar plot displaying the proportion of fibroblast subclusters within obese BMI KOA-IFPs compared to normal BMI KOA-IFPs. No significant differences were found in proportions of nuclei contributed to subclusters from KOA-IFPs from obese versus normal BMI study participants (q<0.05). Fibroblast subcluster proportions were analysed by arcsin-transformation of the absolute proportions across all samples and performing multiple unpaired t-tests with FDR correction using the Benjamini, Krieger and Yekutieli two stage step up method. Top five DEGs within each cluster are indicated. (C) Volcano plot showing the log2 fold change (FC) of genes that are uniquely differentially expressed in obese BMI compared to normal BMI KOA-IFPs. DEGs were defined by a minimum of 50% of nuclei expressing a marker, genes with a log2FC>0.5, q<0.05 are upregulated while genes with a log2FC<−0.5, q<0.05 are downregulated. (D) Dot plot (left) with average expression and percent of population expressing each DEG based on obesity status identified in snRNA-seq data (top) and within spatial sequencing data (bottom). Spatial resolution (right) of DEGs significantly upregulated within obese BMI compared to normal BMI KOA-IFPs in both snRNA-seq and spatial sequencing, visualised within spatial sequencing data. (E) GO biological processes and pathDIP pathways enriched for the upregulated genes from obese BMI compared to normal BMI KOA-IFP samples. (F) GO biological processes and pathDIP pathways enriched for downregulated genes from obese compared to normal BMI KOA-IFP samples. (G) Interaction network showing protein−protein interactions and transcription factor-gene interactions with enriched biological processes or pathDIP pathways linked to DEGs (see online supplemental figure 21, online supplemental table 6A-F). BMI, body mass index; DEGs, differentially expressed genes; ECM, extracellular matrix; FDR, false discovery rate; GO, gene ontology; KOA, knee osteoarthritis; IFP, infrapatellar fat pad; snRNA-seq, single-nucleus RNA sequencing; UMAP, uniform manifold approximation and projection.

in culture supernatants of obese versus normal BMI KOA-IFP fibroblasts were modified when stimulated by TGF-β or TNF-α, compared to stimulation by vehicle control (phosphate-buffered saline). When comparing fibroblast cultures from obese versus normal BMI KOA-IFPs, nine metabolites were significantly differentially detected ($p<0.05$) in response to TGF-β treatment, compared to vehicle control (figure 8C; online supplemental table 7B). Mean levels of homocitrulline, ethanolamine, C16:1OH (2-hydroxypalmitoleylcarnitine), TG (52:5) and Hex2Cer (34:1) (di-hexosyl ceramide) were increased by TGF-β-treated fibroblasts from obese BMI KOA-IFPs versus vehicle control and decreased in normal BMI KOA-IFPs. In contrast, mean levels of cholesteryl esters (17:0) and (20:1), alpha-ketoglutaric acid and phosphatidylcholine diacyl (PCaa) C26:0 were increased in TGF-β-treated fibroblast cultures from normal BMI KOA-IFPs and decreased in obese BMI KOA-IFPs (figure 8C; online supplemental table 7B). Pathway enrichment analysis identified enriched metabolism and neuron-related pathways associated with the differentially secreted metabolite signature by BMI after profibrotic TGF-β stimulation (figure 8E).

Additionally, when comparing fibroblast cultures from obese versus normal BMI KOA-IFPs treated with TNF-α, levels of 10 metabolites were significantly differentially detected ($p<0.05$) compared to vehicle control (figure 8D; online supplemental table 7C). Mean levels of serotonin, 3-hydroxybutyric acid, 3-hydroxyisobutyric acid, glutaric acid, TGs (54:7) and (52:5) and N-acetyl-glycine were increased in TNF-α-treated fibroblast cultures from obese BMI KOA-IFPs and decreased in normal BMI KOA-IFPs (figure 8D; online supplemental table 7C). In contrast, mean levels of sphingomyelins C24:0, C16:0 and C16:1 were increased in TNF-α-treated normal BMI KOA-IFPs and decreased in obese BMI KOA-IFPs (figure 8D; online supplemental table 7C). Pathway enrichment analysis identified a single enriched pathway, cAMP signalling, associated with the differentially secreted metabolite signature from fibroblasts by obesity status with proinflammatory TNF-α stimulation (figure 8E). Overall, these data show differential metabolite levels in supernatants of fibroblasts from obese compared to normal BMI KOA-IFPs under normal conditions and in response to profibrotic and proinflammatory stimuli, with enrichment for metabolism and/or neuronal-related pathways.

DISCUSSION

Here, we generated a transcriptomic map of the IFP, identifying and spatially resolving major cell types and subtypes using snRNA-seq, spatial transcriptomics and advanced bioinformatic analyses. We revealed that each cell type subcluster had a unique transcriptomic profile. Furthermore, we identified transcriptomic differences within IFP fibroblasts based on KOA, sex and obesity status, and metabolic alterations based on obesity status. To our knowledge, our study is the first comprehensive, tissue-specific, patient-matched transcriptomic map of the IFP, including transcriptomic analyses for KOA, sex and obesity status and using spatial transcriptomics to localise major cell populations, subclusters and transcriptomic profiles.

Similar fibroblast populations have been previously identified. A recent study investigated combined synovium and IFP tissues, identifying four fibroblast subclusters [7], in line with those we identified within IFP only. Additionally, when comparing subclusters of macrophages, adipocytes and endothelial cells identified in the IFP within our study, similar populations have been observed in other adipose tissue sources [13]. Thus, it is likely that the IFP is another white adipose depot with similar composition to those previously described.

Within combined synovium and IFP analysis of mouse models, in silico analyses and lineage tracing have established that DPP4+/PI16+ fibroblast cells can differentiate into mature fibroblasts of the synovium and adipocytes within the IFP [30–32]. Additionally, trajectory analysis of both human synovium and IFP suggests that DPP4+ cells can differentiate into adipocytes of the IFP and mature fibroblasts of the synovium [7]. Our trajectory analysis also defined that IFP fibroblasts expressing universal markers (DPP4+PI16+CD34+) are likely precursors for other fibroblast subclusters and adipocytes, suggesting that fibroblasts residing in the IFP have the capacity to promote IFP-related OA pathologies through differentiation.

By employing CellChat, we determined putative communications between major cell types identified within the IFP. CD44 and ITGAV/IGTB8 receptors on fibroblasts had the highest proportion of communications with other major cell types, with this signalling retained when comparing KOA-IFPs to healthy donor control IFPs. Interestingly, CD44 binds fibronectin and collagen while ITGAV/ITGB8 binds fibronectin [33,34]. We found that fibronectin ligands were expressed by macrophages and endothelial cells, while all major cell types were involved in the collagen signalling pathway (figure 4A,C). This may indicate an overexpression of collagen and fibronectin as ligands from macrophages, adipocytes and endothelial cells resulting in modification of fibroblast activity through CD44 and integrins.

After establishing transcriptomic profiles of fibroblast subclusters, we revealed transcriptomic differences based on KOA, sex and obesity status, with some DEGs being important transcription factors related to fibrosis, cell proliferation, differentiation, senescence, inflammation and ECM composition, mechanisms typically associated with joint homeostasis or KOA pathogenesis [35–47]. Interestingly, some upregulated and downregulated transcription factors were found to putatively interact, a regulatory mechanism likely influencing gene expression based on KOA, sex or obesity status. Of note, the transcription factor CREB5 directly regulates the expression of lubricin, important for joint lubrication and encoded by PRG4 [40]. In female versus male KOA-IFPs, CREB5 was upregulated, as was PRG4, suggesting that lubrication mechanisms in fibroblasts may be enhanced in females. In obese versus normal BMI KOA-IFPs, CREB5 and PRG4 were downregulated, suggesting that joint lubricating mechanisms by IFP fibroblasts may be reduced in obese OA individuals. When comparing KOA-IFPs versus healthy control donor IFPs, DEG-associated enriched pathways were related to cell adhesion and signalling pathways, indicating that these pathways may be linked to KOA-related functions of fibroblasts. Additionally, our data showed DEG-associated enrichment for biological processes and pathways related to ECM, connective tissue and metabolism-associated processes when comparing KOA-IFPs by sex and obesity status, suggesting that these pathways may be differentially regulated in females versus males and obese BMI versus normal BMI KOA-IFPs, which requires further investigation. Overall, KOA, sex and obesity status likely impact gene expression in fibroblasts, in part through modifications of transcription factor expression, impacting overall joint biology.

While investigating DEGs of fibroblasts from obese compared to normal BMI KOA-IFPs, metabolism-related pathways were enriched (figure 7G). Differentially secreted metabolites identified from fibroblasts based on obesity status have been linked to various cellular and physiological mechanisms including lipid transport, metabolism, inflammation and pain [48–51].

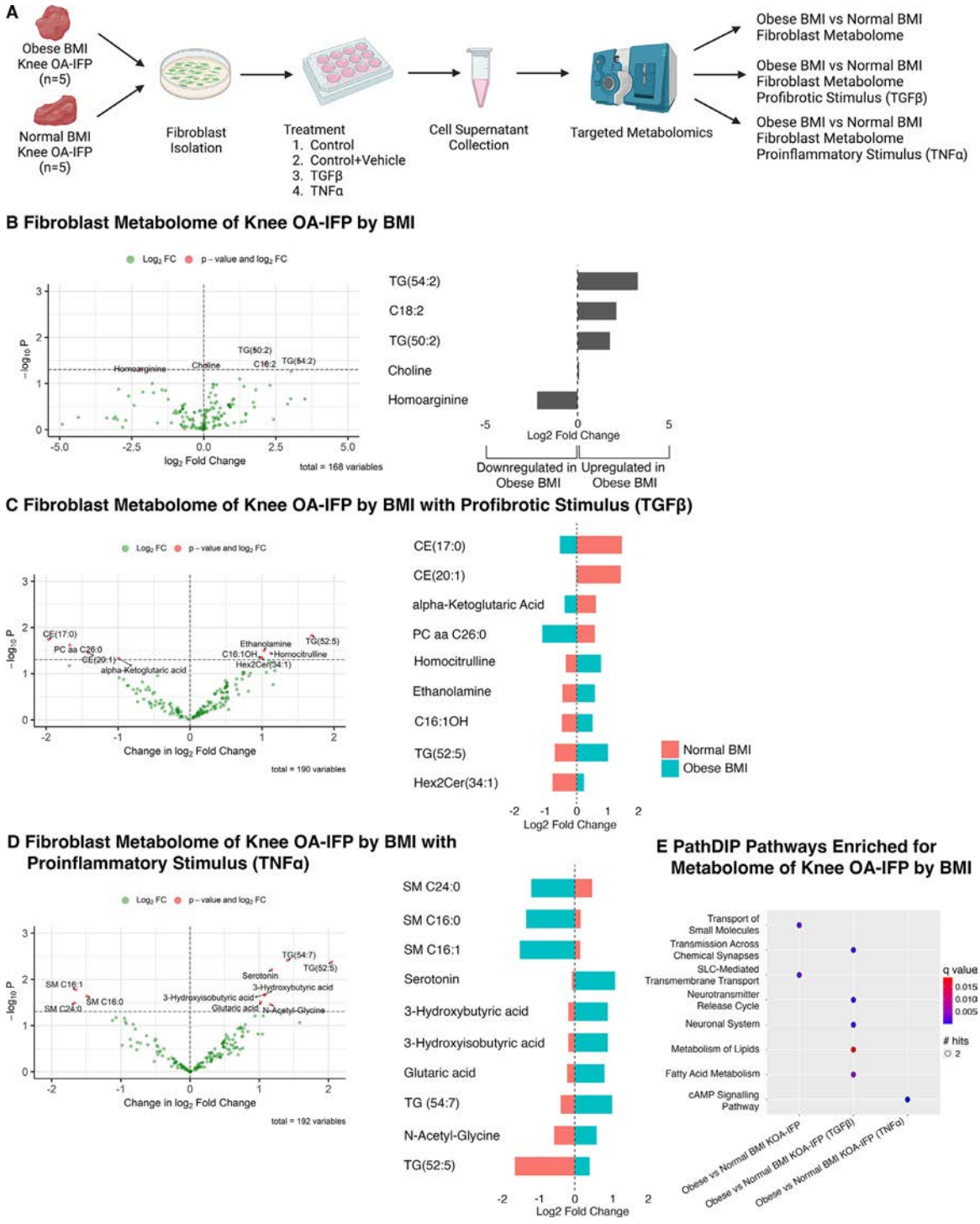

Figure 8. Differences in metabolite secretome in fibroblasts from KOA-IFPs based on obesity status. (A) Schematic workflow to identify differences in the metabolite levels within supernatants of fibroblast cultures of obese compared to normal BMI KOA-IFPs, stimulated with or without profibrotic or proinflammatory stimulus (created with BioRender.com). (B) Violin plot (left) and bar plot (right) showing the log2 fold change (FC) of metabolites differentially found in supernatants of fibroblast cultures from obese compared to normal BMI KOA-IFPs. Positive log2FC indicates an increase in the metabolite level within supernatants of cultures from obese compared to normal BMI KOA-IFP fibroblasts. (C) Volcano plot (left) showing the change in log2FC of metabolites differentially found in supernatants of obese compared to normal BMI KOA-IFP fibroblast cultures when treated with TGF-β compared to vehicle control. Positive values indicate a greater upregulation of metabolite level in obese versus normal BMI KOA-IFP fibroblast culture supernatants when treated with TGF-β versus vehicle control. Bar plot (right) showing the log2FC of metabolites differentially found in supernatants of obese compared to normal BMI KOA-IFP fibroblast cultures when treated with TGF-β compared to vehicle control, with positive values indicating an upregulation in levels found in supernatant. (D) Volcano plot (left) showing the change in Log2FC of metabolites differentially found in supernatants of obese compared to normal BMI KOA-IFP fibroblast cultures when treated with TNF-α compared to vehicle control. Positive values indicate a greater upregulation of a metabolite level in obese versus normal BMI KOA-IFP fibroblast culture supernatants when treated with TNF-α versus vehicle control. Bar plot (right) showing the log2FC of metabolites differentially found in supernatants of obese compared to normal BMI KOA-IFP fibroblast cultures treated with TNF-α compared to vehicle control, with positive values indicating an upregulation in secretion. Please refer to C for the legend. (E) Dot plot displaying pathways enriched for the differentially secreted metabolites by fibroblasts from obese compared to normal BMI KOA-IFPs and after treated with TGF-β versus vehicle control or TNF-α versus vehicle control (see online supplemental figure 22, online supplemental table 7A-C). BMI, body mass index; KOA, knee osteoarthritis; IFP, infrapatellar fat pad; TG, triglycerides; TGF-β, transforming growth factor β; TNF-α, tumour necrosis factor α.

Additionally, metabolite level changes in response to profibrotic and proinflammatory stimuli, and associated enriched pathways, indicate that fibroblasts from obese BMI KOA-IFPs may promote inflammation, fibrosis, pain and dysregulated metabolism, as compared to fibroblasts from normal BMI KOA-IFPs, based on previously published reports [52–59]. Further investigations to identify differences in the functions of fibroblasts and other major KOA-IFP cell types in KOA pathogenesis based on obesity status should be considered.

One limitation of this study may be that we analysed IFPs from n = 21 study participants, which could be considered a small sample size. However, given the current literature available, the multiomic technologies used and the total number of nuclei sequenced, our sample size is large in context. It is also notable that age and BMI groups were not significantly associated in our dataset, nor were sex and BMI, suggesting unlikely confounding effects of age and sex on our results (online supplemental table 1). Since the age range of the study participants in our KOA cohort for snRNA-seq is relatively small, ranging from 50 to 64, analysing the impact of age on the KOA-IFP was not feasible in the current study. However, future studies should be directed towards understanding how age impacts the transcriptomic and cellular diversity of the IFP during KOA. Considering the IFP is a highly innervated tissue, it was surprising that we did not identify Schwann cells in our sequencing dataset. Thus, future studies should use alternative methods to attempt to identify these cells and the contribution of neuronal populations to the IFP. While this study used flow cytometry to identify cell surface markers associated with the major fibroblast subclusters (0, 1 and 2), future studies should focus on the detection of the other fibroblast subclusters and additional major cell types within the IFP tissue, which was beyond the scope of the current study. Furthermore, future investigations should also focus on understanding the transcriptomic differences of other major cell types, including macrophages, adipocytes and endothelial cells, within the IFP, with consideration for sex and obesity status.

This study has used snRNA-seq, spatial transcriptomics and advanced bioinformatic approaches to generate comprehensive transcriptomic and spatial profiles of the human IFP. By applying these high throughput methods, we identified unique transcriptomic profiles of major cell populations and subtypes present within the IFP, including fibroblasts, macrophages, adipocytes and endothelial cells. We identified fibroblasts expressing universal markers that may contribute to both other fibroblast populations and differentiated adipocytes. We revealed putative cell–cell communications between fibroblasts and all other major cell types within the IFP and based on OA status. Furthermore, we identified transcriptomic differences within fibroblasts of the IFP based on OA, sex and obesity status, and metabolic alterations based on obesity status using metabolomics. Thus, our data suggest that IFP fibroblasts are likely major contributors to IFP biology and play a role in OA pathology through transcriptional, metabolic and cell differentiation mechanisms influenced, in part, by KOA, sex and obesity status. Overall, this study provides a comprehensive map of the cellular and transcriptomic diversity of the human IFP using a multiomic approach.

Correction notice

This article has been corrected since it published Online First. Figures have been replaced for clarity.

Acknowledgments

This work is supported by the Arthritis Society of Canada Strategic Operating Grant (23-0000000271), Canada Research Chairs Program (CRC# 1019359), Tony and Shari Fell Platinum Chair in Arthritis Research (University Health Network Foundation, University Health Network, Toronto). IJ was supported in part by funding from Natural Sciences Research Council (NSERC #203475), Canada Foundation for Innovation (CFI #225404, #30865), and Ontario Research Fund (RDI #34876, RE010-020). Thank you to the Schroeder Arthritis Institute Orthopaedic Research Team for consenting and collecting study participant data. We thank Edwin Speck from Princess Margaret Flow Cytometry (https://pmflow.ca), University Health Network for their assistance in FACS cell sorting. Thank you to Melanie Peralta from the Pathology Research Program within University Health Network's Laboratory Medicine Program–Pathology Department for their assistance with the OCT-embedded samples. We would also like to thank Farzaneh Aboualizadeh from the Princess Margaret Genomics Center, University Health Network, for their assistance with spatial sequencing within this study.

Contributors

HP contributed to study design, selection study participants for IFP samples, acquisition of data, interpreting of all analyses, fibroblast culture experiments and writing of the manuscript and generation of figures. PP contributed to the analysis and interpretation of single-nucleus RNA sequencing data, CellChat analysis and generation of associated figures. JSR contributed to the analysis and interpretation of all experiments and the acquisition of funding for this study. TT contributed to the analysis and interpretation of spatial sequencing data and generation of associated figures. CP and IJ contributed to all GO biological process and pathway enrichment analysis, protein interaction and TF-target networks, and generation of associated figures. KDS contributed to tissue preparations and the completion of single-nuclei RNA sequencing experiments and data analysis. SV has contributed to the analysis pipeline used for single-nucleus RNA sequencing data, the completion of trajectory analysis and generation of associated figures. NF contributed to the completion of flow cytometry, cell experiments and data analysis. SL contributed to study design and the experimental pipeline used for single-nucleus RNA sequencing. KP contributed to the acquisition and storage of all KOA-IFP samples and clinical data through the Schroeder Arthritis Institute Orthopaedics Biobank. NL, SHL and VC contributed to the completion of all targeted metabolomics experiments. KH contributed to the analysis and interpretation of all targeted metabolomics experiments and generation of associated figures. PK contributed to fibroblast culture experiments. AVP and RR contributed to collection and interpretation of data from LEAP OA clinical database. NNM and KS contributed to the collection of KOA-IFP samples and data collection. EG contributed to data interpretation. RK contributed to the collection of healthy control donor IFP samples and data analysis. MBB contributed to the study planning and interpretation of cell population mapping using previously published literature. RG contributed to the conception and acquisition of funding for this study, the acquisition of KOA-IFPs, and interpretation of the data. MK designed the original study design, contributed to the conception and acquisition of funding for this study, directed the entire study and was involved in the interpretation of all experiments. All authors have contributed

significantly to the critical revision of the manuscript and approved the final version of the manuscript. MK is the author responsible for the overall content as the guarantor.

Funding

This study was funded by the Arthritis Society of Canada Strategic Operating Grant (23-0000000271), Canada Research Chairs Program (CRC#1019359), Tony and Shari Fell Platinum Chair in Arthritis Research (University Health Network Foundation, University Health Network, Toronto) (N/A), Canada Foundation for Innovation (225404, 30865), Natural Sciences Research Council (203475) and Ontario Research Fund (34876, RE010-020).

Competing interests

None declared.

Patient and public involvement

Patients and/or the public were not involved in the design, or conduct, or reporting, or dissemination plans of this research.

Patient consent for publication

Not applicable.

Ethics approval

This study involves human participants and was approved by University Health Network Research Ethics Board: REB #07-0383, #14-7592, #21987. Participants gave informed consent to participate in the study before taking part.

Data availability statement

Data are available in a public, open access repository. SnRNAseq and spatial sequencing data were submitted to GEO data repository with a superseries GEO accession ID: GSE253200.

Supplementary materials

Supplementary material associated with this article can be found in the online version at doi:10.1136/ard-2024-225928.

REFERENCES

[1] Steinmetz JD, Culbreth GT, Haile LM, et al. Global, regional, and national burden of osteoarthritis, 1990–2020 and projections to 2050: a systematic analysis for the Global Burden of Disease Study 2021. Lancet Rheumatol 2023;5:e508–22. doi: 10.1016/S2665-9913(23)00163-7.

[2] Katz JN, Arant KR, Loeser RF. Diagnosis and Treatment of Hip and Knee Osteoarthritis: A Review. JAMA 2021;325:568–78. doi: 10.1001/jama.2020.22171.

[3] Jang S, Lee K, Ju JH. Recent Updates of Diagnosis, Pathophysiology, and Treatment on Osteoarthritis of the Knee. Int J Mol Sci 2021;22:2619. doi: 10.3390/ijms22052619.

[4] Jiang LF, Fang JH, Wu LD. Role of infrapatellar fat pad in pathological process of knee osteoarthritis: Future applications in treatment. World J Clin Cases 2019;7:2134–42. doi: 10.12998/wjcc.v7.i16.2134.

[5] Mantripragada VP, Piuzzi NS, Bova WA, et al. Donor-matched comparison of chondrogenic progenitors resident in human infrapatellar fat pad, synovium, and periosteum - implications for cartilage repair. Connect Tissue Res 2019;60:597–610. doi: 10.1080/03008207.2019.1611795.

[6] Favero M, El-Hadi H, Belluzzi E, et al. Infrapatellar fat pad features in osteoarthritis: a histopathological and molecular study. Rheumatology (Oxford) 2017;56:1784–93. doi: 10.1093/rheumatology/kex287.

[7] Tang S, Yao L, Ruan J, et al. Single-cell atlas of human infrapatellar fat pad and synovium implicates APOE signaling in osteoarthritis pathology. Sci Transl Med 2024;16:eadf4590. doi: 10.1126/scitranslmed.adf4590.

[8] Wang T, He C. Pro-inflammatory cytokines: The link between obesity and osteoarthritis. Cytokine Growth Factor Rev 2018;44:38–50. doi: 10.1016/j.cytogfr.2018.10.002.

[9] Tschon M, Contartese D, Pagani S, et al. Gender and Sex Are Key Determinants in Osteoarthritis Not Only Confounding Variables. A Systematic Review of Clinical Data. J Clin Med 2021;10:3178. doi: 10.3390/jcm10143178.

[10] Afzali MF, Sykes MM, Burton LH, et al. Removal of the infrapatellar fat pad and associated synovium benefits female guinea pigs in the Dunkin Hartley model of idiopathic osteoarthritis. Ann Transl Med 2024;12:43. doi: 10.21037/atm-23-1886.

[11] Peters H, Potla P, Rockel JS, et al. Cell and transcriptomic diversity of infrapatellar fat pad during knee osteoarthritis. NCBI GEO database. Available: https://www.ncbi.nlm.nih.gov/geo/query/acc.cgi?acc=GSE253198; 2024.

[12] Saelens W, Cannoodt R, Todorov H, et al. A comparison of single-cell trajectory inference methods. Nat Biotechnol 2019;37:547–54. doi: 10.1038/s41587-019-0071-9.

[13] Emont MP, Jacobs C, Essene AL, et al. A single-cell atlas of human and mouse white adipose tissue. Nature 2022;603:926–33. doi: 10.1038/s41586-022-04518-2.

[14] Merrick D, Sakers A, Irgebay Z, et al. Identification of a mesenchymal progenitor cell hierarchy in adipose tissue. Science 2019;364:eaav2501. doi: 10.1126/science.aav2501.

[15] Hepler C, Shan B, Zhang Q, et al. Identification of functionally distinct fibro-inflammatory and adipogenic stromal subpopulations in visceral adipose tissue of adult mice. Elife 2018;7:e39636. doi: 10.7554/eLife.39636.

[16] Buechler MB, Pradhan RN, Krishnamurty AT, et al. Cross-tissue organization of the fibroblast lineage. Nature 2021;593:575–9. doi: 10.1038/s41586-021-03549-5.

[17] Peters H, Potla P, Rockel JS, et al. Cell and transcriptomic diversity of infrapatellar fat pad during knee osteoarthritis. NCBI GEO database. Available: https://www.ncbi.nlm.nih.gov/geo/query/acc.cgi?acc=GSE253199; 2024.

[18] Liu N, Martin J, Bhuva DD, et al. HoodscanR: profiling single-cell neighborhoods in spatial transcriptomics data. bioRxiv. Available: https://www.biorxiv.org/content/10.1101/2024.03.26.586902v1; 2024.

[19] Jin S, Plikus MV, Nie Q. CellChat for systematic analysis of cell-cell communication from single-cell and spatially resolved transcriptomics. bioRxiv. Available: https://www.biorxiv.org/content/10.1101/2023.11.05.565674v1; 2023.

[20] Oike Y, Yasunaga K, Suda T. Angiopoietin-related/angiopoietin-like proteins regulate angiogenesis. Int J Hematol 2004;80:21–8. doi: 10.1532/ijh97.04034.

[21] Elango J, Hou C, Bao B, et al. The Molecular Interaction of Collagen with Cell Receptors for Biological Function. Polymers (Basel) 2022;14:876. doi: 10.3390/polym14050876.

[22] Beer HD, Longaker MT, Werner S. Reduced expression of PDGF and PDGF receptors during impaired wound healing. J Invest Dermatol 1997;109:132–8. doi: 10.1111/1523-1747.ep12319188.

[23] DeLisser HM, Christofidou-Solomidou M, Strieter RM, et al. Involvement of endothelial PECAM-1/CD31 in angiogenesis. Am J Pathol 1997;151:671–7.

[24] Pastrello C, Kotlyar M, Abovsky M, et al. PathDIP 5: improving coverage and making enrichment analysis more biologically meaningful. Nucleic Acids Res 2024;52:D663–71. doi: 10.1093/nar/gkad1027.

[25] Wu T, Hu E, Xu S, et al. clusterProfiler 4.0: A universal enrichment tool for interpreting omics data. Innov Camb 2021;2:100141. doi: 10.1016/j.xinn.2021.100141.

[26] Fava R, Olsen N, Keski-Oja J, et al. Active and latent forms of transforming growth factor beta activity in synovial effusions. J Exp Med 1989;169:291–6. doi: 10.1084/jem.169.1.291.

[27] van Beuningen HM, Glansbeek HL, van der Kraan PM, et al. Differential effects of local application of BMP-2 or TGF-β1 on both articular cartilage composition and osteophyte formation. Osteoarthr Cartil 1998;6:306–17. doi: 10.1053/joca.1998.0129.

[28] Benito MJ, Veale DJ, FitzGerald O, et al. Synovial tissue inflammation in early and late osteoarthritis. Ann Rheum Dis 2005;64:1263–7. doi: 10.1136/ard.2004.025270.

[29] Orita S, Koshi T, Mitsuka T, et al. Associations between proinflammatory cytokines in the synovial fluid and radiographic grading and pain-related scores in 47 consecutive patients with osteoarthritis of the knee. BMC Musculoskelet Disord 2011;12:144. doi: 10.1186/1471-2474-12-144.

[30] Li J, Gui T, Yao L, et al. Synovium and infrapatellar fat pad share common mesenchymal progenitors and undergo coordinated changes in osteoarthritis. J Bone Miner Res 2024;39:161–76. doi: 10.1093/jbmr/zjad009.

[31] Knights AJ, Farrell EC, Ellis OM, et al. Synovial fibroblasts assume distinct functional identities and secrete R-spondin 2 in osteoarthritis. Ann Rheum Dis 2023;82:272–82. doi: 10.1136/ard-2022-222773.
[32] Collins FL, Roelofs AJ, Symons RA, et al. Taxonomy of fibroblasts and progenitors in the synovial joint at single-cell resolution. Ann Rheum Dis 2023;82:428–37. doi: 10.1136/ard-2021-221682.
[33] Govindaraju P, Todd L, Shetye S, et al. CD44-dependent inflammation, fibrogenesis, and collagenolysis regulates extracellular matrix remodeling and tensile strength during cutaneous wound healing. Matr Biol 2019;75–76:314–30. doi: 10.1016/j.matbio.2018.06.004.
[34] Moyle M, Napier MA, McLean JW. Cloning and expression of a divergent integrin subunit beta 8. J Biol Chem 1991;266:19650–8.
[35] Lizarraga G, Lichtler A, Upholt WB, et al. Studies on the role of Cux1 in regulation of the onset of joint formation in the developing limb. Dev Biol 2002;243:44–54. doi: 10.1006/dbio.2001.0559.
[36] Shi S, Wan F, Zhou Z, et al. Identification of key regulators responsible for dysregulated networks in osteoarthritis by large-scale expression analysis. J Orthop Surg Res 2021;16:259. doi: 10.1186/s13018-021-02402-9.
[37] Mirando AJ, Liu Z, Moore T, et al. RBP-Jκ-dependent Notch signaling is required for murine articular cartilage and joint maintenance. Arthritis Rheum 2013;65:2623–33. doi: 10.1002/art.38076.
[38] Konopka G, Bomar JM, Winden K, et al. Human-specific transcriptional regulation of CNS development genes by FOXP2. Nature 2009;462:213–7. doi: 10.1038/nature08549.
[39] Zwickl H, Niculescu-Morzsa E, Halbwirth F, et al. Correlation Analysis of SOX9, -5, and -6 as well as COL2A1 and Aggrecan Gene Expression of Collagen I Implant-Derived and Osteoarthritic Chondrocytes. Cartilage 2016;7:185–92. doi: 10.1177/1947603515615388.
[40] Zhang C-H, Gao Y, Jadhav U, et al. Creb5 establishes the competence for Prg4 expression in articular cartilage. Commun Biol 2021;4:332. doi: 10.1038/s42003-021-01857-0.
[41] Kieslinger M, Folberth S, Dobreva G, et al. EBF2 regulates osteoblast-dependent differentiation of osteoclasts. Dev Cell 2005;9:757–67. doi: 10.1016/j.devcel.2005.10.009.
[42] Swahn H, Li K, Duffy T, et al. Senescent cell population with ZEB1 transcription factor as its main regulator promotes osteoarthritis in cartilage and meniscus. Ann Rheum Dis 2023;82:403–15. doi: 10.1136/ard-2022-223227.
[43] Ai J, Zhao F, Zhou X. HMGA1 Aggravates Oxidative Stress Injury and Inflammatory Responses in IL-1β-Induced Primary Chondrocytes through the JMJD3/ZEB1 Axis. Int Arch Allergy Immunol 2023;184:279–90. doi: 10.1159/000526680.
[44] Xiong B, Chen L, Huang Y, et al. ZBTB16 eases lipopolysaccharide-elicited inflammation, apoptosis and degradation of extracellular matrix in chondrocytes during osteoarthritis by suppressing GRK2 transcription. Exp Ther Med 2023;25:276. doi: 10.3892/etm.2023.11975.
[45] Xu L, Wang Z, Wang G. Screening of Biomarkers Associated with Osteoarthritis Aging Genes and Immune Correlation Studies. Int J Gen Med 2024;17:205–24. doi: 10.2147/IJGM.S447035.
[46] Chen S, Tao J, Bae Y, et al. Notch gain of function inhibits chondrocyte differentiation via Rbpj-dependent suppression of Sox9. J Bone Miner Res 2013;28:649–59. doi: 10.1002/jbmr.1770.
[47] Dankel SN, Grytten E, Bjune J-I, et al. COL6A3 expression in adipose tissue cells is associated with levels of the homeobox transcription factor PRRX1. Sci Rep 2020;10:20164. doi: 10.1038/s41598-020-77406-2.
[48] Ramsden CE, Domenichiello AF, Yuan Z-X, et al. A systems approach for discovering linoleic acid derivatives that potentially mediate pain and itch. Sci Signal 2017;10:eaal5241. doi: 10.1126/scisignal.aal5241.
[49] Zhang N, Li Y, Feng Z. Inhibition effect of choline and parecoxib sodium on chronic constriction nerve injury-induced neuropathic pain in rats. BMC Anesthesiol 2023;23:22. doi: 10.1186/s12871-022-01913-0.
[50] Nitz K, Lacy M, Bianchini M, et al. The Amino Acid Homoarginine Inhibits Atherogenesis by Modulating T-Cell Function. Circ Res 2022;131:701–12. doi: 10.1161/CIRCRESAHA.122.321094.
[51] Wang Z, Nicholls SJ, Rodriguez ER, et al. Protein carbamylation links inflammation, smoking, uremia and atherogenesis. Nat Med 2007;13:1176–84. doi: 10.1038/nm1637.
[52] Dasgupta S, Ray SK. Diverse Biological Functions of Sphingolipids in the CNS: Ceramide and Sphingosine Regulate Myelination in Developing Brain but Stimulate Demyelination during Pathogenesis of Multiple Sclerosis. J Neurol Psychol 2017;5. doi: 10.13188/2332-3469.1000035.
[53] Xiang L, Wei J, Tian XY, et al. Comprehensive Analysis of Acylcarnitine Species in db/db Mouse Using a Novel Method of High-Resolution Parallel Reaction Monitoring Reveals Widespread Metabolic Dysfunction Induced by Diabetes. Anal Chem 2017;89:10368–75. doi: 10.1021/acs.analchem.7b02283.
[54] Mann DA, Oakley F. Serotonin paracrine signaling in tissue fibrosis. Biochim Biophys Acta 2013;1832:905–10. doi: 10.1016/j.bbadis.2012.09.009.
[55] Fu S-P, Li S-N, Wang J-F, et al. BHBA suppresses LPS-induced inflammation in BV-2 cells by inhibiting NF-κB activation. Mediators Inflamm 2014;2014:983401. doi: 10.1155/2014/983401.
[56] Nilsen MS, Jersin RÅ, Ulvik A, et al. 3-Hydroxyisobutyrate, A Strong Marker of Insulin Resistance in Type 2 Diabetes and Obesity That Modulates White and Brown Adipocyte Metabolism. Diabetes 2020;69:1903–16. doi: 10.2337/db19-1174.
[57] Ferreira G da C, Viegas CM, Schuck PF, et al. Glutaric acid administration impairs energy metabolism in midbrain and skeletal muscle of young rats. Neurochem Res 2005;30:1123–31. doi: 10.1007/s11064-005-7711-9.
[58] Su K-J, Chen X-Y, Gong R, et al. Systematic metabolomic studies identified adult adiposity biomarkers with acetylglycine associated with fat loss in vivo. Front Mol Biosci 2023;10:1166333. doi: 10.3389/fmolb.2023.1166333.
[59] Torretta E, Barbacini P, Al-Daghri NM, et al. Sphingolipids in Obesity and Correlated Co-Morbidities: The Contribution of Gender, Age and Environment. Int J Mol Sci 2019;20:5901. doi: 10.3390/ijms20235901.

Ann Rheum Dis 84 (2025) 368–369

Contents lists available at ScienceDirect

Annals of the Rheumatic Diseases

journal homepage: https://www.sciencedirect.com/journal/annals-of-the-rheumatic-diseases

Images in rheumatology

Mutilating arthropathy with skin nodules

Tsz On Lam, Edric Chi Ching Ip, Wendy Wan Hang Lau, Agnes Wai Sze Chan, Christina Man Tung Cheung, Joshua Jing Xi Li, Joanna Ka Man Ng, Lai-Shan Tam*

The Chinese University of Hong Kong Faculty of Medicine, Hong Kong, Hong Kong

Keywords:
Arthritis
Inflammation
Immune System Diseases

PRESENTATION

A 68-year-old woman attended the rheumatology clinic for hand polyarthralgia and deformity for over 1 year, together with weight loss of 10 kg in the past 6 months. On examination, there were no tender or swollen joints. There were deformities over multiple proximal interphalangeal (PIP) and distal interphalangeal (DIP) joints, as well as innumerable soft papulonodular skin lesions over her hands (figure 1A), arms and face. These lesions did not appear on the lower extremities. There was no mucosal lesion in the oral or anterior nasal cavity. These skin lesions also began 1 year ago, similar to the onset of joint symptoms. There was no psoriasiform rash. The radiograph of her hands (figure 1B) revealed bony erosions at multiple DIP joints, PIP joints, metacarpal and carpal bones. There was bone resorption at multiple phalanxes. Rheumatoid factor, anticyclic

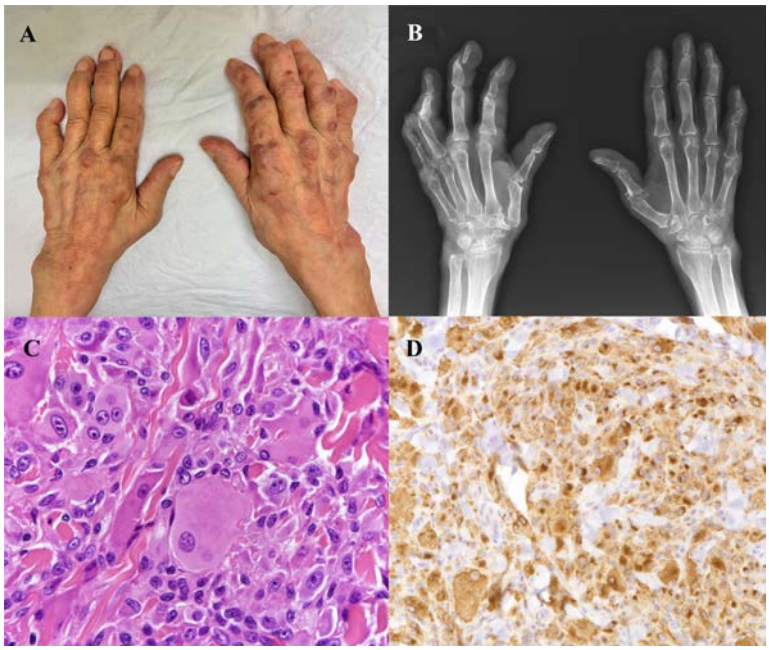

Figure 1. (A) Dorsal sides of the patient's hands, showing deformities at multiple interphalangeal joints, as well as innumerable erythematous papulonodular skin lesions. (B) Radiograph of the patient's hands, showing severe periarticular and marginal bone erosion, as well as resorption affecting phalanxes, metacarpal and carpal bones. (C) Histopathology photos of the skin nodule biopsy showing giant cells with abundant glassy cytoplasm on H&E staining. (D) Histopathology photos of the skin nodule biopsy showing positivity to CD 68, a histiocytic marker.

*Correspondence to Professor Lai-Shan Tam.
E-mail address: tamls_813@yahoo.com (L.-S. Tam).
Handling editor Josef S. Smolen.

https://doi.org/10.1136/ard-2024-226186
Received 30 May 2024; Accepted 27 July 2024

citrullinated peptide antibody and antinuclear antibody were negative. There was normocytic anaemia (haemoglobin 100 g/dL). The erythrocyte sedimentation rate was raised (80 mm/hour) but the C-reactive protein level was normal. A skin nodule was biopsied and the histological features are illustrated in figure 1C,D.

DISCUSSION

Biopsy confirmed the diagnosis of multicentric reticulohistiocytosis (MRH). MRH is a rare histiocytic disorder characterised by concurrent skin nodules and destructive arthropathy. Unlike rheumatoid arthritis, the DIP joints are typically affected in MRH. There were only approximately 300 cases of MRH reported worldwide. Patients tend to be female in their 50s [1]. A quarter of the patients have an underlying malignancy, but no particular type of malignancy is more prevalent in MRH [1]. A metastatic liposarcoma was subsequently found in our patient. She received prednisolone 30 mg daily from the rheumatology team for treatment of MRH. Due to the concurrent malignancy and chemotherapy, she did not receive any additional antirheumatic drugs for example, methotrexate or cyclophosphamide [2]. Her constitutional and cutaneous symptoms significantly improved afterwards. However, the phalangeal bone loss progressed and a dose of intravenous zoledronic acid was given [3]. Unfortunately, the liposarcoma progressed after failure of multiple lines of chemotherapy and the patient finally succumbed to tumour haemorrhage 6 months after the diagnosis.

Acknowledgments

We would like to thank our rheumatology nurse who first attended this patient at triage clinic and noticed the atypical presentation, so that timely diagnostic investigations could be arranged. We would also like to thank the patient and her family for trusting us in the management of this challenging disease.

Contributors

TOL and L-ST took the lead in writing this manuscript and patient management. ECCI, WWHL, AWSC and CMTC provided dermatological assessment and performed the skin biopsy. JJXL and JKMN performed the histological analysis and provided the histopathological photos and descriptions. L-ST is the guarantor.

Funding

The authors have not declared a specific grant for this research from any funding agency in the public, commercial or not-for-profit sectors.

Competing interests

None declared.

Patient and public involvement statement

The patient of this case participated in the consent to provision of her clinical information. There was no public involvement.

Ethics approval

This study involves human participants but it was exempted from the Joint Chinese University of Hong Kong-New Territories East Cluster Clinical Research Ethics Committee as it does not involve patient intervention or potential harm to patient. It is an anonymised descriptive report of the patient's clinical condition with the patient's full and written consent.

Data availability statement

Data are available on reasonable request.

REFERENCES

[1] Sanchez-Alvarez C, Sandhu AS, Crowson CS, et al. Multicentric reticulohistiocytosis: the mayo clinic experience (1980-2017). Rheumatology (Oxford) 2020;59:1898–905. doi: 10.1093/rheumatology/kez555.

[2] Liang GC, Granston AS. Complete remission of multicentric reticulohistiocytosis with combination therapy of steroid, cyclophosphamide, and low-dose pulse methotrexate. Case report, review of the literature, and proposal for treatment. Arthritis Rheum 1996;39:171–4. doi: 10.1002/art.1780390125.

[3] Goto H, Inaba M, Kobayashi K, et al. Successful treatment of multicentric reticulohistiocytosis with alendronate: evidence for a direct effect of bisphosphonate on histiocytes. Arthritis Rheum 2003;48:3538–41. doi: 10.1002/art.11362.

Ann Rheum Dis 84 (2025) 370–372

Contents lists available at ScienceDirect

Annals of the Rheumatic Diseases

journal homepage: https://www.sciencedirect.com/journal/annals-of-the-rheumatic-diseases

Letter

CD-19 CAR-T cells for polyrefractory rheumatoid arthritis

'Poly-refractory' disease affects 2.7% of patients with rheuma- toid arthritis (RA) who have failed different groups of biologic disease-modifying antirheumatic drugs (b-DMARDS) and targeted synthetic DMARDs (ts-DMARDS) [1]. Recently, chimeric antigen receptor T-cell (CAR-T) therapy has emerged as a prom- ising approach in autoimmune diseases [2].

We present a 39-year-old woman with erosive seropositive RA who had failed all available biologic and ts-DMARDS therapies over a 20-year disease course (figure 1).

She remained corticosteroid-dependent with persistently active disease manifested on ultrasound and MRI, a Disease Activity Score (DAS)-28-C reactive protein (CRP) of 7.46 and a CRP level of 104 mg/L (normal <5 mg/L). Rheumatoid factor (RF) 339/mL (normal <14 U/mL) and anticitrullinated protein antibodies (ACPA) 489.68 U/mL (normal <2.99 U/mL) were significantly elevated. Health Assessment Questionnaire Disability Index score (HAQ-DI) of 2.88 correlated with severe impairment of daily activities. Given the failure of all classes of therapies that had resulted in persistent peripheral B cell depletion (6 CD19+ cells/μL) yet with an abundance of CD19+ B cells (>70%) on synovial biopsy, CAR-T therapy was proposed. Anti-CD-19 CAR-T were produced on our institutional plat- form using an FMC63-28-CD3ζ CAR [3]. Following lymphodeple- tion with fludarabine (total 75 mg/m^2) and cyclophosphamide (900 mg/m²), 1×10^6 CAR-T/kg were infused. The patient developed grade 3 cytokine release syndrome (CRS) on day 2 and grade 4 immune effector cell-associated neurotoxicity (ICANS) on day 5, which necessitated tocilizumab, anakinra and high-dose corticosteroids for resolution.

100 days post-therapy, the patient was in drug-free remission with a DAS-28-CRP score of 2.5 with no neurological sequelae. Imaging findings have shown improvement; inflammatory markers normalised, and RF/ACPA levels decreased by more than 80% (figure 1).

This is the first documented case of CAR-T therapy in polyre- fractory RA. Recently, a case of a patient with myasthenia gravis and seropositive RA who responded to CAR-T therapy with respect to both diseases has been published, which in line with our findings [4]. Preclinical studies have shown CAR-T utility in eliminating autoreactive B cells both in vitro and in RA animal models [5,6]. CAR-T therapy was efficacious in patients with auto- immune diseases who failed treatment with rituximab, poten- tially as it also targets short-lived CD19+ plasma cells and due to their penetration into tissues [2]. Indeed, the synovium of sero- positive patients with RA frequently reveals a lymphomyeloid pattern dominated by the presence of CD19+ B cells, which is associated with disease progression and the accrual of damage [7]. Our patient suffered from relentless disease with high RF and ACPA levels despite peripheral B cell depletion resulting from multiple previous therapies. Disease remission was attained rapidly post-CAR-T therapy in unison with plunging RF, ACPA and CRP levels, suggesting the eradication of synovial CD19 B cells, which were present in abundance prior to therapy (figure 1). This discrepancy highlights the challenges in fully depleting B cells in soft tissues with standard therapies [8], which may be overcome by CAR-T therapy [9].

Our patient experienced both CRS and ICANS, far more severe than hitherto reported in patients with other autoimmune diseases following CAR-T therapy [2]. This can be attributed to the high burden of CD19 B cells within the synovium despite the low level in the periphery, to the potency of the CAR construct in use (having CD28 co-stimulation), to the number of cells given or to our patient's extreme inflammatory state at baseline with a CRP 20-fold higher than the upper limit of normal.

Recently, bispecific T-cell engager therapy has also shown preliminary success in managing refractory RA, emphasising the importance of CD19 B cells in RA [6].

In conclusion, we suggest that autologous CD19 CAR-T therapy with CD28 co-stimulation, which we have introduced here for the first time, be further evaluated in randomised controlled trials, taking into account potential benefits as well as the risk of severe adverse events in this population [8].

Social media: @doronrimar@gmail.com (D. Rimar)

Handling editor Josef S. Smolen.

ML and DR are joint first authors.

https://doi.org/10.1136/ard-2024-226437
Received 19 July 2024; Accepted 31 October 2024

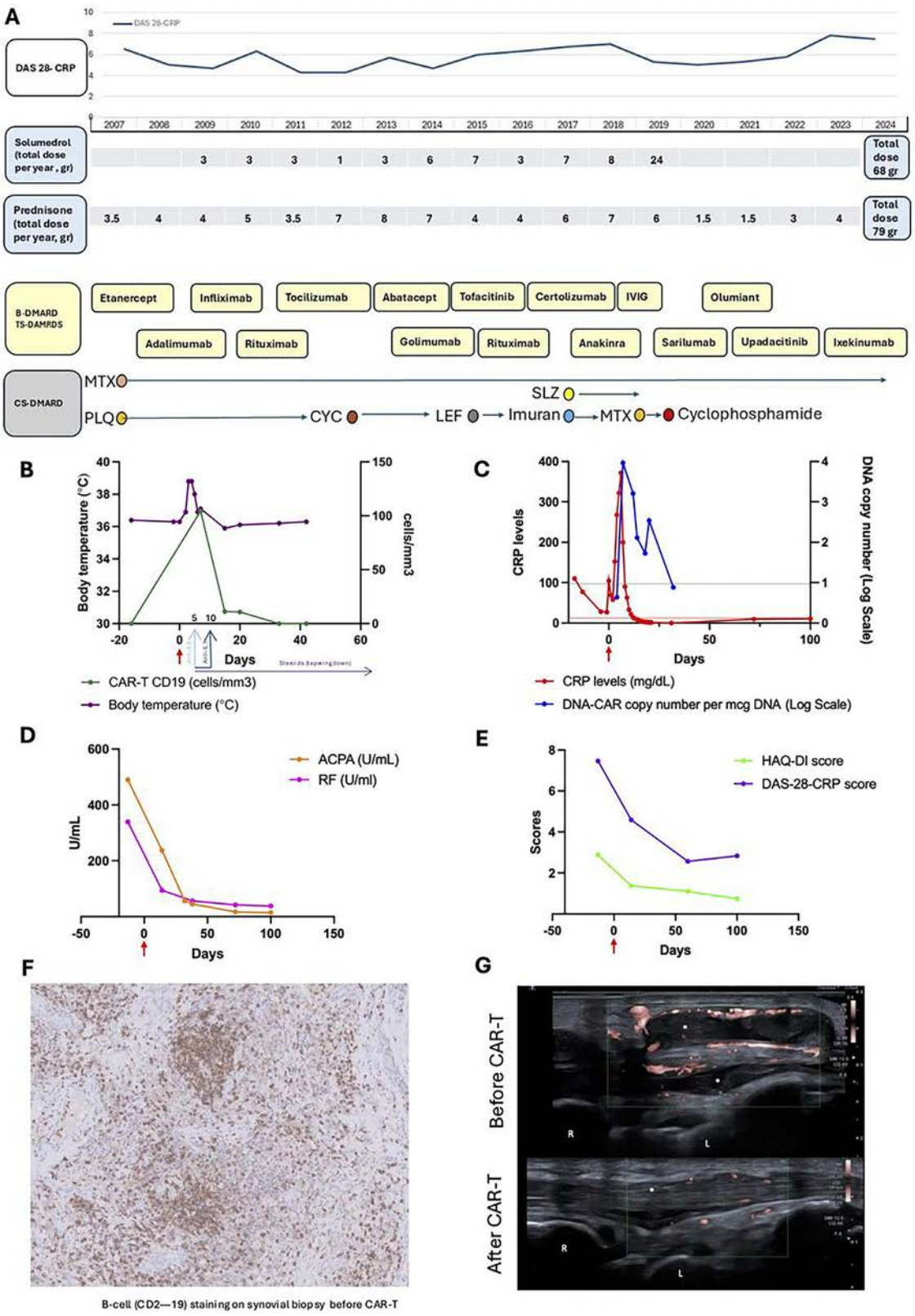

Figure 1. (A) Graphical overview of disease course and therapeutic regimen. (B) Body temperature (purple) and CAR-T cell expansion (green) over time. On day 5 post-CAR-T therapy (day 0), the patient was treated with methylprednisolone (1000 mg/day for 3 days), a single dose of intravenous tocilizumab (8 mg/kg) and anakinra (400 mg/day from days 5 to 10). (C) DNA-CAR copy number (blue, log scale) and CRP levels (red) following CAR-T cell infusion. (D) Reduction in RF and ACPA levels post-CAR-T cell infusion. (E) Improvement in disease activity and quality of life scores post-CAR-T cell infusion. (F) Graph showing peripheral B-cell depletion in counter to synovial CD-19 B cell abundance (70%) prior to CAR-T infusion. (G) Colour Doppler ultrasound images in the long axis to the extensor tendons of the wrist showing fluid distension (*) of the tendon sheath with the increased flow on colour Doppler imaging before CAR-T infusion Marked improvement with almost normal appearing extensor tendons after CAR-T cell infusion. ACPA, anticitrullinated protein antibodies; B-DMARDs, biologic disease-modifying drugs; CRP, C reactive protein; CAR-T, chimeric antigen receptor T-cell; CS-DMARDs, conventional synthetic disease-modifying drugs; CYC, cyclosporin; DAS-28, Disease Activity Score-28; HAQ-DI, Health Assessment Questionnaire Disability Index; IVIG, intravenous immunoglobulins; LEF, leflunomide; MTX, methotrexate; PLQ, plaquenil; RF, rheumatoid factor; SLZ, sulfasalazine; TS DMARDS, targeted synthetic DMARDs.

Acknowledgements

Rivka Adgo, our CAR-T cell coordinating nurse for providing compassionate and expert care.

Contributors

ML and DR contributed equally to this paper. ML, DR, PD, EJ, RSF, AS and AA conceived the idea and prepared the treatment protocol. ML, DR, PD, EJ and AA and wrote the letter. OI prepared the CAR-T cells. MDS and IE performed the radiological assessment of the patient. TS performed the pathological analysis of biopsy. GS, RM, RY, NST and ID completed patient assessments. All authors approved the letter. ML is the guarantor for this paper.

Funding

The authors have not declared a specific grant for this research from any funding agency in the public, commercial or not-for-profit sectors.

Competing interests

None declared.

Patient and public involvement

Patients and/or the public were not involved in the design, or conduct, or reporting, or dissemination plans of this research.

Patient consent for publication

Consent obtained directly from patient(s).

Ethics approval

This study involves human participants. The Sheba Medical Center's Internal Review Board gave permission for the study (approval number 1433-24-SMC). Participants gave informed consent to participate in the study before taking part.

Orcid

Doron Rimar: http://orcid.org/0000-0002-9137-2322
Paula David: http://orcid.org/0000-0003-0075-5895

REFERENCES

[1] David P, Di Matteo A, Hen O, et al. Poly-Refractory Rheumatoid Arthritis: An Uncommon Subset of Difficult to Treat Disease With Distinct Inflammatory and Noninflammatory Phenotypes. Arthritis Rheumatol 2024;76:510–21.
[2] Müller F, Taubmann J, Bucci L, et al. CD19 CAR T-Cell Therapy in Autoimmune Disease - A Case Series with Follow-up. N Engl J Med 2024;390:687–700.
[3] Itzhaki O, Jacoby E, Nissani A, et al. Head-to-head comparison of in-house produced CD19 CAR-T cell in ALL and NHL patients. J Immunother Cancer 2020;8:e000148.
[4] Haghikia A, Hegelmaier T, Wolleschak D, et al. Clinical efficacy and autoantibody seroconversion with CD19-CAR T cell therapy in a patient with rheumatoid arthritis and coexisting myasthenia gravis. Ann Rheum Dis 2024;83:1597–8.
[5] Whittington KB, Prislovsky A, Beaty J, et al. CD8$^+$ T Cells Expressing an HLA-DR1 Chimeric Antigen Receptor Target Autoimmune CD4$^+$ T Cells in an Antigen- Specific Manner and Inhibit the Development of Autoimmune Arthritis. J Immunol 2022;208:16–26.
[6] Zhang B, Wang Y, Yuan Y, et al. In vitro elimination of autoreactive B cells from rheumatoid arthritis patients by universal chimeric antigen receptor T cells. Ann Rheum Dis 2021;80:176–84.
[7] Bucci L, Hagen M, Rothe T, et al. Bispecific T cell engager therapy for refractory rheumatoid arthritis. Nat Med 2024;30:1593–601.
[8] Kowolik CM, Topp MS, Gonzalez S, et al. CD28 costimulation provided through a CD19-specific chimeric antigen receptor enhances in vivo persistence and antitumor efficacy of adoptively transferred T cells. Cancer Res 2006;66:10995–1004.
[9] Tur C, Eckstein M, Velden J, et al. CD19-CAR T-cell therapy induces deep tissue depletion of B cells. Ann Rheum Dis 2024.

Merav Lidar[1,2,*], Doron Rimar[3,4], Paula David[2,5], Elad Jacoby[2,6], Ronnie Shapira-Frommer[2,7], Orit Itzhaki[7], Gleb Slobodin[3,4], Myriam D Stern[2,8], Iris Eshed[2,8], Tamer Sanalla[2,9], Ronit Marcus[2,10], Avichai Shimoni[2,10], Ronit Yerushalmi[2,10], Noga Shem Tov[2,10], Ivetta Danylesko[2,10], Abraham Avigdor[2,10]

[1] *Rheumatology Unit, Sheba Medical Center, Tel Hashomer, Tel Aviv, Israel*
[2] *Faculty of Medical and Health Sciences, Tel Aviv University, Tel Aviv, Tel Aviv, Israel*
[3] *Rheumatology Unit, Bnai-Zion Medical Center, Haifa, Israel*
[4] *Rappaport Faculty of Medicine, Technion Israel Institute of Technology, Haifa, Haifa, Israel*
[5] *Internal Medicine B, Sheba Medical Center, Tel Hashomer, Tel Aviv, Israel*
[6] *Division of Pediatric Hematology and Oncology, The Edmond and Lily Safra Children's Hospital and Cell Therapy Lab, Sheba Medical Center, Tel Hashomer, Israel*
[7] *Ella Lemelbaum Institute for Immuno Oncology, Chaim Sheba Medical Center, Tel Hashomer, Israel*
[8] *Department of Diagnostic Imaging, Sheba Medical Center, Tel Hashomer, Israel*
[9] *Institute of Pathology, Affiliated to Tel Aviv University, Sheba Medical Center, Tel Hashomer, Tel Aviv, Israel*
[10] *Division of Hematology and Bone Marrow Transplantation, Chaim Sheba Medical Center, Tel Hashomer, Israel*
*__Correspondence to__ Dr. Merav Lidar
E-mail address: Merav.Lidar@sheba.health.gov.il (M. Lidar).

Ann Rheum Dis 84 (2025) 373

Contents lists available at ScienceDirect

Annals of the Rheumatic Diseases

journal homepage: https://www.sciencedirect.com/journal/annals-of-the-rheumatic-diseases

Corrigendum

Correction: Olokizumab plus methotrexate: safety and efficacy over 106 weeks of treatment

Feist E, Fleischmann RM, Fatenejad S, *et al*. Olokizumab plus methotrexate: safety and efficacy over 106 weeks of treatment. *Annals of the Rheumatic Diseases* 2024;83:1454-1464.

The correct figures 2 and 3 including descriptions provided on y-axis are below:

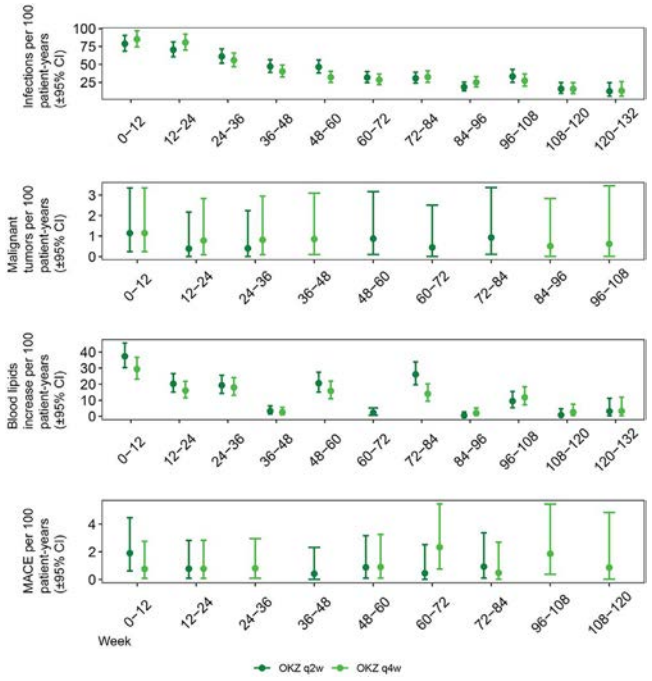

Figure 2.

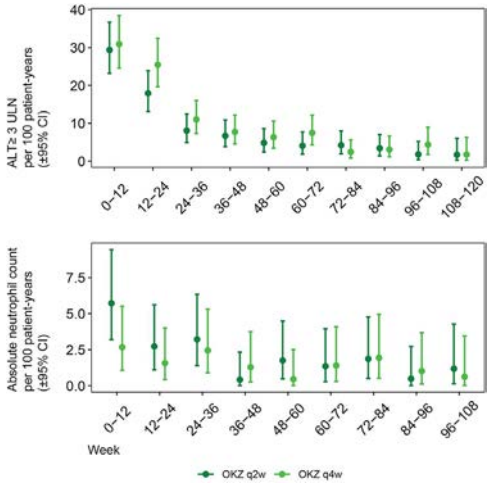

Figure 3.

https://doi.org/10.1136/ard-2023-225473corr1